

16TH

INTERNATIONAL SYMPOSIUM

Water Management &
Hydraulic Engineering


WMHE
2019

Proceedings

5-7TH September

SKOPJE, NORTH MACEDONIA



GDAŃSK UNIVERSITY
OF TECHNOLOGY

STU
SVF

SLOVAK UNIVERSITY OF
TECHNOLOGY IN BRATISLAVA
FACULTY OF CIVIL ENGINEERING



BRNO
UNIVERSITY
OF TECHNOLOGY

Editors

Petko Pelivanovski, Milorad Jovanovski, Ljupcho Petkovski, Katerina Donevska

Technical editors

Stevcho Mitovski, Goce Taseski

Cover Design

Todor Lazarovski

Published by

Ss Cyril and Methodius University, Civil Engineering Faculty – Skopje

Printed by

LT 978

Printing run

120 copies

Web site

www.wmhe2019.gf.ukim.edu.mk

© All rights reserved. The publication can not be translated or copied at full or any part of it without written permission from the publisher.

ISSN 2410-5910

CIP - Каталогизација во публикација

Национална и универзитетска библиотека "Св. Климент Охридски", Скопје

556.18(062)(048.3)

626/628(062)(048.3)

16TH International simposium Water management & hydraulic engineering
WMHE (2019 ; Skopje)

Book of abstracts / 16th International simposium Water management &
hydraulic engineering WMHE 2019, 5-7th September, Skopje, North
Macedonia ; editors Petko Pelivanovski ... [и др.]. - Skopje : Faculty
of civil engineering, 2019. - 85 стр. ; 25 см

ISBN 978-608-4510-33-8

1. Pelivanovski, Petko [уредник]

а) Водени ресурси -- Управување -- Собири -- Апстракти б) Хидротехника
-- Собири -- Апстракти

COBISS.MK-ID 110982666

Note: The Proceedings contains original author's papers reviewed and accepted by the
Scientific Advisory Committee. (for e-Proceedings]

Symposium Chairmen

Cvetanka Popovska,
Ss. Cyril and Methodius University, Civil Engineering Faculty, Skopje, N. Macedonia

Damir Bekić
University of Zagreb, Faculty of Civil Engineering, Zagreb, Croatia

Michał Szydłowski
Gdansk University of Technology, Faculty of Civil and Environmental Engineering,
Gdansk, Poland

Andrej Soltesz
Slovak University of Technology, Faculty of Civil Engineering, Bratislava, Slovak
Republic

Helmut Habersack
University of Natural Resources and Life Sciences, Vienna, Austria

Jaromir Riha
Brno University of Technology, Faculty of Civil Engineering, Brno, Czech Republic

Scientific Advisory Committee

Petko Pelivanovski, Milorad Jovanovski, Ljupcho Petkovski, Katerina Donevska
Ss. Cyril and Methodius University, Faculty of Civil Engineering, Skopje, N. Macedonia

Živko Vuković, Neven Kuspilić, Goran Lončar
University of Zagreb, Faculty of Civil Engineering, Zagreb, Croatia

Adam Szymkiewicz, Magdalena Gajewska, Piotr Zima Gdansk
University of Technology, Faculty of Civil and Environmental Engineering, Gdansk,
Poland

Peter Šulek, Silvia Kohnová, Štefan Stankoi
Slovak University of Technology, Faculty of Civil Engineering, Bratislava, Slovak Republic

Johannes Hübl, Gerhard Kammerer, Petr Lichtneger
University of Natural Resources and Life Sciences, Vienna, Austria

David Duchan, Miroslav Špano Brno
University of Technology Faculty of Civil Engineering, Brno, Czech Republic

Organizing Committee

Vladimir Vitanov, Josif Josifovski, Zlatko Zafirovski, Stevcho Mitovski, Goce Taseski,
N. Macedonia

Damir Bekić, Dražen Vouk, Dalibor Carević, Croatia

Lea Čubanová, Martin Orfánus, Slovak Republic

Wojciech Artichowicz, Poland

Petr Lichtneger, Austria

Tomáš Julínek, Czech Republic

PREFACE

The 16th International Conference on Water Management and Hydraulic Engineering (WMHE) is organized by the Faculty of Civil Engineering at the University of Ss Cyril and Methodius in Skopje, from 5-7 September 2019, in Skopje, Macedonia. The main goal of the WMHE Conferences is to achieve on long-term perspective the integrated approach and application of the concepts of integrated water resources management in a context of regional climate change and anthropogenic pressure on the environment.

The key objectives of WMHE Conferences are to improve the scientific knowledge and networking between scientist, to favor multidisciplinary approach and to disseminate information on educational experiences, new technologies, practices and strategies to the end-users in order to improve the education and to preserve the water resources and the biodiversity of the aquatic ecosystems.

This Conference provided a setting for discussing recent developments in a wide variety of topics including: Integrated Water Resources Management (I), Hydraulic Engineering and Environmental Impacts (II), Sanitary Engineering and Sustainable Water Use (III), Hydraulic Structures (IV), Ecohydrology and Water Bodies Protection (V), River Basin Restoration Strategies and Experiences (VI) and Climate Change and Flood Risk Management (VII).

All these topics are interconnected and related to the changes of the environment. The physical environment and resource availability are being affected by global climate change, which in turn is being driven by human development and growth. It feeds into cycles of water resources degradation affecting both human well-being and the environment. In such cycles, climate change and natural hazards play significant roles. Impacts related to climate change are evident across regions and in many sectors important to society – such as human health, agriculture, water supply, transportation, energy, ecosystems, and others are expected to become increasingly disruptive in the coming decades. Hence, WMHE conferences aim to encourage participants to exchange knowledge and experience and to cope with the water related problems and environment protection.

The Faculty of Civil Engineering in Skopje organizes the WMHE conference for the second time. The conference was announced widely on Internet by creation its web page: <http://wmhe2019.gf.ukim.edu.mk>. The host Organizing Committee prepared templates for abstracts and full papers, as well as templates in Power Point for oral and poster presentations.

During the Conference there were 5 plenary lectures covering the different topics:

Andrej Šoltész (Slovak University of Technology, Faculty of Civil Engineering, Bratislava): *Flood protection design for municipalities of Slovakia in various hydrological conditions.*

Tomás Julínek (Brno University of Technology, Faculty of Civil Engineering, Czech Republic): *Flood hazards related to effects of groundwater flow.*

Tomasz Kolerski (Gdańsk University of Technology, Faculty of Civil and Environmental Engineering, Poland): *Mathematical modelling of river ice processes.*

Gordon Gilja (University of Zagreb, Faculty of Civil Engineering, Croatia): *Experimental investigation of flow field in a physical fishway mode.*

Milorad Jovanovski (University Ss Cyril and Methodius, Faculty of Civil Engineering, Skopje, Macedonia): *Floods and post-recovery of landslides.*

To manage the tasks related to this Conference an International Scientific Advisory Committee was set up:

Petko Pelivanovski, Milorad Jovanovski, Ljupčo Petkovski, Katerina Donevska, Violeta Gješovska (University of Ss Cyril and Methodis, Skopje, Macedonia), Živko Vuković, Neven Kuspilić, Goran Lončar (University of Zagreb, Croatia), Adam Szymkiewicz, Magdalena Gajewska, Piotr Zima (Gdańsk University of Technology, Poland), Peter Šulek, Silvia Kohnová, Štefan Stanko (Slovak University of Technology, Bratislava, Slovakia), Johannes Hübl, Gerhard Kammerer, Petr Lichtneger (BOKU University, Austria), Jan Jandora, Miroslav Špano (Brno University of Technology, Czech Republic).

All accepted papers are published in Proceedings in digital form and in the Book of Abstracts published in printed form. For the first time out of two-annual WMHE Conferences there will be organized a post-conference publishing activity. Selected papers by the Scientific Advisory Committee will be published in the following journals:

1. Slovak Journal of Civil Engineering (Bratislava)
2. Acta Hydrologica Slovakia (Bratislava)
3. Scientific Journal of Civil Engineering (Skopje)

The members of the Organizing Committee made a great effort on preparation of the conference materials and organizing the events which is certainly not less important than the other issues, and the editors would like to express their warm gratitude to the people:

Josif Josifovski, Vladimir Vitanov, Zlatko Zafirovski, Stevčo Mitovski, Goce Taseski (University of Ss Cyril and Methodis, Skopje, Macedonia), Damir Bekić, Dražen Vouk, Dalibor Carević (University of Zagreb, Croatia), Wojciech Artichowicz (Gdańsk University of Technology, Poland), Lea Čubanová, Martin Orfánus (University of Technology, Bratislava, Slovakia), Petr Lichtneger (BOKU University, Austria), and Tomáš Julínek (Brno University of Technology, Czech Republic).

Special thanks should go to Nikola Jankulovski, the Rector of the University Ss Cyril and Methodius in Skopje, who has demonstrated understanding and strong support to the conference. His support make possible achieving relaxing atmosphere during the final steps of conference preparation which is usually the most stressed work.

Skopje, September, 2019

Cvetanka Popovska

Contents

Preface

Invited speakers

IS1	EXPERIMENTAL INVESTIGATION OF FLOW FIELD IN A PHYSICAL FISHWAY MODEL G. Gilja, E. Ocvirk, A. Cikojević	1
IS2	FLOOD PROTECTION DESIGN FOR MUNICIPALITIES OF SLOVAKIA IN VARIOUS HYDROLOGICAL CONDITIONS A. Šoltész, L. Čubanová, A. Janík, D. Baroková	13
IS3	MATHEMATICAL MODELING OF RIVER ICE PROCESSES T. Kolerski	22
IS4	MAPPING OF GROUNDWATER FLOW CHANGES AND RELATED HAZARDS T. Julinek, J. Řiha	33
IS5	POST-FLOOD RECOVERY OF LANDSLIDES M. Jovanovski, C. Popovska, I. Pesevski	34
T1 Integrated Water Resources Management		
P28	ASSESSMENT OF MULTI-OBJECTIVE OPERATION OF THE “BOVAN” RESERVOIR DUE TO SILTATION J. M. Brankovic, M. Markovic, J. Protic	55
P42	APPLICATION OF SIMULATION MODEL IN CASE OF MULTI-RESERVOIR SYSTEM PLANNING F. Panovska, S. Mitovski, L. Petkovski	61
T2 Hydraulic Engineering and Environmental Impact		
P27	APPLICATION OF THE SWAT TO MODEL THE IMPACT OF POLLUTION FROM AGRICULTURAL AREAS ON COASTAL WATERS OF THE BALTIC SEA IN PUCK BAY REGION D. Kalinowska, P. Wielgat, T. Kolerski, M. Szydłowski, P. Zima	77
P32	IMPACT OF RIVER TRAINING WORKS ON THE DRAVA RIVER FLOW REGIME G. Gilja, N. Kuspilić, N. Golubović	89
P33	SENSITIVITY ANALYSIS OF EMPIRICAL EQUATIONS APPLICABLE ON BRIDGE PIERS IN SAND-BED RIVERS A. Cikojević, G. Gilja, N. Kuspilić	100
P36	EROSION SEVERITY ESTIMATION USING MULTI-CRITERIA ANALYSIS N. Dragičević, B. Karleuša	109
P39	INTERNAL EROSION INCIDENT AT THE WEIR SLUICE J. Řiha, T. Julinek	118
P51	SIMULATION OF THE FLOOD FORMATION, TIME AND SPATIAL DISTRIBUTION BY USING ADVANCED HYDRODYNAMIC MODELING M. Orfanus, A. Šoltész, D. Buček	126
P55	NUMERICAL MODELS FOR ANALYSIS OF HYDRAULIC TRANSIENTS G. Lončar, Ž. Šreng, T. Kulić, H. Miličević, S. Ostojjić	133

P59	HYDRAULIC ANALYSIS OF WATER SUPPLY SYSTEM WITHOUT TANKS G. Taseski, P. Pelivanoski	146
P60	HYDRAULIC ANALYSIS OF EXISTING SEMI-SEPARATE SEWAGE SYSTEM BY USING SWMM G. Taseski, P. Pelivanoski	154
P54	A COMPARISON OF FLOOD ROUTING BY MODIFIED LINEAR MUSKINGUM AND KINEMATIC WAVE APPROACHES ON THE DRAVA AND MURA RIVERS D. Bekić, T. Kulić, K. Bašić	161
P08	THE IMPACT ON THE ENVIRONMENT WITH THE CONSTRUCTION OF ALL PHASES FROM THE MULTI-PURPOSE HYDRO SYSTEM ZLETOVICA E. A. Dosevska	162
P09	APPLICATION OF ADCP IN SUSPENDED SEDIMENT MONITORING N. Cvijanović, M. Kostić, M. Ivljanin	172
P34	WATER LEVELS OF THE MAJOR RIVERS IN SLAVONIA S. Maričić, T. M. Svetinović	181
P35	A REVIEW OF EROSION POTENTIAL METHOD MODIFICATION AND APPLICATION ON DUBRAČINA RIVER BASIN N. Dragičević, B. Karleuša, N. Ožanić	194
P57	HYDRAULIC CONSIDERATION OF THE FISH PASS CROSS SECTION USING VELOCITY-AREA METHOD L. Čubanová	206
T3 Sanitary Engineering and Sustainable Water Use		
P48	PILOT-PLANT EXPERIENCES WITH MEMBRANE FILTRATION AT THE WTP JASNÁ D. Barlokova, J. Ilavsky, M. Marton, M. Kunštek	216
P21	CRITICAL INFLUENCING FACTORS FOR THE CAUSES OF PIPE FAILURES AND LEAKAGE IN WATER SUPPLY SYSTEMS S. Spirovska, P. Klingel	224
P40	SETTLING CHARACTERIZATION OF ELECTROCOAGULATED FLOCS I. Halkijević, I. SOKOL, H. Posavčić	232
P41	REMOVAL OF PHOSPHATES FROM WASTEWATER BY ELECTROCOAGULATION I. Halkijević, G. Lončar, D. Dizdar	244
P58	DETERMINATION OF THE POPULATION EQUIVALENT AND THE REQUIREMENT OF WATER IN THE EXISTING WATER SUPPLY SYSTEMS AS INPUT PARAMETERS FOR HYDRAULIC ANALYSIS, A CASE STUDY ON THE WATER SUPPLY SYSTEM FOR THE TOWN OF GOSTIVAR G. Taseski	255
P63	EFFICIENCY OF ELECTROCHEMICAL PROCESSES IN REMOVAL OF AMONIUM FROM URINE D. Vouk, G. Lončar, A. Musa, M. Pandžić, A. Vekić, M. Drušković, A. Bubalo, R. Kollar	263

P17	ELECTROCHEMICAL PROCESS FOR MUNICIPAL WASTEWATER TREATMENT – A REVIEW H. Posavčić, D. Vouk, I. Halkijević	272
P50	HYDRODYNAMIC DISPERSION IN SEWER: DETERMINATION OF DEAD ZONES PARAMETERS Y. Veliskova, M. Sokač	282
T4 Hydraulic structures		
P23	RESEARCH ON THE OUTLET CAPACITY OF THE LAKE MONDSEE TO IMPROVE FLOODRISK MANAGEMENT P. Lichtneger, H. Holzmann, C. Sindelar, J. Schobesberger, H. Habersack	293
P6	POLYMERIC GEOMEMBRANES IN NEW ROCKFILL DAMS: 2 CASE HISTORIES G. Vaschetti, V. Verdel, A. Scuero	305
P45	WAVE TRANSMISSION BELOW BREAKWATERS WITH SEMI-IMMERSED CURTAIN D. Carevic, D. Bujak, K. Potočki, J. Drašković	315
P53	THE WATER WAY DUNAV – MORAVA – VARDAR – AEGEAN SEA, UP TO NOW REAMARKS OF THE TECHNICAL DOCUMENTATION A. Radevski	327
P67	CONSTRUCTION OF DAMS AND HYDROPOWERS, AS A MEASURE FOR THE LEVEL OF DEVELOPMENT OF THE STATE S. Milevski	336
P68	SOLUTIONS FOR THE REHABILITATION IN THE HYDROTECHNICAL TUNNEL Z. Zafirovski, V. Gacevski, I. Peshevski, M. Jovanovski	348
P25	SEDIMENTATION VELOCITY OF SAUALM CRYSTALLINE USING IMAGE PROCESSING METHODS D. Worf, J. Schobesberger, P. Lichtneger, H. Habersack, C. Sindelar	353
T5 Ecohydrology and Water Body Protections		
P11	NUMERICAL ANALYSIS OF ESCHERICHIA COLI TRANSPORT THROUGH THE KARST ENVIRONMENT (EXAMPLE OF BOKANJAC-POLIČNIK AQUIFER, REPUBLIC OF CROATIA) G. Lončar, Ž. Šreng, H. Miličević, S. Ostojić	366
T6 River Basin Restoration Strategies and Experiences		
P38	MULTICRITERIAL EVALUATION OF THE BÍLINA RIVER REVITALIZATION T. Julinek, J. Řiha	377
T7 Climate Change and Flood Risk Management		
P13	FLOOD RISK MANAGEMENT: AN INSTITUTIONAL DEVELOPMENT PERSPECTIVE C. Popovska, D. Sekovski, D. Barbalić	387
P12	BUILD BACK BETTER APPROACH TO RECOVERY OF FLOOD-DAMAGED TRANSPORT AND WATER INFRASTRUCTURE C. Popovska, M. Jovanovski, D. Sekovski	398
P14	ENHANCING RESILIENCE THROUGH RECOVERY OF FLOOD-DAMAGED INFRASTRUCTURE IN MACEDONIA: AN	409

	OVERVIEW OF LESSONS AND CHALLENGES	
	D. Sekovski, C. Popovska	
P37	DROUGHT AND PRECIPITATION CONCENTRATION INDEX (PCI) ANALYSIS IN CONTINENTAL CROATIA	
	L. Tadić, T. Brleković	420
P46	POSSIBILITIES OF DESIGN OF FLOOD PROTECTION MEASURES ON THE ONDAVA RIVER	
	J. Mydla, A. Šoltesz, M. Orfanus	430
P07	CLIMATE CHANGE IMPACT ON IRRIGATION WATER REQUIREMENTS: CASE STUDY OF IRRIGATION SYSTEM IN SKOPJE VALLEY	
	K. Donevska, A. Panov	438
P19	PROTECTION FROM EROSION AND RIVER SEDIMENTS BY TORRENTIAL RIVERS AND GULLIES NEAR LOCAL ROADS IN THE MUNICIPALITY OF KONCHE	
	D. Dimitrievski, S. Stoshevska, D. Ilievski, L. S. Trendafilova, K. Veleska	447
P73	REDEFINITION OF FLOOD WATERS FOR THE KALIMANCI DAM	
	V. Gjesovska, I. Lefkova, G. Taseski	455
	T8 Geotechnical aspects of Hydraulic Engineering	
P61	EXPERIMENTAL AND NUMERICAL MODELLING OF RAINFALL-INDUCED SLOPE INSTABILITIES IN UNSATURATED SANDY SOIL	
	J. Josifovski, B. Susinov, M. Tasevska	466
P52	COMPARISON OF CALCULATED AND MEASURED FILTRATION RATES	
	J. Škvarka, E. Bednarova	478
P65	STABILIZATION OF SURFACE EROSION ON SLOPES USING POLYMERS AND VEGETATION	
	A. Nikolovska, J. Josifovski, B. Susinov	488
P26	HYDROGEOLOGICAL ASPECT IN DETERMINING THE PROTECTION ZONES OF THE “NEREZI – LEPENEC” WELL SYSTEM	
	Z. Ilijovski, S. Mihailovski, M. Makeshoska	500
P43	HAZARD AND RISK ASSESSMENT OF EARTHQUAKE GEOTECHNICAL INSTABILITIES	
	J. Bojadjieva, V. Sheshov, K. Edip, T. Kitanovski, J. Chaneva, D. Ivanovski	511
P44	NUMERICAL SIMULATION OF SOIL CONSOLIDATION AS A GEOTECHNICAL PHENOMENON	
	K. Edip, V. Sheshov, J. Bojadjieva, T. Kitanovski, J. Chaneva, D. Ivanovski	522
P62	HYDROLOGICAL ANALYSIS OF HIGH INTENSITY RAINFALLS OVER TOPOLNICA TAILING DAM	
	B. Susinov, M. Naumovski, J. Josifovski	529
P66	MANAGEMENT, EXPLOITATION AND MONITORING OF THE GROUNDWATER	
	D. Dimitrievski	540

Invited lectures

EXPERIMENTAL INVESTIGATION OF FLOW FIELD IN A PHYSICAL FISHWAY MODEL

GORDON GILJA¹, EVA OCVIRK², ANTONIJA CIKOJEVIĆ³

¹University of Zagreb Faculty of Civil Engineering, Croatia, ggilja@grad.hr

²University of Zagreb Faculty of Civil Engineering, Croatia, ocvirk@grad.hr

³University of Zagreb Faculty of Civil Engineering, Croatia, acikojevic@grad.hr

1. Abstract

This paper describes the detailed testing of the characteristic velocity fields on the physical model of pool-type and vertical slot fishway. For the physical model setup, a 18m long, 0.9m wide and 0.9m high hydraulic flume with rectangular cross-section was used. Each type of fishway was tested by a physical model in geometric scale 1:3 for the different gradient (12.5%, 10% and 7.5%), the pool length (45cm, 60cm and 90cm) and orifices or slots geometry. Raster of the measuring points is defined longitudinally, transversely and by the flow depth so that it includes all relevant positions that are of interest to estimate the hydraulic efficiency of the fishways. The results of experimental measurements were analysed by comparing the velocity field in pools for both types of fishways and all configurations within them. Flume experiments have shown that local variability of the flow field heavily influences the measurement quality and consequently the results.

Keywords: pool-type fishway, vertical slot fishway, physical model, ADV, recirculation zone, slot zone.

2. Introduction

Small watercourses are currently being more and more exploited, *i.e.* for small hydropower facilities or restoration of traditional mills, whose construction has adverse effect on fish populations [1]. These structures usually traverse the entire river profile, thus disconnecting its longitudinal connectivity and blocking the movement of some fish species that require migration during different stages of their life cycle [2]. Fishways are structures used for mitigation of negative effects of aforementioned obstacles on fish migration which can facilitate both upstream and downstream fish migration [3] [4]. Their value is in visible through ecological engineering approach which involves creating and restoring a sustainable ecosystem for fish migration [5]. Fishways are usually designed for each location individually, adjusting their hydraulic efficiency (discharge, velocity, depth, power, turbulence fields, etc.) to the dominating fish population in the area, taking into account their swimming capacity, behaviour, and motivation [6]. Most common classification of fishways is based on their design type, where 4 main groups are recognized: pool-type, vertical slot, Denil, and culvert fishways [1]. Swimming ability and desired flow path of the target fish species are the key factors in hydraulic design of fishways - hydraulic conditions in each fishway type are suitable

for target fish species, while at the same limiting factor for the other.

Guiny *et al.* [7] investigated different types fishways and found that majority of fish species moved through submerged orifices and vertical slots rather than through overflow weirs, independent of discharge, flow velocity and head loss. They also found that at equal velocities orifices may be more suitable than vertical slots. The pool-type fishway is oriented towards the strong swimming fish species. It is composed of consecutive vertical walls that divide the fishway into pools, with orifice(s) on the bottom. Main goal of such design is to ensure adequate energy dissipation contained within the single pool, and to offer resting sections within them [8]. The downside of the pool-type fishway installation is the narrow range of operating flow [9]. Vertical slot fishway design enables fish to pass through the fishway at any desired depth of water column. Rajaratnam *et al.* [10] conducted initial investigation for 7 different designs of vertical slot fishways and defined a linear relationship between the dimensionless discharge and relative flow depth. Later on, they experimentally investigated 18 different designs of vertical slot fishways experimentally and recommended some for practical use.

The complex 3D turbulent flow field in fishways can be most conveniently investigated using 3D numerical models [11] [12] which allow for detailed numerical mesh computation, as well as adaptive display of relevant results. In this regard, they have advantage over experimental investigations on physical models, but on the other hand they require extensive mesh preparation and must be calibrated using field surveys or physical model results. Therefore, in order to fully exploit the advantages of numerical model for understanding of turbulent structures and flow pattern in fishways, they must be complemented/preceded with investigations on physical model conducted in smaller extent.



Figure 1. Conversion of baffle fishway into pool fishway on SHPP Ilovac

In hydraulic laboratory under University of Zagreb, Faculty of Civil Engineering, physical and numerical model of fish passes for typical weir obstacles in small watercourses is established [13] [14] [15]. Physical model is used for calculation of reference flow field characteristics in one pool under current constraints of the infrastructure in the laboratory (*e.g.* flume width, length and height and pump capacity). Numerical model is used to calculate hydraulic characteristics across several pools that form single fishway with finer step in discretization of discharge, flow depth and fishway geometry. This paper presents the results of the first phase of pool-type and vertical slot type fishway investigation: experimental investigations of the flow velocity field and turbulence structure that affect the hydraulic performance on physical model.

3. Experimental setup

The experiments were designed to examine the hydraulic conditions of several different geometries and boundary conditions on two types of fishway: pool-type and vertical slot fishway. For the establishment of a physical model, a 18m long, 0.9m wide and 0.9m high recirculating hydraulic flume with rectangular cross-section was used. Working section of the flume is currently 13m long, 0.9m wide and 0.7m deep. The discharge in the flume is controlled by frequency-regulated pump with maximum capacity of 35l/s, and water level is controlled by hinged flap gate. A permeable flow straightening system was constructed on the pump inlet in the upstream flume boundary to reduce turbulence in the inflow section. The fishway model itself was built in scale 1:3 to prototype, using Froude scaling which results with following equations for extrapolation of the results to prototype scale:

$$L_P = 3 \cdot L_M \quad (1)$$

$$v_P = \sqrt{3} \cdot v_M \quad (2)$$

$$Q_P = \sqrt{243} \cdot Q_M \quad (3)$$

where: L = length [m], v = flow velocity [m/s], Q = discharge [m^3/s], subscripts P and M denote prototype and model values, respectively.

Model scale was selected in order to fully exploit the flume capacity, taking into account the limitations of flume, where the flume depth was proven to be limiting dimension. Therefore, the fishway model width and length had to be reduced to 0,45cm and 3m, respectively. Fishway models were constructed in the flume using waterproof plyboard as its inner wall and the flume glass as the outer wall, using best practices [16]. Fishway walls are fixed, while its bottom and cross-walls, are modular so that model geometry can be adjusted to desired gradient, orifice/slot opening size and pool length. Following figure shows the flume with fishway model constructed inside (Figure 2).



Figure 2. Hydraulic flume (left), hinged flap gate (right).

Measurement of flow velocity field characteristics was performed by a Vectrino Acoustic Doppler Velocimeter (ADV) mounted on a cart, which was supported on the walls of the hydraulic flume allowing it to be positioned on pre-set positions. ADV selected for the application is able to collect data with a 25Hz sampling frequency. Seeding particles were introduced into the pumping basin to increase the number of acoustically reflective particles in the water, and subsequently the measured data quality. To ensure the statistical significance of the velocity record, velocity measurements were recorded over 3 min duration [17]. Values of quality control variables, correlation

coefficient COR and signal/noise ratio SNR, was within the limits reported in the literature for the highly turbulent flow [18] [19]: correlation coefficient fluctuated between 30% and 85%, while signal/noise ratio varied between 50dB and 80dB for all experiments. For flow over rough boundaries, the lower correlation values can be used [20]. Therefore, the raw data were filtered to eliminate poor signals based on a filtering scheme of $SNR \geq 30\text{dB}$ and $COR \geq 55\%$ [17], and spikes were eliminated using the method of Goring and Nikora [21] using Velocity Signal Analyser [22] before calculating the flow field characteristics. After filtering, more than 70% of the original velocity time series data was preserved, which is deemed enough for Reynolds stress calculation [19]. If all of the noise could be filtered out, the velocity spectra exhibit “ $-5=3$ ” slope at higher frequencies, *i.e.* the inertial subrange [23].

The following convention was used when referring to the measured instantaneous velocity: u represents streamwise velocity component, positive in the downstream direction; v represents spanwise velocity component, positive towards the right and w represents vertical velocity component, positive in the direction opposite of gravity. Sampling volume of the ADV is set 5cm from the instrument, which has influenced the raster of measurement points. Raster of the measuring points is defined longitudinally, transversely and by the flow depth so that it includes all relevant positions that are of interest to estimate the hydraulic efficiency of the fishways. Raster of velocity measurement points is defined with constant spacing of 7cm between points across the fishway and 9cm along the fishway. Points nearest to the wall were displaced from it up to 5cm, depending on the configuration. Measurements were taken at 3 different depths: surface (level A), middle (level B) and bottom (level C).

4. Experimental procedure

The fishway model has been built according to the schematic below (Figure 3,

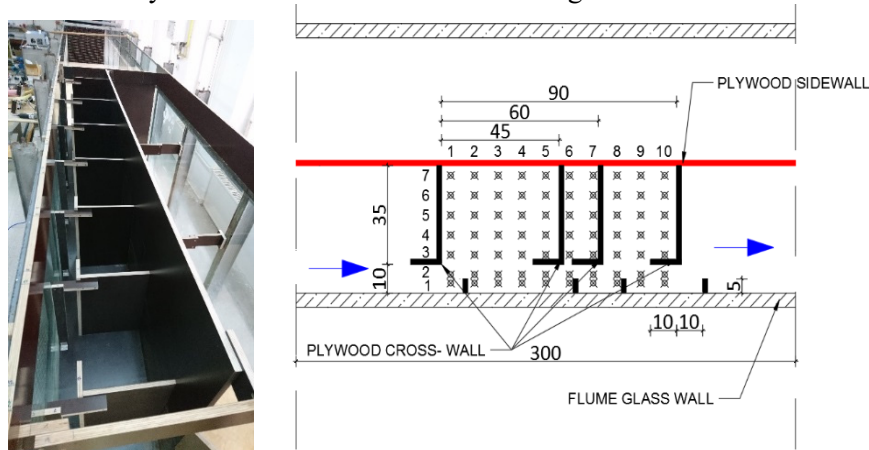


Figure 4). Depending on the pool length, at least three pools were formed for the tests: a head pool receiving the water from an upstream reservoir, at least one active pool and a tail pool. Each fishway type was tested by a physical model for the different gradient (12.5%, 10% and 7.5%) [24] [1], the pool length (45cm, 60cm and 90cm) and orifices 8cmx8cm, 10cmx10cm, 12cmx12cm or slots geometry. Investigations on pool fishway

type consisted of 27 different gradient/pool length/orifice size combinations: gradient was varied for 12.5%, 10% and 7.5%, pool length was varied for 45cm, 60cm and 90cm, orifice size was varied for 8cmx8cm, 10cmx10cm and 12cmx12cm. For distinctive purposes, configurations were labelled “gradient – pool length – orifice”. Orifices are positioned on the bottom of cross-wall, with alternating positions between successive cross-walls, next to the fishway sidewall (Figure 3).

Investigations on vertical slot fishway type consisted of 9 different gradient/pool length combinations, same as for the pool fishway, and configurations were labelled accordingly “gradient – pool length”. Slot is formed using two cross-walls [25], in such a way that its vertical section that forms the slot is L-shaped cross-wall with baffle protruding into the upstream pool

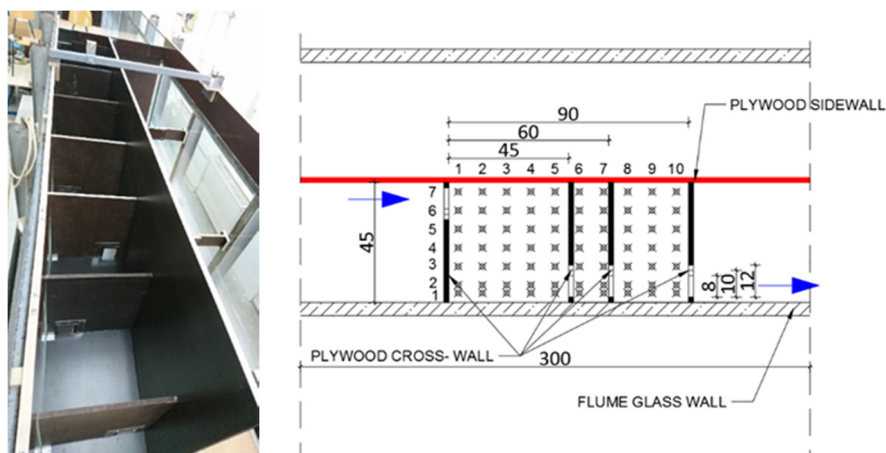


Figure 3. Physical model of pool-type fishway: photo (left), design scheme for all pool lengths (right)

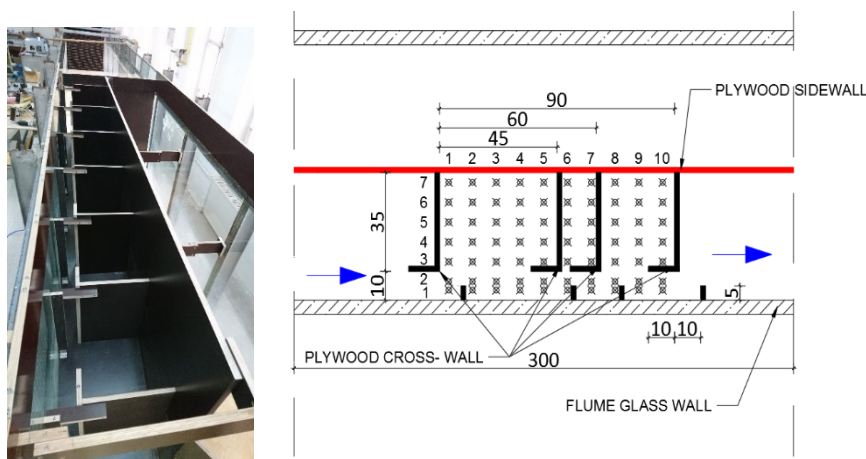


Figure 4. Physical model of vertical slot type fishway: photo (left), design scheme for all pool lengths (right).

For each configuration velocity measurements were conducted in representative active pool, selected in the middle section of the fishway which is unaffected by the upstream

and downstream boundary conditions. For pool length of 45cm and 60cm third pool from the upstream was selected, while for pool length of 90cm it was second pool. Defined raster of measurement points consisted of 25 measurement points in a single level for pool length 45cm, 49 measurement points for pool length 60cm and 70 measurement points for pool length 90cm. Naming convention was defined according to the matrix, level, row, column, where number of rows is for all configuration 7 because fishway width is constant across all experiments, column number varies from 5 to 10, depending on the pool length. The following figure shows schematic of a measurement point raster for both fishway types.

5. Results and discussion

The results of experimental measurements were analysed by comparing the velocity field in pools for both types of fishways and all configurations within them. Each configuration contains three measured flow velocity components at all three planes for slopes 7.5%, 10% and 12.5%, different orifice opening and discharge span from 6.5l/s to 12.9l/s, depending on the orifice size. Observations of the flow velocity field characteristics in the pools and at the slots are described and derived conclusions regarding the design guidelines conforming to requirements and restrictions for specific locations on small watercourses. Flow velocity vectors in analysis are represented by scaled arrows in horizontal plane view, by coneplot in 3D view for comparison between different models. Results are singled out for fishway with slope 12.5% because it enables the use of the most space-consuming fishway, and gives representative values for other slopes at the same time.

The following figure (Figure 5) shows plane view of flow velocity vectors for pool fishway model 125-45-10 at each of the three measured planes (from top to bottom: A, B and C). All 3 planes have similar flow velocity pattern: at the pool inlet orifice situated on the left side of the upstream cross-wall flow velocity vectors are immediately deflected towards the left sidewall. Flow entering the pool creates the clockwise vortex on the outside of the pool that spans across the entire pool. Flow vortex has clockwise orientation due to the position of the inlet orifice and alternate positioning of the outlet orifice next to the right-side pool wall. Flow velocity vortex is largest for the plane C, which is expected because height position of the measurement points on plane C corresponds to the orifice position. Flow velocity vector with the largest magnitude of 1.15m/s was measured on point 1-7, adjacent to the inlet orifice. Largest flow velocities were measured along the vortex next to the left and downstream pool cross-wall after which majority of the flow momentum is transferred to the downstream pool through the orifice. This part of the vortex is formed by two lines of measurement points along the left sidewall (rows 1-5, columns 1-2) and one line of points next to the downstream wall (5,3-5,7), with velocity magnitude on average 0.52m/s. On the point 5-1 flow velocity is negligible because it is situated between the orifice and the right sidewall, therefore relatively unaffected with the general flow field. The remainder of the vortex is formed by two lines of measurement points along the right sidewall and one line of measurement points along the upstream cross-wall (1,1-2,5 and 1,1-7,1). Flow velocity magnitude, on average, in this part of vortex is 0.36m/s. The middle part of the pool, points 3,2-5,4 also follow the direction of the large vortex, but velocities in this zone are negligible, on

average 0.26m/s.

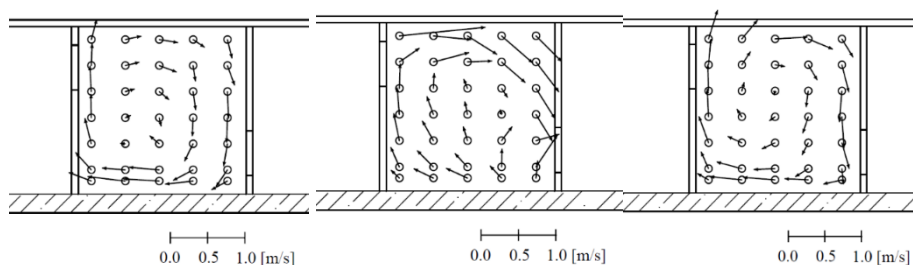


Figure 5. Plane view of flow velocity vectors for pool fishway model 125-45-10 at measurement planes A (left), B (centre) and C (right).

The plane C is most appropriate for comparison of different fishway geometry due to the majority of fish species using bottom zone for migration. On the C plane flow velocity vectors have greatest magnitude, induced by the flow entering and exiting the pool, while on the other two upper planes, A and B, flow velocity field in general is of lower magnitude. Outside vortex is visible on both A and B planes, as well as low velocity zone in the inner pool. Size of the outside vortex is larger for the A and B plane than plane C - vortex is formed by two lines of measurement points along the downstream cross-wall, rather than one as for plane C. Consequently, the inner low velocity zone is smaller, spanning the points from 3,2 to 5,3. Average velocity of the outer vortex is 0.30m/s and 0.31m/s for planes A and B, respectively, while in the inner zone flow velocity is less than 0.14m/s. It can be seen that orifice opening has influence on flow velocity field magnitude and size of the outer vortex – both flow velocity and vortex size are increasing with the increase of the orifice opening. Average flow velocity of the outer vortex of the model 125-45-8 is vortex is 0.23m/s, 0.28m/s and 0.47m/s for planes A, B and C, respectively, while in the inner zone flow velocity is less than 0.20m/s. Average flow velocity of the outer vortex of the model 125-45-12 is vortex is 0.39m/s, 0.42m/s and 0.47m/s for planes A, B and C, respectively, while in the inner zone flow velocity is less than 0.23m/s. The following figure shows comparison of flow velocity field for plane C of pool fishway with all analysed orifice sizes and the same slope (12.5%) and pool length (45cm).

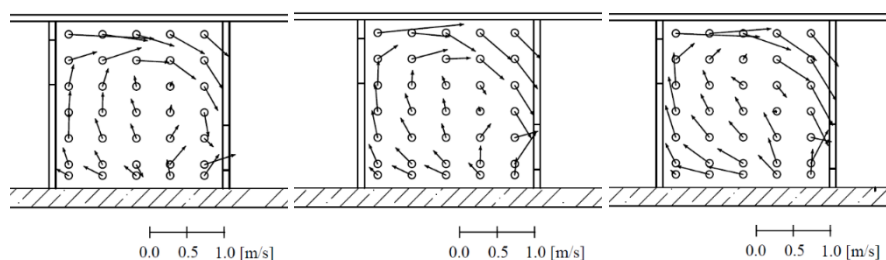


Figure 6. Plane view of flow velocity vectors for pool fishway model 125-45-8 (left), 125-45-10 (centre) and 125-45-12 (right) at measurement plane C

If comparison is made of the same slope (12.5%) and orifice size (10x10cm) and different pool lengths (45cm, 60cm and 90cm) similar flow velocity field characteristics are observed, with characteristic outer vortex. For all pool lengths the largest velocity

magnitudes were measured on the bottom plane C. For the pool length of 60 cm outer vortex is formed by two lines of measurement points along the left and downstream cross-wall, while on the right and the upstream cross-wall it is formed by three lines of measurement points (Figure 7). Low flow zone is then reduced to only 4 inner points (4,4-5,5). At the B plane outer vortex is smallest, formed by two lines of measurement points along the all of the pool walls, reducing the low flow zone to 9 inner points (3,3-5,5). On the plane A outer vortex is formed by one line of measurement points along the upstream pool cross-wall, three measurement points along the left sidewall, and two measurement points along the right and downstream sidewall, with the low flow zone consisting of 8 inner points (3,2-5,5).

For the pool length of 90 cm outer vortex has the largest area on the C plane: it is formed by two lines of measurement points along the left and upstream cross-wall, one measurement point on the downstream cross-wall and four measurement points on the right sidewall (Figure 7). Low flow zone is then reduced to only 7 inner points on one line (5,3-5,9). At the B plane outer vortex is smallest, formed by two lines of measurement points along the all of the pool walls, reducing the low flow zone to 14 inner points along the 2 measurement lines (3,3-5,9). On the plane A outer vortex is formed by two measurement points along the left, right and downstream pool wall. Along the upstream cross-wall one there are no significant velocity magnitudes and are part of the low flow zone (3,1-5,9).

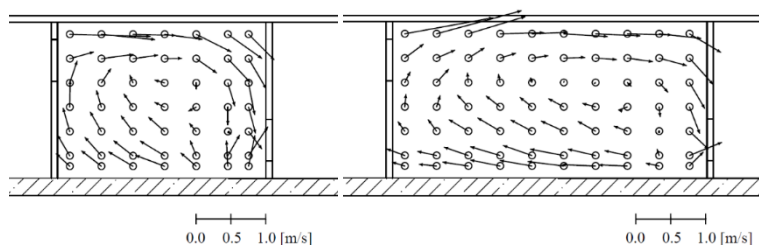


Figure 7. Plane view of flow velocity vectors for pool fishway model 125-60-10 (left) and 125-90-10 (right) at measurement plane C

From the analysis it can be concluded that larger pools with same slope and orifice size area of low flow velocity increases. Flow velocity lower than 0.5m/s is favourable for rest of fish migrating through the fishway before continuing to next pool [26]. Therefore, this area is desirable to be as large as possible, and according to the applied scale this cut-off velocity in model conditions is 0.29m/s. The following figure (Figure 8) shows measured flow velocity vectors in measurement plane C with highlighted area of velocities $<0.29\text{m/s}$ for model with slope 12.5%, length 60cm and different orifice openings. It can be seen that the largest area of resting flow velocities is for the smallest orifice, and smallest for largest orifice. For 8x8cm orifices low flow zone is adjacent to the inlet and outlet orifice, enabling fish to enter resting zone immediately upon entry to the pool, and exit the pool almost directly from it. For 10x10cm and 12x12cm orifices low flow zone is adjacent to the downstream orifice, but rather dislocated from the upstream orifice.

Most important flow field characteristics for fishway with the steepest slope are summarized in the following table (Table 1), including discharge, maximum flow

velocity in the orifice, maximum flow velocity in the pool and percentage of the pool suitable for resting.

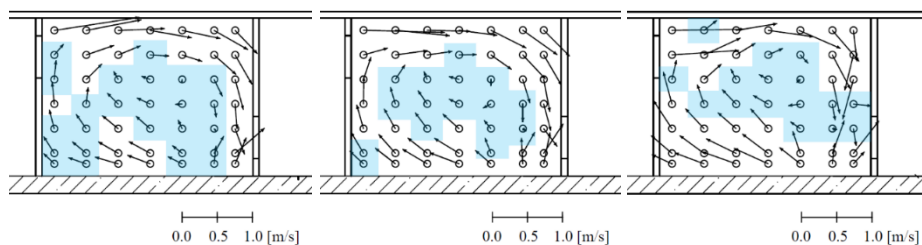


Figure 8. Plane view of flow velocity vectors for pool fishway model 125-60-8 (left) 125-60-10 (centre) and 125-60-12 (right) at measurement plane C with highlighted areas $<0.29\text{m/s}$

Table 1. Flow velocity field characteristics

Model		Discharge [l/s]	Maximum flow velocity in the orifice [m/s]	maximum flow velocity in the pool [m/s]	Pool area with $v < 0.29\text{m/s}$ [%]
Pool-type	125-45-8	6.5	2.39	2.24	45
	125-45-10	8.5	1.14	1.15	37
	125-45-12	11.5	1.05	1.13	35
	125-60-8	6.4	1.32	1.22	48
	125-60-10	9.0	1.10	1.15	34
	125-60-12	11.5	1.14	1.02	36
	125-90-8	5.9	1.17	1.26	61
	125-90-10	9.2	1.20	1.28	55
Vertical slot type	125-90-12	12.9	1.35	1.29	34
	125-45	17.7	1.21	0.88	49
	125-60	17.7	1.46	1.10	47
	125-90	17.7	1.35	1.05	27

For all pool fishways flow at the inlet is concentrated next to the left sidewall, and highest velocities are measured along this wall. After colliding with the downstream wall flow is deflected towards the right side and downstream orifice, with still large velocity magnitude, but in smaller jet width. Majority of the flow momentum is transferred into the downstream pool, and part of it is deflected upstream in the pool along the right sidewall, forming clockwise vortex and consequently low flow velocity zone in the middle pool area. Largest flow velocities are concentrated in the bottom plane, while the lowest velocities occur in the surface layer. This flow characteristics are mutual to all pool fishway configurations. For vertical slot fishways flow is concentrated next to the right sidewall, following the shortest path between the inlet and outlet. Majority of the flow momentum is transferred into the downstream pool, while part of it is deflected upstream in the pool along the downstream cross-wall and left sidewall, forming counter-clockwise vortex and consequently low flow velocity zone in the middle pool area. Flow field does not differ significantly between measurement planes, regarding flow velocity magnitude and direction. The following coneplot shows comparison of 3D flow velocity field for pool-type and vertical slot type fishway with same geometric and flow conditions (slope 12.5%, pool length 60cm Figure 9).

Flow depth in pools depends mostly on the orifice size and position, and less on the flow velocity characteristics. Average flow velocity through the orifice increases with increase in discharge, as well as head loss. Flow velocity increase rate is related to the local flow velocity next to the orifice that influences flow contraction and local loss. Flume experiments have shown that local variability of the flow field heavily influences the measurement quality and consequently the results. Instrument setup needs to be changed between the slower recirculation zone and accelerated slot zone. Transition between the recirculation zone and slot zone is not easily distinguished, therefore, the results have to be reviewed in real-time during survey to recognize the flow characteristics and adjust measurement accordingly.

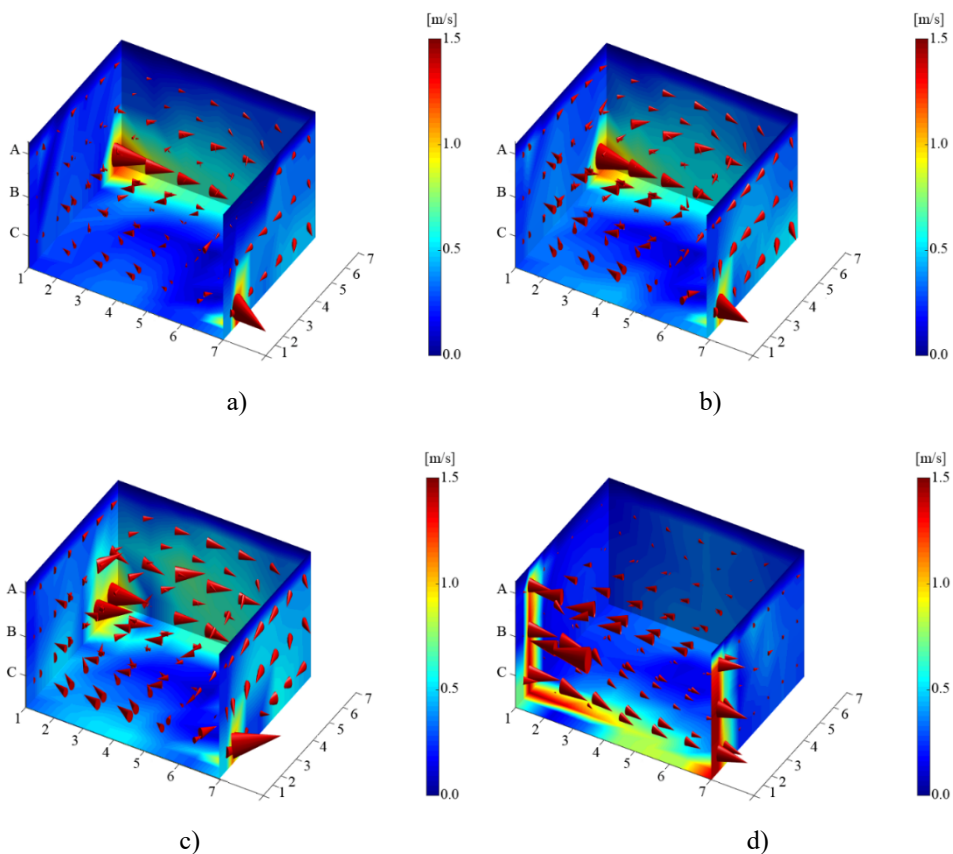


Figure 9. Coneplot of 3D flow velocity field for 125-60 pool-type and vertical slot type fishway with same geometric and flow conditions: a) 125-60-8, b) 125-60-10, c) 125-60-12, d) 125-60

6. Conclusion

Flume experiments conducted for series of fishway geometry and discharges have shown that complex flow field in fishways require detailed flow velocity measurements. Formation of the outer vortex and inner low flow zone needs to be measured with fine grid in order to accurately define the size of the vortex, low flow zone and transition between them. Special care needs to be taken near the orifice where the flow is deflected

into the downstream pool and contracted, which occurs in the vicinity of the orifice, making flow velocity measurements challenging if model scale is small. Therefore, investigations of flow pattern in the fishways must always be complemented with numerical model that can augment the information on the flow field collected in physical model. Vertical discretization of measurement planes is one more aspect that can be investigated in more detail if numerical model is used, considering that this research has shown significant differences of flow field in respect to its vertical position. For all models it was shown that highest velocities that affect the head loss, size of the vortex and rest zone are concentrated next to the pool walls. More turbulence is observed for smaller pool lengths, while in largest pools more energy is dissipated within the pool. Also, independent of the model it was shown that for pool fishways high velocity zone next to the downstream wall doesn't exceed one point from the cross-wall. This might be key information for fishway design used to maximise the low flow zone in the pools.

References:

- [1] Yagci, O.: Hydraulic aspects of pool-weir fishways as ecologically friendly water structure, *Ecological Engineering*, 36 (2010) 1, pp. 36-46
- [2] Branco, P., Segurado, P., Santos, J.M., Pinheiro, P., *et al.*: Does longitudinal connectivity loss affect the distribution of freshwater fish?, *Ecological Engineering*, 48 (2012) pp. 70-78
- [3] FAO: Fish passes – Design, dimensions and monitoring, Rome, Italy, pp. 119, 2002
- [4] Larinier, M.: Pool fishways, pre-barrages and natural bypass channels, *Bulletin Français de la Pêche et de la Pisciculture*, (2002) 364, pp. 54-82
- [5] Jelić, D., Ocvirk, E., Gilja, G., Cikojević, A.: Functionality of fish passes, *7th Croatian Water Conference with International Participation - Croatian waters in environmental and nature protection*, Opatija, Croatia, pp. 975-984, 2019
- [6] Bermúdez, M., Puertas, J., Cea, L., Pena, L., *et al.*: Influence of pool geometry on the biological efficiency of vertical slot fishways, *Ecological Engineering*, 36 (2010) 10, pp. 1355-1364
- [7] Guiny, E., Ervine, A.D., Armstrong, J.D.: Hydraulic and Biological Aspects of Fish Passes for Atlantic Salmon, *Journal of Hydraulic Engineering*, 131 (2005) 7, pp. 542-553
- [8] Larinier, M., Marmulla, G.: Fish passes: types, principles and geographical distribution an overview, *Proceedings of the Second International Symposium on the Management of Large Rivers for Fisheries*, Phnom Penh, Kingdom of Cambodia, pp. 183-205, 2003
- [9] Bates, K.: Fishway guidelines for Washington State, Department of Fish and Wildlife, pp. 53, 2000
- [10] Rajaratnam, N., Van der Vinne, G., Katopodis, C.: Hydraulics of vertical slot fishways, *Journal of Hydraulic Engineering*, 112 (1986) 10, pp. 909-927
- [11] Marić, M., Ocvirk, E., Gilja, G., Bujak, D.: Analysis of hydraulic flow conditions in Denil fish passes, *10th Eastern European Young Water Professionals Conference - New Technologies in Water Sector*, Zagreb, Croatia, pp. 75-76, 2018
- [12] Gilja, G., Marić, M., Bujak, D., Ocvirk, E.: Analysis of hydraulic flow conditions in Denil fish passes, *7th Croatian Water Conference with International Participation - Croatian waters in environmental and nature protection*, Opatija, Croatia, pp. 985-994, 2019
- [13] Ocvirk, E., Gilja, G., Bujak, D.: Pool fishway hydraulic analysis, *15th International Symposium Water Management and Hydraulics Engineering*, Primošten, Croatia, pp. 184-192, 2017
- [14] Martinović, D., Ocvirk, E., Gilja, G., Bujak, D.: Analysis of hydraulic flow conditions in pool fish pass, *10th Eastern European Young Water Professionals Conference - New*

- Technologies in Water Sector*, Zagreb, Croatia, pp. 77-78, 2018
- [15] Đerek, I., Ocvirk, E., Gilja, G., Bujak, D.: Analysis of hydraulic flow conditions in vertical slot fish passes, *10th Eastern European Young Water Professionals Conference - New Technologies in Water Sector*, Zagreb, Croatia, pp. 37-38, 2018
- [16] HAP: Best Practice Catalog - Flumes and Open Channels, Hydropower advancement project, Tennessee, pp. 19, 2011
- [17] Baki Abul Basar, M., Zhu David, Z., Rajaratnam, N.: Turbulence Characteristics in a Rock-Ramp-Type Fish Pass, *Journal of Hydraulic Engineering*, **141** (2015) 2, pp. 04014075
- [18] Wahl, T.L.: Analyzing ADV Data Using WinADV, *Joint Conference on Water Resources Engineering and Water Resources Planning & Management*, Minneapolis, Minnesota, pp. 1-10, 2000
- [19] Martin, V., Fisher, T.S.R., Millar, R.G., Quick, M.C.: ADV Data Analysis for Turbulent Flows: Low Correlation Problem, *Hydraulic Measurements and Experimental Methods Specialty Conference*, Estes Park, Colorado, United States, pp. 1-10, 2002
- [20] Cea, L., Puertas, J., Pena, L.: Velocity measurements on highly turbulent free surface flow using ADV, *Experiments in Fluids*, 42 (2007) 3, pp. 333-348
- [21] Goring Derek, G., Nikora Vladimir, I.: Despiking Acoustic Doppler Velocimeter Data, *Journal of Hydraulic Engineering*, 128 (2002) 1, pp. 117-126
- [22] Jesson, M.A., Bridgeman, J., Sterling, M.: Novel software developments for the automated post-processing of high volumes of velocity time-series, *Advances in Engineering Software*, 89 (2015) pp. 36-42
- [23] Nikora Vladimir, I., Goring Derek, G.: ADV Measurements of Turbulence: Can We Improve Their Interpretation?, *Journal of Hydraulic Engineering*, 124 (1998) 6, pp. 630-634
- [24] Wu, S., Rajaratnam, N., Katopodis, C.: Structure of Flow in Vertical Slot Fishway, *Journal of Hydraulic Engineering*, 125 (1999) 4, pp. 351-360
- [25] Luís, P., Jerónimo, P., María, B., Luis, C., *et al.*: Conversion of Vertical Slot Fishways to Deep Slot Fishways to Maintain Operation during Low Flows: Implications for Hydrodynamics, *Sustainability*, 10 (2018) 7, pp. 1-16
- [26] Liao, J.C.: A review of fish swimming mechanics and behaviour in altered flows, *Philosophical transactions of the Royal Society of London. Series B, Biological sciences*, 362 (2007) 1487, pp. 1973-199.

FLOOD PROTECTION DESIGN FOR MUNICIPALITIES OF SLOVAKIA IN VARIOUS HYDROLOGICAL CONDITIONS

ANDREJ ŠOLTÉSZ¹, LEA ČUBANOVÁ¹, ADAM JANÍK¹, DANA BAROKOVÁ¹

¹ Slovak University of Technology in Bratislava, Faculty of Civil Engineering, Department of Hydraulic Engineering, Radlinského 11, 810 05 Bratislava, Slovakia, andrej.soltesz@stuba.sk, lea.cubanova@stuba.sk, adam.janik@stuba.sk, dana.barokova@stuba.sk.

1. Abstract

The goal of the contribution is to present possibilities of comprehensive and complex procedures for proper design of flood protection measures in several parts of Slovakia. It highlights the need of flood protection of municipalities as a consequence of changes in hydrological parameters, uncontrolled build-up near the streams as well as the sedimentation of the river bed by deposits, rubbish or vegetation. The complex approach consisted of mutual integration of results of several mathematical models. All modelling works were done in DTM coming from aerial photography or in conditions of detailed morphological and geodetic survey of investigated rivers basins. According to the modelling process appropriate preventive flood protection measures have been designed and afterwards realised in the territory, i.e. detention reservoirs in the mountain region above the urban regions. Proposed flood protection measures should help to mitigate the impact of flash floods on the urban regions of small and even larger cities.

Several case studies are presented in the contribution all over the Slovak Republic to emphasize the variety of flood wave progress, its reduction in discharge and postponing in time in different hydrological, morphological and geological conditions of mountain regions. Most of the presented proposals of flood protection measures have been projected and some of them have been already realized.

Keywords: flood wave, hydraulic simulation, flood protection measures, detention reservoir.

2. Introduction

Flash floods sometimes called sudden or storm floods are specific type of rainfall floods characterized by rapid increase of the surface water level in very short time (in order of hours) [1]. Mostly they occur on small streams in upper parts of river basins and their starter is extremely high storm rainfall. The threshold intensity and duration of the rainfall required for formation of a flash flood cannot be uniquely determined because it depends on various factors as type and morphology of the terrain, soil moisture saturation as well as on anthropogenic activities in the watershed [1].

Accompanying phenomenon of these floods is significant erosion of soil and enormous property damages due to high kinetic energy of water stream. Due to extremely short time of flood forming it is very complicated to warn the population and mostly there is

no more time to perform really proper flood protection measures as mobile flood protection barriers of other measures. Therefore, it is reasonable to prepare appropriate flood protection measures which do not need any operation, i. e. they will “work automatically”.

All over the Slovakia there is lot of municipalities situated at the foot of a mountain where flash floods occurred. It is apparent from the Figure 1. River basins of these streams are in mountain regions and are mostly forested. Storm rainfalls which induce flash floods are however so extreme that even forest management as well as soil protection from erosion seem not to be sufficient. Therefore it is reasonable to take into account technical flood protection measures. Recently, the most convenient (most used) solution in valleys of these streams are detention reservoirs. Their volume can serve for transformation of the flood wave, its temporal lag and – for all – the reduction (attenuation) of the maximum flow rate [1], [2].

Very important is the location of the detention reservoir. In principle, there are two variants – location in upper parts of the catchment or to build it up directly above the protected locality. The advantage of location of detention reservoirs in upper parts of the river basins is the accumulation of the run-off directly in the area of its creation to avoid the possible fusion of flood waves from different streams. Possible problems of detention reservoirs consist of very fast fulfilling by flood water accompanied by higher risk of occurrence of filtration instability of the dam.

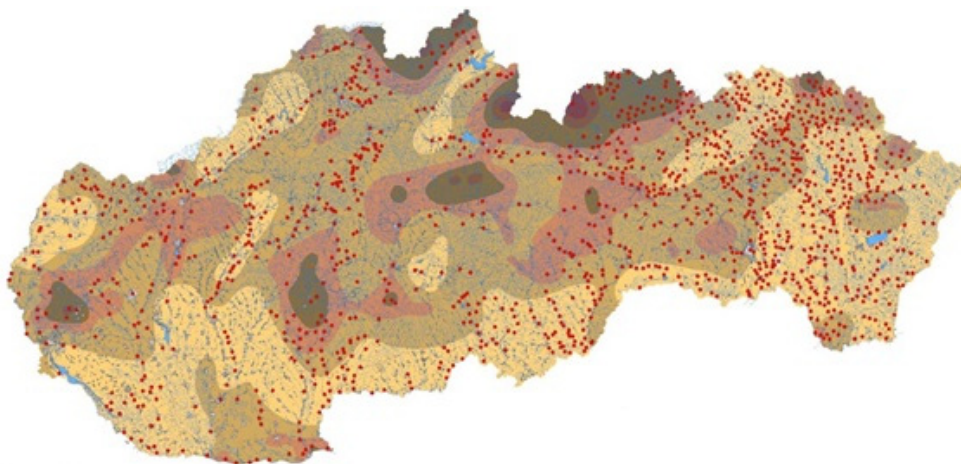


Figure 1. Presentation of municipalities in Slovakia where flash flood occurred in years 1997 - 2010

On base of former information and data it can be stated that each locality of interest which is endangered by floods, requires an individual approach to proposed appropriate flood protection measures. Each flood protection proposal itself comes out from particular situation depending on existing morphological and hydrological conditions in the area of interest. The proposed measure is hydraulically analysed by mathematical model of the current state where the effects of proposed measures are determined [2], [3].

In the next chapter some case studies which were analysed by the Department of

Hydraulic Engineering at STU in Bratislava in last years will be presented. They are showing possible solution of flood protection in the river basins with different geological, morphological and hydrological conditions. Some of proposed flood protection measures have been just analysed, some of them are presently in projection and some of them are after successful realization already.

3. Methods, results and discussion

3.1 The case study Pila village, Gidra stream and its tributary Kamenný stream

The Pila village was affected by destructive flood in 2011. After this flood many buildings, roads and bridges had to be repaired but the flood protection was still non-existent. After the simulation of flood without proposed measures it was determined to design detention reservoirs according to spatial conditions and existing structures (bridges and culverts) on the stream. On base of created hydraulic model based on measured morphological and hydraulic data the maximum capacity of the main Gidra stream was determined. Moreover, it was decided to propose detention reservoirs in valleys above the confluence of two streams (Gidra, Kamenný) over the village. In this case, earth fill dams were proposed because of their more natural appearance. In frame of the modelling several scenarios have been taken into consideration. All these scenarios have been loaded by Q_{100} flood wave and the most proper solution was evaluated for the sufficient flood protection of the Pila village. The best variant involved the proposal of two detention reservoirs (Figure 2), each on one of the streams. By synergy of proposed detention reservoirs the peak flow rate has been reduced from original $24.6 \text{ m}^3 \cdot \text{s}^{-1}$ to value $11.10 \text{ m}^3 \cdot \text{s}^{-1}$ [2], [4]. Due to wide valleys the sufficient height of dams was approximately in the range of 5.5 – 6.0 m.



Figure 2. Location of proposed detention reservoirs (Kamenný stream – left, Gidra stream – right).

3.2 The case study Levice town, Podlužianka River, its tributaries Čajkovský and Rybnický streams

Slovak lowlands are suffering from floods, as well. The floods are formed in connection with rainfalls, arising water in rivers and rising groundwater above the terrain. The river which flows through the district of Levice is the Podlužianka River with right-bank tributaries Čajkovský stream and Rybnický stream. This area is often naturally flooded from all rivers during floods. Present flood protection conditions in the Levice district town are not sufficient. The river bed training of the Podlužianka River in the central part of Levice town was realized in 2004. The town is protected by walls situated along the river bed and in the location of bridges mobile barriers were installed (Figure 3) [3], [5].



Figure 3. Levice district town – Podlužianka River (normal conditions, during the flood).

For sufficient town protection, it is necessary to ensure increasing of the capacity of the river bed, to remove obstacles from the river bed, to adjust river banks and to store flood flow rates in detention reservoirs. Various alternatives were examined (up to 7 detention reservoirs were proposed and simulated in one mathematical unsteady model) and - on the basis of the economical and water management assessment – an alternative with 3 detention reservoirs (Figure 4) was chosen [5], [6].

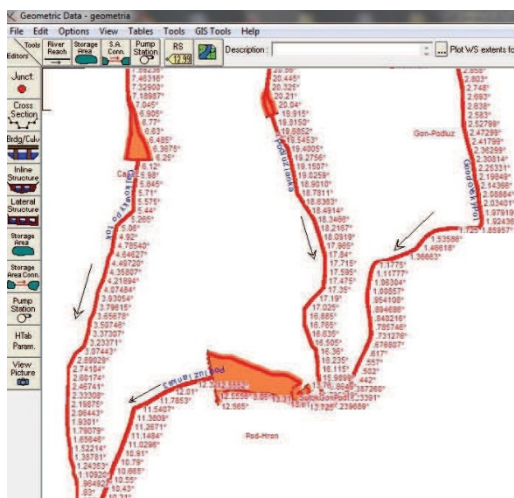


Figure 4. Graphic presentation of the area of interest including tributaries of the Podlužianka River and location of proposed detention reservoirs (HEC-RAS) [6]

From flood protection point of view introducing mentioned measures a reduction from $Q_{100}=65.0 \text{ m}^3 \cdot \text{s}^{-1}$ in the Podlužianka River in front of the Levice district town down to $Q=37.0 \text{ m}^3 \cdot \text{s}^{-1}$ would be achieved [5], [6].

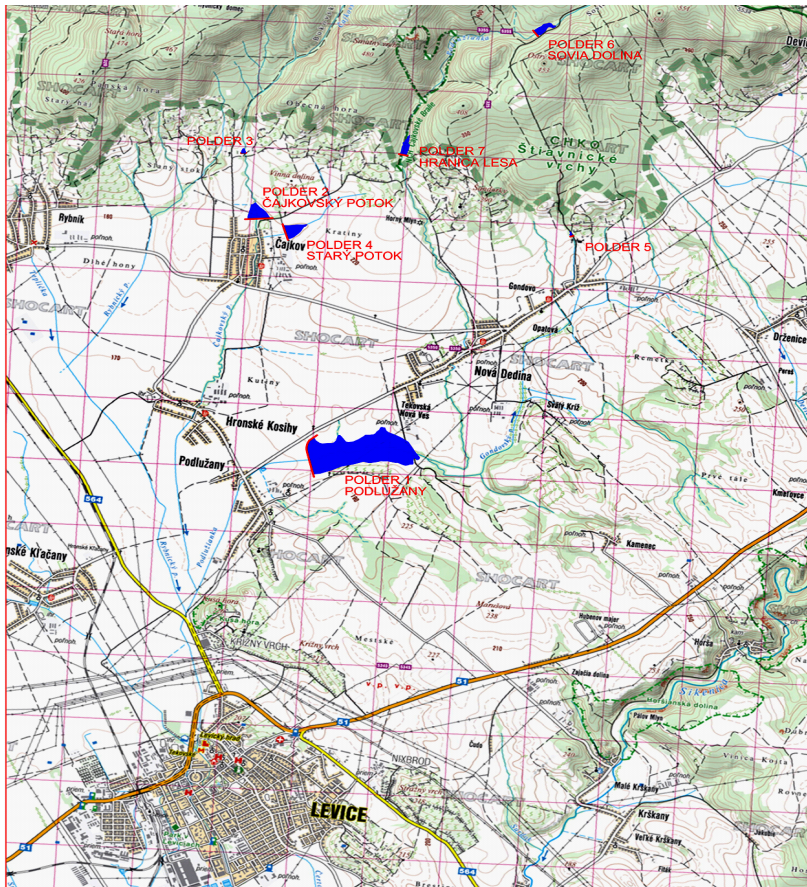


Figure 5. Location of proposed detention reservoirs in river basin of the Podlužianka River [6].

3.3 The case study Bardejov town, Topla River

Analysis of the flood protection of the Bardejov town was performed due to insufficient flood protection of the centre of the city. Capacity of the Topla River bed in the urban area of the Bardejov district town is insufficient, resulting in repeated floods. The last historical flood happened in 2010. Due to the fact that it is a downtown with dense building development, it was not possible to enlarge the dykes by earth, also river bed could not be trained or extended. Therefore, the flood protection of the middle part of the city was already realized by building of concrete walls along the river. This realization was assessed by one dimensional open channel flow model of the Topla River in Bardejov in non-uniform steady flow conditions. The results of mathematical modelling showed, that flood protection walls designed and realized in the central part of the town (phase I.) must be supplemented in upstream and downstream sections (phases II. and III.) to ensure flood protection in whole solved section (Figure 6). Recommended measures will increase flood protection of the town of Bardejov [7].



Figure 6. Bardejov – orthophoto map of planned phases of the d flood protection walls (phase I.)



Figure 7. Gauging station on the Topľa River and realized flood protection walls (phase I.) [8]

3.4 The case study Veľká Lúka village, Lukavica stream

A typical example of problems connected with the individual residential construction close to flood plains of water courses. The Lukavica stream flows through the small village Veľká Lúka (located between towns Sliach and Zvolen). The stream flows in ordinary hydrological situation as a stream with minimum water level (few centimetres). The problem is that family houses in the central part of the village are built close to the stream. Training of the Lukavica river bed was done only partially in different periods and for different capacities. In addition, there are two road bridges as well as a railway bridge (culvert) and a ford on the stream.

Mentioned new building development in the central part of the village which was already affected by floods (heavy storms and rapid snow melting - 2009, 2013, 2016). The river bed is loaded with sediments and overgrown with bush and willows. By the hydraulic

analyses and simulations, based on the actual geodetic measurements of the area of interest, it has been proved that even by clean-up of the river bed (sediment dredging) there is insufficient flood protection of the municipality (Figure 8). Expansion and training of the river bed nor the dyke construction is impossible, therefore a detention reservoir was proposed above the village (Figure 9). However, the volume of the flood wave volume is so great that a relatively large detention reservoir has been proposed whereas the river bed in the village must be refined. In the part of expected planned house building damming of river banks by small walls was proposed, so that the outflowing discharge from the detention reservoir could not cause damages, anymore [9].



Figure 8. Cleaning of the Lukavica River bed in the central part of the Veľká Lúka village.



Figure 9. Ortho-photo map with the situation of the planned detention reservoir above the village.

For the needs of hydraulic calculation of the flood wave mitigation a HEC.RAS mathematical model was created in steady and unsteady conditions, as well. The dimension of the bottom outlet has been determined according to the dam height and the flood wave propagation for $Q_{100} = 49 \text{ m}^3 \cdot \text{s}^{-1}$. The diameter was modified so that the water level in detention reservoir would not reach the level of the emergency spillway. In this case, a circular outlet with a diameter of 1.5 m was proposed. This proposal resulted in a flood wave mitigation with a peak flow of $49 \text{ m}^3 \cdot \text{s}^{-1}$ reduced to a maximum outflow of $15.9 \text{ m}^3 \cdot \text{s}^{-1}$ (Figure 10). This proposal has been evaluated as sufficient due to the capacity

of the river channel in the municipality [9].

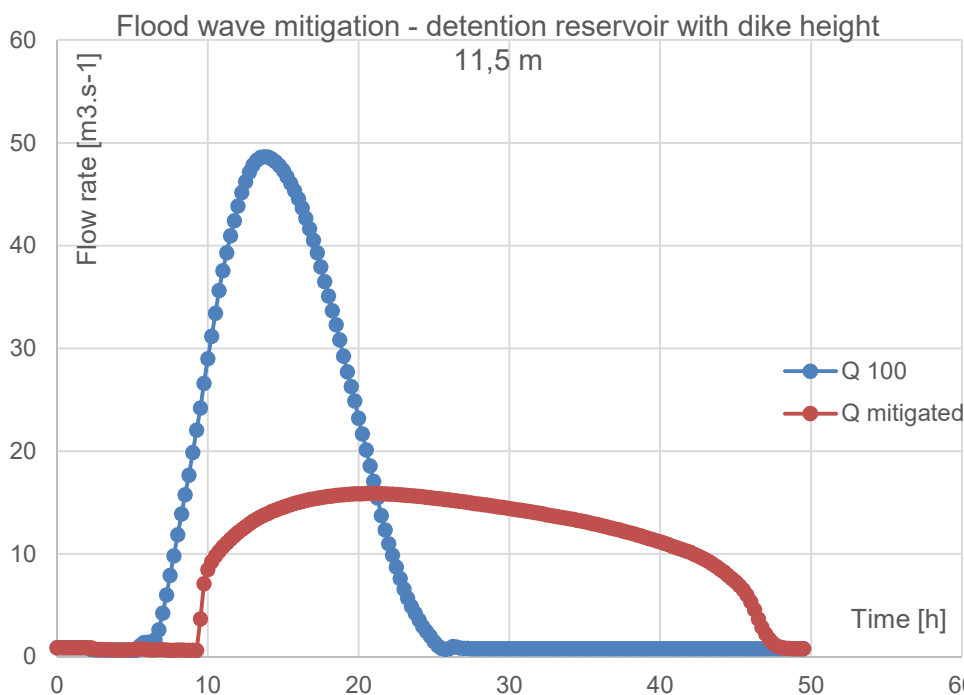


Figure 9. Flood wave mitigation of the design flood wave (height of the dam 11.5 m, bottom outlet $D=1.5$ m).

4. Conclusion

Flash floods are becoming a phenomenon that troubles people more and more often in many Slovak under-mountain regions. Flash floods also called storm or sudden floods are a specific type of rain floods which typical sign is an intensive increase of water level in the river in a short time period (usually couple of hours). Mostly there are floods on small streams in upper parts of river basins and their starters are extreme storm rainfalls. Rainfall intensity and duration limits are not possible to determine exactly due to dependence on many factors as type and shape of landscape, soil water saturation and nonetheless they depend on anthropogenic activity (inadequate operation in the landscape). Due to the extremely short time of flood beginning it is difficult to alarm inhabitants and for carrying out operative flood protection measures like mobile flood-protection barriers it is mostly too late. That is the reason why it is necessary to prepare appropriate flood-protection measures, which do not need any operation and work automatically.

The above presented case studies showed the possibilities of the flood protection measures design in different hydrological conditions of small municipalities with relatively small river catchments but high flood flow rates. Every proposal was sensitively tested for given location capabilities with regard to maximum flood protection, functionality as well as from ecological point of view.

Acknowledgements

The paper was developed within the frame of and based on the financial support of the VEGA 1/0800/17 project “Optimization of the flood protection of municipalities in river basin of mountain streams” and of the Slovak Research and Development Agency under Contract No. APVV-16-0278 project „Use of hydromelioration structures for mitigation of the negative extreme hydrological phenomena effects and their impacts on the quality of water bodies in agricultural landscapes”.

References:

- [1] Best practices on flood prevention, protection and mitigation 2003. [online]. [cit. 2018-06-20]. Available at: https://www.floods.org/PDF/Intl_BestPractices_EU_2004.pdf
- [2] Janík, A., Šoltész, A.: Flash flood mitigation modeling – Case study Small Carpathians. *Pollack Periodica*, Vol. 12, no. 2, pp. 25 – 34, 2017.
- [3] Pindjaková, T., Kelčík, S., Šoltész, A.: Simulation of flood progress on the river Gidra. *Pollack Periodica*, Vol. 11, no. 1, s. 25-34, 2016.
- [4] Šoltész, A., Janík, A.: Flood protection proposal in the Gidra River basin. *FCE STU Bratislava*, 36 p., 2017.
- [5] Kelčík, S., Pindjaková, T., Šoltész, A.: Assessment and design of the flood protection measures in the district of Levice (Slovakia). *Pollack Periodica*, Vol. 11, no. 1, pp. 35-41, 2016.
- [6] Šoltész, A., Bednárová, E., Minárik, M., Gramblička, M. a kol.: Podlužany – Gondovo, flood protection measures in Podlužianka River basin – detention reservoirs. *FCE STU Bratislava*, 71 p. p., 2014.
- [7] Šoltész, A., Janík, A., Čubanová, L.: Štúdia protipovodňovej ochrany Bardejova. In: Vplyv antropogénnej činnosti na vodný režim nížinného územia, zborník recenzovaných príspevkov, 1. vyd. Bratislava: *Ústav hydrologie SAV*, pp. 281-289, 2018
- [8] Kupa, J., Šoltész, A., Kolesárová, E., Janík, A.: Hydraulic assessment of flood protection in Bardejov City, In: Proc. of *Inter. Symposium on Management of river basins and extreme hydrologic phenomena*, Vyhne, pp. 214 – 220, 2017.
- [9] Šoltész, A., Čubanová, L., Janík, A., Živčicová, K.: Veľká Lúka – flood protection measures in river basin of the Lukavica stream, *FCE STU Bratislava*, 39 p., 2018.

MATHEMATICAL MODELING OF RIVER ICE PROCESSES

TOMASZ KOLERSKI¹

¹*Department of Civil and Environmental Engineering, Gdańsk University of Technology, Narutowicza 11/12, 80-233, Gdańsk Poland*

1. Abstract

The paper presents the results of research on mathematical modeling of ice phenomena on rivers and in water reservoirs. The performed analysis included the processes leading to ice formation on rivers, its transformation and break-up. A significant part of this work refers to ice jam formation and break-up. The knowledge of ice-related processes was a basis for the presentation of an adequate mathematical description.

The main objective of the paper was to gain more knowledge about the course of ice phenomena on rivers and mathematical presentation of these processes. Indirectly, the paper also aims at determining the possibilities of applying a mathematical model in the context of aspects that are important for management of water areas in winter. Due to the lack of an adequate tool, a significant part of this information is obtained through approximation or on the basis of subjective expertise. By referring to examples, it was shown how the results obtained from a mathematical model can support decision-making when designing hydrotechnical objects, or in other situations.

This paper presents mathematical equations necessary to build a model which will be able to reproduce ice phenomena on rivers. With this objective in mind, it presents the equations for the hydrodynamics of rivers, considering the influence of ice cover, equations for the description of thermal balance of water surface, equations regarding dynamic ice processes on water surface, and equations for presenting ice thickness increase rate resulting from external factors. In addition, an ice barrier served as an illustration of a method of determining ice-originating forces which may affect hydrotechnical objects.

On the basis of knowledge and experience gained during many numerical experiments conducted in idealized conditions and in the actual area, several significant conclusions have been drawn regarding calculations for ice dynamics on rivers and in reservoirs.

2. Introduction

The presence of ice in rivers is an important aspect to be considered in the development of water resources in cold regions including Poland. River ice research has largely been driven by engineering and environmental problems that concern society. Ice formation can affect many fields of hydraulics, hydrology, civil engineering, ship design and ecology such as for example:

- Ice jamming and flood protection

- Ice damage on shoreline and onshore facilities
- Ice load on bridge and bridge piers
- Sediment transport problems
- Design of Icebreakers and arctic ships
- Habitat improvements projects and river restoration in cold regions

River hydraulics is well examined and its mathematical description allows to model river hydrodynamics with high accuracy (Szymkiewicz, 2010). The presence of ice can seriously interfere with utilization of lakes and rivers and an adequate mathematical model has to be formulated. During the last decades river ice is a rapidly growing subject area in hydraulic engineering. Several reviews on river ice processes and the state of research have been published (Ashton, 1986; Beltaos, 1995). Formulations for the hydraulics of flow in rivers with continuous ice cover have been developed (Lal and Shen, 1991; Potok and Quinn, 1979). Also numerical models for the dynamic transport of surface ice and ice jam evolution have been developed (Shen, 2016, 2010).

Flow in an open channel with ice forms is in fact a two-phase process, involving a liquid phase (water) and a solid phase (ice). Water hydrodynamics in a two-dimensional approach is described in a form of shallow water equations of mass and momentum conservation with additional terms including mutual relations between ice and water. To include ice movement on the water surface, shear stress at the ice–water interface is an effect of velocity difference. All details about mathematical modeling of river hydrodynamics with ice cover are presented in Chapter 2. A significant part of this work refers to velocity distribution under the ice cover and composite ice roughness coefficient. I also presented wind effect on ice dynamics; this is also presented there.

River ice processes involve complex interactions between hydrodynamic, mechanical, and thermal processes, as well as the ambient hydro-meteorological conditions and channel morphology. The ice dynamic equations consider all the external and the internal forces which act on an ice parcel. These forces include water drag, gravity, internal resistance of ice, and bed friction on grounded ice. The momentum balance of an ice parcel at any location can be written in Lagrangian form as shown in (Shen et al., 2000). A Lagrangian discrete-parcel method based on smoothed particle hydrodynamics is used to solve the ice dynamic equations. The basic concept of the discrete-parcel method is that the ice, considered as a continuum, can be represented by a sufficiently large number of individual parcels carrying mass, momentum and energy. In a flow field, the mass density at any point is obtained by summing up the contribution from all the particles surrounding that point. The mathematical model is described in Chapter 3 of the monograph and numerical method adapted to ice dynamics in Chapter 3.

3. River hydrodynamics with ice cover

3.1 One dimensional model of unsteady flow with ice cover

All described below methodology is related to the case with floating ice cover, which is the most commonly observed in natural rivers. The floating ice cover means that ice is able to follow changing water levels and no pressure is built under the cover. It is consistent with field observations: for majority of cases ice cover does not remain in

suspension while water level drops. Also while due to increased water discharge, water level is raised ice cover usually floats on the water surface. It is caused by mechanical property of the ice which has not significant strength for bending and cracks easily. Thus while the hole is drilled in the ice cover the water level will typically remain on 1/10 of the total ice cover thickness measured from the top of the ice. This is caused by the density relation between water and ice ($\rho_L \approx 920 \text{ kg}\cdot\text{m}^{-3}$). The assumption will limit the model application to the large rivers only. For narrow streams the conditions will be not satisfy and this approach cannot be used. Even though there is some limitation for model application, the assumption of floating ice cover will allow using modified form of shallow water equations (Yapa and Shen, 1986):

$$\frac{\partial Q}{\partial x} + \frac{\partial A}{\partial t} = 0, \quad (0-1)$$

$$\rho \frac{\partial Q}{\partial t} + \rho_w \left(\frac{2Q}{A} \frac{\partial Q}{\partial x} - \frac{Q^2}{A^2} \frac{\partial A}{\partial x} \right) + \rho_w g A \frac{\partial h}{\partial x} + P_d \tau_d + P_L \tau_L + B_o \tau_a = 0. \quad (0-2)$$

where: Q – water discharge [$\text{m}^3\cdot\text{s}^{-1}$]; A – net cross section area under the ice cover [m^2]; x [m] i t [s] variables related to distance [m] and time [s]; ρ_w – water density [$\text{kg}\cdot\text{m}^{-3}$]; g – gravitational acceleration. [$\text{m}\cdot\text{s}^{-2}$]; h – water Surface elevation [m]; B_o – width of the cross section at the water Surface [m]; P_d i P_L – wetted perimeter for river bed and underside of the ice cover [m]; τ_d i τ_L – share stress in the river bed and on the underside of the ice cover [Pa]; τ_a – share stress caused by the wind [Pa] (Shen et al., 1990):

$$\tau_a = \tau_{aL} \frac{N}{N_{\max}} + \tau_{aw} (N_{\max} - N), \quad (0-3)$$

In which N – Surface ice concentration [-]; τ_{aw} i τ_{aL} – share stresses build on the water and ice surface by the wind [Pa], proportional to the difference between ice (or water) surface velocity and wind velocity:

$$\tau_{aw} = C_w \rho_a (V_p - W)^2, \quad (0-4)$$

Where C_w [-] is a wind coefficient: $C_w = 0,00155$ (Wu, 1973), ρ_a [$\text{kg}\cdot\text{m}^{-3}$] is air density, V_p [$\text{m}\cdot\text{s}^{-1}$] is water or ice surface velocity, W [$\text{m}\cdot\text{s}^{-1}$] is wind velocity 10 m above the water surface.

Bed and ice share stresses may be determined with respect to Manning's roughness coefficient and logarithmic velocity profile. By assuming wide river channel (width much larger than depth) the composite roughness coefficient can be derived as:

$$n_o = \left[\frac{1}{2} (n_L^{3/2} + n_d^{3/2}) \right]^{2/3}. \quad (0-5)$$

Introducing composite roughness formula and wind share stress to the equation (1-2) the Saint Venant equation for ice covered channel can be presented in following form:

$$\frac{\partial Q}{\partial x} + \frac{\partial A}{\partial t} = 0, \quad (0-6)$$

$$\rho \frac{\partial Q}{\partial t} + \rho \left(\frac{2Q}{A} \frac{\partial Q}{\partial x} - \frac{Q^2}{A^2} \frac{\partial A}{\partial x} \right) + \rho g A \frac{\partial h}{\partial x} + \frac{\rho g Q^2}{AR^{4/3}} \left[\frac{1}{2} (n_L^{3/2} + n_d^{3/2}) \right]^{4/3} = (0-7)$$

3.2 Two dimensional model DynaRICE

One dimensional modeling has obvious limitations for reproducing river ice formation, dynamic transport and jamming. For this reason the two dimensional concept of river flow with ice was introduced in last century (Shen et al., 1997), which evaluated in Dynamic River Ice Comprehensive Environment (DynaRICE), which allow to forecast ice jam formation and release. The DynaRICE model is fully conceptual model thus modeling of ice jams is on the base of dynamic force balance without user interference.

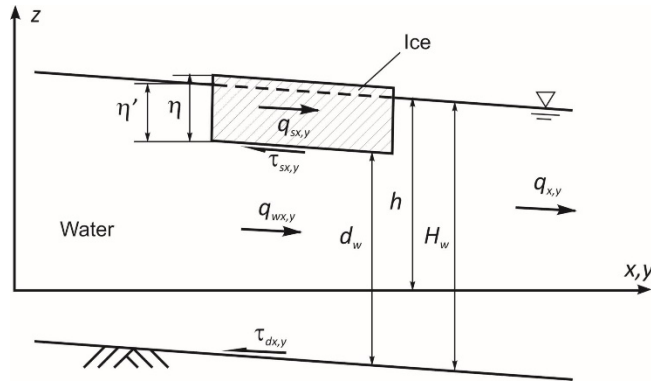


Figure 10. River hydrodynamics under the ice cover; based on (Liu and Shen, 2000)

The DynaRICE model allows unsteady ice and water simulation driven by dynamic balance of all internal and external forces and was calibrated and validated to a number of real case scenarios, i.e. (Kolerski, 2018, 2015; Kolerski et al., 2013; Shen et al., 1997). Hydrodynamic module is a solution of two-dimensional shallow water equation including mutual interaction between ice and water flow (variables used in equations below are shown on Figure 10.):

$$\frac{\partial H_w}{\partial t} + \frac{\partial q_x}{\partial x} + \frac{\partial q_y}{\partial y} = \frac{\partial}{\partial t} (N\eta'), \quad (0-8)$$

$$\begin{aligned} \frac{\partial q_x}{\partial t} + \frac{\partial}{\partial x} \left(\frac{q_x^2}{H_w} \right) + \frac{\partial}{\partial y} \left(\frac{q_x q_y}{H_w} \right) \\ = \frac{1}{\rho} (\tau_{sx} - \tau_{dx}) + \frac{1}{\rho_w} \left(\frac{\partial T_{xx}}{\partial x} + \frac{\partial T_{yx}}{\partial x} \right) - g H_w \frac{\partial h}{\partial x}, \end{aligned} \quad (0-9)$$

$$\begin{aligned} \frac{\partial q_y}{\partial t} + \frac{\partial}{\partial x} \left(\frac{q_y^2}{H_w} \right) + \frac{\partial}{\partial x} \left(\frac{q_x q_y}{H_w} \right) \\ = \frac{1}{\rho} (\tau_{sy} - \tau_{dy}) + \frac{1}{\rho_w} \left(\frac{\partial T_{xy}}{\partial x} + \frac{\partial T_{yy}}{\partial x} \right) - g H_w \frac{\partial h}{\partial y}. \end{aligned} \quad (0-10)$$

In which q_x, q_y – water discharge in x and y directions [$\text{m}^3 \cdot \text{s}^{-1}$], which are the flow under the ice cover q_{wx}, q_{wy} and seepage flow through the ice q_{sx}, q_{sy} ; h – water Surface elevation [m]; η' – ice thickness from the underside surface to the water level [m]; τ_{sx}, τ_{sy} – share stresses on the water surface in x and y direction [Pa], could be share stress on the underside surface of the ice ($\tau_{Lx,y}$) or on the water surface caused by the wind ($\tau_{ax,y}$); τ_{dx}, τ_{dy} – share stress on the river bed in x and y [Pa]; N – ice concentration lodu [-]; ρ_w – water density [$\text{kg} \cdot \text{m}^3$]; H_w – total water depth underneath an equivalent ice-water interface $H_w/d = q/q_s$ [m]. T_{xy} is a turbulence tensor calculated as follows :(Su et al., 1997)

$$T_{xy} = \varepsilon_{xy} \left(\frac{\partial q_x}{\partial y} + \frac{\partial q_y}{\partial x} \right), \quad (0-11)$$

$$T_{xx} = \varepsilon_{xx} \left(\frac{\partial q_x}{\partial y} + \frac{\partial q_x}{\partial x} \right), \quad (0-12)$$

$$T_{yy} = \varepsilon_{yy} \left(\frac{\partial q_y}{\partial y} + \frac{\partial q_y}{\partial x} \right). \quad (0-13)$$

Where $\varepsilon_{xy}, \varepsilon_{xx}, \varepsilon_{yy}$ are generalized eddy viscosity coefficients [$\text{Pa} \cdot \text{s}$]. Bed share stress is calculated from (Shen et al., 1990):

$$\tau_{dx} = \frac{n_d^2}{(\alpha_d d_w)^{1/2}} \rho g \frac{q_x (q_x^2 + q_y^2)^{1/2}}{d_w^2}, \quad (0-14)$$

$$\tau_{dy} = \frac{n_d^2}{(\alpha_d d_w)^{1/2}} \rho g \frac{q_y (q_x^2 + q_y^2)^{1/2}}{d_w^2}. \quad (0-15)$$

Parameter α_d is the fraction of the water depth affected by the bed friction, $\alpha_d = A_d/A$.

In case of grounded ice jam the cross section is totally filed with the ice and there is no water flow under the ice. The only way for water to pass is a seepage flow through the ice rubble and additional force will be generated causing immediate stoppage of ice run:

$$\tau_{g,x} = -\rho g \frac{q_f q_{f,x}}{\lambda_f \eta'} (1 - N)^2, \quad (0-16)$$

$$\tau_{g,y} = -\rho g \frac{q_f q_{f,y}}{\lambda_f \eta'} (1 - N)^2. \quad (0-17)$$

4. Mathematical model of river ice dynamics

River ice processes are affected by hydrodynamics, thermodynamics, and mutual relations between ice forms. Dynamic transport of river ice is mathematically described as a movement of the number of particles carrying all ice properties and being subjected to force balance. The governing equation for ice dynamics can be presented in the following form (Shen et al. 2000):

$$M_L \frac{d\vec{V}_L}{dt} = \vec{R} + \vec{F}_a + \vec{F}_w + \vec{G} \quad (0-1)$$

In which M_L is mass per area of parcel, \vec{V}_L is ice velocity vector, $\frac{d\vec{V}_L}{dt}$ is surface ice acceleration, \vec{R} is an ice internal resistance force, \vec{F}_a is a wind drag force, \vec{F}_w jest is a water drag force, \vec{G} is gravitational force. The forces acting on the ice are shown on

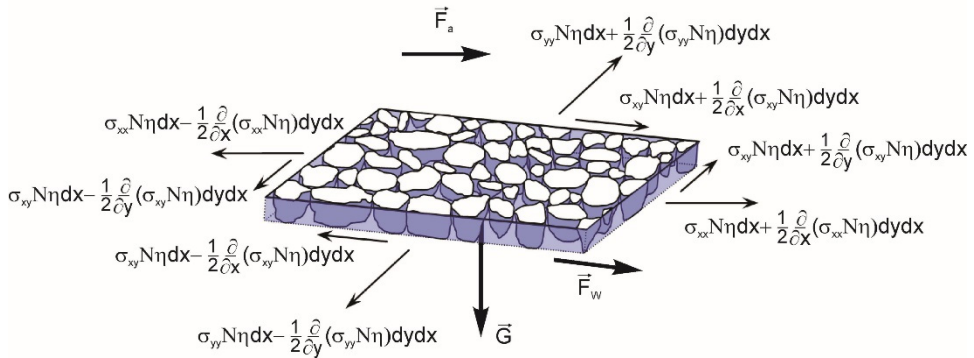


Figure 11. Schematic force balance on ice parcel on the water surface

In two dimensional coordinate system (depth averaged), internal ice resistance can be described in following way (Shen et al., 2000):

$$\vec{R} = \vec{i}R_x + \vec{j}R_y, \quad (0-2)$$

$$R_x = \frac{\partial}{\partial x} (\sigma_{xx} N \eta) + \frac{\partial}{\partial y} (\sigma_{xy} N \eta), \quad (0-3)$$

$$R_y = \frac{\partial}{\partial x} (\sigma_{yx} N \eta) + \frac{\partial}{\partial y} (\sigma_{yy} N \eta), \quad (0-4)$$

In which, σ_{xx} i σ_{yy} are internal ice stresses in normal direction build up in ice rubble, $\sigma_{xy} = \sigma_{yx}$ are internal ice stresses in tangential direction. Internal stresses are calculated from viscoelastic–plastic constitutive model with Mohr-Coulomb yielding criterion for the ice as described in (Ji et al., 2005) Other terms from equation (0-1) i.e. wind and water drag as well as gravitational force can be calculated as follows:

$$\vec{F}_a = \vec{i} \left[\rho_a C_w \left| \vec{V}_L - \vec{W} \right| (u - W_x) N \right] + \vec{j} \left[\rho_a C_w \left| \vec{V}_L - \vec{W} \right| (v - W_y) N \right] \quad (0-5)$$

$$\vec{F}_w = \vec{i} \left[\rho \frac{n_L^2}{(\alpha_d d_w)^{1/2}} |\vec{V}_L - \vec{V}_w| (u - u_w) N \right] + \vec{j} \left[\frac{n_L^2}{(\alpha_d d_w)^{1/2}} |\vec{V}_L - \vec{V}_w| (v - v_w) N \right] \quad (0-6)$$

$$\vec{G} = -\vec{i} M_L g \left(\frac{\partial \eta}{\partial x} \right) - \vec{j} M_L g \left(\frac{\partial \eta}{\partial y} \right) \quad (0-7)$$

C_w [-] is a wind drag coefficient, $C_w = 0,00155$ (Wu, 1973), ρ_a is air density [$\text{kg}\cdot\text{m}^{-3}$], $\vec{V}_w = u_w \vec{i} + v_w \vec{j}$ [$\text{m}\cdot\text{s}^{-1}$] is water velocity vector, $\vec{V}_L = u \vec{i} + v \vec{j}$ [$\text{m}\cdot\text{s}^{-1}$] is surface ice velocity vector, $\vec{W} = \vec{i} W_x + \vec{j} W_y$ [$\text{m}\cdot\text{s}^{-1}$] is a wind velocity vector referred to the wind velocity on 10 m height above the water surface, n_L is ice roughness, d_w [m] is a water depth under the ice (see Figure 10), α_d [-] jest parametrem mówiącym o proporcji powierzchni czynnej przekroju poprzecznego będącej pod wpływem oddziaływania lodu.

5. Ice jams

In the beginning of winter, when the water temperature drops to the freezing point, further heat loss will lead to supercooling and frazil ice formation. Subsequently, various types of ice formation can develop in the river. In slow flowing areas, where the turbulence intensity is not strong enough to mix the water or frazil ice crystals formed on the water surface over the depth, skim ice can form in the river even before the cross-section-averaged water temperature drops to the freezing point. The most severe phenomena related to river ice evolution is an ice jam. Jamming is observed and described by many researchers (i.e. (Beltaos, 1995; Majewski, 1985; Uzuner and Kennedy, 1976, 1974), however mechanism of ice jam formation and evolution is usually omitted.

The ice jam is an extreme phenomenon that occurs during the winter season when the river freezes or as the result of the ice run. The consequence of the jam on the river is an increase in the flow resistance and a freshet caused by the jam. Many ice jam floods can be distinguished such as flood on the Vistula River in Plock (Kolerski, 2011; Majewski, 1985), ice jam on the Thames River in Chatham (Beltaos, 1988; Beltaos and Moody, 1986) or the ice jam on the St. Clair River (Derecki and Quinn, 1986; Kolerski and Shen, 2015). In view of the associated flood risk, extensive measures should be taken to neutralise or prevent jams. Still occurring jam caused floods are to a large extent the result of ice jams, which could not have been liquidated in time for technical reasons.

The frequency of ice jams is to a great extent related to hydraulic conditions occurring in a particular river. Meteorological conditions are an additional factor, which may increase the risk of jam formation. The causes of formation of ice jams are both natural phenomena that we cannot control (high sea stages in the river estuaries and wind) and causes related to the negligence in the river regulation (shallows, narrow river beds, sharp bends). In addition, we can mention the impact of obstacles in the current (bridge pillars) and the supply of ice to the river from the tributaries. Every effort should be

made to eliminate as many causes of ice jams as possible. In this way we will not additionally increase the already high jamming potential of the river.

River ice breakup is a complicated process, still not fully identified. The ice breakup is currently studied from the perspective of causes and mechanisms. Ice cover will break if its strength is weak due to the high air and water temperature. Also it could be pushed downstream if the downside forces will exceed the ice resistance force. Typically in natural condition both mechanisms are mutually related and will affect the breakup at the same time (Jasek, 2003).

5.1 Mathematical modeling of the river ice jam, Odra River case study

From practical and technical perspective field measurements of river ice jams are difficult and dangerous, which is caused by the highly dynamic process which are hard to predict. Thus the river ice jam formation will be analyzed on the base of mathematical model application to the Odra River section near Słubice-Frankfurt. The previously described DynaRICE model base on the dynamic force balance, therefore all observed processes are not affected by the user interference.

The mathematical model has been implemented in the section of river in the Słubice region, which is indicated as the section with a high jamming potential. The town of Słubice is located in the upper section of the Odra river, about 40 km from the mouth of the Nysa Łużycka river. The bridge that connects Słubice with Frankfurt (Odra) is a critical point for ice jam formation. The reason for this is the narrowing of the cross-section of the Odra river from about 120 m to the clearance width of the bridge span of about 65 m. In addition, the lead-in pier built above the bridge makes it impossible for the ice run-off under the next bridge span (Figure 12).

The implementation of the mathematical model boiled down to the creation of a finite element grid based on the measured bathymetry and the bank line of the Odra area from km 581 to km 586. Due to the lack of bathymetric data on the German side of the border, the river bed layout was extrapolated. Calculations were carried out for low flow $NQ = 160 \text{ m}^3/\text{s}$ and for the ice inflow with the concentration of 0,5. Ice parameters such as internal friction angle and roughness of the lower surface were selected on the basis of typical values, which were calibrated and verified on such rivers as the Lower Wisła, the St. Lawrence river or the Niagara river. The values of critical parameters concerning the dynamic formation of jam, i.e. the critical Froude number for the incoming ice ($Fr = 0,09$) and the erosion velocity for ice jam ($V_{cr} = 1,5 \text{ m}\cdot\text{s}^{-1}$) were adopted according to the instructions in the literature.

The results of mathematical modelling indicate that ice jams can form in a very short period of time on the border Odra. The results obtained from the numerical calculations indicate a clear tendency to stop ice in the area of the border bridge in Słubice-Frankfurt. When simulating the inflow of ice of medium concentration ($N=0.5$), the beginnings of the jam are observed already after 3 hours of simulation and the extended jam occurs after 18 hours of simulation. The thickness of the jam face is not significant as it reaches from 0.6 to 0.75 m, and in some places even up to 1 m. The jam develops over the length of about 2 km, reaching the upper edge of the calculation area after 24 hours (about 3 km in length).

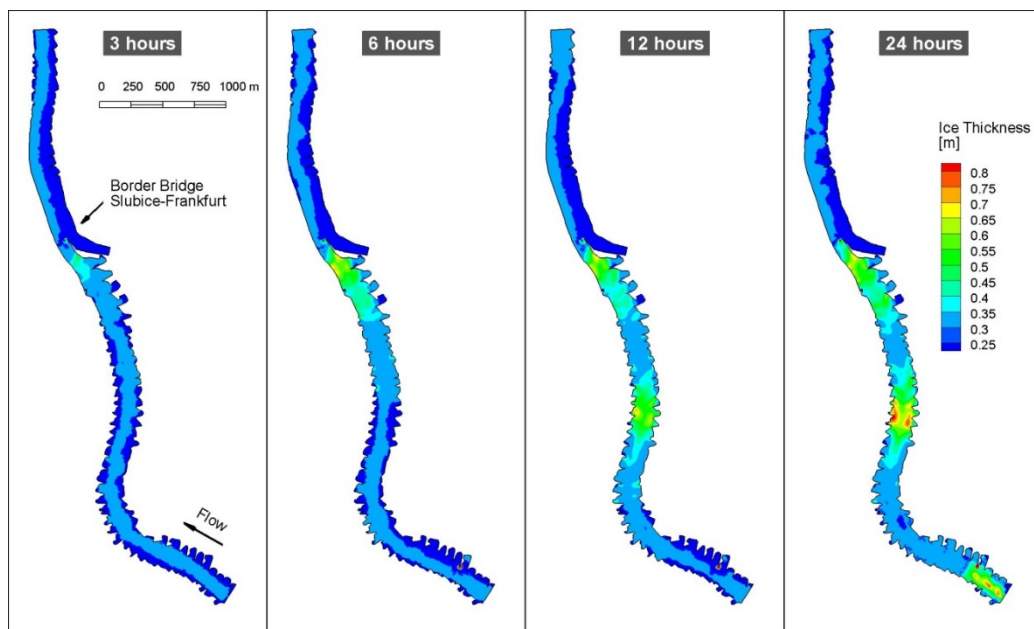


Figure 12 Results of the numerical simulation, presenting the process of ice jam formation in the Słubice region (from (Kolerski, 2018)).

6. Conclusions

Mathematical modeling of ice phenomena is a complicated process due to the large number of factors affecting the behavior of ice on the river. Strength and hydraulic parameters of ice are affected by meteorological factors such as air temperature, wind, solar radiation, precipitation and water temperature. These factors change the strength of ice and can significantly contribute to an increase or decrease in the roughness of the ice's bottom surface.

The most important factor that determines the dynamic behavior of ice is the river hydrodynamics in terms of flow velocity and slope of the water surface elevation. The morphometry of the river channel is not without significance, i.e. its decline and tortuosity, which can affect ice accumulation and pile up as well as jam formation.

The meteorological factors and hydraulic parameters of the flow affect jointly the formation of ice in rivers, and any of them it cannot be ignored. It is especially significant to properly estimate the volume of ice in the river. In a situation where the movement of ice is simulated during spring thaws, the temperature of the water will also affect the melting of ice, but in case of simulating a short episode, the thermal loss of ice volume can be skipped.

Jamming or bridging of the surface ice run by congestion initiates the accumulation of incoming surface ice into an ice cover or ice jam was shown here. By using characteristic boundary and initial flow condition ice transport and jam formation was investigated.

This study showed that the formation of an ice jam is a result of congestion of ice due to the convergence of ice flow. The other mechanism which lead to jam formation shows that ice will start to accumulate if its concentration will increase. The first process is usually related to ice bridge or other obstacle which could be reduction of flow area or bending of the channel. The next mechanism of jamming is related to hydraulic slope change affecting the retardation of ice movement (not shown here – could be upstream reach of the reservoir). Both processes taking place in relatively small area in which in consequences ice jam will be formed. Jamming is self-perpetuating process and once initiated will lead to complete blocking of the river channel if hydraulic conditions didn't change.

It is worth noticing that in final stage of ice jam formation process shown in chapter 0, the ice velocity is significantly reduced. It is caused by increase of internal resistance and concentration of the ice rubble within the ice jam toe. Obviously while the concentration reaches its maximum, further ice compaction will lead to the increase of the jam thickness which is normal phenomena observed in the jam toe. All above discussion can be present in a form of following relation (Shen et al., 2008):

$$\nabla \cdot N < 0 \Rightarrow N \uparrow \Rightarrow \sigma_L \uparrow \Rightarrow V_L \downarrow \Rightarrow \nabla \cdot N < 0 \quad (0-1),$$

The relationship presented above can be understood in such a way that due to increased ice concentration N , the internal resistance σ_L , will build up inside the ice rubble, and decrease of ice velocity V_L , will be observed. Ice concentration will than increase consequently. This process will continue to the point where no more ice will move into the toe region, which means equilibrium form of ice jam which is fully stopped.

Reference

- Ashton, G.D., 1986. River and lake ice engineering. Water Resources Publication, Littleton Co, USA.
- Beltaos, S., 1995. River Ice Jams. Water Resources Publication.
- Beltaos, S., 1988. Configuration and properties of a breakup jam. *Can. J. Civ. Eng.* 15, 685–697.
- Beltaos, S., Moody, W.J., 1986. Measurements of the configuration of a breakup jam. *Hydraulics Division, National Water Research Institute, Canada Centre for ...*
- Derecki, J.A., Quinn, F.H., 1986. Record St. Clair River Ice Jam of 1984. *J. Hydraul. Eng.* 112, 1182–1193. [https://doi.org/10.1061/\(ASCE\)0733-9429\(1986\)112:12\(1182\)](https://doi.org/10.1061/(ASCE)0733-9429(1986)112:12(1182))
- Jasek, M., 2003. Ice jam release surges, ice runs, and breaking fronts: field measurements, physical descriptions, and research needs. *Can. J. Civ. Eng.* 30, 113–127.
- Ji, S., Shen, H.T., Wang, Z., Shen, H.H., Yue, Q., 2005. A viscoelastic-plastic constitutive model with Mohr-Coulomb yielding criterion for sea ice dynamics. *ACTA Oceanol. Sin.-Engl. Ed.-* 24, 54.
- Kolerski, T., 2018. Mathematical modeling of ice dynamics as a decision support tool in river engineering. *Water* 10, 1241.
- Kolerski, T., 2015. Ice cover progression due to flow regulation at the Wloclawek dam. *Acta Sci. Pol. Form. Circumiectus* 14, 229–240.
- Kolerski, T., 2011. Numerical modeling of ice jam formation in the Wloclawek Reservoir. *Task Q.* 15, 283–295.
- Kolerski, T., Shen, H.T., 2015. Possible effects of the 1984 St. Clair River ice jam on bed changes. *Can. J. Civ. Eng.* 42, 696–703.

- Kolerski, T., Shen, H.T., Kioka, S., 2013. A Numerical Model Study on Ice Boom in a Coastal Lake. *J. Coast. Res.* 291, 177–186. <https://doi.org/10.2112/JCOASTRES-D-12-00236.1>
- Lal, A.W., Shen, H.T., 1991. Mathematical model for river ice processes. *J. Hydraul. Eng.* 117, 851–867.
- Liu, L., Shen, H.T., 2000. Numerical simulation of river ice control with booms (Technical Report No. ERDC/CRRE: TR-00-10), Engineer Research and Development Center. Cold Regions Research and Engineering Laboratory, Hanover, NH, USA.
- Majewski, W., 1985. Powódź zatorowa na Wiśle w rejonie Zbiornika Włocławek w zimie 1982 r. Wydawnictwa Geologiczne.
- Potok, A.J., Quinn, F.H., 1979. A HYDRAULIC TRANSIENT MODEL OF THE UPPER ST. LAWRENCE RIVER FOR WATER RESOURCES STUDIES 1. JAWRA J. Am. Water Resour. Assoc. 15, 1538–1555.
- Shen, H.T., 2016. River Ice Processes, in: *Advances in Water Resources Management, Handbook of Environmental Engineering*. Springer, Cham, pp. 483–530. https://doi.org/10.1007/978-3-319-22924-9_9
- Shen, H.T., 2010. Mathematical modeling of river ice processes. *Cold Reg. Sci. Technol.* 62, 3–13. <https://doi.org/10.1016/j.coldregions.2010.02.007>
- Shen, H.T., Gao, L., Kolerski, T., Liu, L., 2008. Dynamics of Ice Jam Formation and Release. *J. Coast. Res.* 52, 25–32. <https://doi.org/10.2112/1551-5036-52.sp1.25>
- Shen, H.T., Lu, S., Crissman, R.D., 1997. Numerical simulation of ice transport over the Lake Erie-Niagara River ice boom. *Cold Reg. Sci. Technol.* 26, 17–33. [https://doi.org/10.1016/S0165-232X\(97\)00005-0](https://doi.org/10.1016/S0165-232X(97)00005-0)
- Shen, H.T., Shen, H., Tsai, S.-M., 1990. Dynamic transport of river ice. *J. Hydraul. Res.* 28, 659–671.
- Shen, H.T., Su, J., Liu, L., 2000. SPH Simulation of River Ice Dynamics. *J. Comput. Phys.* 165, 752–770. <https://doi.org/10.1006/jcph.2000.6639>
- Su, J., Shen, H.T., Crissman, R.D., 1997. Numerical study on ice transport in vicinity of Niagara River hydropower intakes. *J. Cold Reg. Eng.* 11, 255–270.
- Szymkiewicz, R., 2010. Numerical modeling in open channel hydraulics. Springer Science & Business Media.
- Uzuner, M.S., Kennedy, J.F., 1976. Theoretical model of river ice jams. *J. Hydraul. Div.* 102.
- Uzuner, M.S., Kennedy, J.F., 1974. Hydraulics and mechanics of river ice jams. IOWA INST OF HYDRAULIC RESEARCH IOWA CITY.
- Wu, J., 1973. Prediction of near-surface drift currents from wind velocity. *J. Hydraul. Div.* 99, 1291–1302.
- Yapa, P.D., Shen, H.T., 1986. Unsteady flow simulation for an ice-covered river. *J. Hydraul. Eng.* 112, 1036–1049.

MAPPING OF GROUNDWATER FLOW CHANGES AND RELATED HAZARDS

TOMÁŠ JULÍNEK¹, JAROMÍR ŘÍHA¹

¹ Faculty of Civil Engineering, Brno University of Technology, Veveří 95, 602 00 Brno, Czech Republic,
E-mail: julinek.t@fce.vutbr.cz, riha.j@fce.vutbr.cz

Abstract

The underground elements of flood protection structures such as levees or floodwalls may significantly influence the groundwater regime. Therefore, it is important to consider such consequences when they are being designed. European Directive 2007/60/EC mentions, although only briefly, the problem of hazard arising due to natural groundwater flooding and related measures. There are several groundwater-related threats, which can be considered as follows:

- during flood – e.g. seepage of groundwater behind levees or potential uplift of the topsoil layer at the protected area,
- without flood – influence of the underground parts to the natural flow regime.

The hazard corresponding to rising groundwater level depends on a number of factors related to the flood course, groundwater regime, geology and topology of the protected area. The increased piezometric head and water pressures at the area protected against flooding can harm the subsurface parts of buildings such as cellars, underground garages and also sewer mains.

Different methods can be applied expressed by mapping technics. The limit state approach recommended in Eurocode 7 is applied to the assessment and mapping of hazard induced by rising groundwater level in the area behind flood protection barriers. The discussed problems are related to groundwater flow issues concerning mainly the flood protection measures placed in urban localities and partly also other type of structures. Hydraulic modelling and risk mapping techniques are applied for the assessment of the impact of groundwater flow and related hazards exposed on flood protection facilities and on structures in protected areas. Additionally, the effect of subsurface parts of floodwalls and levees on the groundwater regime in adjacent areas is discussed. The limit state condition for topsoil layer uplift or seepage threat are usually defined as over-design factor. To describe the factor in space it is expressed using mapping techniques as a function of the spatial co-ordinates (x, y) .

Floods are characterized by a growth in river flow rates, increased water stages in streams, overbanking and the inundation of floodplains. Increased water stages during the flood event may significantly affect the groundwater flow regime in the aquifer adjacent to the river. In the case of the construction of flood control works, their subsurface parts can affect the natural groundwater regime during periods when flooding is absent, at which times groundwater usually flows from higher-lying areas towards streams which drain adjacent aquifers. Therefore, to maintain free communication between the river and aquifer (Directive 2006/118/EC), seepage barriers such as cut-off walls, injection walls, etc. should be designed to be partially penetrable.

The method of evaluating groundwater hazard due to uplift during floods consists of the following steps:

- identification and conceptual description of hazard arising from solved scenarios,
- limit state definition, potential hazards arise according to local conditions,
- input data collection, verification and analysis. Data from geological and hydrogeological surveys and groundwater flow modelling are used to evaluate individual terms in the limit state condition. Uncertainties in the input data are expressed via partial factors,
- hydraulic modelling techniques are chosen according to solved problem,
- quantification of hazard due to considered hazard via flood mapping.

Keywords: groundwater, reliability, limit state, European Directive 2007/60/EC, hazard mapping.

POST-FLOOD RECOVERY OF LANDSLIDES

MILORAD JOVANOVSKI¹, CVETANKA POPOVSKA², IGOR PESEVSKI³

¹Faculty of Civil Engineering, Macedonia, jovanovski@gf.ukim.edu.mk

²Faculty of Civil Engineering, Macedonia, popovska@gf.ukim.edu.mk

³Faculty of Civil Engineering, Macedonia, pesevski@gf.ukim.edu.mk

1. Abstract

Floods and landslides present most frequent natural hazards, causing in average yearly damage of about 50 billion US dollars or 40 000 human lives. Some analyses indicate that 2 billion people could be vulnerable to floods and landslides as a result of global warming, deforestation and population growth in flood prone areas. In order to improve management of such hazards, many studies focus on the different topics related to qualitative and quantitative flood and landslide risk assessment at local to national scales. Post recovery from flood and landslides is another hot topic. With aim to underline again the importance of these hazards for society, here we are presenting some analyses, connected with floods and post-recovery from landslides. The experiences are mainly for case histories from Macedonia, but we believe that these findings can help in improvement of legislative in line with the flood and landslide risk management strategies to be developed in affected regions on international scale.

Keywords: Flood, landslide, experiences, post-recovery, legislation.

2. Introduction

Well known fact is that floods and landslides are among the most dangerous and costly of all natural hazards. In general, frequency of such events, especially floods and induced landslides from flash floods, has been on the rise globally in the past decades. There is a lot of data that clearly presents the importance of such events. For example, Kalsnes, Nadim, Lacasse 2010, reports that, in average yearly damage, about 50 billion US dollars or 40 000 human lives [1]. Over the period 1900—1976, 3006 people have lost their lives due to landslides (36 per year) out of a total of 4.8 million killed in all natural disasters [2].

Having this in mind, at present there are many strategic documents, projects and published deliverables worldwide, which are specifying the significance of floods and landslides. Some of them are listed below:

- Safe land, Living with landslide risk in Europe
- RECARE;
- Horizon 2020 Transport Advisory Group – TAG;
- FEHRL Vision 2025 for Road Transport in Europe;
- ECTP reFINE;

- Sendai Framework for Disaster Risk Reduction;
- UNDP-implemented EU Recovery Program to support Macedonia recovery efforts after 2015-floods;
- Sri Lanka rapid post disaster needs assessment;
- Technical assistance for preparation of climate resilience design, Guidelines for the Public Enterprise for state roads in Macedonia (in print), and many others.

Safe Land is a Large-scale integrating collaborative research project funded by The Seventh Framework Program for research and technological development (FP7) of the European Commission. The aim of Safe Lands is to develop generic quantitative risk assessment and management tools and strategies for landslides at local, regional and European scales and establish the baseline for the risk associated with landslides in Europe. It is in correlation with the EU Soil Thematic Strategy and its associated Proposal for a Soil Framework Directive, and for achieving interoperability and harmonization in agreement with the INSPIRE European Directive [3].

The RECare project has an aim to develop effective prevention, remediation and restoration measures using an innovative trans-disciplinary approach, actively integrating and advancing knowledge of stakeholders and scientists in 17 Case Studies, covering a range of soil threats in different bio-physical and socio-economic environments across Europe [4].

Documents which are specifying the significance of transport infrastructure for coming decades as Horizon 2020 Transport Advisory Group (TAG), FEHRL Vision 2025 for Road Transport in Europe, ECTP reFINE and ELGIP position paper. In principle they are focused on three aspects: sustainability, availability and affordability [1], [5], [6], [7].

The “Sendai Framework for Disaster Risk Reduction 2015-2030” was prepared by United Nations International Strategy for Disaster Reduction (UNISDR) and adopted at the Third UN World Conference in Sendai, Japan. This document is the successor instrument to the Hyogo Framework for Action (HFA) 2005-2015: Building the Resilience of Nations and Communities to Disasters [8].

The Post Disaster Need Assessment (PDNA) project in Sri Lanka is developed after floods and landslides in 2017 as a collaborative effort of the Government of Sri Lanka with its partners - the United Nations agencies, the World Bank, the European Union, and other organizations [9].

For a local scale in Republic of Macedonia, we can mention UNDP-implemented EU Recovery Program. It has a main objective to support country’s recovery efforts after 2015 floods. Special emphasis is placed on the general design guidance for recovery of the most common types of flood-damaged transport and water infrastructure contained in the country’s first-ever Build Back Better manual [10]. Another important document is still in final preparation with a title: Technical assistance for preparation of climate resilience design, Guidelines for the Public Enterprise for State Roads in Macedonia by IMC Worldwide, with a help from World Bank. The aim is to support policy and decision makers in establishing a foundation for taking climate hazard resilience considerations in the road transport management and response plans [11].

Beside mentioned and other strategic documents, there are a lot of scientific papers related to different aspects of landslide and flood susceptibility, qualitative and quantitative flood and landslide risk assessment, early warning systems, post-recovery from flood and landslides etc. Large number of landslide susceptibility models in last two decades have been published, usually being prepared by GIS technology on continental and national scale [12], [13] [14], [15], [1].

Another important issue in risk management is to develop adequate Landslide Early Warning Systems (LEWSs). This helps a lot in appropriate reaction and gives sufficient time to reduce the possibility of harm or loss (UNISDR, 2009). The details can be found in paper [16].

The Slope Safety System has proven successful in containing landslide risk within an As Low as Reasonably Practicable (ALARP) methodology. General ideas are developed by the United Kingdom Health and Safety Executive (HSE 1988, 1992) in the form of Tolerability of Risk (TOR) [17], [18] [2].

The importance of the topic is a reason to organize a lot of specific Conferences or Symposiums devoted to landslide and flood risks. Here we can mention few as: “Geotechnical Safety and Risk”, [19], 16th European Danube Geotechnical conference: “Geotechnical hazard and risks, experiences and practices”, held in Republic of Macedonia in June 2018 [20], “Seventh International Conference on Debris-Flow Hazards Mitigation” in Golden, Colorado 2019 [21] and others. The major objective of such conferences is to develop numerical, empirical and combined methods to face with these problems, and provide a forum for international researchers, engineers, and policy makers to exchange ideas and promote communication to advance the scientific understanding of flood and landslide hazards.

Beside all previously mentioned facts, unfortunately, still public perception of flood and landslide hazard does not correspond to reality, and McGuire note from 2002 that “landslides are the most widespread and undervalued natural hazard on Earth” is still actual. Therefore, the outline of the paper is to provide overview of basic principles for landslide analyses, and recovery design guidelines, aiming to enhance resilience levels and overall preparedness to future disaster events.

3. Methods for landslide hazard analyses

It is well known fact that the rational physical planning largely depends on the knowledge of different geohazards. At today’s practice, there exist numbers of methods for analysis of hydrology and landslide data which enable definition of the flood and landslide hazard and risk level.

In relation to landslide hazard in particular, the first step is to prepare landslide inventory (see example in Figure 1) and susceptibility maps for particular region which will enable recognition of most critical zones that will be subjected to further investigation on higher level – landslide hazard and risk. In order to prepare such maps, appropriate landslide database is needed.

Model for establishment and operation of a GIS databases for Republic of Macedonia is

given in [23]. The procedure of landslide susceptibility includes generating and combining a set of conditioning factors, as: lithology, slope, land cover and rainfall influences. Recently, the susceptibility map from above mentioned publication was used as base layer for preparation of additional susceptibility maps for different rainfall scenarios (that can be expected from the climate change scenarios). This work was done in a frame of analyses for State Roads in Republic of Macedonia [11]. Switching from susceptibility to Landslide Hazard (LH) required involvement of triggering process and its spatial-temporal influence. It can be based on interpolated rainfall measurements depicting conditions of severe rainstorms or periods of prolonged rainfall (maximal recorded daily values and annual totals, respectively) within a baseline period (Rainfall). The models are presented in Figure 2.

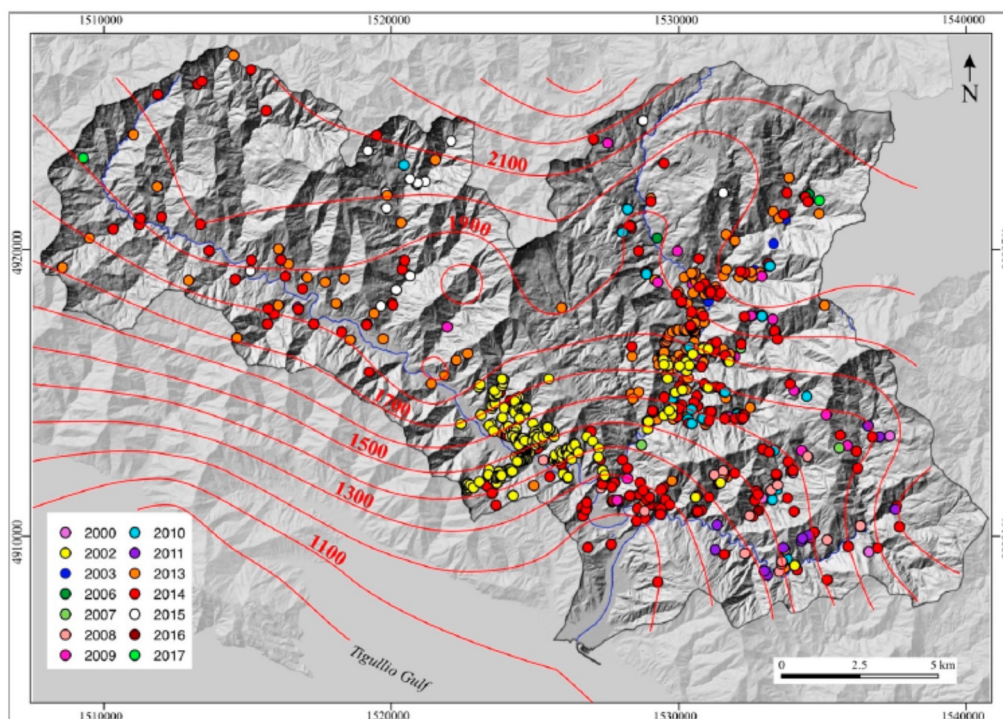


Figure 1. Spatial distribution of rainfall-induced shallow landslides which occurred in Entela River Basin in Italy from 2000-2017 (red lines show values of mean annual precipitation in the catchment area) [22].

The optimal model includes the rainfall influences, and it is presented with following formulas:

$$LH = 0.3 \times \text{Lithology} + 0.175 \times (\text{Slope} + \text{Land Cover} + \text{Earthquake}_{100 \text{ year r.p.}} + \text{Rainfall}) \quad (1)$$

Finally, the Rainfall Factor (RF) normalized to 0-1 range, was used to predict the hazard change in the future, for 2021-2050 and 2071-2100 period, respectively:

$$RF1 = 90^{\text{th}} \text{ percentile rainfall} \times \text{expected annual sum for 2021-2050} \quad (2)$$

$$RF2 = 90^{\text{th}} \text{ percentile rainfall} \times \text{expected annual sum for 2071-2100} \quad (3)$$

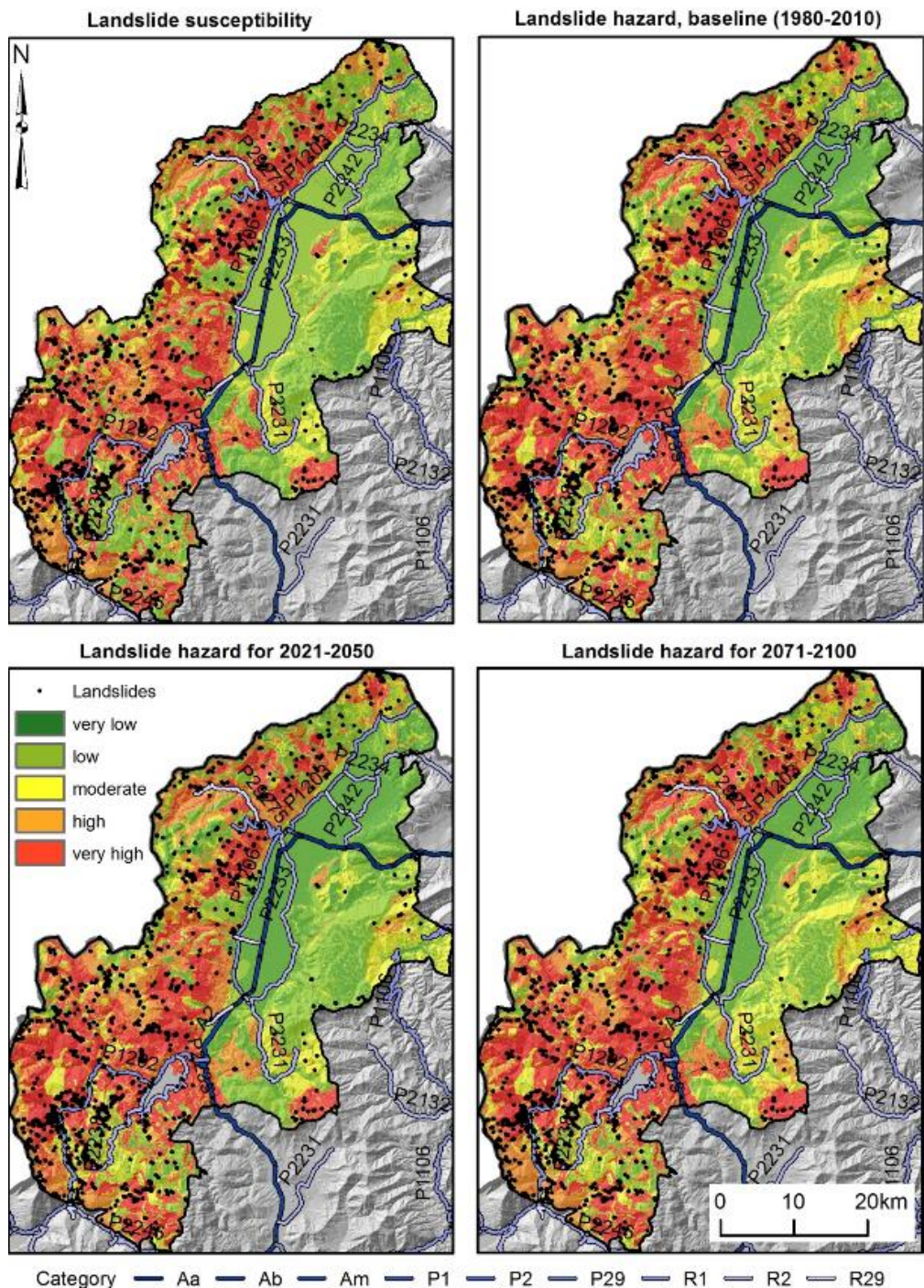


Figure 2. Landslide susceptibility and hazard models for respective periods, case for the Polog region in Macedonia [11]

Both factors were introduced by using the worst climate change scenario, i.e., gas emission RCP85. Since it represents the factor of change of the baseline levels, it was introduced in the optimal model equation by using:

$$LH1 = 0.3 \times \text{Lithology} + 0.175 \times (\text{Slope} + \text{Land Cover} + \text{Earthquake}_{100} + (1+RF1) * \text{Rainfall}) \quad (4)$$

And

$$LH2 = 0.3 \times \text{Lithology} + 0.175 \times (\text{Slope} + \text{Land Cover} + \text{Earthquake}_{100} + (1+RF2) * \text{Rainfall}) \quad (5)$$

The need for the use of quantitative interpretation and modeling in the assessment of landslide hazard is underlined by several authors and they are summarized in Cotecchia et al. [12]. The authors suggest to use stage-wise methodology presented in Figure 3.

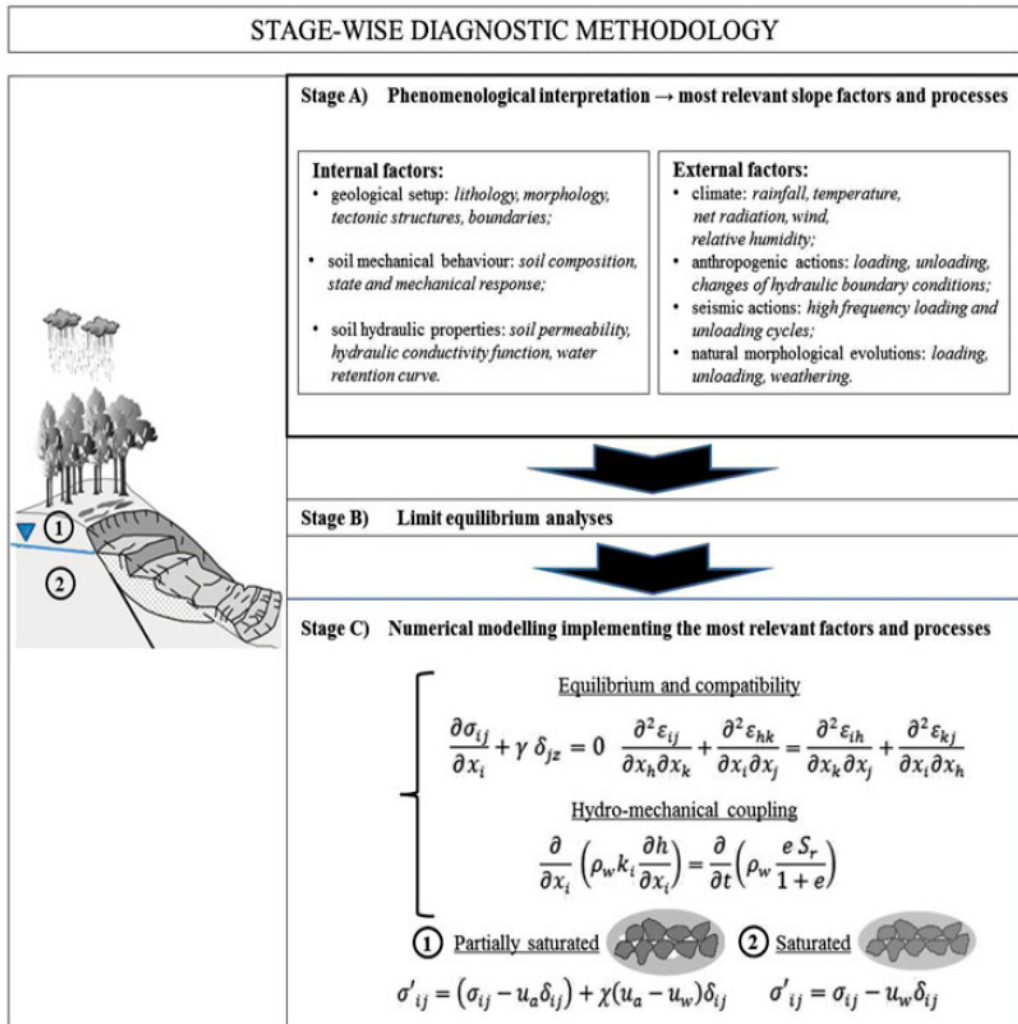


Figure 3. Stage-wise methodology for the diagnosis of the landslide mechanism [12]

Almost in every methodology, it is evident that infiltration of water (from rainfalls or snow melt) in the ground and rise of ground water level is usually dominant factor for slope stabilities. Some methods that present such influences are presented in following Figures 4 to 6.

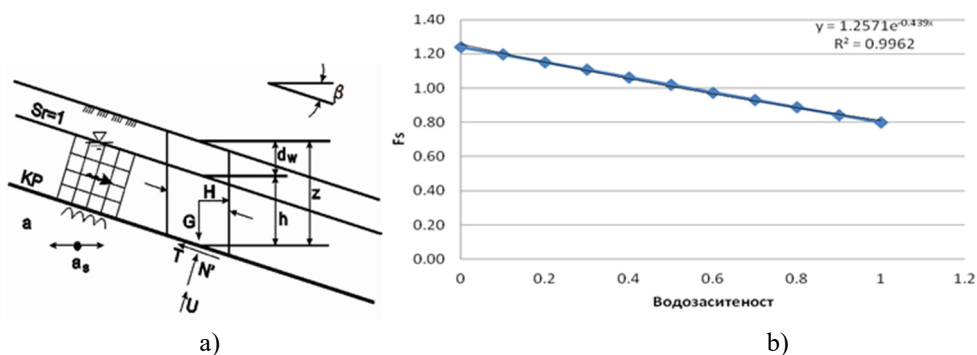


Figure 4: a) Simple model for calculation of Safety factor (F_s) for infinite slope analyses; b) influence of saturation on Safety factor

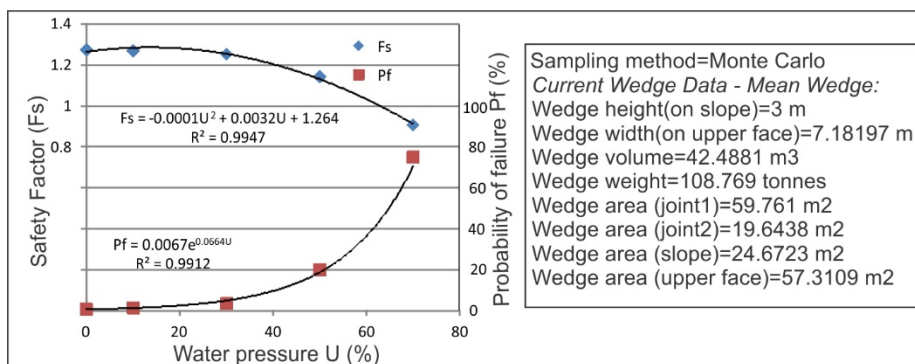


Figure 5. Presentation of influence of water pressure (U) on the decreasing of Safety Factor (F_s) and increasing of probability of failure (P_f) for a wedge failure (case for road from Stip to Radovis in Macedonia)

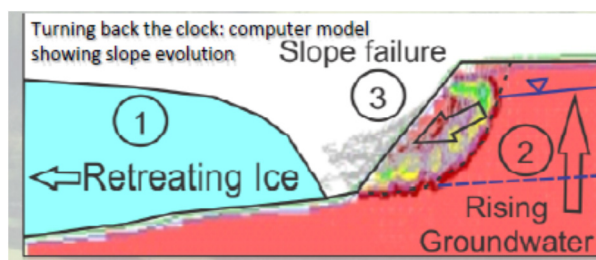


Figure 6. Model for reactivation of old large landslides as a result of retreating of ice in Britain [24].

It is evident that rainfall influences must be one of the main factors in quantification and management of landslide risk. Here we will mention Hong Kong's experience (Figure 7). The Hong Kong area is known with a number of disastrous landslides with serious fatalities in the 1970s. That was the reason to establish GEO (Geotechnical Engineering Office) system in 1977. Over the years, a comprehensive Slope Safety System has been developed and implemented by the GEO with a goals to: (i) to minimize landslide risk to the community through a policy of priority and partnership for reducing landslide frequency and consequence, and (ii) to address public attitude and tolerability of landslide risk to avoid unrealistic expectations [4], [19].

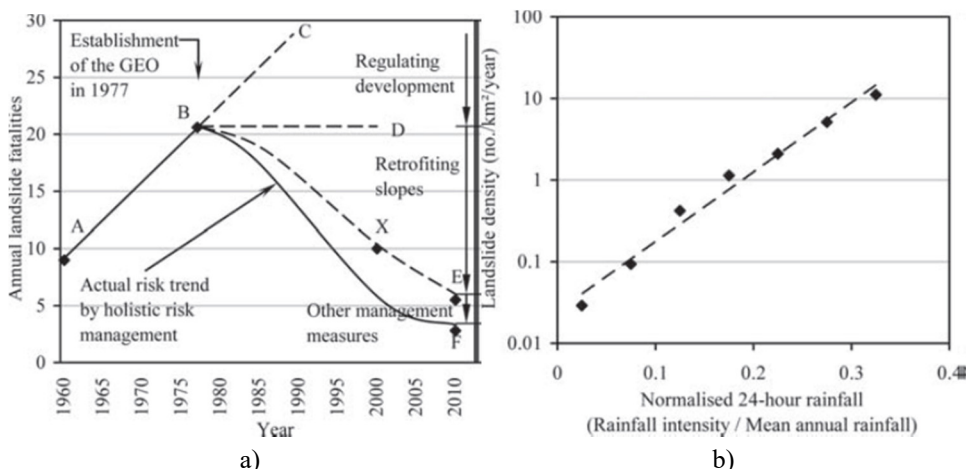


Figure 7: a- Reducing of fatalities in Hong Kong after establishing of the GEO system; b- simple diagram for prognosis of landslide density with a help of normalised rainfall intensity [4].

The Slope Safety System has proven successful in containing landslide risk within an As Low as Reasonably Practicable (ALARP) level, via: (i) improving slope safety standards, technology and administrative and regulatory frameworks, (ii) ensuring safety standards of new slopes, (iii) rectifying substandard Government slopes and maintaining them, (iv) ensuring that private owners take responsibility for slope safety, and (v) promoting public awareness in and response to slope safety [4].

An interesting tool for forecasting of siliding is established in using radar techniques by Meteorological Service of Catalonia (SMC). This tool is a part of Landslide Early Warning System, and in helps in identification of the type of precipitation, extrapolation of elevated reflectivity measurements to surface and conversion of reflectivity to rain-rate. To assess if a given rainfall event has the potential of triggering a debris flow, four rainfall hazard levels have been defined: “very low”, “low”, “moderate” and “high” (Figure 8).

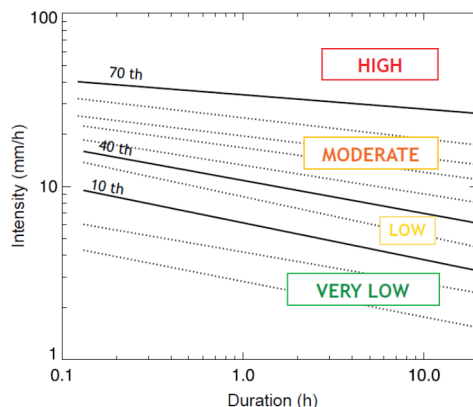


Figure 8. Rainfall intensity-duration thresholds adapted from Guzzetti et al. (2008) and selected rainfall hazard levels. The continuous lines represent the 10th, 40th and 70th percentiles of rainfall that were selected as thresholds [21].

Numerical modelling of the slope processes can provide further interpretation of the landslide mechanism, but it overcomes the frame of this paper. As a short conclusion is, that knowledge of possible failure modes is an essential prerequisite, both for a reliable assessment of existing failures, but also for optimised modeling of new events, using best principles and practices for post recovery.

4. Some examples for recent floods and landslide influences

The impact of floods and landslides are always in the forefront of publicity. Here we will present short list as an overview of large landslides that have occurred recently. In Southeastern and Central Europe from the last two decades, there are a lot of catastrophic events. In Austria, for instance a 2 000 to 10 000-year flood event was back-calculated from the flood disaster in the year 2002 (Figure 9). As a result of that, the risk of dykes or levees failure increased a lot [1], [20].

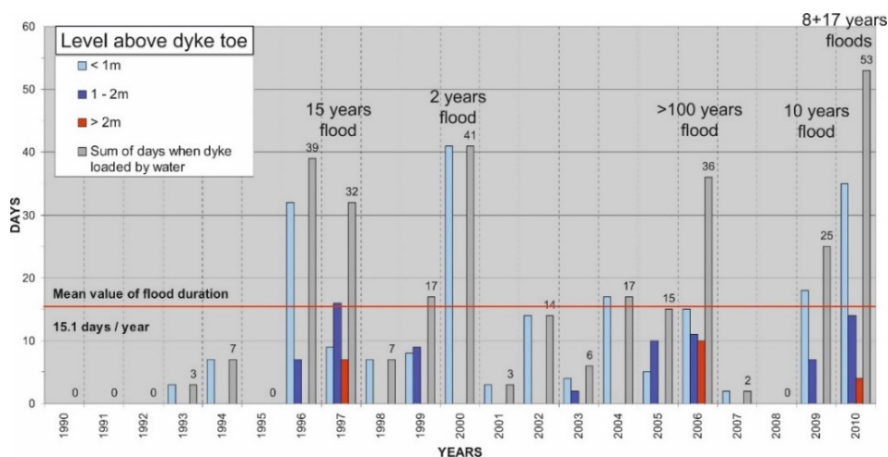


Figure 9. Duration of floods along the River March dykes (Water level at Dürnkrot – Austria/Slovakia; Two floods within three weeks in 2010 [20].

Extreme flooding in Central Europe in late May and early June 2013 affected south and East German states, western regions of the Czech Republic and Austria. In addition, Switzerland, Slovakia, Belarus, Poland, Hungary and Serbia were affected to a lesser extent. Twenty-five deaths were recorded as a result of the floods; eleven in the Czech Republic, six in Austria, and eight in Germany. Overall losses are estimated to €12Bn.

Between 13 and 18 May 2014 a low-pressure cyclone affected a large area in Southeast Europe, causing floods and landslides. Serbia and Bosnia and Herzegovina suffered the greatest damage. By 20 May, at least 62 people had died as a result of the flooding, and hundreds of thousands had been forced from their homes. Floodwaters caused over 2.000 landslides across the Balkan region. Official counts indicate that over 1.6 million people were affected in Serbia and Bosnia and Herzegovina, after a week of flooding. Croatia was affected by the floods to a lesser extent. The embankment on the Sava River was breached near Rajevo Selo and Račinovci, and thus evacuation was ordered for Gunja, Rajevo Selo and Račinovci. Some illustrations of influences are presented in following Figures.



Figure 10 Breach of a Sava River dyke with an extensive scour on the landside (120 x 300 x 12m) due to internal erosion of the ground below the dyke in 2014 [20].



Figure 11. Piping through a railway embankment during an already sinking flood. Train traffic was stopped in 2014 [20].

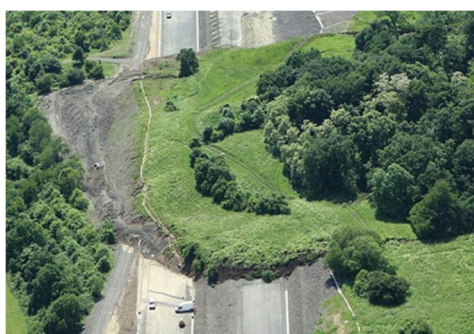


Figure 12. Landslide covering the constructed motorway D8 in Czech Republic in 2013, [1].



Figure 13. The result of surface erosion of the crest with asphalt pavement during a flood in Czech Republic 2002, [1].

Landslide processes in Macedonia in the past have caused significant economic loss and unfortunately loss of life, Peshevski et al 2013, [14]. The key findings were that almost 70% of the landslides have been caused by heavy rain falls, and the rest have been caused in combination of excavation and water saturation as the main prerequisite. The precipitations in Macedonia are unequally spread through the space and time, with relatively small intensity and amount (500-700 mm/y). Based of analyses by Jovanovski et al [25], this and other average values have been increased mainly due to the large precipitations in 2009. Excessive rainfalls and snowfalls during and especially at the end of 2009, were followed by similar trend at the beginning of 2010. Similar occurrences are typical for beginning of 2015 and in 2016.

The event in November-January 2004 was caused by overflow of the major rivers Vardar, Crna Reka, Treska, Strumica, and Bregalnica. Besides this kind of flooding caused by long rainy periods and intensive snowmelt (or combination of both), there are flash floods caused by short and intensive rains, most frequently in summer periods, in smaller river basins. The floods in 2004 affected 26 municipalities with an estimated damage of approximately EUR 15 million. Floods from January and February 2015

affected 43 out of 80 municipalities in the country, causing a damage of over €35 Mn, [10].

A subsequent disaster occurred on 3 August 2015, when flash floods and mudslides struck the northwest Polog Region, killing six people and causing damage to municipal infrastructure and houses in the city of Tetovo and villages in the surrounding mountainous areas. The trigger for flooding and landslides on 3 August from 17.30 to 21.00 hours was heavy rainfall combined with hail. Relevant seismic events were not recorded before and during the rainfall event. People from one of the most affected villages Shipkovicica witnessed that a 10cm thick layer of hail fell during the event. Along the watercourse of river Pena there was flooding and debris flow sliding.

Moreover, the night between 6 and 7 August 2016 heavy torrential rain affected country's capital suburbs, causing tragic loss of 23 lives and an estimated cost of over €30Mn, resulting from the severely damaged infrastructure and affected agricultural land, occurrences of several landslides in catchment area etc. The Hydrometeorological Service measured 92.9 mm of rain that fell in just a few hours, which is considered an event with a return period of 1,000 years, [10]. To present the scale of the events



Landslide on the road Bitola – Resen in 2010



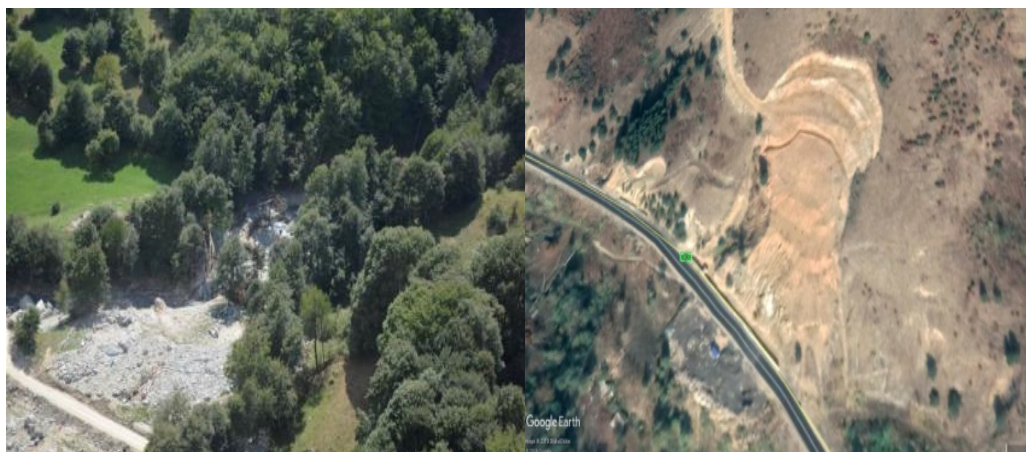
Rockfall on the railway Gostivar – Kichevo in 2010



Landslide on the road Mavrovo – Debar in 2010



Rockfall on the road Kochani – Shtip in 2013



Debris on the road Shipkovica – Brodec in 2013

Landslide on the road Bitoyal – Resen in 2015

Figure 14. Recent rockfalls and landslides on transport infrastructure in Macedonia

The presented floods and landslides in the world and in country caused major damages to transport infrastructure, and resulted in negative impact on many productive activities, and access to social services in the affected areas. The drastic consequences are unfortunately followed by lot human lost. Some of the events has the elements of real catastrophes, expressed in high percentage on the costs in many countries (Table 1).

Table 1. Annual economic losses and fatalities (GDP data from EUROSTAT 2015 or [https://en.wikipedia.org/wiki/List_of_countries_by_GDP_\(nominal\)](https://en.wikipedia.org/wiki/List_of_countries_by_GDP_(nominal)))

Country	Annual economic losses	Some data about fatalities	% Country GDP
BOSNIA & HERZEGOVINA (FOR THE YEAR 2014)	€ 2.03 billion	Annually 4	15%
ITALY (ANNUAL AVERAGE FOR THE PERIOD 1968-2015)	€5.5 billion	137	3.5%
POLAND (ESTIMATED ANNUAL FOR THE PERIOD 2004-2009)	€260 million	0- 51	0.07%
SLOVENIA (ANNUAL AVERAGE FOR THE PERIOD 1994-2008)	€86 million	-	0.19%
SWITZERLAND	€300 million	Annually 4	0.05%
SPAIN (ANNUAL AVERAGE FOR THE LAST 20 YEARS)	€650 million	25	0.23%
SERBIA, 2013	€ 1,5 billion	12	About 3%
MACEDONIA 2015 AND 2016	About 40 millions	30	0.55 - 0.85%
JAPAN GEJE	US\$5.5 trillion	About 16 000	2,5 %

Unofficial data on human loses from landslides in Macedonia is presented in Table 2. However, authors consider that this data incomplete and underestimates the real situation by far. Efforts are being made to enlarge the database.

Table 2. Database on landslide fatalities. Authors own data, update of data presented in [27]

Location name	Date	Deaths	Event	Description
Access road to dam Sveta Petka	21.3.2007	1	Rockfall	rockfall during preparations for blasting
Preseka (Gostivar-Kicevo road)	30.9.2008	0	Rockfall	hit rockfall sitting on carriageway
Rudina (road to Rakovec near Tetovo town)	25.4.2010	1	Rockfall	rockfall hits shepherd
Access road to Knezevo dam	21.6.2010	0	Rockfall	workers cleaning one rockfall hit by another one
road to mount.Bistra (Gostivar-Kicevo road)	9.2.2011	0	Rockfall	rockfall hits car while driving
Senecki livadi (road Mavrovo-Debar)	5.5.2012	1	Rockfall	rockfall hits car while driving
Railway Veles - Skopje	29.01.1946	15	Rockfall	rockfall sitting on railway
Gradot Kavadarci	05.09.1956	11	debris flow	slow moving landslide turned into debris flow
Avalanche-Landslide Radika catchment	11.02.1956	52	Avalanche (rock+sno w+trees)	construction workers on the Mavrovo hydrosistem sleeping in barracks
Road Mavrovo Debar	197?	2	Rockfall	truck hit rockfall sitting on carriageway
Debar-Melnicki most	21.04.2008	1	Rockfall	construction works Debar Melnicki most
Tetovo - Poroj	03.08.2015	4	Flash flood + mud slide	Severe thunderstorm with intense precipitation

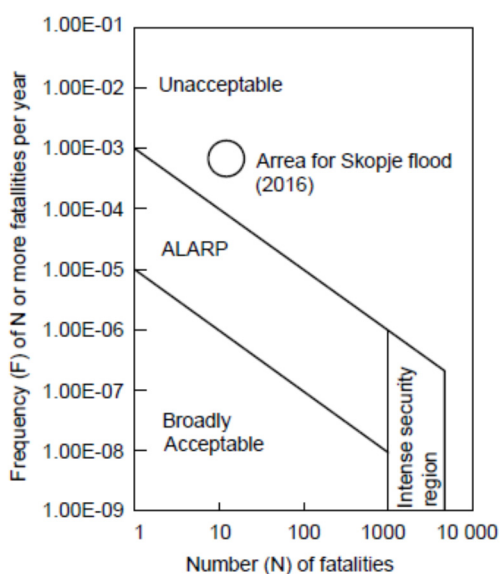
Just to have a picture of magnitude of events, the cases in a frame of Table 1 can be compared with the effects from Great East Japan Earthquake (GEJE) and tsunami of 11 March 2011 and the ensuing Fukushima nuclear incident. It is well known that the Japanese economy is the third largest in the world, with GDP of US\$5.5 trillion in 2010, but as an effect from this disaster, Japan's north east coast, known as the Tohoku region, suffered the greatest damage as a result of the GEJE. However, the Tohoku region produces only 2.5 per cent of the total Japanese economy.

If take a more specific insight on the floods, it can be seen that the most devastating flood in Macedonia since it gained its independence in 1991 occurred in 1995 and caused nearly \$400 million in damage. More recently, flooding in 2004 affected over 100,000 people and caused almost \$5 million in damage (Source: World Bank). The annual average population affected by flooding in Macedonia is about 70.000 and the annual average affected GDP about \$500 million. For most provinces, the 10 and 100 year impacts do not differ much, so relatively frequent floods have large impacts on these

averages (World Bank). Also, in the last few years, Macedonia has black statistics regarding the floods (Centre for Research on the Epidemiology of Disasters - CRED). Both in 2015 and 2016, Macedonia is among the top 10 countries, with the greatest economic damages and mortality also, as a result of the floods, some more specific statistics are the following:

- 6th of top 10 countries in terms of disaster mortality in 2016 (1.06/100.000)
- 3th of top 10 countries by damages in 2016 (0.55% of GDP)
- 8th of top 10 countries by damages in 2015 (0.85% of GDP)

Just to have a clearer picture of events in a term of societal risks, some data are presented in Figure 15. Figure 15 is connected with Figure 16, which presents calculations related to estimating the loss of life, which as a problem is very difficult to determine with one simple value. Some recommendations for the “value of life” estimates used by a number of countries are listed in Figure 15b.



a)

Country	Value of life loss (million £)
USA	1.67
New Zeland	0.75
Great Britain	3
France	4
Germany	2.1
Netherlands	0.3

b)

Figure 15. a) Presentation of occupied area of recent Skopje flood in an ALARP diagram proposed for evaluation of societal risk; b) typical figures of "value of life" (ERM-Hong Kong 1998 [17]).

However, the preparation and use of such diagrams will always remain a controversial topic from many aspects, but it is more than evident that damages and losses caused by floods and landslides have a significant impact on the economies and societal aspects, and that the need of application of post recovery methodologies is more than necessary in such cases.

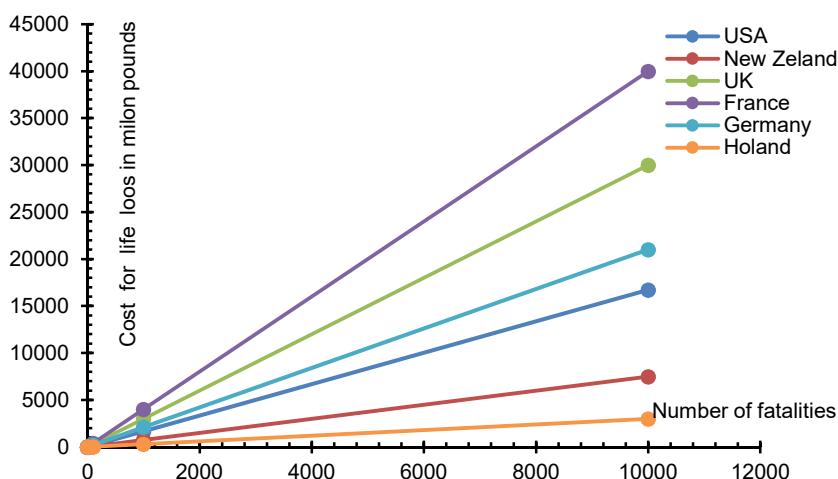


Figure 16. Diagram for prognosis of costs for life loss for different countries

5. Landslide post-flood recovery examples

In a frame of this article, we are presenting one case for post recovery from Sri Lanka, as well as some domestic experiences. Both experiences can be related to Build Back Better concept, and can be an example how to manage with such problems.

Connected with first case, it shall be underlined, that in May 2016 and May 2017, Sri Lanka faced catastrophic floods and landslides that affected almost the entire country. The combined fatalities of the two events amounted to 317 persons. The estimated damages and losses from the floods and landslides in May 2016 were over LKR 90 billion and in the aftermath of the events in May 2017 it was estimated at LKR 70.2 billion (1US\$=LKR150). Nearly five million people were affected by the May 2016 events, while that of May 2017 exceeded 8 million people [9].

Both events left close to 10,000 houses fully damaged, and over 100,000 partially damaged. In response to these disaster events, the Government of Sri Lanka in partnership with the United Nations, the World Bank and the European Union conducted a Post-Disaster Needs Assessment (PDNA), assessing both the effects and the recovery needs, across all affected sectors and districts.

Presentation of total damages, estimated recovery needs for main sectors and recovery needs timeline are presented in Figure 17. The highest recovery needs are concentrated in social sector (Housing, Land and Settlements sector), amounts to 71% and in Infrastructure sector, consisting of Irrigation, Transport, Power Supply, and Water and Sanitation, amounts to 24% of the recovery needs in 2017. The recovery needs timeline is divided in short term, medium term and long term actions.

Experience from Macedonia is relatively well documented only by Public Enterprise for State Road (PESR). Besides the unfortunate human losses, the landslides present major challenge in the maintenance of the roads. Peshevski et al. 2013, for a period of 2000-2013, found that remedial measures have been undertaken for 62 landslides (authors consider that this number is far greater).

Rehabilitation works mostly consist of construction of support walls, road nets, water drainage systems under road, concrete piles, gabion walls, etc. Each year from the budget of the Public enterprise for state roads large amount of money is spent on preparation of design documentation and civil works for landslide remediation. Some data for post recovery of landslides on road network are presented in Table 3.

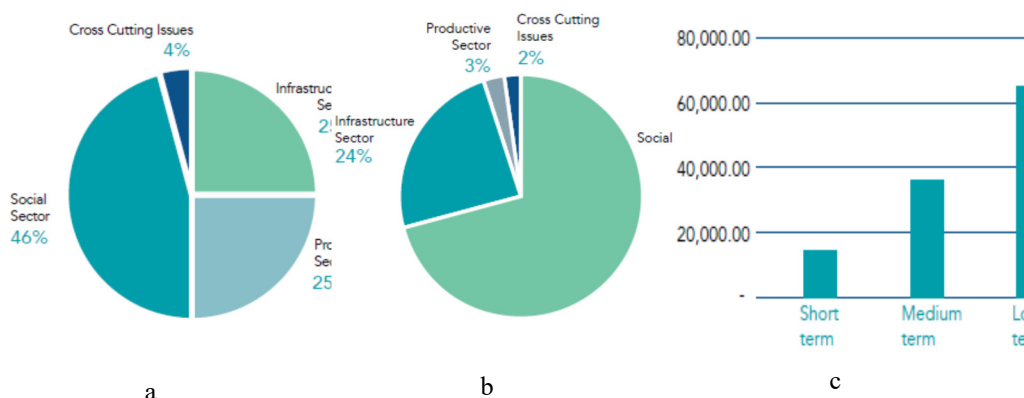


Figure 17. Main data from Sri Lanka Post Disasters Needs Assessment: a) Total damages by main sectors equal to = 70 bilions LKR; b) Recovery needs by main sectors=118 70 bilions LKR; c) Recovery needs timeline [9]

Some applied solutions for landslide and rockfall remediations are presented in Figure 18, Figure 19 and Figure 20.

Table 3. Cost on postflood recovery landslides in Macedonia

Location	COST FOR POST-RECOVERY (EUR)
Road R-2433, Resen-Greek border, place Markova noga	1.700.000,00
Veles, road R-1102, km 49+300	894.000
Kratovo, road R-1205, km 18+125	305.000,00
Kratovo, road r-1205, km 18+165	850.000,00
Kozuf mountain, road r-1105, seven landslide zones	3.500.000,00
Magistral Road A3, location Bukovo	195.000
Magistral road Resen - Bitola	600.000,00
Landslide on section Gradsko-Prilep, place Farish	155.000
Landslide Konce, road R-2433, km 11+500	290.000
Rock fall zones along access road to dam "Sveta Petka"	1.900.000,00

Case presented in Figure 20, presents also an used approach for fast way of cost estimation for used support type. Similar diagrams can be found in [28],[29]. They are constructed according to the detailed bill of quantities for several slope types protective measures, and they can be used for fast estimation of costs for post recovery in a case of emergencies in a short time recovery period.

Of course, for analyses in cases of middle and long term planing, detailed analyses are needed.

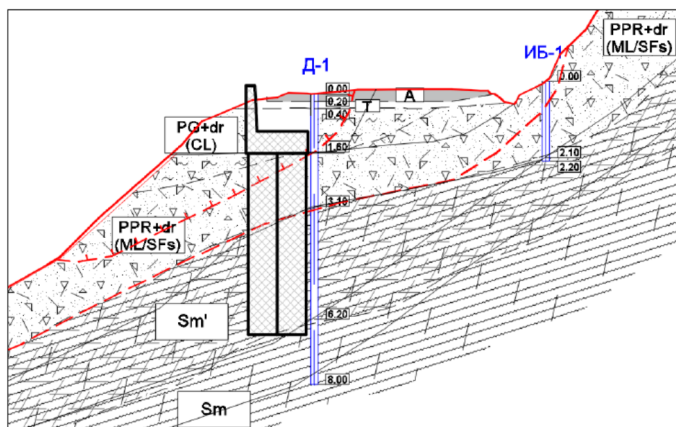


Figure 19 Typical section for repair solution of landslide on regional road to village Konce with retaining wall founded on piles

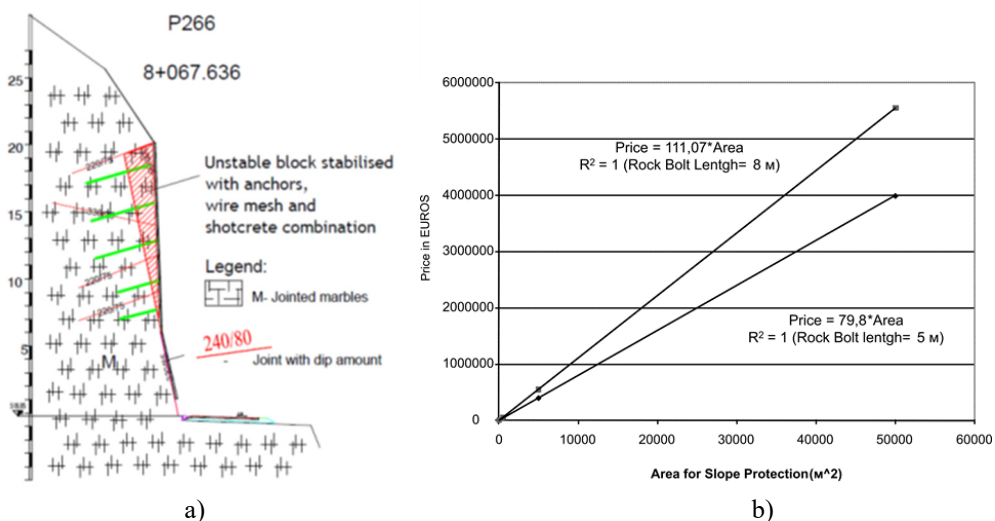


Figure 20 a) Typical section for repair solution of rockfall zones along access road to arch dam Sveta Petka; b) Cost estimation for Slope Protection Type for different rock bolt length.

When we come to the post-recovery measures, main questions that arise are:

- What design criteria to be used?
- Which strategy for post-recovery to be used?
- What is the best approach for long-term measures etc.

Authors experiences leads to the concept for design, where possible cost can be related also to concepts of definition of acceptable risk and allowable values for Safety factors and Probability of failures using so-called Protection Effect (PE), defined with following formula:

$$PE = \frac{Fs(san) - Fs(prir)}{Fs(prir)} * 100(\%) \tag{5}$$

Where:

PE - Effect from applied measures in increasing of FS (%);

Fs (san) – Factor of Safety obtained with applied measure;

Fs (prij) - Initial Factor of Safety without applied measure.

Application of this concept for the one case analysed by the authors is presented in Figure 21. From the given analyses, it is clear that all problems have to be considered in terms of the particular set of circumstances, as: rock types, design loads and end uses for which it is intended.

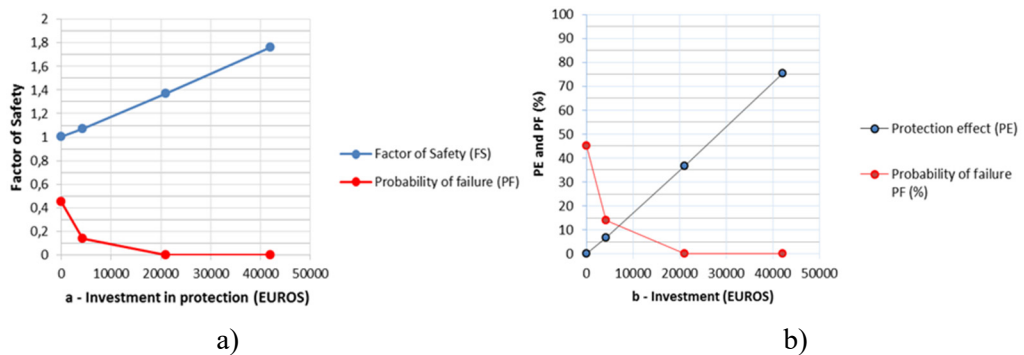


Figure 21. a) Diagrams presenting influence of investment on FS and PF for one analysed case along road to “Sveta Petka”; b) influence of investment (I) on increasing of PE and decreasing of PF [28]

Implementation of the recommendations from this article leads to the conclusion, that in terms of climate resilience design, it is good to apply concept presented in Figure 22.



Figure 22. a) Spider Evaluation Chart Risk Management; b) Operations and maintenance framework

6. Conclusions

Based on practical experiences and theoretical analyses, the paper presents some experiences with post recovery from floods and induced landslides. It is a chance to promote again “Build Back Better” concept on country level and provides an overview of its basic principles and how to ensure a greater level of resilience and preparedness to future disaster events.

Capacities of government Ministries and Municipalities and all affected Enterprises at local, district and central levels should be strengthened to adequately carry out this problems. These shall be combined with probability theories, risk assesment methods and an urgent need for application of integrated flood risk and in particular landslide risk management strategies. It is always better to prevent problems, so systematic investment in rehabilitation of old structures is necessary. For these, the short, middle and long term strategies shall be applied.

The responsibility of the engineering community is to apply new approaches, and to find a safe and economical solutions which is compatible with all the constraints which apply to the projects. Solutions should be based upon detailed analyses, but also on engineering judgement guided by practical and theoretical studies.

References:

- [1] Vanicek I, Jirasco D., Vanicek M.: Interaction of transport infrastructure with natural hazards (landslides, rock falls, floods) Geotechnical hazards and risks, experiences and practices Proceedings of the 16th Danube – European Conference on Geotechnical Engineering, 7-9 June 2018, Skopje, Republic of Macedonia
- [2] Lee, E.M., Jones D.K.C (2004): Landslide risk assessment, Thomas Telford, London.
- [3] Van Den Eeckhaut M., Hervás J., Safe Land, Living with landslide risk in Europe: Assessment, effects of global change, and risk management strategies 7th Framework Program Cooperation Theme 6 Environment (including climate change), Sub-Activity 6.1.3 Natural Hazards, 2011
- [4] Frelüh L., A., B. Görlach, S. Ittner, S. Naumann, M. Schock, L. Röschl: Integrated impact assessment of European soil protection policies, RECARE PROJECT REPORT, 2018
- [5] ECTP reFINE (2012): Research for Infrastructure Network in Europe initiative – Building up Infrastructure Network of a Sustainable Europe - Strategic targets and expected impacts – ECTP, Retrieved from www.ectp.org, 2012
- [6] ELGIP position paper (2016): Geotechnical risk reduction for transport infrastructure. Presentation for ECCREDI, Jan. 21st, 2016, Bruxelles.
- [7] FEHRL Vision 2025 for Road Transport in Europe - <http://www.fehrl.org/>.
- [8] Sendai Framework for Disaster Risk Reduction (2015-2030), UN Office for Disaster Risk Reduction
- [9] Post-disaster Recovery Plan (PDRP) for Sri Lanka, floods and landslides, May 2017
- [10] Build Back Better Manual: Roadmap towards resilient transport and water infrastructure (2018) EU Flood Recovery Programme, UNDP
- [11] Abolmasov B., Pesevski I., White J., Reeves J., Panov A., Technical assistance preparation of climate resilience design Guidelines for the Public Enterprise for State Roads in Macedonia, DRAFT Climate Resilience Design Guidelines, 2019 (personal communications)
- [12] Cottechia F., Santolia F., Tagarelli.: Geo-hydro-mechanics for quantitative landslide hazard assessment (QHA) Geotechnical hazards and risks, experiences and practices Proceedings of the 16th Danube – European Conference on Geotechnical Engineering, 7-9 June 2018, Skopje, Republic of Macedonia
- [13] Marteos R.M, Herrera G., García-Davalillo J.C.: Integration of geohazards into urban and land-use planning. Towards a Landslide Directive. The EuroGeoSurveys questionnaire Proceedings of World Landslide Forum 4, May 29 - June 2, 2017, Ljubljana, Slovenia
- [14] Peshevski I., Jovanovski M., Markoski B., Petrusseva S., Susinov B. (2013) Landslide inventory map of the Re-public of Macedonia, statistics and description of main historical landslide events, Landslide and flood hazard assessment, Proceedings of the Regional

- Symposium on Landslides in the Adriatic-Balkan Region. 6-9 march, 2013, Zagreb, Croatia. pp 207-212
- [15] Peshevski I., Jovanovski M., Peternel T., Jovanovski M., Urgent need for application of integrated landslide risk management strategies for the Polog region in R. of Macedonia Proceedings of World Landslide Forum 4, May 29 - June 2, 2017, Ljubljana, Slovenia
- [16] Segani S., Piciullo U., Luigi G.S.: Landslide early warning systems: monitoring systems, rainfall thresholds, warning models, performance evaluation and risk perception Nat. Hazards Earth Syst. Sci., 18, 3179–3186, 2018, <https://doi.org/10.5194/nhess-18-3179-2018>
- [17] ERM-Hong Kong (1998): Quantitative Risk Assessment of Boulder Fall Hazards in Hong Kong: Phase 2 Study. GEO Report No. 80. Report prepared for the Geotechnical Engineering Office, Hong Kong.
- [18] Fell, R. (1994): Landslide risk assessment and acceptable risk. Canadian Geotechnical Journal 31, 261-272.
- [19] Wong H.N., Zhang et al. (eds): Geotechnical Safety and Risk IV : Is landslide risk quantifiable and manageable? 2014 Taylor & Francis Group, London, ISBN 978-1-138-00163-3
- [20] Brandl H., Szabo M.: Hydraulic failure by underseepage of dykes and levees, Geotechnical hazards and risks, experiences and practices, Proceedings of the 16th Danube – European Conference on Geotechnical Engineering, 7-9 June 2018, Skopje, Republic of Macedonia
- [21] Palau R.M, Hürlimann M., Berenguer M., Sempere-Torres D.: Debris-flow early warning system at regional scale using weather radar and susceptibility mapping, 7th International Conference on Debris-Flow Hazards Mitigation, 2019
- [22] Roccati A., Faccini F., Luino F., Ciamaplini A., Turconi L.: Heavy Rainfall Triggering Shallow Landslides: A Susceptibility Assessment by a GIS-Approach in a Ligurian Apennine Catchment (Italy), Water 2019, 11, 605; doi:10.3390/w11030605
- [23] Peshevski I., Jovanovski M., Papic J., Abolmasov B., Model for landslide database establishment and operation in Republic of Macedonia, Geologica Macedonica, vol.29 No.1, pp75-86 (2015)
- [24] Boon D., Wilby P., Chambers P., Hobbs P., Kirkham M., Foster C., Evans H., Merritt A & The BGS Drilling Team: Will Britain’s landslides ‘wake up’ to climate change? Giant prehistoric landslides lurk in the UK landscape, but why, how and when did they form, and are they still dangerous? Poster of British Geological Survey, 2019
- [25] Jovanovski M., Milevski I., Papic J., Pesevski I., Markovski B: Landslides in Republic of Macedonia triggered by extreme event in 2010, D. Lochy (ed)., Chapter 17, Geomorphological impacts of extreme weather: Case studies from Central and eastern Europe, Springer Geography, DOI 10.1007/978-94-007-6301-2_17, Springer Science + Business Media, Dordrech 2013, ISBN 978-94-007-6300-5. pp.265-279.
- [26] Collins T., Great East Japan Earthquake: economic and trade impact Trade Competitiveness & Advocacy Branch statssection@dfat.gov.au
- [27] Haque U., Blum Ph., F. da Silva P., Andersen P., Pilz J., R. Chalov S., Malet J.P, Jemec Auflič M., Andres N., Poyiadji E., C. Lamas P, Zhang W., Peshevski I., G. Pétursson H., Kurt T., Dobrev N., Garcia-Davalillo J.C., Halkia M., Ferri S., Gaprindashvili G., Engström J., Keellings D.: Fatal landslides in Europe, Technical Note, Landslides pp 1-10, First online: 07 May 2016.
- [28] Jovanovski, M., Peshevski I., Papic J., Abazi S.: An approach for slope protection on the access road to arch dam “Sveta petka“ in Republic of Macedonia, Naucni skup, Geoexpo, 2017, Sarajevo.
- [29] Jovanovski M., Dimitrov B.: Experiences, methodology and principles for rock slope stabilisation, case for a road to arch dam “Sveta petka”, Savremena Gradjevinrska praksa, Novi Sad.

Topic no. 1 - Integrated Water Resources Management

ASSESSMENT OF MULTI-OBJECTIVE OPERATION OF THE “BOVAN” RESERVOIR DUE TO SILTATION

JELENA MARKOVIC BRANKOVIC¹, MILICA MARKOVIC¹, JELICA PROTIC²

¹ Faculty of Civil Engineering and Architecture, University of Nis, Republic of Serbia, gaf@gaf.ni.ac.rs

² Public Water Management Company “Srbijavode”, Country, office@srbijavode.rs

1. Abstract

Dams and their reservoirs have been constructed to serve various human needs as storing, using and diverting water for consumption, irrigation, power generation and flood control, but also made an important contribution to human development in many ways. The reservoir aging and progressive loss of water storage capacity, resulting from ongoing sedimentation, coupled with increasing societal needs, results in continuously increasing social, economic and environmental importance of reservoirs. In this paper results of silting measurements at “Bovan” reservoir are presented. Further, the new reservoir volume was calculated in order to assess multi-objective “Bovan” reservoir operation. Specifically is highlighted and assessed the reservoir role in flood management, mainly its storage capacity.

Keywords: reservoir aging, dam, fluvial processes.

2. Introduction

The longevity, usefulness and sustainable operations of dams and reservoir storage is significantly threaten by sedimentation process (Palmieri et al. 2003).

The traditional “dam design life” paradigm, entails calculation of the sedimentation rate and estimation of the trap efficiency and provision of a sediment storage pool volume - dead volume equivalent to the design life (50 or 100 years).

Many dams built during the 1930-70s, an era of intensive dam construction, have an expected life of 50 to 100 years. Due to inadequate maintenance and/or for environmental reasons, some of these dams will fail or be removed. The end-of-life scenario may require project decommissioning with its attendant costs and impacts.

New dams constructing implies severe economic, social and environmental issues. Moreover, the best dams sites are already used.

The key to sustaining operation is to identify the desired outcome and management strategy as early as possible and to implement the required modifications while there is still time to save a significant portion of the storage volume.

In this paper results and analysis from the second control measurement of “Bovan” reservoir silting are presented. First measurement is done in the year 1990. Zero geodetic measurement is done in the year 1978.

3. Methods

3.1 Characteristics of Bovan dam and reservoir

The dam "Bovan" is a rockfill dam with a central clay core. The reservoir "Bovan" extends from Ljiljac to Strazevica municipality in the length of about 6500 m.

The Bovan reservoir has multi-objective purpose, the main objective is sediment trading and protection of HP «Iron Gates» from silting, than water supply of municipality of Aleksinac, small water level rising, small hydropower and irrigation.

The Bovan dam is maintained by Public Water Management Company and Bovan reservoir is operated by Municipal Communal Company.

The reservoir Bovan main characteristics are presented in the Table 1.

Table 1: Main characteristics of the reservoir Bovan

Location	
Watercourse	Moravica
Nearest settlement	Aleksinac
Construction information	
Beginning of a construction	Year 1971.
Completion of construction	Year 1980.
Beginning of the reservoir filling	Year 1984.
Completion of the reservoir filling	Year 1984.
Main characteristics of the reservoir	
Total reservoir volume	60 000 000 m ³
Minimal water level	243.00 m.a.s.l.
Normal water level	252.00 m.a.s.l.
Maximal water level	261.50 m.a.s.l.
Number of measuring profiles	26

3.2 Measurement concept / method

Sediment storage volume is measured by performing repeated bathymetric surveys using an echo sounder in combination with GPS equipment. Survey track lines consist of a series of tracks designed to create a complete topographic contour map of the reservoir (Figure 1). The table below, shows the types of instruments used for the measurement, with the details and installation location.

Table 2: The instruments details

Measurement type	Instrument	Instrument type	Location

Shore of the cross sections	Distomat	DI-3	Boat
Reservoir bed level	Echo Sounder	E-SEA SOUND 103, 200 KHz	Boat

Bathymetric mapping of sedimentation consist of:

- Cross section surveys
- Reservoir bed modeling.

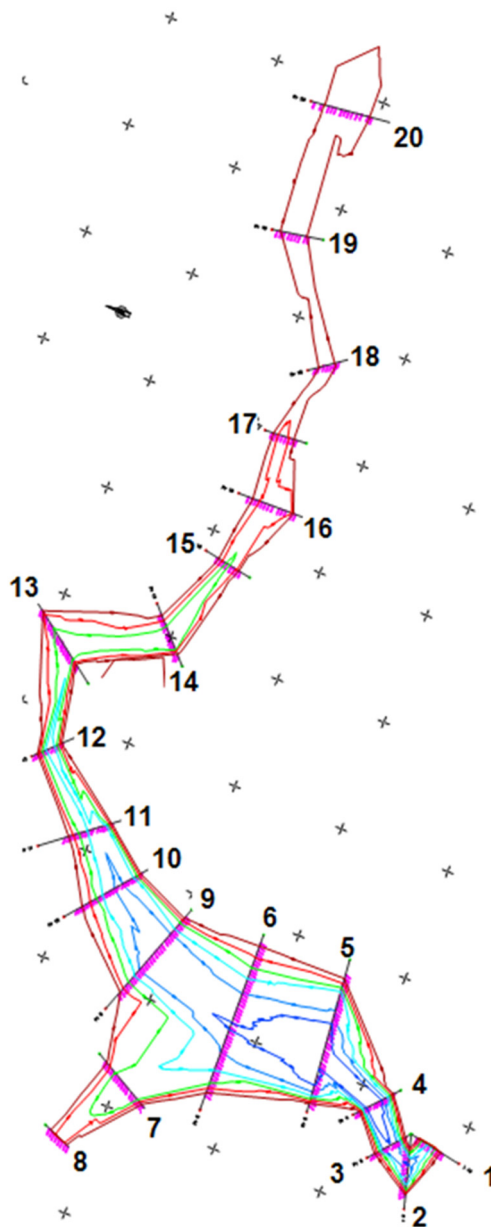


Figure 1. Reservoir bed level with cross sections

Bathymetric mapping of sedimentation surveys have heretofore been undertaken to document the changes in the storage capacity over time and determine its impact on the various reservoir pools and the reservoir’s “useful life.”

4. Results and discussion

4.1 Calculation of the volume curve for a reservoir

Based on cross section surveys and reservoir bed level, the volume curve for a reservoir is calculated. For the calculation, truncated pyramid pattern is applied.

Table 3: Surveying results

Water Level	Water surface area m ²	Equidistance	Reservoir volume x10 ⁶ m ³	Volume curve 2010	Volume curve 1984
215					0,00
220					0,10
225	103684,38	5	0	0,00	1,00
230	331588,94	5	1,03	1,03	2,10
235	556355,93	5	2,20	3,23	5,00
240	856327,98	5	3,50	6,74	10,00
245	1152344,45	5	5,00	11,74	16,00
250	1567024,33	5	6,77	18,51	24,20
255				30,31	36,00
260				46,31	52,00
265				68,71	74,40

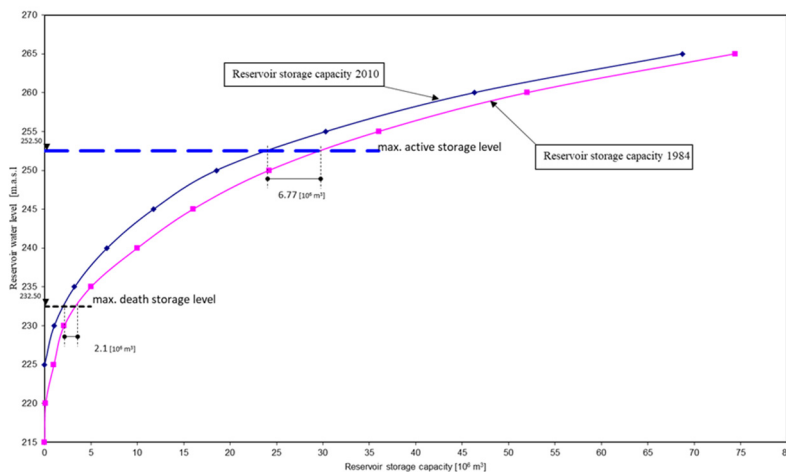


Figure 2. Reservoir capacity volume curve

4.2. Reservoir sediment deposition rate

Rate of sediment deposition presents a part of the initial storage capacity which was silted during a year; it is defined by the expression:

$$r = \frac{W_r}{V}$$

Where:

W_r – Sediment volume in the reservoir (m³/year)

V – Initial volume in the reservoir (m³).....31 000 000 m³ (NWL)

T – Period of the reservoir silting.....26 years (1984 -2010)

$$W_r = \frac{6770000,00}{26} = 260384.61 \text{ m}^3 / \text{god.}$$

$$r = \frac{W_r}{V} = \frac{260384.61}{31000000} \times 100 = 0.84\%$$

4.3 Reservoir silting analysis

The designed dead storage capacity equals 3.000.000 m³. It was designed to trap the estimated amount of sediment transported by river Moravica for the period of 50 years.

The estimated annual sediment yield is 60.000m³/year. As the measured sediment deposit in reservoir equals 6.770.000 m³ respectively 260.384 m³/year one can be concluded that the river sediment yield is 434% greater than the estimated during the dam design phase.

It also deposited the 178% of the actual dead volume.

4.4 The time required for complete reservoir backfilling

Total time required for complete reservoir backfilling up to normal water level (252.50m above the sea) is defined with the expression:

$$T_a = \frac{1}{r} = \frac{1}{0.0084} = 119$$

If this silting trend continues, reservoir will be filled up to the normal water level in 119 years. In other words, for full reservoir silting is 119-26=93 years left.

5. Conclusion

The silting of the reservoir has numerous negative consequences, which should be analyzed from the time of reservoir release into the operation and monitored during exploitation. Negative effects are not shown only in the reservoir zone, but they are

spreading even upstream such as:

- Loss of active storage capacity, which decreases reservoir capacity in regulating flows towards the user; in the last 26 years, active storage of reservoir decreased. Usable storage decreased for 4,67 hm³, from 26.7 hm³ to 22,00 hm³.
- Loss of reservoir capacity to be used for effective flood management requires enough reservoir storage space to temporarily store flood waters for gradual release downstream. The degree to which a flood can be attenuated is determined by the amount of reservoir storage available, and by the operating procedure at the reservoir.
- Dead storage is decreased for 2,1 hm³. Average yearly silting rate is 0.84%. If this trend continues, dead storage will be at maximal active storage level in 93 years.
- Changing in water quality.

The results presented in this paper show that the periodical monitoring and estimation of the amount of silted sediment in reservoirs important for evaluating the impacts of reservoir sedimentation.

Concerning all above, it is essential to have existing projects in sustainable use insofar as is possible.

Before the storage capacity has been seriously depleted the operating rule and project's structures may be modified to achieve a sediment balance and sustainable operation.

References

- [1] Marković, V. et al.: Akumulacija "Bovan"-Izveštaj o snimanju zasipanja nanosom, GAF, Institut za građevinarstvo i arhitekturu, 2010
- [2] Palmieri, A. et al.: Reservoir conservation volume I: the RECON approach, economic and engineering evaluation of alternative strategies for water storage assets worldwide. International Bank for Reconstruction and Development, The World Bank, Washington, DC, 101002E, 2003

APPLICATION OF SIMULATION MODEL IN CASE OF MULTI-RESERVOIR SYSTEM PLANNING

FROSINA PANOVSKA¹, STEVCHO MITOVSKI², LJUPCHO PETKOVSKI³

¹ Ss. Cyril and Methodius University, Civil Engineering Faculty, Republic of North Macedonia, frosinapanovska@yahoo.com

² Ss. Cyril and Methodius University, Civil Engineering Faculty, Republic of North Macedonia, smitovski@gf.ukim.edu.mk

³ Ss. Cyril and Methodius University, Civil Engineering Faculty, Republic of North Macedonia, petkovski@gf.ukim.edu.mk

1. Abstract

In this paper an analysis of the future hydropower utilization of Crna Reka is conducted with application of simulation models for different configuration alternatives and reservoir operation policies.

Crna Reka is one of the largest tributary of river Vardar, with average annual flow of $Q_{aver}=30 \text{ m}^3/\text{s}$ before entering Tikvesh lake, and a 5890 km^2 river basin in the south-west of North Macedonia. Back in 1968 the first hydropower plant on river Crna Reka was built – Tikvesh, with an overall installed capacity of $Q_{ins}=4 \times 36 \text{ m}^3/\text{s}$ and $P_{ins}=113 \text{ MW}$. The alternatives of potential water utilization of Crna Reka, analysed with the simulation models, are defined based on existing technical documentation, design plans and development analyses made for river Crna Reka.

The modelling of the complex multi-reservoir cascade system was done by application of HEC ResSim software. Within the paper are analysed Alternative 0, as existing state, composed of dam and reservoir Tikvesh with hydropower plant, incorporating both hydropower and irrigation water use, with hydropower as priority user and Alternative 1, where beside Tikvesh hydro-system, Chebren and Galishte dams with reservoirs and hydropower plants are included in model, with conventional hydropower units.

Hydropower production in both alternatives is analysed for three different operation policies: (1) Low non-linear policy, where power capacity of the plant is high for low reservoir levels, (2) Linear policy, where power capacity is in linear correlation with reservoir level, and (3) High non-linear policy, where power capacity of the plant is high for higher reservoir levels.

The upgrade of the existing state of utilization of water at Crna Reka watershed is estimated upon the annual hydropower production within period of 60 years.

Keywords: water resources systems, simulation models, hydropower generation, multi-reservoir systems, HEC ResSim.

2. Introduction

In an era where electricity power is constantly on high demand and environmental issues arise from using conventional power resources such as fossil fuels, more and more pressure is put on hydropower as one of the cleanest, high efficacy sources of energy (Jermar, 1987). In Republic of North Macedonia alone, over 1/3 of all annual production of electricity comes from hydropower (AD ELEM, 2016). However, not even half of the potential of electricity production of hydropower is utilized in the Republic, so there is still a lot to be done in this sector.

In North Macedonia, only a few rivers' hydropower potential is completely utilized – the one on Crn Drim river and Treska river. Vardar is our largest river and no hydropower plant has been built on this mighty stream. The case is similar with Crna Reka, where only one hydropower plant is in operation since 1969 – Tikvesh HPP. Many other smaller streams are waiting on investments in hydropower use, some being built at the moment.

Possibilities of implementation of hydropower are open to incorporating power plants to existing water resources systems where hydropower lacks, such as single purpose reservoirs with dams (irrigation, water supply, flood control water systems).

In both cases – building completely new hydropower systems from scratch, or incorporating hydropower to existing ones – an extensive analyses on electricity production should be done. The analyses should answer the question on the plant's capacity for power production for a certain time series of registered/generated inflows on the stream.

Such analyses are done with simulation models – mathematical models that reproduce the potential real behaviour of the plant under certain input (inflows) and physical parameters of the system (Votruba, 1988). Simulation models have been developed since mid 90's and are improved by the day – alongside technology development. Many software are available for the purpose of water resources simulation and analysis, such as MITSIM, WEAP, HEC ResSim, RIBASIM.

In this paper, simulation model on hydropower potential is conducted on Crna Reka as a case study, by implementation of HEC ResSim software. In the model, input parameters such as observed water inflows registered at three gauging stations are used, physical parameters of the systems as planned or built, and operation policies for hydropower production. Crna Reka is one of the largest tributary of river Vardar, with average annual flow of $Q_{aver}=30 \text{ m}^3/\text{s}$ before entering Tikvesh lake, and a 5890 km^2 river basin in the south-west of North Macedonia. Back in 1968 the first hydropower plant on river Crna Reka was built – Tikvesh, with an overall installed capacity of $Q_{ins}=4 \times 36 \text{ m}^3/\text{s}$ and $P_{ins}=113 \text{ MW}$. The concept of utilization of the waters in Crna Reka exists since the middle of 20th century, when very first conceptual solution has been made on multipurpose and multi reservoir use of the river. This solution consisted of building three cascade dams with hydropower plants on Crna Reka – Chebren, Galishte and Tikvesh Lake and HPPs (XEP Ckonje, 1961). Later on, this concept somewhat changed and different concepts were made, dividing the capacity of the river in more, smaller reservoirs with dams and hydropower plants. However, not to this day any of these

concepts lived the light of the day except Tikvesh dam and hydropower plant, which was built as first of the three cascade dams.

The purpose of this paper is to emphasize the importance of building these capacities in numbers of produced electrical energy annually.

3. Methods

Simulation mathematical model is used to perform the analyses. Simulation model is a mathematical replica of the original system, describing the system with logical relations and mathematical equations (Votruba, 1988). Often, the simulation model is a simplified version of the original system. The convenience of simulation models is the possibility of applying different input parameters, physical parameters or operation rules, and analysing the response of the system without implementing them on the real system (Votruba, 1988).

HEC ResSim software for simulation of complex water resources systems operation is applied. The software consists of three basic modules: (1) Watershed setup, (2) Reservoir network, and (3) Simulation module. In the first module, the model is set up and relationships between the elements is defined. In the second module, physical parameters of the elements and operation rules for the whole systems are defined. In the third, defined configurations are called upon and analyses are conducted, with an overview of the results.

Two different models are elaborated. For the purpose of comparing results, the first model – Alternative 0, represents the current situation – Tikvesh dam, reservoir and hydropower plant in operation. The second model – Alternative 1 is an upgrade to the first one, where alongside Tikvesh, both Chebren and Galishte dams, reservoirs and hydropower plants are included and in power (Panovska, 2019).

In both alternatives, three sub alternatives are made in relation to three different operating rules for the hydropower plants. Basically, in order to explore the optimal operating rules for the hydropower plants, we created three operating curves: (1) Low non-linear, (2) Linear, and (3) High non-linear curves. All curves represent a relationship between water level in the reservoir (Power Storage) and engaged power capacity in the power plant (Plant Factor).

Low non-linear operating curve defines an operation rule for the plant where it will work with high capacity when low water levels in the reservoir (Figure 1).

Linear operating curve defines an operation rule for the plant where the relationship between water level in the reservoir and engaged power capacity is linear (Figure 2).

High non-linear operating curve defines an operation rule for the plant where it will work with high capacity for high water levels in the reservoir only (Figure 3).

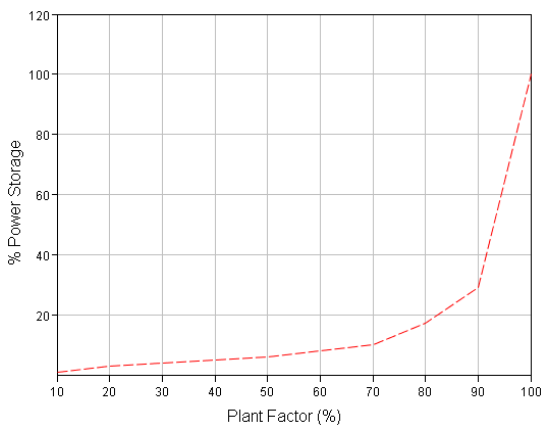


Figure 1. Operating rule 'Low non-linear'.

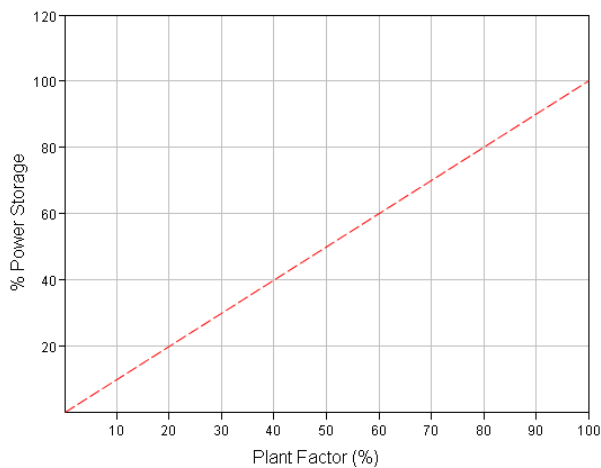


Figure 2. Operating rule 'Linear'.

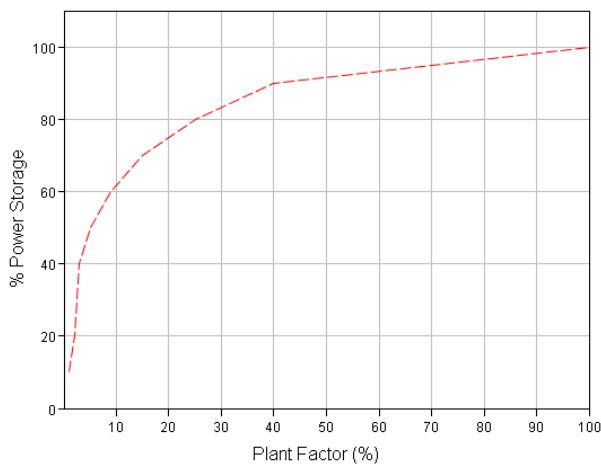


Figure 3. Operating rule 'High non-linear'.

3.1 Alternative 0

Alternative 0 consists of Tikvesh reservoir, dam and hydropower plant. This system serves two major consumers: irrigation of Tikveshko Pole, and production of electricity. Physical elements that are modelled in the simulation run, are: (1) reservoir Tikvesh, (2) hydropower plant Tikvesh with penstock characteristics, (3) uncontrolled spillway, (4) irrigation channel, and (5) bottom outlet.

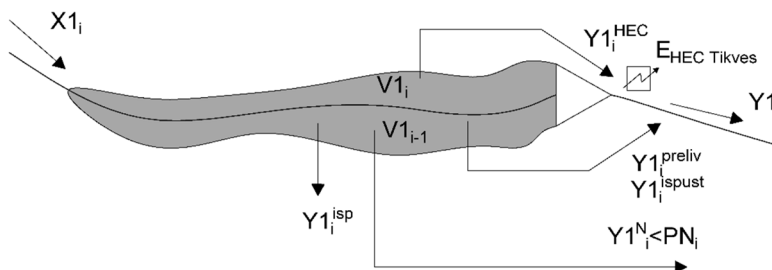


Figure 4. Schematic of simulation model Alternative 0.

Mass balance equation for the system is:

$$V1_i = V1_{i-1} + X1_i - [Y1_i + Y1_i^N + Y1_i^{isp}] \dots \quad (1)$$

Outflows of the reservoir are defined as:

$$Y1_i = Y1_i^{preliv} + Y1_i^{ispust} + Y1_i^{HEC} \dots \quad (2)$$

$$Y1_i^N \leq PN_i \dots \quad (3)$$

$$Y1_i^{isp} = f(Z_{akum}, T) \dots \quad (4)$$

Abbreviations in the equations (1) and (2) have the following meaning:

- $X1_i$ - inflow in the reservoir at i-moment,
- $Y1_i^{isp}$ - water loss due to evaporation at i-moment,
- $Y1_i^{HEC}$ - water flow through penstock, at i-moment,
- $Y1_i^{preliv}$ - spillway flow at i-moment,
- $Y1_i^{ispust}$ - bottom outlet flow at i-moment,
- $Y1_i^N$ - delivered water quantities for irrigation purposes, at i-moment,
- PN_i - water needs for irrigation at i-moment,
- $Y2_i$ - total outflows from reservoir Tikvesh, at i-moment,
- $V1_i$ - volume of water at the reservoir at i-moment.

Inflow hydrograph is gauged hydrograph for the period of 1946 – 2005 (60 years in total)

(Figure 54), at gauging station Tikvesh. Since the hydrograph is of measured values, the model itself is deterministic. The time step of simulation run is 1 Day, common for analyses of this type.

Irrigation needs are implemented as average monthly values, obtained by gauged values from delivered water quantities for the period of 2005 – 2012. Basically, irrigation only occurs in vegetation period – starting from march until the end of september. Average irrigation needs vary from 2 – 8 m³/s of water per day.

3.2 Physical characteristics of the model

Physical characteristics of the model are implemented for the following elements: (1) reservoir Tikvesh, (2) hydropower plant Tikvesh with penstock characteristics, (3) uncontrolled spillway, (4) irrigation channel, and (5) bottom outlet.

The reservoir's physical capacity is defined through surface and volume curves.

The hydropower plant is defined through several characteristics:

- (1) Penstock capacity,
- (2) Installed capacity of the aggregates,
- (3) Energy loss through the penstock,
- (4) Relation between coefficient of efficiency and flow,
- (5) Flow curve for downstream riverbed.

All these parameters are necessary in the model for it to calculate produced energy at every time step, using the equation:

$$E = \frac{\rho g Q H t}{\eta} = \dots [W] \dots \quad (5)$$

,where:

- E - produced energy in Watts,
- Q - turbine flow in m³/s,
- H - water head minus loss, in m,
- t - time frame, in hrs,
- η - coefficient of efficiency.

Overall installed capacity of the modelled power plant is 4 turbines with installed capacity of 28.83 MW – the same as in Tikvesh hydropower plant.

The spillway is defined through a flow curve, with maximum capacity of Q_{10 000} = 2150 m³/s and H_p = 3.5m. Spillway elevation is H_{spill} = 265 m.a.s.l. Maximum elevation at the reservoir is H_{max} = 268.5 m.a.s.l. and crest elevation is H_{crest} = 270 m.a.s.l.

In HEC ResSim it is mandatory to divide the reservoir in different zones. Each zone has its one, specific characteristics and rules that apply only for the zone itself. When creating a basic model, three zones are automatically generated: (1) Flood Control zone, (2) Conservation zone, and (3) Dead zone. Flood control zone is normally the zone above H_{spill}, when the elevation in the reservoir rises above the normal level and spills out. Conservation zone is the zone where all normal functioning rules are applied, such as

rules for hydropower generation, irrigation, water supply or whatever the purpose of the reservoir is. Basically, the volume of water in the conservation zone is the water that we want to operate with. Conservation zone is located between H_{min} and H_{spill} . Below H_{min} its the dead zone, where no rules can be applied since this water levels are considered to be below the physical capacities of the outflow structures.

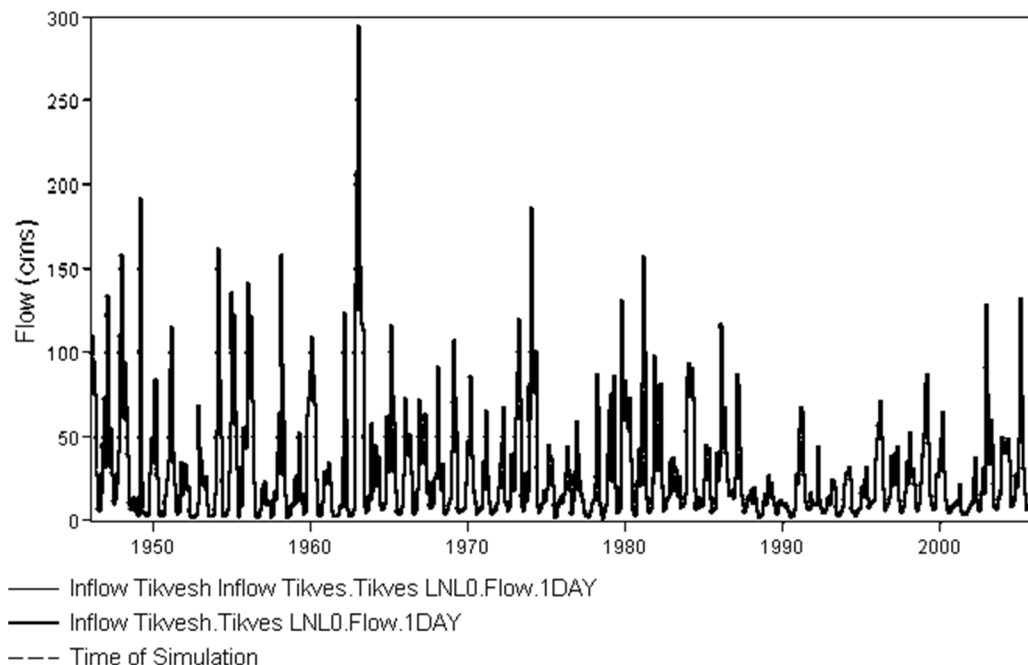


Figure 5. Hydrograph of gauged flows for station Tikvesh, 1946 – 2005.

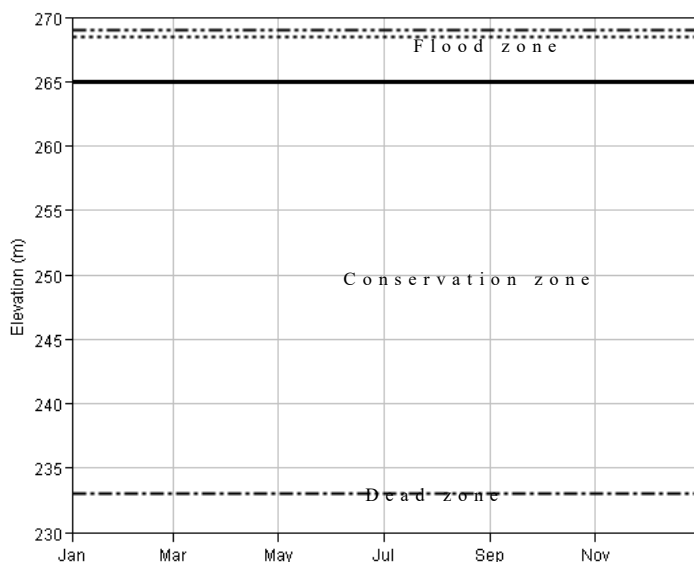


Figure 613. Definition of zones in the reservoir Tikvesh for the purpose of simulation model in HEC ResSim.

In the case of Tikvesh reservoir, Flood control zone is between elevation 265 m.a.s.l. and 270 m.a.s.l., where rules for including the spillway and bottom outlet for quick reservoir draining are defined. Conservation zone is between elevation 265 m.a.s.l. and 233 m.a.s.l. where operating rules for the power plant are defined and rules for irrigation purposes as well. Dead zone is under 233 m.a.s.l (Figure 6).

3.3 Alternative 1

This alternative is an upgraded alternative 0, with two more added systems: Chebren and Galishte. The configuration model can be seen in Figure 7. Chebren is the first and largest reservoir and dam in the cascade, with capacity of $555 \cdot 10^6 \text{ m}^3$. Galishte is the second in line, similar in capacity of reservoir as Tikvesh, with volume of $256 \cdot 10^6 \text{ m}^3$. The furthest in line is the existant Tikvesh reservoir.

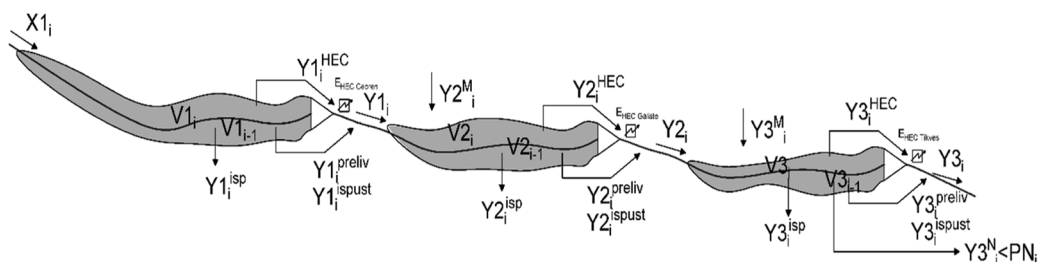


Figure 714. Schematic of Alternative 1.

In order to connect the reservoir's operating rules and make them 'work for one another', there is a Tandem Operatin Rule definition in HEC ResSim. What this rule does, is basically make the upper reservoir work for the lower reservoir in order for it to achieve mass balance (HEC Ressim 3.1, User's Manual, 2013).

Mass balance equation for the system Alternative 1 is shown as follows:

$$V1_i = V1_{i-1} + X1_i - [Y1_i + Y1_i^{isp}] \dots \quad (6)$$

$$V2_i = V2_{i-1} + X2_i^M - [Y2_i + Y2_i^{isp}] \dots \quad (7)$$

$$V3_i = V3_{i-1} + X3_i^M - [Y3_i + Y3_i^N + Y3_i^{isp}] \dots \quad (8)$$

Outflow from the reservoirs is shown as follows:

$$Y1_i = Y1_i^{preliv} + Y1_i^{ispust} + Y1_i^{HEC} \dots \quad (9)$$

$$Y2_i = Y2_i^{preliv} + Y2_i^{ispust} + Y1_i^{HEC} \dots \quad (10)$$

$$Y3_i = Y3_i^{preliv} + Y3_i^{ispust} + Y3_i^{HEC} \dots \quad (11)$$

$$Y3_i^N \leq PN_i \dots \quad (12)$$

$$Y1,2,3_i^{isp} = f(Z_{akum}, T) \dots \quad (13)$$

$$Q_{TIKVES}^{BASIN} = Q_{TIKVES}^{GAUGED FLOW} - Q_{GALISTE}^{GAUGED FLOW} \dots \quad (23)$$

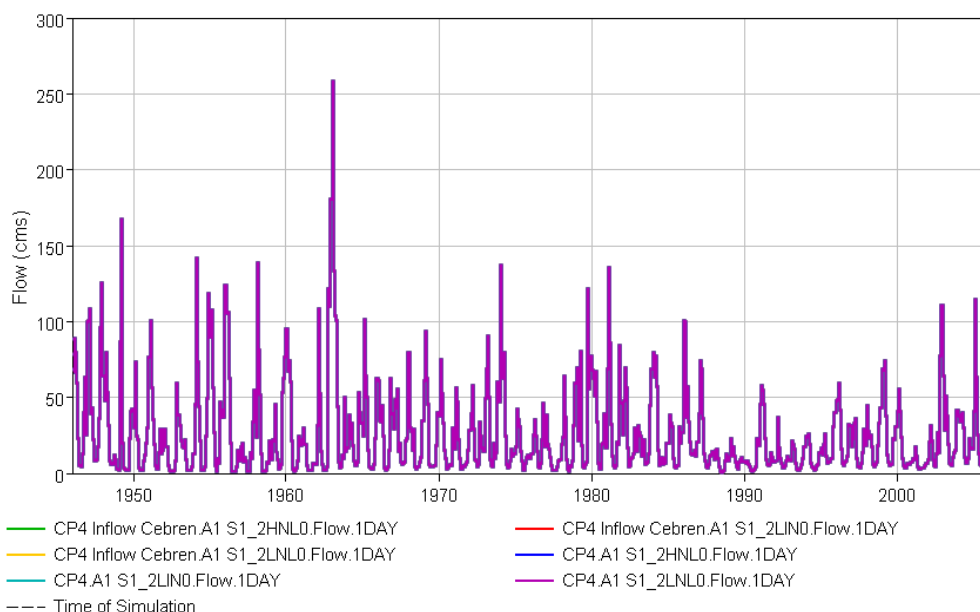


Figure 8. Hydrograph of gauged flows for Chebren reservoir (1946 - 2005).

Mass curve for Chebren is an observed hydrograph in the period from 1946 – 2005 (60 years) at gauging station Rasimbegov most on Crna Reka (Figure8). There are gauged flows for Galishte and Tikvesh, however, those cannot be used in the model since they have been once included in the measured flow in Chebren (Figure 9159). In order to extract the mass curve entering the reservoirs of Galishte and Tikvesh, measured values had to be extracted:

$$Q_{GALISTE}^{BASIN} = Q_{GALISTE}^{GAUGED FLOW} - Q_{CEBREN}^{GAUGED FLOW} \dots \quad (14)$$

$$Q_{TIKVES}^{BASIN} = Q_{TIKVES}^{GAUGED FLOW} - Q_{GALISTE}^{GAUGED FLOW} \dots \quad (23)$$

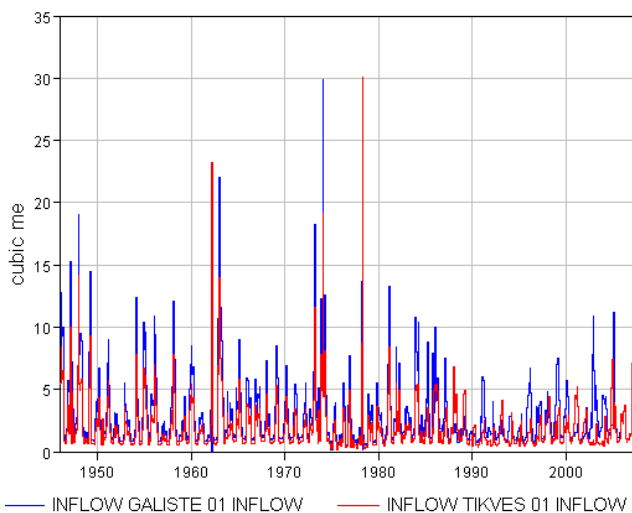


Figure 915. Hydrograph of extracted flows for Galishte and Tikvesh reservoir (1946 - 2005).

Physical characteristics of the model

Physical parameters of the system are concisely shown in Table 2. The parameters for Tikvesh reservoir, dam and power plant are as existant. Galishte and Chebren have higher installed capacities, according to the Water Master Plan of Macedonia, adopted back in 1973. The parameters, as shown, are implemented in a simulation model for hydropower generation, where hydropower is the primary user and irrigation is implemented only for Tikvesh reservoir.

Zones are also defined in order to apply rules for the reservoirs. Same operating rules for the hydropower plant apply as described in Alternative 0 – Low non linear, Linear and High non linear curves for hydropower engagement.

Table 2. Physical parameters of Alternative 1.

System	Physical parameter	Alternative 1	
Tikvesh	Normal operating level	265	[m.a.s.l.]
	Minimal elevation	233	[m.a.s.l.]
	Volume of reservoir	310 10 ⁶	[m ³]
	Crest level	269	[m.a.s.l.]
	Capacity of power plant	115.32	[MW]
		144	[m ³ /s]
Galishte	Normal operating level	392	[m.a.s.l.]
	Minimal elevation	342	[m.a.s.l.]
	Volume of reservoir	256 10 ⁶	[m ³]
	Crest level	398	[m.a.s.l.]
	Capacity of power plant	190.83	[MW]
		180	[m ³ /s]
Chebren	Normal operating level	565	[m.a.s.l.]
	Minimal elevation	515	[m.a.s.l.]
	Volume of reservoir	555 10 ⁶	[m ³]
	Crest level	567	[m.a.s.l.]
	Capacity of power plant	324.48	[MW]
		231	[m ³ /s]

4. Results

Results are discussed on: (1) electricity generation [MWh/day, MWh/year], (2) engagement of power [MW], and (3) average water levels in reservoirs [m.a.s.l.].

4.1 Alternative 0

In this alternative, a simulation run was conducted for a single reservoir with main use – production of electricity and secondary use - irrigation. As described in detail in section 0 and with implementation of three different operating rules for power plant engagement, results will be discussed for the operating rule that contributed to highest results.

When comparing water level fluctuation during the analysed period of 60 years (1946 – 2005), highest maintained water level in the reservoir is achieved with implementation of operating rule High non-linear, with average elevation in the reservoir of H_{high} =

259.95 m.a.s.l (Figure 1010).

It is only logical to expect that the implementation of operating rule High non-linear will give out the highest values for energy production as well. Mainly, the average power engaged on daily is $P_{aver}= 18.84$ MW and average production of electricity is $E_{aver}=452.28$ MWh/day. Annually, the production of electricity would exceed 160 GWh/year.

Implementation of operating rules Low non-linear and Linear result in annual production of electricity of $E_{aver}=149.4$ GWh/year and $E_{aver}= 156.6$ GWh/year respectively.

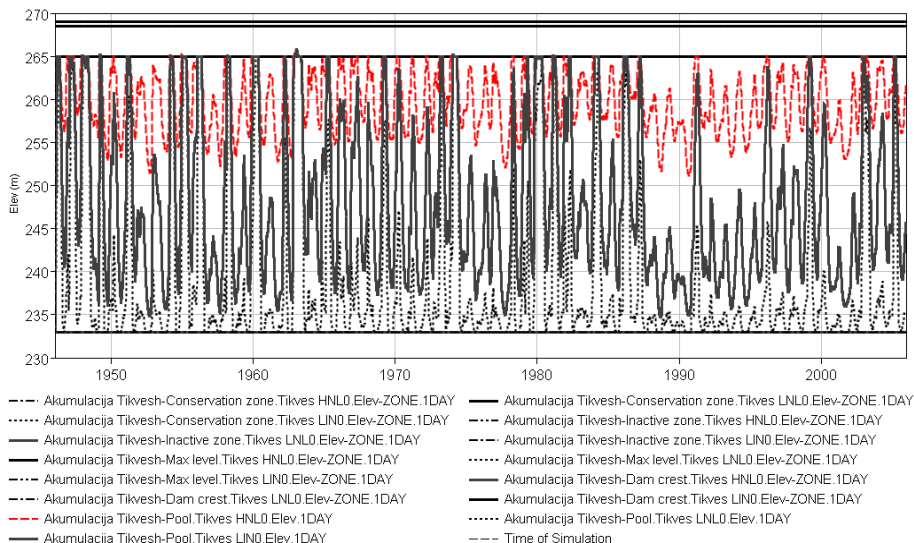


Figure 10. Water level fluctuations under operating rules and physical limitation of the Tikvesh system.

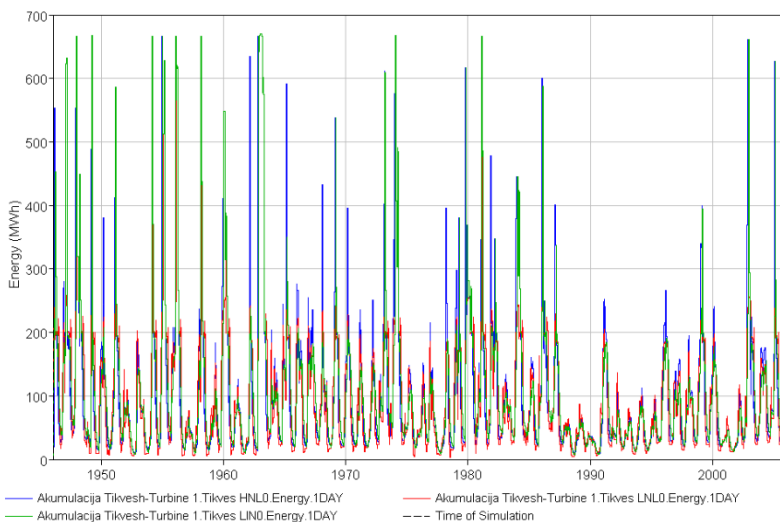


Figure 11. Energy production of each turbine in Tikvesh HPP for the 60 year simulation run.

In comparison to produced electricity from Tikvesh HPP for the period of 1994 to 2016 (Figure 121612), the results we got with the simulation model are matching to the real values. Namely, with the simulation run, we got an average production of electricity of around 160 GWh/yearly. Real delivered values show somewhat of 150 GWh in average produced electricity of Tikvesh HPP for the period of 1994 to 2016.

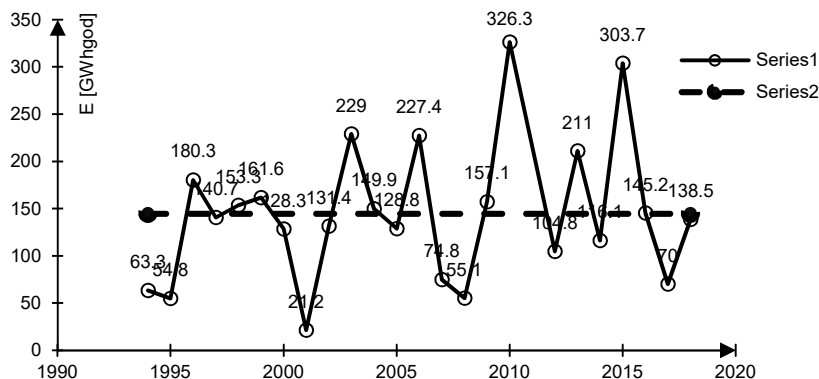


Figure 1216. Produced electricity in Tikvesh HPP in the period from 1994 – 2016 (AD ELEM, 2016).

4.2 Alternative 1

The simulation model of Alternative 1 consists of three cascade reservoirs with hydropower plants: Chebren, Galishte and Tikvesh. All plants are equipped with conventional units and their physical characteristics are in details explained in section 0. Three operating rules for hydropower generation are applied, of which only the highest results will be discussed.

In Figure 131713 and Figure 14 water fluctuating levels are given for Galishte and Chebren reservoirs, with implementation of operating rules 1,2 and 3. Highest water levels are obtained with implementation of High non-linear operating rule for the hydropower plant, with $H_{aver} = 386.31$ m.a.s.l. for Galishte and $H_{aver} = 558.68$ m.a.s.l. for Chebren. Maximal obtained water level for Tikvesh reservoir in this configuration is $H_{aver} = 260.90$ m.a.s.l.

The annual production of energy per plant is highest when implementing operating rule High non linear for each and one of the power plants. The average annual production of electricity in Chebren HPP is $E_{aver} = 243.1$ GWh/year, in Galishte HPP is $E_{aver} = 196.7$ GWh/year and in Tikvesh HPP is $E_{aver} = 153.1$ GWh/year. Adding up the numbers, when putting HPPs Chebren and Galishte in operation, our state would get over 439 GWh/year clean electricity:

$$E_{Chebren} + E_{Galishte} = 243.1 + 196.7 = 439.8 \text{ GWh/year} \dots \quad (16)$$

Implementation of operating rules Low non-linear and Linear results in lesser production of electricity annually. Namely, for Chebren HPP these numbers are $E_{aver} = 193.4$ GWh/year for Low non-linear, and $E_{aver} = 216.6$ GWh/year for Linear operating rules. For Galishte HPPs, these numbers are $E_{aver} = 142.9$ GWh/year for Low non-linear, and $E_{aver} = 167.1$ GWh/year.

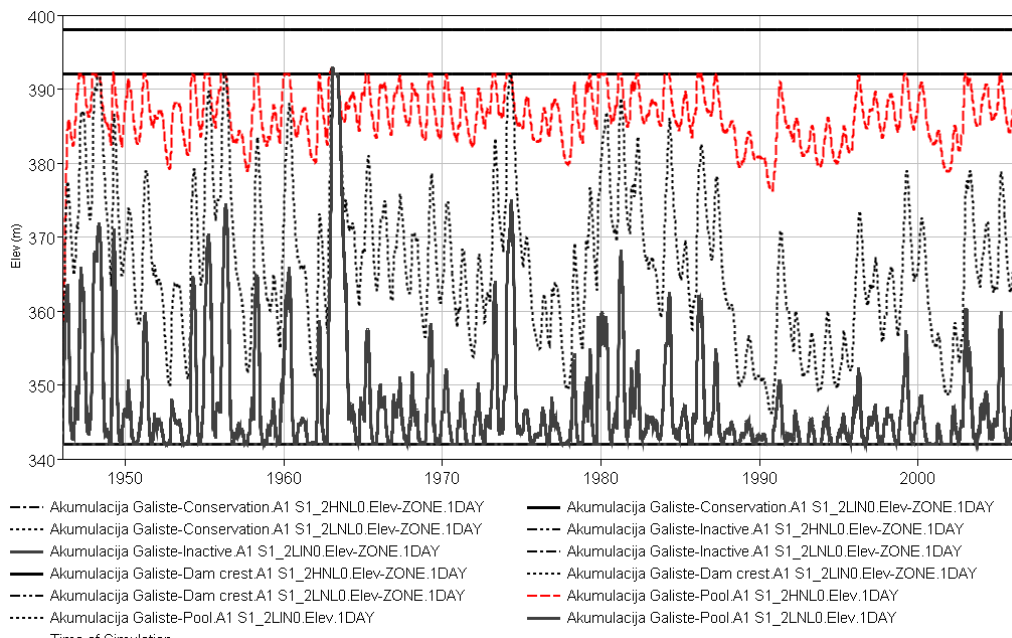


Figure 1317. Fluctuation of water level in Galiste reservoir.

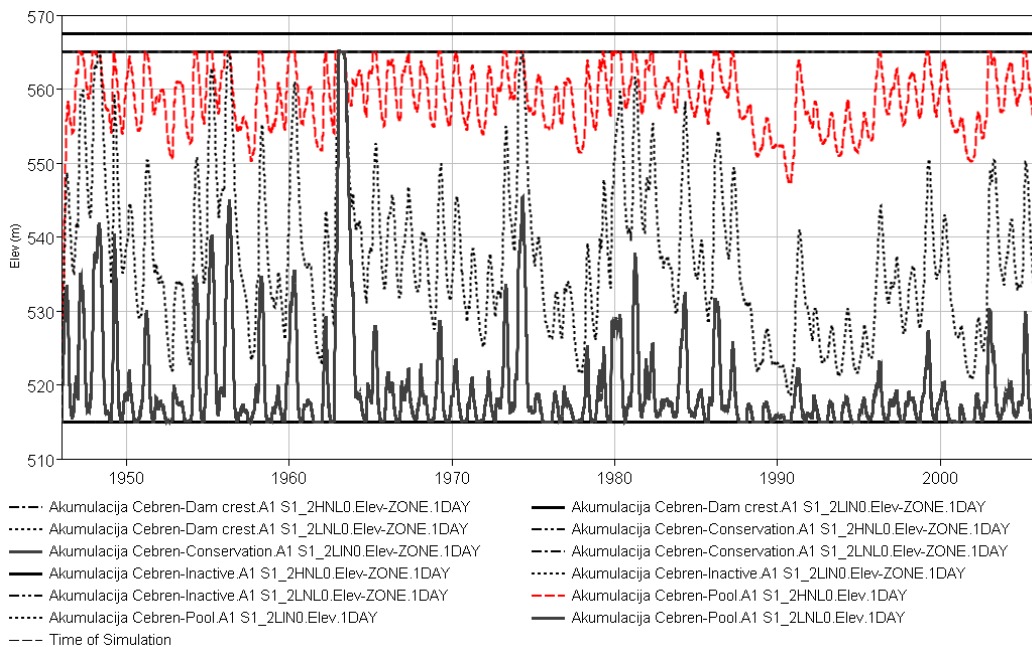


Figure 14. Fluctuation of water level in Chebren reservoir.

5. Conclusion

Simulation models for hydropower generation in complex water resources system is

applied. For each simulation run, hydrological inflow, physical parameters and operation rules are defined. HEC ResSim software is used for the analyses. A 60 year time frame is analysed with gauged flows on river Crna Reka.

Alternative 0 consists only of one water resources system – Tikvesh reservoir, dam and hydropower plant. Three different operating rules are applied to investigate the optimal operating rule and maximize electricity production. Alternative 1 consists of three cascade reservoirs with dams and hydropower plants – Chebren, Galishte and Tikvesh.

Results show that implementation of operating rule High non-linear in both alternatives give the maximal values for electricity production. This operating rule runs the power plant under high capacity only when the reservoir is full.

Average annual production of electricity of Tikvesh hydropower plant alone in Alternative 0 varies from 149 GWh/year for Low non-linear, 154 GWh/year for Linear and 160 GWh/year for High nonlinear operating rule. It is interesting to notice that only by changing the operating rule, generated electricity can exceed 10 GWh/year in this configuration alone.

Average annual production of electricity of all capacities simulated in Alternative 1 varies from 456.83 GWh/year for Low non-linear, 517.33 GWh/year for Linear and 592.98 GWh/year for High non-linear operating rules. Excluding the existing plant Tikvesh, when putting Chebren hydropower plant and Galishte hydropower plant in operation, with physical parameters as implemented in the simulation run, over 350 GWh/year would be placed on the national grid as clean and renewable energy.

References

- [1] AD ELEM. (2016). 2016 Annual report on AD ELEM. Skopje: AD ELEM.
- [2] Association, M. (2014). Modelica (R) - a unified object-oriented language for systems modeling language specification, version 3.3, revision 1.
- [3] Brenan, K., Campbell, L., & Petzold, L. (1989). Numerical Solution To Initial Value Problems in Diferential-Algebraic Equations. New York: Society for Industrial and Applied Mathematics.
- [4] Elmqvist, H., Tummescheit, H., & Otter, M. (2003). Object Oriented Modeling of Thermo-Fluid Systems. 3rd International Modelica Conference. Linköping.
- [5] Fritzson, P. (2004). Principles of Object Oriented Modelling and Simulation with Modelica 2.1 (1st ed.). Wiley IEEE Press.
- [6] HEC Ressim 3.1, User's Manual. (2013). USACE, Hydrologic Engineering Center.
- [7] Jermar, M. K. (1987). Water resources and water management. Munich: ELSEVIER.
- [8] Jović, V. (1995). Finite elements and method of characteristics applied to water hammer modelling. International Journal for Engineering Modelling, 51-58.
- [9] Jović, V. (2013). Analysis and Modelling of Non-Steady Flow in Pipe and Channel Networks. John Wiley & Sons.
- [10] Panovska, F. (2019). Simulation model of multi reservoir system for hydropower generation - master thesis. Skopje: Faculty of Civil Engineering in Skopje.
- [11] Tummescheit, H., Eborn, H., & Wagner, F. (2003). Development of a Modelica Base Library for Modeling of ThermoHydraulic Systems. Modelica Workshop 2000, (pp. 41-51). Lund.
- [12] Veersteg, H., & Malalasekera, W. (2007). An Introduction To Computational Fluid Dynamics (2nd ed.). Harlow: Pearson Education Limited.

- [13] Votruba, L. (1988). Analysis of water resources. Prague: Technical University of Prague.
- [14] Wood, D., Lingireddy, S., & Boulos, P. (2005). Pressure wave analysis of transient in pipe distribution systems, MWH Soft.
- [15] Wylie, E., & Streeter, V. (1967). Hydraulic Transients. New York: McGraw-Hill Education.
- [16] ХЕП Скопје. (1961). Основен проект за енергетско искористување на Црна Река. Скопје.

Topic no. 2 - Hydraulic Engineering and Environmental Impact

APPLICATION OF THE SWAT TO MODEL THE IMPACT OF POLLUTION FROM AGRICULTURAL AREAS ON COASTAL WATERS OF THE BALTIC SEA IN PUCK BAY REGION

DOMINIKA KALINOWSKA¹, PAWEŁ WIELGAT¹, TOMASZ KOLERSKI¹,
MICHAŁ SZYDŁOWSKI¹, PIOTR ZIMA¹

¹Gdańsk University of Technology, Faculty of Civil and Environmental Engineering, Poland,
piotr.zima@pg.edu.pl

1. Abstract

This paper presents the complex hydrological model of runoff of contaminated agricultural surface waters from the area of Puck District to the Puck Bay. Computer-based hydrologic model the Soil And Water Assessment Tool (SWAT) was used for this purpose. For the calibration of the model, available (from last 20 years) and acquired meteorological and hydrological data as well as the results of physicochemical measurements were used. The impact of the choice of the type of fertilizer and the time of its application on the amount of nutrients found in the watercourses outflow to the Puck Bay is presented.

Keywords: Baltic Sea, coastal waters, eutrophication, pollution impact, Puck Bay, WaterPuck

2. Introduction

In recent years, the problem of pollution of coastal waters by pesticides and nutrients fluxes from livestock and agricultural production fertilizers becomes very important [1]. This may be the cause of eutrophication and water hypoxia. This is particularly important in the case of the Baltic Sea ecosystem, considered as one of the most polluted seas in the world [2]. Puck Bay is a western branch of the Gulf of Gdańsk in the southern Baltic Sea, separated from the open sea by the peninsula (Figure 1).

Established in 1978 Polish Coastal Landscape Park covers large portion of the bay. Another part is a special protection area for birds and a popular place for water sports in Poland, especially kitesurfing. It is shallow bay with an average depth of 3 m and numerous shoals, not deeper than 1 m which hampers the exchange of water in the Bay. For this reason, it is important to keep its waters clean and to prevent excessive pollution having its source in the adjacent agricultural catchment located in the Puck District drained by numerous rivers and springs including, but not limited to: Płutnica, Reda, Gizdepka, Bładzikowski Creek and Mrzezino Canal.

Despite many tourist values, the area of the Puck Commune is mainly used for agricultural purposes [3]. To determine the impact of agricultural anthropopression on shallow coastal waters, a predictive environmental information service based on the SWAT model [4], [5],

[6], [7] was prepared. The catchment model in the SWAT program is an interactive prognostic tool powered by meteorological data from the ICM UW (Interdisciplinary Centre for Mathematical and Computational Modelling at University of Warsaw) forecast. One of the possibilities of this model is the calculation of (among others) approximate loads of biogens and pesticides migrating to the Puck Bay from the area of the Puck Commune [8]. The catchment model of Puck Bay was based on the numerical terrain model [9], geological maps, soil and agricultural maps and meteorological data obtained from Institute of Meteorology and Water Management - National Research Institute (IMWM-NRI). The model analyzes 17 sub-basins, designated for the following watercourses: Reda, Gizdepka, Bładzikowski Creek (Żelistrzewo Canal) and Płutnica, with a total area of 168 km² (Figure 2). The model was calibrated based on the results of field measurements made in 2017-2019 and information provided by the catchment monitoring system, created for the needs of this project.

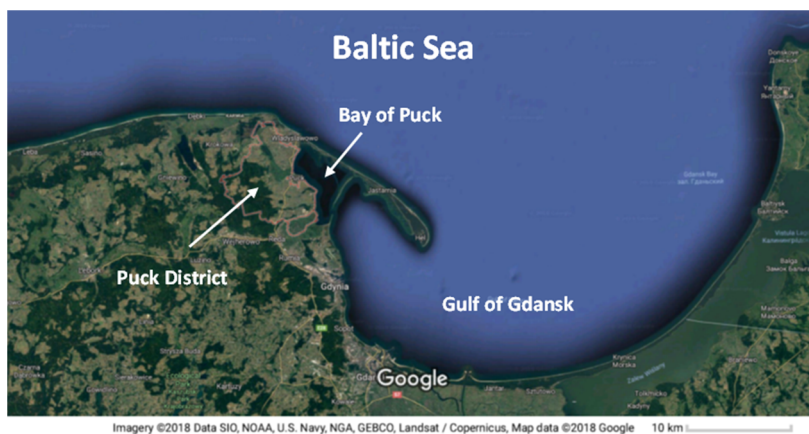


Figure 1. Map of the study area (source: Google Maps, accessed 25 March 2019)

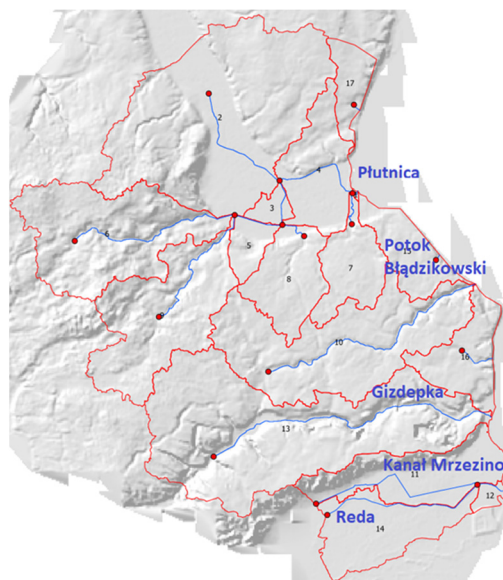


Figure 2. The system of watercourses and subbasins in the analyzed area

2. Methods

2.1 Computer model

Computer-based hydrologic model SWAT [4], [5] was used for hydrological modeling of runoff of contaminated agricultural surface waters from the area of Puck District to the Puck Bay. The conversion of precipitation data into surface runoff was achieved with the SCS (Soil Conservation Service) Curve Number procedure [10], [11] through the accumulated runoff volume and the time of concentration, denoted as the time from the beginning of a storm event until the moment when the entire sub-basin area is contributing to flow at the outlet. Therefore detailed data on land use, land cover and digital terrain model were subjected to extensive study [12]. Out of 168 km² of the analyzed area, 17 sub-basins were separated (Figure 3), divided into 353 HRUs (Hydrologic Response Unit). In addition, to model basin behavior, numerous meteorological data were required including daily climatic information about rainfall, solar radiation, wind speed and direction, relative humidity, and maximum and minimum temperatures [13], [14], [15].

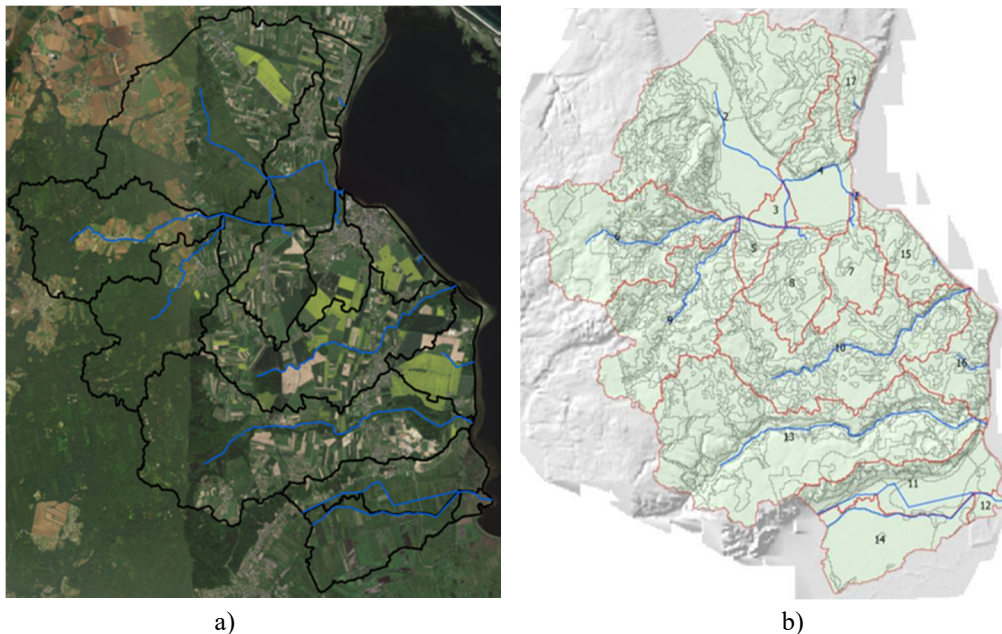


Figure 3. Location of watercourses and sub-basins included in the SWAT model (a) and division into HRU (b)

The SWAT model enables quantitative and qualitative analysis of the impact of catchment management on the water balance [4], [5]. By means of physical equations, the program describes the relationships between input data and results. Processes occurring on the catchment surface, in the ground and during river transport are modeled. The main element of the SWAT model are units of uniform hydrological response of HRU, dividing the area of each sub-division into areas with the same land development and soil coverage. The percentage distribution of land development in the Puck commune is summarized in Table 1.

Table 1. Land use of the catchment area of the Puck Bay

Land use	[ha]	[%]
URBAN	1336.50	7.95
WETLAND	260.25	1.55
AGRICULTURAL	8563.50	50.95
PASTURES	1978.25	11.77
FOREST	4647.50	27.65

Computer simulations were carried out with a daily time step. To increase accuracy, the first 20 years of simulation were treated as a start-up period - necessary to stabilize water relations, among others saturation of aquifers and determining the initial content of nitrogen and phosphorus in the soil profile.

The SWAT model analyzes the circulation of water, nitrogen and phosphorus. These processes depend on many factors, including meteorological data. Based on IMWM-NRI archival data from the vicinity of the analyzed area, for 1979 - 2019 a summary of parameters such as: daily sum of rainfall, minimum and maximum temperature, relative humidity, wind speed and solar radiation were prepared. In addition, these data were verified in 2018-2019 by placing a meteorological station in the town of Żelistrzewo, located in the central point of the catchment. In addition, these data were verified in 2018-2019 by placing a meteorological station in the town of Żelistrzewo (as part of the monitoring network for the implementation of the WaterPuck project [6], [7], [8]), located in the central point of the catchment. In the case of the amount of biogen's reaching the Pucka Bay, the most important parameter was the precipitation value determining the amount of surface runoff. These values are summarized in Table 2.

Table 2. Monthly average: precipitation and surface runoff of the catchment area of the Puck Bay.

MON	RAIN	SNOW FALL	SURFACE RUNOFF
	(MM)	(MM)	(MM)
1	56.57	28.05	12.18
2	43.52	19.97	13.03
3	48.39	8.92	10.50
4	35.31	2.55	8.79
5	48.52	0.00	7.42
6	63.35	0.00	9.17
7	116.08	0.00	32.42
8	77.5	0.00	10.52
9	70.69	0.00	13.28
10	57.71	0.28	6.35
11	69.4	2.40	12.94
12	74.26	22.48	14.24

The amount of biogens coming from the land surface to watercourses is related to changes in the ground. The analysis of ground parameters, including content of individual fractions and organic carbon was important. The identification of these

parameters was made on the basis of field research - several dozen soil samples were taken and tested from areas used for agriculture [16]. In addition, the results of surveys conducted among farmers in terms of the type and doses of fertilizers used were analyzed.

2.2 Model of nutrients metabolism

SWAT analyzes both inorganic and organic forms of nitrogen contained in the soil and transported in watercourses [4], [5]. In mineral soils, organic nitrogen is associated with humus, additionally it can be added through fertilization, crop residues, bacterial processes, rainfall. Nitrogen losses are associated with vegetation growth (nitrogen uptake from soil), leaching, oxidation, denitrification and erosion. In a similar way, SWAT simulates the phosphorus circulation, monitors organic compounds associated with humus, mineral and plant phosphorus.

2.2.1 Transport of substances to watercourses

Transport of nutrients from the catchment area to watercourses is the result of weathering of soils and erosion processes. These compounds can be transported by surface run-off, under-surface flow or percolation. To calculate the substance load, calculate the amount of water flowing out of the basin and the concentration of individual compounds leached from the ground.

On the example of nitrates, the concentration is calculated as follows [17]:

$$conc_{NO_3} = \frac{NO_{3ly} \cdot (1 - \exp\left[\frac{-w_{mob}}{(1 - \theta_e) \cdot SAT_{ly}}\right])}{w_{mob}} \quad (1)$$

where:

$conc_{NO_3}$ – the concentration of nitrate in mobile water for a given layer [kg N/mm H₂O],

NO_{3ly} – the amount of nitrate in the layer [kg N/ha],

w_{mob} – the amount of mobile water in the layer [mm H₂O]:

for top 10mm $w_{mob} = Q_{surf} + Q_{lat} + w_{perc}$,

for lower layers $w_{mob} = Q_{surf} + w_{perc}$,

θ_e – the fraction of porosity from which anions are excluded,

SAT_{ly} – the saturated water content of the soil layer [mm H₂O].

Surface runoff is calculated according to the SCS method [10], [11], [17]:

$$Q_{surf} = \frac{(R_{day} - I_a)^2}{R_{day} - I_a + S} \quad (2)$$

where:

Q_{surf} - the accumulated runoff or rainfall excess [mm H₂O],

R_{day} - the rainfall depth for the day [mm H₂O],

I_a - the initial abstractions which includes surface storage, interception and infiltration prior to runoff [mm H₂O],

S - the retention parameter [mm H₂O].

Lateral flow [17]:

$$Q_{lat} = 0.024 \cdot \left(\frac{2SW_{ly} \cdot K_{sat} \cdot slp}{\phi_d \cdot L_{hill}} \right) \quad (3)$$

where:

SW_{ly} – soil water content of layer [mm H₂O],

K_{sat} – saturated hydraulic conductivity [mm/h],

slp – average slope of the sub-basin [-],

ϕ_d – drainable porosity of the soil [mm/mm],

L_{hill} – hillslope length [m].

Percolation [17]:

$$w_{perc} = SW_{ly} \cdot \left(1 - \exp \left[\frac{\Delta t}{TT_{perc}} \right] \right) \quad (4)$$

where:

Δt – length of the time step [h],

TT_{perc} – the time travel for percolation [h].

2.2.2 Transformation of nitrogen compounds in watercourses

In river streams, oxygen changes of nitrogen take place, part of organic nitrogen is retained in bottom sediments. The concentration of organic nitrogen in watercourses can increase due to nitrogen changes from biomass of vegetation (algae) to organic nitrogen or reduced by the transition to NH_4^+ , whose concentration can be reduced by the conversion to NO_2^- or by absorption through algae. Daily concentration changes are calculated according to the formulas [17]:

$$\Delta orgN_{str} = \left(\alpha_1 \cdot \rho_a \cdot algae - \beta_{N,3} \cdot orgN_{str} - \sigma_4 \cdot orgN_{str} \right) \cdot TT \quad (5)$$

$$\Delta NH4_{str} = \left(\beta_{N,3} \cdot orgN_{str} - \beta_{N,1} \cdot NH4_{str} + \frac{\sigma_3}{1000 \cdot depth} - frNH4 \cdot \alpha_1 \cdot \mu_a \right) \cdot TT \quad (6)$$

$$\cdot algae) \cdot TT \quad (7)$$

$$\Delta NO2_{str} = \left(\beta_{N,1} \cdot NH4_{str} - \beta_{N,2} \cdot NO2_{str} \right) \cdot TT \quad (8)$$

$$\Delta NO3_{str} = \left(\beta_{N,2} \cdot NO2_{str} - (1 - frNH4) \cdot \alpha_1 \cdot \mu_a \cdot algae \right) \cdot TT$$

where:

$\Delta orgN_{str}$ – the change in organic nitrogen concentration [mg N/L],

- $\Delta NH4_{str}$ - the change in ammonium concentration [mg N/L],
 $\Delta NO2_{str}$ - the change in nitrite concentration [mg N/L],
 $\Delta NO3_{str}$ - the change in nitrate concentration [mg N/L],
 α_1 - the fraction of algal biomass that is nitrogen [mg N / mg alg biomass],
 ρ_a - the local respiration or death rate of algae [day^{-1}],
 σ_3 - the sediment source rate for ammonium [$\text{mg N/m}^2 \cdot \text{day}^{-1}$],
 σ_4 - the rate coefficient for organic nitrogen settling [day^{-1}],
 μ_a - the local growth rate of algae [day^{-1}],
 $\beta_{N,1}$ - the rate constant for biological oxidation of ammonia nitrogen [day^{-1}],
 $\beta_{N,2}$ - the rate constant for biological oxidation of nitrite to nitrate [day^{-1}],
 $\beta_{N,3}$ - the rate constant for hydrolysis of organic nitrogen to ammonia nitrogen [day^{-1}],
 fr_{NH4} - the fraction of algal nitrogen uptaken from ammonium pool [/],
 $algae$ - the algal biomass concentration at the beginning [mg alg/L],
 TT - the flow travel time in reach segment [day].

2.3 Hydraulic and hydrology study

In order to calibrate the SWAT model [17], hydrometeorological data obtained from a nearby meteorological station in Puck, Żelistrzewo station (launched as part of the WaterPuck project) and hydrometric and marker measurements made in 2017-2019 on the main watercourses in the Puck Commune were used. Hydrometric measurements were made using various devices, depending on the local hydraulic conditions [13], [14]. In the case of the Reda river (high flow, large sections, respectively), measurements were made using the ADCP device RIVERSURVEYOR® S5 from SonTek. In the case of smaller cross-sections (Gizdepka, Płutnica, Bładzikowski Creek and Mrzezino Canal), measurements were made using HEGA hydrometric current meters with electronic recorders. Flow measurements in the culverts with a stabilized cross-section were made by means of ultrasonic flowmeters type PCM4 (Portable Channel Monitoring) by Nivus with recording in memory at the assumed time intervals. In addition, tracer study were made to identify the parameters of pollutant transport and to measure the flow rate in the natural part of the channels of the analyzed watercourses [18], [19], [20]. For these measurements, the rhodamine WT was used as a tracer, and the Trilogy fluorometer from Turner Designs was used to determine its concentration. Taken field samples were determined in the laboratory. Results in characteristic cross-sections of watercourses are presented in Table 3. This data was used to calibrate the model in the SWAT program [17].

Table 3. Flows in characteristic sections on the main watercourses: at the mouth - Płutnica, Gizdepka, Reda Out and at the inlet – Reda In.

Płutnica		Gizdepka		Reda In		Reda Out	
Date	Q[m ³ /s]	Date	Q[m ³ /s]	Date	Q[m ³ /s]	Date	Q[m ³ /s]

19-Jul-18	0.469	18-Jul-18	0.785	14-Jun-18	3.726	14-Jun-18	3.856
20-Jul-18	0.239	18-Oct-18	0.104	17-Jul-18	4.525	17-Jul-18	4.795
20-Jul-18	0.166	29-Nov-18	0.181	18-Oct-18	3.757	18-Oct-18	4.719
8-Nov-18	0.018	6-Dec-18	0.160	8-Nov-18	4.003	8-Nov-18	5.684
29-Nov-18	0.299	6-Feb-19	0.211	29-Nov-18	4.042	29-Nov-18	4.373
6-Dec-18	0.271	2-Mar-19	0.059	6-Dec-18	4.011	6-Dec-18	5.396
6-Feb-19	0.745	23-Mar-19	0.192	6-Feb-19	5.058	6-Feb-19	6.563

3. Results

The aim of the work is to present the impact of the choice of the type of fertilizer and the time of its application on the amount of nutrients found in the watercourses outflow to the Puck Bay [21]. A simulation was prepared for 20 years of start-up (needed to determine water relations, eg establishing the level of groundwater) and 16 years (1999-2014) of calculation. Several calculation variants were made that differed in dose and type of fertilizer. The analysis covered the estuary sections of watercourses, for nitrates leached out of fields after rain, and the total amount of organic nitrogen and phosphorus going to watercourses from the catchment.

Table 4. Monthly average values at the mouth of Płutnica

STREAM	MONTH	Q [m ³ /s]	Norg [kg]	Porg [kg]	NO ₃ [kg]	NH ₄ [kg]	NO ₂ [kg]	Pmin [kg]
Płutnica	1	0.88	377.03	76.75	157.46	7.60	0.01	6.02
	2	1.09	505.28	107.43	186.20	9.67	0.01	7.99
	3	1.01	382.19	82.99	95.62	7.79	0.02	5.54
	4	0.96	484.66	106.15	48.98	10.10	0.02	5.82
	5	0.80	466.03	108.57	34.53	12.07	0.03	6.13
	6	0.68	722.66	166.09	19.21	21.63	0.07	9.60
	7	1.28	2147.94	483.38	45.48	57.06	0.16	28.09
	8	0.58	337.42	74.57	51.85	11.96	0.07	5.94
	9	0.68	358.49	78.43	8.00	9.29	0.03	5.81
	10	0.44	143.28	30.57	2.38	3.76	0.01	2.42
	11	0.70	293.98	63.59	5.89	6.36	0.01	4.98
	12	0.85	274.57	59.31	18.93	5.64	0.01	4.96

The results obtained by model simulation in the SWAT program were presented for each of the watercourses (from the area of Puck Commune - Płutnica, Bładzikowski Creek and Gizdepka), at its mouth to the Puck Bay. The results are presented in graphical form (graph of variability in the whole nutrient calendar year - organic nitrogen and phosphorus) and in tabular form (monthly average values of individual biogenic indicators in the estuary section) for each of the watercourses: Płutnica (Table 4 and Figure 4), Bładzikowski Creek (Table 5 and Figure 5) and Gizdepka river (Table 6 and Figure 6).

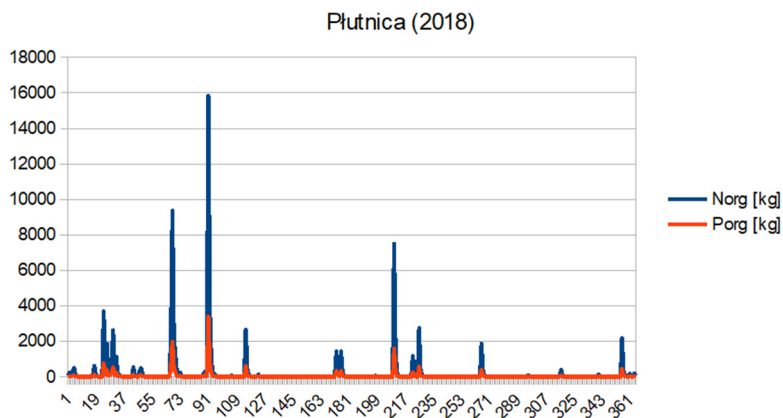


Figure 4. Graph of variability of nutrients at the mouth of Plutnica in 2018

Table5. Monthly average values at the mouth of Bładzikowski Creek

STREAM	MONTH	Q [m3/s]	Norg [kg]	Porg [kg]	NO3 [kg]	NH4 [kg]	NO2 [kg]	Pmin [kg]
Bładzikowski	1	0.20	98.85	20.97	31.49	1.32	0.00	0.99
	2	0.25	143.30	31.52	34.42	1.76	0.00	1.37
	3	0.23	101.97	22.74	19.40	1.46	0.00	1.01
	4	0.22	123.00	27.98	11.06	1.81	0.00	0.98
	5	0.19	115.79	27.23	8.62	2.12	0.00	0.99
	6	0.18	178.51	41.77	5.49	3.76	0.00	1.28
	7	0.34	547.34	127.27	12.45	9.52	0.00	3.39
	8	0.16	99.86	22.58	18.19	2.72	0.00	0.93
	9	0.18	102.65	23.09	2.86	1.66	0.00	0.90
	10	0.11	42.55	9.39	0.27	0.81	0.00	0.44
	11	0.17	79.86	17.93	0.29	1.13	0.00	0.78
	12	0.20	88.53	19.81	0.92	1.21	0.00	0.86

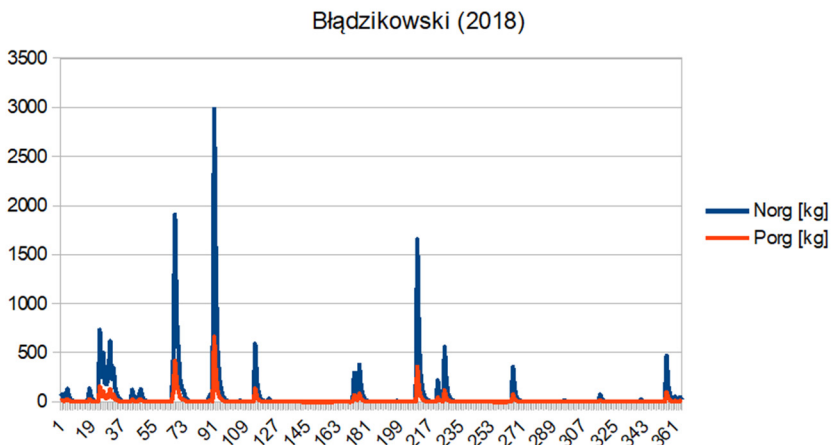


Figure 5. Graph of variability of nutrients at the mouth of Bładzikowski Creek in 2018

Table 6. Monthly average values at the mouth of Gizdepka

Stream	month	Q [m ³ /s]	Norg [kg]	Porg [kg]	NO3 [kg]	NH4 [kg]	NO2 [kg]	Pmin [kg]
Gizdepka	1	0.32	136.39	28.27	29.30	2.28	0.00	1.55
	2	0.39	197.69	42.93	33.03	3.09	0.00	2.09
	3	0.36	144.51	32.16	16.98	2.61	0.00	1.58
	4	0.34	185.13	42.99	9.52	3.39	0.00	1.61
	5	0.27	188.12	46.55	9.63	4.41	0.00	1.58
	6	0.22	292.16	74.57	19.99	8.10	0.00	1.90
	7	0.40	754.38	179.49	39.81	17.54	0.00	5.04
	8	0.20	118.62	26.75	24.69	4.35	0.00	1.33
	9	0.22	130.20	29.15	1.87	2.77	0.00	1.36
	10	0.15	50.88	11.11	0.77	1.28	0.00	0.65
	11	0.23	101.65	22.46	1.24	1.90	0.00	1.20
	12	0.30	105.77	23.48	3.21	1.92	0.00	1.26

Gizdepka (2018)

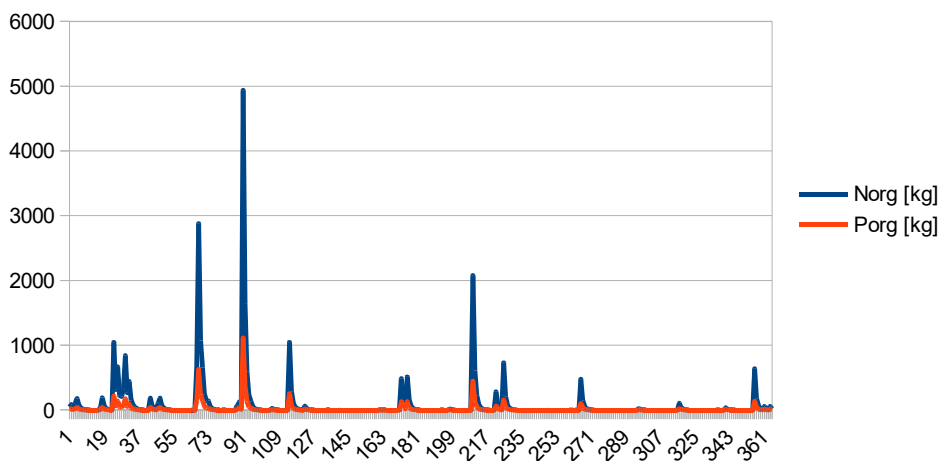


Figure 6. Graph of variability of nutrients at the mouth of Gizdepka in 2018

The obtained results allowed to simulate the effect of fertilization practices on the pollution of the Puck Bay.

4. Conclusions

As result of the conducted research, the following is stated.

1). In the case of the analyzed catchments of the Puck commune (Płutnica, Potok Bładzikowski and Gizdepka), despite many differences (in the catchment geometry, land development and soil coverage), no significant differences were observed in the outflow characteristics of nitrogen and phosphorus derivatives in watercourses.

2). By comparing the seasonal variation in the concentration of nitrogen and phosphorus

compounds with precipitation episodes, one can notice a rapid increase in substances transported via watercourses to the Puck Bay associated with precipitation. This is particularly evident in the non-vegetative season. The highest recorded nitrogen and phosphorus content in 2018 occurred after the heavy rainfall of 1 April (20.9 mm), the rainfall of 29 July (33.1 mm), which occurred in the peak of the growing season, generated on average twice less nitrogen and phosphorus in inflow to the Puck Bay.

3). It is important to properly choose the date of fertilization. This will allow the use of an appropriate dose of compounds that should be put into the ground, by limiting excessive leaching of them together with surface runoff from arable fields until the maximum absorption by the plants.

Acknowledgements

The article is the results obtained within WaterPuck Project financed by the National Centre for Research and Development within BIOSTRATEG III program (No. UMO-2016/21/B/ST10/0121).

References:

- [1] Łysiak-Pastuszek, E., Drgas, N., Piątkowska, Z.: Eutrophication in the Polish coastal zone: the past, present status and future scenarios, *Marine Pollution Bulletin*, 49, pp.186-195, 2004.
- [2] Ning, W., Nielsen, A.B., Ivarsson, L.N., Jilbert, T., Åkesson, C.M., Slomp, C.P., Andrén, E., Broström, A., Filipsson, H.L.: Anthropogenic and climatic impacts on a coastal environment in the Baltic Sea over the last 1000 years, *Anthropocene*, 21, pp. 66–79, 2018.
- [3] Wojciechowska, E., et al.: Seasonal changes of the concentrations of mineral forms of nitrogen and phosphorus in watercourses in the agricultural catchment area (Bay of Puck, Baltic Sea, Poland), *Water Science and Technology: Water Supply*, 19 (3), pp. 986-994, 2018.
- [4] Arnold, J.G., Fohrer, N.: SWAT2000: Current capabilities and research opportunities in applied watershed modelling, *Hydrological Processes*, 19(3), pp. 563–572, 2005.
- [5] Arnold, J.G., et al.: Soil and Water Assessment Tool input/output file documentation: Version 2012, Texas Water Resources Institute, TR-439, 2012.
- [6] Dzierzbicka-Głowacka, L., et al.: Integrated information and prediction Web Service WaterPUCK General concept, *Proceedings of 22nd International Conference on Circuits, Systems, Communications and Computers (CSCC 2018)*, EDP Sciences, pp.1-7, 2018.
- [7] Dzierzbicka-Głowacka, L., et al.: A new approach for investigating the impact of pesticides and nutrient flux from agricultural holdings and land-use structures on the coastal waters of the Baltic Sea, *Polish Journal of Environmental Studies*, 28(4), pp. 2531–2539, 2019.
- [8] Dzierzbicka-Głowacka, L., et al.: Impact of agricultural farms on the environment of the Puck Commune: Integrated agriculture calculator – CalcGosPuck, *PeerJ* 7:e6478.
- [9] Kalinowska, D., Wielgat, P., Kolerski, T., Zima, P.: Effect of GIS parameters on modelling runoff from river basin. The case study of catchment in the Puck District, *Seminary on Geomatics, Civil and Environmental Engineering (2018 BGC)*, E3S Web Conf., 63, pp.1-5, 2018.
- [10] Hjelmfelt, Jr.A.T.: Investigation of curve number procedure, *Journal of Hydraulic Engineering*, 117, pp. 725–737, 1991.
- [11] SCS: National Engineering Handbook, Section 4: Hydrology, Soil Conservation Service, USDA, Washington, D.C., 2004.
- [12] Dile, Y.T., et al.: Introducing a new open source GIS user interface for the SWAT model, *Environmental Modelling & Software*, 85, pp. 129-138, 2016.

- [13] Maidment, D.R.: Handbook of hydrology, McGraw-Hill, 1992.
- [14] Eslamian, S.: Handbook of engineering hydrology: fundamentals and applications, CRC Press, Taylor and Francis NY, 2014.
- [15] Srinivasan, R., et al.: Large area hydrologic modeling and assessment part II: model application, Journal of the American Water Resources Association, 34(1), pp. 91-101, 1998.
- [16] D. Potrykus, et al.: Assessing groundwater vulnerability to pollution in the Puck region (denudation moraine upland) using vertical seepage method, E3S Web of Conferences, 44, 00147, 2018.
- [17] Soil & Water Assessment Tool, Theoretical Documentation: <https://swat.tamu.edu/media/99192/swat2009-theory.pdf>.
- [18] Zima, P.: Modeling of the Two-Dimensional Flow Caused by Sea Conditions and Wind Stresses on the Example of Dead Vistula, Polish Maritime Research, 97, pp. 166-171, 2018.
- [19] Zima, P.: Numerical analysis of an impact of planned location of sewage discharge on Natura 2000 areas - the Dead Vistula region case study, Polish Maritime Research, 102, pp. 76-84, 2019.
- [20] Sawicki, J.M., Zima, P.: The influence of mixed derivatives on the mathematical simulation of pollutants transfer, 4th International Conference on Water Pollution, Slovenia, pp. 627–635, 1997.
- [21] Zima, P.: Simulation of the impact of surface water pollution from agricultural areas on the quality of the Baltic Sea in the Bay of Puck region, Euro-Mediterranean Journal for Environmental Integration, 4:16, 2019.

IMPACT OF RIVER TRAINING WORKS ON THE DRAVA RIVER FLOW REGIME

GORDON GILJA¹, NEVEN KUSPILIĆ², NINA GOLUBOVIĆ³

¹University of Zagreb Faculty of Civil Engineering, Croatia, gordon.gilja@grad.hr

²University of Zagreb Faculty of Civil Engineering, Croatia, kuspa@grad.hr

³PRONING DHI Ltd., Croatia, nina@proning-dhi.hr

1. Abstract

The 32% of the most downstream Drava River section for low navigable water level of freeflow river does not meet minimal requirements for navigation due to the insufficient fairway depth. Aim of this paper is to estimate impact of proposed river training structures on long term morphologic development for 4 critical locations and evaluate the layout of structures on fairway conditions. For this purpose, 4 types of river training structures are proposed to be strategically grouped on critical locations. Evaluation of proposed river structures effectiveness is done using coupled flow/sediment transport 2D numerical model results: flow depth, width and local flow velocity within the fairway. Results have shown that construction of river training structures has local impact on hydraulic and sediment regime, while its influence on hydrologic regime has global character throughout the river section.

Keywords: groynes, T-shape groynes, detached groynes, Chevron dikes, Drava River fairway

2. Introduction

The 14 km long Drava River section from its mouth into Danube to the international port Osijek is classified as international class IV waterway. This section has been heavily modified throughout the history in order to accommodate sufficiently wide and deep navigable fairway, confining morphodynamic processes on this river mostly to the main channel with limited sand-bar development. Nevertheless, for low navigable water level of freeflow river 32 % of this river section does not meet minimal requirements for navigation due to the insufficient fairway depth. Fairway management issues related to sediment transport are well documented on this Drava River reach, including sedimentation in port Osijek [1], sand-bar blockage of the fairway at the confluence [2] or problems with the fairway depth and clearance [3].

Most efficient and at the same time cost-effective measures for securing the fairway geometry are installation of groynes in rivers, with purpose of flow concentration in the fairway, thus initiating erosion of the river channel in the fairway while protecting the banks. Groynes can be classified into different types according to their construction, angle of orientation and shape. Conventional groynes are simple and durable structures built mainly from rock, with effective length most often greater than one third of river

width. They have trapezoidal shape with narrow crest and different lateral slopes: steeper upstream slope and gentler downstream slope. T-shaped groynes have the same design parameters, except the head where additional perpendicular wings that can provide more sediment deposition and better performance in wide rivers and are most often used to secure fairway conditions in large rivers. More recently, in the context of enhancing the biodiversity and of morphological riparian features alternative shapes of groynes were suggested, among which detached groynes [4] and Chevron dikes [5], which are not connected to the riverbank as conventional groynes. Angle between the groyne centerline and riverbank is important because it is used to attract the flow towards alongside the near bank of the river, resulting with more efficient erosion in the fairway and less scour around the groyne head compared to the conventional groynes. Therefore, detached groynes are rotated for 15° downstream, according to the best practices on Danube River [6]. Chevron dikes utilize plan form in shape of the letter “V” or “U” pointing upstream, which is significantly different from the conventional design.

Groyne installation design includes definition of crest length, height and width and side slopes. Traditionally, groynes on Drava River are constructed with constant cross-sectional trapezoidal geometry. Their crest width is 1m, height is 1m above mean water level, upstream and downstream slope H:V 1:1 and 1:2, respectively. Slope of the groyne head is 1:1.5. These values were used in this research in order to conform to traditional construction practices on this river reach. Groynes are often constructed in groups, or fields in order to maximize their effect on the flow and sediment transport, not only inside the fields, but along the main stream. Installation of groyne fields result with more sediment being deposited inside the groyne field, making these regions the most habitable areas for the aquatic fauna and biota [7].

Existing Drava River fairway conditions are analysed using ship’s navigation logs from River Information Services. Based on the analysis [8] it was concluded that fairway axis needs to be adjusted in order to minimise excavation and river training works during future fairway management. On the analysed river section 4 critical locations, *i.e.* “bottlenecks”, were identified on which groynes need to be installed in order to achieve the required fairway depth during low flows. The following locations are selected for groyne field installation: from rkm 2+730 to rkm 3+032 (groyne field I), from rkm 4+667 to rkm 5+375 (groyne field II), from rkm 9+842 to rkm 10+342 (groyne field III) and from rkm 10+942 to rkm 11+652 (groyne field IV). These locations are shown in the following picture:



Figure 18. Drava River section from rkm 0+000 to 12+000 with surveyed cross-sections

Aim of this paper is to analyse flow field characteristics, estimate impact of proposed river training structures on Drava River's long-term morphologic development for 4 critical locations and evaluate the layout of structures on fairway conditions under relevant characteristic flow conditions. Two numerical models were used to simulate flow conditions: 1D flow model HEC-RAS and 2D coupled flow/sediment transport model MIKE 21 fm. 1D model domain covers the entire river section with 120 numerical cross-sections equally spaced from rkm 0+000 to rkm 12+000. 2D model was divided into 2 models to save computational time: downstream section from rkm 1+500 to rkm 5+500 (focused on groyne fields I and II) and upstream section from rkm 9+400 to rkm 12+000 (focused on groyne fields III and IV).

2. Methodology

Flow and sediment transport regime for analyzed river section was calculated using coupled 2D flow and sediment transport numerical model. Current flow and sediment transport regime were calculated using discharge curve and sediment curve from the upstream section as inflow boundary condition [9]. Nearest gauging stations used for hydrologic analysis are located immediately on the Drava River confluence (GS Aljmaš) and 8 km upstream from the upstream boundary of the analysed section (GS Osijek, rkm 20+000). Nearest GS with continuous discharge data is located further upstream, GS Belišće on rkm 53+800, and available data from it was used to calculate characteristic discharge data. Flow regime that affects the fairway conditions on this river section is historically known and in context of this study $Q_{94\%}$, $Q_{60\%}$ and Q_{mean} were selected as reference values [8]. $Q_{94\%}$ is discharge associated with low navigable water level of freeflow river below which ship transport is suspended. Data acquired from discharge duration curve had to be corrected in order to compensate the inflow from 40 km of basin from the GS Belišće until the analysed section boundary. Data was corrected using specific inflow theory, which describes functional relationship between the basin area and discharge increase. Characteristic discharges adjusted from GS and used in analysis are 296 m³/s, 483 m³/s and 573 m³/s, for $Q_{94\%}$, $Q_{60\%}$ and Q_{mean} , respectively, which is approximately 4% increase through correction. This section is heavily influenced by the Danube which creates backwater effect more than 20 km upstream, which means that water levels corresponding to the aforementioned discharges cannot be calculated directly from GS data. Therefore, new discharge curve had to be constructed that represents freeflow conditions. For this purpose, data collected by FCE in the period from 2008 until 2018 was used [10, 11]. From the Q - H scatter plot data pairs that are not influenced with backwater effect were singled out and used in regression analysis to obtain boundary data for the model (Figure 19).

For calibration of the 1D model the same data was used, resulting with local and friction losses coefficient for the three characteristic discharges. Results of water levels from 1D model were fed into the 2D model since it covers its sub-domain. Validation of 2D model was conducted using recorded detailed flow field data on 4 Drava River cross-sections [2, 8, 12]. Each of the 2D models used was validated using surveyed flow velocity field on 3 independent surveys conducted in 2014 represented with vectors averaged throughout the water column depth. Downstream model was validated on profile 5+000, while upstream model was validated on profile 11+000 (Figure 19).

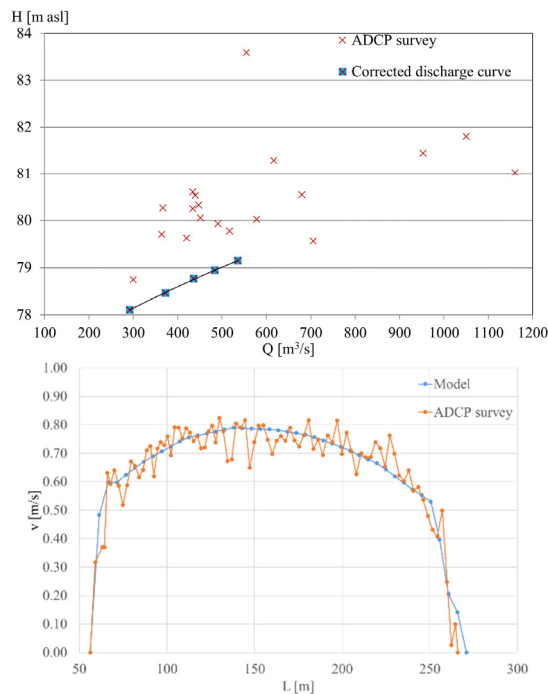


Figure 19. Discharge curve corrected for backwater effect (left); example of 2D model validation (right)

2D model validation has shown that for defined discharge span model results correspond well with measured flow profile. Apart from magnitude, flow velocity vectors show good alignment with local flow distortion near the banks, although the model cannot reflect sudden changes in flow velocity observed in the field. Based on the validation, current model setup is considered reliable for flow simulations on this Drava River section. Impact of proposed river training structures on flow regime was evaluated through comparison of flow field for existing and design state. Analysis included longitudinal profile of depth-averaged flow velocity in fairway axis, longitudinal water surface elevation, scalar flow field characteristics and flow velocity profile in the groyne field. Results are analysed separately for each groyne field for all 3 characteristic flow events.

3. Results

Numerical model results show that proposed groyne fields have significant effect on flow regime. Flow contraction from groyne placement in the river resulted in water level increase at each groyne field, where biggest increase was observed locally at the groynes. For all 4 groyne fields water level increase was observed to be similar: under $Q_{9.4\%}$ conditions smallest increase (6 cm) compared to existing state was observed for Chevron dikes, followed by 8 cm increase for detached and T-shaped groynes, while the biggest increase was observed for conventional groynes (9 cm). Between individual groynes in each of the groyne fields local water surface depression was observed, resulting from local flow contraction and acceleration immediately downstream of the groynes (Figure

20). Flow conditions regarding the water levels are observed to be similar for the other two discharges $Q_{60\%}$ and Q_{mean} as well: for both discharges smallest increase (7 cm) was observed for Chevron dikes, followed by 9 cm increase for T-shaped groynes and detached, while the biggest increase was observed for conventional groynes (10 cm). When groynes are positioned next to the right bank have less influence on water level depression for adjacent groyne downstream.

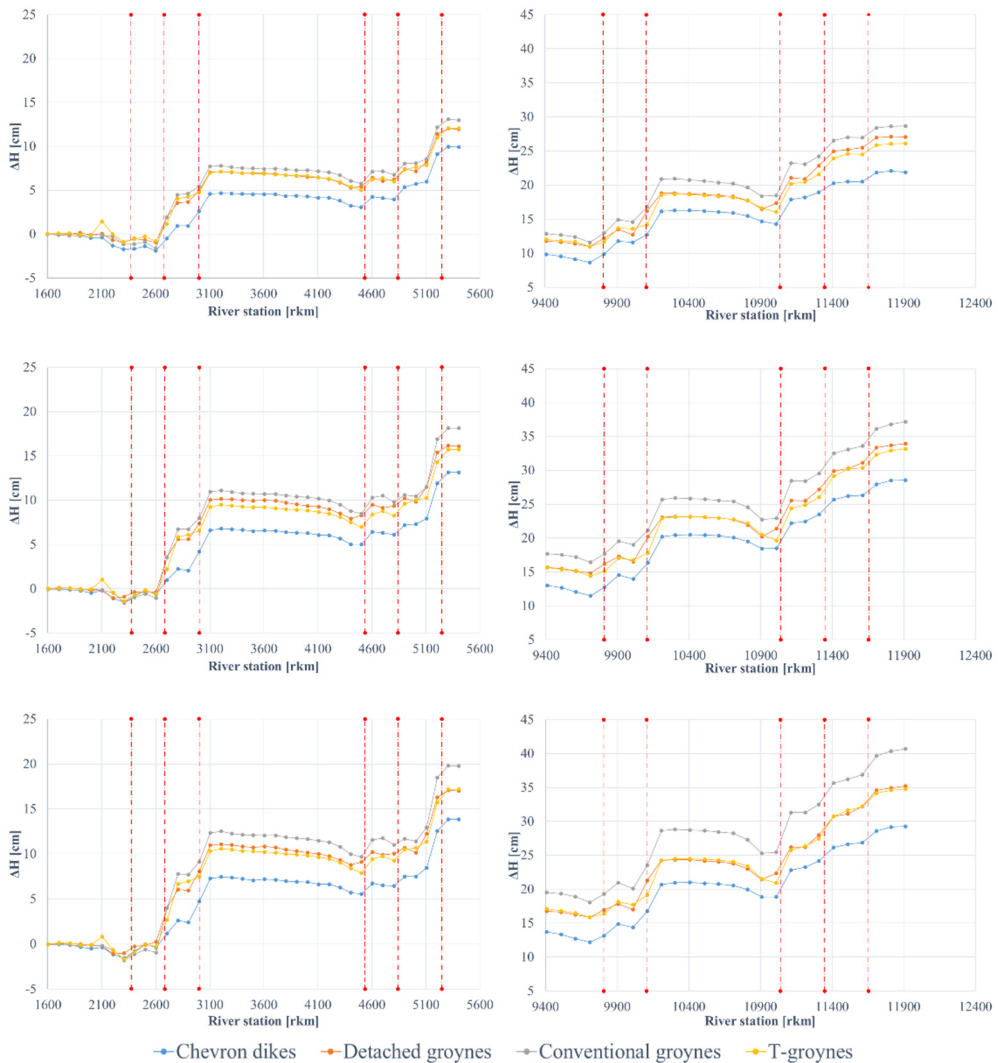


Figure 20. Longitudinal water surface elevation profile: from top to bottom: $Q_{94\%}$, $Q_{60\%}$ and Q_{mean} ; left column for the downstream model and right for the upstream model

The biggest increase in flow velocity is observed immediately downstream of the groyne head (Figure 21), as expected based on previously observed trend of depressions in water surface elevations profile (Figure 20). Trend of flow velocity increase through groyne field is not uniform – location of largest velocity increase varies between different groyne fields. As for water levels, smallest velocity increase for all discharges was for

Chevron dikes and largest for conventional groynes, while detached and T-shaped groynes have approximately the same velocity increase. On freeflowing river section between adjacent groyne fields there is no significant difference in velocity, compared to existing state.

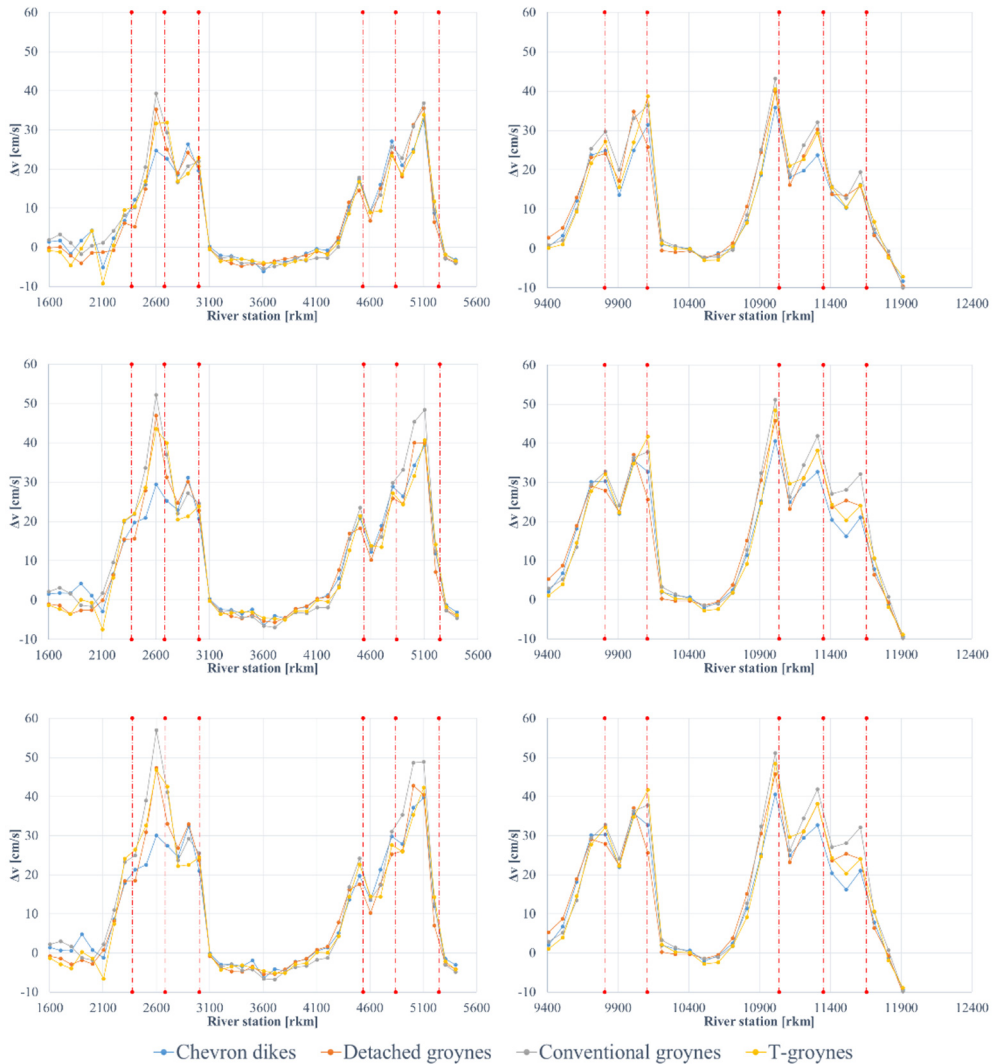


Figure 21. Longitudinal flow velocity profile: from top to bottom: $Q_{94\%}$, $Q_{60\%}$ and Q_{mean} ; left column for the downstream model and right for the upstream model

Groyne layout in groyne field I reveals that their positioning follows the existing river island and river branch behind it, emphasizing the alignment of flow towards the left bank. For all types of groynes the most upstream one has small effect on the flow field due to its positioning in shallow depth downstream of the river island. Velocity increase for all discharges, $Q_{94\%}$, $Q_{60\%}$ and Q_{mean} , is similar: for conventional, T-shaped groynes and detached groynes affect the flow field the most, while Chevron dikes affect the flow field the least. Downstream of the last groyne river bend is located in which effect of the

proposed groynes is negligible. Groynes in Groyne field II are positioned in such a way that their construction augments existing structures on the same location, where river flows in straight section gradually transitioning into the right bend. Flow is deflected towards the left bank and therefore groyne field II has less impact on flow field than previously observed groyne field I. Most significant impact on flow field is visible on the most upstream groyne, which is consistent for all groyne types. Similarly, all groyne types equally affect the flow field, with least visible impact for detached groynes. Upstream river section around groyne fields III and IV is characterized with uniform flow width and flow velocity field distribution, without isolated hotspots. River section at groyne field III is straight, and groyne impact on flow velocity field is significant, causing the shift of the flow towards the left bank. For characteristic discharges $Q_{94\%}$ and $Q_{60\%}$ changes in resulting flow field is similar, independent of groyne types. Largest velocity increase is observed for conventional, smallest for Chevron dikes, while T-shaped groynes and detached groynes have similar impact. Groyne field shadow follows the river continuity into the natural low flow area where flow field is deflected towards the left bank. For Q_{mean} most significant impact on flow field is visible for conventional groynes, and the least for T-shaped groynes. Groynes in the groyne field IV are positioned on the concave river bend at the end of flow bifurcation through port Osijek. Complex flow field on the entrance in the port results with saddle formed river bathymetry where maximum flow velocity wanders from one bank to another. Therefore, primary role of the groynes in this field is not to influence morphologic development, rather to deflect the flow towards the right bank and entrance to the port. Flow expansion on this section is significant and therefore groynes have the least effect on the flow velocity, compared to the other groyne fields. Under $Q_{94\%}$ flow conditions largest velocity increase is observed for conventional groyned, while Chevron dikes, T-shaped groynes and detached groynes have similar impact. Groyne field shadow is relatively because the most downstream groyne is already in the transitioning section where flow attacks the same bank where groynes are positioned. Under $Q_{60\%}$ flow conditions largest velocity increase is observed for conventional groynes, while least impact is observed for Chevron dikes. Under Q_{mean} flow conditions largest velocity increase is observed for conventional groynes and detached groynes, while least impact is observed for Chevron dikes and T-shaped groynes. The following figures show numerical model results for flow velocity field for under Q_{mean} for existing and design state: downstream model (Figure 22 - Figure 26); upstream model (Figure 27 - Figure 31).

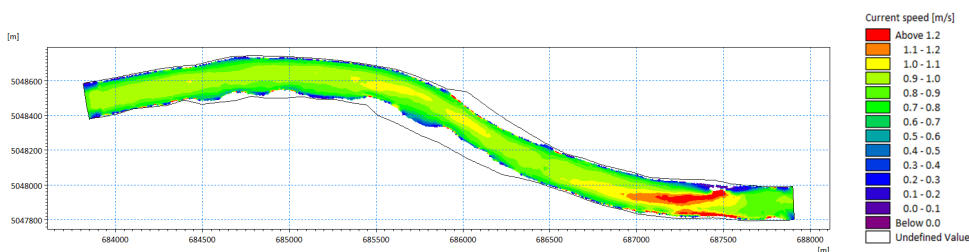


Figure 22. Downstream numerical model results for flow velocity field under Q_{mean} in existing state

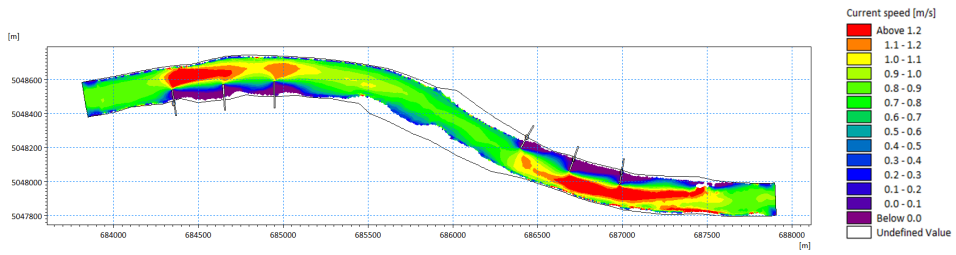


Figure 23. Downstream numerical model results for flow velocity field under Q_{mean} for conventional groynes

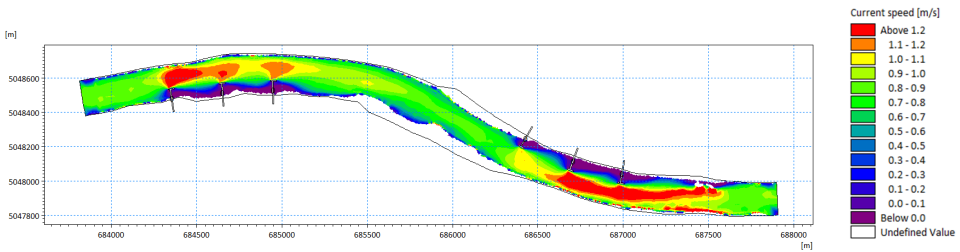


Figure 24. Downstream numerical model results for flow velocity field under Q_{mean} for T-shaped groynes

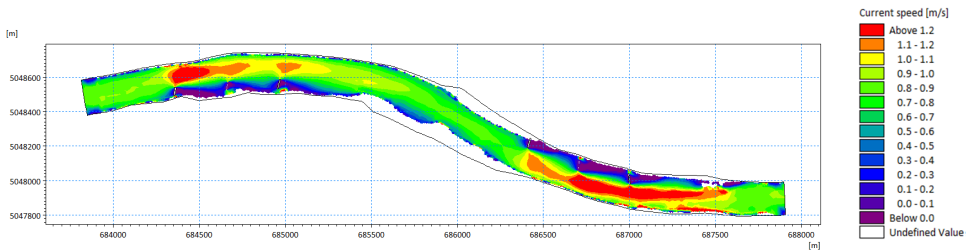


Figure 25. Downstream numerical model results for flow velocity field under Q_{mean} for detached groynes

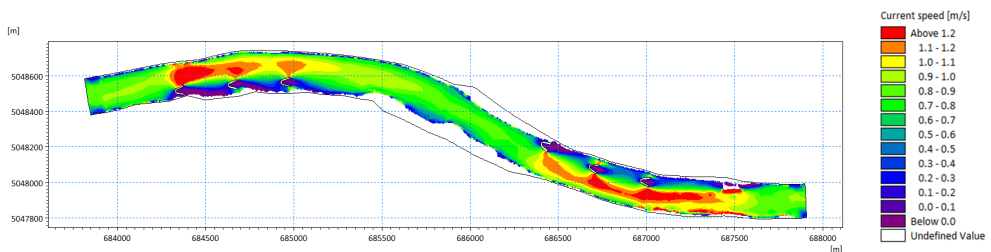


Figure 26. Downstream numerical model results for flow velocity field under Q_{mean} for Chevron dikes

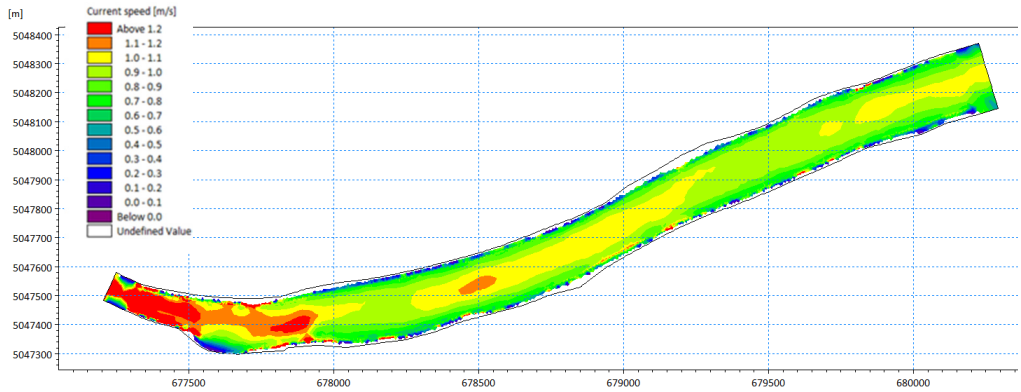


Figure 27. Upstream numerical model results for flow velocity field under Q_{mean} in existing state.

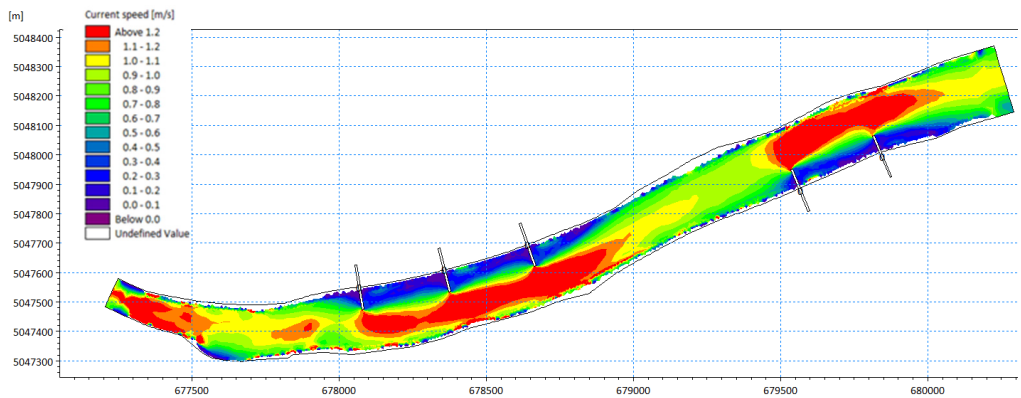


Figure 28. Upstream numerical model results for flow velocity field under Q_{mean} for conventional groynes

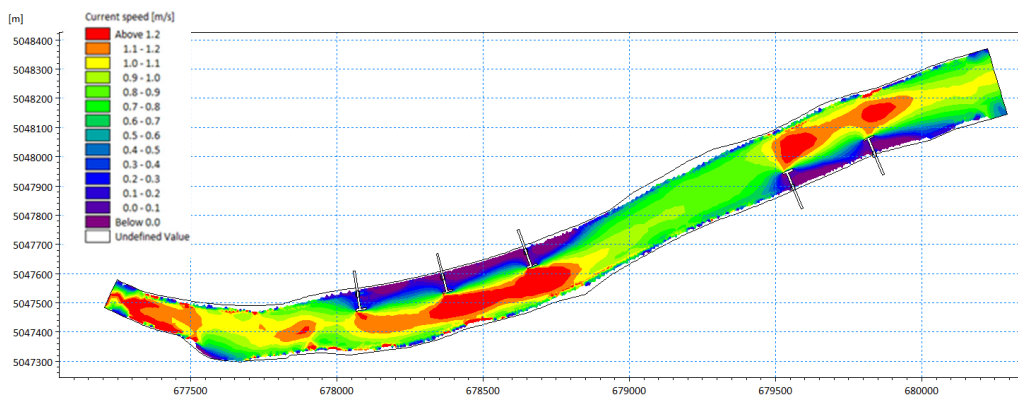


Figure 29. Upstream numerical model results for flow velocity field under Q_{mean} for T-shaped groynes

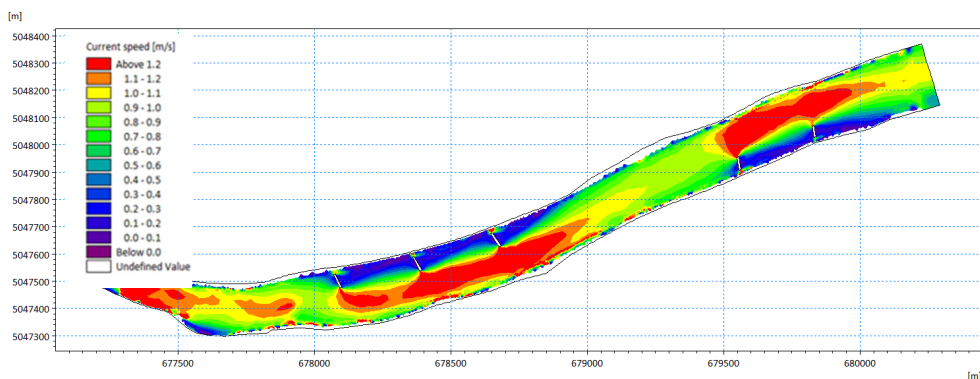


Figure 30. Upstream numerical model results for flow velocity field under Q_{mean} for detached groynes

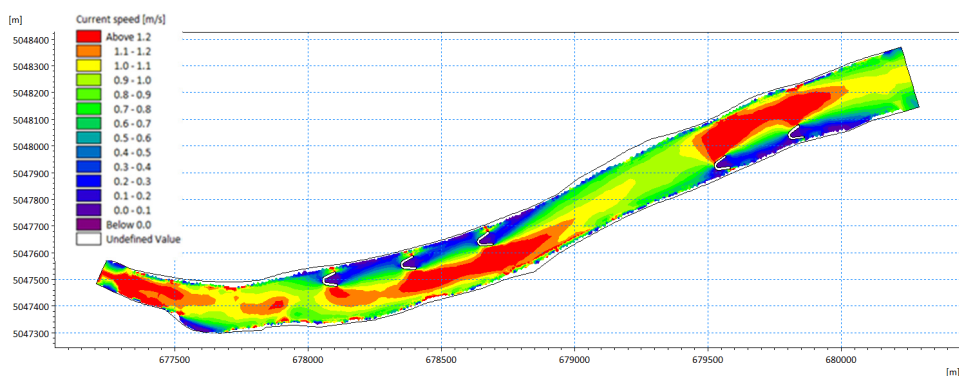


Figure 31. Upstream numerical model results for flow velocity field under Q_{mean} for Chevron dikes

Cross-sectional flow velocity profile analysis is conducted for existing and design state on three characteristic cross-sections of each respective groyne field: upstream of the groyne field, downstream of the groyne field and between individual groynes inside the groyne field. Upstream of the groyne field flow velocity profile is affected only next to the bank where groynes are positioned, i.e. flow is decelerated compared to the existing state, while flow in the river channel remains unaffected. Flow velocity distribution doesn't differ significantly for different types of groynes. Within the groyne field flow velocity profile is completely altered in comparison to the existing state. In the groyne shadow next to the riverbank flow is decelerated, while it is accelerated in the fairway, with little or no difference of flow pattern between different groyne types. Downstream of the groyne field flow velocity profile is completely altered in comparison to the existing state, and flow velocity distribution is similar to the one within the groyne field.

4. Conclusions

This paper presents results of analyses for impact of 4 different types of groynes installed as groyne fields on Drava River flow velocity field characteristics. Numerical models used for flow velocity computations were calibrated and verified using detailed ADCP flow field surveys. For all of the characteristic discharges associated with fairway it is

evident that installation of groyne fields significantly affects the flow velocity field. Groyne influence on flow velocity has global and local effect: globally, groynes cause backwater effect through increased local and friction losses while they locally alter the velocity through acceleration in contracted flow profile. Aforementioned changes in flow velocity distribution enable sediment deposition within the groyne field, thus contracting the flow area during low flows and initiating erosion of the river channel in the fairway zone which secures sufficient fairway geometry under low flow conditions. Maximum flow velocity patterns remain unaffected with groyne installation, due to its placement on the shallow inner bank, which in turn means that there is no additional hydraulic loading on the banks, apart from the design ones. Chevron dikes are shown to have the least effect on the flow velocity field pattern, while conventional ones are shown to have the most effect. Detached groynes have the common positive environmental impact as the Chevron dikes, while at the same time contribute more to the fairway geometry. Therefore, between all analysed structures in this paper detached groynes are estimated as good compromise between achieving environmental and navigational goals in this Drava River section.

References:

- [1] Gilja, G., Kuspilić, N.: Modeling of long-term sedimentation in the Osijek port basin, *14th International Symposium on Water Management and Hydraulic Engineering*, Brno, Czech Republic, 590-600, 2015
- [2] Gilja, G., Jelić, D., Kuspilić, N.: Morphodynamic analyses of the variant river training solutions for the Drava confluence, *7th Croatian water conference – Croatian waters in environmental and nature protection*, Opatija, Croatia, 701-711, 2019
- [3] UniZag: Estimation of sediment yield on critical Drava River sections during concession, Agency for Inland Waterways, Zagreb, 2017
- [4] ICPDR: PLATINA - Manual on Good Practices in Sustainable Waterway Planning, International Commission for the Protection of the Danube River, Vienna, pp. 107, 2010
- [5] Remo, J.W.F., Khanal, A., Pinter, N.: Assessment of chevron dikes for the enhancement of physical-aquatic habitat within the Middle Mississippi River, USA, *Journal of Hydrology*, 501 (2013), 146-162
- [6] Sommer, M., Eberle, M.: Possibilities to improve the ecological status of Federal waterways in Germany: A collection of case studies, Federal Institute of Hydrology, Koblenz, pp. 38, 2009
- [7] Mansoori, A.R.: Study on Flow and Sediment Transport around Series of Spur Dikes with Different Head Shape, Kyoto University, Kyoto, Japan, pp. 167, 2014
- [8] UniZag: Concept of Drava River fairway improvement from the confluence (rkm 0) to port Osijek (rkm 12) – Water regime analysis, Agency for Inland Waterways, Zagreb, 2015
- [9] Gilja, G., Bekić, D., Oskoruš, D.: Processing of Suspended Sediment Concentration Measurements on Drava River, *11th International Symposium on Water Management and Hydraulic Engineering*, Ohrid, Republic of Macedonia, 181-191, 2009
- [10] Gilja, G., Kuspilić, N.: Dune geometry estimation using apparent bedload velocity as predictor variable, *E3S Web of Conferences*, 40 (2018), 02054
- [11] Gilja, G., Kuspilić, N., Potočki, K.: Review of empirical models for estimation of dune field characteristics, *Građevinar*, 69 (2017) 6, 427-436
- [12] UniZag: Monitoring of morphodynamic changes and river training measures for Drava River fairway management at the confluence into Danube, Agency for Inland Waterways, 2017

SENSITIVITY ANALYSIS OF EMPIRICAL EQUATIONS APPLICABLE ON BRIDGE PIERS IN SAND-BED RIVERS

ANTONIJA CIKOJEVIĆ¹, GORDON GILJA², NEVEN KUSPILIĆ³

¹ *University of Zagreb Faculty of Civil Engineering, Croatia, acikojevic@grad.hr*

² *University of Zagreb Faculty of Civil Engineering, Croatia, ggilja@grad.hr*

³ *University of Zagreb Faculty of Civil Engineering, Croatia, kuspa@grad.hr*

1. Abstract

Adverse effect of local scour on bridge safety is well documented throughout the history, most notably in cases when scouring causes bridge collapse. Most straightforward way to assess scour hole depth is to employ one of readily available empirical equations, using flow field and riverbed characteristics as predictor variables. The aim of this paper is to identify empirical equations applicable for pier scour calculation in sand-bed rivers and estimate resulting scour depths. Based on the results sensitivity analysis was conducted in order to quantify range of values that can be expected in specific site conditions for variation in the input variables.

Keywords: local scour, bridge pier, empirical equations, sand-bed rivers, sensitivity

2. Introduction

Croatian rivers are exposed to significant river-bed changes since the last century when the extensive river training works were undertaken on largest Croatian rivers, mainly for flood protection [1] and for water use for industry [2]. Both, natural general river degradation and anthropogenic factors such as installation of river training works [3], construction of dams, weirs and bridges [4] [5] [6] has had significant effect on the sediment transport regime, resulting mostly with deepening of the rivers channel since banks are stabilized [7]. Local scour is phenomenon caused by disturbance of velocity field in vicinity of bridge piers, whose adverse effect on bridge safety is well documented throughout the history, most notably in cases when scouring causes bridge collapse [2] [4] [7]. Scour holes around bridge piers lead to greater depths in vicinity of bridges especially during flood events when scour depth attain the most significant growth [8]. Most straightforward way to assess scour hole depth is to employ one of readily available empirical equations, using flow field and riverbed characteristics as predictor variables [9]. This approach, while it has advantage in its simplicity, also has disadvantages in its limited applicability of each empirical equation overtaken from state of the art literature. In order to reliably estimate scour depth, equations developed for flow environment similar to the one that needs to be estimated in prototype scale must be used. More often than not, several empirical equations will be appropriate for predefined constrictions and decision must be made which one is most suitable for application in specified site conditions.

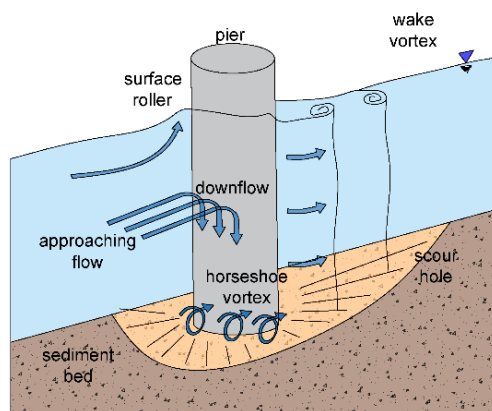


Figure 32. Mechanism of local scour; adapted from [10]

Input data for this research were overtaken from survey database obtained from field measurements [6] [7]. Dataset used in this research was developed using flow rate and depth data from several gauging stations to obtain relevant flow environment conditions encompassing river characteristics with diverse flow regimes. In combination with river cross-section, flow velocity and energy slope can be calculated, thus completing the set of governing hydraulic variables. Hydraulic variables were calculated by using HEC-RAS numerical model for 100-year flood, taking into account detailed bathymetry in the bridge opening.

Focus of this study is testing sensitivity of the empirical equations on scouring around bridge piers on large Croatian rivers: Sava, Drava, Kupa and Danube. The aim of this paper is to identify empirical equations applicable for pier scour calculation in sand-bed rivers and estimate resulting scour depths. Empirical equations used in this paper can be found in commonly used state of the art literature. Based on the results sensitivity analysis was conducted in order to quantify range of values that can be expected in specific site conditions for variation in the input variables.

3. Methods

The estimate of the maximum local scour depth is necessary for designed bridge safety. For this purpose, many theoretical equations have been derived throughout history to predict scour depth d_s at bridge piers. Most of them were derived on scaled models in idealized laboratory conditions which consequently limits applicability of such equations due to the scaling issues. Some of those limiting features that cannot be found in watercourse are [10]:

- Straight rectangular river sections
- Steady uniform approach flows
- Noncohesive, homogeneous and uniform size bed materials

Based on bathymetry survey, HEC-RAS model is established with input parameters from upstream and downstream gauging stations. Results from HEC-RAS hydraulic model are input data in equations for scour depth. From HEC-RAS were extracted mean approach flow velocity (\bar{v}), flow depth (y) and Froude number ($F_r = \bar{v} / (g \cdot y)^{0.5}$). Other

relevant parameters that differ by specific site conditions i.e. pier width (b), median of the sediment particle size distribution (d_{50}), threshold velocity by Laursen criteria (v_c), Froude number for critical velocity (F_{rc}) and flow angle (Θ) are presented in Table 4. In theoretical equations figure a lot of empirical coefficients as follows: mean flow depth and pier width (K_{yb}), flow intensity (K_I), sediment size (K_d), pier shape (K_s), flow angle of attack (K_θ), approach channel geometry (K_G), bed condition (K_b), armouring by bed material size (K_a) and pier width (K_w).

For the calculation of the scour depth, ideally the empirical equation that gives minimum error in the estimation must be chosen [11]. In this research 13 different empirical equations were selected for calculating scour depth on bridge piers in sand-bed rivers: *Laursen* [12], *Hanco* [12], *Inglis* [12], *Neill* [12], *Richardson and Davis* [10], *Breusers* [10], *Jain and Fischer* [10], *Ansari and Qadar* [10], *Larras* [10], *Shen et al* [10], *Melville* [13], *Coleman* [14], and *Ettema et al* [15].

Table 3 List of all equations for sensitivity analysis

Laursen	$d_s = 1,11 \cdot b \cdot \left(\frac{y}{b}\right)^{0,5}$ – live-bed	(1)
	$d_s = 1,34 \cdot b \cdot \left(\frac{y}{b}\right)^{0,5}$ – clear-water	(2)
Hanco	$d_s = 3,3 \cdot b \cdot \left(\frac{d_{50}}{b}\right)^{0,2} \cdot \left(\frac{y}{b}\right)^{0,13}$	(3)
Inglis	$d_s = 4,2 \cdot b \cdot \left(\frac{y}{b}\right)^{0,78} \cdot (Fr)^{0,52}$	(4)
Neill	$d_s = 1,5 \cdot b \cdot \left(\frac{y}{b}\right)^{0,3}$	(5)
Richardson and Davis	$d_s = 2 \cdot b \cdot K_s \cdot K_\theta \cdot K_b \cdot K_a \cdot K_w \cdot \left(\frac{y}{b}\right)^{0,35} \cdot (Fr)^{0,43}$	(6)
Breusers	$d_s = 1,4 \cdot b$	(7)
Jain and Fischer	$d_s = 1,84 \cdot b \cdot \left(\frac{y}{b}\right)^{0,3} \cdot (F_{r,c})^{0,52}$ – clear-water	(8)
	$d_s = 2 \cdot b \cdot \left(\frac{y}{b}\right)^{0,5} \cdot (F_r - F_{r,c})^{0,52}$ – live-bed	(9)
Ansari i Qadar	$d_s = 0,86 \cdot (b_p)^3$ – $b_p < 2,2$	(10)
	$d_s = 3,6 \cdot (b_p)^{0,4}$ – $b_p > 2,2$	(11)
Larras	$d_s = 1,05 \cdot K_s \cdot K_\theta \cdot (b)^{0,75}$	(12)
Shen et al	$d_s = 0,000223 \cdot \left(\frac{v \cdot b}{\nu}\right)^{0,619}$	(13)
Melville	$d_s = K_{yb} \cdot K_I \cdot K_d \cdot K_s \cdot K_\theta$	(14)
Coleman	$d_s = b \cdot 1,49 \cdot \left(\frac{v^2}{g \cdot \nu}\right)^{0,1}$	(15)
Ettema et al	$d_s = 1,34 \cdot (b \cdot y)^{0,5}$	(16)

Laursen recommended equation in which observed parameters are flow depth and pier width. He described formula for scour depth neglecting grain size and approach velocity because it's given for bridge piers set in sand bed and for live-bed scour conditions. Hanco develop simplified formula for general case in which sediment particle size in laboratory flume were $d_{50} = 0.5, 2, 5$ mm. Hanco explicitly included pier widths $b = 3,$

4, 7, 6, 13 and 20 cm by providing required condition $y/b > 1$ (which is case for all bridges). Inglis suggested equation which included the Froude number $F_r = \bar{v} / (g \cdot d)^{0.5}$. Tests were performed on a rectangular round-nosed pier. Neill described scouring with ratio of flow depth and pier width like many other empirical equations. Neill's equation considers live-bed conditions, rectangular round-nosed pier for pier alignment parallel with flow direction. However, the effects of grain size distribution and local conditions should be investigated in more detail. Another experimental equation expressed by Richardson and Davis is modified CSU equation. Equation is based on almost all parameters that influence scour depth throughout 5 empirical coefficients. Considering that equation gives greater deviations for larger particle sizes, the most accurate results are just for sand river-bed. Breusers gave simplified relation expressing scour depth as a function of pier diameter, with neglected water depth and grain size. Although it satisfies basic linear relationship between scour depth and pier dimension, which is considered as essential for model studies. Jain and Fischer bring another formula for local scour depth at the round pier nose under unsteady flow but with distinction whether clear-water or live-bed scour conditions prevail. Ansari and Qadar derived equation on more than 100 field measurements of pier scour depth from 12 different sources. They brought projected pier width into consideration as a consequence of locating bridges in river curvature where flow attack is not parallel to the pier alignment. Larras proposed a design equation for estimating maximum scour depth near the threshold velocity of the undisturbed bed material. Shen et al have analysed flow field and the horseshoe-vortex system near a circular pier and based on that derived formula which indicates that viscosity may affect the scouring phenomenon. Melville's design method rests on product of 5 different coefficients. Equation tends to predict much greater scour depths than other expressions. The scour depth variations under live-bed conditions are a consequence of the particle size distribution at particular flow velocities. As Melville reported, the steeper and higher the bed forms, the lesser the observed scour depth because the sediment supplied with the passage of a given bed form is not fully removed from the scour hole prior to the arrival of the next bed form. Using dimensional analysis Coleman obtained the scour predictive formula for circular piers in sand beds. Formula consider continuous sediment transport conditions. Ettema et al's data show that scour depth, relative to pier width, may increase with pier Froude number. Froude number is useful for describing energy gradients for flow around a pier. The experiments were conducted with velocities lower than critical.

Comparison of the chosen equation was made for seven case studies on large Croatian rivers. For 100-year flow, scouring can occur under live-bed (Drava and Danube) or clear-water conditions (Sava and Kupa) which are defined by mean velocities that are larger than threshold velocity value.

The Botovo bridge is the railway bridge on Drava river near Koprivnica. The bridge is constructed across the bend of the river. Positions of the two round nosed bridge piers are in the main channel and their alignment is deviated 25 degrees of the flow attack which additionally contributes to development of the scour hole. The Osijek bridge is also part of the railway network on the Drava river which piers are round nosed and 9 degrees deviated from flow course. In the past, the bridge was exposed to development of scour holes which were remediated with riprap. This resulted with reducing of flow profile and it led to significant erosion of river bed and phenomenon of scour hole

downstream of remediated pier. The Varaždin bridge is a railway bridge located in Varaždin on the Drava river. All of 5 bridge piers are round nosed, located in the main watercourse and aligned at an angle of 5 degrees to the flow attack. Although the bridge is on a flat stream section, just behind the river starts meandering. The railway bridge Erdut is in Bogojevo in straight section on the Danube river. It is one of the longest bridge on Danube with span of over 600 meters. 5 bridge piers are in the main river channel and 6th is on bank slope. All of 6 bridges are round nosed and aligned parallel to the flow attack. The Karlovac bridge is located in Karlovac on the Kupa river. The bridge has 2 round nosed piers and both are in the main channel. Piers alignment is 3 degrees deviated from flow course. The Gunja is railway bridge in the straight Sava river section. 2 round nosed piers are sited in the main channel of the river and aligned 4 degrees deviated of the flow attack. The Šamac bridge is railway and road bridge on the Sava river that is lying on 14 piers, of which 5 are sited in the main river channel. Although alignment of bridge piers is almost parallel with flow attack, the bridge is preceded by sharp rived bend. All bridges are sited in rivers whose bed are made of sand or mixture of sand and gravel. All other influential parameters from specific site conditions are shown in following Table 4:

Table 4 Input parameters from specific site for calculating scour depths [m]

	BOTOVO	OSIJEK	VARAŽDIN	ERDUT	KARLOVAC	GUNJA	ŠAMAC
v	2.2	2.1	2.4	1.0	1.3	0.9	1.4
y	4.0	7.8	5.6	11.6	8.4	12.5	5.9
Fr	0.27	0.23	0.32	0.09	0.14	0.08	0.14
b	3.5	3.6	2.1	4.2	3.6	4.2	2.3
d50	10	0.25	20	0.7	3	5	20
v _c	1.7	0.5	2.2	0.8	1.3	1.6	2.3
Fr _c	0.27	0.06	0.30	0.08	0.14	0.15	0.30
Θ	25	9	5	0	3	4	1

Boxplot is a visual representation of a given data set through five statistical parameters: minimum, first quartile, median, second quartile and maximum. Boxplot graph gives a good indication of how the values in the data are spread out. The main box present 25th to the 75th interquartile range and contain median line between two parts of box. Other elements of boxplot are whiskers which present minimum and maximum values with 0,35th percentile, as well as the mean value that is illustrated by sign X. Furthermore, if there are some outliers, they are illustrated as points [16]. There is a similar article in literature that describes local scouring around complex bridge piers established in laboratory by using boxplot [17]. The purpose of presenting boxplot in that paper was to show variability of a ratio between depth of scour hole and pier width. Most of articles about scouring statistically process database representing graphs that have predicted scour hole and pier width ratio on the ordinate and approaching flow depth and pier width ratio on the abscissa. Moreover, usual graphs bring particle size and development time in correlation with scour depth. [12], [15], [14]

4. Results and discussion

In order to determine the most applicable equations for specific sites, results of the

theoretical scour depths are shown in Table 5 for all bridges. Moreover, data were analysed using statistical method called box plot, presented in Figure 33. Box plot display variation of data through their quartiles. The aim of this paper is to analyse sensitivity by quantifying range of values that can be expected in specific site conditions for equation variations.

Table 5. Scour depths [m] obtained by using empirical formulas

	Botovo	Osijek	Varazdin	Erdut	Karlovac	Gunja	Šamac
Laursen	4.2	5.9	3.8	7.8	7.4	9.7	5.0
Neill	5.5	6.9	4.3	8.6	7.0	8.7	4.6
Inglis	8.3	12.9	10.5	11.2	10.5	11.1	7.3
Richardson and	5.4	10.2	7.4	8.5	7.3	8.9	4.5
Hanco	3.7	1.9	3.1	2.8	3.2	4.2	3.3
Jain	6.8	8.4	5.2	10.5	8.5	10.7	5.7
Melville	14.7	10.9	6.0	10.1	9.3	11.3	5.9
Breusers	5.0	5.1	3.0	5.9	5.0	5.9	3.2
Ansari and Qadar	9.0	6.9	5.4	6.4	6.3	6.8	5.2
Larras	5.3	3.4	2.2	3.1	2.9	3.4	2.1
Coleman	4.3	4.1	2.5	3.9	3.6	3.8	2.5
Shen et al	4.1	4.1	3.1	2.8	2.9	2.7	2.4
Ettema et al	5.06	7.13	4.62	9.36	7.37	9.69	4.96
Average:	6.1	6.4	4.6	6.6	6.0	6.8	4.1
Standard deviation:	3.0	3.2	2.3	2.9	2.4	2.7	1.4

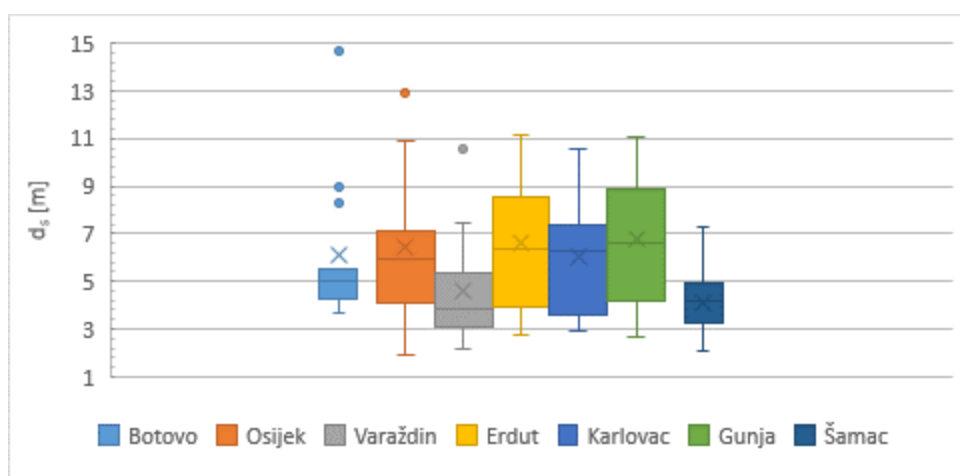


Figure 33. Boxplot of whole dataset presenting distribution of the scour depth

Based on the conducted analysis, some of the used equations exhibit similar output pattern independently of the bridge on which it was deployed: equations of Inglis and Melville predict the highest values of scour depth across all bridges, while the lowest

values are predicted by the equations Hanco, Larras and Shen et al. Inglis's equation predicts scour on average 79% greater than the mean value of all equations, and 86% for reduced dataset from which aforementioned 5 equations are excluded. In the same regard, Melville's equation predicts scour on average 47% and 54% greater compared to entire and reduced dataset, respectively. Hanco's, Larras's and Shen et al.'s empirical equations predict scour on average 43%, 45% and 45% lower compared to entire dataset, and 41%, 42% and 42% lower compared to reduced dataset.

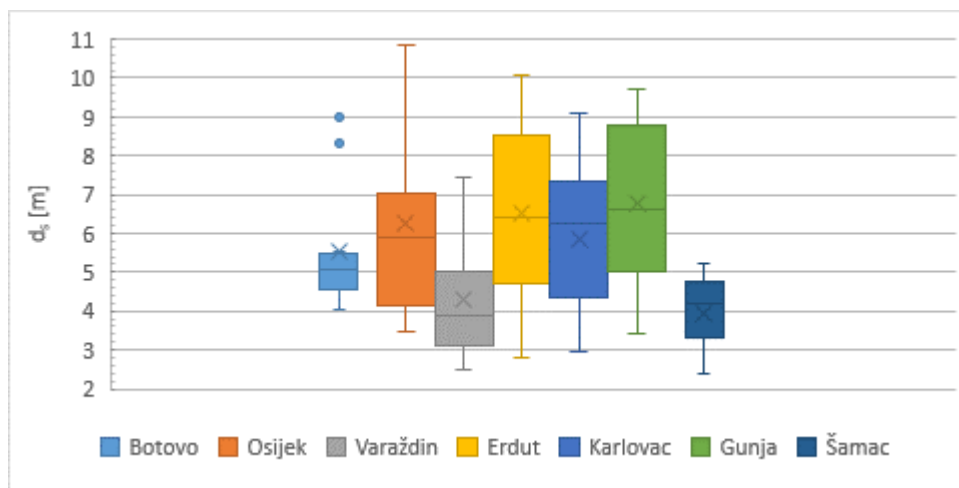


Figure 34. Boxplot presenting reduced dataset distribution of the scour depth

Taking into account the results from conducted analyses, it can be concluded that aforementioned equations cannot be used for specific site to reliably predict scour depth, considering the deviation from expected values. Observing standard deviation that is presented in Table 5, the greatest dispersion of results can be noticed for Drava-Osijek bridge, and the lowest for Sava-Šamac bridge. Many factors can be reasons for such deviations. Primary reason for sensitivity of specific site could be bed characteristics and different composition of bed material mixture. Secondary reason could be technique of remediation of scour holes that has led to secondary scour hole downstream of the pier. [18] Third reason could be quantification of approaching flow using averaged values of flow rate, flow depth, velocity, etc. Similar results have been presented in other papers [13], [12].

Results of the analyses show that the Laursen, Neill, Richardson and Davis, Jain and Fischer, Ansari and Qadar, Breusers and Coleman equations can be used as first approximation for the reliable local pier scour calculation. The following equations estimate both similar scour depths with near average values at the same time: Ansari and Qadar, Jain and Fischer, Ettema et al and Neill. Common for these equations is that they contain few easily calculated parameters that make their use simple and straightforward. However, it is found that considering all equations sensitivity of results are in range of 3 to 7 meters, which is considerable span compared to the depth of the pier foundation. Some of the reasons for large span of results are phenomenon of secondary scour hole downstream of the pier. Furthermore, none of empirical equations used in scour calculation is applicable to all analysed sites because every site has specific hydraulic environment and geometry, both for riverbed and piers.

5. Conclusion

In conclusion, there is no universal equation that provides reliable results for all analysed bridge sites. Although all bridge sites correspond to equations established for specific flow depth and pier width ratio as well as for sand bed rivers at suitable sediment transport conditions, some of those sites are more sensitive in selecting suitable equation and gives greater dispersion of results. Planned follow-up of this paper is to conduct analyses of recorded scour depths and produce empirical equation that would be suitable for bridges over Croatian rivers, and others with similar flow regime and riverbed material characteristics.

References:

- [1] Bašić, K., Gilja, G., Bujak, D., Kuspilić, N.: Design criteria for levees, *10th Eastern European Young Water Professionals Conference - New Technologies in Water Sector*, Zagreb, Croatia, pp. 27-33, 2018
- [2] Gilja, G., Oskoruš, D., Kuspilić, N.: Erosion of the Sava riverbed in Croatia and its foreseeable consequences, *BALWOIS Conference on Water Observation and Information System for Decision Support*, Ohrid, Republic of Macedonia, pp. ffp-1826(p9), 2010
- [3] Gilja, G., Kuspilić, N., Bekić, D.: (Chapter), *Impact of morphodynamical changes on the bridge stability: Case study of Jakuševac bridge in Zagreb*, (ur. Sawicki, J.M.& Zima, P.), Gdansk University of Technology, Gdansk, pp. 112-122, 2011
- [4] Kuspilić, N., Bekić, D., Gilja, G., McKeogh, E.: Monitoring of river channel morphodynamical changes in the zone of bridge piers, *First International Conference on Road and Rail Infrastructure (CETRA 2010)*, Opatija, Croatia, pp. 107, p8, 2010
- [5] Gilja, G., Kuspilić, N., Tečić, D.: Morphodynamic impact of scour countermeasures on riverbed topography, *15th International Symposium Water Management and Hydraulics Engineering*, Primošten, Croatia, pp. 176-183, 2017
- [6] Kuspilić, N., Gilja, G.: Influence of watercourse flow on bridge safety, *e-Zbornik: Electronic collection of papers of the Faculty of Civil Engineering*, **8** (2018) 16, pp. 26-41
- [7] Gilja, G., Kuspilić, N., Bekić, D.: Influence of riverbed degradation on bridge safety, *Congress of Croatian builders 2012*, Cavtat, Croatia, pp. 795-806 2012
- [8] Tabarestani, M.K., Zarrati, A.R.J.K.J.o.C.E.: Local scour calculation around bridge pier during flood event, **21** (2017) 4, pp. 1462-1472
- [9] Gilja, G., Marić, M., Kuspilić, N.: Calculation of local scour at bridges over large Croatian rivers, *Geophysical Research Abstracts - EGU General Assembly 2019*, **21** (2019) pp. EGU2019-1917
- [10] Melville, B.W., Coleman, S.E.: *Bridge Scour*, Water Resources Publications, 2000
- [11] Mohammad, T., Megat Mohd Noor, M.J., Ghazali, A.: *Validation of Some Bridge Pier Scour Formulae Using Field and Laboratory Data*, 2005
- [12] Ghorbani, B.: *A Field Study of Scour at Bridge Piers in Flood Plain Rivers*, 2008
- [13] Gaudio, R., Grimaldi, C., Tafarojnoruz, A., Calomino, F.: *COMPARISON OF FORMULAE FOR THE PREDICTION OF SCOUR DEPTH AT PIERS*, 2010
- [14] Breusers, H.N.C.: Lecture notes on local scour, pp. 1979
- [15] Junke Guo, O.S., Haoyin Shan, and Jerry Shen: Pier Scour in Clear-Water Conditions with Non-Uniform Bed Materials, pp. 62, May 2012
- [16] boxplot: Towards Data Science, <https://towardsdatascience.com/understanding-boxplots-5e2df7bcbd51>, 3.7.2019.,
- [17] Amini Baghbadorani, D., Ataie-Ashtiani, B., Beheshti, A., Hadjzaman, M., *et al.*: Prediction of current-induced local scour around complex piers: Review, revisit, and integration,

Coastal Engineering, **133** (2018) pp. 43-58

- [18] Board, T.R., National Academies of Sciences, E., *Medicine: Countermeasures to Protect Bridge Piers from Scour*, The National Academies Press, 2007

EROSION SEVERITY ESTIMATION USING MULTI-CRITERIA ANALYSIS

NEVENA DRAGIČEVIĆ¹, BARBARA KARLEUŠA²

¹ *University of Rijeka, Faculty of Civil Engineering, Croatia, nevena.dragicevic@uniri.hr*

² *University of Rijeka, Faculty of Civil Engineering, Croatia, barbara.karleusa@uniri.hr*

1. Abstract

On the case study of Dubračina River catchment (situated in the Vinodol Valley, County of Primorsko-Goranska, Croatia) two MCA methods: SAW (as a simple method) and AHP (as a pairwise comparison method), are applied to estimate the erosion severity of 12 sub-catchments prone to erosion. The results are compared and verified using Erosion Potential Method (EPM) on the case study. Both methods have given similar results and have pointed to sub-catchments more effected by soil erosion. AHP method has given slightly better results in comparison to EPM method results than SAW method. Overall for both methods the results differ in somewhat to EPM result but this can be improved by integrating more criteria into MCA analysis.

Keywords: multi-criteria analysis, erosion, severity, water, management

2. Introduction

The soil erosion and the investigation on erosion processes have been the topic of the scientific research for many decades and still are [1]. In recent decades there has been a significant development of erosion assessment methods that simultaneously followed the development of computer technologies, thus enabling more detailed information on topography, land use and vegetation cover. The concept behind these models differs extremely, wherein each model integrates different scientific methods and modelling approaches [1].

Water erosion models differ not only in the output information they provide (e.g. erosion sediment production, sediment transportation and/or erosion intensity) but also in terms of complexity, a process considered and the data required for model calibration and model use [2]. According to [3] till today there hasn't been a model that best fits all catchments and all purposes but when choosing a model one needs to consider the initial purpose of the model and the catchment characteristics among other factors affecting the model selection.

Multi-criteria analysis has been applied worldwide in the various soil erosion related problems [4 – 7]. Vulević et al. [7] applied AHP (Analytic hierarchy process) and TOPSIS (Technique for Order Preference by Similarity to Ideal Solution) MCA methods with the purpose to identify areas vulnerable to soil erosion that are in need for conservation measures in the Topčiderska River Catchment in Serbia. They used three

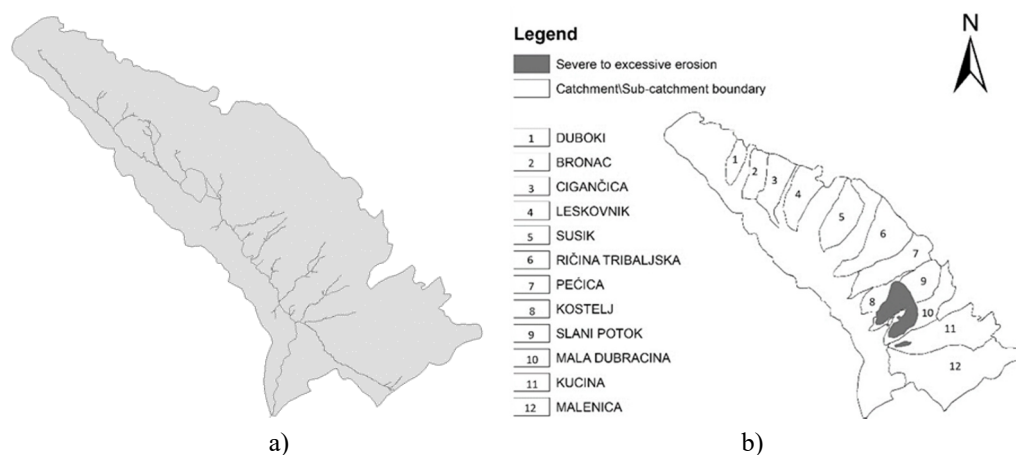
criteria: (i) mean sub-watershed slope, (ii) land use and (iii) soil type. Their research has shown strong correlation between the ranking results of applied multi-criteria analysis (MCA) methods. Rezaian and Jozi [8] used MCA to identify environmental risk on Karoon 3 dam during its construction in Iran using AHP and TOPSIS too. Their analysis has pointed a high risk of erosion and sedimentation. Another research related to erosion vulnerability was conducted by Pal [9] on the Chandrabhaga River catchment in West Bengal. They applied WLC (weighted linear combination method) using six parameters: slope, soil texture, land cover, drainage frequency, rainfall, and proximity to stream link. RUSLE method was used to quantify soil loss production in the catchment and for the model verification using comparison of RUSLE with vulnerable areas defined by WLC.

Similar research was conducted in Spanish mountain olive plantations by Nekhay et al. [10]. ANP (Analytic Network Process) was used for the evaluation of soil erosion risk and Benisagar dam catchment system in India [4]. A spatial decision support system (SDSS) was applied in Ethiopia [11]. It combined multi-criteria and multi-objective decision analysis. Several criteria were used such as land cover-land use, altitude, potential erosion, proximity to roads, water and the relative soil protective capacity of crop. ELimination and Choice Expressing REality (ELECTRE III) method was applied in Normandy, France to identify erosion risk and with an aim to make decision making process easier [12].

This paper has the aim to evaluate the application of different multi-criteria methods as the erosion intensity/severity preliminary estimation in the river catchments. Two different MCA methods were applied (Simple Additive Weighting - SAW and Analytic Hierarchy Process - AHP) and their result compared with the erosion coefficient, the output of Erosion Potential Model (EPM), a method used for estimation of erosion severity and sediment production [2].

2.1 Case study

Dubračina catchment, is situated in Primorsko-Goranska County in Croatia. It has a size of 43 km². The main river Dubračina has 12 torrential tributaries: Duboki, Bronac, Cigančica, Leskovnik, Susik, Ričina Tribaljska, Pečica, Kostelj, Slani Potok, Mala Dubračina, Kučina and Malenica (Figure 1).



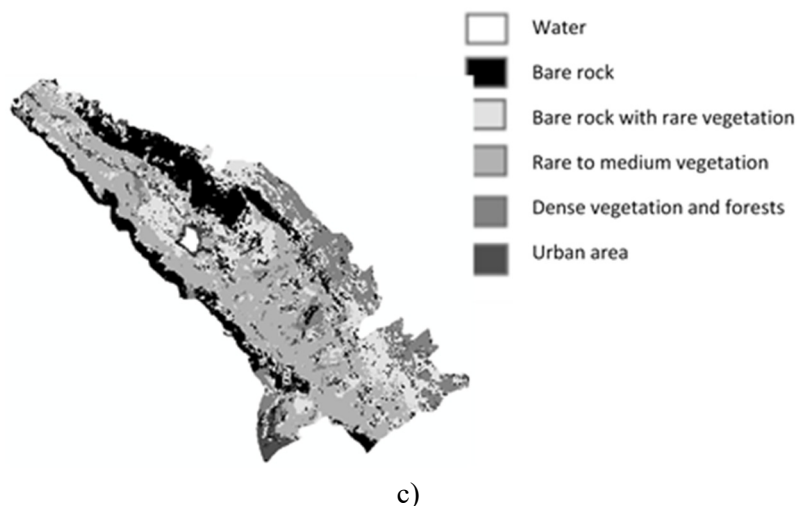


Figure 1. Dubračina catchment: (a) river network, (b) sub-catchments and areas covered with excessive erosion processes [13]; (c) Land cover

The characteristics of the Dubračina catchment and its sub-catchments are given in Table 1.

Table 1. Characteristic of Dubračina catchment and its sub-catchments

TRIBUTARY	Area [km ²]	River/Tributary length	Average slope [%]	Average Elevation [masl]	Excessive erosion affected areas [% of sub-catchment area]
Duboki	0.67	0.96	44.85	342.5	0
Bronac	0.99	1.62	41.33	293.3	0
Cigančica	1.49	3.03	42.31	298.0	0
Leskovnik	1.62	0.87	44.70	384.5	0
Susik	1.93	0.78	40.47	418.9	0
Ričina Tribaljska	2.74	1.71	34.83	428.5	0
Pečica	2.23	2.32	29.59	385.4	0
Kostelj	0.82	1.04	18.76	128.7	11.07
Slani Potok	2.21	3.22	33.78	358.4	38.5
Mala Dubračina	2.09	3.0	29.29	341.5	28.08
Kučina	3.29	1.52	24.75	438.1	1.89
Malenica	5.54	4.0	26.60	341.8	0
Dubračina catchment	43.5	13.69 (River Dubračina) 40.23 (overall)	32.44	303.1	4.42

2 Methods

2.1 Erosion Potential Method

The Erosion Potential Method, also known as Gavrilović method is used worldwide for erosion intensity and sediment production assessment. The method encompasses erosion mapping, sediment quantity estimation and torrent classification. In this paper only one model output, Erosion coefficient Z (Eq. 1) will be used for the verification and comparison of MCA methods application results.

$$Z = Y * X_a * (\phi + \sqrt{J_a}) \quad (1)$$

where

Z – erosion coefficient

Y – soil erodibility coefficient [-]

X_a – soil protection coefficient [-]

ϕ – coefficient of type and extent of erosion

J_a – average slope of the study area

Input parameters soil erodibility coefficient, soil protection coefficient and coefficient of type and extent of erosion are based on soil type, land cover (Figure 1c) and visual and noted signs of erosion processes in the catchment (Table 1).

EPM erosion coefficient model output provides estimation on erosion intensity in the area of interest classifying the area in five categories by erosion severity: very slight erosion (value 0-0.2), slight erosion (value 0.2-0.4), medium erosion (value 0.4-0.7), severe erosion (value 0.7-1.0) and excessive erosion (value ≥ 1.0).

2.2 AHP

Analytic Hierarchy process (AHP) is a priority method applicable to problems that can be represented by a hierarchical structure [14,15] where the hierarchy consists of the goal at the highest level, one level lower are criteria and even lower sub-criteria, while the lowest level is represented by alternatives. AHP method is based on estimating relative priorities (weights) of criteria and alternatives on which pair-wise comparison criteria matrix and pair-wise comparison alternatives matrices (one matrix for each criterion) are generated. The matrices are normalized in order to calculate the priority weightings for criteria and for alternatives on the basis of each criterion. Combining the criteria priorities and the priorities of each alternative relative to each criterion enables the development of an overall priority ranking of the alternatives. Pairwise comparison of criteria and of alternatives is done using the scale presented in Table 2.

Table 2. AHP pair-wise comparison scale [15]

Intensity of weight, importance, preference	Definition
1	Equal importance (no preference)
3	Moderate importance (moderate preference)
5	Strong importance (strong preference)
7	Very strong importance (very strong preference)
9	Extreme importance (extreme preference)
2, 4, 6, 8	Intermediate values

2.3 SAW

Simple additive weighting (SAW) is the best known and widely used method for MCA for its simplicity. It is also known as weighted linear combination or scoring method. The method is based on evaluating each alternative by each criterion and multiplying this value with the importance (weight) of that criteria, and finally summarising these

products to calculate the alternative overall evaluation score [16].

2.4 MCA Input Data

For the purpose of MCA analysis four parameters are used:

1. Average slope of the sub-catchment
2. Visual signs and extent of excessive erosion in the sub-catchment
3. Soil erodibility coefficient Y
4. Soil protection coefficient X_a

These four parameters are equivalent to the parameters used for the calculation of erosion coefficient in the EPM method. Soil erodibility coefficient and soil protection coefficient are based on EPM and used in both MCA and EPM methods (Figure 2 and Table 3).

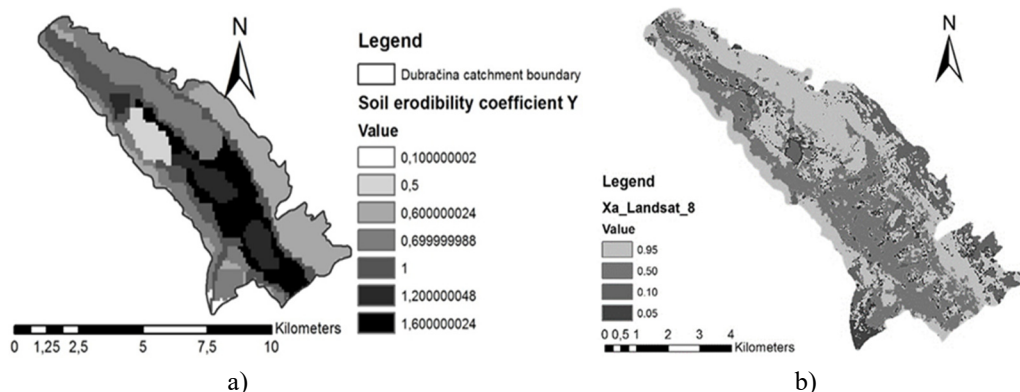


Figure 2. (a) Soil erodibility coefficient Y (b) Soil protection coefficient X_a

For evaluating parameters with SAW method the scale 1 to 5 was chosen, with 1 representing the less prone to erosion and 5 highly prone to erosion (Table 4).

Table 3. Average soil erodibility coefficient and soil protection coefficient on sub-catchments

TRIBUTARY	Soil protection coefficient Y [-]	Soil protection coefficient X_a [-]
Duboki	0.82	0.38
Bronac	0.83	0.37
Cigančica	0.85	0.32
Leskovnik	0.86	0.33
Susik	0.81	0.25
Ričina Tribaljska	0.95	0.30
Pečica	1.08	0.34
Kostelj	1.38	0.44
Slani Potok	1.15	0.26
Mala Dubračina	1.12	0.34
Kučina	0.85	0.31
Malenica	1.05	0.36

Table 4. SAW scale for MCA analysis

Soil erodibility coefficient [Y]	Scale [1-5]	Soil protection coefficient [Xa]	Scale [1-5]	Average slope [%]	Scale [1-5]	Visual signs and extent of excessive erosion [% of sub-catchment area]	Scale [1-5]
0.2-0.6	1	0.05-0.19	1	0-14.9	1	0-0.99	1
0.6-1.0	2	0.2-0.39	2	15-19.9	2	1-9.99	2
1.0-1.3	3	0.4-0.59	3	20-26.9	3	10-19.99	3
1.3-1.8	4	0.6-0.79	4	27-34.9	4	20-29.99	4
1.8-2.0	5	0.8-1.0	5	> 35.0	5	>30	5

3. Results and discussion

The evaluation process and results for the analysis using SAW method are presented in Table 5. As it can be seen sub-catchments Kostelj, Slani Potok and Mala Dubračina are the most prone to soil erosion according to SAW.

Table 5. SAW evaluation and results

		Soil erodibility coefficient	Soil protection coefficient	Average slope	Visual signs of excessive erosion	Result
Weight [1-100]		25	45	25	5	
TRIBUTARY	Duboki	2	2	5	1	270
	Bronac	2	2	5	1	270
	Cigančica	2	2	5	1	270
	Leskovnik	2	2	5	1	270
	Susik	2	2	5	1	270
	Ričina Tribaljska	2	2	4	1	245
	Pećica	3	2	4	1	270
	Kostelj	4	3	2	3	300
	Slani Potok	3	2	4	5	290
	Mala Dubračina	3	2	4	4	285
	Kučina	2	2	3	2	225
	Malenica	3	2	3	1	245

In the flowing table (Table 6) AHP pair-wise criteria weights are presented and result of AHP application are shown in Table 7 and Figure 3 along with results form SAW and EPM. According to conducted analysis using AHP method sub-catchments Kostelj, Mala Dubračina and Slani Potok are the most prone to soil erosion. This results corresponds to results obtained using SAW method.

The small difference between the criteria weights in SAW and AHP are the result of pair – wise criteria comparison in AHP.

When comparing AHP and SAW results with EPM erosion coefficient, Slani Potok is the only sub-catchment that is in all three applied methods among three most prone sub-

catchments. Although, Mala Dubračina is not in the three most prone to erosion sub-catchments according to EPM model, for erosion assessment it is also the catchment with noted excessive erosion by visual on field survey.

Table 6. AHP pair-wise criteria weights

	Soil erodibility coefficient	Soil protection coefficient	Average slope	Visual signs of excessive erosion
Weight	0.2346	0.4488	0.2346	0.0819

Table 7. Comparison of SAW, AHP and EPM results

TRIBUTARY	EPM (Erosion coefficient Z)	SAW	AHP
Duboki	0.297	270	0.1005
Bronac	0.272	270	0.0923
Cigančica	0.29	270	0.0685
Leskovnik	0.388	270	0.0799
Susik	0.334	270	0.0413
Ričina Tribaljska	0.216	245	0.0440
Pečica	0.178	270	0.0620
Kostelj	0.211	300	0.1744
Slani Potok	0.315	290	0.1127
Mala Dubračina	0.275	285	0.1213
Kučina	0.204	225	0.0323
Malenica	0.236	245	0.0706

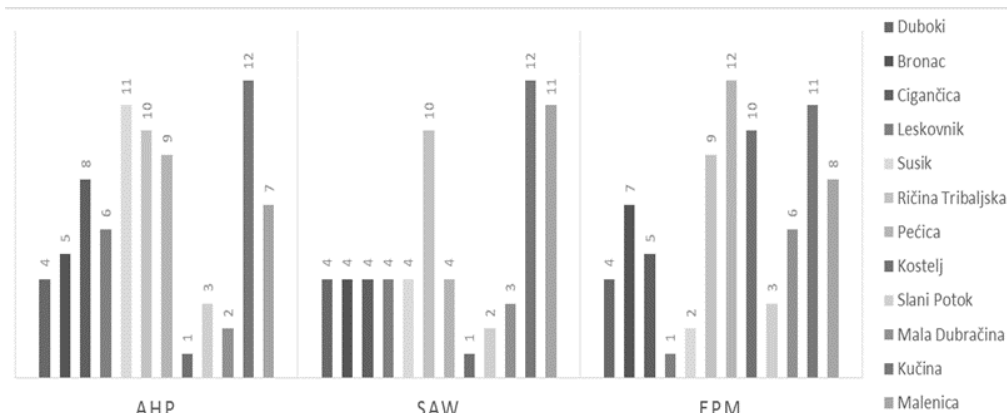


Figure 3. Comparison of results

4. Conclusion

The analysis has shown that MCA can be a very useful tool for preliminary erosion assessment. Both methods have given similar results and have pointed to sub-catchments more effected by soil erosion. AHP method has given slightly better results in comparison to EMP method results so based on that it can be concluded that AHP method corresponds better to EPM results than SAW method. Overall in both methods results differ in somewhat to EPM result but this can be improved by integrating more

criteria into MCA analysis such as rainfall, temperature, and etc.

Acknowledgements

This research was conducted within the University of Rijeka funded projects: Implementation of innovative methodologies, approaches and tools for sustainable river basin management (uniri-tehnic-18-129 5570) and Hydrology of water resources and risk identification of flooding and mudflows in the karst areas (uniri-tehnic-18-54 5766).

References:

- [1] Thiemann S.D.: Detection and Assessment of Erosion and Soil Erosion Risk in the Watershed of the Bilate River-Southern Ethiopian Rift Valley, PhD thesis, Freie University Berlin, Institute for Geographic Sciences, Berlin, 2006.
- [2] de Vente, J. and Poesen, J.: Predicting soil erosion and sediment yield at the basin scale: scale issues and semi-quantitative models, *Earth-Science Reviews*, 71, 1-2, pp. 95-125, 2005.
- [3] Merritt, W., Letcher, R., Jakeman, A.: A review of erosion and sediment transport models, *Environmental Modelling & Software*, 18, 8-9, pp. 761-799, 2003.
- [4] Jaiswal, R.K, Ghoshm N.C., Galkate, R.V., Thomas, T.: Multi criteria decision analysis (MCDA) for watershed prioritisation, *Aquatic Procedia*, 4, pp. 1553-1560, 2015.
- [5] Chowdary, V.M., Chakraborty, D., Jeyaram, A., Krishna Murthy, Y.V.N., Sharma, J.R., Dadhwal, V.K.: Multi-criteria decision making approach for watershed prioritisation using analytic hierarchy process technique and GIS, *Water Resource Management*, 27, pp. 3555-3571, 2013.
- [6] Saini, S.S., Jangra, R., Kaushik, S.P.: Vulnerability assessment of soil erosion using geospatial techniques a pilot study of upper catchment of Markanda River, *International Journal of Advancement in Remote Sensing, GIS and Geography*, 3, 1, pp. 9-21, 2015.
- [7] Vulević, T., Dragović, N., Kostandinov, S., Belanović Simić, S., Milovanović, I.: Prioritization of soil erosion vulnerability areas using multi-criteria analysis methods, *Polish Journal of Environmental Studies*, 24, 1, pp. 317-323, 2015.
- [8] Rezaian, S., Ali Jozi, S.: Environmental risk analysis by using multi-criteria decision making method (case study: Karoon 3 dam of Iran), in: *Proceedings of the 2nd International conference of environmental engineering and application IPCBEE*, vol. 17, Singapore, pp. 159-163, 2011.
- [9] Pal, S.: Identificaiton of soil erosion vulnerable areas in Chandrabhaga river basin: a multi-criteria decision approach, *Modelling Earth Systems and Environment*, 2, 5, pp. 1-11, 2016.
- [10] Nekhay, O., Arriaza, M., Boerboom, L.: Evaluation of soil erosion risk using Analytic Network Process and GIS: A case study from Spanish mountain olive plantations, *Journal of Environmental Management*, 90, pp. 3091-3104, 2009.
- [11] Dragan, M., Feoli, E., Ferneti, M., Zerihun, W.: Application of a spatial decision support system (SDSS) to reduce soil erosion in northern Ethiopia. *Environmental Modelling & Software*, 18, pp. 861-868, 2003.
- [12] Macary, F., Ombredane, D., Uny D.: A multicriteria spatial analysis of erosion risk into small watersheds in the low Normandy bocage (France) by ELECTRE III method coupled with a GIS, *International Journal of Multicriteria Decision Making*, 1, 1, pp. 25-48, 2010.
- [13] Dragičević, N., Karleuša, B., Ožanić, N.: Different approaches to estimation of drainage density and their effect on the erosion potential method, *Water*, 11, 3, pp.1-14, 2019.
- [14] Saaty, T. L.: *Fundamentals of Decision Making and Priority Theory*, RWS Publications, Pittsburg, USA, 1994.

- [15] Saaty, T. L.: The Analytic Hierarchy Process, second edition, RWS Publications, Pittsburg, USA, 1996.
- [16] Abdullah, L., Adawiyah, C.W.R.: Simple additive weighting methods of multi criteria decision making and applications: a decade review, International Journal of Information Processing and Management, 5, 1, pp. 39-49, 2014.

INTERNAL EROSION INCIDENT AT THE WEIR SLUICE

JAROMÍR ŘÍHA¹, TOMÁŠ JULÍNEK²

¹*Faculty of Civil Engineering, Brno University of Technology, Veveří 95, 602 00 Brno, Czech Republic, riha.j@fce.vutbr.cz*

²*Faculty of Civil Engineering, Brno University of Technology, Veveří 95, 602 00 Brno, Czech Republic, julinek.t@fce.vutbr.cz*

1. Abstract

On 11 June 2018, the Hubalov weir suddenly collapsed close to the right abutment at the vicinity of small hydropower plant. Detailed assessment of available data including the video record of the collapse was carried out. Two potential seepage paths were identified, one below the sluice gate and the second one between the sluice and the hydropower plant. In the paper, the hydraulic structure is described and the log of historical events at the structure is compiled. Possible reasons of the failure are identified and discussed based on the available data and detailed site investigation after the collapse.

Keywords: weir, small hydropower plant, seepage, piping

2. Introduction

The Hubalov weir is located in the north of the Czech Republic at the Jizera River that is the right bank tributary of the Elbe River. The purpose of the weir is river slope stabilization and generation of hydropower. The hydraulic structure consists of 93.6 m long and 10.3 m weir body. The height of the weir is 1.56 m. At the right bank, the weir is equipped with the gated sluice. This serves for flushing down the gravel deposited in front of the inlet to the small hydropower plant located at the right bank of the Jizera river (Figures 1, 2).

Due to the minor significance and low potential consequences in case of weir collapse, it has been classified as a hydraulic structure of the category IV, i.e. the lowest consequence class with only limited extent of surveillance and measurements.

The weir was built in 1877 as a fixed weir with the mill equipped with two water wheels. In 1903, the mill was transferred into the hydropower plant (HPP) with two Francis turbines. During the 19th century, several improvements and changes were carried out at the scheme, the most important of which was establishing the sheet pile wall along the upstream toe of the weir and constructing the sand sluice equipped with the slide gate (1957/58). However, the sheet pile wall was not prolonged along the sluice and inlet to the hydropower plant.

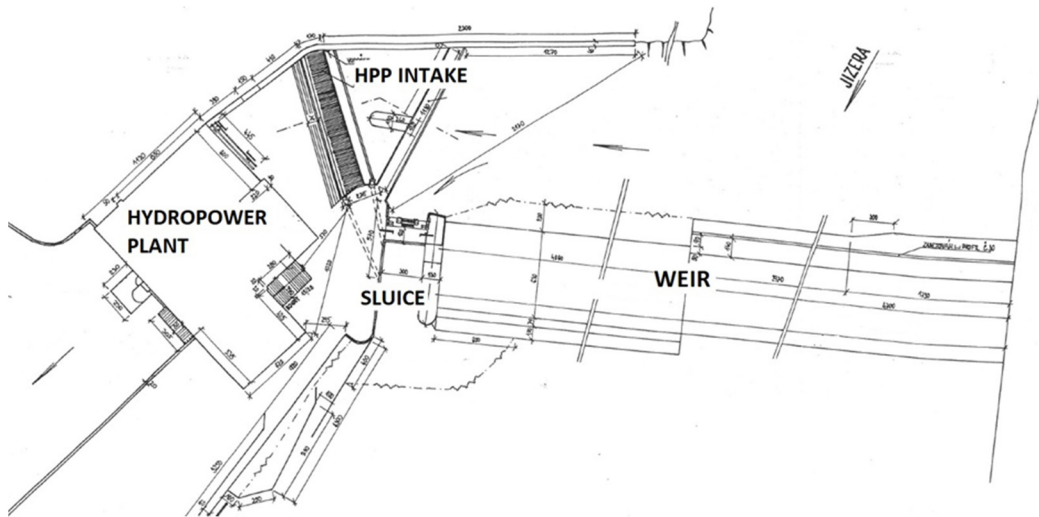


Figure 1. The layout of the weir



Figure 2. The layout of the scheme before the reconstruction in 1957/58

3. Description of the scheme

3.1 Geological conditions

The geological conditions at the site are only poorly documented. The overall geological map shows glauconitic calcareous-clayey sandstones that on the left bank of the Jizera river outcrop to the terrain (Figure 3). Towards the right bank, permeable gravels and

sandy gravels overlay the sandstone. The thickness of permeable layer was documented to be exceeding 6 m.

With this knowledge, the original documentation of the weir is rather confusing when expecting the sandstone just at the foundation joint of the weir and hydropower plant.

3.2 Weir

The weir body was originally composed of timber frame filled with quarry stone; the overflow surface was made of stone paving.

During the reconstruction at the years 1957-1958 the weir was equipped with 6 m deep sheet pile wall along the upstream toe of the weir and with 0.3-0.7 m thick concrete slab at the overflow section. During the service life of the weir the structure suffered by cavities below the concrete slab causing its cracks. This resulted in repairs of the weir in years 1972 and 1985.



Figure 3. The sandstone outcrops at the left bank of the Jizera River

3.3 Sluice

The sand sluice equipped with the slide gate (Figure 4) was built during the weir reconstruction in 1957-1958.

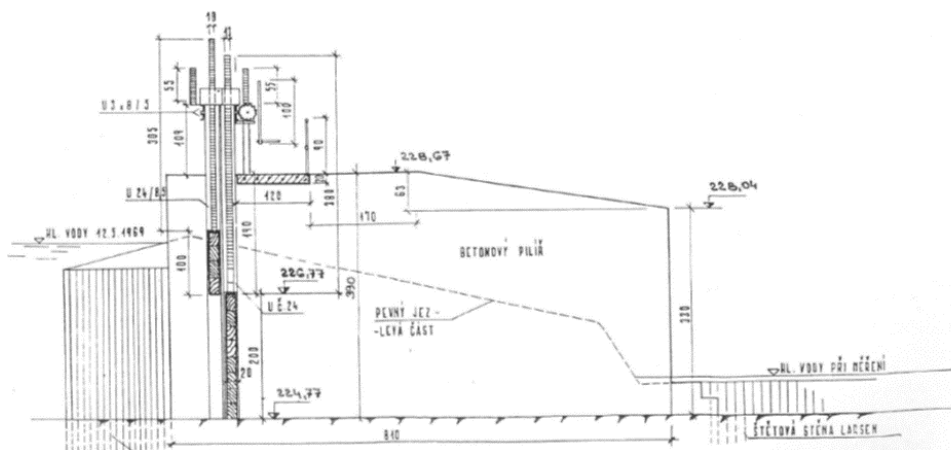


Figure 4. The section along the sand sluice

The sluice is connected with the weir via concrete pier with the length 8.10 m and width 1.30 m. Since 1972, the pier at its upper part has been damaged by the crack caused probably by the thermal stresses raised from reinforced footbridge. Possible minor inclination of the pier should not be ignored. The clearance width of the sluice corresponding with the span of the gates is 3.0 m. The massive concrete pier forms the right side of the sluice.

An important fact is that the sheet pile driven to the gravel subbase was not extended to the sluice section and was terminated at the right pier of the weir at the left side of the sluice opening (Figure 1). Stones embedded in 100 mm thick concrete bed paved the bottom of the inlet channel to the sluice and hydropower plant. The sluice bottom was made of the same material (total thickness approx. 150 mm) except of an upstream concrete sill below the slide gates. This does not correspond with available drawings of the sluice (Figure 2) which expect rock foundation at the bottom of the sluice. The sluice is not equipped by the stilling basin.

There were several signs of erroneous expectations and poor interpretation of geological conditions. After each higher discharge through the sluice, the scour was identified at the downstream toe. Therefore, riprap from quarry stone was put downstream of the sluice. Its stabilisation was made by additional sheet pile driven to the riverbed below the sluice (Figure 1).

3.4 Hydropower plant

The HPP is located at the right bank of the Jizera River adjacent to the sand sluice. The trash racks and inlet to the turbine chamber follow the approach footbridge with concrete sill. Site investigation after the weir collapse showed that the hydropower base slab is founded on the frame made of wooden piles. The space between the hydropower plant and the right pier of the sluice has been filled by random backfill composed of refuse material and debris (bricks, stones, ash, and soil).

4 The collapse of the sluice

4.1 Description of the collapse

The video documentation indicates that the damage started downstream behind the right-bank massive pier between the sluice and the hydropower plant (Figure 5).

The collapse continued by gradual subsidence of the right pier by approximately 1.8 m. Intensive vortex developed fast in front of the sluice gates, which indicated intensive flow below the sluice (Figure 5). At the same time, gates and the footbridge over the sluice inclined and collapsed. This propagated to the left sluice pier, which inclined towards the sluice and separated from the weir body. To the stability of the left pier contributed the sheet pile supporting its lower part (Figure 6). It sunk about 0.7 m following the left pier. An overall aerial view on the collapsed weir can be seen from Figure 7.



Figure 5. The downstream view at the sluice, the arrow indicates subsidence of the backfill and platform behind the right sluice pier.



Figure 6. The detailed view at the collapsed right sluice pier with sunk sheet pile.



Figure 7. An overall view on the collapsed weir

4.2 The mechanism of the failure

Detailed assessment of available data including the video record of the collapse was carried out to clarify the causes of the incident. Two potential seepage paths (A, B in Figure 8) were identified, one below the sluice gate and the second one between the sluice and the HPP.

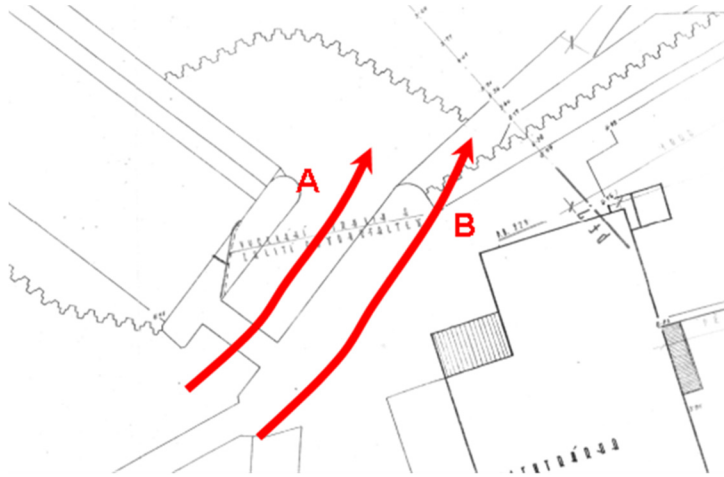


Figure 8. Two expected seepage paths

From the available data, it is clear that continuous seepage paths developed at the sandy gravel subbase and/or in the debris backfill behind the right sluice pier. It may be expected that process started by local instability of soil which was flushed out from the subbase or behind the right sluice abutment. It is also likely that the initiation process was long and might take several years. When looking back to the documentation of repairs it can be seen that the right bank wall downstream of the sluice adjacent to the hydropower plant suffered from the subsidence and cracks and had to be equipped by sheet pile wall and concrete support of the toe (Figures 7, 8, 9).



Figure 9. Cracked toe of the right bank wall (upstream view)

The development of the local seepage paths below the concrete structures supported by wooden piles (Figure 10) was hardly to be identified. The seepage was also possible via not-sealed contraction joints between right sluice pier and the HPP and damaged bottom pavement in front of the sluice and HPP intake.

Taking into account the first subsidence of the HPP platform (Figure 5), the more probable is the development of the seepage path B (Figure 8). Further on the right sluice pier started to subside and incline (Figures 5, 6, 9) and ripped off the bottom slab of the sluice. Thus, extremely short seepage path developed below the sluice gates, which resulted in bursting out the slab and the scour with the depth about 1.7 m. This phase took about 15-20 minutes.



Figure 10. Piles supporting the undermined foundation slab of the HPP inlet

4.3 The main causes of the collapse

As is usual at the failures of technical facilities the collapse was caused by the combination of several unfavourable factors:

- Structural deficiencies at the upstream intake channel to the HPP, which enabled seepage into the subbase. These are not sealed contraction joints, cracks and defects in the intake channel bed (missing pavement, cracks).
- Upstream sheet pile wall was not extended to the sluice and HPP intake.
- The absence of the stilling basin, scouring the riverbed downstream of the weir and the stilling basin. The stabilizing riprap did not improve this situation and did not extend the seepage path.

- Former demolition and construction works might contribute to the seepage behind the right sluice wall.
- The effective stress in the sand gravel soil below the foundation slabs supported by wooden piles was practically zero; the material lost its resistance against internal erosion. Certain role may be attributed to vibrations coming from the turbines.
- The dry period resulted in historically highest head, i.e. difference between upstream and downstream water levels at the weir.

5. Conclusions

The collapse of the Hubalov weir was caused by internal erosion of permeable sandy gravel soils in the subbase of the sand sluice and its right pier. The local defect started probably behind the right sluice pier where flushed out material caused subsidence of the platform in front of the HPP. At the continuation phase, subsidence of the right pier caused a collapse of the bottom slab of the sluice and total collapse of the structure.

The contributing factors were structural deficiencies upstream of the sluice like open contraction joints, cracks and defects in the intake channel bed and a fact that upstream sheet pile wall was not extended to the sluice and HPP intake. Other factors were the absence of the stilling basin below the sluice, the fact that wooden piles, vibrations coming from the turbines and high head during the dry period, supported foundation slabs. Poor knowledge about true geological conditions at the site was also crucial.

Due to minor importance of the scheme and low consequence class, the structure was not equipped by any measuring device. The surveillance was carried out only by visual inspections and did not contain any special measurements. Therefore, the identification of initiation of the internal erosion process was practically impossible also due to the method of foundation of the HPP slab supported by wooden piles.

Acknowledgements

This study is a part of the projects FAST-S-19-5714 – Probability assessment of internal instability in earth structures and in hydraulic structures' foundations and FAST-J-19-5744 – Hydraulic and erosion conditions in the seepage path during backward erosion.

SIMULATION OF THE FLOOD FORMATION, TIME AND SPATIAL DISTRIBUTION BY USING ADVANCED HYDRODYNAMIC MODELING

MARTIN ORFÁNUS¹, ANDREJ ŠOLTÉSZ², DANIEL BUČEK³

¹ *Department of Hydraulic Engineering, Faculty of Civil Engineering, STU in Bratislava, Slovak republic, martin.orfanus@stuba.sk*

² *Department of Hydraulic Engineering, Faculty of Civil Engineering, STU in Bratislava, Slovak republic, Andrej.soltesz@stuba.sk*

³ *Department of Hydraulic Engineering, Faculty of Civil Engineering, STU in Bratislava, Slovak republic, Daniel.bucek@stuba.sk*

1. Abstract

The project aims to strengthen the joint of the regional framework for mitigation consequences of floods, droughts and pollution by increasing absorption capacity of the landscape. This will happen by systematic use of nature close (small) measures for water retention in the country. Project will develop methods, which apply existing knowledge of nature close (small) retention measures water management practices in river basin management. The result will improve water balance, reduce sediment transport and restore nutrient cycles.

Floods affect the river basin; there have been identified 31 geographical areas with significant flood risk, which are connected with 8 water bodies. For pilot area in the catchment the ability of HEC-RAS was used as the primary tool to determine hydrodynamic runoff. In terms of simulation of the flash flood formation, time and spatial distribution, the 2D HEC-RAS option was chosen. At this step the creation calibration and validation took a place to determine the effects of flash floods on the catchment.

To develop a 2D flow area model, an understanding of how the 2D flow model works is required. This article covers the basics of 2D flow modeling. HEC-RAS provides two methods for computing the flow field in a 2D mesh, both of which may be selected from the Unsteady Flow Computational Options dialog box available from the Analysis ribbon menu.

The 2D Diffusion Wave computational method is the default solver and allows the computations to run faster and with greater stability. Most 2D modeling situations, such as flood modeling, can be accurately modeled using this solver, where inertial forces tend to dominate frictional and other forces.

Keywords: hydrodynamic model, 2D numerical model, flood simulation, HEC-RAS, runoff, flash floods

1. Introduction

The project aims to strengthen the joint of the regional framework for mitigation consequences of floods, droughts and pollution by increasing absorption capacity of the landscape.

This will happen by systematic use of nature close (small) measures for water retention in the country. Project partners will develop methods, which apply existing knowledge of nature close (small) retention measures water management practices in river basin management. The result will improve water balance, reduce sediment transport and restore nutrient cycles.

The project will be provided by the executive appropriate instruments to incorporate the nature of nearby measures to retention of water in the country to the next cycle of river basin management plans. It will also be support and provide guidance on the horizontal integration of different strategic ones documents and plans in this area.

The river basin is affected by floods, there have been identified numerous geographical areas with significant flood risk which are connected with 8 water bodies. The pilot area has 271 km² with 26 sub-catchment in the region.

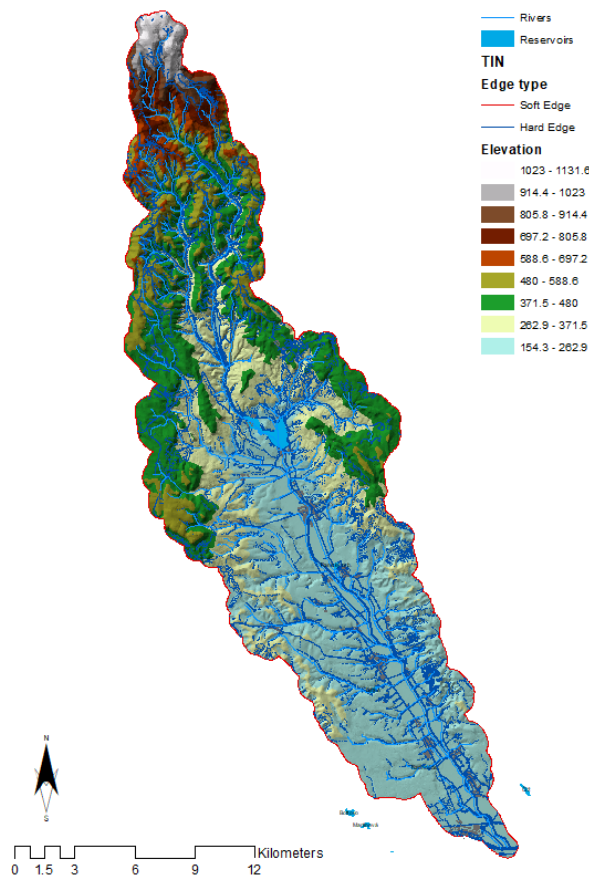


Figure 1. The caption heading for a figure should be placed below the figure, centered.

2. Methods

For the catchment the ability of HEC-RAS was used as the primary tool to determine hydrodynamic run off. In terms of simulation of the flash flood formation, time and spatial distribution, the 2D HEC-RAS option was chosen [1].

. HEC-RAS 2D flow modeling can be used in a variety of different situations:

- Detailed 2D channel and floodplain modeling
- Combined 1D channel flow with 2D floodplain flow areas
- Combined 1D channel and overbank flow with 2D flow areas behind levees
- Simplified to detailed dam failure (i.e., dam breach) analyses
- Simplified to detailed levee failure (i.e., levee breach) analyses
- 1D flow that suddenly expands laterally into the floodplain overbank area
- Flow outside of well-defined single channel
- Interconnected or braided creeks, meanders, loops
- Alluvial fans and estuaries
- And many other situations

To develop a 2D flow area model, an understanding of how the 2D flow model works is required. This article covers the basics of 2D flow modeling. HEC-RAS provides two methods for computing the flow field in a 2D mesh, both of which may be selected from the Unsteady Flow Computational Options dialog box available from the Analysis ribbon menu.

The 2D Diffusion Wave computational method is the default solver and allows the computations to run faster and with greater stability. Most 2D modeling situations, such as flood modeling, can be accurately modeled using this solver, where inertial forces tend to dominate frictional and other forces.

The Diffusion Wave computational method can be used in the following situations:

- Flow is mainly driven by gravity and friction
- Fluid acceleration is monotonic and smooth (i.e., no waves)
- Compute rough global estimates (i.e., flood extents)
- Assess interior flooding (i.e., levee breach)
- Quick estimate for using the Full Momentum computational method
-

The 2D Full Momentum computational method, often referred to as the Saint Venant equations for shallow flow, can account for turbulence and Coriolis effects, making it applicable to a wider set of conditions. However, solving the 2D Saint Venant flow equations requires more computational power and thereby results in longer run times. In addition, the 2D Saint Venant flow equations can become numerically unstable in regions of the 2D mesh where the water surface profile or flow direction is changing rapidly. To avoid an unstable model, a finer mesh and a corresponding smaller time step will need to be used [2].

The Full Momentum computational method should be used in the following situations:

- Dynamic flood waves (i.e., dam failure, rapid rise and fall)
- Sudden expansion or contraction of flow with high velocity changes

- Detailed flow solutions around hydraulic structures and obstacles (i.e., bridge openings, piers and abutments)
- Detailed mixed flow regime (i.e., hydraulic jumps, critical flow, etc.)
- Wave propagation (i.e., waves reflecting off walls and objects)
- Tidal boundary conditions (i.e., upstream wave propagation)
- Super elevation around river bends

Both the 2D Diffusion Wave and 2D Saint Venant solvers use an Implicit Finite Volume solution algorithm. The implicit solution method allows for larger computational time steps than explicit solution methods. In addition, the finite volume method provides a greater degree of stability and robustness over traditional finite difference and finite element methodologies[3]. This computational algorithm is very robust and allows 2D cells to wet and dry. 2D flow areas can start completely dry and can handle a sudden rush of water into them. In addition, this algorithm can handle flow regimes that change with time:

- Subcritical flow
- Supercritical flow
- Mixed flow (contains both subcritical and supercritical flow, including moving hydraulic jumps)
-

For the HEC-RAS 2D computational methodology, the following modeling guidance and assumptions are provided:

- Vertical fluid motion is negligible
- Velocity is vertically averaged at the cell center (depth averaged flow)
- Energy head is computed at the cell center
- Manning's roughness assigned on cell face using roughness value at cell face center
- Manning's roughness assumed constant across each cell face, although each cell face can have its own value
- Rain on grid is applied uniformly to all cells of the 2D flow area
- Rainfall initial abstraction and other losses need to be accounted for prior to assigning precipitation data
- At least one external boundary condition must exist on the 2D mesh
- Time step selection should consider cell size and wave speed.[4]

3. Results and discussion

2D flow areas are created by constructing polygon areas representing the regions to be modeled. Along the 2D flow area polygon mesh boundary, boundary condition polylines are defined to represent different flow conditions or constraints that are to be applied to the 2D flow area. Two main boundary conditions were applied for the purpose of hydrodynamic simulation of runoff in the pilot area. One type of boundary condition is precipitation. Precipitation is "area type" of boundary condition set for every computation node (mm per time unit) in the domain. The precipitation boundary condition should be set either as constant or time depended with defined time step. Outflow boundary condition represents **flux boundary**, where flow leaves the 2D

flow area. (Boundary conditions can also be defined within the interior of the 2D flow area, to represent additional discharge that enters the 2D flow area—such as flow from a wastewater treatment plant.)

Examples of flux boundaries are:

- Inflow hydrograph
- Stage hydrograph (time series)
- Fixed water surface elevation
- Normal depth (given user-defined energy slope)
- Tidal (time-series)

The Normal depth boundary condition was set as the outflow.

As the primary results are the map of depths, stage hydrographs and velocity maps considered for every important catchment region. The precipitation run-off should be characterized as flash flood. Such an extreme run-off at the geographical area with these condition, the high intensities and quick progress is characteristic as well as the quick subsidence.

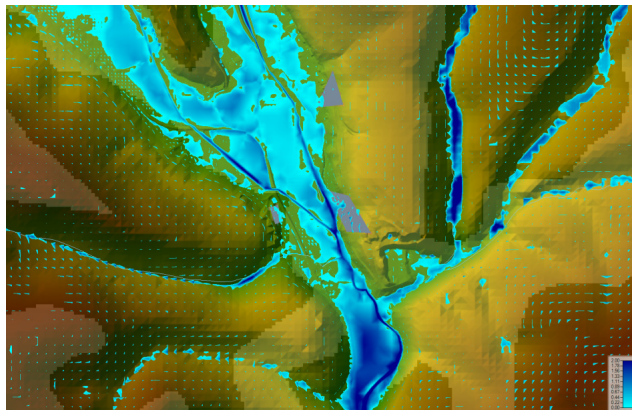


Figure 2. The map of depths

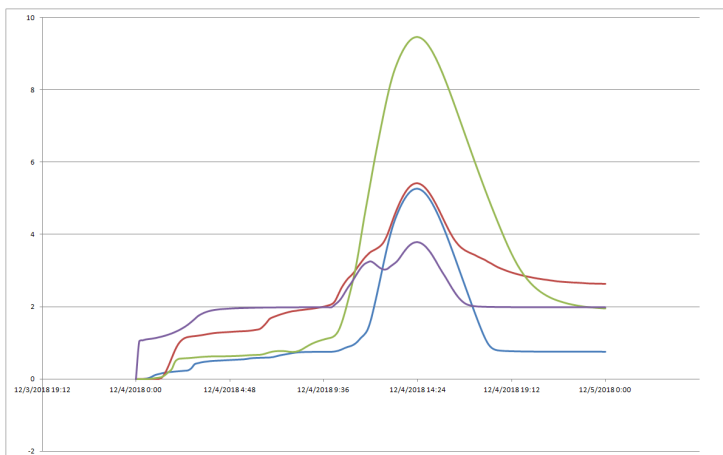


Figure 3. The stage hydrographs of tributary sub-catchment creeks

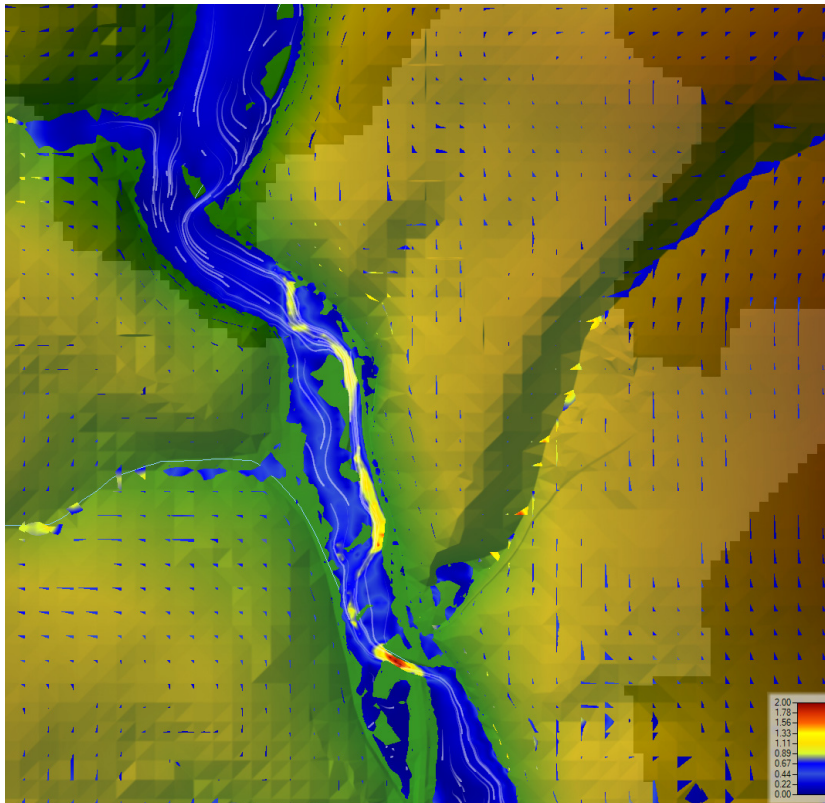


Figure 4. The velocity map

4. Conclusion

The main objective at current project stage was to develop, calibrate and verify simulation model of the pilot area in Slovakia. The area has 271 km². 2D hydrodynamic model HEC-RAS was adopted to simulate precipitation runoff and the flood formation due the heavy rain event.

Despite the simplification of landcover/landuse parameterization only through the roughness evaluation it can be concluded that the calibration and verification process was successfully realized. The results are reliable for the flood formation simulations and prepared for next possible exploitation such as

- floodplain mapping,
- velocity mapping,
- flood intensity mapping,
- potential of erosion and sedimentation in the catchment, stream power
- assessment of flood protecting objects already constructed / planned to be realized
- proposal and optimization of the flood protecting objects [5]
- other objectives in relation to the flood formation with spatial and time distribution

Acknowledgements

The Slovak Research Grant Agency supported the research presented in this paper under VEGA project No. 1/1011/12.

This publication is the result of the project implementation: „Centre of Excellence of Integrated Flood protection of Territory“, ITMS 26240120004, supported by the Research & Development Operational Programme funded by the ERDF.

This work was supported by the Slovak Research and Development Agency under Contract No. APVV-15-0489.

This paper was supported by the Grant agency VEGA under contract No.

References:

- [1] Gary W Brunner; United States. Army. Corps of Engineers.; Institute for Water Resources (U.S.); Hydrologic Engineering Center (U.S.), HEC-RAS river analysis system : hydraulic reference manual. Davis, CA : US Army Corps of Engineers, Institute for Water Resources, Hydrologic Engineering Center, 2010.
- [2] Dvořák, Ladislav. 2012. *Hydraulické poměry v předpolí hrázového přelivu*. Brno : Vysoké učení technické v Brně, 2012.
- [3] Fošumpaur, Pavel. 2010. *Kombinace numerického a fyzikálního modelování ve výzkumu vodních staveb*. Praha : ČVUT v Praze, Fakulta stavební, 2010.
- [4] Kay, Malvin. 2008. *Practical Hydraulics, second edition*. New York : Taylor & Francis, 2008.
- [5] Martin, Kantor. 2007. *Hydraulika bezpečnostních přelivů vodních děl za extrémních průtoků*. Praha : ČVUT Praha, Fakulta stavební, 2007.

NUMERICAL MODELS FOR ANALYSIS OF HYDRAULIC TRANSIENTS

GORAN LONČAR ¹, ŽELJKO ŠRENG ², TIN KULIĆ ³, HANNA MILIČEVIĆ ⁴, SANJA OSTOJIĆ ⁵

¹ *University of Zagreb, Faculty of Civil Engineering, Croatia, gloncar@grad.hr*

² *J.J. Strossmayer University of Osijek, Faculty of Civil Engineering Osijek Country, zsreng@gfos.hr*

³ *University of Zagreb, Faculty of Civil Engineering, Croatia, tkulic@grad.hr*

⁴ *University of Zagreb, Faculty of Civil Engineering, Croatia, hanna.milicevic@student.grad.hr*

⁵ *University of Zagreb, Faculty of Civil Engineering, Croatia, sanja.ostojic@student.grad.hr*

1. Abstract

This paper focuses on the analysis of standard hydraulic transients in pressure systems: water-mass oscillations, water hammer and changes in pump operation regime due to the rupture in pipeline. The research has been conducted on the open-source numerical models based on the method of characteristics (Allievi) and finite-volume method (OpenModelica). Parameters defined within the numerical models have been calibrated based on the measurements on physical models.

The model simulation results show that OpenModelica is superior to Allievi when pressures during transient stages are being analysed. OpenModelica considers full thermodynamic formulations while simulating pressure flow what makes it more complicated regarding defining a model as well as manipulating with the numerical model. On the other hand, Allievi is simpler and more applicable if practical engineering problems are analysed. Furthermore, it can be used as an upgrade of the existing numerical models of pressure systems such as Epanet.

Keywords: hydraulic transients, pressured systems, numerical modelling, Allievi, OpenModelica

2. Introduction

Besides time-prevailing steady states, hydraulic pressured systems are often being exposed to transient events which are caused by sudden changes in operation of system elements. Transition between initial to final state within transient period of a system is followed by significant temporal and spatial pressure and flow fluctuations. If water supply systems are analysed, the main causes for such phenomenon of changes in pressures and flow could be found in rapid closure or opening of the valves, sudden changes in pump operation regimes such as pump start or failure in operation. Unfavourable events such as pipe ruptures will further cause the phenomenon of significant transition of hydraulic state inside observed pressured pipeline (Jović, Finite elements and method of characteristics applied to water hammer modelling, 1995),

(Wood, Lingireddy, & Boulos, 2005). However, pressured pipelines are often exposed to transient events, such as dynamic changes in water consumption or changes in water levels in reservoirs, that have less significant effect on the functionality of a whole system.

During transient period on a location of transient event there is an exchange of pressure and kinetic energy in pipeline what further causes pressure and flow velocity fluctuations within ranges of corresponding maximum and minimum values. Both extreme states can endanger the stability and functionality of a system. So, it is necessary to conduct numerical simulations of potential transient events that might occur in a system even during phase of preparation of project documentation for a new or existing pipeline that needs to be recovered.

This paper consists of analysis of three standard transient events in a pressured pipe system. The first event is oscillation of water mass in a system which consists of reservoir, pipeline, surge tank and valve. Also, this event is considered to have mild changes where fluid is assumed to be incompressible with pipe as a rigid element. The other two analysed events, water hammer and sudden pipe rupture in pressured system, are transient events with sudden changes in pressured system operation. This means that pressure and velocity fluctuations occur significantly faster with assumption that fluid is compressible, and pipe is elastic. Tools that have been used for the purpose of conducting the necessary simulations are software Allievi that is based on method of characteristics (Jović, Finite elements and method of characteristics applied to water hammer modelling, 1995), and modelling environment OpenModelica that is based on method of finite volumes (Tummescheit, Eborn, & Wagner, 2003), (Veersteg & Malalasekera, 2007). Calibration of the values of coefficients of local and friction losses, that had to be defined within numerical models, was conducted by comparing the simulated results with the ones obtained from the measurements on physical models.

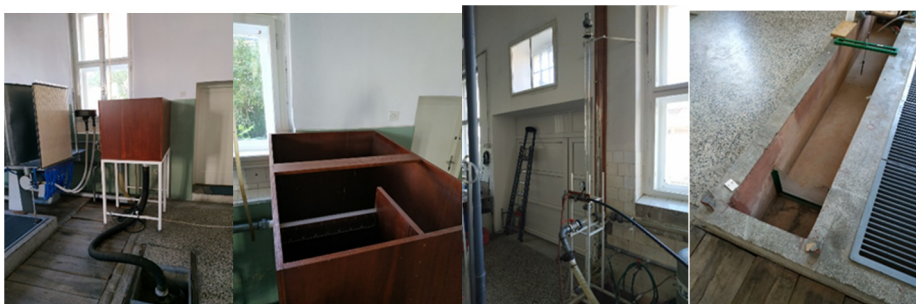
3. Methods

3.1 Physical models of pressured systems

Analysed physical models of pressured systems were made and are currently located in laboratory for hydraulic and hydrological research of Faculty of Civil Engineering, University of Zagreb. Photos and schemes of physical models are shown below.



a)

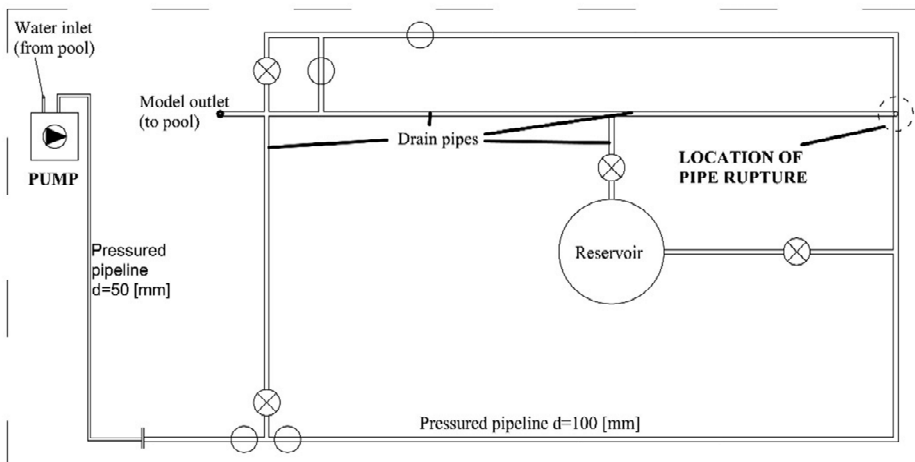


b)



Figure 35 Analysed physical models of pressured systems located in laboratory for hydraulic and hydrological research, Faculty of Civil Engineering, University of Zagreb – a) model of water supply system; b) model for the analysis of water mass oscillations; c) model for the analysis of water hammer

MODEL GROUND PLAN



- ⊗ - closed valves
- ⊖ - opened valves

a)

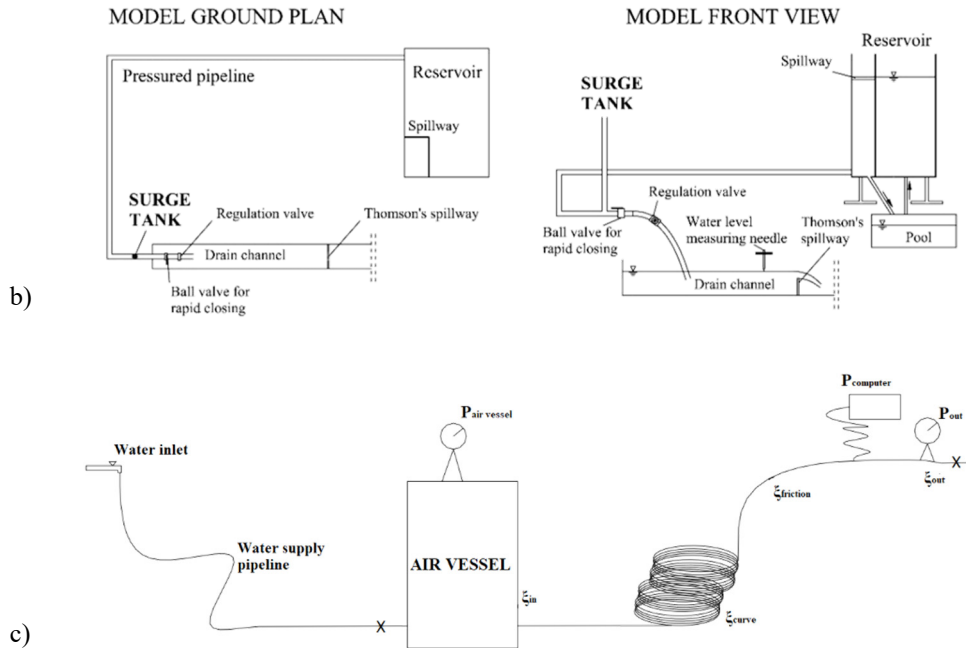


Figure 36 Schemes of physical models for the analysis of a) pipe rupture, b) water mass oscillations, c) water hammer

Water enters the model shown on Figure 35a through underground channel with bed level equal to -2 m. Water level in a channel is on -1.5 [m]. Water intake of a pump is dipped on -1.75 m. Pump characteristics are listed below:

- Installed power of a pump $P = 15$ [kW]
- Nominal flow $Q_P = 36$ [m³/h], or 10 [l/s]
- Nominal head $H_P = 7.5$ [bar] when $N = 3000$ [rpm]
- Efficiency coefficient $\eta = 0.9$ [1]
- Pump type – Etachrom B, 065-040-200, manufacturer KSB

This system also contains a series of typical fittings (air release valve, reduction valve, gate valve, knee fitting, etc.), but this research focused on nozzle with diameter $d_N = 20$ [mm] that has a gate valve with a short polyethylene (PE) pipe connected to it, and another gate valve on the end of the pressured system. Pipeline is designed of a series of short iron and PE pipes with inner diameter $d = 100$ [mm]. Data about the pressure in pump water inlet and outlet (Figure 36a) are obtained by manometer measurements connected to the acquisition system designed by PDL-AG. Data sampling frequency is equal to 10 [Hz]. Besides pressure, pump flow Q_P and power P are recorded. Simulation of pipe rupture has been conducted by applying the following procedure. After the establishment of steady state in a system for three experiments of different pump revolutions per minute, $N = 1800, 2100$ and 2400 [rpm], the gate valve was rapidly opened. Time of the valve opening is equal to approximately 0.1 [s]. Valve opening rate on the model outlet is equal to 5 [%]. Basic hydraulic characteristics of the conducted experiments are shown in Table 6.

Model for simulating the oscillations of water mass water is directly supplied from laboratory's pipeline to reservoir. System is filled while valves on a pipe between reservoir outlet and surge tank base (zero level) are closed. Measurement of steady state flow Q_0 before transient event is obtained on the Thomson's spillway. By manipulating the regulation valve on the outlet, energy loss equal to $\Delta h_0 = -0.4$ [m] is obtained (loss is measured from the initial level in reservoir). Boundary conditions are defined as constant water level and steady state conditions in reservoir which are maintained with a spillway inside reservoir. After establishing the steady state flow conditions, rapid closure of a valve at the outlet of a system causes the water mass oscillations in surge tank. Maximum and minimum water levels in surge tank during the first oscillation period (h_{MAX} and h_{MIN}) were registered visually, and duration of this period was measured with a stopwatch. Length of a water supply pipeline is $L = 8.1$ [m] (pressured pipeline), and a diameter of this pipeline and a surge tank is $d = 49$ [mm]. Hydraulic characteristics of this experiment (experiment 4) are presented in Table 6.

Physical model used for simulating water hammer is supplied from the water supply network that is connected with an elastic pipe to air vessel. Air vessel has an installed analogue manometer for pressure measurement on the pressured pipeline inlet. Outlet of air vessel is connected to a PE pressured pipeline with length $L = 200$ [m], inner diameter $d = 21.2$ [mm], and thickness of pipe wall equal to $s = 1.9$ [mm]. On the end of this pipeline there are two valves and one manometer. First valve is a ball valve that was used for rapid stopping of flow what caused the occurrence of water hammer. The second one is regulation valve which was used for manipulating the flow through pipeline for the purpose of measuring the pressure rate during rapid and total closure of valve at different values of flow. Manometer is located directly upstream of the ball valve and is connected to PDL-AG acquisition system. The measurement frequency is 10 [Hz]. Regulation valve was initially set to obtain the value of pressure $h_{P_1} = 30$ [m] upstream of the ball valve. Manometer located on air vessel recorded pressure is $h_{P_2} = 69.2$ [m]. Steady state flow Q_0 before transient period was measured on Thomson's spillway. Closing time of ball valve was equal to approximately 0.1 [s]. The overview of hydraulic characteristics of this experiment (Experiment 5) are shown in Table 6.

Table 6 Hydraulic characteristics of the conducted experiments of pipe ruptures (experiment 1, 2, 3), water mass oscillations (experiment 4), and water hammer (experiment 5). Presented values are related to steady state flow conditions before and after the transient event

Experiment.	N (1/min)	t_{LEAK} (s)	$h_{p_IN_0}$ (m)	$h_{p_OUT_0}$ (m)	Q_{p_0} (l/s)	$h_{p_IN_1}$ (m)	$h_{p_OUT_1}$ (m)	Q_{p_1} (l/s)	$P_{0_P_1}$ (kW)
1	2400	0.1	-2.5	45.0	1.9	-8.4	36.4	5.3	3.76_5.34
2	2100	0.1	-2.4	34.0	2.2	-6.9	28.0	5.2	2.76_3.77
3	1800	0.1	-2.1	24.5	2.2	-5.2	20.3	5.1	1.89_2.53
	Q_0 (l/s)	$t_{CLOSURE}$ (s)	Δh_0 (m)						
4	2.46	0.1	-0.4						
	Q_0 (l/s)	$t_{CLOSURE}$ (s)	h_{p_1} (m)	h_{p_2} (m)					
5	0.62	0.1	30	69.2					

3.2 Numerical models for the analysis of unsteady flow in pressured systems

Unsteady flow in pipes is generally described with continuity (1) and momentum (2) equations for compressible fluid which are given below (Jović, Finite elements and method of characteristics applied to water hammer modelling, 1995), (Wylie & Streeter, 1967):

$$\frac{\partial p}{\partial t} + v \frac{\partial p}{\partial l} + \rho c^2 \frac{\partial v}{\partial l} = 0 \quad (17)$$

$$\frac{\partial v}{\partial t} + v \frac{\partial v}{\partial l} + \frac{1}{\rho} \frac{\partial v}{\partial l} + g(J_e - J_0) = 0 \quad (18)$$

$$J_e = \frac{\lambda}{2gD} v|v| \quad (19)$$

$$J_0 = -\frac{\partial z}{\partial l} \quad (20)$$

where v is average flow velocity, p is pressure, ρ is fluid density, t is time, c is sound wave celerity, J_e energy gradient, and J_0 is pipe axis gradient.

Continuity and momentum equation consist of three unknown variables (p , v , ρ) so it is necessary add another equation in which relationship between pressure and density is given by (equation of state):

$$F(p, V, T) = 0 \quad (21)$$

Equation of state (21) provides a new variable – temperature T . Allievi software assumes isothermal process ($T = \text{const.}$), so three equations are sufficient for simulating a complete unsteady flow conditions in pressured pipeline (Jović, Analysis and Modelling of Non-Steady Flow in Pipe and Channel Networks, 2013). Furthermore, state of equation defines functional relationship between density ρ and sound wave celerity c . However, OpenModelica model uses the expanded system which considers full thermodynamic formulations (Elmqvist, Tummescheit, & Otter, 2003).

Transient states within hydraulic system are developed from steady states as a result of manipulating with the elements in a system. Both Allievi and OpenModelica models are initially calculated under steady state conditions with all the elements having the same regime in time. Numerical models of the analysed systems consist of number of connected elements on model boundaries. All the system elements have starting and ending node.

For the analysis of pipe rupture by using Allievi, following elements were used that are shown on Figure 37a:

- Open channel element (*rule*) – IN as a steady boundary condition defined as;
- Pipe elements – c_1 , c_2 and c_3 ;
- Pump element;
- Orifice with gate valve – LEAK, OUT

For the analysis of water mass oscillations by using Allievi, following elements were defined as it is shown on Figure 37b:

- Reservoir element (rule) – *IN* as a steady boundary condition;
- Pipe elements – c_1 , c_2 and c_3 ;
- Surge tank element – *ST*;
- Valve element – *VALV*;
- Open channel element (rule) – *OUT* as a steady boundary condition.

For water hammer analysis by using Allievi, following elements were defined as it is shown on Figure 37c:

- Reservoir (tank) element – *IN* as a steady boundary condition;
- Pipe elements – c_1 , c_2 and c_3 ;
- Air vessel element – *AIR_CHAMB*;
- Valve element – *VALV*;
- Open channel element – *OUT* as a steady boundary condition.

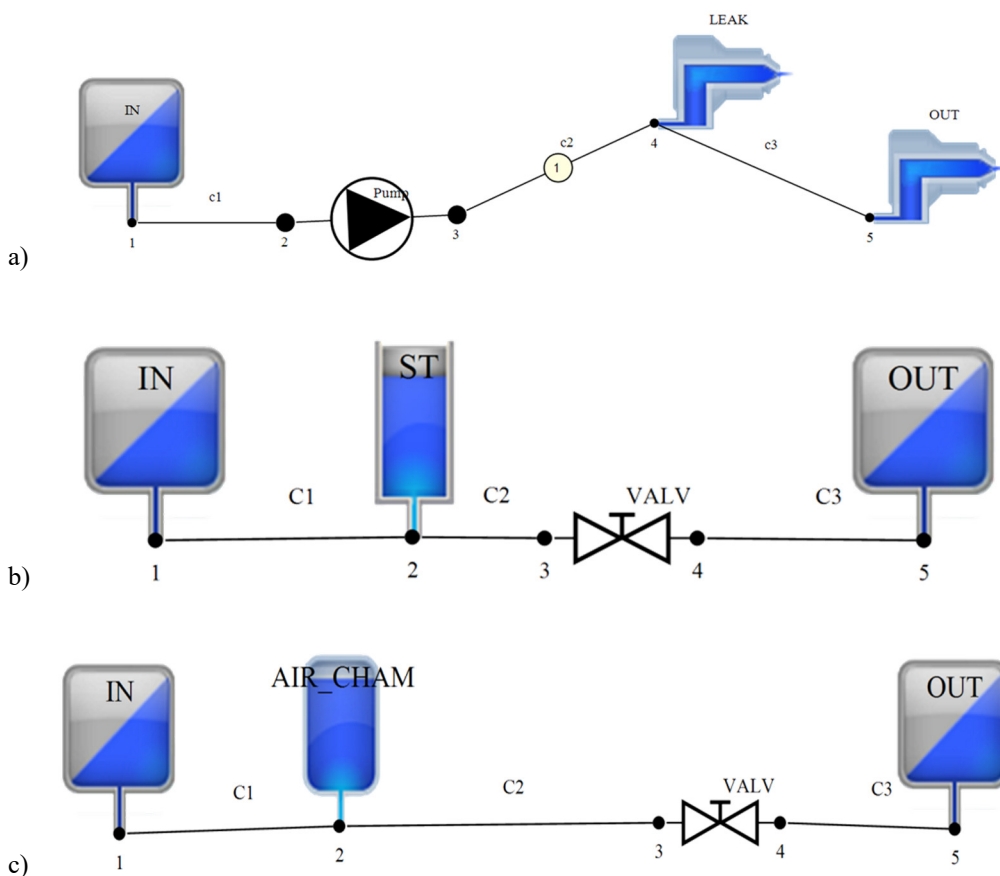
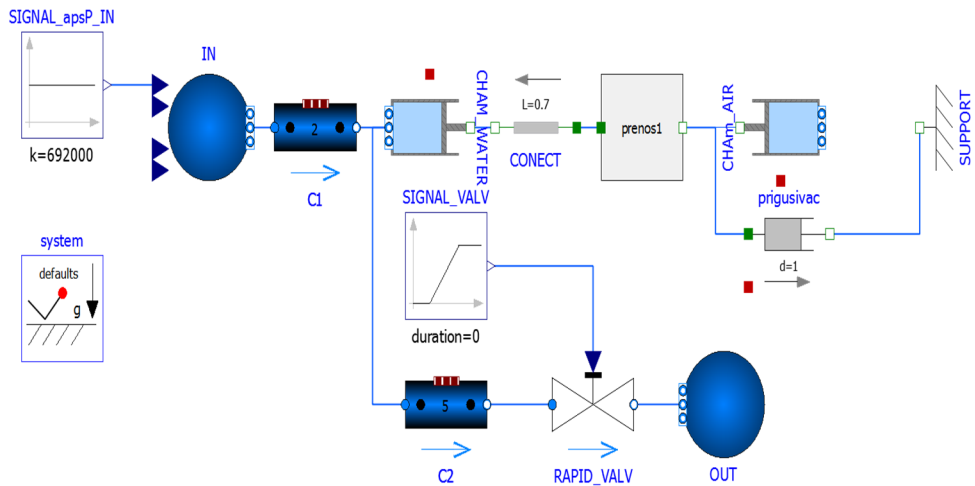


Figure 37 Schemes of the analysed pipeline systems in Allievi software for the analysis of a) pipe rupture, b) water mass oscillations, and c) water hammer

OpenModelica has been developed by Open Source Modelica Consortium (OSMC) and is an open-source modelling environment available on www.openmodelica.org. The available versions are supported by Windows, Linux and Mac operating systems (Association, 2014), (Fritzson, 2004). Basic component of this modelling environment



c)

Figure 38 Schemes of the analysed pipeline systems in OpenModelica environment for the analysis of a) pipe rupture, b) water mass oscillations, and c) water hammer

4. Results and discussion

Parametrization of the numerical models was conducted based on the measured pressures and flows obtained by physical models. Table 7 presents the values of the calibrated coefficients defined within numerical models with the following labels:

- k_C – coefficient of local energy losses in pipes;
- ε – absolute pipe roughness;
- k_{VALV} – coefficient of local energy loss on gate valve on the location of pipe rupture;
- k_{OUT} – coefficient of local energy loss on gate valve on the pipeline outlet;
- k_{ST_IN} – coefficient of local energy loss on the inlet to surge tank;
- k_{ST_OUT} – coefficient of local energy loss on the outlet of surge tank;
- k_{CHAM_IN} – coefficient of local energy loss on the inlet to air vessel;
- k_{CHAM_OUT} – coefficient of local energy loss on the outlet of air vessel;
- dP_{VALV_LEAK} – pressured drop under the conditions of nominal flow through valve used for simulating the pipe rupture;
- dP_{VALV_OUT} – pressured drop under the conditions of nominal flow through valve at the outlet of pipeline;
- dP_{VALV_LEAK} – pressured drop under the conditions of nominal flow through valve used for simulating the water mass oscillations and water hammer.

It's important to note that models defined in Allievi compared to the ones in OpenModelica use different formulations for local energy loss coefficients. Allievi based models use coefficients that are related to the squared values of flow. So, coefficients values are greater than the ones that would be obtained when relationship with squared velocities is considered.

Table 7 Values of calibrated coefficients in Allievi numerical model

Experiment	k_{C1} [1]	k_{C2} [1]	k_{C3} [1]	ϵ_{C1} [mm]	ϵ_{C2} [mm]	ϵ_{C3} [mm]	k_{VALV} [1]	k_{OUT} [1]
1	3.75	650	650	0.25	0.25	0.25	1000	100
2	2.00	650	650	0.25	0.25	0.25	500	100
3	1.00	650	650	0.25	0.25	0.25	100	100
	k_{C1} [1]	k_{C2} [1]	k_{C3} [1]	ϵ_{C1} [mm]	ϵ_{C2} [mm]	ϵ_{C3} [mm]	k_{ST_IN} [1]	k_{ST_OUT} [1]
4	0	0	0	0.10	0.01	0.01	55000	0
	k_{C1} [1]	k_{C2} [1]	k_{C3} [1]	ϵ_{C1} [mm]	ϵ_{C2} [mm]	ϵ_{C3} [mm]	k_{CHAM_IN} [1]	k_{CHAM_OUT} [1]
5	0	0	0	0.01	0.005	0.01	0	0

Table 8 Values of calibrated coefficients in OpenModelica numerical model

Experiment	k_{C1} [1]	k_{C2} [1]	k_{C3} [1]	ϵ_{C1} [mm]	ϵ_{C2} [mm]	ϵ_{C3} [mm]	dP_{VALV_LEAK} [Pa]	dP_{VALV_OUT} [Pa]
1	3.85	0	0	0.25	1.00	1.00	5000	10000
2	2.00	0	0	0.25	1.00	1.00	5000	10000
3	0.70	0	0	0.25	1.00	1.00	5000	10000
	k_{C1} [1]	k_{C2} [1]		ϵ_{C1} [mm]	ϵ_{C2} [mm]		dP_{RAPID_VALV} [Pa]	k_{ST_IN} / OUT [1]
4	0	0		0.2	0.025		5000	2.7 / 0.1
	k_{C1} [1]	k_{C2} [1]		ϵ_{C1} [mm]	ϵ_{C2} [mm]		dP_{RAPID_VALV} [Pa]	$k_{CHAM_IN} /$ OUT [1]
5	0	0		0.1	0.015		1000	0.0 / 0.0

Measured and simulated pressure time series for Experiments 1, 2 and 3 on the locations of manometers P1 (h_{P-IN}) and P2 (h_{P-OUT}) for different number of pump revolutions per minute are shown on Figure 39. Results of measured and simulated surge tank water level time series for Experiment 4 are presented Figure 40 while the results of measured and simulated pressures on P1 (h_{P_1}) and P2 (h_{P_2}) manometers for Experiment 5 are provided on Figure 41.

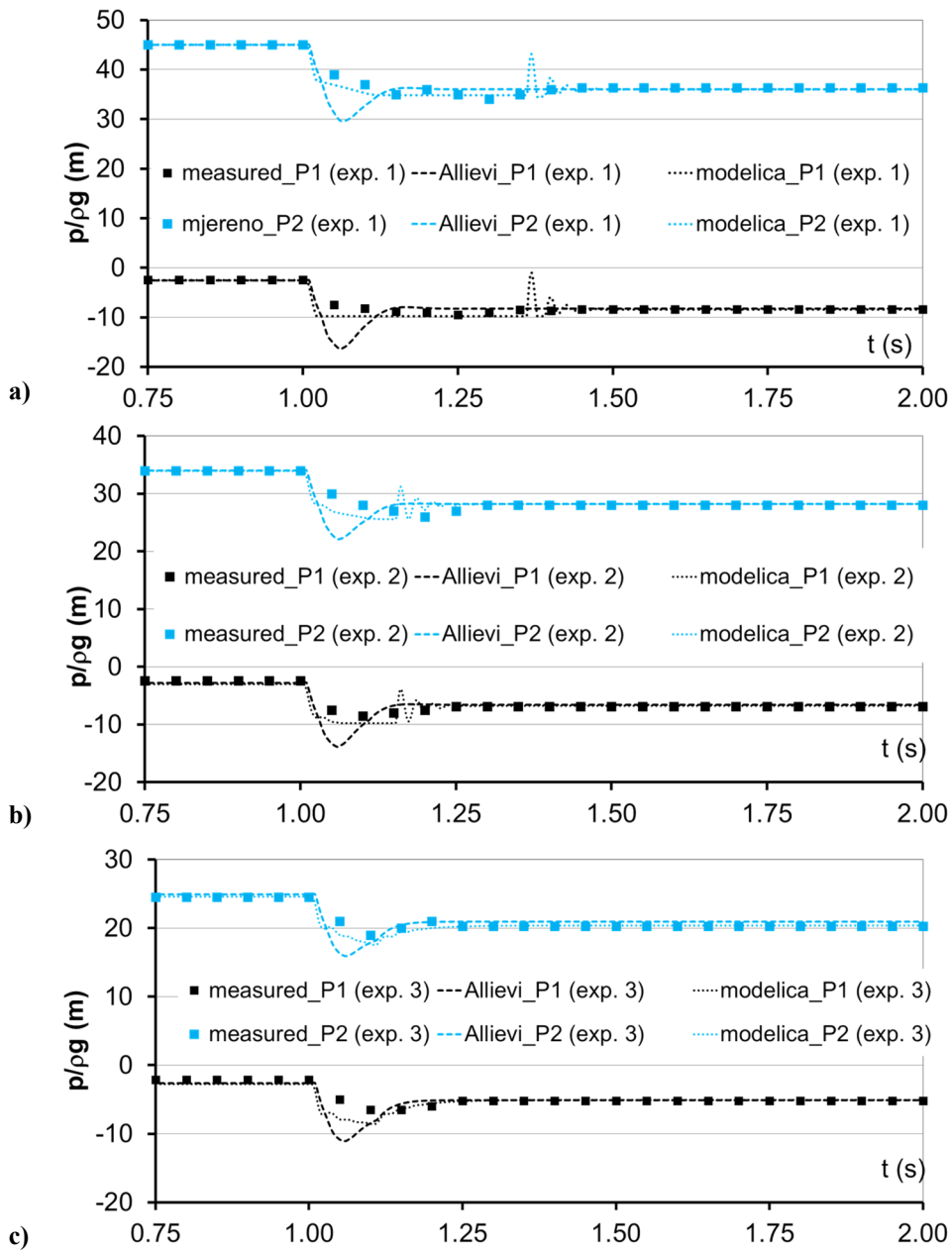


Figure 39 Measured and simulated pressure time series on the locations of P1 (h_{P-IN}) and P2 (h_{P-OUT}) for a) Experiment 1, $N = 2400$ [rpm]; b) Experiment 2, $N = 2100$ [rpm]; c) Experiment 3, $N = 1800$ [rpm]

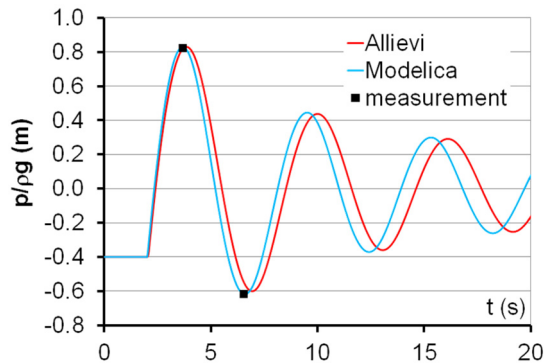


Figure 40 Measured and simulated surge tank water level time series for Experiment 4

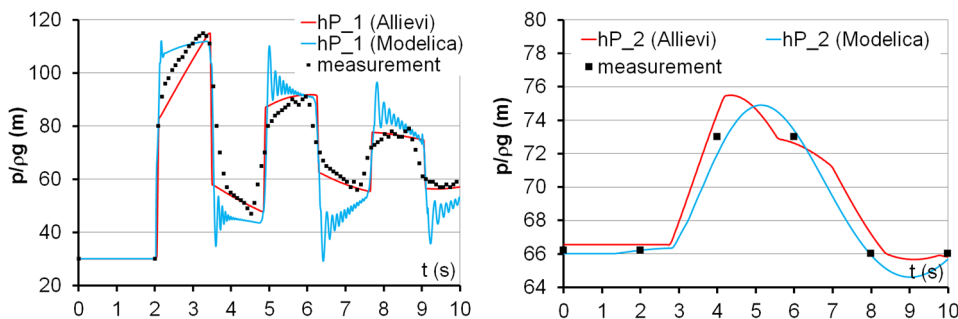


Figure 41 Measured and simulated pressure time series on the locations of P1 (h_{P_1}) and P2 (h_{P_2}) for Experiment 5

5. Conclusion

This paper provided the analysis of transient events in pressured systems. By the conducted experiments, temporal changes of pressures during transient periods was recorded on the characteristic locations for the events of pipe rupture, water mass oscillations and water hammer occurrence due to the rapid closure of a valve. Results were obtained by physical and numerical models. Simulations in numerical models were conducted within Allievi software and OpenModelica modelling environment.

The results for five experiments provided in the previous section confirm that the simulated results correspond to the measurements on physical models. Pressure time series for the pipe rupture event modelled by using OpenModelica provide more realistic results during transient period than the results obtained by using Allievi software, especially on the location of pump inlet. OpenModelica applies full thermodynamic formulations during analysis of flow regimes in pressured systems what disables the occurrence of unrealistic values of the calculated pressure depression at pump inlet. However, Allievi model performed better in the analysis of pressure changes during water hammer primarily since this software uses method of characteristics which superior to model of finite volumes in this case. The latter method shows the problem of inadequate accuracy in approximation of integration procedure. If the experiment of

water mass oscillations is considered, both models provided satisfying results when compared to the measurements.

Based on the conducted analysis, it can be concluded that Allievi software is a simple and easy-to-learn tool that can be used for the analysis of hydraulic transients. The fact that it is an open source software that can be easily used as an extension to the other open source softwares that are commonly used in hydraulic modelling of pressured systems (i.e. Epanet) gives this software an advantage when compared to other commercial softwares with similar functionalities. For the purpose of analysis of hydraulic transients, it can be said that Allievi is simpler than OpenModelica. However, OpenModelica is applicable not only in hydraulic transient analysis, but in other domains of physics and engineering. It's also an open source modelling environment with a bunch of useful tools which facilitate the work in it. Furthermore, the users are enabled to create their own elements, functions and libraries, and, in such way, contribute to the development of OpenModelica. Both Allievi and OpenModelica are powerful engineering tools, but the engineers are the ones to decide which one is appropriate for the problems they confront with.

References

- [1] V. Jović, "Finite elements and method of characteristics applied to water hammer modelling," *International Journal for Engineering Modelling*, pp. 51-58, 1995.
- [2] D. Wood, S. Lingireddy and P. Boulos, *Pressure wave analysis of transient in pipe distribution systems*, MWH Soft, 2005.
- [3] H. Tummescheit, H. Eborn and F. Wagner, "Development of a Modelica Base Library for Modeling of ThermoHydraulic Systems," in *Modelica Workshop 2000*, Lund, 2003.
- [4] H. Veersteeg and W. Malalasekera, *An Introduction To Computational Fluid Dynamics*, 2nd ed., Harlow: Pearson Education Limited, 2007, p. 503.
- [5] E. Wylie and V. Streeter, *Hydraulic Transients*, New York: McGraw-Hill Education, 1967, p. 416.
- [6] V. Jović, *Analysis and Modelling of Non-Steady Flow in Pipe and Channel Networks*, John Wiley & Sons, 2013.
- [7] H. Elmqvist, H. Tummescheit and M. Otter, "Object Oriented Modeling of Thermo-Fluid Systems," in *3rd International Modelica Conference*, Linköping, 2003.
- [8] M. Association, *Modelica (R) - a unified object-oriented language for systems modeling language specification*, version 3.3, revision 1, 2014.
- [9] P. Fritzson, *Principles of Object Oriented Modelling and Simulation with Modelica 2.1*, 1st ed., Wiley IEEE Press, 2004.
- [10] K. Brenan, L. Campbell and L. Petzold, *Numerical Solution To Initial Value Problems in Differential-Algebraic Equations*, New York: Society for Industrial and Applied Mathematics, 1989

HYDRAULIC ANALYSIS OF WATER SUPPLY SYSTEM WITHOUT TANKS

GOCE TASESKI ¹, PETKO PELIVANOSKI ²

¹ Ss. Cyril and Methodius University Faculty of Civil Engineering – Skopje, taseski@gf.ukim.edu.mk

² Ss. Cyril and Methodius University Faculty of Civil Engineering – Skopje, pelivanoski@gf.ukim.edu.mk

1. Abstract

Whether a particular water supply system needs a tank or not depends primarily on the available capacities of the springs used for water supply and their altitude at which they are located in relation to the inhabited place. If the spring capacity is larger than the maximum water consumption per hour, there is no need for tank. Alternatively, the requirement of a tank in order to provide 100% provision for the water supply system is mandatory. In practice, the water supply systems which have not required building of tank for equalizing the consumption with the inflow of water have been very rare. Such example of a larger water supply system in our country is the water supply system of the town of Gostivar and the surrounding inhabited places, which will actually be the subject of analysis in this paper.

According to the previously stated, the aim of this paper is, through the hydraulic analysis of water supply system without tank, to define how big the maximum and minimum pressures are in the water supply network, the losses of water in the system, and by that the possible disadvantages/advantages of the water supply systems without a tank to be considered.

Keywords: Water tank, hydraulic model, water supply, water pressure water fow

2. Introduction

Creating hydraulic-simulation model of an existing water supply system is a complex process for which it is firstly necessary to have entire knowledge of the geometrical characteristics of all the constituent parts of the water supply system, such as: intakes of water, tanks (if any), pipelines, hydro-mechanic equipment, etc. After the geometrical characteristics of the water supply system have been entered into the model, it is necessary to define the initial and the boundary conditions of the model which represent the grounds for the hydraulic analysis of one water supply system. In the hydraulic models of the water supply systems, the tanks are one of the basic elements in which the initial and the boundary conditions for modelling are defined. This paper will analyze the specific system which does not have tank space built, i.e. the water supply is done from a water intake structure where, by means of the gravitation, the water will be transported to all consumers in the system. Thus, the water spring structure will represent a basic element in which the initial and the boundary conditions in modelling will be defined.

According to the previously stated, the aim of this paper is to define the performances

of the system through the hydraulic analysis of one water supply system without tank, i.e. to determine the following: the maximum and minimum pressures in the water supply network, the total losses of water in the system, "black points" along the lines in the water supply network, possible requirement of a reservoir, etc.

3. Geometrical characteristics of the system

Subject of analysis in this paper is the water supply system for the town of Gostivar (Figure 1) and the surrounding inhabited places which are supplied with water from the mutual spring "Vrutok", located at an altitude of 684 m above sea level and with the capacity of 400 – 1200 l/s depending on the season [1].

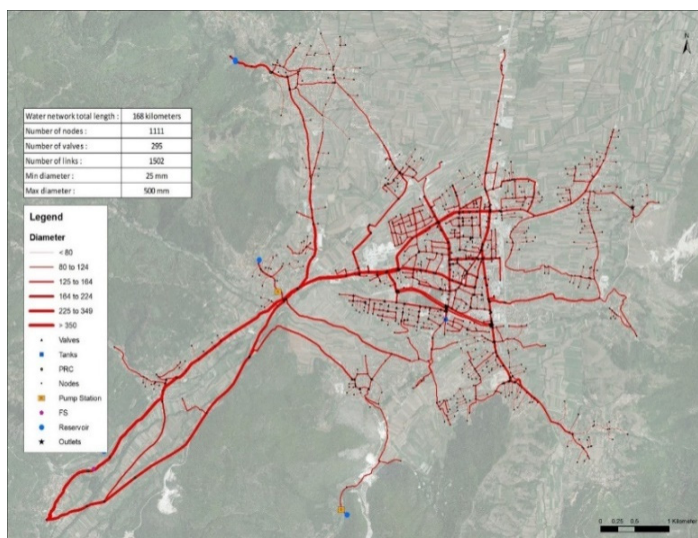


Figure 1. Disposition of the analyzed water supply system

From the spring "Vrutok", the distribution of water to the town of Gostivar (average altitude above sea level of 530 m) and the surrounding settlements is done by two main gravitational supply pipelines, i.e.:

- Right main supply pipeline: made of asbestos cement pipes, with internal diameter of AC DN 250 mm. This pipeline has a break pressure chamber at 644 m above sea level.
- Left main supply pipeline: made on the left side of the river Vardar, where practically two pipelines exist, one of AC DN 350 mm, and the other is PVC DN 380 mm. At 1000 m from the beginning of the left main pipelines, there is a break pressure chamber at 647 m above sea level, in which the two pipelines are connected into one which represents left main pipeline, of AC DN 500 mm.

The two main supply pipelines right at the entrance to the water supply network of the town of Gostivar are connected into one pipeline of AC DN 500 mm.

The characteristics of the water supply network for the town of Gostivar and the surrounding inhabited places are presented in Table 1.

Table 1. Geometrical characteristics of the sewage system

Parameter	Unit measure	Detected in total	Modelled in total
Water supply network:	[km]	168	122
Number of junctions:	N	1111	721
Number of valves:	N	295	259
Number of connections:	N	1502	1073
Min Diameter:	[mm]	25	50
Max Diameter:	[mm]	500	500

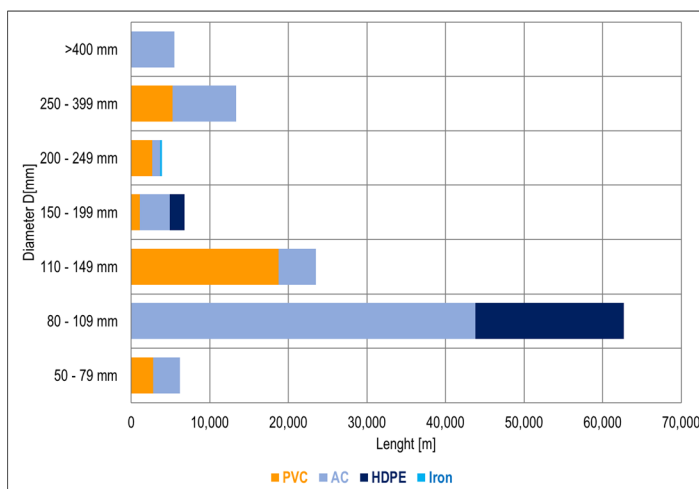


Figure 2. Graphic presentation of the length and diameters of pipelines depending on the material.

In the Figure 2 presents the length of pipes depending on the material and the pipe diameter which are used in the hydraulic model.

Water requirements are analyzed through relevant - reliable data and in this case, it is the General and the Detailed Urban Plan from which the total requirements of water are obtained in the moment of performing the hydraulic analysis. The total net requirements of water which include the requirements of water for the population living in apartment buildings and houses, livestock, commercial and collective buildings are presented in Table 2.

Table 2. Net requirements of water in the moment of the hydraulic analysis of the water supply system

Inhabited place	Consumer type				Total [m3/d]
	Households [m3/d]		Collective buildings [m3/d]	Industry [m3/d]	
	Houses	Buildings			
Town	1,776.0	3,649.0	1,085.0	554.0	11,364.0
Village	3,909.0	0.0	391.0	0.0	

Here we should mention that such calculated requirements of water represent net requirements of water and they do not include the calculations of losses of water whether they are technical or administrative.

4. Hydraulic model

For the hydraulic analysis of the system under pressure such as the water supply systems, the software package WaterGEMS is used, which represents the most sophisticated package for this kind of hydraulic models [2].

The geometry of the network which is imputed from the data base consists of the following elements:

- Pipes (initial and end point, material, length and diameter)
- Junctions (X-Y coordinates, altitude above sea level and water consumption)
- Valves (X-Y coordinates, altitude above sea level, type, material, diameter and connection to the pipes)

For the purpose of obtaining a model that will be close to the real system at creating the model for the water supply system without tanks, the following hypotheses have been used [3, 4, 5]:

- All the pipes of diameter longer than 80mm have been modelled
- Pipes of diameter shorter than 80mm have also been modelled only in the parts where this line is situated between pipes of diameter longer than 80 mm. This has been done for the purpose of observing the concept of that particular part of the network.
- For distribution of the required quantities of water per lines, the automatic function of the software package WaterGEMS has been used – proportional distribution per junctions, separately for the population, livestock, collective buildings and the small-scale industry.
- Large consumers of water are recorded as concentrated consumers in the nearest junction point.

5. Calibration and verification of the results from the hydraulic model

5.1 Calibration of the hydraulic model

For the purpose of performing calibration of the hydraulic model with the actual water supply system, there have been two measurement campaigns performed, where in the first campaign only the flow at 12 points – pipes in total has been measured, while in the second campaign a parallel measurement of the flow and pressure at 13 points in total has been performed, Figure 3.

For the calibration of the hydraulic model, certain hypotheses originating from the results obtained from the measurements have been used, i.e.:

- The water head line does not start from the spring of water but it is at a lower peak elevation from the spring of water, which results in different starting peak elevation in both main supply pipelines.
- The pressure in the measurement points is changeable during the day.
- Four types of variations of the water consumption have been applied depending on the location of measurement.

- There have not been any available relevant data on the coefficient of pipe roughness which, according to the data from the literature, depends on: type of the material, age and the diameter of the pipes.
- Also, there have not been any available relevant data on how big the administrative losses of water are compared to the technical losses of water. Due to that, only the total losses of water in the water supply system have been analyzed in the model, which are modelled in function of the pressure in the water supply network, larger pressure – larger losses and vice versa, with separate coefficient for the town and separately for the villages.

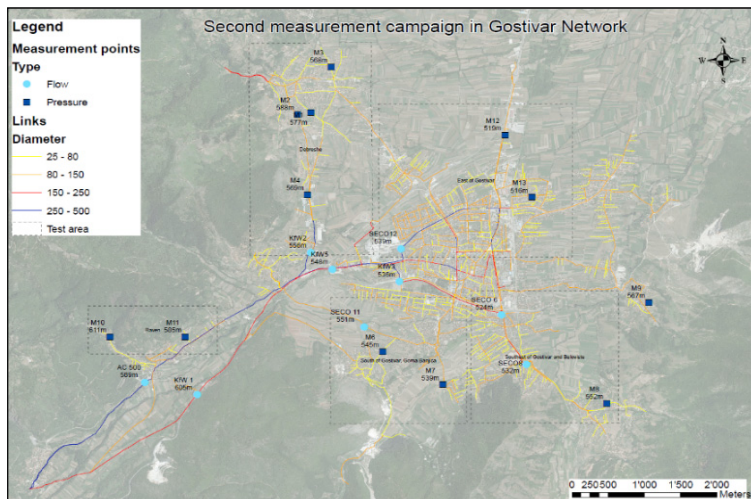


Figure 3. Location of the measurement points from the second campaign

5.2 Verification of the hydraulic model

By applying all the previously mentioned hypotheses in the hydraulic model, verification to the model with the actual water supply system has been performed. Results from the verification on the flow and the pressure of one analyzed point have been presented in Figure 4 and 5.

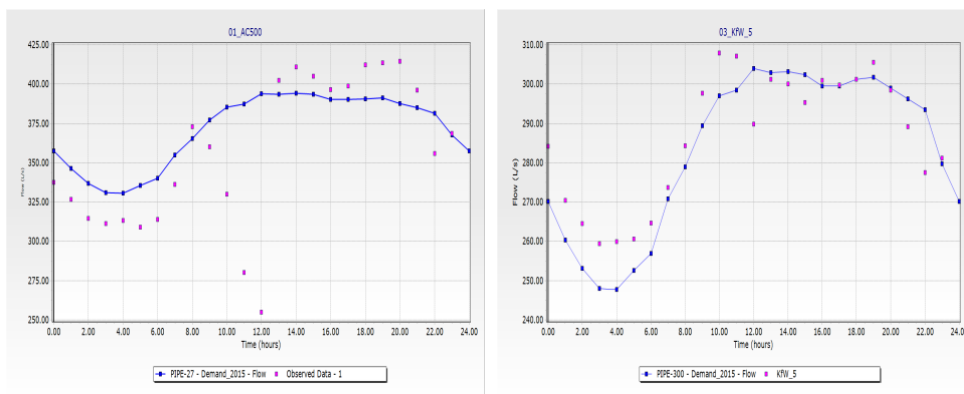


Figure 4. Presentation of the results from the calibration and the verification of the model – pressure

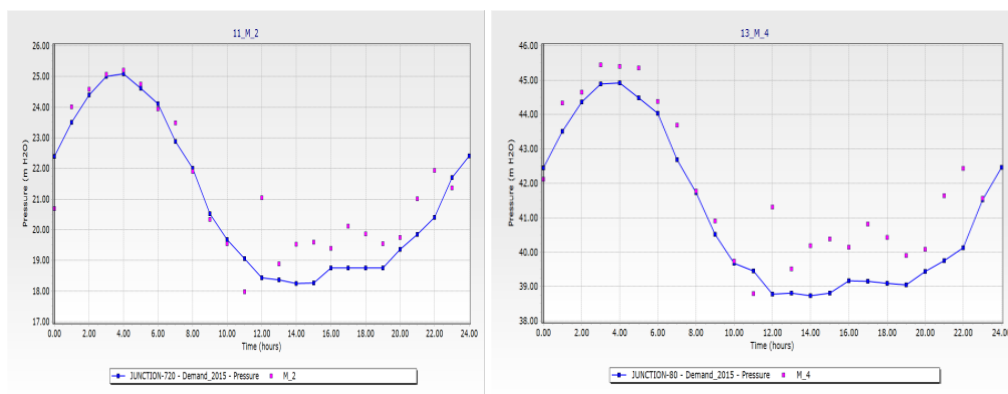


Figure 5. Presentation of the results from the calibration and the verification of the model – flow

6. Analysis of the results obtained from the hydraulic model

From the hydraulic analysis of the water supply system without tanks, the following two significant characteristic states within the system can be realized:

- Certain higher parts of the inhabited places do not have enough pressure for water supply, Figure 6, red color.
- Whereas the pressure in the central town area is larger from the optimal pressure (>6bar) which results in increased losses of water in that part of the system, Figure 6, blue color.

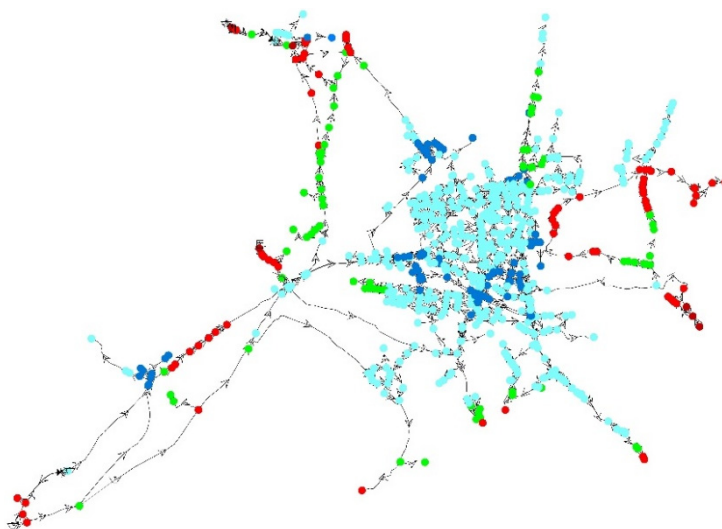


Figure 6. Minimum and maximum pressure

Regarding the fact that the capacity of the spring is much larger than the requirements of water within the system, and not having reservoir space by which the large pressure in the water supply network would be reduced, it has been concluded according to the hydraulic analysis that the total losses of water amount to:

- 71% in the central town area
- 67% in total in all the villages

Also, by means of the hydraulic analysis there have been pipelines - lines detected where the slope of water head is very big, although such states do not have any particular influence to the function of the system as long as the pressure in the town network is high. However, by future reduction to the system it should be taken into consideration that there are “black spots” in the water supply network, and the locations of the pipelines are given in Figure 7 – red color.

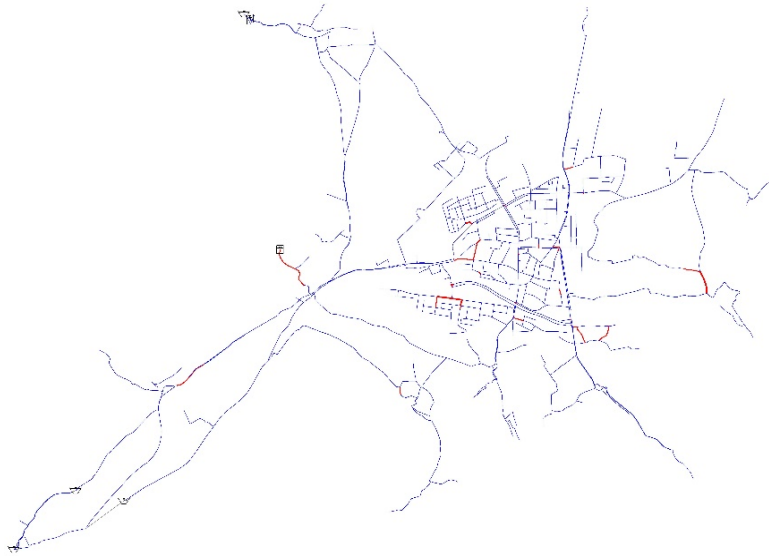


Figure 7. “Black spots” in water supply network

7. Conclusion

From the hydraulic analysis performed for the water supply system without reservoirs, where the capacity of the water spring is bigger than the maximum requirements of water per hour, the following conclusions can be drawn:

- High percentage of total losses of water (71% in the town area, up to 67% in the villages) which owes primarily to the fact that "there is enough water" and there is no need for special attention to be paid to it.
- High pressures in the bigger part of the town water supply network which in certain points are nearly 10 bar.
- In small number of inhabited places, in their higher parts, there is not enough pressure, which owes to the large losses of water in the system and the fact that the entire system is supplied with water as one zone.
- In certain parts – lines there is a short diameter of the pipelines observed – large hydraulic losses per m'

According to the previously stated, as a general conclusion it can be said that even in the case when the capacity of the water spring meets the requirements of water in one water supply system, before making the decision whether to have reservoirs in the system or

not, the remaining parameters of the system should be considered, the working pressure within the water supply network above all.

References:

- [1] Pelivanoski P., Taseski G., Hydraulic model for water supply Gostivar, 2016.
- [2] Bentley WaterGEMS V8i User's Guide, 2017
- [3] Fulvio Boano, Marco Scibetta, Luca Ridolfia, Orazio Giustolisi: Water Distribution System Modeling and Optimization: A Case Study, 13th Computer Control for Water Industry Conference, CCWI 2015, pp. 719 – 724, 2015
- [4] Prabhata K. Swamee & Ashok K. Sharma: „Design Water Supply Pipe Networks“, 2008.
- [5] O. Giustolisi, T.M. Walski, A Demand Components in Water Distribution Network Analysis. *J. Wat. Resour. Plan. Manage.*, 138(4) (2012)
- [6] O. Giustolisi, D.A. Savic , Z. Kapelan, Pressure-driven demand and leakage simulation for water distribution networks. *J. Hydr. Eng.*, pp/ 626–635, 2008.
- [7] Z. Veljanovski ; „Water supply“, 2008.

HYDRAULIC ANALYSIS OF EXISTING SEMI-SEPARATE SEWAGE SYSTEM BY USING SWMM

GOCE TASESKI ¹, PETKO PELIVANOSKI ²

¹ Ss. Cyril and Methodius University Faculty of Civil Engineering – Skopje, taseski@gf.ukim.edu.mk

² Ss. Cyril and Methodius University Faculty of Civil Engineering – Skopje, pelivanoski@gf.ukim.edu.mk

1. Abstract

Sewage systems in the Republic of North Macedonia are designed and constructed as separate sewage systems for sanitary and storm water, but in practice, in the majority of cases they function as semi-separate or combined systems. This owes to the fact that a small number of the inhabited places have a completely built system, i.e. in parts of the urban area there is no sanitary or storm water sewage system. In such case, users of the system, regardless of the network type and the wastewater type, use the existing sewage system by which mixing of water in the collectors occurs.

The aim of this paper is, through the hydraulic analysis of an existing semi-separate sewage system, by means of the software package SWMM, to determine the influence of storm water on the maximum capacities - permeability of the collectors. Also, it is well known that storm water carries solid particles such as sand, soil, gravel which subsequently deposit in the collectors since they have not been anticipated in the phase of designing and construction to receive deposit particles. Therefore, the model will present the influence of pipe fullness with deposits on collector capacity.

Keywords: Sewer system, Storm system, hydraulic model, SWMM

2. Introduction

The need for hydraulic analysis of an existing sewage system of the town of Radovish in the Republic of North Macedonia is imposed by the project for construction of Wastewater Treatment Plant when, in the phase of designing and managing it, there is a large influence of the quantity and quality of water being treated on how economical the technical solution would be. On the other hand, the type and state of the sewage network also influences directly both quantity and quality of the wastewater, which, as it was mentioned before, the sewage network for the town of Radovish was initially planned as a separate system (storm water sewage plus sanitary sewage). Regarding the fact that the storm sewage is poorly developed – there is only a small part of the area and therefore, in the meantime, the storm water sewage under the necessity has been turned into sanitary sewage due to frequent clogging of the existing sanitary sewage [1].

According to the previously mentioned, the current system for which the hydraulic model in SWMM has been made represents a combined sewage system which receives sanitary household wastewater, light industry wastewater, as well as storm water. This concept of sewage system imposes making of hydraulic analysis on the existing sewage

network during dry weather and during precipitations. Also, for the needs of this analysis a complete video recording (CCTV) of the sewage pipes has been made for the purpose of assessing the state of the pipes.

3. Description of the existing sewage system

On the basis of the design documentation and the insight into the existing situation in the field, it has been established that there are 4 drain areas of wastewater in Radovish, two on each side of the river Radovishka, and one drain area in the settlement of Raklish. Collectors at the drain areas in Radovish discharge water at a same location which is at a distance of 800m downstream from the town.

- Collector 100 covers the utmost western part of the town including the industrial zone. In 2010, expanding of the collector was made by using concrete pipes of $D=600\text{mm}$ so that discharge could be carried out at a same location with the other collectors.
- Collector 200 is the oldest collector whose encompassing area covers the oldest part of the town on the right side along the river. This collector functions as a combined collector in its largest part, and the collector for storm water $D=1000\text{mm}$ flows into it, among the rest. It is constructed from concrete pipes of different diameters, from 300 to 1000mm.
- Collector 300 is a relatively new collector whose route leads to the river bed up to the town limits where it turns and continues into the right river bank. At the town limits, a newly constructed line is joined to it, by which one part of the encompassing area of the collector 400 is redirected, and thus this collector covers the largest area. It is constructed from polyethylene corrugated pipes with nominal diameter 500 mm.
- Collector 400 covers storm water from the utmost eastern parts of the town. It was built in the 1990s, from asbestos-cement pipes with diameter of $D=400\text{mm}$.
- Collector 500 has the smallest encompassing area which stretches to the boundaries of the inhabited place of Raklish. The waters collected by this collector are released in the south of Raklish, in the river bed of Raklishka.

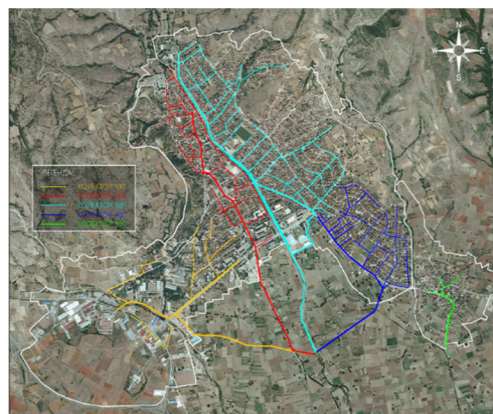


Figure 1. Map of the analyzed system.

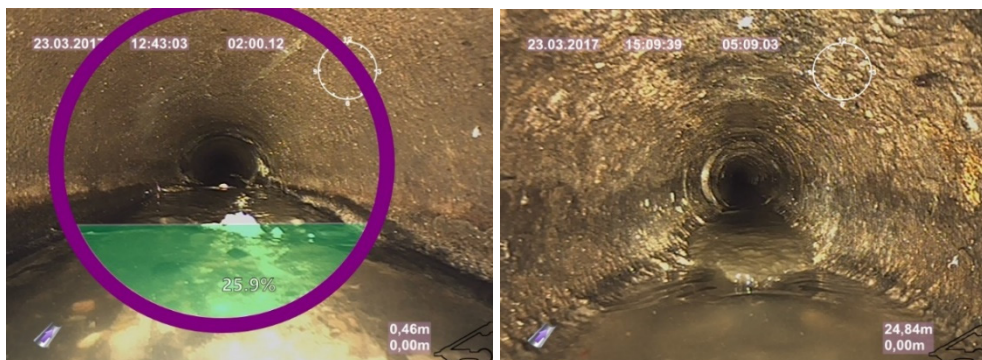
The secondary network consists of predominantly asbestos-cement pipes, with diameter of 250mm. At a small part, concrete pipes (up to 500mm) can also be seen, usually at lines where general sewage is lead, as well as PVC and HDPE pipes (200-300mm), on the lines constructed in more recent period.

Slopes of the network in a large range result from the terrain configuration which is quite mild along the river flow, but quite steep in the high zones of the town. In these parts there are drop manholes constructed for the purpose of moderating the slopes.

Table 1. Geometrical characteristics of the sewage system

Sewage Network									
Collector	Material		Diameter [mm]			Slope [%]			
	ACC	PE	<= 200	300	>= 300	< 4	4-20	20-40	> 40
100	45	55	11	74	16	0	65	25	10
200	67	33	3	70	27	1	75	18	6
300	78	22	10	75	15	0	48	22	30
400	97	3	6	94	0	0	20	28	52
500	100	0	0	100	0	0	0	57	43

For the purpose of making detailed overview of the existing sewage network, visual checks of all the manholes from the system were firstly performed, from which it was concluded that a large number of secondary collectors are filled with sand deposits. Therefore, a complete video recording of the sewage pipes with a special camera (CCTV) was performed, which gave a detailed image of the existing sewage system regarding the existing slope of the pipes, internal pipe diameter, height and fullness with deposit, other possible obstacles in the pipes, etc. In Figures 2 and 3 below, the current state of the manholes and the sewage system pipes is presented.



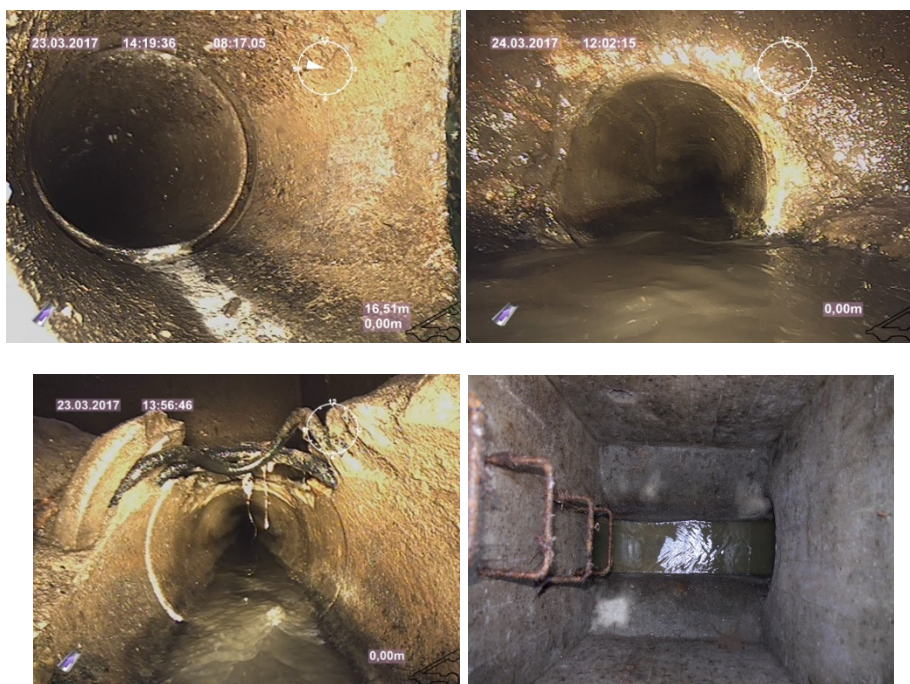


Figure 2. Current situation of manhole and sewerage network - CCTV

4. Wastewater quantity

Regarding the fact that although the sewage system was initially designed and constructed as a separate sewage network, in practice it functions as a general sewage system, which primarily owes to the insufficiently built storm water sewage and clogging in part of the collectors from the sanitary sewage. Therefore, as realistic wastewater quantities for the hydraulic analysis, sanitary water from households and light industry was taken, as well as storm water with rainfall in duration of 10 minutes and frequency of 2 years.

4.1 Sanitary Water Quantity

The quantities of sanitary water for the town of Radovish have previously been defined by the Study for Construction of Wastewater Treatment Plant in Radovish and they are presented in Table 2 below [1].

Table 1. Sanitary Water Quantities

Description	Units	Values
Average daily dry weather flow, (DDWF _{aver.})	m ³ /d	3,895
Maximum daily dry weather flow, (DDWF _{max.})	m ³ /d	5,134
Peak hour dry weather flow, (HDWF _{max.})	m ³ /h	344
Peak wet weather flow under normal conditions, (HWWF _{norm.})	m ³ /h	508
Peak wet weather flow under extraordinary conditions, (HDWF _{extr.})	m ³ /h	923

4.2 Storm Water Quantity

Data on realistic rainfall are taken from the nearest weather station, for which measurements exist, Figure 3. In the analysis for wet weather, rainfall with frequency of 2 and 5 years is taken and duration of 10 min.

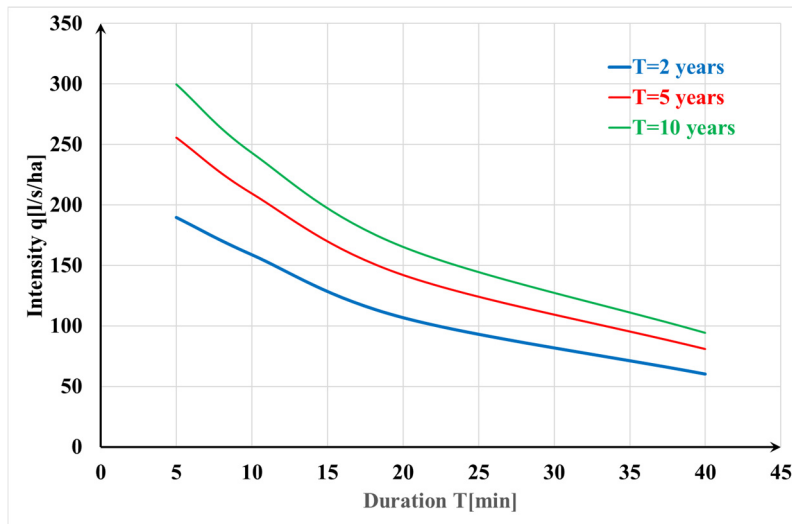


Figure 3. IDF curve

5. Hydraulic model

The efficiency of the system for wastewater drainage, through the hydraulic analysis presents possible weaknesses and bottlenecks in the network, and by that it helps in optimizing the means for reconstruction and planning. Today's advanced mathematical models enable analysis of complex sewage systems for various scenarios. A model in the software package "Storm Water Management Model" (SWMM)[2] was created for the needs of this paper. The following scenarios have been reviewed in it:

- Peak hourly flow at dry weather,
- Peak hourly flow at wet weather for combined system of 10-minute rain and frequency T=2 and 5 years.

As it was previously mentioned, part of the sewage pipes are filled with deposit, most frequently the pipes which are placed normally on main collectors and because of that, for both scenarios there are hydraulic analyses made in the state when the sewage pipes are completely clean and in the state when part of them are filled with deposit.

According to the images made, in all sewage pipes in the parts which have deposits, the deposit height ranges from 15 to 29% of the internal pipe diameter.

The quantities of wastewater and storm water are distributed per encompassing area of the network manholes. The transformation of rainfall into flow is done by the rational formula ($Q=F \cdot C \cdot i$), where for the coefficient of discharge, the value of 0.40 has been taken, while the pipe roughness is adopted according to experiences, but also recommendations in literature depending on pipe material and age.

6. Analysis of results from the hydraulic model

The results from hydraulic model for both scenarios are shown in the following figure.

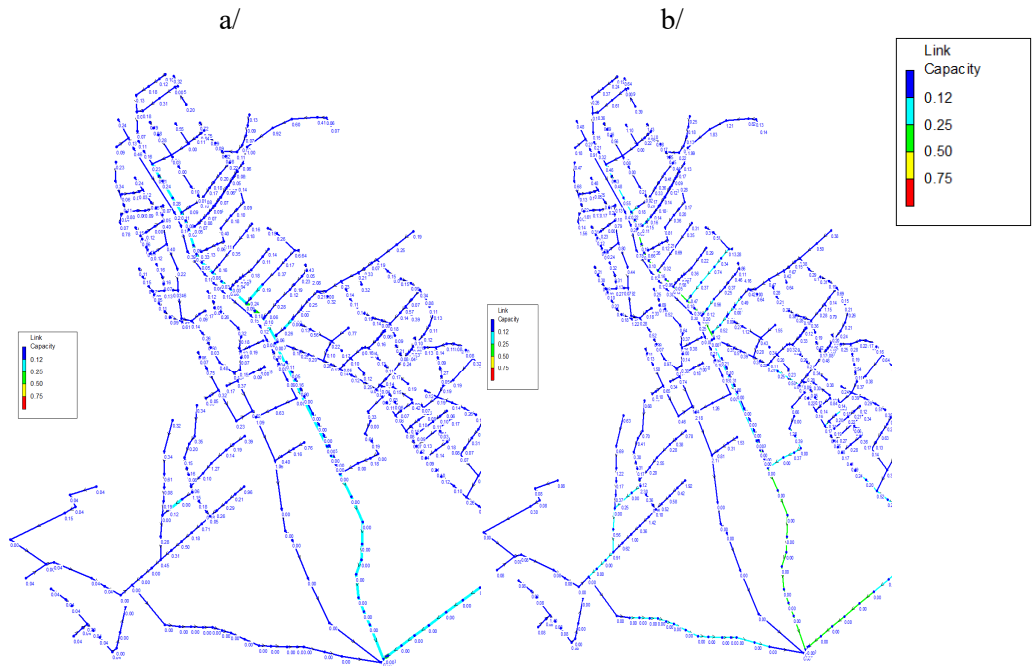


Figure 5. Peak hour dry weather flow: a/ clean network; b/ filled with sediment

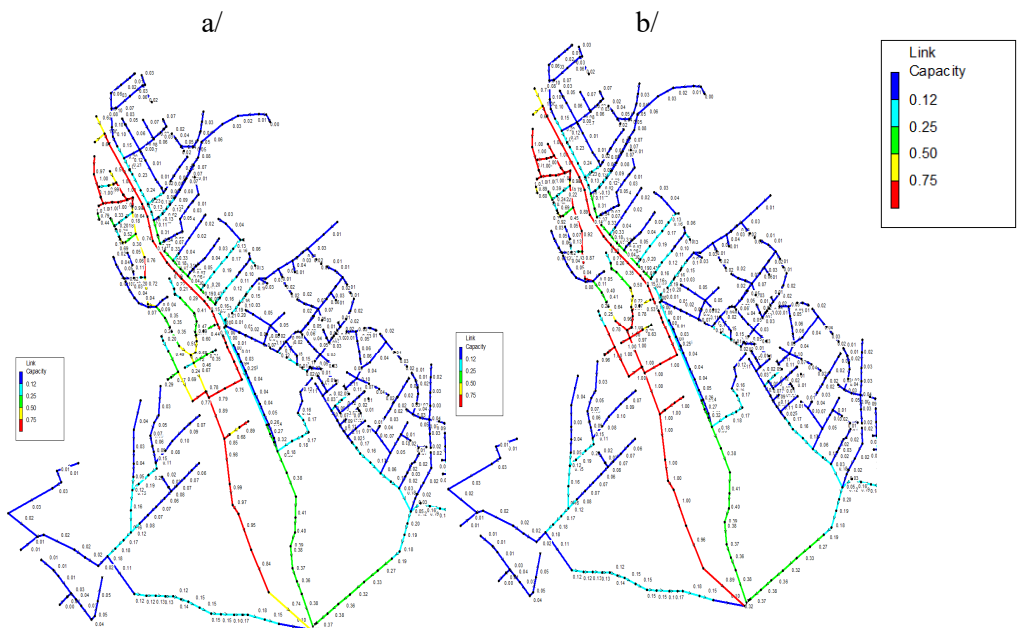


Figure 6. Peak hour wet weather flow: a/ clean network and rainfall with frequency of 2 years and duration of 10 min; b/ network with sediment and rainfall with frequency of 1 year and duration of 20 min

The following significant characteristic states in the system can be observed from the hydraulic analysis of the system regarding all scenarios:

- During dry weather and in the state of decreased permeability of the pipes and in the state when they are completely clean, there are no existing parts of the sewage network where the capacity exceeds.
- In the state when the sewage system functions without decreased permeability - without deposit inside the pipes, except for the maximum quantities of sanitary water, it can receive rainfall of 10-minute intensity and frequency of 2 years without manhole overflow except on one branch of the sewage network, Figure 6.
- While in the situation when there is deposited material in one part of the pipes, the sewage overflow happens during 20-minute rainfall with frequency of each year, Figure 7 shows the places where the sewage system overflows (red color).

7. Analysis of results from the hydraulic model

By last year construction of the first larger wastewater treatment plants in the Republic of North Macedonia, the need for analysis increasingly occurs for the sewage systems in towns where in the past their function has not been considered very much. Namely, majority of them are designed as separate systems, and in practice they function as combined sewage systems by which the quantity significantly increases and the quality of wastewater ending in the wastewater treatment plant decreases. Also, large amounts of sand are transported in them which incidentally deposit inside the pipes, and part of it goes towards the wastewater treatment plant, which has negative impact of both technical and economic character on the wastewater treatment process.

Regarding the sewage system in Radovish, it can be observed that it is above its dimensioning for receiving sanitary water, which is its primary function, while for receiving storm water there needs to be a new sewage system constructed, by which these waters would be received and safely evacuated from the inhabited place. That would enable the future functioning of the wastewater treatment plant in optimal technical and economic conditions, and also the manhole overflows would be avoided, which currently happens practically with every rainfall.

References:

- [1] Pelivanoski P., Taseski G., Study for updating of the existing sewage system in Radovish, 2017.
- [2] Gironas J, Roesner LA, Davis J. Storm water management model applications manual, EPA, United States. 2009; p. 180.
- [3] Rossman LA. Storm water management model user's manual, version 5.0, EPA. United States. 2009; p. 233.
- [4] American Society of Civil Engineering. Gravity Sanitary Sewer Design and Construction. ASCE Manual of Practice. 1982; 60: p. 275.
- [5] Gironas J, Roesner LA, Davis J. Storm water management model applications manual, EPA, United States. 2009; p. 180.
- [6] Butler D, Davies J. Urban Drainage, Chapter 7. System component and design, Taylor & Francis. 2011; p. 28
- [7] Richard Field "Storage/Sedimentation Facilities for Control of Storm and Combined Sewer Overflows", U.S. Environmental Protection Agency (EPA)

A COMPARISON OF FLOOD ROUTING BY MODIFIED LINEAR MUSKINGUM AND KINEMATIC WAVE APPROACHES ON THE DRAVA AND MURA RIVERS

DAMIR BEKIĆ¹, TIN KULIĆ², KLAUDIJA BAŠIĆ³

¹ University of Zagreb, Faculty of Civil Engineering, Croatia, damir.bekic@grad.hr

² University of Zagreb, Faculty of Civil Engineering, Croatia, tkulic@grad.hr

³ University of Zagreb, Faculty of Civil Engineering, Croatia, kbasic@grad.hr

Abstract

During flood events hydrographs may experience significant transformation in the downstream reaches due to translation, physical dispersion and lateral inflow/outflow. The overland flow is more complex than the in-channel flow and routing is usually calculated by non-linear approaches. This paper presents the development of modified linear Muskingum-McCarthy (MM) and kinematic wave (KW) approaches for routing of flood hydrographs and the results of hydrograph calculations on the Mura and Drava rivers. The original MM and KW approaches were modified so that inflow hydrograph to a reach is separated based on a flow rate, and separated hydrographs are then routed independently in a reach. In such a way the overland flow is routed independently and differently from the in-channel flow but is transformed by using linear approximation. This idea is applied in HEC-HMS model by using different K , x parameters (MM approach) and Manning's roughness coefficients n (KW approach) for the in-channel and overland flows. Such approach is physically based as the overland attenuation is significantly larger than the in-channel flow. The modified linear Muskingum-McCarthy and kinematic wave models were applied for the calculation of flood hydrographs on the Drava and Mura rivers. The subject area covers the 106.6 km long section of the Mura river (from g.s. Gornja Radgona in Slovenia to its confluence into the Drava river in Croatia) and the 27.5 km long section of the Drava river in Croatia (from hydroelectric power plant Dubrava to g.s. Botovo). Input dataset included hourly discharges on several gauging stations for 19 historical flood events in period 1996-2018. Model calibration was performed for 4 events on trial-and-error basis by comparing measured and calculated hydrographs on six hydrological stations, and model verification is done for other 15 events. The goodness of fit was evaluated for peak discharge, time of peak discharge and volume of hydrograph by using mean absolute error (MAE), relative mean absolute error (RMAE), root mean square error (RMSE) and Nash-Sutcliffe efficiency coefficient (NSE). It was shown that the modified Muskingum-McCarthy model performs better for routing of flood waves on the Mura and Drava river than the modified kinematic wave approach.

Keywords: Muskingum-McCarthy method, kinematic wave method, flood routing, HEC-HMS, Drava river, Mura river.

THE IMPACT ON THE ENVIRONMENT WITH THE CONSTRUCTION OF ALL PHASES FROM THE MULTI-PURPOSE HYDRO SYSTEM ZLETOVICA

ELENA ALEKSOVA-DOSEVSKA ¹

¹ PE HS Zletovica- Republic of Macedonia, e.aleksova@hszletovica.com.mk

1. Abstract

The construction of Hydro system Zletovica (pic. 1) is planned in few phases, such as:

- Phase I-water-supply of approximately 100.000 inhabitants in municipalities Probishtip, Shtip, Sveti Nikole, Lozovo and Karbinci
- Phase II- irrigation of 4.500 ha in municipalities of Probishtip and Kratovo
- Phase III-production of electricity with the construction of 6 small hydro power plants with installed power of 9,7 MW and planned production of 50 GWh.

First phase – water-supply is completed and is in operation since 2011, since when with drinking water are supplied municipalities Probishtip and Sveti Nikole, while others are in preparation for receiving raw water from the system.

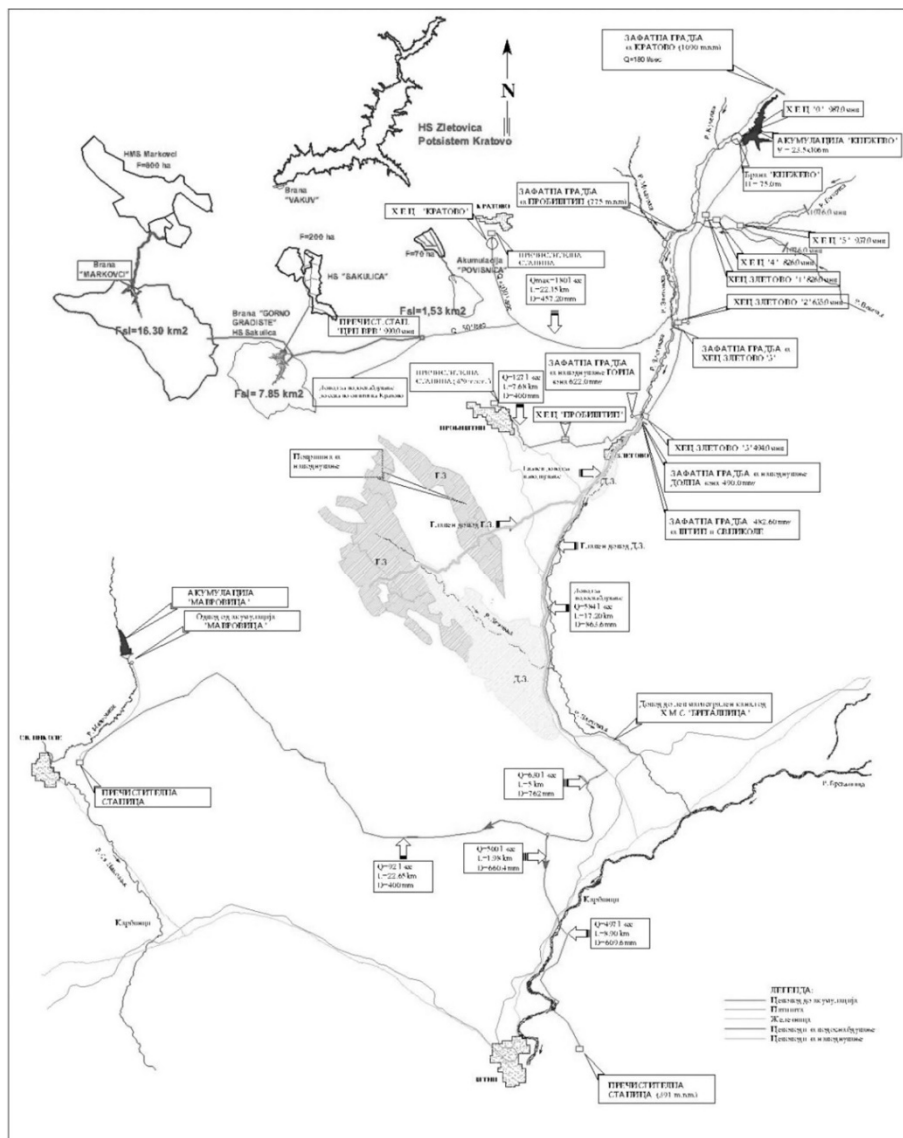
According to the Environmental Impact Assessment Study and permits for water capture, the construction of the hydro system does not cause an environmental disorder on flora and fauna, but on the contrary reduces the risks to human health and ecosystems had improved life in the region.

The remaining two phases- irrigation and production of electrical energy are in the final phase of preparation of technical documentation where, according to the Integrated Environmental and Social Impact Assessment Study (ESIA) for Phase II and Phase III, negative impacts on the environment are expected in the construction phase, but it is the responsibility of the investor to clearly implement the environmental management and monitoring plan, as well as the further maintenance of all systems.

2. Introduction

A critical problem confronting humankind today is how to manage the intensifying competition for water between expanding urban centres, traditional agricultural activities and in-stream water uses dictated by environmental concerns.

In the agricultural sector, the dwindling number of economically attractive sites for largescale irrigation and drainage projects limits the prospects of increasing the gross cultivated area. Irrigated agriculture is the third biggest sector after services and industry in the economy of the Republic of Macedonia. Therefore, it is a challenge to increase agricultural production, which will necessarily require application of new technologies, more accurate estimation of crop water requirements, major improvements in the construction, operation and management of existing irrigation, as well as drainage systems and construction of new irrigation networks



Picture 1. Display of all phases of HS Zletovica

Irrigation by its nature is an integral part of crop production and it is treated as one of the technical measures that agricultural producers have applied to their surfaces.

Based on the forecasts for population growth and the improvement in the living standard, it is expected that food production will grow rapidly in the next years. In addition, it is expected that 90% of the increase in food production will have to come from existing cultivated land and only 10% from new land reclamations, either in the highlands, or in the lowlands. It is not expected that cultivated area without a proper water management system can contribute to the future improved food production. Zletovska river represents a unique source of pure and healthy water for long-term solving of water economy problems of this region. This river is the right tributary of Bregalnica River and runs through the east driest region of Macedonia.

2.2 Data for Hydro system "Zletovica"

Zletovica Hydro System presents a multipurpose water economy system, located in the eastern and north-eastern part of Macedonia, which provides complete usage of the available water and hydropower potentials of Zletovska River. The realization of this regional and extremely important hydro system will provide a long-term supply of water to about 100.000 people, irrigation of 4.500 ha of agricultural land and an annual production of electric power of about 49.5 GWh.

At the same time, the general benefit of the realization of the Project is the development of the East and North-East regions of Macedonia, greater economic growth and better living conditions.

The realization of the multipurpose project HS "Zletovica" is planned to be carried out in three phases as follows:

- Phase I: Water supply - Access road, Knezevo Dam with an asphalt core with a height of 75.0 meters with its associated structures, intakes and main water supply inlets (completed in 2011)
- Phase II: Irrigation of some 4.500 ha in the region of municipalities of Probishtip and Kratovo; and
- Phase III: Construction of small hydroelectric power plants.

3. Phases of the project Zletovica

3.1 Phase I: Water supply

The overall realization of this project was conditioned by elaboration impact assessment study, whose main goal is to determine the measures for protection of the human health and ecosystem's quality. Therefore, besides the environmental impact assessment, the study will also analyze the demographic, economic, social and cultural aspects, including the development aspect and interests of the affected space users.

It is known that each intervention taken in the environment, even its most favorable variant, causes certain direct and indirect changes of some environmental parameters, which in a long-term run, could cause several unwanted effects.

The environmental impact assessment has a goal to determine the compatibility of the activities planned in the watershed of Zletovica River and in the locality of Knezhevo Dam, and to point out an efficient way for maximal reducing of the harmful impact resulting from the planned activities in the space. Therefore, in the frameworks of this ecological study, appropriate, comprehensive analysis of the environmental impact has been carried out.

Dams transform landscapes and create risks of irreversible impacts. Therefore, protecting and restoring ecosystems at river basin level is essential to foster equitable human development and the welfare of all species. The natural environment couldn't be preserved completely. Principal task is to provide conditions for maximum possible protection. One particular change leads to chain of changes and therefore it is necessary to institute some measures aimed at ensuring the sustainable and integrated management of the Hydro system Zletovica.

Construction of the hydro system Zletovica might influence the conditions in the upstream and downstream areas of the dam site, in the area of the storage reservoir even around the large region. These changes might be of positive or negative connotation.

Main benefit од изградбата на hydrosistem will generally solve the current problems of drinking water for almost 100.000 inhabitants in municipalities in the semiarid area of eastern part (Shtip, Probishtip, Sveti Nikole, Lozovo and Karbinci), as well as flood protection and regulation of water flows.

During the construction of the dam as well as in exploitation, all the measures and recommendations given in the above study the summary assessment of the Hydro system Zletovica points out that this object does not present dangers for the environmental mediums, human, fauna, flora and cultural heritage. On the contrary it will significantly reduce the risk upon the human health and ecosystem and will improve the quality of living of more inhabitants livings in affected municipalities related to the project.

3.1.1 Activities undertaken during the exploitation of phase 1-water supply

With the commissioning of the Hydro system, a permit for water capture (2012) was obtained by the Ministry of Environment of the Republic of Macedonia, which has been extended in 2018, where the hydro system has a legal obligation to maintain the regime and the quality of the river Zletovica and the Ash it is regularly realized as follows:

- Providing continuous biological minimum flow in the Zletovska River, as follows:
 - ✓ Profile Knezhevo: 95 l/s for the cold season and 155 l/s for a warm season
 - ✓ Water station Zletovo: 200 l/s for the cold season and 300 l/s for the hot season
- Regular monitoring of the condition of the quality of the affected water in the two intakes individually, the accumulation of dam Knezhevo, the tributaries of Zletovska river (total of 10 measuring points) and the data from the performed measurements are submitted to all competent bodies in accordance with the Law on Waters, Water and Water Safety Rules.
- Elaborate for the Protective Zones of the Hydro system "Zletovica" has been prepared, which has been approved by the Ministry of Environment, Ministry of Health on the basis of which a Decision was adopted for determining the protection zones for protection of the waters for the area of the Zletovska River, and the accumulation of Knezhevo with the approval of the Government of the Republic of Macedonia defining three protection zones (Fig. 2):
 - First closer zone of protection, or a zone of strict sanitary supervision
 - Second wide zone of protection, or a zone of sanitary restriction(limitation)
 - Third wider zone of protection, or a zone of hygienic-epidemiological monitoring
- PE HS Zletovica performed forestation on an area of 40ha, in the area Drtavica municipality Kratovo with: spruce, fir, white pine, daglasia and pitted chestnut in exchange for the destroyed forest during the construction of the accumulation.

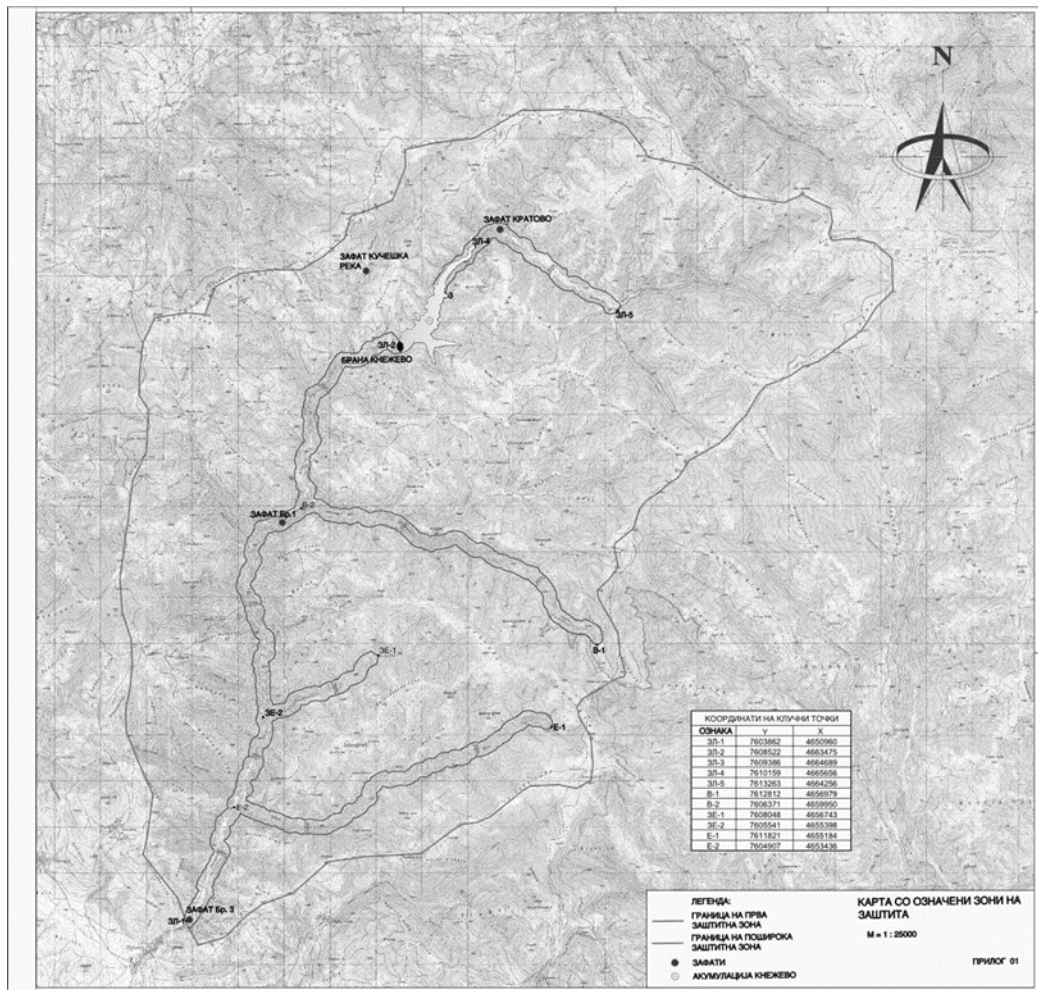


Figure 2 Protective zones of Hydro system Zletovica

3.2 Characteristics of future planned phases of Hydro system Zletovica

3.2.1 Phase II-irrigation

Planning and construction of the Phase II-irrigation system from the multi-purpose system Zletovica is based on analyzing several alternatives. The main criteria for evaluation of each alternative are financial cost, environmental and social impacts.

This alternative is most useful for investment, it is also the least harmful to the environment in the project area.

The technical solution envisages irrigation in the municipalities of Probishtip and Kartovo, as follows:

- Probishtip irrigation system
 - ✓ Subsystem Upper zone with irrigation area for 2300 ha
 - ✓ Subsystem Down zone with irrigation area for 1500 ha

- Kratovo irrigation system
 - ✓ Subsystem Markovica with irrigation area for 800 ha
 - ✓ Subsystem Sakulica with irrigation area for 200 ha
 - ✓ Subsystem Povishnica with irrigation area for 70 ha

3.2.2 Phase III - production of electricity

In this phase, several solutions on the basis of technical, economic and environmental aspects have been considered, which show the most optimal utilization of the potential of Zletovska river, thus envisaging the planned production of 49.5 GWh with installed power of 9.7 MW with the construction of 6 small hydro power plants, three of them along the Zletovska River: HPP Zletovo 1, HPP Zletovo 2 and HPP Zletovo 3, one hydropower plant at the biological minimum of the Knezhevo HPP B dam and two hydro power plants for the supply pipelines for water supply of the municipalities Probishtip and Kratovo, both HPP Probishtip and HPP Kratovo.

4. Impact assessment on the environment and social aspects for the future planned phases of the Zletovica project

4.1 Methodology for assessment of the impacts

The analysis of the impacts takes into account any potential changes, positive or negative, on the environment and socio-economic aspects, which may result from the realization of the Project. The Environmental and Social Impact Assessments Study presents details of the Project's potential impacts and effects in the assessments. For that purpose, the following distinction between impacts and effects was made:

- Impacts are the predicted changes in the current conditions of the environment, resulting from the implementation of the Project; and
- Effects are the consequences of impacts on the environmental resources or receptors with particular value or sensitivity.

The assessment in the Environmental and Social Impact Assessments Study examines:

- Collection of environmental data by research and monitoring;
- Consultation with relevant stakeholders/parties concerned in order to identify the key problems and to obtain further data, where necessary;
- Evaluation of appropriateness and limitations of the assessment methodology;
- Identification of resources and receptors;
- Prediction of the impacts;
- Identification of the effects;
- Evaluation of the intensity;
- Identification of the mitigation measures; and
- Evaluation of residual effects And after implementation of the mitigation measures or risks.

The Environmental and Social Impact Assessments Study (ESIA) identify the environmental impacts resulting from implementation of the project in its different phases: pre-construction, construction, operational and decommissioning phase

Pre-construction phase covers activities for preparation of designs and plans, as well providing necessary permits/signed contracts, which will allow proper project implementation.

Construction phase includes preparation of site and construction activities for Phase II construction

of irrigation system for the municipality of Probishtip and Kratovo (which include construction of intakes, dams, main pipelines, irrigation networks and other required structures for irrigation of agricultural land, access roads etc.) and activities for Phase III preparation of the sites and construction of six small hydroelectric power plants in the Municipality of Probishtip and Kratovo (which include construction of intakes, sedimentation tanks, tunnels, siphons, penstocks, powerhouse, electricity transition lines, access roads etc.).

Operational phase include activities for operation of the both systems, its regular maintenance, repair and reconstruction. Impacts that may be caused by these activities are subject of analysis in the operational phase.

Decommissioning phase comprises the impacts on the environment and social aspects, which are similar to the construction phase, because of similar activities for excavation, digging, dismantling of facilities, pipelines and other structures, usage of machinery, transport of waste and other similar activities, which are expected to be performed in the decommissioning phase. It cannot be foreseen which approaches will be taken at the time of decommissioning of both systems and separate facilities. Impacts will depend of future available dismantling techniques at the time of decommissioning.

4.2 Cumulative impacts from the construction of all phases of the project

As it was described above, HS "Zletovica" with all designed phases (I, II, III) will be of benefit for two Regions in the Republic of Macedonia (East and North East) and especially two municipalities Probishtip and Kratovo, which are low developed municipalities.

The HS will provide healthy potable water for about 100 000 inhabitants, irrigation of agricultural land, intensifying of farming and production of electricity from renewable sources (which will reduce emission of greenhouse gases).

Thus, the Project results will have positive cumulative impact to the economic development of the two regions, improve human life/well-being.

4.2.1 Environmental positive cumulative impacts

Changes in the environment caused by predicted activities in combination with other activities from the past, present or future activities that are similar with the activities planned within the observed area are assessed as cumulative impacts. Project, in general, will have cumulative positive impact in the two project areas (subsystem-Probishtip and subsystem-Kratovo). The positive effects will be related to: improving the water supply and human health in the Region, improving the existing agricultural practices and yield, better ecological status of the surface water body and subsequently of the ground water, improving the quality of the soil, due to controlled and efficient use of fertilizers and management and in general sustainable development of the municipalities of Probishtip

and Kratovo. The electricity production is a benefit of the entire project due to replacement of significant quantities of fuel for electricity production with renewable energy/hydro-potential.

4.2.2 Adverse cumulative impacts to the environment

The possible adverse cumulative impacts is in the construction phase, because of the planned activities for construction of the irrigation system and small hydropower plants (HPPs), planned in Phase II and Phase III of the Project "Hydro system Zletovica".

As a result of the past construction activities and future planned activities for construction of HPPs and irrigation system, some degradation of the environment already have been done or will occur in the future, so the cumulative impacts are expected on the geology and soil, biodiversity, hydrological characteristics of the water body.

The expected cumulative effects include noise emission, air emissions, waste, wastewater, which may cause negative impact on the air quality, soil, surface and ground water, biodiversity, landscape, human health, labor engagement, land use, use of resources (raw materials, water supply, electricity, use of roads, landfills, etc.).

With implementation of good planning and construction practice and regular monitoring of the affected media and receptors, the cumulative impact could be minimized.

Productions of electricity from small HPPs is considered as environmentally friendly energy sources and give great contribution for reduction of GHG and mitigation of climate changes. Production of electricity of these HPPs will replace the production and use of energy from non-renewable sources of energy that generate greenhouse gases.

Irrigation system and small HPPs will cause cumulative impact on the rivers related with changes of the flow, morphological characteristic of the rivers as a result of removal of sediment, etc. This impact will be expressed more on Zletovska River in the area downstream from Knezhevo dam to village of Zletovo where will be located more intakes for water supply, irrigation and production of electricity (operation of four HPPs).

4.3 Measures to reduce environmental impacts and social aspects

Environmental mitigation measures are designed to avoid or mitigate the identified negative environmental impacts that may be caused by the implementation of the project. Pursuant to the legislation, the Monitoring Plan aims to assess the extent and effects of the implementation of the mitigation measures of the project.

As part of the Site Management Plan, the Contractor will develop and implement a Construction Environmental and Social Management Plan to support good environmental and social management practices. The CESMP will be developed and implemented in line with the international standards (i.e. ISO 14001 & SA 8000) and will include:

- ✓ Organization, responsibilities and resources;
- ✓ Construction Environmental and Social Management Plan, including supplementary plans (e.g. Dust Management Plan, Blasting Management Plan,

Noise and Vibration Management Plan, Traffic Management Plan, Vegetation Removal Management Plan, Water Management Plan, River Crossing Management Plan, Fish Stock Management Plan, Flood Protection Management Plan, Waste Management Plan, Hazardous Materials and Spill Prevention Management Plan, Emergency and Response Management Plan (which will include Firefighting Management Plan), Vegetation Management Compensation Plan, Raw Materials Management, Soil and Erosion Management Plan, Occupational Health and Safety Plan (OHSP) with implemented Employee grievance mechanism etc.);

- ✓ Procedures for each plan;;
- ✓ Construction Monitoring Plan;;
- ✓ An audit process and program (including performance audits, audits on labor & working conditions);
- ✓ Training program; and
- ✓ Reporting of environmental and social performance.

4.3.1 Mitigation Measures

The magnitude of cumulative impacts in the construction phase is moderate and mitigation measures are required. The mitigation measures for the cumulative social impacts on the environment and social aspects in the construction and operational phase will primary include:

- ✓ Communication and coordination of activities with other institutions/companies that are developing and implementing plans and projects in the project area;
- ✓ Adjustment of construction activities between investors in relation to the period of implementation of special projects;
- ✓ Adjustment of the planned activities within the project (HS Zletovica), the Plan of measures and activities of Bregalnica River Basin Management Plan;
- ✓ To establish a harmonized allocation of water for priority supply of HS "Zletovica";
- ✓ Training for all users of the planned systems

4. Conclusion

With the construction of all projected phases (Phase I-water supply, II-irrigation, III-energy) within the HS "Zletovica" will have a positive impact on the economic development of both regions, will improve people's lives and well-being by providing new hiring and reducing poverty through the development of agriculture.

The project as a whole will have cumulative positive impacts in both project areas by improving the water supply and health of the people in the region, enhancing the existing agricultural practices and yields, the ecological status of surface waters, and consequently the groundwater, improving the quality of the soil, control and efficient use of fertilizers.

The production of electricity for the benefit of the whole project is due to the replacement of a significant amount of fuel for the production of electricity with renewable sources / hydro potential.

References:

- [1] Basic project for Branka Knezhevo with accompanying objects, Book 1-General part, GIM-Skopje, Faculty of Civil Engineering-Skopje, April 2008
- [2] Phase II Phase Studies Irrigation Book 1-Text Contributions, Sweco Aqua Hydro Consortium, December 2013
- [3] Environmental Impact Assessment Study of the Construction of Irrigation System and Hydro Power Plants in the Hydro System Zletovica, Sweco Aqua Hydro Consortium, October 2015

APPLICATION OF ADCP IN SUSPENDED SEDIMENT MONITORING

NEVENA CVIJANOVIĆ¹, MLADEN KOSTIĆ² AND MIRA IVLJANIN³

¹ Jaroslav Černi Water Institute, Serbia, nevena.cvijanovic@jcerni.rs

² Jaroslav Černi Water Institute, Serbia, mladen.kostic@jcerni.rs

³ Republic Hydrometeorological Service of Serbia, Serbia, mira.ivljanin@hidmet.gov.rs

1. Abstract

Suspended sediment is a natural component of any river system. It is important to continuously monitor the suspended sediment transport, given the effects of changes to erosion and sedimentation patterns will depend on whether the change results in an increase or decrease in sediment availability.

Over the past decades, human activities within the Danube River and its tributaries have led to strong changes in the natural sediment load. These changes negatively influence important water management issues such as flood risk, inland navigation, ecology and hydropower production. The International Commission for the Protection of the Danube River (ICPDR) has recognized a lack of sediment management in the Danube River Basin and to tackle this challenge, 14 partners from nine countries came together in the DanubeSediment project. Their goal is to improve water and sediment management as well as the morphology of the Danube River. The project team proposed that the sediment monitoring in Danube River Basin should be based on coordinated national monitoring programs, having a common or at least comparable methodology, instruments and techniques. In order to achieve this task, future sediment monitoring system should include contemporary methods such as optical and acoustic backscatter sensors (OBS and ABS). The initial results in utilization of backscatter sensor (Acoustic Doppler Current Profiler - ADCP) for suspended sediment monitoring will be presented in this paper, as well as the reliability assessment relative to the data collected using conventional methods.

Keywords: suspended sediment monitoring, backscatter intensities, ADCP, data correlation

2. Introduction

Conventional measurement techniques for collecting of data on suspended-sediment concentration (SSC) are real challenge considering the time and effort to collect all necessary data. Furthermore, it is often unfeasible to perform measurements during the floods, which leads to a lack of data in this range of flow. For those reasons, there is a need to establish a contemporary and sustainable methods in sediment monitoring systems which will enable continuous data acquisition. Instead of conventional monitoring methods, optical and acoustic backscatter sensors (OBS and ABS) are widely used in sediment monitoring programs all around the world. The ultrasound method

(Acoustic Doppler Current Profiler - ADCP) is primarily designed for measuring velocity profiles. Since the measurement of flow velocity with ADCP is based on particles velocity in river flow, it can be assumed there is a correlation between the acoustic backscatter intensities and SSC.

For more than two decades, Acoustic Doppler Current Profilers have been in common use measuring current profiles. In recent years, the acoustic sensors such as ADCP have become a more widely used in means of estimating suspended solids. Plenty of studies have indicated that there is a strong relation between acoustic backscatter intensity and SSC. However, these studies also pointed out that the use of ABS for estimating the SSC has a lot of limitations factors, which affect the measurement results. Those factors include variations in water salinity and temperature, sediment particle size and concentration, water depth and surface conditions, and other that can result in unreliable data. For this reason, the acoustic sensor must be periodically calibrated to the water sample data, in order to obtain reliable SSC results. Regardless of these shortcomings, acoustic sensors offer some advantages over traditional methods in SSC monitoring. For example, water samples only provide information at a specific point or the water column, while ADCP can provide information through the entire cross section. To collect the same amount of information with conventional methods such as periodic sampling in different layers of the water column, much more time and effort is needed.

Recent studies found good correlation between acoustic backscatter from ADCP and measured concentration by direct measurement. The method of converting backscatter into SSC can be done by the principle of sonar equation [1]. The direct measurement of SSC can then be correlated with echo intensity from ADCP using simple regression linear equations. These equations can then be used to estimate time series data of SSC from ADCP backscatter values. This paper describes the results of a field experiment in which SSC values were estimated at multiple layer of depth from the ADCP data.

3. Methods

3.1 Study area and data collection

1. Introduction

As the second largest river in Europe after the Volga, the Danube River passes through or bordering 18 different countries and integrates different impacts. From its source in the Black Forest Mountains of Germany, it flows east over 2850 km across the continent to the Black Sea. Many countries have built dams on the Danube with the purpose of hydropower generation, water supply, and flood control. Located on the Lower Danube (Serbia), approximately 900 km upstream from the Black Sea, the Iron Gates (Figure 1) is the largest dam and reservoir system by volume, area and hydropower potential. Sediment regime is very significant factor in case of river dams, due to the inevitability of sedimentation process in reservoirs and consequential reduction of its active storage.

To provide an assessment of the sediment transport and deposition processes in the Iron Gates Reservoir, a monitoring program has initiated in 1974 by the Jaroslav Černi Water

Institute (JCI) and it is still going on. The sediment monitoring has been performed within the annual program which includes:

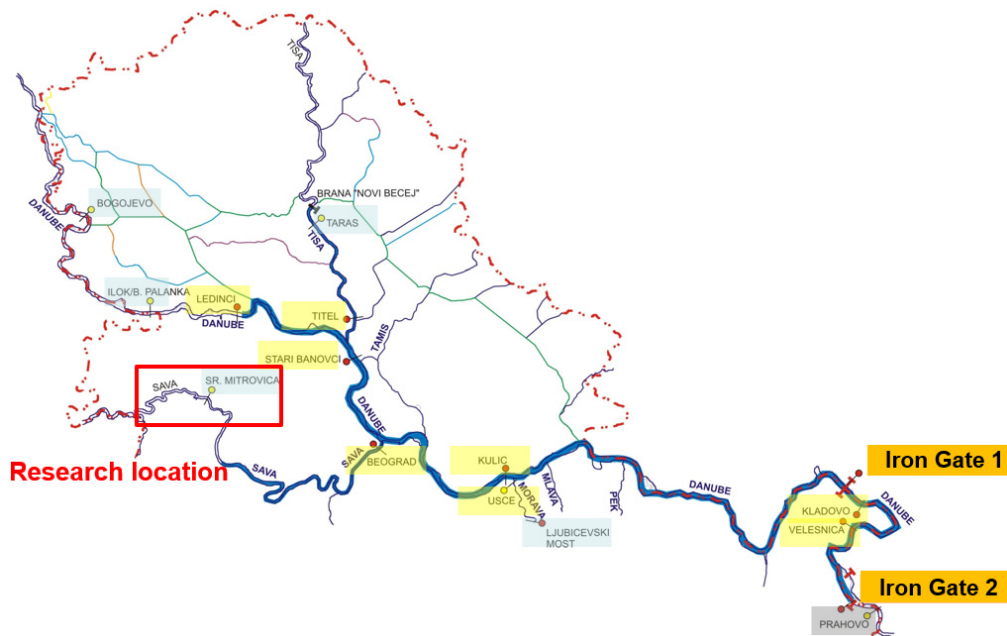


Figure 1. Monitoring profiles along the Iron Gate Reservoirs

- Measurements and observations of water and suspended sediment:
 - Daily observations of suspended sediment concentrations at monitoring profiles (Figure 1)– samples taken from fixed point at water surface,
 - Field measurements of water and sediment discharge (1-2 times/year),
- Occasional special measurements of deposits and
- Surveys of the reservoir (1976, 1981, 1984, 1989, 1997, 2006, 2010, 2014), 250 cross sections along the Danube.

3.1.2 Data collection

This research was conducted in April 2019 at monitoring site Sremska Mitrovica, within the annual monitoring program. Sremska Mitrovica is located at 140 r.km of the Sava River (Figure 1), a right tributary of the Danube River and constituent of the Iron Gate Reservoir.

Water samples Five water columns were placed along the survey line and water samples were collected in five different layers of those columns. All water samples were collected with vacuum bathometer in 40 L bottle (25 samples in total). Wet sieving, water evaporation, sediment drying, and weighing were then performed in laboratory for each sample to finally assess SSC in the sampled volume.

ABS Data Velocity, discharge, and acoustic backscatter data was collected with the RDI 600 kHz ADCP. The ADCP was mounted to the boat and lowered so that the transducers were 20 cm below the water surface. The boat heading, velocity and location were

recorded with a Hemisphere vector GPS system. Prior to collecting water samples, two ADCP survey lines were run along the monitoring profile (one in each direction) to collect discharge, average velocity, and acoustic backscatter. The boat is then moved to each water sampling location along the measurement cross-section and recorded ADCP data simultaneously while water samples were collected (Figure 2).

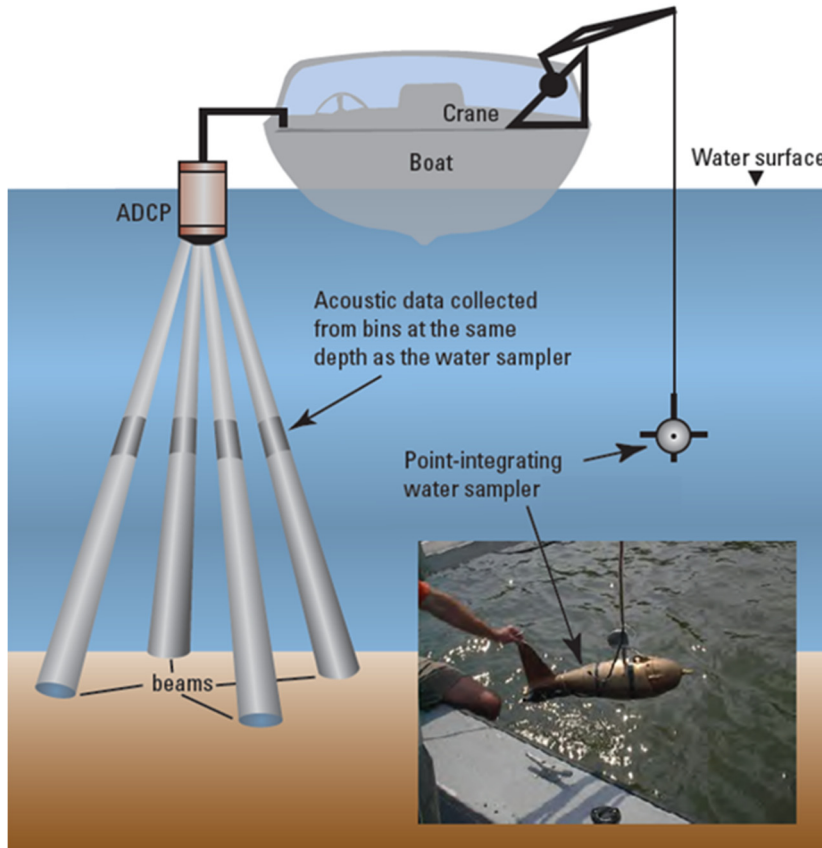


Figure 2. Schematic diagram showing position of acoustic Doppler current profiler (ADCP) and water sampler for ADCP calibration

3.2 Data analysis

3.2.1 Theoretical background

According to basic underwater acoustics theory, the equality between received signal level and background masking level can be expressed by the active sonar equation [1]:

$$DT + NL = SL + 2 \cdot TL + TS + DI \quad (1)$$

where DT represents detection threshold, NL is noise level, SL is source level, TL is transmission loss, TS is target strength, and DI is receiving directivity index. The source level (SL) and the directivity index (DI) are usually determined by the manufacturer of the acoustic transducer and can be regarded as constants for a specific instrument. Therefore, the output of acoustic signal ($DT + NL$) is influenced by the 2-way

transmission loss (2 TL) and the target strength (TS) parameters, both of which are influenced by the amount of backscatterance within the water column. The 2-way transmission losses include attenuation by seawater and spreading and attenuation by the sediment particles. The target strength (TS) of suspended sediment is also a function of particle shape, size, rigidity, and acoustic wavelength.

Based on the power (or energy) of acoustic intensity, Deines simplified the theoretical sonar equation for the broadband RDI ADCP [1]:

$$S_v = C + 10 \cdot \log_{10} \left((T_x + 273.16) \cdot R^2 \right) - L_{DBM} - P_{DBW} + 2 \cdot \alpha_w \cdot R + K_c \cdot (E - E_r) \quad (2)$$

where S_v = volume scattering strength (in dB), T_x = temperature of the transducer (in C), R = range along the beam to the scatter (in m), $L_{DBM} = 10 \log_{10}$ (transmit pulse length), $P_{DBW} = 10 \cdot \log_{10}$ (transmit power), α_w = absorption coefficient of water, K_c = received signal strength indicator scale factor, E = echo strength (in counts), and E_r = received noise (in counts). The first right hand term of the simplified sonar Eq (2) is parameter C - a constant that incorporates many of the combined parameters (e.g., noise power, transducer efficiency), which are impossible to be measured independently. The parameters L_{DBM} , P_{DBW} and E_r can also be regarded as constants for specific ADCP instruments and constant power supply. Based on the above assumptions, Eq (2) can be simplified further as follows

$$10 \cdot \log_{10} (SSC) = C_k + 10 \cdot \log_{10} (R^2) + 2 \cdot \alpha_w \cdot R + K_c \cdot E \quad (3)$$

where SSC is suspended sediment concentration (in kg/m^3), and C_k is a combined constant. The attenuation coefficient due to water absorption (α_w) depends primarily on the frequency of the transmitted pulse and partially on the temperature, salinity, density and depth of the water column [2]. For an acoustic frequency of 600 kHz, frequency of the ADCP we used, 0.153 dB m^{-1} is a typical α_w value [1],[2]. Although C_k and K_c cannot be measured directly, they can be estimated through calibration with acoustic data backscattered by sedimentary particles of known concentration.

Once the constants K_c and C_k are calculated through the calibration, the inversion process can be done through calculating suspended sediment concentration from ADCP echo intensity (Eq (3)).

3.2.2 Calibration procedure

The purpose of calibrating an ADCP is to determine unknown constants K_c and C_k in Eq (2) and Eq (3). The scale factor (K_c), that converts the received signal strength indicator value (RSSI – the number of counts) to decibels, is obtained by calibrating the ADCP in the field where known sediment concentrations, such as those obtained from water samples, are used to determine the scaling factor. The constant C_k is also estimated by using the field calibration method. Linear regression analysis was used to estimate the best values for the constants K_c and C_k . The echo intensity directly monitored from the ADCP and the volume scattering coefficient have linear correlations, which are shown in Figure 3.

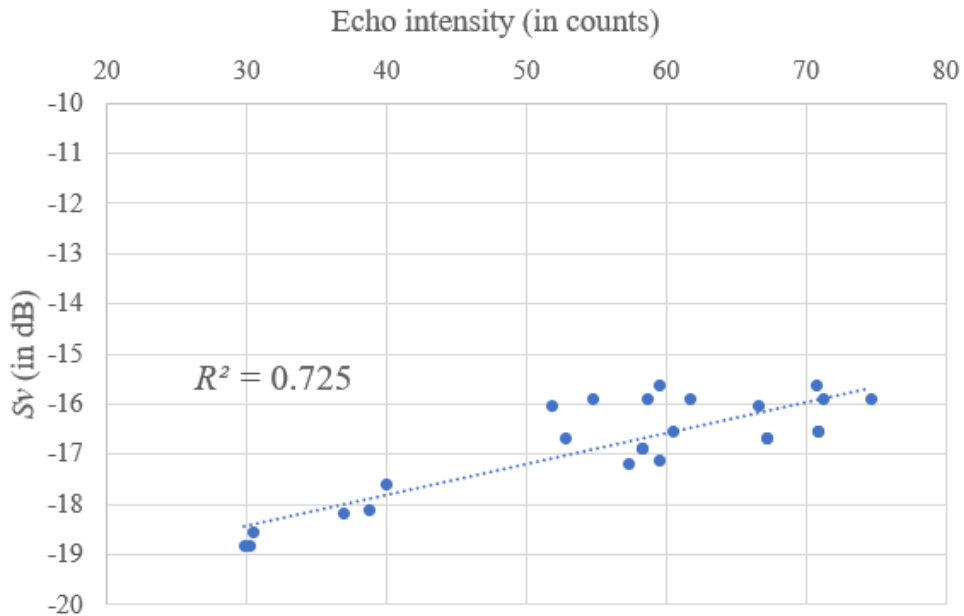


Figure 3. Linear correlation between echo intensity directly monitored by ADCP and the volume scattering strength

3.2.3 Verification procedure

Using Eq (3) with estimated values of K_c and C_k , the SSC values were determined using the ADCP recorded acoustic intensity data. Figure 4 shows a comparison of vertical distributions of SSC derived from water samples and the ADCP acoustic intensity data in water columns. Five different graphs are shown corresponding to a water column locations along the monitoring profile. In addition to the qualitative comparison shown in Figure 4, the direct measured and ADCP-derived SSC values are compared to each other in Figure 5, demonstrating a significant correlation ($R^2=0.85$).

Eq (3) was applied to the ADCP records collected along the entire measurement profile and the time-averaged SSC for each segment was calculated for the whole survey line. The results are shown in Figure 6. As expected, the highest values of SSC are recorded near the riverbed.

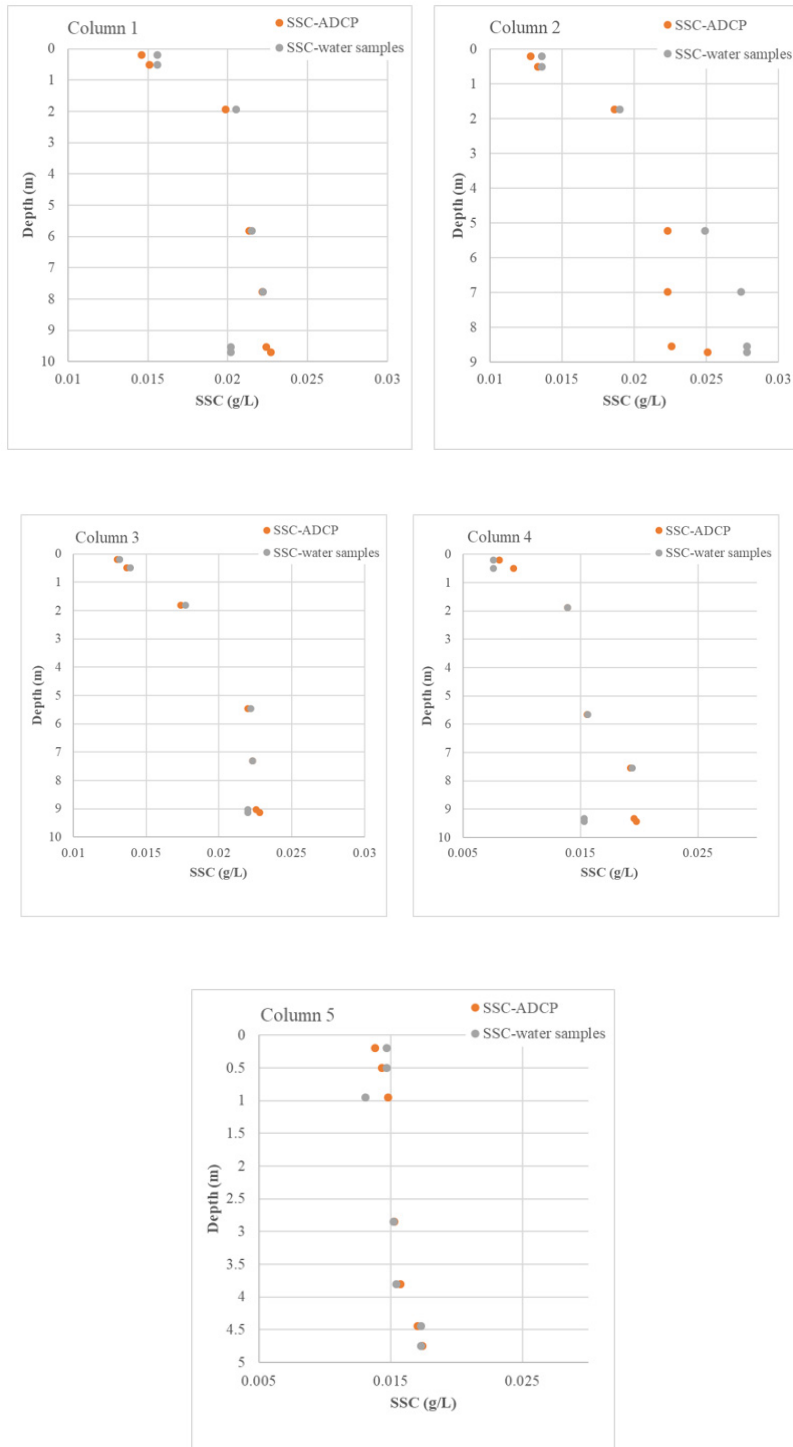


Figure 4. Comparison between acoustic-retrieved and SSC directly estimated from water samples in water columns layers

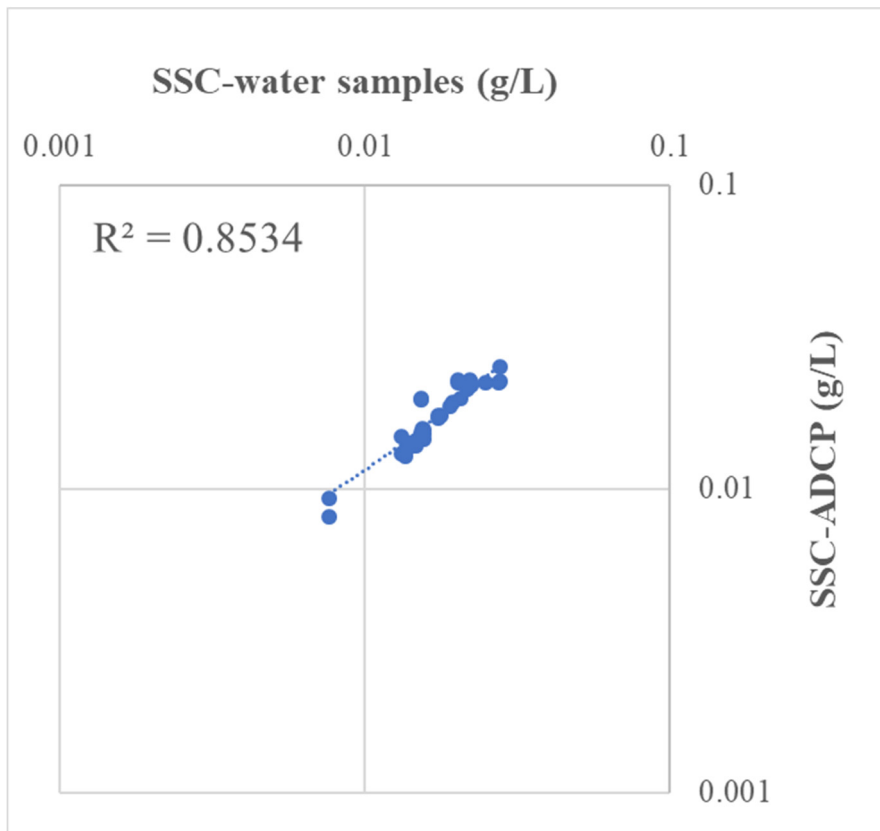


Figure 5. Correlation between ADCP and directly (water samples) derived SSC

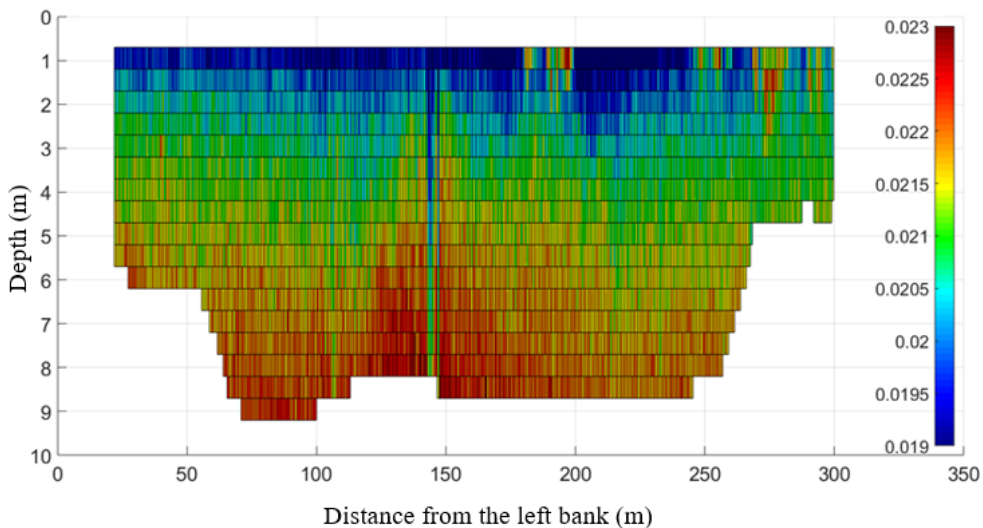


Figure 6. SSC distribution along the entire monitoring profile derived from the ADCP records.

4. Conclusion

An acoustic backscatter method was applied in the Sava River, at monitoring profile Sremska Mitrovica to estimate suspended sediment concentration. The estimation methodology was based on the modified sonar equation. The two immeasurable constants in the sonar equation were calculated through a calibration process using intensity of acoustic signals from ADCP. These constants are then used to estimate SSC values from acoustic signals strength recorded by ADCP. Verification of this results is obtained by comparing the ADCP-derived SSC with SSC values derived from water samples analysis. The correlation coefficient was found to be 0,85.

The analysis and calibration procedures indicate that acoustic signals from ADCP provide reasonable vertical distributions of the SSC. Although the ADCP-based SSC slightly differs from water samples SSC, the estimated SSC from the acoustic technique showed acceptable correlation with lab-based SSC. Therefore, the ADCP-based sediment monitoring could be considered as a practical method for evaluating accurate suspended sediment concentration values.

Although ADCP show potential for estimating SSC quickly, several issues remain to be explored such as impact of particle size distribution on recorded data and a better understanding of instrument error, especially when it comes to concentration ratios between fine and coarse material using instruments with different acoustic frequency.

References:

- [1] Deines, K.L., Backscatter estimation using broadband acoustic Doppler current profilers.
- [2] Proceedings of the IEEE Sixth Working Conference on Current Measurement, San Diego, CA, March 11-13, 249-253, 1999.
- [3] Rehman, S. S. The Development of High Frequency Acoustics for the Measurement of Suspended Sediment. Ph.D. thesis, University of East Anglia, 235 pp, 1990.
- [4] Gary R.W., Elizabeth A.N. and Simon L., Use of an ADCP to Compute Suspended-Sediment Discharge in the Tidal Hudson River, New York, Scientific Investigations Report 2006-5055, U.S. Geological Survey, Reston, Virginia, 2006.
- [5] Hoitink A.J.F. and Hoekstra P., Observations of suspended sediment from ADCP and OBS measurements in a mud-dominated environment, Coastal Engineering 52, pp. 103- 118, 2005.
- [6] CPSD technical report: Using the Acoustic Doppler Current Profiler to Estimate Suspended Sediment Concentration, University of South Carolina Columbia, 2004.
- [7] Latosinski F.G., Szupiany R.N., Garcia C.M., Guerrero M. and Amsler M.L., Estimation of Concentration and Load of Suspended Bed Sediment in a Large River by Means of Acoustic Doppler Technology, Journal of Hydraulic Engineering, ASCE, 2014.
- [8] Dwinovantyo A., Manik H.M., Prartono T. and Ilahude D., Estimation of suspended sediment concentration from Acoustic Doppler Current Profiler (ADCP) instrument: A case study of Lembah Strait, North Sulawesi, IOP Conference Series Earth and Environmental Science. Sci., 2017.
- [9] Ghaffari P., Azizpour J., Noranian M., Chegini V., Tavakoli V. and M. Shah-Hosseini, Estimating suspended sediment concentrations using a broadband ADCP in Mahshahr tidal channel, Ocean Sci. Discuss., 8, 1601-1630, 2011.

WATER LEVELS OF THE MAJOR RIVERS IN SLAVONIA

SINIŠA MARIČIĆ ¹, TATJANA MIJUŠKOVIĆ - SVETINOVIĆ ²,

¹ Josip Juraj Strossmayer University of Osijek, Faculty of Civil Engineering and Architecture Osijek, Croatia, smaricic@gfos.hr

² Josip Juraj Strossmayer University of Osijek, Faculty of Civil Engineering and Architecture Osijek, Croatia, tatjanam@gfos.hr

1. Abstract

A large lowland region in the east part of the Republic of Croatia, known as Slavonia, is surrounded by three large rivers. In the north flows the Drava River, which turns right and flows into the Danube, close to Aljmaš. In the south is the Sava River bed, which connects with the Danube downstream in Serbia. It can be said that the Danube River extends along the eastern border of this lowland. Slavonia is the main granary and agriculturally most developed part of Croatia. Measuring of Water levels at Slavonian hydrological gauging stations have been conducting for many years. But this measuring period, historically is very small because the space has changed constantly. Very long ago there was the Pannonian Sea. Later, large forest areas were developed, but wetland areas remained. Recent history (that of anthropocene) is characterized by regulatory and ameliorative procedures and constructions.

The paper presents an overview of the Sava – Drava - Danube hydrological gauging stations in Slavonia as well as their characteristics. There is a respectable water fund database collected over the last three centuries (strings and over 120 years). Further, the paper discusses data from six stations, two from each major river. Various observation periods (10, 40 and 120 years) are used and their characteristic water levels (mean, minimum and maximum) are expressed. Appropriate analyses and graphical displays indicate water levels change over time. Generalized decrease in both the minimum and average annual water levels were observed across studied periods at all locations. By analysing more successive periods, two phenomena can be observed. First, with each new period the rise of water levels have been appearing earlier and more rapid in hydrological years. Second, with each new period there is a greater dispersion in the appearance of extreme high water levels.

Changes in the hydrological characteristics of the rivers in Slavonia also indicates the condition of the groundwater of this basin, which is largely protected from high waters by embankments. Changes are evident and warning and needs to be accepted in future development plans. Perhaps a new concept is needed in solving water management problems.

Keywords: Slavonia, Drava, Sava, Dunav, water levels, gauging stations, hydrological analyse

2. Introduction

Since ages, the man has realized that the only constant in life is a change. The ancient

Greek saying "Panta rei" (Latin form) is just as known as the quote 'No man steps into the same river twice' (by Heraklitus) because things are always in the state of flux and nothing remains the same (there are no two similar natural processes). The Croatian poet Petar Preradović also wrote about the change as the only constant in the world. While in the Far East, for thousands of years Buddhism has taught that all things in the world are impermanent, insubstantial and imperfect.

We most easily understand the changes around us. Since the authors of this paper come from Osijek, a town in the east Croatia, the focus is on the changes of the Sava-Drava-Danube inter-river area, which can be said to represent the wider surrounding of the town. It is the south-western part of the Pannonian Basin, which hundreds of thousands of years ago was covered by the sea. If we tracked the history of the said area over the past millions of years, we would find that tens of millions of years ago Europe and the Mediterranean Sea were covered by Tethys Ocean. A few tens of millions of years ago, due to strong tectonic disturbances, the mountain massifs (Alps, Dinarides and Carpathians) have emerged, and today's Pannonian lowland was covered by the Sea of Paratethys (Pannonian Sea). Approximately 13 million years ago, it lost the connection with the Mediterranean Sea and became the Pannonian shallow sea whose salinity gradually decreased. There lived some shells and snails that had been able to adapt to brackish (less salty) water, together with fish, whales and other marine organisms. About ten million years ago, the Pannonian Sea continued to lose its salinity, and species characteristic for the Sarmatian Stage were lost, while new species developed. Over the time, the sea split into less salty or freshwater pools and lakes. The rich flora (meadows and forests) developed on the newly formed land because the climate was considerably warmer than today. Along the banks of the lakes, huge rhinoceros and elephants found their sanctuary, feeding on the leaves of trees. Following that era, large lakes disappeared – no evidence of lake sedimentation nor characteristic fossils were found. This (quaternary) period has lasted from 2 million years to this day. Sedimentation included gravel, clay and sands, but no longer in the sea or in the lake but as stream or river deposits, or wetland sediments [1, 2]. In the same area, from thousands of years ago originated the traces of humans. Near Papuk were remains of ancient camps, erected some 12,000 years ago, by mammoth and bison hunters. That time was a breaking point for the human species - the end of the Ice Age, when the ice-captured remains of the Pannonian waters could sink into the Black Sea. The time of the "Neolithic Revolution" emerged, when for the first time organic species opposed nature by changing it [3]. The Neolithic was characterized by mitigating the harsh continental climate, rising of precipitation and watercourses, and the formation of wetlands in the lowlands. The herbal cover was made up of mixed oak forests. The first communities of farmers came to the intercessions of the Drava, Sava and the Danube rivers more than 8,000 years ago, bringing ceramics, domesticated animals and plants, as well as new social relationships, ideology and religion. The result of a farming-based economy is a sedentary lifestyle and the construction of durable dwellings [3]. Settlements of many prehistoric cultures are usually found along the waterways, on elevated riverbanks or on low hills, and very often on the site of older settlements. According to a rich archaeological and cultural-historical heritage, it may be the oldest inhabited area in Europe. Especially (in global terms) important is the Vučedol culture that appeared in Eastern Slavonia and Srijem five thousand years ago. With further development of water coexistence (water

protection, fishing, construction and navigation of boats) in the Vučedol culture, new Indo-European elements such as new residential buildings, heavy-duty four-wheel drive and the application of new metallurgy were recognized. This is where the epic civilized discovery was made – the production of bronze. Vučedol inhabitants were also the creators of the oldest comprehensive European (Indo-European) calendar. [3].

About 2,000 years ago, still a large part of Southeast Slavonia and northwest of Srijem above Sava, to the loess plain in the north was covered by the shallow, yet spacious Spacva Lake (Gr. Syrmie Limna, Latin Lacus Syrmius). The swampy forests of today's pedunculated oak, ash and similar kinds grew along the lower shores of the lake [3]. Such a wild environment and its assimilated inhabitants Illyrias (the Breuci subtribe) posed problems to the spread of the Roman Empire. However, nearly half a millennium of the Roman influence brought an extraordinary development to this region. By draining the swamplands, creating waterways, deforestation, formation of cities and creation of agricultural land at the time of the Roman Empire, human society has begun to seriously change the natural determinants in this region [4]. Around 1.5 thousand years ago, the Slavs migrated bringing the features of their way of life into these parts. Since then, the Croatian people have survived and built their own identity in that mixture of peoples, cultures and religions. Up to a thousand years ago, we may say that the area where Sava – Drava - Danube rivers connect was, in political terms, "no man's land", with the predominant Slavic population, and under the influence of different peoples. In those turbulent times, that area became a hostile territory (with large forest-wetland covered areas and frequent flooding, insects and infections), so that its population remained small for quite some time. In the period between one thousand to half a thousand years ago, this area was under the Hungarian supreme territorial authority and the influence of Hungarian culture. The recent history, traced through the centuries, has been marked by the great technical advancement, which has enabled human domination over many natural processes. The centennial penetration and influence of Islam has again formed the so-called "no man's land." Despite the war activities, this was a new opportunity for nature to recover, and the waters themselves shaped their paths, so-called hydrographic network, while forests were thriving. With the collapse of the Ottoman Empire and the emergence of the Austro-Hungarian monarchy, many decades of intensive industrial development have been taking place. In the area concerned (Sava-Drava-Danube), numerous regulatory interventions were carried out. The forest areas were intensively exploited, which was particularly encouraged by the development of rail traffic, and more than 30% of waterways were shortened; and additionally, the systematic construction of anti-flood dams started. With the development of the wood industry, there were large interventions in the Slavonian forest area which in the 19th century resulted in huge reduction of forest covered areas in Slavonia, from 70% to 35%. Hydro amelioration (flood protection and land drainage) was intensified during the existence of three states of Yugoslavia. It culminated in the second half of the 20th century with a construction of a very dense drainage network, creating therefore modern agricultural surfaces. Consequently, the natural appearance and characteristics of this region have again changed significantly, thus supporting the use of the "Anthropocene" term [4, 5, 6, 7].

This paper is focused on hydrological changes during a large number of decades in which river water levels were measured.

2. Methods

2.1 Study area and water level observations

2.1.1 Study area

The study area is not strictly (or precisely) defined. The main feature includes the plain, mostly located in Croatia, which is the edge of the Pannonian valley, on its south and south-west. This area borders with the surrounding countries (Hungary, Serbia and Bosnia and Herzegovina), and the borders are mostly formed on the Drava, Danube and Sava rivers. It is about large rivers in its middle (Danube, Sava) and lower flow (Drava, Sava). The Drava River flows north and turns right into the Danube. In the south, there is the Sava bed, which further downstream connects to Danube. Thus, it may be concluded that Danube stretches alongside the east side of the plain. Throughout the history, the name commonly used for the parts of this area are Slavonia, Baranja and Srijem. Most of the area observed includes Slavonia which extends to the west Croatia, too. The smaller parts include Baranja and Srijem, with their larger extent in neighbouring countries of Hungary and Serbia. Therefore, in this work, we use the common term of Slavonia for the entire space (including the neighbouring countries) effected by the observed hydrological characteristics.

Table 1. Characteristics of selected hydrological stations on the major river in Slavonia

GAUGING STATION		RIVER	START OF WORK	"0" ELEVATION (a. s. l.)	LOCATION (r. km)	DATA LENGHT (YEAR)		MISSING RECORDS PERIOD
CODE	NAME					FROM	TO	
5063	TEREZINO POLJE	DRAVA	1872	100,67	152,3	1925	2018	1941; 1944 -1945
5150	DONJI MIHOLIJAC	DRAVA	1890	88,57	80,6	1900	2018	1913 - 1922; 1944 -1945
42010	BEZDAN (R SERBIA)	DUNAV	1856	80,64	1425,6	1920	2018	1934; 1999 - 2000
5170	BATINA	DUNAV	2001	80,45	1424,85	2001	2018	
5070	VUKOVAR	DUNAV	1856	76,19	1333,45	1900	2018	1913 -1922; 1945; 1948; 1992 -1998
3098	SLAVONSKI BROD	SAVA	1855	81,8	360	1900	2016	1913 - 1919
3211	ŽUPANJA ST.	SAVA	1886	76,28	262	1900	2017	1913 -1928; 1943 -1944

2.1.2 Gauging stations

The hydrology is science based on the measurements of the elements of the hydrologic cycle. Among the most important and earliest ones are measurements of river water levels. Several hydrological river stations have been established in the area concerned. They are maintained by the relevant state-run Hydrology Offices in all four countries, carefully monitoring water levels of said rivers. The National Hydrometeorological Institute (DHMZ), headquartered in Zagreb, and similar offices in other countries, provides information about their work and services, available on their websites. Figure 1 and Table 1 give an insight into the Sava-Drava-Danube hydrological stations on the territory of Slavonia.

It is obvious that there is a respectable set of water data collected during the last three centuries. The measurements of longest duration were: on Sava near Stara Gradiska (started in 1817), on Drava near Varaždin (1821), on Danube near Bezdan, Vukovar and Ilok (all began in 1856), [8]. In the largest urban center of the area in question, the town of Osijek, the hydrological monitoring level of the Drava River, along which the town stretches, started in 1827. Unfortunately, no data of the earliest measurements were available for the analysis in subject. The data that has been disposable, however, were collected around the beginning of the last century, but because of different beginning and interruptions of work (caused by wars) their series were not completely unified. Due

to these problems and positioning benefits, two hydrological stations were selected from each major river. On the Drava River these are Terezino Polje and Donji Miholjac, Sava - Županja and Slavonski Brod, and on Danube - Bezdán (Batina) and Vukovar. Among them, the most deficient data set was collected for the Terezino Polje (Drava) station. We included medium daily water levels in the period from 1925 to 2018 (without 1941 and, end the period between 1944-1945), thus data representing 91 years. The most extensive set was collected for the Slavonski Brod (Sava) hydrological station. Water levels were analyzed from 1900 to 2016 (without the period between 1913-1919), which covered 110 years in total.

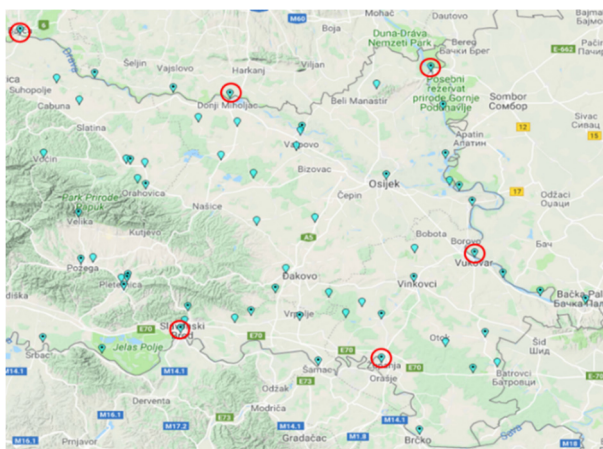


Figure 1. Location of analyzed hydrological stations of the major rivers in Slavonia (DHMZ gauging stations)

2.1.3 Rivers

In the observed area, there are three great rivers, one of which is at the last section of its flow, one at the beginning of the second half of the flow, and one is in the middle section of the flow. The analysis refers to their about 200 km long sections, positioned approximately by river kilometres (distance from the river mouth): on Drava from 80 to 150 rkm, on Sava from 260 to 360 rkm, on Danube from 1330 to 1430 rkm. All three rivers, Drava and Sava as tributaries to Danube, run along the Danube River (gravitating) to the Black Sea.

The Danube River is (after Volga) the second largest river in Europe, about 2 850 km long and with the catchment area of around 817 000 km². On this part, the Danube River is characterized as a lowland river with an average drop of about 4 to 7 cm/km. The average bed width is about 450 m, but the width of the river ranges from 250 to 880 meters, and the average flow rate is 0.9 m/s. The Drava River, which flows into the Danube River in Croatia, has a total length of about 750 km and a catchment area of over 40 000 km². About 100 km of lowland flow of this river makes the Croatian-Hungarian state border. The drop of the Drava River in the observed area is larger than the Danube's, and is about 7 to 20 cm/km. Among the Pannonian rivers, Drava has the highest average drop, so it is very fast in its lower course (about 1.7 m/s in Varaždin, 1.14 m/s in Osijek). The dimensions of the bed vary considerably, its width ranges from 240 to 600 m. Sava is about 945 km long, with the surface of the basin of about 96 000

km². The observed section is characterized by large differences in average drops on small distances. The values of drops range from 5 to 60 cm/km. For middle and lower Sava, the average drop is 9.1 cm / km, and the width of the bed ranges from 250 to 400 m.

All three rivers in the area observed show the features of the pluvial-glacial (rainy-snowy) water regime. It is characterized by the low water quantity in winter, and high in spring and early summer due to melting snow and ice, as well as rain in the mountains. Another characteristic refers to an increased water quantity in autumn, due to then abundant rainfall (precipitation peak). There are discrepancies, i.e. differences in regimes due to different basin conditions. The Alpine and Carpathian waters travel longer along Danube, and their catchment area is larger in comparison to waters coming from the Alps, by Drava. On the other hand, the Sava water regime from the Alps is modified by the significant water quantities of its southern, Bosnian tributaries. Due to small drops, large quantities of Danube water cause deceleration of Drava, which may be observed even 50 kilometres upstream from the mouth.

3. Results and discussion

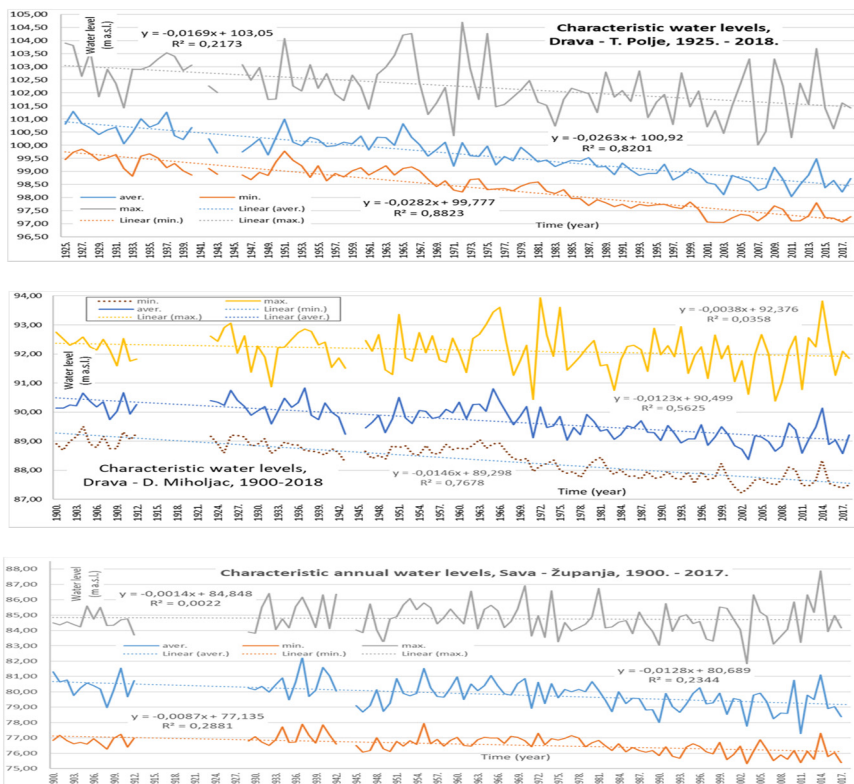
In order to detect changes in water levels, we selected the (sub)periods for analysis of the period of about 120 years of observation of daily water levels, so that they approximately coincide with the observed cyclical changes of wet and dry episodes (high and low water levels). For the six selected representative stations, different successive periods (1, 10, 40 years for targeted 120 years) were analyzed and their characteristic mid-day water levels (mean, minimum and maximum) were reported.

In Figure 2, each individual water station is presented by a graph containing annual data: mean daily water level, as well as water levels with minimal and maximal daily value. Expectedly, the annual maximum daily water levels oscillate the most during time. Annual minimum and average daily water levels are considerably more uniform. Based on these annual changes of statistically characteristic water levels, linear trends of their changes are determined and presented on graphs. It is noteworthy that all considered water levels have a downward trend. These are annual reductions: for medium water levels - 0.9-2.6 cm/year, for minimums - 0.1-2.8 cm/year and for maxima - 0.1-1.7 cm/year. The data from the Drava River at Terezino Polje point out a more noticeable decrease in water levels (1.7-2.8 cm/yr), in comparison to other monitored sites where the decreases are more even (0.1-1.4 cm/year). Particularly interesting is the reduction in mean daily water levels during the years considered, which is 2.6 cm/year in Terezino Polje, and 0.9-1.4 cm/year at other locations. This means that the entire surrounding area experienced an average decrease of indicative water levels of about 1.2 cm/year, i.e. 1.2 m over the past 100 years. In Figure 3, each individual water station is presented by a graph showing the mean daily water levels of different processing periods (for annual, 10-year and 40-year periods). Their changes over time are noticeable. Average daily water levels of successive 10-year periods are not continuously in the declining sequence, but within each 40-year period there is a (higher/lower) deviation (increase in a water level compared to the previous one). By contrast, mean daily levels of successive 40-year periods indicate a constant, significant (apparent) decline in water levels. During the 40-year period, everywhere it was larger than 25 cm, but the largest occurred at Drava

near Terezino Polje, where it was about 1.2 m.

Figure 4 shows graphs of annual flow of daily water levels, calculated as mean values of daily water levels of a certain day of the year for the selected 40-year period (Three periods were considered: 1900-1940, 1940-1980 and 1980-2018). Based on that, we can see what the water regimes of the large Slavonian rivers are like. The following differences may be observed:

- According to the mean values, there is a bigger difference between the small and the large waters of the annual flow of Sava (about 10 m) than Drava (about 7 m) and Danube (about 9);
- Big waters (on average) occur earlier in Sava, then in Drava, while in Danube they occur at the latest
- Sava and Drava have the spring peak and secondary one in the autumn, while the two highest peaks are visible on Danube - at the very beginning and, usually the larger one at the end of spring;
- The phenomenon of extreme high water is most likely to be: in Drava - from late spring to mid- autumn, in Sava - late winter to mid spring, but also during the majority of the autumn period to the beginning of winter, in Danube - throughout spring and summer, especially in June/July.



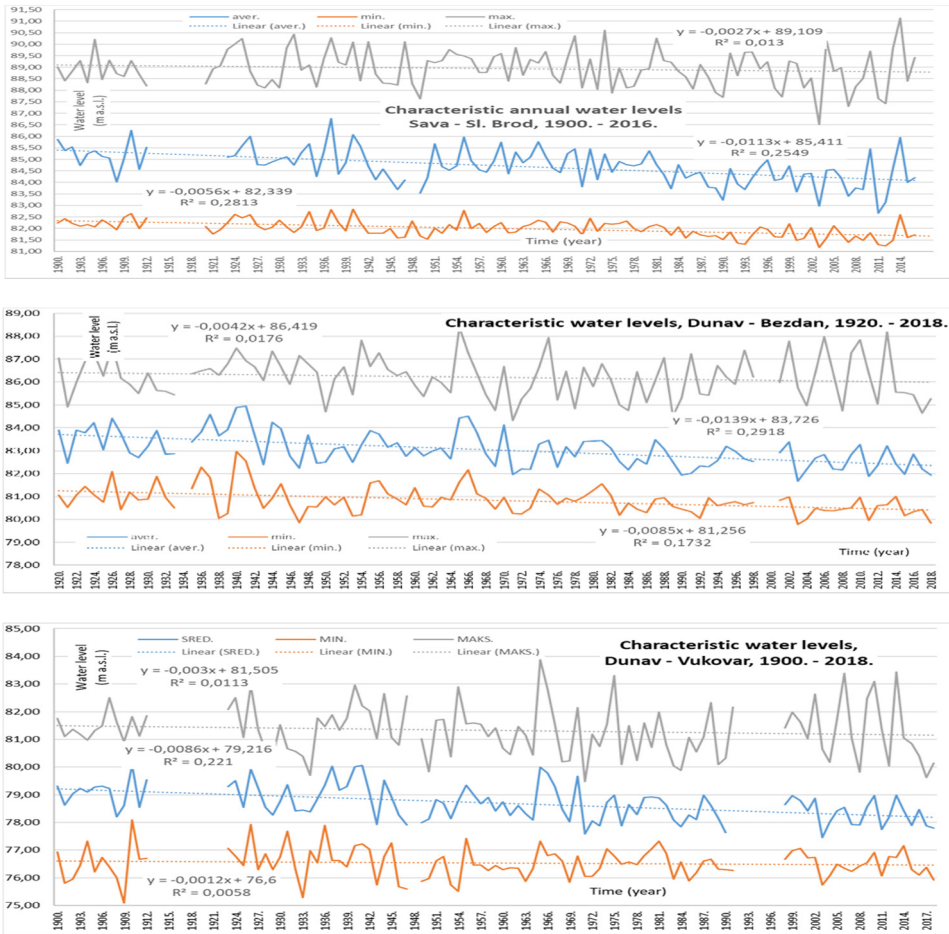
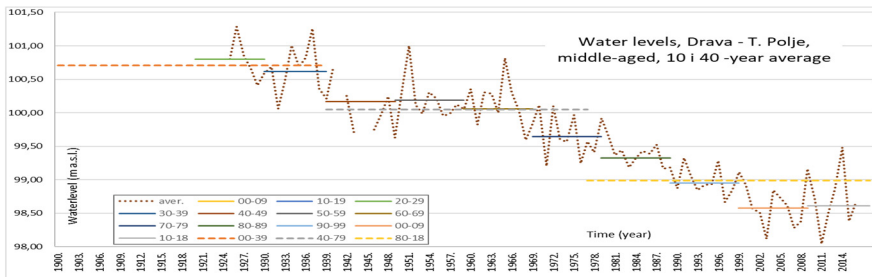


Figure 2. Characteristic water levels of major rivers in Slavonia (Drava – w.g.s. Terezino Polje and Donji Miholjac, Sava – w.g.s. Županja and Slavonski Brod, Danube – w.g.s. Bezdán and Vukovar)



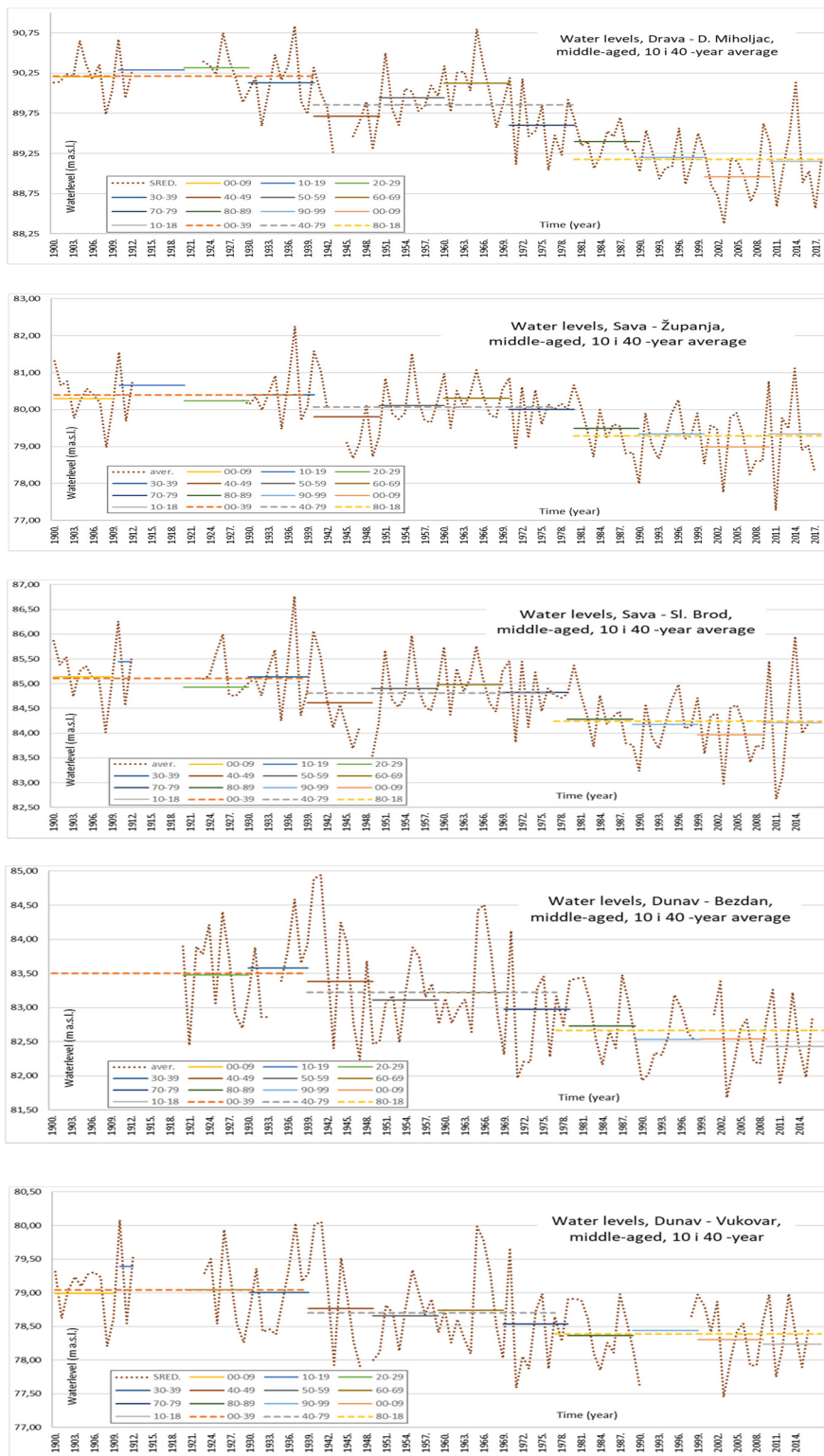
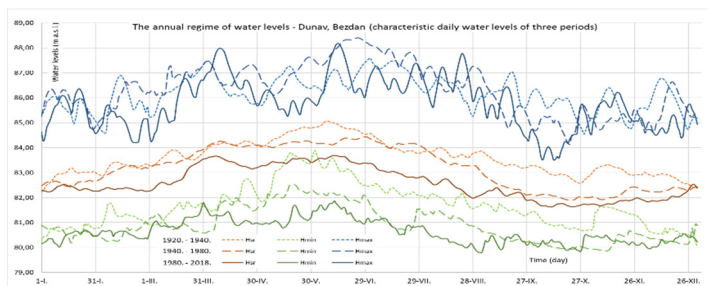
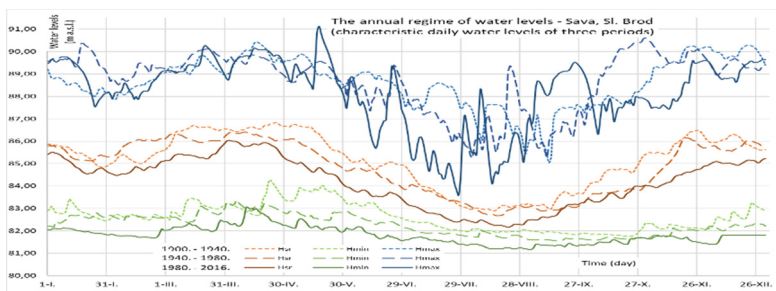
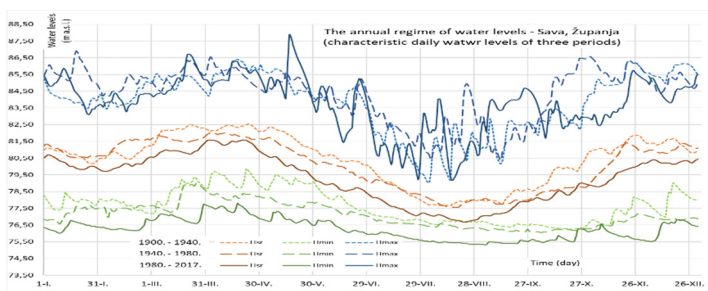
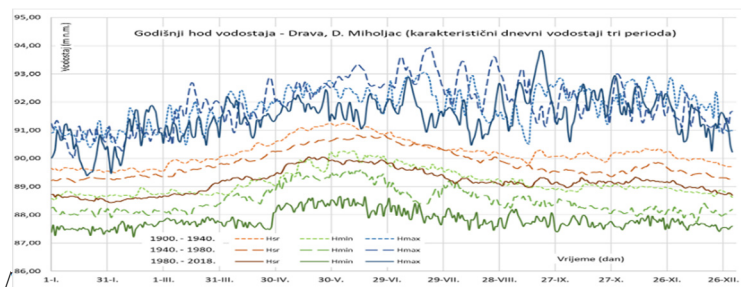
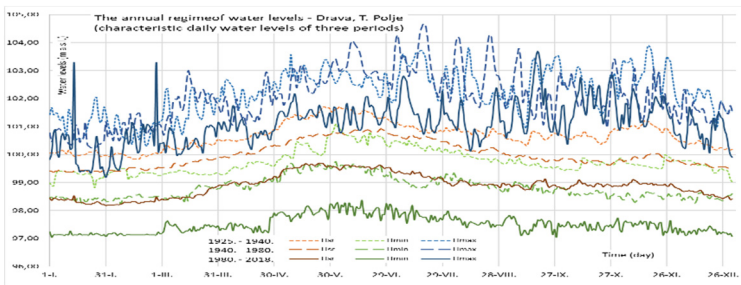


Figure 3. Middle-aged, 10 and 40-year average water levels of major rivers in Slavonia



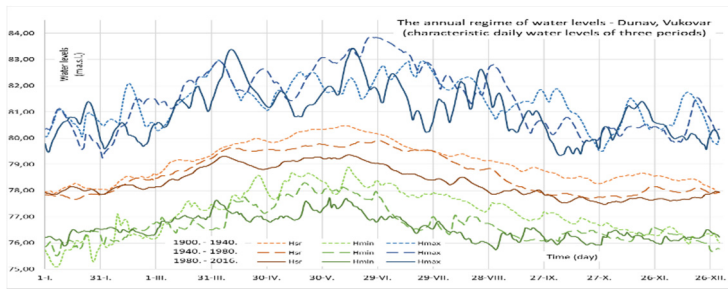
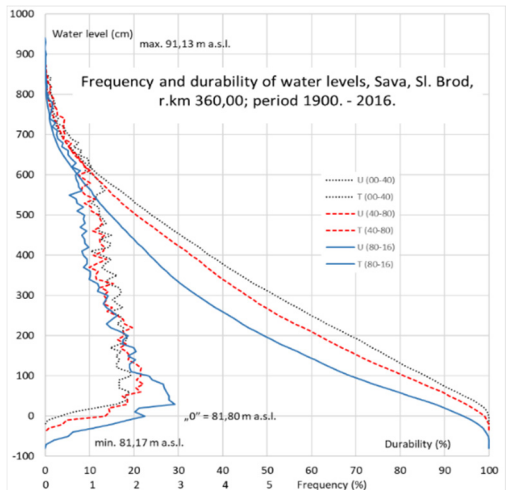
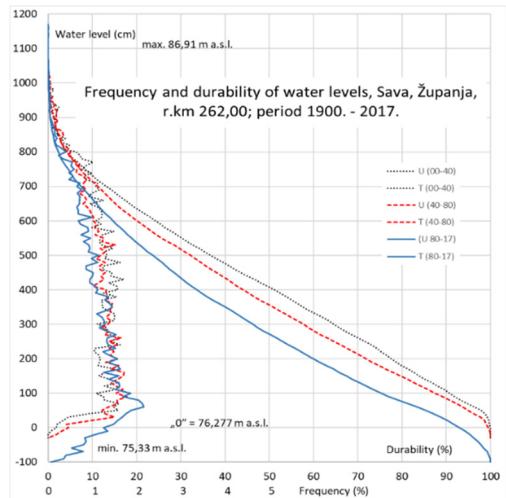
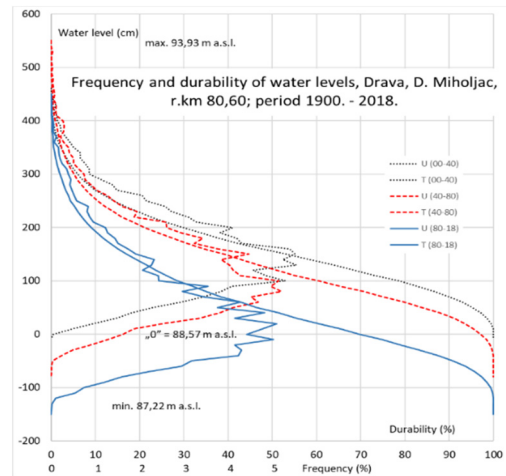
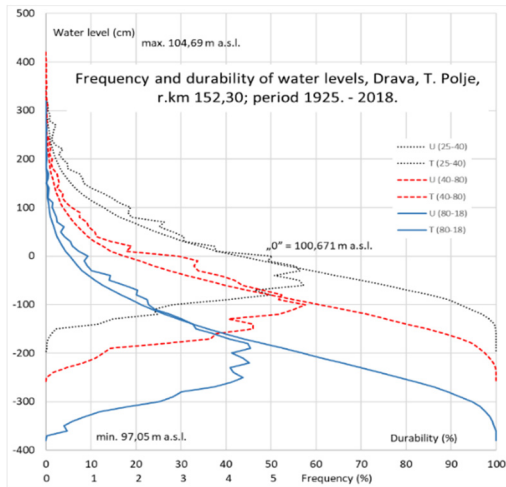


Figure 4. Annual water levels at different gauging station of major rivers



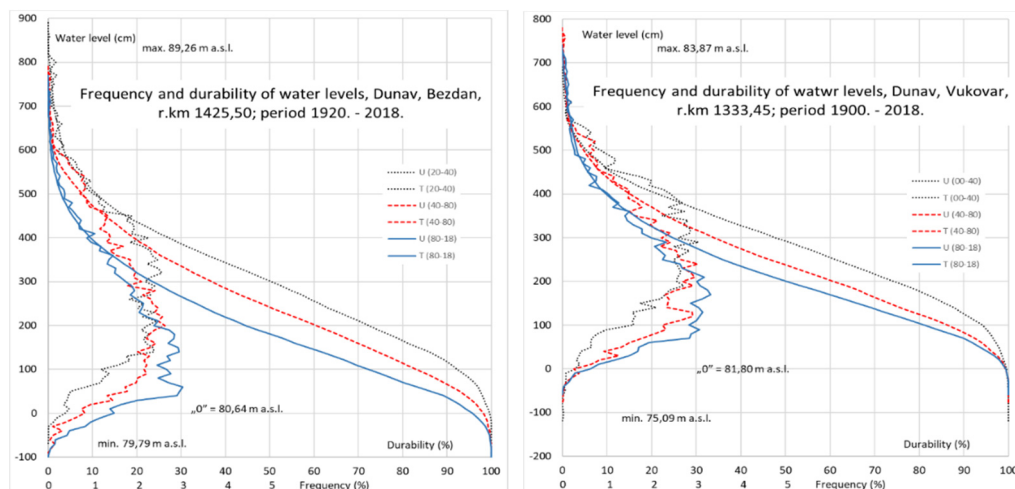


Figure 5. Water level frequency/duration curves of major rivers in Slavonia for three different periods

Separation by period allows us to observe changes in the regime of the large Slavonian rivers. There is a significant reduction in the mean and minimum water levels observed for all three rivers, while at maximum water levels, besides the occurrence of lower values, there are also higher values than the previous periods. The phenomenon of extremely high-water levels is more recent in the wider annual range, which means that flood problems cannot be linked only to certain periods of the year, but the caution is always necessary. Even better insight into the changes is given by Figure 5, which shows the frequency and duration curves for all observed rivers and locations. According to the data observed, the Sava River has the highest registered water level range (86.21 a. s. l. - 76.28 a. s. l. = 10.71 m). Drava, as the smallest one, has also the smallest oscillation of water levels. With Danube, and especially with Drava, there is a great concentration of water level around the middle and then below, while with Sava there is more even distribution of the presence of certain water levels. Considering the successive periods, what is noticed refers to: lowering the curve of the frequency to the lower; concentration to lower water levels and increasing the range (max. min.) of the water level.

4. Conclusion

The hydrological analysis in the observed area of Slavonia noted more and more lower mean water levels and higher occurrence (presence) of the lower water levels of its large rivers, as well as the appearance of extremely high water levels even beyond the expected time periods. Such a situation requires from both nature and society to constantly adapt to new living conditions. Changes are evident and alerting, and should be considered in future development plans. Perhaps, it is necessary to develop a new resolution concept of water management problems.

References:

- [1] Magyar, I., Geary, D.H. & Müller, P.: Paleogeographic evolution of the Late Miocene Lake Pannon in Central Europe; *Palaeogeography, Palaeoclimatology, Palaeoecology*, 147 (3-4),

- pp. 151-167, 1999.
- [2] Mandić, O., Kurečić, T., Neubauer, T.A. & Harzhauser, M.: Stratigraphic and palaeogeographic significance of lacustrine molluscs from the Pliocene Viviparus beds in central Croatia; *Geologia Croatica*, 68 (3), pp. 179-207, 2015.
 - [3] Parat, J.: Šume i drveće u antici južne Panonije (Forests and Timber in Ancient Southern Pannonia); *Slavonske šume kroz povijest; Bibliotheca Croatica: Slavonica, Sirmiensa et Baranyensia, Knjiga 17; Hrvatski institut za povijest, Slavonski Brod, str. 15-40, 2017.*
 - [4] Gračanin, H., Pisk, S.: Pisani izvori o šumama u savsko - dravskom međuriječju u kasnoj antici i srednjem vijeku (Written Sources on Forests between the Sava and Drava River in Late Antiquity and the Middle Ages); *Slavonske šume kroz povijest; Bibliotheca Croatica: Slavonica, Sirmiensa et Baranyensia, Knjiga 17; Hrvatski institut za povijest, Slavonski Brod, str. 41-62, 2017.*
 - [5] Andrić, S.: Šuma Garavica i „ničija zemlja“ na slavonsko-turskom pograničju u 16. i 17. stoljeću (Garavica forest and “no man’s land” on the Slavonian - Turkish frontier in the 16th and 17th centuries); *Slavonske šume kroz povijest; Bibliotheca Croatica: Slavonica, Sirmiensa et Baranyensia, Knjiga 17; Hrvatski institut za povijest, Slavonski Brod, str. 63-110, 2017.*
 - [6] Kale, E.: *Povijest civilizacija, IRO Školska knjiga, Zagreb, 1990.*
 - [7] Gračanin, H.: Rimske prometnice i komunikacije u kasnoantičkoj južnoj panoniji, *Scrinia Slavonica 10 (2010.)*, Zagreb, str. 9-69, 2010.
 - [8] Oskoruš, D.: Hidrološki monitoring i obrada podataka; *Zbornik radova Seminar Gospodarenje vodom i zaštita okoliša, Društvo građevinskih inženjera Zagreb; Zagreb; str. 23-38, 2013.*

A REVIEW OF EROSION POTENTIAL METHOD MODIFICATION AND APPLICATION ON DUBRAČINA RIVER BASIN

NEVENA DRAGIČEVIĆ¹, BARBARA KARLEUŠA², NEVENKA OŽANIĆ³

¹ *University of Rijeka, Faculty of Civil Engineering, Croatia, nevena.dragicevic@uniri.hr*

² *University of Rijeka, Faculty of Civil Engineering, Croatia, barbara.karleusa@uniri.hr*

³ *University of Rijeka, Faculty of Civil Engineering, Croatia, nevenka.ozanic@uniri.hr*

1. Abstract

An overview of the research related to soil erosion and carried on Dubračina River basin and its most important conclusions will be presented in this paper. The research consisted of: data gathering; methodology selection; modelling of soil erosion using GIS and remote sensing technology; method sensitivity analysis; model uncertainty analysis, Erosion Potential Method (EPM) modification, soil erosion intensity and production assessment using EPM, erosion observation and model verification on the case study Dubračina River basin.

Keywords: erosion assessment, Erosion Potential Method, modification, soil erosion

2. Introduction

One of eight leading processes causing soil degradation in the European Countries is soil erosion. Soil erosion is a process of mechanical detachment of the soil under the influence of erosive agents such as water and wind that consists of detachment of soil particles, transportation of detached soil and its deposition. The dominant geomorphic process for much of Earth's land surface is soil erosion by water agent. The main influence on erosion processes are considered to have climate, soil, topography, vegetation cover and anthropogenic factors. All these elements make environment more or less resistant to climate events [1].

The method and model for the erosion assessment are described in this paper and based on research and gathered data from Dubračina River Basin, situated in the Vinodol Valley in the County of Primorsko-Goranska, Croatia.

2.1 Dubračina River Basin

Dubračina River Basin is a small basin, 43 km² in size (Figure 1). It is characterised by its valuable natural and cultivated landscape, biodiversity, cultural, historical heritage and also high annual rainfall, steep topography and variable geology all of which contribute to its land instability such as landslides and excessive erosion processes. Dubračina River and its twelve tributaries, all with torrential characteristic, count approximately 41 km in length. The overall catchment can roughly be divided into the upper karstic part with steep slopes and active sediment movement and lower Flysh as less permeable area. Complex geological structure, spatial valley cross section with

distinct steep slopes affected by erosion, local landslides and torrents are the reason this area has been known for many years as an area of potential hazard risk. Water erosion related problems on Dubračina catchment have been known to exist from 19th century till today. First land instability map was made in the 1970s after the severe flash flood in the 1960s causing major damage on river structures and initiating numerous landslides in the area. During the years several attempts were made in order to mitigate erosion processes in the catchment and included reforestation measures, river regulation, construction and maintenance off structures for prevention and mitigation of erosion and flash flood with no significant affect upon the intensity of erosion processes in the area. One of the main problems is the nonexistence of erosion observations in the catchment for a longer period and their comparison in time. For this reasons, the first objective of this research were observations of erosion processes in the catchment and their comparison and evaluation in time.

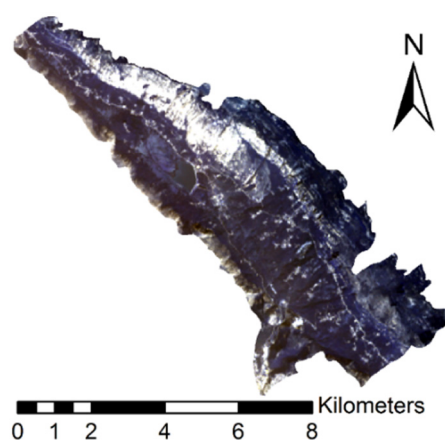


Figure 1. Dubračina catchment

Till now the maps showing erosion intensity and sediment production in the catchment on annual or seasonal level, distinguishing the areas that are more or less prone to erosion processes do not exist. This maps would enable more appropriate and on time definition of erosion mitigation and protection measures which would potentially reduce structural measures, as they are the most expensive ones, to its minimum. Structural measures have been planned on various locations in the Dubračina catchment but most of them due to the high cost have not been realised. From this problem, the third and fourth objective are defined, the third that includes the derivation of erosion intensity and sediment production, and the fourth defining the appropriate mitigation and prevention measures upon them. In order to produce such maps a detailed and comprehensive data collection for the Dubračina catchment needed to be conducted using a variety of academic, governmental and nongovernmental institutions. Since there is no unified database from which those data could be obtained the main problem in a form of multiple information sources for the same model input data has occurred. One of the main objectives and also the fifth, is to define the most appropriate information source to be used for one input data and define model uncertainty that arises from such problem. The model was verified using the visual survey method. Short review of this research will be presented in the following sections of this paper.

3. Methods used and analysis conducted

3.1 Erosion Potential Method (EPM)

The Erosion Potential Method (EPM), also known as the Gavrilović method, was developed by Slobodan Gavrilović and was based on erosion field research in the Morava River Catchment area in Serbia in the 1960's [2]. The method encompasses erosion mapping, sediment quantity estimation, and torrent classification. Since 1968, the method has been extensively applied to erosion and torrent-related problems in the Balkan countries [3].

The most often calculated outputs of the method (equations 1-6) are (i) the total annual volume of detached soil W_a (Eq. 3), (ii) the erosion coefficient (Z) (Eq. 1), and (iii) the actual sediment yield G_y (Eq. 4).

$$Z = Y * X_a * (\phi + \sqrt{J_a}) \quad (1)$$

$$W_a = T * P_a * \pi * \sqrt{Z^3} * F \quad (2)$$

$$T = \sqrt{\frac{T_0}{10} + 0.1} \quad (3)$$

$$G_y = \xi * W_a \quad (4)$$

$$\xi = \frac{\sqrt{O * z}}{(l_p + 10)} * D_d \quad (5)$$

$$D_d = \frac{l_p + l_a}{F} = \frac{L}{F} \quad (6)$$

where

Y - the soil erodibility coefficient (-),

X_a - the soil protection coefficient (-),

ϕ - the coefficient related to the type and extent of erosion (-),

J_a - the average slope of the study area (%),

T - the temperature coefficient [-],

P_a - the average annual precipitation [mm],

F - the contributing catchment area [km²]

T_0 - the average annual temperature [°C],

ξ - the sediment delivery ratio [-],

O - the perimeter of the study area [km],

z - the mean difference in the elevation of the study area [km],

l_p - the length of the principal waterway [km],

D_d - the drainage density [km/km²],

l_a - the cumulative length of the secondary waterways [km],

L - the cumulative length of the principal and secondary waterways.

According to de Vente [4], this method can be characterised as a semi-quantitative method because it is based on a combination of descriptive and quantitative procedures. It uses a descriptive evaluation of its three parameters: soil erodibility; soil protection, which represents land use/cover and type; and extent of erosion in the catchment. All other parameters represent quantitative catchment descriptors. Table 1 shows the procedure for the evaluation of three method parameters that are defined using the descriptive attributes of the analysed catchment/cell.

Table 1. Descriptive evaluation of Gavrilović method parameters [4, 5]

Soil protection coefficient [Xa]	
Mixed and dense forest	0.05-0.2
Low density forest with grove	0.05-0.2
Coniferous forest with little grove, scarce bushes, bush prairie	0.2-0.4
Damaged forest and bushes, pasture	0.4-0.6
Damaged pasture and cultivated land	0.6-0.8
Areas without vegetal cover	0.8-1.0
Soil erodibility coefficient [Y]	
Hard rock, erosion resistant	0.2-0.6
Rock with moderate erosion resistance	0.6-1.0
Weak rock, schistose, stabilised	1.0-1.3
Sediments, moraines, clay and other rock with little resistance	1.3-1.8
Fine sediments and soils without erosion resistance	1.8-2.0
Coefficient of type and extent of erosion [ϕ]	
Little erosion on watershed	0.1-0.2
Erosion in waterways on 20-50% of the catchment area	0.3-0.5
Erosion in rivers, gullies and alluvial deposits, karstic erosion	0.6-0.7
50-80% of catchment area affected by surface erosion and landslides	0.8-0.9
Whole watershed affected by erosion	1.0

3.2 Input data availability

The necessary model input data can be subdivided into spatially variant input parameters (precipitation, temperature and land cover/use, soil erodibility, average slope of the study area, coefficient of type and extent of erosion and mean difference in elevation of the study area) and spatially invariant parameters (study area, perimeter of the watershed, length of the principal waterways and cumulated length of the principal and the secondary waterways).

The spatial distributions for average annual precipitation P_a and temperature T_0 , with a resolution of 1000x1000 m, were obtained from the Croatian Meteorological and Hydrological Service for the time period of 1961 to 1990, representing past. Maps representing the present were generated based on the changes in precipitation and temperature in 24 year time period (Talbe 2) [6].

Table 2. Average seasonal temperature and precipitation based on Crikvenica meteorological station (based on data obtained from Croatian Meteorological and Hydrological Service)

Average seasonal temperature T_0 [°C]/ Time series	January (Winter)	April (Spring)	July (Summer)	October (Autumn)
1961-1990	5.8	12.4	23.3	15.1
1991-2020	6.7	13.5	24.9	16.0
ΔT_0	+0.9	+1.1	+1.6	+0.9
Average seasonal precipitation P_a [mm]/ Time series	Winter	Spring	Summer	Autumn
1961-1990	287.6	283.7	237.5	434.1
1991-2020	305.0	249.4	227.0	517.3
ΔP_a	+17.4	-34.3	-10.4	+83.2

Two different soil erodibility maps were derived for the Dubračina catchment. First is based on Geological map of Dubračina catchment with the scale 1:25 000. The second variant of Soil erodibility coefficient is based on Pedological map of Primorsko-goranska County with a scale 1: 100 000 [7].

Two different land cover/use data sets were initially available [7, 8]; the 1:100,000 scale CORINE land cover map produced by the European Commission (EC) in 2006 and the 1:25,000 Spatial Plan of land use produced by the Croatian Government in 2004. The CORINE data were available at a spatial resolution of 100x100 m whilst the Spatial Plan was converted to raster format at a spatial resolution of 25x25 m. A third data set, based on supervised classification of a recent (August, 2013) Landsat 8 scene was subsequently included in the study to provide a more up-to-date and higher resolution (15x15m) assessment of land cover than the CORINE data set. The land cover map based on Landsat scene was obtained using supervised classification of the data with the help of the ERDAS Imagine 2014 software (Figure 2).

Four different Landsat 8 images, with resolution 15x15 m, were used for the derivation of seasonal land cover maps upon which soil protection coefficient is created. For the classification of these images ERDAS Imagine 2014 software was used to obtain land cover classes and later ArcGIS 10.2 for the derivation of soil protection coefficient [9].

The coefficient of type and extent of erosion was based on the Spatial Plan map of known erosion - affected areas (scale 1:25,000). LIDAR data were used to generate a digital elevation model with a 2x2-m cell size spatial resolution, from which the average slope of the study area map (Figure 24) and mean difference in elevation of the study area was derived.

The drainage density map is based on river (primary and secondary) density calculated from the centre point of each map cell taking into account the values of all cells within the rectangle 1000 x 1000 m [10].

Spatially invariant parameters are those that are constant in their values for each cell size throughout the catchment area and include:

- Study area
- Perimeter of the study area

both of which are considered basic catchment descriptors and used in the model as a constant values.

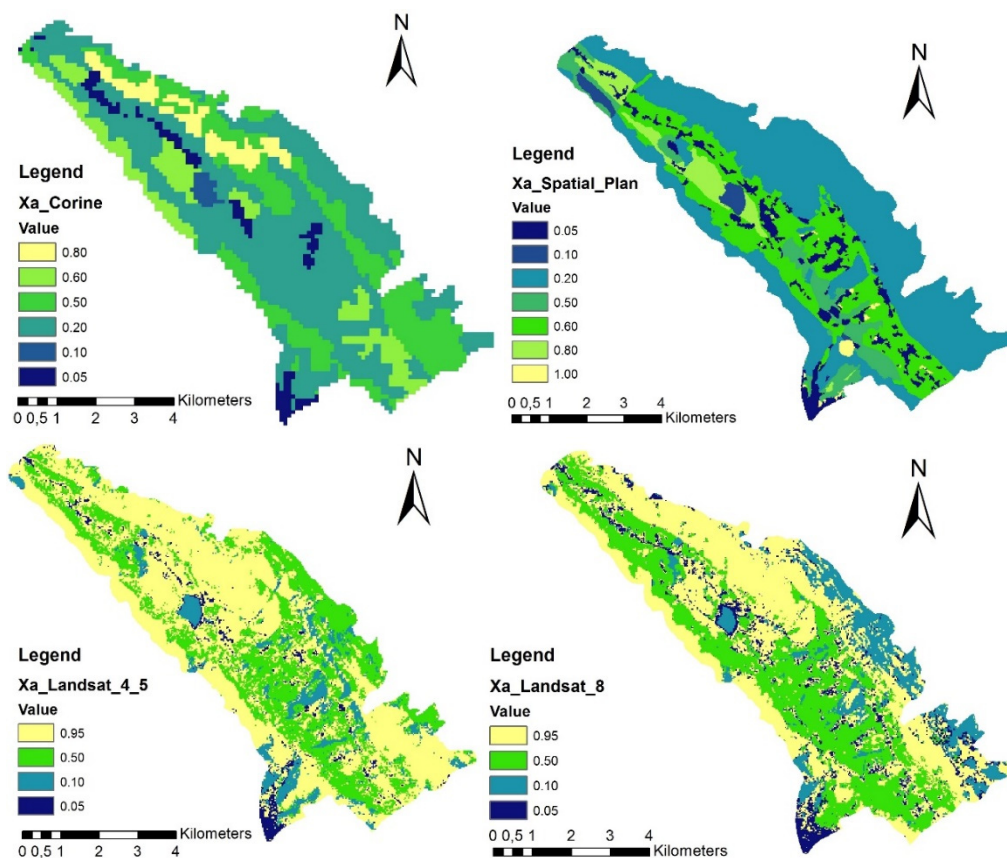


Figure 2. Soil protection coefficient according to numerical evaluation of different land cover/use maps

3.3 Method sensitivity and model uncertainty analysis

For the EPM method sensitivity analysis [6], twenty-nine model variations were derived, and a total of fourteen model parameters were analysed and varied by $\pm 10\%$ to obtain the values for the Sensitivity index I for each affected model output. Included parameters can be divided into three categories: (A) the parameters that affect all three model outputs (W_a , G_y and Z), (B) the parameters that affect both W_a and G_y , and (C) the parameters that only affect G_y .

Sensitivity classes were assigned to each of fourteen different parameters included in the method, with the objective of providing a better understanding of the method and the contributions of each parameter to different model outputs. The model outputs are mainly based on the multiplication of the model parameters; thus, for example, when varying the Average annual temperature P_a , the model outcome Total annual volume of detached soil W_a will vary proportionally. Not all parameters are included in the model through multiplication, e.g., Average slope off the study area J_a , Average annual temperature T_0 and Drainage density D_d . Most of these parameters are categorised as

high or medium sensitivity, whereas those in the multiplication form are classified as very-high-sensitivity parameters.

The model uncertainty analysis was conducted to examine the model response to variations in time and source of information. For this purpose, seven different model scenarios were selected, each varying only one parameter in relation to scenario I, as seen in Table 3.

Table 3. scenarios for uncertainty analysis and input data for spatially and time-varying parameters

Scenario	Average annual precipitation P_a	Average annual temperature T_0	Land cover/use data on which the Soil protection coefficient X_a is based	Soil type data on which the Soil erodibility coefficient Y is based
I	$P_{a(1991-2020)}$	$T_{0(1991-2020)}$	Landsat 8	Pedology map
II	$P_{a(1961-1990)}$ *	$T_{0(1991-2020)}$	Landsat 8	Pedology map
III	$P_{a(1991-2020)}$	$T_{0(1961-1990)}$ *	Landsat 8	Pedology map
IV	$P_{a(1991-2020)}$	$T_{0(1991-2020)}$	Spatial Plan*	Pedology map
V	$P_{a(1991-2020)}$	$T_{0(1991-2020)}$	Corine*	Pedology map
VI	$P_{a(1991-2020)}$	$T_{0(1991-2020)}$	Landsat 4,5*	Pedology map
VII	$P_{a(1991-2020)}$	$T_{0(1991-2020)}$	Landsat 8	Geology map*

*Changed parameter in relation to basic scenario I

The uncertainty analysis was divided into two main elements. The first, parameter uncertainty analysis based on a chosen sample size selected out of the population that encompasses all the cells in the Dubračina catchment and the second that reflects overall uncertainty of a model output when the entire population is taken into account [7].

The analysis consisted of several model scenarios, each changing one parameter at a time. Both, soil protection coefficient and soil erodibility coefficient were found to strongly impact the outcomes of the EPM model and are highly sensitive model parameters. The analysis indicates that, when changing the data source, significant changes in the model outcome values (up to approximately 47%, as shown for the Dubračina River catchment study area) can occur without the awareness of an expert as to the nature of the error (Table 4). Such changes are related to input data errors and depend on detailed preliminary research and data gathering as well as applied criteria for appropriate data selection. To conclude, the EPM can result in a large range of model output uncertainty due to the use of input data with unknown errors from approximations in data measurement, incorrect assumptions, etc [7].

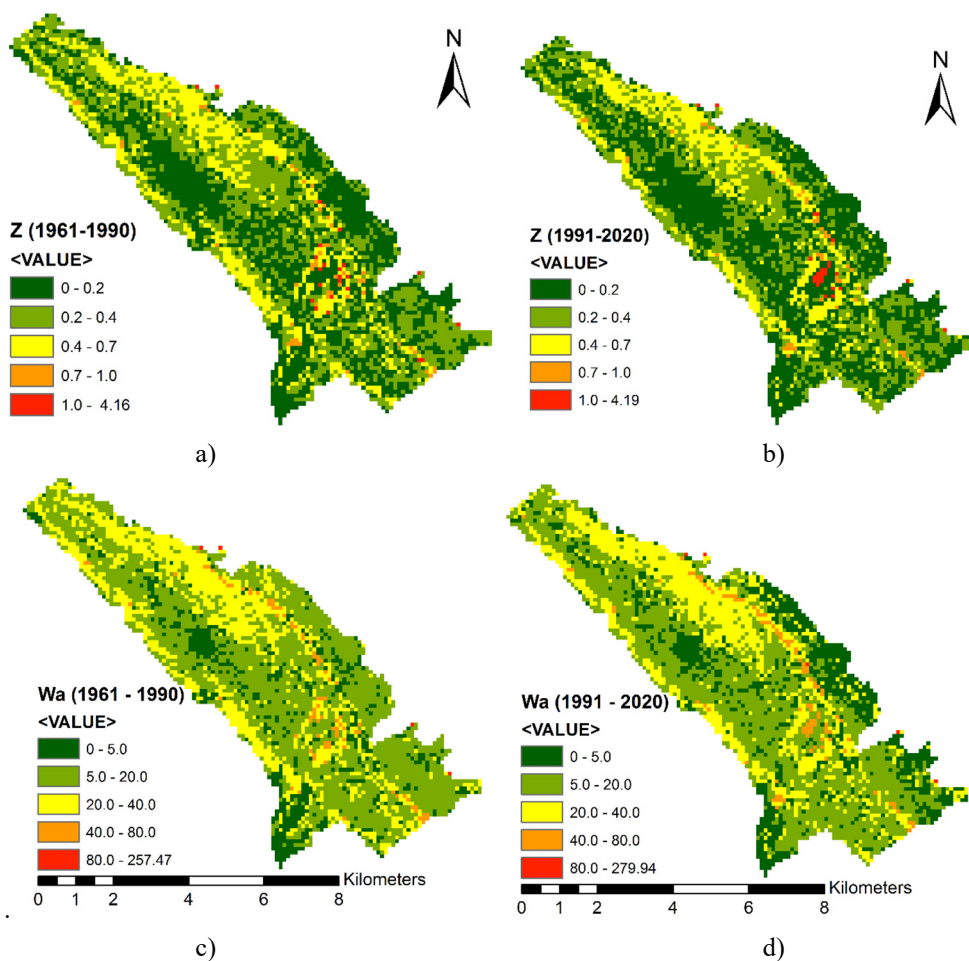
Table 4. Model uncertainty shown in percent change in the model output

Parameter	Change in parameter data set [%]	Change in model output values		
		[% $W_{a,I}$]	[% Z_I]	[% $G_{y,I}$]
Average annual precipitation P_a	-2.5	/	-2.4	-3.5
Average annual temperature T_0	-3.3	/	-3.4	-3.2
Soil protection coefficient X_a	-45.5	-46.0	-46.9	-23.5

(source Spatial Plan)				
Soil protection coefficient X_a (source Corine database)	-45.0	-45.0	-44,7	-50.9
Soil protection coefficient X_a (source Landsat 4,5)	-2.5	+9.9	+9.8	+11.8
Soil erodibility coefficient Y	-37.8	-41.2	-41.7	-33.9

3.4 Soil erosion assessment using EPM method

The estimated values and maps (Figure 3, Table 5) derived by the EPM model include outputs for erosion coefficient (intensity), total annual volume of the detached soil and actual sediment yield for the past (1961 – 1990) and present time (1991 – 2020) [11]. The most noticeable spatial change in erosion coefficient between the two time series is around Slani Potok and Mala Dubračina sub-catchments, where the area affected by excessive erosion was found to increase from past to present time. The overall decrease in average values of the total annual volume of the detached soil is noted from past (15.64 m³/cell/year) to present (15.12 m³/cell/year) time but this change in values was not found to be significant, in contrast to the change in the spatial distribution visible on the maps.



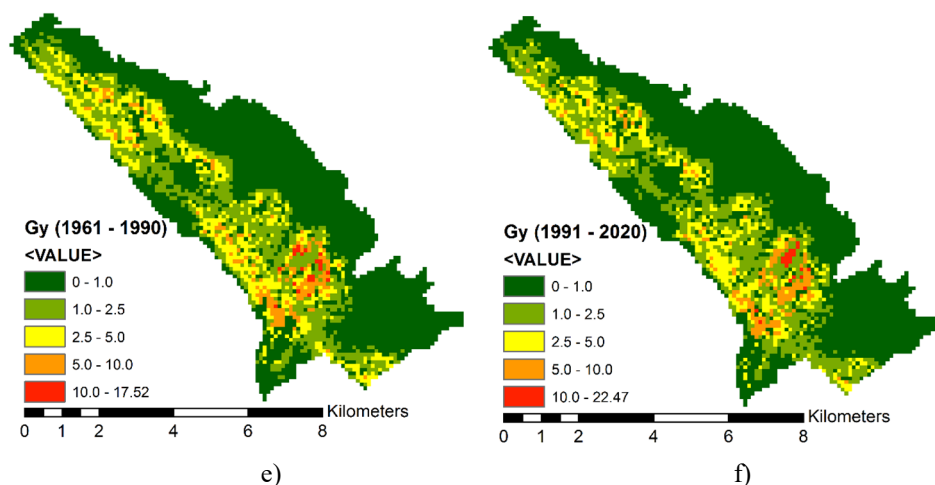


Figure 3. Gavrilović model outputs for the past and present time series for the Dubračina catchment: a) Erosion coefficient Z for the time period 1961-1990, b) Erosion coefficient Z for the time period 1991-2020, c) Total annual volume of the detached soil W_a for the time period 1961-1990 in $\text{m}^3/\text{cell}/\text{year}$, d) Total annual volume of the detached soil W_a for the time period 1991-2020 in $\text{m}^3/\text{cell}/\text{year}$, e) Actual sediment yield G_y for the time period 1961-1990 in $\text{m}^3/\text{cell}/\text{year}$, f) Actual sediment yield G_y for the time period 1991-2020 in $\text{m}^3/\text{cell}/\text{year}$

Table 5. Descriptive statistics for derived past and present model outputs (Z , W_a , G_y) for the entire catchment Dubračina

Time-series	Statistical parameter	Z [-]	W_a [$\text{m}^3/\text{cell}/\text{year}$]**	G_y [$\text{m}^3/\text{cell}/\text{year}$]**
1961-1990	Minimum	0.0009	0.044	0
	Mean	0.274	15.649	1.30
	Maximum	4.163	257.47	17.51
	Sum*	/	67 072.91*	5573.21*
	Standard deviation	0.297	11.442	1.855
1991-2020	Minimum	0.0009	0.048	0
	Mean	0.250	15.12	1.244
	Maximum	4.189	279.93	22.47
	Sum*	/	64810.75*	5331.86*
	Standard deviation	0.219	13.701	1.908

*[$\text{m}^3/\text{catchment}/\text{year}$]

** cell size is $100 \times 100 \text{m}$ or 0.01 km^2

The current erosion intensity in the catchment and the erosion sediment production and transportation is represented by the model outputs from 1991-2020 time-series. The very slight erosion covers the largest area of the catchment, approximately 44.98%, followed by slight erosion with 34.19%, then moderate erosion with 17.11%, and severe and excessive erosion covering together approximately 3.72% of the catchment area. Overall, average erosion coefficient for the Dubračina catchment is 0.25 which classifies it as the area of slight erosion.

3.5 Modification of EPM method and seasonal soil erosion production

The most often used time interval for which the erosion sediment production is calculated is one year. Although, today more and more interest is given on event based calculation of sediment production but those models are mainly complex physical based model. When choosing and applying the method and model for erosion assessment, consequently one or the other time interval for which the model was developed is chosen. However, till today, less attention is given on seasonal erosion sediment production assessments which can actually highly contribute to the planning strategies and implementation of erosion mitigation and prevention measures and benefit local community.

There are three main parameters that are changed in relation to the existing version of the EPM model [9]. These parameters are:

- Average annual temperature T_0
- Average annual precipitation P_a and
- Soil protection coefficient X_a .

Instead, Average seasonal temperature $T_{0,s}$, Average seasonal precipitation $P_{a,s}$ and Soil protection coefficient $X_{a,s}$ representing season soil cover are used. Average seasonal temperature $T_{0,s}$ is derived based on the calculated change in average values from past to present and later integrated into the temperature maps representing four different seasons, obtained from DHMZ for the past time seasons (1961-1990) in order to produce seasonal $T_{0,s}$ maps for the present time. The same procedure was used to obtain average seasonal precipitation $P_{a,s}$ maps. The soil protection coefficient $X_{a,s}$ is based on Landsat 8 data from January 2016, April 2014, August 2013 and October 2014 representing in the same order winter, spring, summer and autumn [9].

From these three parameters, only soil protection coefficient affects all three model outputs while average seasonal temperature and precipitation affect only total seasonal volume of the detached soil $W_{a,s}$ and actual sediment yield $G_{y,s}$. Although, when changing the soil protection coefficient based on different land cover maps, each representing one season, the value range of the model output erosion coefficient Z_s is not changed but the spatial distribution of its values.

The mean values for erosion coefficient indicate that the catchment should be the most exposed to erosion processes during the summer (0.25) and winter (0.24) while less during the spring (0.22) and autumn (0.2). This is not actually the case since for the derivation of the erosion coefficient not all significant factor influencing erosion such as temperature and precipitation are taken into account. So in reality, the higher values for erosion coefficient indicate the soil type characteristic and vegetation cover effectiveness to protect the top soil surface in a given time of the year. That corresponds to the change in land cover in time cycle of one year, where during the winter and summer vegetation cover is in its decrease and less dense, while during the spring the vegetation is in its peak (Figure 4).

When comparing the values obtained and presenting annual values for W_a for the present time and ones representing seasonal values $W_{a,s}$ it can be noted that the overall sum of values obtained for season (56 152.23 m³/catchment/year) is approximately 13% less than one obtain for the entire year (64 810.75 m³/catchment/year).

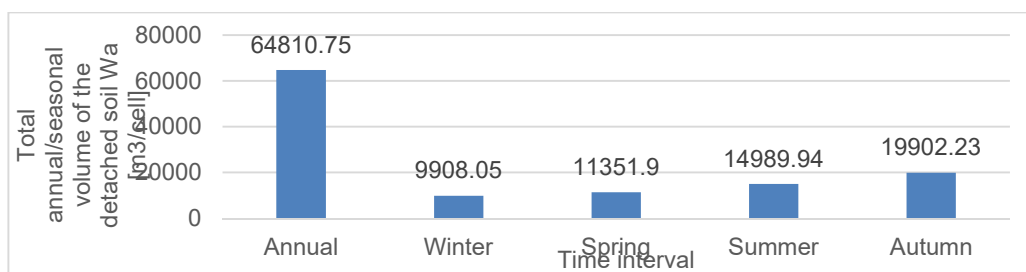


Figure 4. Redistribution of the soil loss within the seasons and comparison with annual soil loss for present time [9]

3.3 Verification of the model

The model output erosion intensity, land cover map for the present and the summer and the soil surface change were verified using a visual survey monitoring method and a GPS device. All verifications revealed good results, and the high accuracy of the derived maps was confirmed [9].

Acknowledgements

This research was conducted within the University of Rijeka founded projects: Implementation of innovative methodologies, approaches and tools for sustainable river basin management (uniri-tehnic-18-129 5570) and Hydrology of water resources and risk identification of flooding and mudflows in the karst areas (uniri-tehnic-18-54 5766)".

References:

- [1] Morgan, R. P.: Soil Erosion & Conservation. Oxford, 3rd edition, Blackweel Science Ltd. Oxford, 2005.
- [2] Gavrilović, S.: Inženjering o bujičnim tokovima i eroziji. Izgradnja (special issue), d. Marković, A. and Jarić, M., Beograd , PPT. 1972.
- [3] Dragičević, N.; Karleuša, B; Ožanić, N.: A review of the Gavrilović method (erosion potential method) application, Građevinar, 67, (2016), 9, pp. 715-725.
- [4] de Vente, J. and Poesen, J.: Predicting soil erosion and sediment yield at the basin scale: scale issues and semi-quantitative models. Earth-Science Reviews 71, (2005), 1-2, pp.95-125.
- [5] Haghizadeh, A.; Teang Shui, L.; Godarzi, E.: Forecasting sediment with erosion potential method with emphasis on Land use changes at basin, electronic. Journal of Geotechnical Engineering, 14, (2009), pp. 1-12.
- [6] Dragičević, N.; Karleuša, B; Ožanić, N.: Erosion Potential Method (Gavrilović method) sensitivity analysis, Soil and Water Research, 12, (2017), 1, pp. 51-59.
- [7] Dragičević, N.; Karleuša, B; Ožanić, N., Kisić, I: Effect of source-varying input data on Erosion Potential Model performance, Geocarto International, (2018), pp. 1-14.
- [8] Dragičević, N.; Whyatt, D.; Davies, G.; Karleuša, B.; Ožanić, N.: Erosion model sensitivity to land cover inputs: case study of the Dubračina catchment, Croatia. In: Proceedings of the GIS Research UK 22nd Annual Conference GISRUUK 2014, Glasgow, pp. 340 -348, 2014.
- [9] Dragičević, N.; Karleuša, B; Ožanić, N.: Modification of erosion potential method using climate and land cover parameters, Geomatics, Natural Hazards and Risk, 9, (2018), 1, pp. 1085-1105.
- [10] Dragičević, N.; Karleuša, B; Ožanić, N.: Different approaches to estimation of drainage density and their effect on the erosion potential method, Water, 11, (2019), 3, pp.1-14.

- [11] Dragičević, N.; Karleuša, B.; Ožanić, N.: Effect of land cover/use change on soil erosion assessment in Dubračina catchment (Croatia). *In: Proceedings of the 10th World Congress on Water Resources and Environment “Panta Rhei”, Athens, pp. 189-195, 2017.*

HYDRAULIC CONSIDERATION OF THE FISH PASS CROSS SECTION USING VELOCITY-AREA METHOD

LEA ČUBANOVÁ¹

¹ *Slovak University of Technology in Bratislava, Faculty of Civil Engineering, Department of Hydraulic Engineering, Radlinského 11, 810 05 Bratislava, Slovakia, lea.cubanova@stuba.sk*

1. Abstract

Cross section of the fish pass, especially of the nature-like bypass channel, should fulfill different requirements defined for each fish zone. Cross section must offer varied velocity field - different velocities through the cross section and also nearly zero velocities areas nearby the banks for weak individuals. The velocity-area method is the most common method for the determination of discharge in open channels, but here is used vice versa for the cross section design bounded by prescribed parameters of the fish zone. There was tested designed biocorridor in the bream fish zone on the prepared water structure at the Váh river in Slovakia lowland.

Keywords: design parameters, fish pass, hydraulics, ichthyofauna, velocity-area method

2. Introduction

In terms of fulfilling Slovakia's commitments to the European Water Framework Directive, the migration barriers on the Slovakia streams are removed.

In the area of implementation of the Water Framework Directive, a list of water bodies of the Water Plan of Slovakia was prepared and assessed, or for Programme of Action of the Water Plan of Slovakia in the section Hydromorphological Measures - Measures for Elimination of Significant Disturbance of Longitudinal Connections of Rivers and Habitats. The environmental objective of measures to ensure longitudinal continuity of rivers and habitats is to eliminate disturbance of longitudinal continuity of rivers and habitats to a level consistent with criteria of good ecological status/potential, it means restoring the possibility of migration of fish and other aquatic animals in rivers and autochthonous water habitats, promoting biodiversity and securing ecosystem services. The output of hydromorphological measures are corrective actions on water structures, such as fish passes or biocorridors, chutes, ramps, changes in operation manuals, removal of barriers and other measures ensuring longitudinal continuity of the streams and biotopes as well as interconnection of branches with streams to ensuring lateral continuity of wetlands and inundations with streams, or revitalization of streams aimed at ensuring their lateral continuity. Passability of the streams and biotopes is carried out in accordance with the Methodological Guideline of the Ministry of the Environment of the Slovak Republic "Identification of the appropriate fish pass types according to water body typology" [1]. According to this methodology, it is necessary to incorporate written biological requirements into all implemented projects of the fish passes, to ensure bioecological (environmental) building supervision and hydroecological and

ichthyological monitoring of the passability of migration barriers during the first three years of fish pass operation.

This Methodological Guideline [1] follows the German standards that have been dealing with the issue of fish passes in such a form since 1996 (DWVK-Merkblatt 232/1996 [2]) as well as Czech standards because we have approximately the same fish species composition and fish zones (TNV 75 2321 - technical standard of water management [3]).

3. Methods

3.1 Application of the velocity-area method for the cross section design

There is a trend of the building of the natural fish passes eventually the hybrid types, which are partly designed as technical, but have elements of natural character. If we are talking about biocorridors the most appropriate geometrical shape of the cross section is irregular trapezoid, in which conditions for various fish species are created. Such cross section must fulfill prescribed requirements for dimensions (top width of the water level, recommended longitudinal slope of the channel, etc.) as well as for the physical parameters (doped discharge, velocities in verticals, average velocity, etc.).

To refine on the calculation of the flow rate in the proposed biocorridor together with the fulfillment of the conditions for a certain fish zone (velocity in shallows at the edge of the fish pass up to $0.40 \text{ m}\cdot\text{s}^{-1}$) it is necessary to use a compound cross-section method (velocity-area method), it means to divide the profile into several parts by vertical lines (Figure 1).

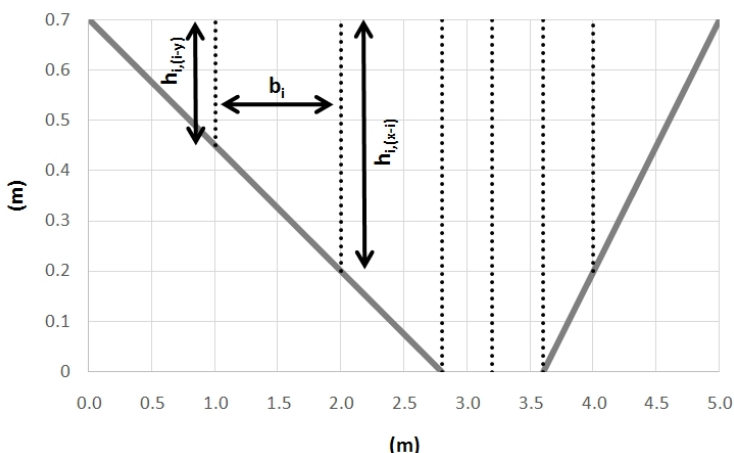


Figure 1. Example of the cross section divided into segments for velocity-area method

The value of the average vertical velocity in the segment with the width b_i , and the depths y_i is determined by the following procedure [1]:

– the profile is divided into several parts - segments, then for each segment p_i is calculated the flow area S_i :

$$S_i = \frac{b_i (h_{i,(x-i)} + h_{i,(i-y)})}{2} \quad (1)$$

S_i – area of the segment,

b_i – segment width in the water level,

$h_{i,(x-i)}$ – the depth on the right side of the segment,

$h_{i,(i-y)}$ – the depth on the left side of the segment,

– wetted perimeter O_i – for the calculation of the wetted perimeter in the velocity-area method, several methods are given in the literature, the method used below is taken from the HEC-RAS mathematical model manual. In this method, only the length of the water-bottom contact is counted into the wetted perimeter of the segment:

$$O_i = \sqrt{b_i^2 + (h_{i,(x-1)} - h_{i,(i-y)})^2} \quad (2)$$

– hydraulic radius R_i :

$$R_i = \frac{S_i}{O_i} \quad (3)$$

– Chezy's factor of flow resistance C_i (Manning equation):

$$C_i = \frac{1}{n} \cdot R_i^{1/6} \quad (4)$$

n – Manning roughness coefficient

– channel conveyance K_i :

$$K_i = C_i \cdot S_i \cdot \sqrt{R_i} \quad (5)$$

– mean vertical velocity v_{mi} in segment i :

$$v_{mi} = C_i \cdot \sqrt{R_i \cdot i_o} \quad (6)$$

Discharge in whole cross section is calculated as sum of the discharges by the individual segments according to the equation [1]:

$$Q = \sum_{i=1}^n Q_i = \sqrt{i_o} \cdot \sum_{i=1}^n K_i \quad (7)$$

Average cross-sectional velocity for whole profile [1]:

$$v = \frac{Q}{S} \quad (8)$$

3.2 Verification tool for the proposed biocorridor cross section

Consequently it is suitable to verify final design also by the 2D model, where is possible

to see detail hydraulic parameters distribution (velocities, etc.) in the model. Suitable tool is software River2D. The River2D model is a two-dimensional, depth averaged hydrodynamic and fish habitat model developed specifically for use in natural streams and rivers. It is a Finite Element model, based on a conservative Petrov-Galerkin upwinding formulation [4].

The hydrodynamic component of the River2D model is based on the two-dimensional, depth averaged St. Venant Equations expressed in conservative form. These three equations represent the conservation of water mass and of the two components of the momentum vector. The dependent variables actually solved for are the depth and discharge intensities in the two respective coordinate directions [4].

Conservation of mass [4]:

$$\frac{\partial H}{\partial t} + \frac{\partial q_x}{\partial x} + \frac{\partial q_y}{\partial y} = 0 \quad (9)$$

Conservation of x-direction momentum [4]:

$$\frac{\partial q_x}{\partial t} + \frac{\partial}{\partial x}(Uq_x) + \frac{\partial}{\partial y}(Vq_x) + \frac{g}{2} \frac{\partial}{\partial x} H^2 = gH(S_{ox} - S_{fx}) + \frac{1}{\rho} \left(\frac{\partial}{\partial x}(H\tau_{xx}) \right) + \frac{1}{\rho} \left(\frac{\partial}{\partial y}(H\tau_{xy}) \right) \quad (10)$$

Conservation of y-direction momentum [4]:

$$\frac{\partial q_y}{\partial t} + \frac{\partial}{\partial x}(Uq_y) + \frac{\partial}{\partial y}(Vq_y) + \frac{g}{2} \frac{\partial}{\partial y} H^2 = gH(S_{oy} - S_{fy}) + \frac{1}{\rho} \left(\frac{\partial}{\partial x}(H\tau_{yx}) \right) + \frac{1}{\rho} \left(\frac{\partial}{\partial y}(H\tau_{yy}) \right) \quad (11)$$

H – depth of flow,

U, V – the depth averaged velocities in the x and y coordinates directions,

q_x a q_y – the respective discharge intensities which are related to the velocity components through:

$$q_x = H \cdot U \quad (12)$$

$$q_y = H \cdot V \quad (13)$$

g – the acceleration due to gravity,

ρ – the density of water,

S_{ox} , S_{oy} – the bed slopes in the x and y directions,

S_{fx} , S_{fy} – the corresponding friction slopes,

τ_{xx} , τ_{xy} , τ_{yx} , τ_{yy} – the components of the horizontal turbulent stress tensor.

The Finite Element Method used in River2D's hydrodynamic model is based on the Streamline Upwind Petrov-Galerkin weighted residual formulation. In this technique, upstream biased test functions are used to ensure solution stability under the full range of flow conditions, including subcritical, supercritical, and transcritical flow. Using the Finite Element Method to solve the hydrodynamic equations results in a system of non-

symmetric, non-linear equations which can be solved by explicit or implicit methods. In River2D, an implicit approach is taken which requires a simultaneous solution of the system of equations. Because the system is non-linear, the Newton-Raphson iterative method is employed [4].

River2D (Depth Averaged Model) solves the basic mass conservation equation and two (horizontal) components of momentum conservation. Outputs from the model are two (horizontal) velocity components and a depth at each point or node. Velocity distributions in the vertical are assumed to be uniform and pressure distributions are assumed to be hydrostatic. Important three-dimensional effects, such as secondary flows in curved channels, are not included. The River2D model is a two-dimensional, depth averaged hydrodynamic and fish habitat model developed specifically for use in natural streams and rivers. It is a Finite Element model, based on a conservative Petrov-Galerkin upwinding formulation. It features subcritical-supercritical and wet-dry area solution capabilities. Ice covers with variable thickness and discontinuous ice covers can be modelled. It is intended for use on natural streams and rivers and has special features for accommodating supercritical /subcritical flow transitions, ice covers, and variable wetted area. It is basically a transient model but provides for an accelerated convergence to steady-state conditions. The fish habitat module is based on the PHABSIM weighted usable area approach, adapted for a triangular irregular network geometrical description. The hydrodynamic component of the River2D model is based on the two-dimensional, depth averaged St. Venant Equations expressed in conservative form. These three equations represent the conservation of water mass and of the two components of the momentum vector. The dependent variables actually solved for are the depth and discharge intensities in the two respective coordinate directions [4].

4. Results and discussion

There was tested designed biocorridor on the prepared water structure at the Váh river in Slovakia lowland. Area of interest belongs to the bream fish zone (metapotamal), long-term annual average discharge is $Q_a = 180 \text{ m}^3 \cdot \text{s}^{-1}$, maximum head $H = 6.2 \text{ m}$ [5, 6].

Table 1. Required parameters for the fish pass - biocorridor in the bream fish zone for $Q_a \geq 5 \text{ m}^3 \cdot \text{s}^{-1}$ [1]

maximum velocity	v_{\max}	($\text{m} \cdot \text{s}^{-1}$)	1.1
minimum depth	y_{\min}	(m)	0.7
minimum top width of the water level	B_{\min}	(m)	5
doped discharge	Q	($\text{m}^3 \cdot \text{s}^{-1}$)	≥ 2
maximum longitudinal slope	$i_{o, \max}$	(-)	1 : 150 (= 7 ‰)

According to the requirements for biocorridor in the bream fish zone (Table 1) given in the Methodological Guideline [1] we proposed top width of the water level $B = 5 \text{ m}$, longitudinal river bed bottom slope of $i_o = 5.7 \text{ ‰}$, depth of $h = 0.7 \text{ m}$. We designed the different slopes of the banks – right bank in slope 1: $m_1 \Rightarrow m_1 = 2$ and left bank in slope 1: $m_2 \Rightarrow m_2 = 4$, giving us an irregular trapezoid with a flat bottom width $b_d = 0.8 \text{ m}$ (Figure 1). It was used the roughness coefficient of the river bed bottom and banks

according to Manning – the river bed bottom of gravel, cobbles and single large stones, then $n = 0.045$.

For estimation of the required doped discharge and approximate mean cross-sectional velocity, we used a simplified method of calculating these parameters for the entire cross section (irregular trapezoid). Simple calculation for proposed parameters of the cross section given these results:

- cross section area $S = 2.03 \text{ m}^2$,
- wetted perimeter $O = 5.25 \text{ m}$,
- hydraulic radius $R = 0.387 \text{ m}$,
- Chézy factor $C = 19.0 \text{ m}^{0.5} \cdot \text{s}^{-1}$,
- channel conveyance $K = 23.9 \text{ m}^3 \cdot \text{s}^{-1}$,
- mean flow velocity $v_m = 0.891 \text{ m} \cdot \text{s}^{-1}$ (it fulfills the condition for maximum velocity given in Table 1),

– doped discharge into the proposed biocorridor with above described parameters $Q = 1.81 \text{ m}^3 \cdot \text{s}^{-1}$ (it is less than the condition for maximum doped discharge given in Table 1).

Using velocity-area method described in the section 3.1 we obtained more detailed distribution of the velocities in the proposed cross section of the biocorridor (Figure 2) and also more precise value of the doped discharge (Table 2).

Table 2. Results for the proposed cross section obtained using velocity-area method

p	h_i	b_i (m)	S_i (m^2)	O_i	R_i	C_i ($\text{m}^{0.5} \cdot \text{s}^{-1}$)	K_i ($\text{m}^3 \cdot \text{s}^{-1}$)	v_{mi} ($\text{m} \cdot \text{s}^{-1}$)	
	0.000								
1	0.250	1.0	0.125	1.031	0.121	15.634	0.681	0.41	
2	0.500	1.0	0.375	1.031	0.364	18.776	4.247	0.86	
3	0.700	0.8	0.480	0.825	0.582	20.306	7.436	1.17	
4	0.700	0.4	0.280	0.400	0.700	20.940	4.905	1.32	
5	0.700	0.4	0.280	0.400	0.700	20.940	4.905	1.32	
6	0.500	0.4	0.240	0.447	0.537	20.033	3.522	1.11	
7	0.000	1.0	0.250	1.118	0.224	17.313	2.047	0.62	
		$B = 5 \text{ m}$	$\Sigma S_i = 2.03$				$\Sigma K_i = 27.743 \text{ m}^3 \cdot \text{s}^{-1}$		
							$Q = 2.10 \text{ m}^3 \cdot \text{s}^{-1}$		
							$v = 1.03 \text{ m} \cdot \text{s}^{-1}$		

It can be stated that velocity in shallow at the edge of the fish pass at the left bank (in the first segment) is $0.41 \text{ m} \cdot \text{s}^{-1}$, maximum vertical velocity reaches up to $1.32 \text{ m} \cdot \text{s}^{-1}$ (in the middle segments of the cross section), mean flow velocity value of $1.03 \text{ m} \cdot \text{s}^{-1}$, doped discharge of bigger value $2.10 \text{ m}^3 \cdot \text{s}^{-1}$.

The straight section of the part of the biocorridor length 100 m with the above described parameters of the cross section, longitudinal slope and roughness coefficient was also

examined with 2D modeling in River2D software (described in the section 3.2) to verify that the required parameters listed in Table 1 were achieved. On the input topography of the proposed biocorridor river bed (each point contains information about coordinates x , y , z and roughness coefficient) was created mesh file with a computational triangular mesh (required mesh quality index must be in the range $QI = 0.1 - 0.5$ [7]) with $QI = 0.436$, the boundary conditions there were set (inflow area – discharge at the upstream boundary $Q = 2 \text{ m}^3 \cdot \text{s}^{-1}$, outflow area – water level at the downstream boundary (river bed bottom at the outflow area in m a. s. l. + estimated depth 0.7 m)). In the final input file of River2D must be set initial condition – the estimation of the upstream water level (river bed bottom at the inflow area in m a. s. l. + estimated depth 0.7 m) and must be chosen the steady or the unsteady flow (for simulation of the fish passes the steady state regime is the most appropriate).

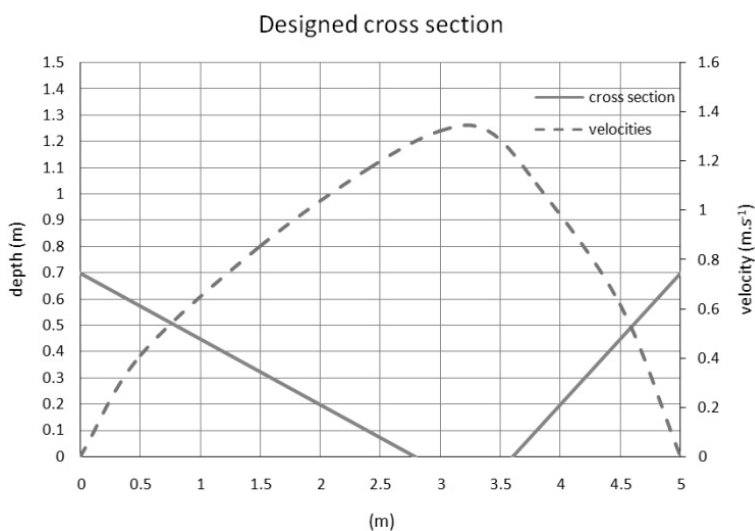


Figure 2. Theoretical distribution of the velocities in the proposed biocorridor cross section

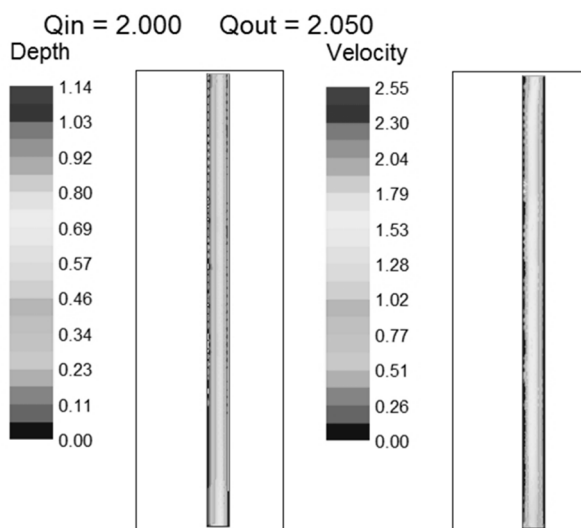


Figure 3. Results - depths and velocities from the 2D modeling (the highest values in the scale are caused by the inaccuracy of the mesh in one point at the edge of the modeled area)

The highest depths in the middle of the cross section reached maximum 0.6 m and at the edge (by banks) about 0.2 m. The highest velocities in the middle of the cross section reached maximum $1.6 \text{ m}\cdot\text{s}^{-1}$ and at the edge (by banks) about $0.2 \text{ m}\cdot\text{s}^{-1}$. For the better comparison of the mean vertical velocities in the cross section results were processed for certain cross section (Figure 4) and projected into the Figure 2 (results from the velocity-area method).

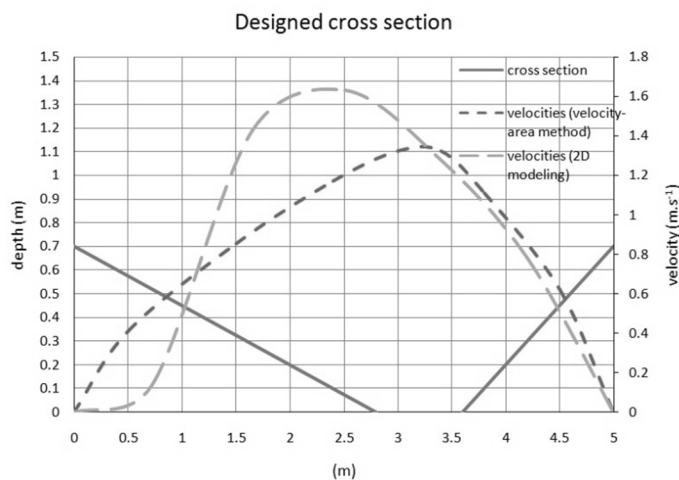


Figure 4. Comparison of the reached results for the mean vertical velocities for the proposed biocorridor using velocity-area method and 2D modeling

5. Conclusion

Cross section of the fish pass, especially of the nature-like bypass channel, should fulfill different requirements defined for each fish zone. The most important is velocity or maximum velocity, but cross section must offer varied velocity field - different velocities through the cross section and also nearly zero velocities areas nearby the banks for weak individuals serving as the rest places. There are also others recommendations as top width of the water level, doped discharge or recommended longitudinal slope of the channel. The velocity-area method is the most common method for the determination of discharge in open channels consists of measurements of stream velocity, depth of flow and distance across the channel between observation verticals. For the cross section design bounded by prescribed parameters of the fish zone is used vice versa. Cross section (its parameters as bottom width, bank slopes, roughness coefficient) is designed (optimized) and by the velocity-area method are verified velocities in verticals (whether rest areas by the banks are achieved), needed doped discharge as well as average velocity. Generally proposed fish pass channel is examined by the 2D mathematical model and results obtained by the calculations are different as simulated outcomes.

Several variants of the cross-sectional shape for the proposed biocorridor on the new water structure in Slovakia were solved (also in connection with the longitudinal slope

of the entire biocorridor routing), but only the presented one met the requirements according to the Methodological Guideline that has been in validity since 2015 and all newly designed and reconstructed fish passes must fulfill it. For the initial design of the non-symmetrical trapezoidal cross section geometry, simplified calculations were used which were put more precisely by the velocity-area method. This method provides a distribution of the mean vertical velocities in the cross section profile, which is important in the design of the biocorridor, because the cross section profile must provide a variable velocities within the range prescribed by the Methodological Guideline. In particular, it is the maximum velocity reached in the cross section profile and the velocities in shallow edges at the banks. Finally, part of the biocorridor was simulated in 2D mathematical software and the results - velocities were compared with the results of the velocity-area method.

Subsequent other verifications of the utilization of the velocity-area method for the cross section design for the nature-like bypass channels could be very strong tool for the designer in practices. It should be tested also curve areas of the fish pass routing and verified them in the hydrotechnical laboratory using methods of hydraulic research.

Acknowledgements

The paper was developed within the frame of and based on the financial support of the VEGA 1/0800/17 project "Optimization of the flood protection of municipalities in river basin of mountain streams" and of the Slovak Research and Development Agency under Contract No. APVV-16-0278 project „Use of hydromelioration structures for mitigation of the negative extreme hydrological phenomena effects and their impacts on the quality of water bodies in agricultural landscapes”.

References:

- [1] Metodické usmernenie MŽP SR: Určenie vhodných typov rybovodov podľa typológie vodných tokov, VÚVH Bratislava, 2015. (Methodological Guideline of the Ministry of Environment of the Slovak Republic: Identification of the appropriate fish pass types according to water body typology).
- [2] DWVK-Merkblatt 232/1996: Fischeaufstiegsanlagen: Bemessung, Gestaltung, Funktionskontrolle (Fish passes: Design, Dimensions and Monitoring). Deutscher Verband für Wasserwirtschaft und Kulturbau, Bonn, 1996.
- [3] TNV 75 2321 - technical standard of water management: Zprůchodňování migračních bariér rybími přechody (The migration barriers passable with fish passes). Hydroprojekt CZ, a. s., 2011.
- [4] Steffler, P., Blackburn, J.: River2D. Two-Dimensional Depth Averaged Model of River Hydrodynamics and Fish Habitat. Introduction to Depth Averaged Modeling and User's Manual. University of Alberta, September, 2002.
- [5] Bombiczová, A.: Hydraulic design of the fish pass and its assessment for the planned Water structure Kolárovo, Diploma thesis, Bratislava, 2019.
- [6] Možiešik, E., Dušička, P., Šulek, P., Rumann, J., Orfánus, M.: Modelový výskum dispozičného riešenia Vodného diela Kolárovo na Váhu s ohľadom na nautické podmienky a podmienky plavebnej bezpečnosti. Záverečná správa, Príloha A. Textová časť, Bratislava, 2015.
- [7] Waddle, T., Steffler, P.: R2D_Mesh. Mesh Generation Program For River2D Two Dimensional Depth Averaged Finite Element, Introduction to Mesh Generation and User's Manual. U.S. Geological Survey, September, 2002.

Topic no. 3 - Sanitary Engineering and Sustainable Water Use

PILOT-PLANT EXPERIENCES WITH MEMBRANE FILTRATION AT THE WTP JASNÁ

DANKA BARLOKOVÁ¹, JÁN ILAVSKÝ, MICHAL MARTON, MICHAL KUNŠTEK

¹*Department of Sanitary and Environmental Engineering, Faculty of Civil Engineering, Slovak University of Technology, Radlinského 11, 810 05 Bratislava, Slovak Republic, danka.barlokova@stuba.sk*

1. Abstract

Ultrafiltration was tested within the pilot-plant experiments at the WTP Jasná during the treatment of surface water originating from the water source Zadná Voda. Water treatment in this locality is focused on turbidity that is caused by storm rainfalls and snow melting. Fully automated ultrafiltration equipment with the membrane modul UA-640 (Microdyn-Nadir) was used. On the base of filtration cycles, the effectiveness of membrane technology was evaluated. By the application of membrane technology used, the required quality of treated water has been achieved.

Keywords: drinking water, water treatment, ultrafiltration, membrane modul UA-640, turbidity, trans-membrane pressure

2. Introduction

Water treatment plant Jasná is located in the region of Liptov, in central Slovakia, more accurately on the top part of Chopok which is located above the village Demänovská Dolina. This particular locality is one of the most famous tourist and ski centre in Slovakia. Hand in hand with the development of tourism, it is important to ensure the sufficiency of water suitable for drinking.

WTP was constructed in 1999. It serves the purpose of drinking-water treatment of the water originating from the water-source Zadná voda, which the water is supplied from after the mechanical pre-treatment to the WTP, to water reservoir and to consumers by using the gravitational transfer of water. Design capacity of the WTP is 15 l/s. Water treatment in this locality is focused on turbidity that is caused by storm rainfalls and snow melting.

This paper deals with the application of ultrafiltration and related operating experiences in the locality of Jasná.

2.1 Ultrafiltration

Ultrafiltration (UF) is a membrane separation process by which the particles of mechanical nature are removed from the water. Thanks to the pore diameter that are the order of tenths nm and the material, constructional and chemical properties of UF membranes, this technology represents the final solution for a secured protection against the turbidity that is caused by content of non-soluble and colloid particles of organic and inorganic origin, bacteria and the majority of viruses [1,2].

Treatment of water from surface water sources that are polluted mechanically or biologically, pre-treatment before the next technological step of water treatment are among the typical applications where the UF is used in. Effectiveness of ultrafiltration is increased by conventional methods such as coagulation, sedimentation and flotation [3].

Ultrafiltration represents a separation process that is powered by the pressure while the pressure impuls is caused by formation of vacuum or by the act of higher pressure from the outer side. The flow throughout the membrane ranges between 40-200 L/m².h⁻¹. Asymmetric membranes are used in ultrafiltration and the separation process is also functional on the principle of sieve mechanism. Pore size of UF-membrane ranges from 0.01 to 0.1 µm and the difference in pressure is from 1-10 bar. Most frequently mentioned is the value for molecular weight cut off, MWCO, that ranges between 5 – 5000 kDa and indicates the lowest molecular weight of testing polymer that is 90% retained on the membrane. For a proper design it is essential to select a membrane with a lower MWCO than is the molecular weight of substances to be effectively removed. Shape of the molecule has a great impact on separation, as the linear molecules do pass the membrane but the spheroidal molecules of the same size can be caught on it [4-6].

UF-modules are available in various constructional versions, e.g. plate-and-frame, spiral wound, with a hollow fibre and tubular. Each version is suitable to be used in different processes. Spiral wound modules are used for clean water, frame modules for high concentrated solutions and tubular modules are used in the treatment of drinking water [3,7].

Membranes of an ultrafilter consist of a bunch of hollow fibres where the functional surface represents an approximately 0,2 µm rough surface film of fiber hollows. Total filtration surface of one membrane standardly ranges between 40–60 m² in industrial modules. Fibers can be made of one or more hollows. Design and size of hollows is selected based on the level of pollution of the raw water. Hollows of larger diameter are preferred when the content of non-soluble substances is higher (> 50mg/L), however the result of it is a smaller filtration surface of the membrane module [8,9].

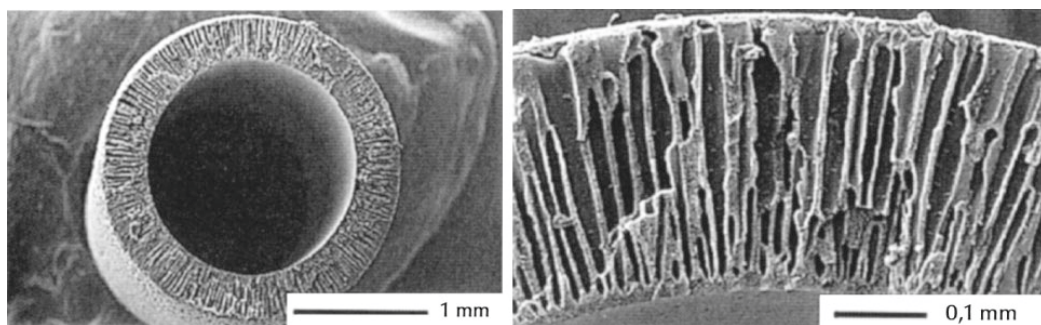


Figure 1. Microscopic zoom into the UF fiber, view of its structure and porous functional surface, functional surface of fibre is thinner from the inside than 1 µm. Flowing of water from the inside to the outside [9].

For manufacturing of the UF-membranes, materials of many kinds can be used, but when taking into account the mechanical and chemical durability, predisposition to siltation

and the price the materials that were approved the most are polysulphone (PSO), polyethersulphone (PES), polyacrylnitrile (PAN), polytetrafluoroethylene (PTFE), polyvinylidene fluoride (PVDF), cellulose acetate (CA), polyamid (PA) and polypropylene (PP). Manufactured are also the more expensive ceramic UF-membranes (Al_2O_3 , TiO_2 , ZrO_2 , SiO_2 , SiC). However, these are rather used in microfiltration, or eventually in applications related with a need for thermic disinfection (food and pharmaceutical industry). Under the constant load on the membrane they are resistant to water with pH 3-10 and for a short term they resist the chemical washing of membrane at the pH ranging between 1-13. Membranes are resistant to the standardly used disinfectants (max. 20 mg/L NaClO) [8,9].

Filtration cycle consists of filtration, forward-flush and upstream washing. Length of one cycle depends on the level of pollution of raw water. Usually, the phase of filtration takes 40-180 minutes and is followed by forward-flushing phase taking 30-50 seconds and upstream washing that takes 40-90 sec. Consumption of washing water ranges regularly between 2-4% from produced water, depending on the non-soluble substances content at the entry point [9].

Fouling of membranes can happen via the series of physico-chemical and biological mechanisms. Those mechanisms contribute to a higher accumulation of solid particles on the surface and within the membranes structure which results in that transmembrane pressure gets increased and the filtration velocity gets decreased. This leads to that the filtration cycle is shortened and the more frequent washing of membrane is needed [5].

We recognize external and internal clogging. External clogging on the membrane surface (scaling) causes the composition of the filtered medium from which the minerals on the membrane surface crystallize to form a filter cake and block the passage through the membrane. This kind of membrane fouling is temporary. External clogging can also cause so-called biofouling by forming biofilms or polymer layers on the membrane surface. The membranes so clogged are cleaned with oxidizing agents, weak sodium hypochlorite solutions are most commonly used. The fouling occurs in the pores of the membranes, representing the physical fouling of the pores by the pores where the pores are blocked and adsorbed, leading to a narrowing of the pores. This clogging is permanent.

3. Methods

3.1 Quality of water source in WTP Jasná

In the Table 1 is presented the analysis of water that was sampled at low values for turbidity at the water source Zadná voda on 18 April 2018. In terms of physico-chemical requirements, water is complying with the provisions of Decree No. 247/2017 Col. which laid down the requirements on water intended for human consumption and on the control of quality of water intended on human consumption. Water from the source Zadná Voda is characterized by a very low mineralisation and an occasional high value for turbidity, what is caused by the type of source of the drinking water.

Table 1. Water quality at the entry point to the mechanical filtration premises

PARAMETER	UNIT	RAW WATER	PARAMETER	UNIT	RAW WATER
pH		7.91	chlorides	mg/l	3.28
Conductivity	mS/m	2.27	nitrites	mg/l	0.86
COD _{Mn}	mg/l	0.56	nitrites	mg/l	0.005
Turbidity	NTU	1.05	sulphates	mg/l	1.92
Colour	mg/L	5	fluorides	mg/l	0.08
Alkalinity	mmol/L	0.268	ammonia	mg/l	0.013
Total dissolved solids	mg/L	20	potassium	mg/l	0.25
Ca+Mg	mmol/L	0.159	sodium	mg/l	0.94
Fe	mg/L	0.02	calcium	mg/l	3.29
Mn	mg/L	0.001	magnesium	mg/l	1.87

3.2 Ultrafiltration module

Fully automated ultrafiltration device, equipped with the membrane module UA-640 (Microdyn-Nadir) and control system and measuring the transmembrane pressure and back-flushing of the membrane with water or air, with chemical washing option, was used within the experiments (Figure 2). Specifications of modul UA-640 are listed in Table 1.

Table 2. Modul UA-640 specifications

Membrane type	Modul with hollow fibres	Peak-flow	do 1.3 m ³ /h
Diameter of fibers	OD/ID: 2.1 mm/1.1 mm	Maximum trans-membrane pressure	1 bar
Membrane material	PAN - polyacrylnitril	Maximum pressure of module	2 bar
Diameter of poruses	0.025 µm	Module diameter	168 mm
Membrane surface	16 m ²	Modul lenght	1210 mm
Regeneration	Back-washing with water and air	Maximum turbidity	300 NTU



Figure 2. A view of the ultrafiltration device, the membrane module itself, the control system and the treated water storage tank

Water was supplied to the UF-device by the pump, so the UF-flow rate was invariably maintained at the 600 L/h. Period of filtration cycle was 30 minutes. Following the end of the cycle, washing of membrane by using the back-flushing by water and air was applied. Filtered water accumulated in the tank was used for back-flushing while the air was supplied by the air-pump connected to the device. Any way of washing of the membrane did last for 30 seconds. On the base of filtration cycles, the effectiveness of membraned technology was evaluated.

4. Results and discussion

Sample of raw water was taken ahead of the membrane within every filtration cycle performed. Filtered water was sampled behind the membrane. Figures 3 to 5 present the turbidity progress in raw water and in filtered water and the difference in trans-membrane pressure over the filtration period (before and after washing of the membrane).

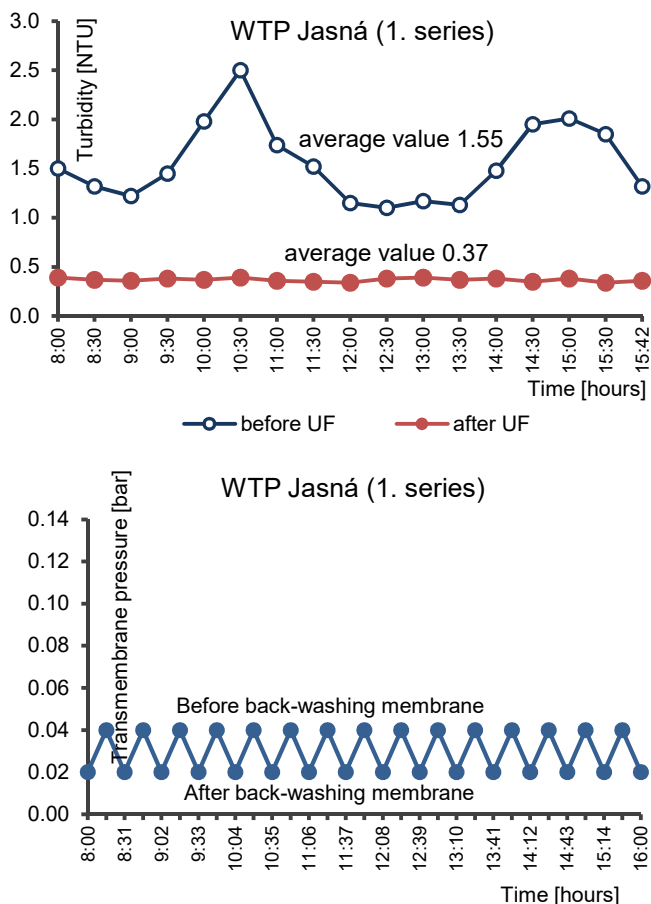


Figure 3. Turbidity progress in a raw water and in treated water by using the ultrafiltration (water with a low turbidity) and difference in pressure before and after washing of membrane.

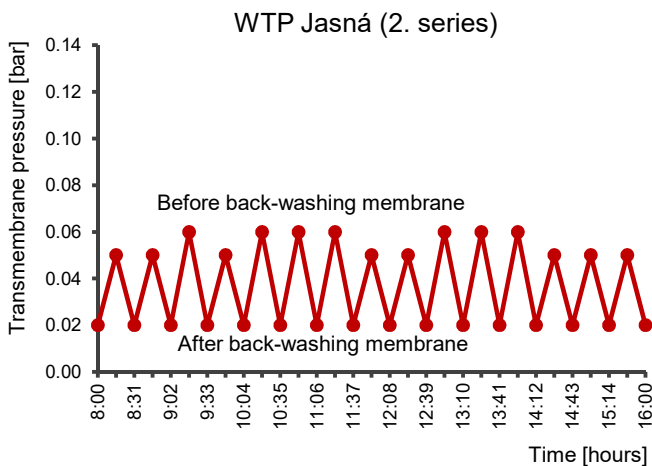
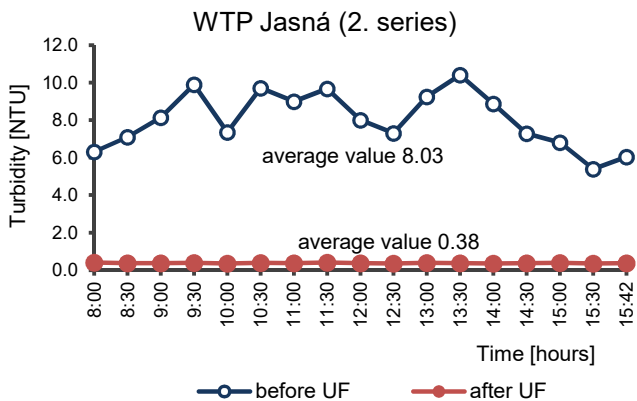
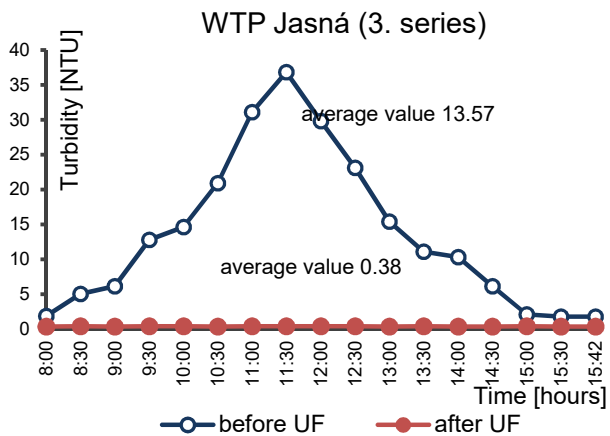


Figure 4. Turbidity progress in a raw water and in treated water by using the ultrafiltration (water with a medium turbidity) and difference in pressure before and after washing of membrane.



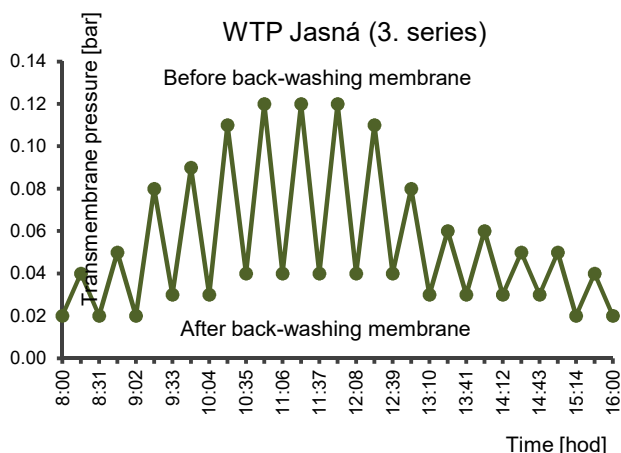


Figure 5. Turbidity progress in a raw water and in treated water by using the ultrafiltration (water with severe turbidity) and difference in pressure before and after washing of membrane.

Under the act of washing by using the air and water, the membrane facing the lower turbidity level managed to get clean again and reached the features as it had in the beginning of the cycle. Higher level of turbidity caused that it was not possible to the membrane to regain the level of initial input pressures that the membrane had in the beginning of the cycle. Only after the turbidity level has been decreased and a few back-flushing has been performed, the initial level of input pressure has been regained. On the other hand, these trans-membrane pressures can still be considered as being very low, so it would be possible to prolong the filtration cycle.

5. Conclusion

Turbidity removal is the major issue at the WTP Jasná. Limit for turbidity 5 NTU is set by Decree No. 247/2007 Col. Measuring data provided that the turbidity level of water treated by using the ultrafiltration device are compliant with the legal limit for drinking water.

By using the ultrafiltration the decrease by 76,1% has been reached in the first experiment (average turbidity in raw water 1,55 NTU). The efficiency of turbidity removal was 95,2% that was reached by ultrafiltration of water with a higher level of turbidity (average turbidity in raw water 8 NTU). High effectiveness of ultrafiltration was reached also with the water with the turbidity 37 NTU. In all of the three experiments, the turbidity of treated water ranged between 0,37 – 0,38 NTU.

Ultrafiltration devices feature the high level of reliability, mechanical firmness of capillars and membrane modules compatibility. On a small built-up area, these devices are capable to provide a high filtration performance. Great chemical endurance of modules in a wide range of pH values represent a standard for chemical treatment performed in cycles. UF devices are nearly maintenance-free.

Acknowledgements

The technological experiments were performed within the APVV-15-0379 grant projects.

References:

- [1] Baker, R.W.: Membrane Technology and Applications, Third edition, John Wiley & Sons Ltd, 2012.
- [2] Zeman, L. J., Zydney, A. L.: Microfiltration and Ultrafiltration: Principles and Applications, Marcel Dekker Inc, New York, 1996.
- [3] Microfiltration and Ultrafiltration Membranes for Drinking Water (M53), Manual of Water Supply Practices, First edition., AWWA, 2005.
- [4] Drioli, E., Giorno, L.: Comprehensive Membrane Science and Engineering. Elsevier Ltd. Oxford, UK, 2010.
- [5] Strathmann, H., Giorno, L., Drioli, E.: An Introduction to Membrane Science and Technology. CNR – Servizio Pubblicazioni e Informazioni Scientifiche, Rome, Italy, 2006.
- [6] Cheryan, M.: Ultrafiltration and Microfiltration Handbook, 2nd edn. CRC Press LLC, Boca Raton, USA, 1998.
- [7] Barloková, D., Ilavský J., Kunštek M., Buchlovičová J.: Membrane Technology in Surface Water Treatment for Drinking Purposes. eds. J. Říha J., T. Julek, Adam K.: 14th International Symposium WHME 2015, Brno, pp. 209-218, 2015.
- [8] Peng, N., Widjojo, N., Sukitpaneelit, P., Teoh, M.M., Lipscomb, G.G., Chung, T.S., Lai, J.Y.: Evolution of Polymeric Hollow Fibers as Sustainable Technologies: Past, Present, and Future. Progress in Polymer Science 37 (10). Elsevier Ltd: pp. 1401–24, 2012.
- [9] Krescanko M. Ultrafiltration - A Progressive Method of Producing Drinking Water. Journal Plynár, vodár, kúrenár + klimatizácia 10(5), pp. 56-57, 2012 (in Slovak).

CRITICAL INFLUENCING FACTORS FOR THE CAUSES OF PIPE FAILURES AND LEAKAGE IN WATER SUPPLY SYSTEMS

SANJA SPIROVSKA ¹, PHILIPP KLINGEL ²

¹ Arcadis Germany GmbH, North Macedonia, sanja.spirovska@arcadis.com

² Stadtwerke Karlsruhe Netzservice GmbH, Germany, philipp.klingel@netzservice-swka.de

1. Abstract

The threat posed by climate change intensifies the need of development of appropriate approaches for water resources management, aimed to establish a balance between water supply and demand. Water loss reduction in the water supply systems is becoming one of the main ways to manage the growing imbalance between water consumption and water availability. The present paper shall contribute to the development of a methodology for identification of critical influencing factors for the causes of pipe failures and leakage in water supply systems. For this purpose, the pipes are categorised and the individual pipe failures are associated with these pipe categories and their specific characteristics respectively and environmental influences, such as bedding condition, traffic loading, level of groundwater and soil type (soil aggressiveness and soil settlement). The degree of influence of these parameters that cause pipe failures is analysed using statistical methods in order to support the planning of water supply systems rehabilitation. Therefore, the Linear Extension of the Yule Process (LEYP) model implemented in the freely available software “Casses” was applied. The water supply system of the city of Pforzheim, Germany, is used as a case study for testing this methodology. From the analysis carried out for the water supply network of the city of Pforzheim, it can be concluded that for the cast iron and polyethylene pipes, where the main cause for the occurrence of leakage is the break of a pipe, significant factors of influence are soil settlement, traffic load and level of groundwater, where soil settlement was proved to be the dominant factor. In the case of ductile iron and steel pipelines, where most of the pipe failures are due to corrosion of pipelines, significant factors of influence are soil aggressiveness, the influence of the power supply cables and the influence of the groundwater, where the soil aggressiveness was proved to be the dominant factor. The results of the study are expected to enable faster and more efficient identification of the factors causing pipe failures and leakage in water supply systems, and thus, to improve the current operational practice of the water utilities.

Keywords: water supply network, water utilities, water loss reduction, water leakage, pipe failures, deterioration of pipelines, statistical modelling

2. Introduction

The pipe network infrastructure of water supply systems, during its lifespan, is exposed to stresses caused by the surrounding environment and its operation and maintenance

that are leading to its deterioration. Considering the fact that pipe networks are located underground and thus the inspection and collection of data on pipe failures is complicated, the identification of causes that lead to the occurrence of failures is complex and not always possible.

The critical influencing factors for the causes of pipe failures in water supply systems have been reviewed by a number of researchers [1], [2], [3]. According to these studies, the factors that influence the deterioration of water pipes, can be classified into three categories: (1) structural factors, (2) environmental factors and (3) operation and maintenance factors.

The main factors of these categories are listed in Table 1.

Table 1. Critical influencing factors for the causes of pipe failures in water supply systems

Structural Factors	Environmental Factors	Operation and Maintenance Factors
pipe material	bedding condition	cathode protection
pipe diameter	traffic loading	water quality
pipe age	external groundwater	water pressure
pipe laying depth	soil aggressiveness	water velocity
joint method	soil consistency	failure history

Statistical modelling of pipe failures is commonly used to identify the dominating influencing factors of a specific water supply network contributing to the occurrence of pipe failures in order to support the rehabilitation planning. This paper presents a case study of the application of a statistical modelling approach called Linear Extension of the Yule Process (LEYP) that relates the physical characteristics of the water pipes, the history of the past failures and the external factors from the water pipes environment, shown in Table 1. The pipe network of the water supply system of city of Pforzheim, Germany, is used to test this method.

3. Methods

3.1 Approach

The approach for development of the analysis method is generalized in the following steps:

- (1) Choice of the statistical model: In this stage of the research the main focus was choosing the proper method for analysis of the relationship between network characteristics, failures and environmental influences. For this purpose, the existing statistical models for describing the technical state of pipes and modelling of the pipe failures have been considered in a literature research.
- (2) Data collection: The application of the chosen method is based on the data collected from the water utility of the city Pforzheim.
- (3) Data analysis: Identification of causes for the occurrence of the pipe failures in the water supply system of the city of Pforzheim by statistical analyses of the relationship between pipeline data, failure data, and environmental influences.

3.2 Choice of the statistical model

In the first stage of the study, the following statistical models, developed by different researchers and used by many European utilities, were reviewed: Poisson Model, Proportional Hazards Model (PHM: Cox's PHM and Weibull PHM), Non-Homogeneous Poisson Process (NHPP) Model, model based on Herz distribution developed within the KANEW software and Linear Extension of the Yule Process (LEYP) model used in the freeware "Casses". The Poisson Model was adapted to water utilities with "poor level" (short period) data. On the other hand, NHPP, PHM, KANEW and LEYP model seem to be more efficient with long maintenance record and complete data, even if they have already been tested on networks with short maintenance record (5 to 10 years) with good results [2], [4], [5], [6], [7], [8]

Based on the necessary data input and the output of the reviewed models the Linear Extension of the Yule Process (LEYP) model implemented in the software "Casses" was chosen for further use. Within the approach, the LEYP intensity function is designed to account for multiplicative effects of: past failures through the so-called Yule factor $(1 + \alpha N(t-))$; ageing through the so-called Weibull factor $\delta t^{\delta-1}$; and covariates, which characterize the pipe and its environment through the so-called Cox factor $e^{z^T \beta}$ [9], [10]. Its intensity function is given as follows:

$$E_{\theta}\{dN(t)|N(t-), Z\} = (1 + \alpha N(t-))\delta t^{\delta-1}e^{z^T \beta} dt \quad (1)$$

The parameter-vector is given in Eq. (2):

$$\theta^T = (\alpha \delta \beta) \quad (2)$$

3.3 Data collection

In the second stage, for the implementation of the statistical model, data from the Pforzheim water utility database was used. In this stage the following activities were conducted: collection of the necessary data, detection of data anomalies, search for missing failure records in the archives of the Pforzheim water utility and digitization of the missing data in the GIS database.

3.4 Data analysis

In the third stage the influence of various factors on the occurrence of pipe failures was analysed using the statistical LEYP model implemented in the software "Casses". For this purpose, the influence of all environmental factors was combined with the material and age of the analyzed pipes. Table 2 presents the analyzed environmental factors and their covariates, where the covariates were grouped to give clear results.

The LEYP calibration model carries out statistical tests to check the significance of the model parameters $(\alpha, \delta, \beta, Z)$ related to chosen covariates. The standard test for significance is an approximate chi-squared valid test that provides a p -value for each parameter. If the p -value is less than 0.05 then the parameter is considered significant.

Table 2. Environmental factors and their covariates

Environmental Factors	Groups of the Covariates					
Soil Consistency	Cov.1 very low cohesion		Cov.2 low cohesion	Cov.3 medium cohesion	Cov.4 strong cohesion	Cov.5 Very strong cohesion
External Groundwater	Cov.1 above groundwater		Cov.2 changing zone		Cov.3 in groundwater	
Traffic Loading	Cov.1 There is none	Cov.2 Light trucks	Cov.3 Heavy goods vehicles (No. < 100 per day)	Cov.4 Heavy goods vehicles (100 ≤ No. < 500 per day)	Cov.5 Heavy goods vehicles (500 ≤ No. < 1000 per day)	Cov.6 Heavy goods vehicles (No. ≥ 1000 per day)
Power Cabels (distance to the analyzed pipeline)	Cov.1 0 - 1 m		Cov.2 1 - 5 m		Cov.3 5 - 10 m	Cov.4 > 10 m
Soil Aggressiveness	Cov.1 Class Ia		Cov.2 Class Ib		Cov.3 Class II	Cov.4 Class III

4. Results and discussion

The database of the Pforzheim water utility contains structural data for the pipes (diameter, material, age), environmental data (bedding condition, traffic loading, groundwater, soil aggressiveness and soil consistency), and operation and maintenance data (causes for the occurrence of the pipe failures, cathodic protection, failure history (type of failure, date of failure, date of repair)).

In the conducted analysis failure data between the years 1994 and 2012 is used. Although the failure observation period is only 18 years, the size and detail of the failure data set is relatively large. Records are available for 841 failures on house connections (414 failures on steel pipes, 252 failures on cast iron pipes, 135 failures on polyethylene pipes and 38 failures on ductile cast iron pipes), where the total length of pipes is 211 km; and 1351 failures on mains and distribution pipes (816 failures on ductile cast iron pipes, 408 failures on cast iron pipes, 4 failures on polyethylene pipes, 122 failures on steel pipes and 1 failure on PVC pipes), with the total length of pipes being 360 km. Figure 1 shows the causes for the occurrence of the pipe failures provided by the records from the water utility of Pforzheim.

Risk factors for the occurrence of the pipe failures have been calculated by analysing the influence of various environmental factors. These risk factors are set by the software "Casses" during the model calculation through the regression coefficient vector β from the Cox factor $e^{z^T \beta}$. To be usable in LEYP calculations, qualitative covariates are converted into $(n-1)$ indices, where n is the number of modalities. The n th modality is called reference modality and it has a value of 1 and the risk factors for all other modalities are calculated considering this reference modality.

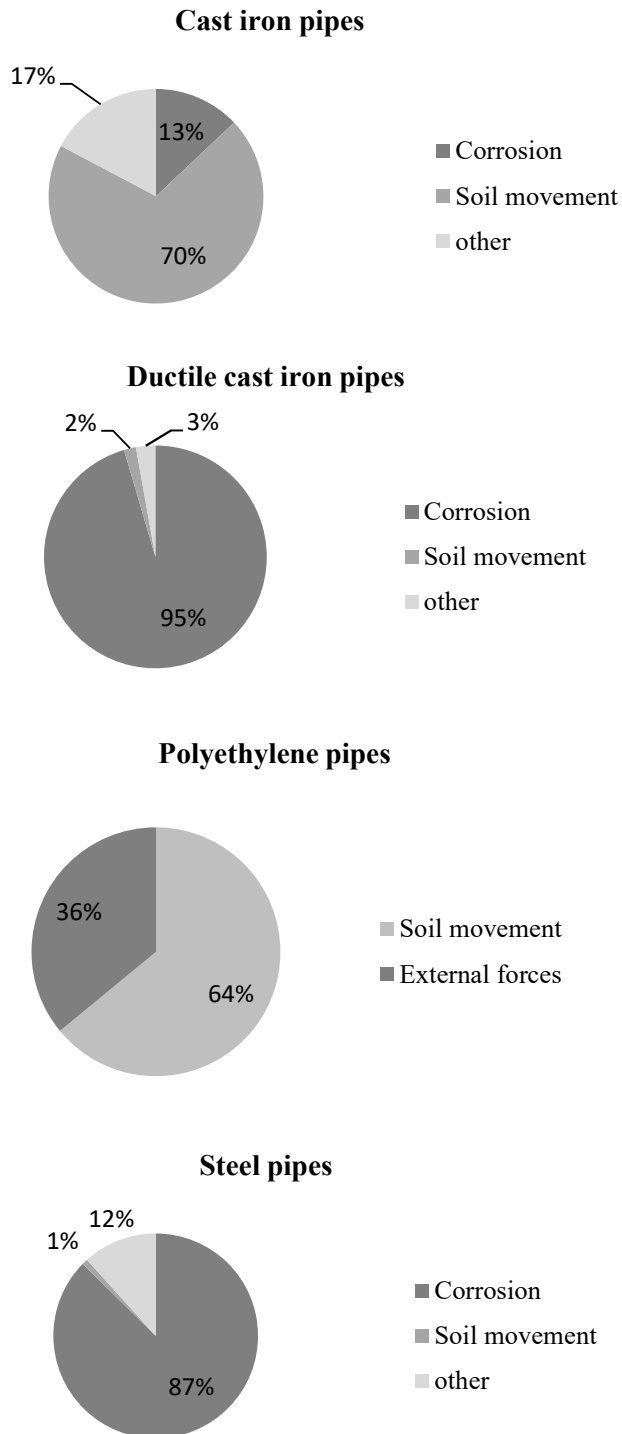


Figure 1. Causes for the occurrence of the pipe failures

Table 3 presents the calculated risk factors for the occurrence of the pipe failures influenced by the environmental factors and their covariates, grouped by pipe material. During the analysis several environmental factors were examined at the same time to determine which dominated. For the soil consistency analysis, the covariates 1, 2 and 3, which are shown in Table 2, are combined as reference modality, and the risk factor, as shown in Table 3, refers to the remaining covariates, namely covariate 4 - strong cohesion and covariate 5 - very strong cohesion. For the traffic load analysis, the covariates 1, 2 and 3 are combined as reference modality and the risk factor refers to the covariates 4,5 and 6, where the number of the heavy goods vehicles is greater than 100 per day. Regarding the groundwater analysis, the covariates 1 and 2 are combined as reference modality and the risk factor refers to the covariate 3, which covers the pipes that are lying in groundwater. For the soil aggressiveness analysis, the covariate 1 is taken as a reference modality and the risk factor refers to the covariates 2, 3 and 4, covering the soil class Ib, II and III. Lastly, regarding the power supply cable analysis, the covariate 4 is taken as a reference modality and the risk factor refers to the remaining covariates, namely the power cables with distance less than 10 m to the existing water pipeline.

Table 3. Calculated risk factors using the software “Casses”

	Cast iron pipes	Ductile cast iron pipes	Polyethylene pipes	Steel pipes
Environmental Factors	Calculated Risk Factors			
Soil Consistency (Cov. 4, 5)	1.5	/	1.46	/
Traffic Loading (Cov. 4, 5, 6)	1.16	/	1.12	/
External Groundwater (Cov. 3)	1.24	1.03/	1.1	1.03
Soil Aggressiveness (Cov. 2, 3, 4)	1.1	1.33	/	1.28
Power Supply Cables (Cov. 1, 2, 3)	/	1.01	/	1.02

Analysis shows that in the case of cast iron pipes, the influence of soil consistency, traffic loading, groundwater and soil aggressiveness is significant and it was calculated that soil consistency has the greatest influence with the calculated risk factor of 1.5. For ductile cast iron pipes, the influence of soil consistency, soil aggressiveness and power supply cables was examined. The dominant factor is soil aggressiveness with the calculated risk factor of 1.33. For polyethylene pipes the influence of soil consistency, traffic loading and groundwater was analysed. It was calculated that the soil consistency has the biggest impact with the calculated risk factor of 1.46. In the case of steel pipes, the influence of groundwater, soil aggressiveness and power supply cables was examined. The dominant factor is soil aggressiveness with the calculated risk factor of 1.28.

The main problem that has been faced within this research was the data collection. Since the pipes of an urban water network have a comparably long average lifetime, usually a sound documentation comprising all components is not available. In the case of the city of Pforzheim the oldest failure recorded in the GIS database is from 1935, but

unfortunately within the period 1935-2001 not all failures have been recorded. Hence analysis of the incomplete failure data would have led to false results. The pipe inventory and failure data available for Pforzheim is typical for many other water works in Europe. Water utilities usually have relatively short failure history documentations comprising the past 20 years when the utilities started to recognize the importance of keeping accurate information.

5. Conclusion

The pipe failure records provided by the water utility of Pforzheim show that the majority of the failures of the cast iron and polyethylene pipes occurred due to soil movement. The main cause for the occurrence of the pipe failures of the ductile cast iron and steel pipes is corrosion.

Pipe failures caused by soil movement are influenced by unfavourable soil consistency, traffic loading and groundwater. With the results obtained by the analyses with the software "Casses" it can be concluded that for non-ductile materials, namely cast iron pipes and polyethylene pipes, the calculated risk for the occurrence of the pipe failures due to unfavourable soil consistency, traffic load and groundwater level is increased (Table 3). Pipe failures caused by corrosion are influenced by groundwater, soil aggressiveness and power supply cables. For this case the analysis has also confirmed that in ductile cast iron pipes and steel pipes, where most of the pipe failures occurred due to corrosion, the calculated risk is higher for increased soil aggressiveness. There are very few pipes located in groundwater, so the results in terms of the factor groundwater are not meaningful. Furthermore, the presented study has shown that the influence of the power supply cables on the occurrence of corrosion of the ductile cast iron pipes and steel pipes is insignificant (Table 3).

The research has shown that statistical methods can be used to identify the failure influences of the most often used pipe materials. This information helps to increase the efficiency of the planning process for the rehabilitation of water supply systems as well as defining the risk of new pipe failures. Both can contribute to a significant improvement of the operational practice of water utilities.

Acknowledgements

This contribution has been made possible as part of the AWaRe project at the Karlsruhe Institute of Technology (KIT) and was funded by the German Federal Environmental Foundation DBU (Deutsche Bundesstiftung Umwelt).

References:

- [1] Mora-Rodríguez, J., Delgado-Galván, X., Ramos, H. M., López-Jiménez, A.: An overview of leaks and intrusion for different pipe materials and failures, *Urban Water Journal*, Volume 11, Issue 1, pp. 1-10, 2014.
- [2] Røstum, J.: Statistical modeling of pipe failures in water networks, Doctoral Dissertation submitted to the Faculty of Civil Engineering, the Norwegian University of Science and Technology, Trondheim, Norway, 2000.

- [3] Le Gat, Y., Kropp, I., Poulton, M.: Is the service life of water distribution pipelines linked to their failure rate, IWA 4th Leading edge conference on strategic asset management (LESAM 2011), Mülheim, Germany, 2011.
- [4] Martins, A.: Stochastic models for prediction of pipe failures in water supply systems, Instituto Superior Técnico, University of Lisbon, Portugal, 2011.
- [5] Hanusch, D. F., Kornberger, B., Friedl, F.: Whole of Life Cost Calculations for Water Supply Pipes, IWA 4th Leading edge conference on strategic asset management (LESAM 2011), Mülheim, Germany, 2011.
- [6] Kasess, D., Hanusch, D. F.: Vienna Waterwork's approach to network maintenance and rehabilitation, Magazine of the International Water Association, United Kingdom, Water21, 2013.
- [7] Sveinung, S., Schilling, W., Røstum, J., Tuhovcak, L.: Computer-aided Rehabilitation of Water Networks (CARE-W), Water Science & Technology Water Supply, 3(1), pp. 19-27, 2003.
- [8] Wang, Y., Zayed, T., Moselhi, O.: Prediction Models for Annual Break Rates of Water Mains, Journal of Performance of Constructed Facilities, Volume 23, Issue 1, 2009.
- [9] Renaud, E., Le Gat, Y., Poulton, M.: Using a break prediction model for drinking water networks asset management: From research to practice, IWA 4th Leading edge conference on strategic asset management (LESAM 2011), Mülheim, Germany, 2011.
- [10] Le Gat, Y.: Extending the Yule process to model recurrent pipe failures in water supply networks, Urban Water Journal, Volume 11, Issue 8, pp. 617-630, 2014.

SETTLING CHARACTERIZATION OF ELECTROCOAGULATED FLOCS

IVAN HALKIJEVIĆ¹, IVAN SOKOL², HANA POSAVČIĆ³

¹ Faculty of Civil Engineering, University of Zagreb, Croatia, halkijevic@grad.hr

² Croatian Motorways, Ltd., Croatia, isokolzg@gmail.com

³ Faculty of Civil Engineering, University of Zagreb, Croatia, hposavcic@grad.hr

1. Abstract

This paper deals with the characterization of settling properties of flocs generated within the electrocoagulation process. Characterization of the settling properties involves the determination of the settling regimes, sludge index, batch settling curve, settling velocity and relation of the suspended matter concentration to settling velocity. An experimental analysis of the settling properties of electrocoagulated flocs was carried out with several tests by using aluminum and iron electrodes with different currents ($I_1 = 10$ [A], $I_2 = 5$ [A]) and different duration of the process ($t_1 = 60$ [min], $t_2 = 90$ [min]). The phosphate contamination was generated by the addition of potassium dihydrogen phosphate (KH_2PO_4). The characterization of settling properties was performed for each test. Other water quality parameters, such as dissolved oxygen concentration, water temperature, pH and conductivity were also monitored.

Settling properties were analyzed by standard settling tests used for the settling characterization of active sludge. During the tests it was not possible to make diluted sludge volume index test (DSVI) and stirred specific volume index test ($\text{SVI}_{3,5}$) due to the low initial concentration of the electrocoagulated flocs. Maximum concentration of electrocoagulated flocs after 90 min was only 1.6 [g/L]. Also, pre-defined intervals in batch settling curve test, in which the height of the water-sludge surface level is read, are too long, especially for longer intervals of 5, 10 and 15 minutes. These intervals can't be used because all the settling occurs quickly after the flocs are merged and the time differences between readings is just too high, resulting in poor and imprecise batch settling curves.

Therefore, some of the standard settling tests are most likely not applicable for electrocoagulated sludge, because electrocoagulation results with significantly less sludge than a biological wastewater treatment process. Thus, further tests on actual sewage samples should be carried out so that more accurate conclusion is reached.

Keywords: settling characterization, electrocoagulated flocs, batch settling curve

2. Introduction

Settling is an important process in several individual operations in wastewater treatment plants. The most prominent of these processes are primary clarifiers (PSTs), which are

pre-biological reactor units, and secondary clarifiers (SSTs), which are the phase of clarification prior to discharging effluent. Settling also plays an important role in the development of new technologies, such as granulated sludge reactors and electrocoagulation. Due to the different nature of the settleable components (raw wastewater, active sludge and granular sludge) and the concentrations in which these compounds occur, these individual processes are characterized by completely different settling characteristics. Different settling regimes occur in which a particle-liquid suspension can be found and these regimes are associated with the specific settling observed in SSTs, PSTs and granulated sludge reactors.

Settling is controlled by its concentration and tendency for flocculation and can be classified in four regimes (classes): discrete settling without flocculation (class I), discrete settling with flocculation (class II), zone settling or obstructed settling (class III) and compression settling (class IV), Figure 1.

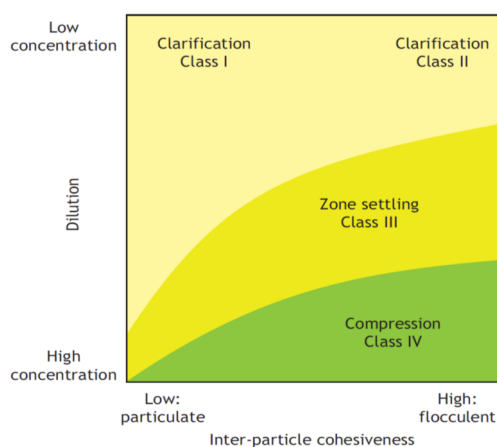


Figure 1. Settling classes [1].

At low concentrations (class I and II), the particles are completely scattered, among them there is no physical contact and the concentration is usually too diluted to cause one particle to deposit the other particle. Each particle precipitates at its own characteristic speed, which depends on the properties of individual particles such as shape, size, porosity and density. If these diluted particles do not show the likelihood for flocculation (e.g. granular sludge), this regime is called discrete settling without flocculation (class I). However, certain suspensions have a natural tendency to flocculation even at low concentrations. In subsequent collisions and cohesion processes, larger flocs are formed, with their settling happening over time. This regime is called discrete settling with flocculation (class II). It is important to note that during the discrete settling with the flocculation, formed flocs still settle at its own characteristic speed. Accordingly, discrete settling without flocculation and discrete settling with flocculation undergo through the same settling dynamics. The difference lies in the fact that, for the discrete settling with flocculation, simultaneously with the settling process, an additional flocculation process occurs, changing the particle properties and hence their settling rate [2].

A transition from discrete settling to hindered settling (class III) occurs if the concentration of solids exceeds the threshold concentration at which the particles no

longer settle independently of each other. This threshold concentration depends on the state of flocculation sludge. For secondary (biological) sludge, the transition usually occurs at concentrations of 600-700 [mgTSS/L], while for the granular sludge limit may increase to 1600-5500 [mgTSS/L] (depending on the granulation state). Above this boundary, each particle is hindered by other particles, and the forces between the particles are strong enough to pull each particle at the same rate, regardless of its size and density. In other words, particles are settling in bulk, as a zone, which is why this regime is called a zone settling.

In this regime, a clear contact surface between the clear supernatant and the particles that are settled is formed. When the solid concentration increases above the critical value (5-10 [g/L]), the settling changes to compression settling (class IV). The exact concentration of the transition once again depends on the particle flocculation condition. At these high concentrations, the solids come into physical contact with each other and are subjected to compression due to the weight of the upper particles. The settling rate will be much lower than in the case of obstructed deposition [3].

3. Methods

To evaluate the performance of the settling tank, it is necessary to quantify the settling characteristics of the sludge, thus flocs. Batch settling experiments are an interesting information source in this respect since they eliminate the hydraulic influences of in and outgoing flows on the settling behaviour. Therefore, several methods aim to determine the settling characteristics of the activated sludge by measuring certain properties during the settling of activated sludge in a batch tank. These measurements range from very simple experiments providing a rough indication of the sample's general settleability to more labour-intensive experiments that measure the specific settling velocity or even determine a relation between the settling velocity and the sludge concentration.

A number of parameters have been developed to obtain a quantitative measure of the settleability of an activated sludge. Sludge settleability is based on the volume that sludge occupies after a fixed period of settling. Among these, the Sludge Volume Index (SVI) is the most known. Number of issues have been reported with the SVI as a measure of sludge settleability of which the most important one is its dependency on the sludge concentration. Particularly at higher concentrations, measured SVI values can deviate significantly between sludge concentrations [1]. Moreover, SVI measurements have been found to be influenced by the dimensions of the settling cylinder. These problems can be significantly reduced by conducting the test under certain prescribed conditions. Hence, number of modifications have been proposed to the standard SVI test in order to yield more consistent information [1], [2]. The SVI test with diluted sludge called the Diluted SVI (DSVI) was proposed. Also, the Stirred Specific Volume Index (SSVI_{3,5}) where the sludge is stirred during settlement was known to provide the most consistent results [4], [5].

3.1 The Sludge Volume Index (SVI)

The Sludge Volume Index (SVI) is defined as the volume (in [mL]) occupied by 1.0 [g] of sludge after 30 minutes of settling in a 1.0 [L] cylinder. After 30 min of settling, the

volume occupied by the sludge in the cylinder (SV₃₀ in [mL]) is read. SVI is calculated according to:

$$SVI = \frac{SV_{30}}{X_{TSS}}$$

where X_{TSS} is the measured concentration of the sample in [g L⁻¹].

3.2 The Diluted Sludge Volume Index (DSVI)

The Diluted Sludge Volume Index (DSVI) differs from the standard SVI by performing an additional dilution step prior to settling. The sludge is diluted with effluent until the settled volume after 30 min is between 150 [ml L⁻¹] and 250 [ml L⁻¹]. The dilutions must be made with effluent where the sludge is obtained to reduce the possibility of foreign substances affecting the settling behaviour.

The advantage of the DSVI lies in its insensitivity to the sludge concentration, allowing for consistent comparison of sludge settleability between different activated sludge plants [6].

3.3 The Stirred Specific Volume Index (SSVI_{3.5})

The Stirred Specific Volume Index (SSVI_{3.5}) was introduced since it was found that stirring the sample during settling reduces wall effects, short circuiting and bridge formation effects, thereby creating conditions more closely related to those prevailing in the sludge blanket in SSTs. The SSVI_{3.5} is determined by performing an SVI test at a specific concentration of 3.5 [ml L⁻¹] while the sludge is gently stirred at a speed of about 1 [rpm]. To determine the SSVI_{3.5}, the sludge concentration is measured with a TSS test and subsequently diluted with effluent to a concentration of 3.5 [ml L⁻¹] in a volume of more than 4 [L].

3.4 The batch settling curve and hindered settling velocity

The sludge settleability parameters presented above provide only a momentary recording of the settling behavior, thus a low level measurement of the general settleability. The volume of a sludge after 30 min of settling will depend on both its hindered settling and compression behaviour, which are both influenced by a number of factors such as the composition of the sludge, floc size distributions, surface properties, rheology, etc. Thus, two different sludge samples with different settling behaviour can result in similar sludge settleability parameters. Detailed information on the settling characteristics of a sludge is obtained from a batch settling curve. Batch settling curve gives information of the settling behaviour of sludge at different settling times. It can be used either to determine, for example seasonal trends in the settling behaviour or to determine the SST capacity limit [1].

In order to measure a batch settling curve, measuring cylinder is filled with a sludge sample. The sludge is allowed to settle and the position of the suspension-liquid interface is measured at different time intervals, Figure 2. The height of the suspension-liquid

interface is recorded at different time intervals giving a curve with the sludge height over time. Standard measurement times for a batch settling curve are 0, 0.5, 1, 2, 3, 4, 5, 10, 15, 20, 30 and 45 min but these can be adapted depending on the settling dynamics of a specific sludge. The suspension-liquid interface is measured more frequently in the beginning as the sludge is settling relatively fast. As the duration of the test increasing, the frequency of the measurements is decreases since the interface is slowing down [7].

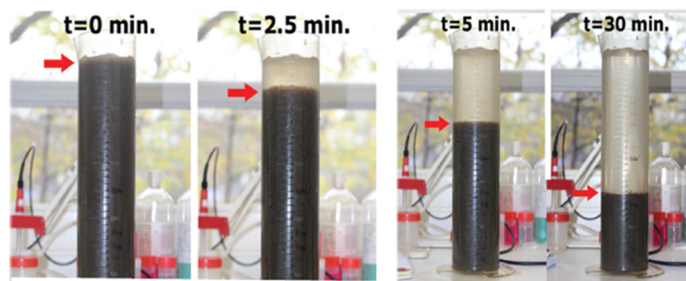


Figure 2. Batch settling at different time intervals with observable suspension-liquid interface [1].

3.5 DSS test

The Dispersed Suspended Solids (DSS) test quantifies sludge's state of flocculation at the moment and location the sample is taken. DSS are defined as the concentration of suspended solids remaining in the supernatant after 30 min of settling. The sample is poured into the container and left for 30 minutes to settle, after which the sample of supernatant is analyzed for TSS. Large, precipitous flocs are precipitated over a period of 30 minutes while dispersed particles, that are not incorporated into the sludge, remain in the supernatant. DSS tests can be performed with samples at several locations in the clarifier (e.g. at the entrance, at the exit from the flocculation chamber or near the effluent overflow) to analyze potential problems (for example flocculation or settling).

3.6 FSS test

A complimentary test to the DSS test is called the Flocculated Suspended Solids (FSS) test. Whereas the FSS test quantifies the flocculation potential of the sludge sample by flocculating the sample under ideal conditions prior to settling. For this test, the sludge sample is collected in a 2 [L] square jar. The sample is mixed with a magnetic stirrer for 30 minutes at 50 [rpm], before it is allowed to settle for an additional 30 minutes, after which the concentration in the supernatant is measured. Mixing increases the flocculation and settling takes place in an ideal conditions (without hydraulic disturbances or vortexing). Since FSS concentration is measured under maximum flocculation and an ideal conditions, its value will not change between reactor and clarifier. For this reason, the sludge sample for FSS can be taken anywhere between the reactor and the clarifier.

4. Results

Two tests with aluminium (Al) and iron (Fe) electrodes were performed on a full-scale batch EC unit made from stainless steel, Figure 3. The unit has two rectangular chambers

(tanks), whose dimensions are 0.80 x 0.55 x 1.10 [m]. In tests 90 [L] of water were used as the operating volume. The first tank is used for electrocoagulation (EC) process, from which water can circulate (by pump) between two rectangular Fe, Al or stainless steel electrode plates, while the second one is used as a settling tank, Figure 4. The total surface of Al electrodes was 0.063 [m²] (2 x 0.98 x 0.032 [m]) and the electrode distance was 0.5 [cm].

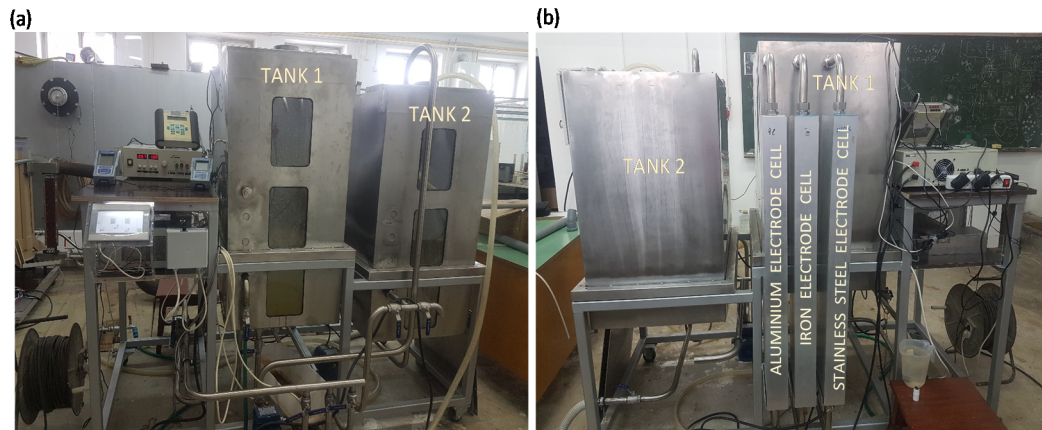


Figure 3. (a) The front and (b) the back of the electrocoagulation unit.

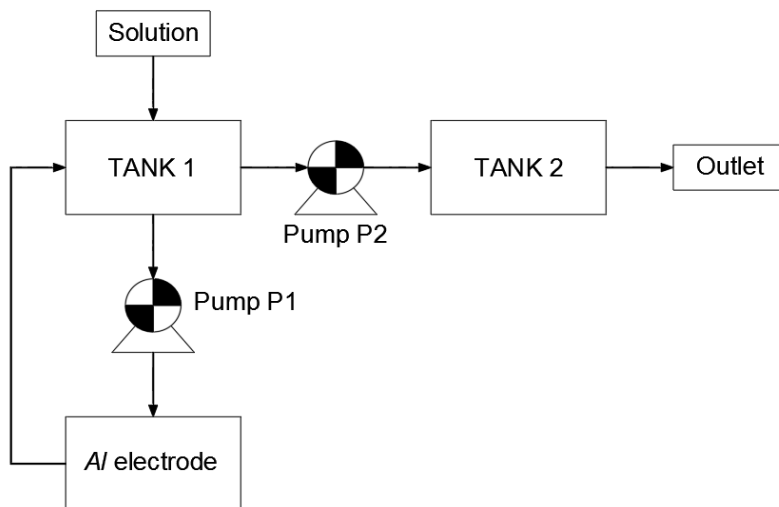


Figure 4. Process scheme of the used EC process

As a contamination, 13 [g] of potassium dihydrogen phosphate (KH₂PO₄) was added to obtain phosphate concentration (PO₄) of 100 [mg/L]. EC efficiency in contamination removal as well as pH, dissolved oxygen (DO) and total dissolved solids TDS were measured during the tests. A total of four set tests, with both electrodes (Al and Fe), were performed with different EC process durations, $t_1 = 60$ [min] and $t_2 = 90$ [min], and different current density ($I_1 = 10$ [A], $I_2 = 5$ [A]). Results of the TSS test with Fe and Al electrode for I_1 , I_2 and t_1 , t_2 are shown in Table 1 and Table 2. The comparison of the TSS tests were given in Figure 5.

Table 1. Measured characteristic parameters during electrocoagulation with Fe electrodes

Sample taken after	Sample volume	Filter mass	Dish mass	Mass of the dish with a wet filter	Mass of the dish with a dry filter	Mass of the dry residue and filter	Mass of the dry residue	X _{TSS}	Voltage	Current
[min]	[l]	[g]	[g]	[g]	[g]	[g]	[g]	[mg/l]	[V]	[A]
15	0,103	0,138	35,288	36,168	35,429	0,141	0,003	29,13	7,1	5
30	0,098	0,137	31,491	32,41	31,637	0,146	0,009	91,84	6,9	5
60	0,099	0,136	27,618	28,612	27,784	0,166	0,03	303,03	6,4	5
90	0,1	0,138	31,136	32,203	31,304	0,168	0,03	300,00	6	5

Sample taken after	Sample volume	Filter mass	Dish mass	Mass of the dish with a wet filter	Mass of the dish with a dry filter	Mass of the dry residue and filter	Mass of the dry residue	X _{TSS}	Voltage	Current
[min]	[l]	[g]	[g]	[g]	[g]	[g]	[g]	[mg/l]	[V]	[A]
15	0,2	0,137	79,998	81,094	80,187	0,189	0,052	260	16,6	10
30	0,1	0,137	54,898	56,288	55,097	0,199	0,062	620	16,4	9,8
60	0,1	0,137	54,8	57,096	55,097	0,297	0,16	1600	16,5	9,9

Table 2. Measured characteristic parameters during electrocoagulation with Al electrodes

Sample taken after	Sample volume	Filter mass	Dish mass	Mass of the dish with a wet filter	Mass of the dish with a dry filter	Mass of the dry residue and filter	Mass of the dry residue	X _{TSS}	Voltage	Current
[min]	[l]	[g]	[g]	[g]	[g]	[g]	[g]	[mg/l]	[V]	[A]
15	0,102	0,137	35,292	36,28	35,431	0,139	0,002	19,61	20	5
30	0,102	0,137	31,494	32,418	31,637	0,143	0,006	58,82	21,4	5
60	0,103	0,137	27,632	28,665	27,779	0,147	0,01	97,09	20	5
90	0,101	0,135	31,086	32,189	31,293	0,207	0,072	712,87	22,7	5

Sample taken after	Sample volume	Filter mass	Dish mass	Mass of the dish with a wet filter	Mass of the dish with a dry filter	Mass of the dry residue and filter	Mass of the dry residue	X _{TSS}	Voltage	Current
[min]	[l]	[g]	[g]	[g]	[g]	[g]	[g]	[mg/l]	[V]	[A]
15	0,14	0,138	35,275	36,438	35,432	0,157	0,019	135,71	60,80	9,60
30	0,081	0,133	31,514	33,06	31,672	0,158	0,025	308,64	60,80	10,00
60	0,075	0,138	27,625	28,77	27,794	0,169	0,031	413,33	60,80	10,00

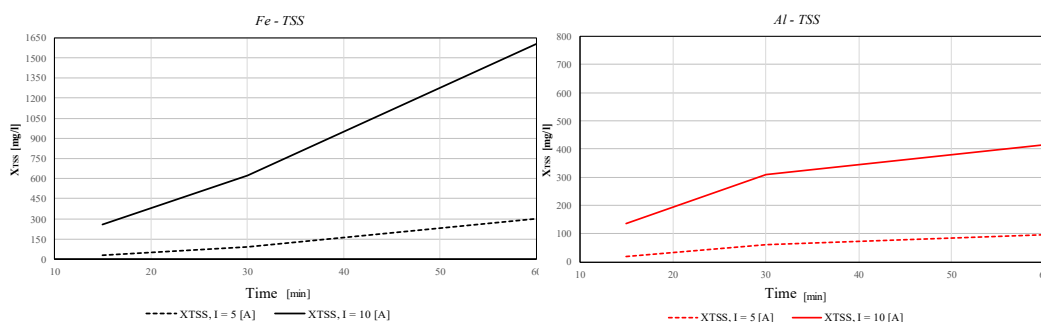


Figure 5. Change of TSS concentration for 60 [min] during electrocoagulation with Fe and Al electrodes

It is seen in Figure 5 that the concentration of suspended solids (XTSS) in the 10 [A] test was significantly different from the same concentration in the 5 [A] current test. After 60 [min] the XTSS is four to five times higher with higher current. It can also be concluded that the Fe electrodes provide three to four times more solids than the Al electrode with the same current. Generally speaking, the sludge obtained with Fe

electrodes has a higher concentration compared to the sludge obtained by the Al electrodes under the same conditions, which means that electrocoagulation by Fe electrodes generates more solids (dissolved electrode mass).

SVI tests are shown in Table 3 (Fe) and Table 4 (Al), while the comparison between electrodes is shown in Figure 6.

Table 3. SVI tests with Fe electrodes ($I = 5$ [A] (90 min); $I = 10$ [A] (60 min))

Uzorak uzet nakon	SVI60	XTSS	SVI	SVI	Uzorak uzet nakon	SVI30	XTSS	SVI	SVI
[min]	[ml/l]	[mg/l]	[ml/mg]	[ml/g]	[min]	[ml/l]	[mg/l]	[ml/mg]	[ml/g]
15	10	29,13	0,34	343,33	15	43	260	0,17	165,38
30	10	91,84	0,11	108,89	30	53	620	0,09	85,48
60	10	303,03	0,03	33,00	60	65	1600	0,04	40,62
90	10	300,00	0,03	33,33					

Table 4. SVI tests with Al electrodes ($I = 5$ [A] (90 min); $I = 10$ [A] (60 min))

Uzorak uzet nakon	SVI30	XTSS	SVI	SVI	Uzorak uzet nakon	SV30	XTSS	SVI	SVI
[min]	[ml/l]	[mg/l]	[ml/mg]	[ml/g]	[min]	[ml/l]	[mg/l]	[ml/mg]	[ml/g]
15	35	19,61	1,79	1785,00	15	70	135,71	0,52	515,79
30	70	58,82	1,19	1190,00	30	106	308,64	0,34	343,44
60	95	97,09	0,98	978,50	60	130	413,33	0,31	314,52
90	113	712,87	0,16	158,51					

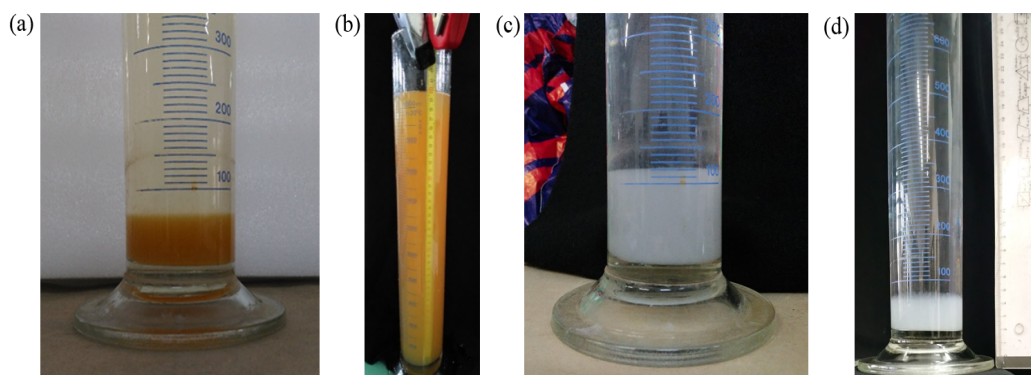


Figure 6. (a) SV30 with Fe electrodes after 30 min, $I = 10$ [A] (b) SV30 with Fe electrodes after 30 min, $I = 5$ [A], (c) SV30 with Al electrodes after 30 min, $I = 10$ [A] (d) SV30 with Al electrodes after 60 min, $I = 5$ [A]

By comparing the results shown above, it can be seen that the sludge obtained by the Al electrode has a significantly higher sludge volume index (SVI) than SVI obtained by the Fe electrodes. This means that such sludge settles more slowly than the one with lower SVI values. Also, by comparing the results for Fe electrodes it can be seen that the 5 [A] test sludge from is settling very slowly, much more slowly than the sludge obtained with the 10 [A].

Figure 6 clearly shows that it was not possible to read the Fe sludge volume after 30 minutes (SV30) in the test with 5 [A] since the sludge was completely dispersed in the measuring cylinder. For that reason SV60 (sludge volume after 60 minutes) was adopted for the calculation of the sludge volumetric index. The flocculation in the 5 [A] test with Fe electrodes happened after 50 minutes when the flocs aggregated and settled. The results of the FSS tests are shown in Table 5 (Fe) and Table 6 (Al).

Table 5. FSS test results with Fe electrodes for I = 5 [A] (90 min) and I = 10 [A] (60 min)

Sample taken after	Sample volume	Filter mass	Dish mass	Mass of the dish with a wet filter	Mass of the dish with a dry filter	Mass of the dry residue	X _{FSS}
[min]	[l]	[g]	[g]	[g]	[g]	[g]	[mg/l]
15	0,101	0,141	25,367	26,182	25,509	0,001	9,90
30	0,076	0,137	20,349	21,159	20,489	0,003	39,47
60	0,101	0,144	15,075	15,193	15,222	0,003	29,70
90	0,100	0,138	24,042	24,885	24,185	0,005	50,00

Sample taken after	Sample volume	Filter mass	Dish mass	Mass of the dish with a wet filter	Mass of the dish with a dry filter	Mass of the dry residue	X _{FSS}
[min]	[l]	[g]	[g]	[g]	[g]	[g]	[mg/l]
15	0,095	0,137	79,988	80,796	80,187	0,062	652,63
30	0,094	0,137	12,084	-	12,230	0,009	95,74
60	0,093	0,137	13,139	-	13,283	0,007	75,27

Table 6. FSS test results with Al electrodes for I = 5 [A] (90 min) and I = 10 [A] (60 min)

Sample taken after	Sample volume	Filter mass	Dish mass	Mass of the dish with a wet filter	Mass of the dish with a dry filter	Mass of the dry residue	X _{FSS}
[min]	[l]	[g]	[g]	[g]	[g]	[g]	[mg/l]
15	0,101	0,137	25,334	26,189	25,483	0,012	118,81
30	0,101	0,132	20,323	21,129	20,461	0,006	59,41
60	0,100	0,134	15,054	15,870	15,190	0,002	20,00
90	0,088	0,141	24,008	24,857	24,153	0,004	45,45

Sample taken after	Sample volume	Filter mass	Dish mass	Mass of the dish with a wet filter	Mass of the dish with a dry filter	Mass of the dry residue	X _{FSS}
[min]	[l]	[g]	[g]	[g]	[g]	[g]	[mg/l]
15	0,098	0,135	25,355	26,241	25,494	0,004	40,82
30	0,084	0,137	20,351	21,250	20,491	0,003	35,71
60	0,108	0,138	15,063	15,939	15,204	0,003	27,78

Comparison of the FSS test results for both electrodes is shown in Figure 7.

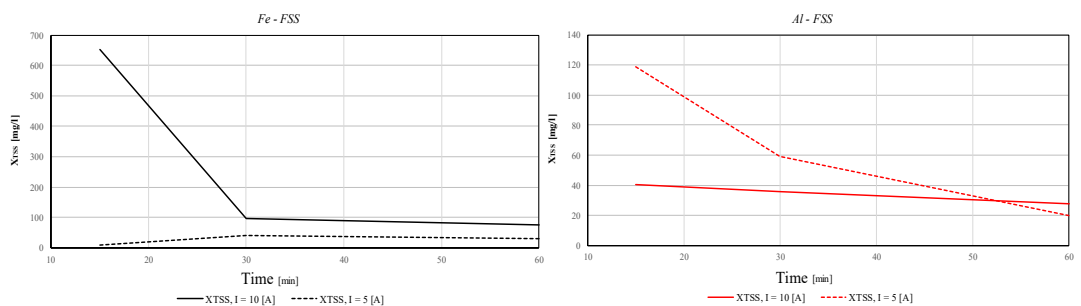


Figure 7. Concentration change of flocculated suspended matter for t = 60 [min] during electrocoagulation with Fe and Al electrodes for current 10 [A] and 5 [A]

The results show that a 15-minute sample of sludge obtained by Fe electrode yields significant deviation, most probably due to the excited sludge during the sampling. Generally, it can be concluded that the sludge obtained by the Fe electrodes with a current of 10 [A] has a higher solids concentration (dissolved mass) than when 5 [A] current is applied. Also, in all the tests, the FSS decreases, meaning that the smaller flocs are aggregated and settled during the process time. The results of the DSS test are shown in Table 7 (Fe) and Table 8 (Al), while the comparison of the results is shown in Figure 8.

Table 7. DSS test results with Fe electrodes for I = 5 [A] (90 min) and I = 10 [A] (60 min)

Sample taken after	Sample volume	Filter mass	Dish mass	Mass of the dish with a wet filter	Mass of the dish with a dry filter	Mass of the dry residue	X_{DSS}
[min]	[l]	[g]	[g]	[g]	[g]	[g]	[mg/l]
15	0,097	0,136	21,809	22,637	21,946	0,001	10,31
30	0,099	0,137	21,605	22,418	21,746	0,004	40,40
60	0,100	0,135	20,442	21,322	20,580	0,003	30,00
90	0,099	0,140	15,207	16,134	15,353	0,006	60,61

Sample taken after	Sample volume	Filter mass	Dish mass	Mass of the dish with a wet filter	Mass of the dish with a dry filter	Mass of the dry residue	X_{DSS}
[min]	[l]	[g]	[g]	[g]	[g]	[g]	[mg/l]
15	0,100	0,137	54,899	55,693	55,097	0,061	610,00
30	0,125	0,137	12,332		12,479	0,01	80,00
60	0,125	0,137	6,759	7,616	6,907	0,011	88,00

It can be concluded that the sludge obtained from Al electrodes has significantly lower concentrations of dissolved suspended solids, that is, that flocs are better aggregated and settled. In a 15-minute sample of Fe electrodes, there is also a significant deviation due to the excited sludge during the sampling.

In the batch settling test an increased reading frequency is required compared to the standard test in which the reading intervals 5, 10 and 15 minutes are too long since all flocs are, after agglomerated, settled in a very short time. Thus, a noticeable change is observed on the suspension-liquid interface. This is particularly obvious in the tests with Al and Fe electrodes with 10 [A]. In the Fe electrodes test with 5 [A], an extremely low settling was observed, whereby the flocs were remaining in a suspension even after 90 min.

Table 8. DSS test results with Al electrodes for I = 5 [A] (90 min) and I = 10 [A] (60 min)

Sample taken after	Sample volume	Filter mass	Dish mass	Mass of the dish with a wet filter	Mass of the dish with a dry filter	Mass of the dry residue	X_{DSS}
[min]	[l]	[g]	[g]	[g]	[g]	[g]	[mg/l]
15	0,103	0,137	21,801	22,634	21,940	0,002	19,42
30	0,100	0,137	21,601	22,420	21,740	0,002	20,00
60	0,100	0,137	20,414	21,279	20,559	0,008	80,00
90	0,100	0,132	15,186	16,000	15,323	0,005	50,00

Sample taken after	Sample volume	Filter mass	Dish mass	Mass of the dish with a wet filter	Mass of the dish with a dry filter	Mass of the dry residue	X_{DSS}
[min]	[l]	[g]	[g]	[g]	[g]	[g]	[mg/l]
15	0,076	0,135	21,795	22,672	21,936	0,006	78,95
30	0,118	0,136	21,609	22,516	21,750	0,005	42,37
60	0,108	0,137	20,434	21,382	20,575	0,004	37,04

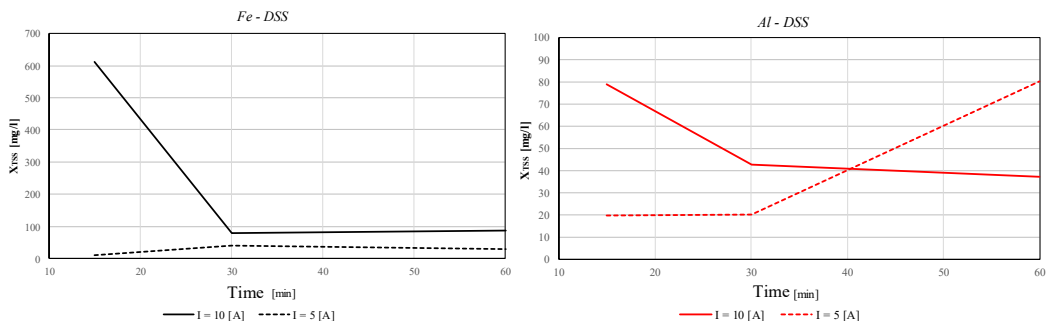


Figure 8. Concentration change of dissolved suspended solids for $t = 60$ [min] during electrocoagulation with Fe and Al electrodes for current 10 [A] and 5 [A]

After readings, the batch settling curves were created and the settling velocity was calculated. The hindered settling velocity is calculated by determining the steepest slope among the three consecutive data points, thus from the slope of the tangent at the steepest part of the batch settling curve. Figure 9 shows the hindered settling velocity for the Al and Fe electrodes. It can be concluded that the sludge obtained from Al electrodes has a significantly higher settling speed compared to the sludge obtained from Fe electrodes.

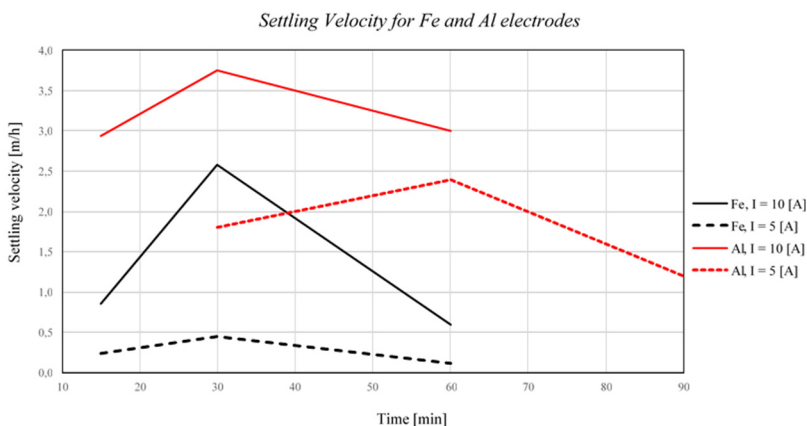


Figure 9. Settling velocities for Fe and Al electrodes

5. Conclusion

The settling characteristics were analyzed by settling tests usually used for biological active sludge testing. During the tests, it was not possible to make a DSVI test and $SVI_{3,5}$

due to the low initial sludge concentration. Therefore, the $SVI_{13.5}$ settling test is probably not applicable to electrocoagulated sludge, because electrocoagulation results in significantly less sludge than by biological process. However, further testing should be carried out so that the conclusion could be more precisely formulated.

In the batch settling test pre-defined intervals can not be used for the suspension-liquid interface reading because the differences between readings are too long. It takes about 10 minutes for flocculation to take place after the sample is poured since flocs are disturbed after the pouring. After that 10 minutes all flocs are settled in a very short time (approx. after 20 minutes in total). This makes intervals of 5, 10 of 15 minutes much too long and does not provide a realistic settling characterization. Therefore, it is necessary to increase the reading frequency for every minute.

Also, in the case of an electrocoagulant sludge, it is difficult to determine the exact suspension-liquid interface i.e. the exact position of the contact surface. Thus, as an interface boundary, a horizontal line is taken below which the apparent settling was observed. The interface boundary could not be established because flocculation and aggregation is taking place throughout the test and larger flocs (not disturbed by the sample pouring) precipitates in the first 20 minutes, while it takes more time for suspended smaller flocs to aggregate and settle.

This results with a new and pronounced settling in the upper zone again, but somewhat slower this time. The conclusion regarding the batch settling curve test is that a settling velocity depends largely on the way how the sample is poured into the measuring jar. Thus, a test should be designed to eliminate this perceived deficiency.

References:

- [1] Mark C. M. van Loosdrecht, Per H. Nielsen, Carlos M. Lopez-Vazquez, Damir Brdjanovic (2016), *Experimental Methods in Wastewater Treatment*, IWA Publishing
- [2] Meunier N(1), Drogui P, Montané C, Hausler R, Mercier G, Blais JF. (2006) Comparison between electrocoagulation and chemical precipitation for metals removal from acidic soil leachate, *Journal of Hazardous Materials*, 137, 1, 581-590, DOI: 10.1016/j.jhazmat.2006.02.050
- [3] De Clercq, J., Nopens, I., Defrancq, J., Vanrolleghem, P.A., (2008). Extending and calibrating a mechanistic hindered and compression settling model for activated sludge using in-depth batch experiments. *Water Res.* 42: 781-791.
- [4] Ekama, G.A., Wilsenach, J.A. and Chen, G.-H. (2010). Some opportunities and challenges for urban wastewater treatment. In: 7th IWA LET conference, Arizona, USA, June 2-4 (keynote presentation), Retrieved in September 2015 from <http://repository.ust.hk/ir/Record/1783.1-16616>
- [5] American Public Health Association (APHA), American Water Works Association (AWWA), and Water Environment Federation (WEF) (2012). *Standard Methods for the Examination of Water and Wastewater*, 22nd Edition. New York. USA.
- [6] Dammal, E.E., Schroeder, E.D., (1991). Density of activated sludge solids. *Scanning*. 25: 841-846.
- [7] Chancelier, J., Chebbo, G., Lucas-Aiguier, E., (1998). Estimation of settling velocities. *Water Res.* 32: 3461-3471.

REMOVAL OF PHOSPHATES FROM WASTEWATER BY ELECTROCOAGULATION

IVAN HALKIJEVIĆ¹, GORAN LONCAR², DINO DIZDAR³

¹ Faculty of Civil Engineering, University of Zagreb, Croatia, halkijevic@grad.hr

² Faculty of Civil Engineering, University of Zagreb, Croatia, gloncar@grad.hr

³ Via Factum, Ltd., Croatia, dino.dizdar94@gmail.com

1. Abstract

The effect of the electrocoagulation process with aluminum (Al) and iron (Fe) electrodes on phosphate reduction from wastewater is presented. The effect was observed in a reactor volume of 90 [L]. Several tests were done with the varying current density and the duration of the process, while the flow rate through the electrodes was maintained constant ($Q = 0.3$ [L/s]).

Initial phosphate concentration of 100 [mg/L PO_4^{3-}] was applied in all tests. Phosphate concentrations are estimated with indicator strips ranging from 0 to 100 [mg/L] in order to monitor the performance of the reactor. 160 [g] of sodium chloride (NaCl) was added to gain more conductivity of the solution. In addition to phosphate concentration, electrical conductivity, pH, total dissolved solids, NaCl concentration, dissolved oxygen concentration and temperature after 15, 30 and 60 minutes were also measured.

It was concluded that aluminum electrodes are better in removing phosphates. After 30 minutes of the electrocoagulation process the phosphate concentration was four times less with Al electrodes. The temperature increased throughout the process as well as the amount of dissolved solids. The concentration of dissolved oxygen was constantly reducing as well as the electrical conductivity which was initially increased by the addition of NaCl. The process with Fe electrodes resulted in slightly more dissolved oxygen, but less total dissolved solids. In addition, the paper also presents the overview of the basic process parameters. The operational costs of the tests, including the cost of materials (electrodes) and operating costs of electricity, were also analyzed.

Keywords: phosphate removal, electrocoagulation, operating costs

2. Introduction

Wastewater treatment procedures must be further developed due to growing effluent and receiving water bodies requirements so that the excessive pollution of water bodies is omitted. Chemical coagulation and flocculation are usually the most frequently used methods for raw and wastewater treatment. Their main function is to improve the separation of particles during sedimentation and subsequently filtration. The most common types of pollutants to be eliminated are nutrients, especially nitrogen and phosphorus, toxic heavy metals and organic matter. The most commonly used

coagulants are aluminum and iron salts such as sulfate and chloride. These salts in water depend on its chemical properties, e.g. pH. Metal cations and hydroxides destabilize colloidal pollutants particles by reducing the repulsive force between the particles which allows their aggregation [1].

Electrochemical water treatment is increasingly analysed and used, particularly in cases of highly polluted water due to the good efficiency / cost ratio. The most commonly used methods are electro-oxidation, electrocoagulation and electrode disinfection. Various types of wastewaters can be treated by these methods which gives them greater importance to research and development [2]. However, researches on the possibility for household wastewater treatment with a large-scale application and case studies are scarce.

Electrocoagulation is an unconventional method of wastewater treatment usually by using metal electrodes and direct current. It connects electrochemical processes with conventional chemical coagulation. Compared to conventional methods, electrocoagulation provides a relatively compact and robust alternative to wastewater treatment by which sacrificial anodes initiate electrochemical reactions that provide active metal cations for coagulation and hydrogen for flocculation. An important advantage of electrocoagulation is that no additional coagulants (chemicals) need to be added, so the salinity of wastewater after treatment does not necessarily have to be changed. Hence, electrocoagulation is a complex process that involves the removal of many pollutants, thus many chemical reactions simultaneously [3].

However, some of the electrocoagulation disadvantages are the electricity costs that may be significant; possible passivation of anode due to the oxygen presence and the deposition on the cathodes; the electrodes need to be regularly replaced; the high conductivity of the wastewater is required; depending on the electrode material, high ion concentrations need to be removed from the water; in some cases, the gelatinous hydroxides may be dissolved in water; it is not effective for the removal of the soluble substances such as ammonia, sugar, organic acids, solvents, phenols, alcohol and similar. In the case of the presence of chlorine carcinogenic chlorinated hydrocarbons are generated [1], [2], [3], [4]. Also, the focus of the relevant research is usually limited on the small-scale batch reactors.

This paper analyzes the possibilities of removing pollutants from the wastewater in the form of phosphate (PO_4) and the possibility of obtaining the continuity of the process through the continuous type of the electrocoagulation reactor.

3. Methods

3.1 Electrocoagulation

Electrocoagulation is used to remove pollution from highly contaminated wastewater by use of electricity and sacrificing electrodes. Electrocoagulation is usually used for water and wastewater treatment. It includes coagulation and precipitation of pollutants by the "in situ" coagulant production. Direct current is usually applied, while the use of electrodes and its material and setup depends on the wastewater pollution and the required effluent quality. Usually, several electrodes of the same material are used to

form an electrode cell.

In the electrocoagulation reactor, the water/wastewater flows between electrodes while the direct current is applied to them. The choice of the electrode material and their arrangement depends on the type of the present contaminants and the required quality of treated water. Usually, aluminium (Al) is used for the drinking water treatment and iron (Fe) for the wastewater treatment. Aluminium and iron are relatively cheap and, compared to the other metals, such as titan and silver, easily available, non-toxic and proven effective [4], [5].

When the current is applied, metal hydroxides are produced in the reaction between either Al^{3+} or Fe^{2+} ions, created in electrolytic oxidation of Al or Fe electrodes, and OH^- ions from a reduction reaction taking place on the cathode where hydrogen gas is also released according to [6]:

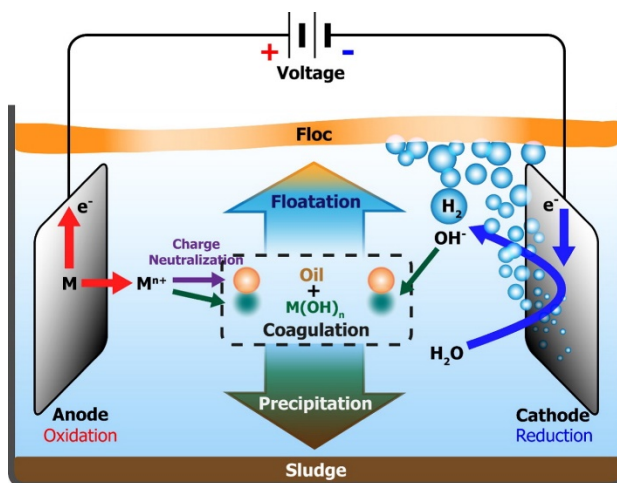
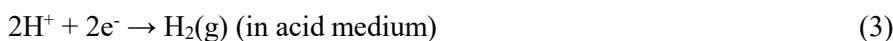
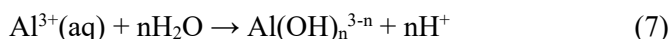
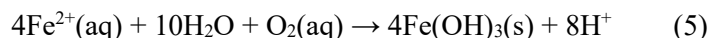


Figure 1. Electrochemical process in water treatment [6]

Metal hydroxides, used in the precipitation process, are produced according to the equations below [47]:



Depending on the pH of wastewater and the oxidation potential, Fe can form divalent or trivalent cations, but Al is only formed as trivalent cation. These hydroxides trap colloidal particles and create flocs which can be easily removed from water by sedimentation or flotation [7]. The evolution of hydrogen bubbles leads to an increase in

pH and it also helps flocculated particles to float out of the water [7].

The amount of generated floats depends primarily on the material and mass of the electrode, duration of the reactor operation and the density of the current. Faraday's law defines the ratio of the current density I and the electrolytically generated mass m :

$$m = \varphi \frac{It}{zF} M \quad (8)$$

where: m weight of the generated metal material [g], t duration [h], I current density [A], M molecular mass of the electrode material [g/mol], z number of the transferred electrons (2 za Fe^{2+} ili 3 za Fe^{3+}), F Faraday constant (96 487 [C/mol]), φ correction coefficient of electrolytic dissociation efficiency. It is noted that the efficiency of dissociation under low pH values can be greater than 100 %, thus greater than specified by the Faraday law (8).

There are various parameters affecting the efficiency of electrocoagulation process for wastewater treatment [8], [9]:

- the material of the electrode may be iron, aluminum or some inert material (usually a cathode),
- pH value of the solution has an effect on the formation of new metal hydroxides in the solution and the ζ -potential of the colloid,
- the current density is proportional to the amount of electrochemical reactions occurring on the surface of the electrode,
- the duration of the process, or the added electric charge per unit volume, is proportional to the number of coagulants generated by electrocoagulation and / or other reactions in the reactor,
- electrode potential defines which reactions will occur on the electrode surface,
- concentration of pollutants affects the efficiency of removal because coagulation does not follow the kinetics of the first order reaction but the kinetics of the pseudo-second order.
- anion concentration, such as sulfate or fluoride, affects the hydroxide composition because it can replace the hydroxide ion in the soil,
- temperature influences the formation of flocs, reaction rate and conductivity. Depending on the type of contamination, the temperature may have a positive or negative influence on the removal efficiency,
- other parameters, such as hydrodynamic conditions and spacing between electrodes, have the impact on the efficiency of the process and the consumption of electricity. However, these parameters are not thoroughly studied.

3.2 Experimental tests

Experimental tests of the phosphate removal efficiency were performed on the pilot electrocoagulation pilot device at the Faculty of Civil Engineering, University of Zagreb. The photo of the device is shown in Figure 2 and its operational scheme is shown in Figure 3.

The device has two tanks whose dimensions are 0.8 x 0.55 x 1.10 [m]. The first tank is used as a reactor for the electrocoagulation process, where the water circulates through

rectangular iron, aluminum or stainless electrodes (2 electrodes for each material), while the other tank is used for settling. The electrode surface is $0.063 \text{ [m}^2\text{]}$ ($0.98 \times 0.032 \text{ [m]}$) and the distance between the electrode is 0.5 [cm] for aluminum and iron, while the distance for the stainless steel electrode is 0.24 [cm] . Concentrations of PO_4^{3-} have been estimated by the Quanto Fix Phosphate indicator tests by Macherey-Nagel for the range of $0\text{-}100 \text{ [mg/L]}$. Flow was measured by an ultrasonic flow meter FLUXUS F601 (by Flexim). Multisond CyberScan PCD 650 (by Eutech) was used water temperature, pH (resolution and accuracy: 0.001 pH , $\pm 0.002 \text{ pH}$) and dissolved oxygen concentration (resolution and accuracy: 0.01 mg / l , $\pm 0.2 \text{ mg / l}$) measurements. The current was controlled by a laboratory power supply with maximum power of 900 [W] (MC Power LBN-1990) and the output current range from 0 to 60 [A] .



Figure 2. Electrocoagulation pilot device installed at the Faculty of Civil Engineering (University of Zagreb) (left - front of the device, right - back of the device)

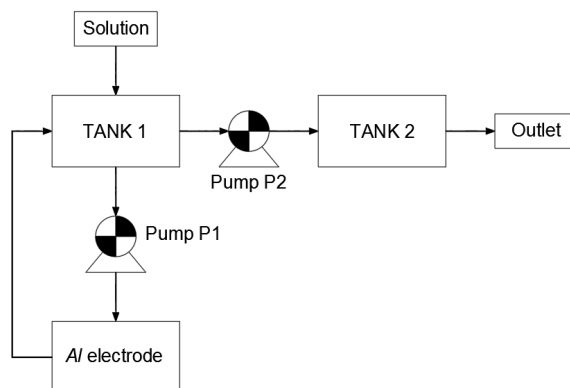


Figure 3. Schematic view of the pilot electrocoagulation reactor

The entire treatment process is divided into several phases. In the first phase, the first tank is filled with a volume of 90 [l] . Then pump P1 is turned on so that water is constantly pumped with flow rate $0,3 \text{ [l/s]}$ from tank 1 through the electrodes. After that 13 [g] of monopotassium phosphate (KH_2PO_4) was added to obtain phosphate

concentration (PO_4) of 100 [mg/l]. The tests were carried out with iron and aluminum electrodes. The total duration of the electrocoagulation process was 1 [h]. For iron electrodes, the current of 10 [A] was set, while the voltage varied in time (16.6 to 17.4 [V]). For aluminum electrodes, the current of 10 [A] was obtained after 30 minutes (initially it was 7.5 [A]), while the voltage varied from 59.1 to 60.8 [V]. For the purpose of improving conductivity, 160 [g] of sodium chloride (NaCl) was added. Electrical conductivity, pH value, total dissolved solids (TDS), NaCl concentration, dissolved oxygen (DO) concentration, temperature and PO_4 concentration were measured in both tests.

4. Results and discussion

Samples were taken after 15, 30, 45 and 60 minutes. The results for the tests with iron electrodes are shown in Figures 4, 5 and Table 1, while the results for aluminum electrodes are shown in Figures 6, 7 and Table 2.

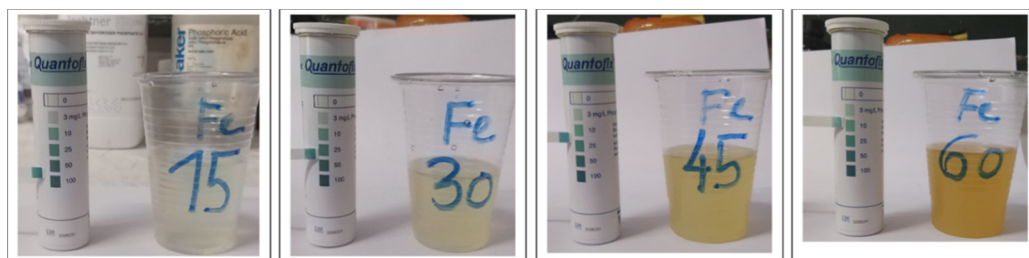


Figure 4. Indicator strips for phosphate concentration after 15, 30, 45, 60, 75 and 90 minutes Fe electrodes

Table 1. Measured characteristic parameters during electrocoagulation with Fe electrodes.

Time	Q	pH	Conductivity	TDS	NaCl	DO	DO	T	PO_4^-	Voltage	Current
[min]	[l/s]	[1]	[mS]	[ppt]	[ppt]	[%]	[mg/l]	[°C]	[mg/l]	[V]	[A]
0 (Drinking Water)	0.3	6.14	0.708	0.302	0.296	76.6	8.79	9.2	-		
0 (NaCl)		6.67	3.594	1.653	1.771	83.3	9.41	10.1	-		
0		7.19	3.981	1.918	2.059	86	9.39	11	100	16.6	10
15		7.15	3.946	2.184	2.345	86.9	9.05	13.2	65	16.4	9.8
30		7.3	3.905	2.335	2.525	86.9	8.72	14.7	30		
45		7.46	3.87	2.453	2.66	85.1	8.38	15.7	-	17.4	9.9
60		7.61	3.847	2.619	2.833	63.2	6.08	17	5		

Figure 4. shows that iron electrodes produce flocs with poor settling characteristics, resulting with increased turbidity. It took about 16 to 24 hours for generated flocs to settle down and to produce obvious supernatant.

Also, the temperature increases throughout the process, which is logical because the electrodes emit the heat through the use of electricity. This, however, shows that the electrocoagulation process use (or lose) most of the input energy for water heating. This also indicates the shortcoming of the process, thus it indicates that some other materials,

which are more reactive, could be used.

The amount of dissolved solids is slightly increased as well as the amount of NaCl, which is caused by the partial dissolution of the electrode and the electrolyte addition. After the addition of salt and potassium monophosphate, the amount of dissolved oxygen is constantly reduced, as well as the electrical conductivity which is initially increased by the addition of NaCl.

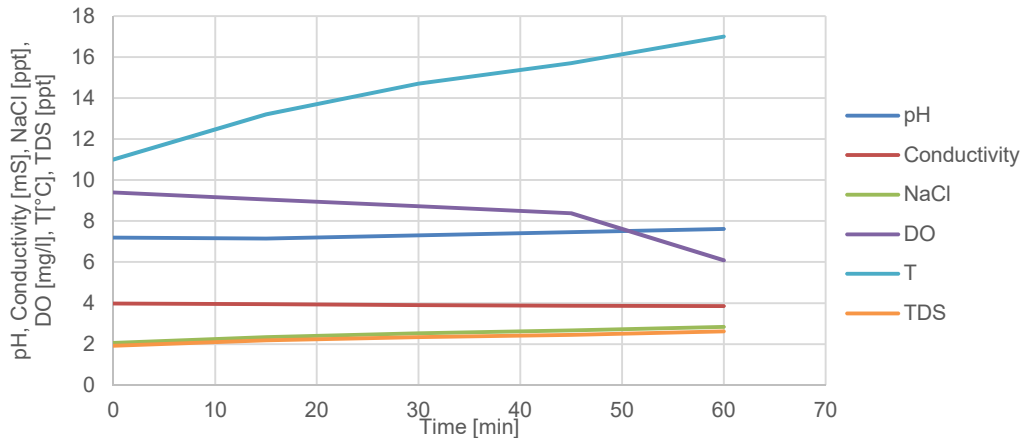


Figure 5. Change of characteristic parameters during electrocoagulation with Fe electrodes

Tests showed that aluminum electrodes produce flocs with good settling characteristics. It took about 15 to 25 minutes for generated flocs to settle down and to produce obvious supernatant, Figure 6, inferring that aluminum electrodes should be used if the continuity of the process is to be achieved. This is the reason why the removal of phosphate is also considerably faster with aluminum electrodes, Table 2.

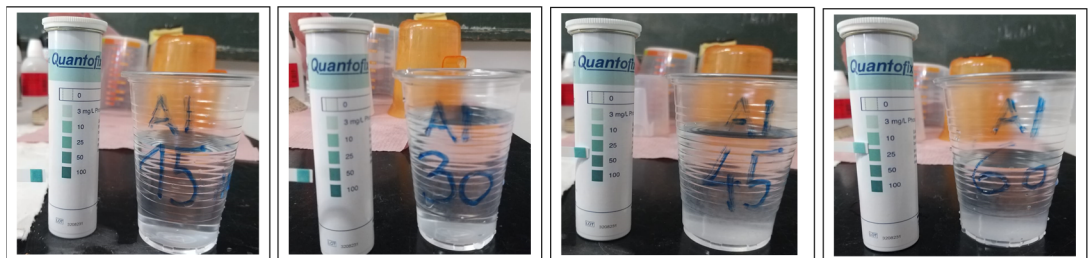


Figure 6. Indicator strips for phosphate concentration after 15, 30, 45, 60, 75 and 90 minutes Al electrodes

Table 2. Measured characteristic parameters during electrocoagulation with Al electrodes

Time	Q	pH	Conductivity	TDS	NaCl	DO	DO	T	PO ₄ ⁻	Voltage	Current
[min]	[l/s]	[l]	[mS]	[ppt]	[ppt]	[%]	[mg/l]	[°C]	[mg/l]	[V]	[A]
0 (Drinking Water)	0.3	6.62	0.694	0.284	0.279	53.30	6.19	8.80			
0 (NaCl)		6.90	3.695	1.628	1.735	73.10	8.32	9.40			

0		6.90	4.069	1.877	2.010	82.00	9.16	10.20	100	60.8	7.5
15		6.78	3.996	2.159	2.318	80.00	8.40	12.50	30	60.8	9.6
30		6.94	3.932	2.448	2.650	77.00	7.68	15.50	8	60.8	10.0
45		7.24	3.882	2.829	3.081	73.90	6.92	18.60		59.1	10.0
60		7.51	3.845	3.170	3.458	71.50	6.35	21.00	3	60.8	10.0

It can be seen that the third of the initial concentration is achieved already after 15 minutes with aluminum electrodes, while the same concentration with iron electrodes is achieved after 30 minutes. Other process parameters with aluminum electrodes show very similar results with iron electrodes.

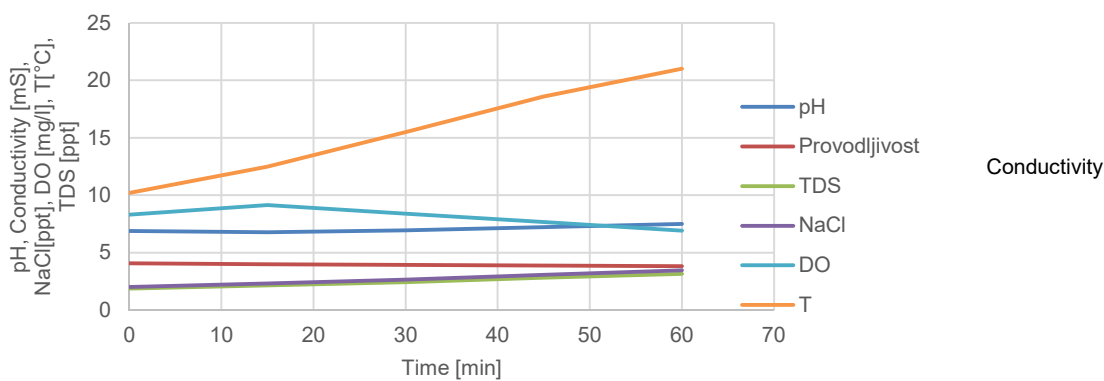


Figure 6. Change of characteristic parameters during electrocoagulation with Al electrodes

According to the results, it can be concluded that aluminum electrodes are better in removing phosphate contamination. When comparing the iron and aluminum electrodes, there is a noticeable similarity in the change of all process parameters except conductivity. Iron electrodes have slightly more dissolved oxygen, but less total dissolved particles. There is also a slight increase in the temperature of aluminum electrodes, probably due to the much higher voltage required to achieve the value of 10 [A] (aluminum proved to be susceptible for lime scale generation thus generation higher electrical resistance). Alkaline electrodes also generate somewhat more NaCl, but phosphate concentrations are removed at the rate of 2 [mg/L] for an hour.

An assessment of the operational costs of the tests are given regarding material (electrodes) cost and the cost of electricity according to:

$$\text{Operational costs} = a C_{\text{energy}} + b C_{\text{material}} \quad (9)$$

where: C_{energy} is electrical energy cost of 1 m³ of treated water [kWh m⁻³] and C_{material} (kg Al m⁻³, kg Fe m⁻³) is the costs of the electrode material used in 1 m³ of the treated water. With the average electricity price of 0.13 Eur/kWh⁻¹ (according to the national tariff models), and the average market price of aluminum given as 1.54 EUR kg⁻¹ and 0.07 EUR/kg⁻¹ for iron. The electricity cost (kWh m⁻³) is calculated according to the following expression:

$$C_{energija} = \frac{U \times I \times t}{V} \quad (10)$$

where: U is the power supply voltage (V), I is the power supply current (A), t the duration of the electrocoagulation process (s), V is the effective volume of the reactor (m^3).

The consumption of electrode material (kg/m^3) is determined according to Faraday's law:

$$C_{elektroda} = \frac{I \times t \times M_w}{z \times F \times V} \quad (11)$$

where M_w is molecular mass ($26.98 \text{ [g mol}^{-1}]$ for Al, $55.85 \text{ [g mol}^{-1}]$ for Fe), z number of electrons transferred ($z = 3$ for Al; $z = 2$ for Fe), F Faraday constant ($96487 \text{ [C mol}^{-1}]$).

Due to the process parameters values used in the tests, as well as the electricity consumption, number of electrodes in the reactor (two electrodes), operational tank volume ($V = 0.09 \text{ m}^3$), mass of electrodes used to generate metal ions and the cost of the electrodes material, operational costs are given in Table 3.

Table 3. Operational costs for energy and materials in conducted tests ($t = 60 \text{ min}$; 2 electrodes)

Electrode	U	I	a	C_{energy}	b	$C_{\text{electrode}}$	Operational Costs
	V	A	EUR/kWh	kWh/ m^3	EUR/kg	kg/ m^3	EUR/ m^3
Al	60	10	0.13	6.7	1.54	0.07	0.96
Fe	16.8	10	0.13	1.9	0.07	0.23	0.25

As the operating reactor volume was 90 [L] and the flow rate was 0.3 [L/s] , it took 5 [min] for the entire volume of the reactor to pass through the electrodes. Since complete removal of contamination is achieved after 60 [min] , it took 12 cycles for the total volume to pass through the electrodes. One can conclude that it is possible to increase the current density 12 times so that water contamination is removed in a single passage of through the electrodes with a sufficient number of metal ions. However, this cannot be done because it has been found that there is an upper current density limit after which the additional increase in current density does not generate additional metal ions.

Therefore, the continuity of the process, at this stage of the development and application in wastewater treatment, is in increased number of reactors/electrodes. If the same reactor had six electrodes instead of two, assuming the same efficiency (the same amount of electrode mass, thus the same coagulant production) it would require 20 minutes in total for the complete removal of contamination. In that case it would take four reactors ($4 \times 90 \text{ [L]}$) connected in series (4 cycles per 5 minutes) for achieving the continuity of the whole treatment process. In that case estimated operating costs are given in Table 4.

It can be seen that operating costs are only 1.22 time higher in average if four reactors with six electrodes are used. However, this assumes the same cost of pumping. In reality slightly higher pumping costs can be expected due to the greater hydraulic losses of water passing between the greater number of electrodes.

Table 4. Operational costs for energy and materials in case with 4 identical reactor tanks ($t = 20 \text{ min}$; 6 electrodes)

Electrode	U	I	a	C _{energy}	b	C _{electrode}	Operational Costs	Operational Costs (4 Reactors)
	V	A	EUR /kWh	kWh/m ³	EUR /kg	kg/m ³	EUR /m ³	EUR /m ³
Al	60	10	0.13	2.2	1.54	0.07	0.21	0.84
Fe	16.8	10	0.13	0.6	0.07	0.23	0.16	0.64

5. Conclusion

Electrocoagulation is relatively simple, adaptable, effective and environmentally friendly (depends on the composition of wastewater due to a possible carcinogens byproduct) process that removes various pollutants, which can also be, depending on the contamination, more economical than conventional treatment. In general, electrocoagulation achieves a high rate of COD and BOD removal, color removal and is faster in eliminating the contamination than conventional coagulation.

Compared to the application of some disinfection methods, such as UV or ozone, it may be considerably cheaper. Biological treatment of wastewater has certain limitation in the treatment of wastewater, while electrocoagulation can handle highly toxic waters with any initial pH value. Further exploration of this method will not only improve its performance, but develop a new modeling technologies that can be used to accurately describe the entire process.

In practice, current density is the primary process parameter that, together with the conductivity, affects the design of the electrocoagulation reactor, which means that the reactor design has to be robust. The design is fairly complex because it includes the geometry of the electrode cell, reactor tanks and hydraulics, which can affect the current density distribution, settling or flotation and ultimately the contamination removal efficiency.

This method can also be used as a pre-treatment in a biological wastewater treatment if the water contains some toxic contaminants. The main disadvantage of this method is the lack of understanding of certain reactions within the process itself. There is no methodology that can simultaneously address the removal of pollution, settling/flotation, technological or economic optimization or scale-up effects. Thus, this is the direction in which electrocoagulation should be developed.

As it was shown metal ions and hydroxides produced by iron electrodes are less effective in the process of colloid destabilization because iron electrodes release more soluble and less charged Fe (II) compounds. Iron electrodes can be more effective in some special applications such as the removal of sulfides and heavy metals. An additional disadvantage of the method is the difficulty of achieving the continuity of the process. The continuity necessary if this method pretends to replace the conventional wastewater treatment process. Higher concentrations of pollutants require longer process duration, increased current density and volume of the reactor to ensure sufficient time for effective

coagulation, settling and flocculation.

References:

- [1] Vepsäläinen, M. (2012) Electrocoagulation in the treatment of industrial waters and wastewaters, doctoral thesis, Retrieved from VTT technical research centre of Finland ltd.
- [2] Ensano, B.M.B., Borea, L., Naddeo, V., Belgiorno, V., de Luna, M.D.G. and Ballestros Jr., F.C. (2017) Removal of pharmaceuticals from wastewater by intermittent electrocoagulation. *Water*, Vol. 9, No. 85, 1-15
- [3] Marriaga-Cabarales, N. and Machuca- Martínez, F. (2014) Fundamentals of electrocoagulation. Evaluation of Electrochemical Reactors as a New Way to Environmental Protection, Editors: Peralta-Hernández, J.M., Rodrigo-Rodrigo M.A. and Martínez-Huitle, C.A., 1-16
- [4] Hakizimana, J.N., Gourich, B., Chafi, M., Stiriba, Y., Vial, C., Drogui, P. and Naja, J. (2017) Electrocoagulation process in water treatment: A review of electrocoagulation modeling approaches. *Desalination*, Vol. 404, No. 1, 1-21
- [5] Moussa, D.T., El-Naas, M. H., Nasser, M. and Al-Marri, M. J. (2017) A comprehensive review of electrocoagulation for water treatment: Potentials and challenges. *Journal of Environmental Management*, 186, 1, 24-41
- [6] Chunjiang An, Gordon Huang, Yao Yao, Shan Zhao (2017) Emerging usage of electrocoagulation technology for oil removal from wastewater: A review, *Science of The Total Environment*, 579, p 537-556, <https://doi.org/10.1016/j.scitotenv.2016.11.062>.
- [7] Shammas, N.K., Pouet, M., Grasmick, A. (2010) *Wastewater Treatment by Electrocoagulation–Flotation*. Flotation Technology, Wang, L., Eds.; Springer: New York, NY, USA, 199-220
- [8] Kuokkanen, V., Kuokkanen, T., Rämö, J. and Lassi, U. (2013) Recent Applications of Electrocoagulation in Treatment of Water and Wastewater - A Review. *Green and Sustainable Chemistry*, Vol. 81, No. 1, 89-121
- [9] Naje, A.S., Abbas, S.A. (2013) Electrocoagulation Technology in Wastewater Treatment: A Review of Methods and Applications. *Civil and Environmental Research*, Vol.3, No.11, 29-4

DETERMINATION OF THE POPULATION EQUIVALENT AND THE REQUIREMENT OF WATER IN THE EXISTING WATER SUPPLY SYSTEMS AS INPUT PARAMETERS FOR HYDRAULIC ANALYSIS, A CASE STUDY ON THE WATER SUPPLY SYSTEM FOR THE TOWN OF GOSTIVAR

GOCE TASESKI ¹

¹*Ss. Cyril and Methodius University Faculty of Civil Engineering – Skopje, taseski@gf.ukim.edu.mk*

1. Abstract

The number of inhabitants including the specific water demand for one inhabited place is a primary input parameter in the hydraulic analysis of a water supply system, i.e. the optimal dimensioning of the water supply systems depends on the accurate assessment of these two parameters.

This paper, through various methods for determining the population growth in the future, i.e. the future number of inhabitants and the specific water demand, shall give a recommendation for selecting the optimal method for their assessment, from which accurate values for the required quantities would be obtained, which would be used as input parameters for the hydraulic analysis of water supply systems. As a case study for the analysis, the Water Supply System of Gostivar was selected.

Keywords: inhabitants, specific water demand, hydraulic model, population growth, water supply

2. Introduction

The basic function of the majority of water supply systems in the underdeveloped countries is to primarily provide water in sufficient quantities and of satisfactory quality for the population, while the remaining users, such as the light industry, livestock, public buildings, etc. usually have lower water demand compared to the water demand for the population. Therefore, in the determination of realistic quantities of water in one water supply system in the underdeveloped countries where the population is the most significant user, an accurate projection of the population that will use the services of the water supply system in its exploitation period should be made - for the following 30 years. In addition, the specific water demand for all the users of the system should be defined, and by that the total net quantity of water demand for water supply to be determined [1].

The aim of this paper is, through the analysis of several methods for determining the population growth, a more accurate projection about the future number of inhabitants in an existing water supply system to be made as much as possible, and that is the water supply system of the town of Gostivar in North Macedonia.

It is well known that the number of inhabitants and the specific water demand in households are primary input parameters in dimensioning the water supply systems. The value of the specific consumption of water in households is taken from the experience with similar systems in the surrounding region, while for the number of inhabitants within the period of exploitation a projection should be made so that the result will be as close as possible to the actual one, i.e. such population growth should be selected that an optimally dimensioned system for the entire period of exploitation would be obtained [1].

3. Forecast / assessment of the number of inhabitants

The term for the number of inhabitants in the water supply system, in the broadest sense means determination of the future demographic development on the basis of assumptions which in the moment of their application may be or may not be probable. Very often, the term projection is identified with the term forecast, although there is a significant difference between them. The projection of the population shows how much the future population growth would be on the basis of the assumptions which are probable for the entire period of the analysis, while the forecast is based only on assumptions which are probable at the time of beginning the analysis. This means that the projection of the population includes the forecast, but also has an aim to present what will happen with the analysis if some assumptions that might occur in the future are different from the initial ones.

Regarding the fact that there is no available relevant data on the current number of inhabitants for the considered water supply system, as population census has not been carried out in the Republic of North Macedonia since the year 2002, in this case a forecast of the population in accordance with the following sources of data has been performed:

- Data source 1: Strategy for demographic development of the Republic of North Macedonia. Methodology used in this method is accorded with the extrapolation of the future forecast about the population on the basis of values of growth taken from the Strategy for Development of the Republic of North Macedonia for the period from 2008 - 2015, where the growth is anticipated to amount to 0.38% for the whole territory of the Republic of Macedonia [2].
- Data source 2: Data from Population Census in the past. In this method, historic rates of population growth are used according to relevant statistical data from the past which have been obtained by population census. By the analysis of this data, the average population growth has been obtained, from 1981 → 2002 which amounts to 1.4%, and this growth is used for obtaining the number of inhabitants in the system exploitation period 2002 → 2015 and 2015 → 2050 [3].
- Data source 3: General Urban Plan of Gostivar. In this methodology, the population growth rates are used as defined by the General Urban Plan for Gostivar (adopted in the year 2005) and the Detailed Urban Plan for the town of Gostivar and its surrounding, where the town of Gostivar is divided into several different blocks, i.e. for the town centre, for the the outskirts and for the villages,

where for each block the population growth rate is different and ranges within the limits from 1.3% to 2% [3,4].

Figure 1 below shows a graph of obtained values on the number of inhabitants for the town of Gostivar about the three analyzed data sources.

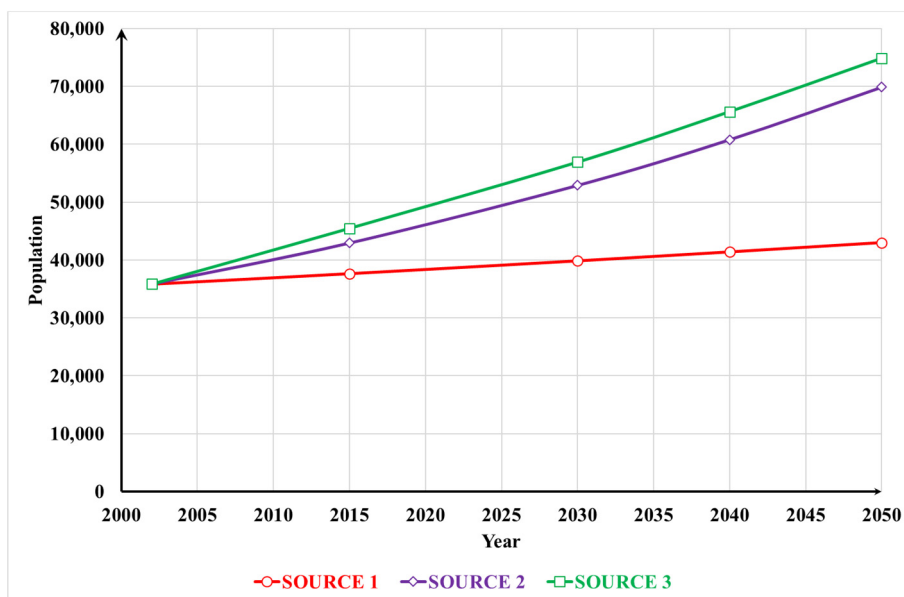


Figure 1. Number of inhabitants for the town Gostivar

From the data obtained, it can be concluded that:

In source data 1, the projection of the growth solely for the town of Gostivar is substantially lower than the actual one, and according to that, this Methodology should not be used for the water supply system of Gostivar.

Data source 2 represents a solid ground regarding the fact that the average population growth in the past 35 years is expected to be similar to the growth in the following 30 years. However, the fact that for the last 17 years there has not been any relevant statistical data on the population in the town of Gostivar, this Methodology has also high probability of an error, and also, the Methodology applied in this manner refers to the entire town, while for the hydraulic analysis of the water supply systems it is important to have data on the population per sectors, both in the town centre and on the outskirts, i.e. with this method the population growth is the same for all the parts of the town, which is different in reality. This method can be used only for some preliminary analyses, whereas it is not recommendable for more precise analyses.

The method with data source 3 is considered as the best one since the assessments are closest to the actual ones and the big advantage with this method is obtaining information on the number of inhabitants per sectors – blocks, both in the central area and on the outskirts. However, close consideration should be taken here for the high rates of growth, especially in the central area, which are expected to decrease in the future since there will be saturation of the space.

According to the previously stated, in the following analyses for determination of the

required realistic quantities of water supply, the third Methodology was used in this paper, for which detailed calculations on the number of inhabitants are given below.

4. Assessment of the number of equivalent inhabitants

4.1 Equivalent populations for the Town of Gostivar

By applying the Methodology for assessment of the population for the town of Gostivar based on the General Urban Plan in order to make classification of the sectors, a separation into four types of blocks has been made as follows:

- Type 1: Central town area, which includes blocks of flats, shopping centers, public buildings and administrative buildings;
- Type 2: Near outskirts, which consists of collective and individual buildings, commercial buildings, which is considered as a zone with possible intensive population growth;
- Type 3: Outskirts, consisting of household buildings;
- Type 4: Remote outskirts, in which only the industry is located.

For all the blocks defined in this way, by using data from the General Urban Plan, the population growth is determined, which is presented in the following table:

Table 1. Population Growth per Blocks for the Town of Gostivar

Block Type	2015 [%]	2015-2020 [%]	2020-2030 [%]	2030-2040 [%]	2040-2050 [%]
1	1.7	2.0	1.4	1.2	1.0
2	1.7	1.8	1.6	1.4	1.0
3	1.7	1.4	1.4	1.4	1.4
4	1.7	0	0	0	0

Whereas the number of inhabitants is determined with the following formula:

$$P=r*(Y-Y_0)*P_0+P_0$$

Where:

P – estimated number of inhabitants

R – growth [%]

Y – year with a number of inhabitants P

Y₀ – year with a number of inhabitants P₀

P₀ – reference number of inhabitants

For the purpose of obtaining more precise results in separating the population in blocks, there has been a separation performed within the blocks into buildings and houses, where it is anticipated that the density of buildings is three times larger than the density in the individual houses. From the results obtained, especially in the centre (Type 1), it can be noticed that the population density is very high (about 85 inhab./ha), and therefore, the density for this type will be reducing in the future, while on the outskirts the situation is opposite and increase in the population density is expected. The results of the analysis

performed in this manner are presented in figures 2 and 3 as follows:

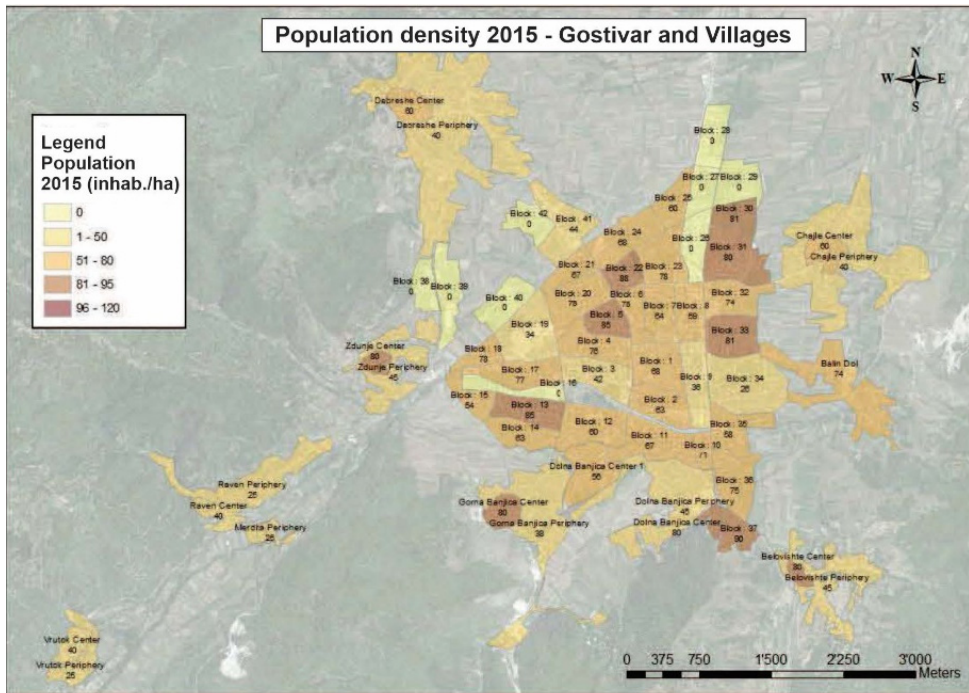


Figure 2. Population Density in 2015 for Gostivar and Villages

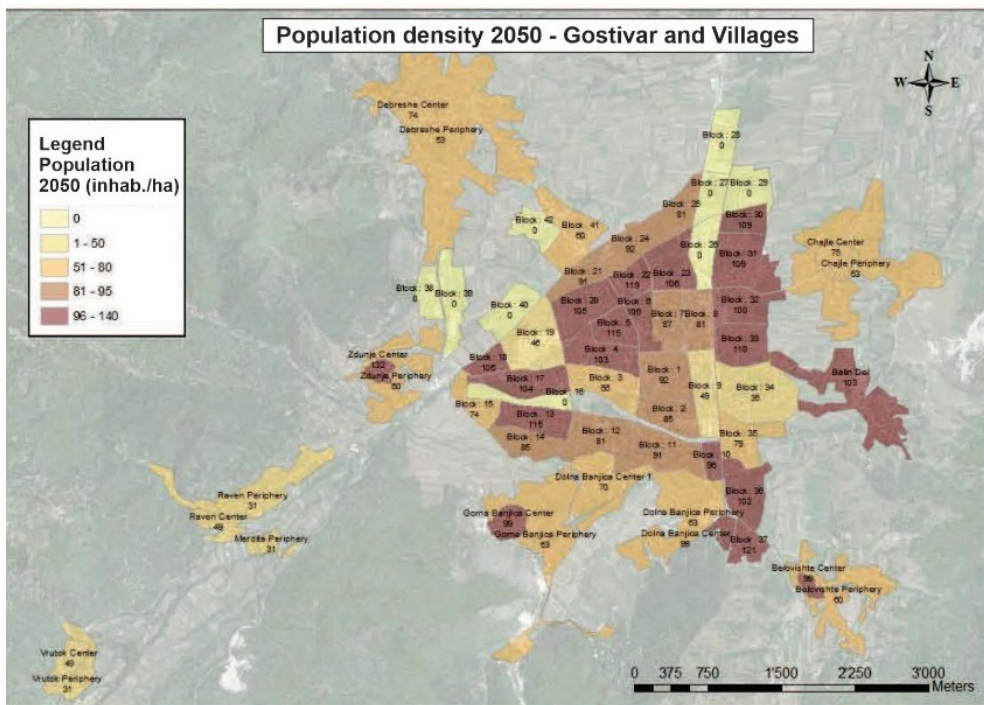


Figure 3. Population Density in 2050 for Gostivar and Villages

4.2 Equivalent populations for the Villages

In the villages, the estimation of the population growth is different from the town of Gostivar as there is no General Urban Plan made for the villages, i.e. the classical method is used for the villages based on using satellite photos in order to define the population density according to the houses for each area, thus identifying three types of villages:

- Type 1: small villages far from the town and with small development in the future,
- Type 2: villages of medium size, with expected development in the future, and
- Type 3: large villages near the town with expected big development in the following years.

Population density values and the expected growth are given in the following table:

Table 2. Population Density and Growth in the Villages

	Density [inhab./ha]		Growth [%]	
	Centre	Outskirts	Centre	Outskirts
Type 1	40	25	0.80	0.9
Type 2	60	40	0.90	1.2
Type 3	80	45	0.90	1.4

5. Net water demand

5.1 Net water demand for the Town of Gostivar

The total water demand for the town of Gostivar consists of the requirements of water for the households, collective demand and the industrial demands, where the water demand for the households are estimated to amount to:

- 110 l/d/PE. for the inhabitants living in buildings, and
- 130 l/d/PE. for the inhabitants living in houses

Since there was no available data on the collective water demand consisting of the public institutions and commercial buildings, this consumption of water has been estimated to amount to 20% of the water requirements for the households.

Regarding the water demand for the industry, also there has not been any available relevant data on the requirements since in this moment there are no larger factories in the town of Gostivar and it is estimated as daily requirements for the area of the industrial complex and amounts to 10 m³/day/ha.

5.2 Net water demand for the Villages

The water demand for the villages consists of the water demand for the households which is estimated to amount to 130 l/d/PE., the collective requirements which are estimated to amount to 10% of the requirements of water for the households and for the livestock which are estimated to amount to 30 l/day per head of cattle and amounts to 5 l/day per head of small animals.

According to the previous, the total net requirements of water are presented in the following graph, figure 4.

In the previous figure, there is a graphic presentation of the total net requirements of

water for the entire water supply system of Gostivar while the losses of water which can be of technical or administrative origin have not been analyzed in this paper since in the models of hydraulic analysis of the water supply systems the losses of water represent a separate input parameter which does not depend on the net required quantities of water.

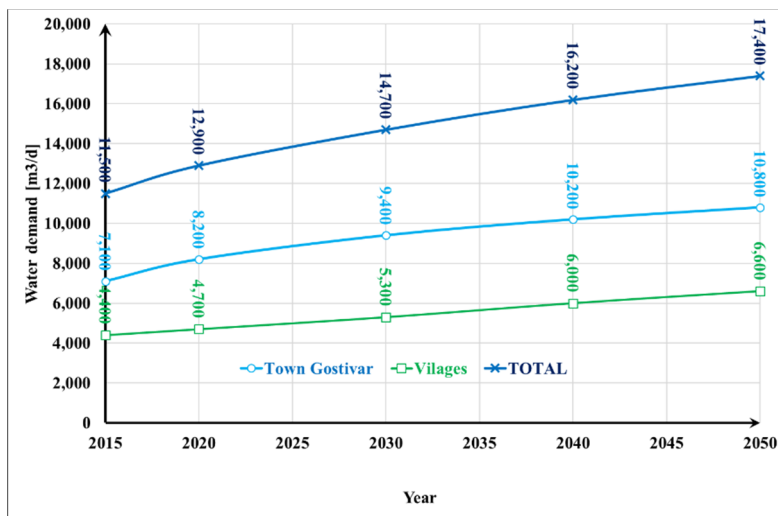


Figure 4. Net water demand

6. Conclusions

From the performed analyses in this paper, it can be concluded that determination of realistic required quantities of water in one water supply system is best to be carried out through relevant – accurate data, and in this case it is the General and the Detailed Urban Plan. This manner of analysis is also significant from the aspect of distribution of the total of required water quantities per junction of the future hydraulic model which is well known to be dependent on the population density per areas, i.e. on the number of inhabitants in the urban blocks.

While using this Methodology, attention should be specially paid on the assessment of the future population growth, especially in the central town areas where satiation of the space is expected in the future, while on the nearby outskirts increase in the population growth should be expected.

As the most significant conclusion, we can say that if we had relevant statistical data from censuses carried out in at least every 10 years, the method of using the growth in the past in that case would also be acceptable for solid assessment of the future number of inhabitants for one water supply system.

References:

- [1] EPD Guidance Document, Method for determining future water demand needs for public/private water systems, 2007
- [2] Strategy for demographic development of the Republic of North Macedonia, 2008
- [3] Detail Urban Plan for town Gostivar, 2015

- [4] Agthe, D.E., R.B. Billings, J.L. Dobra, and K. Raffiee. "A Simultaneous Equation Demand Model for Block Rates." *Water Resources Research* 22(1):1–4., 1986
- [5] State Statistical Office of Republic North Macedonia, 2015
- [6] SGI Ingenierie SA, Master plan for water supply system of town Gostivar, 2015.
- [7] C. Nauges, D. Whittington "Estimation of Water Demand in Developing Countries: An Overview" Published by Oxford University Press on behalf of the International Bank for Reconstruction and Development / THE WORLD BANK. November 11, 2009 25:263–294
- [8] Z. Veljanovski ; „Water supply“, 2008.

EFFICIENCY OF ELECTROCHEMICAL PROCESSES IN REMOVAL OF AMONIUM FROM URINE

DRAŽEN VOUK¹, GORAN LONČAR², ANTONELA MUSA³, MATEO PANDŽIĆ⁴, ANTE VEKIĆ⁵, MORANA DRUŠKOVIĆ⁶, ANĐELINA BUBALO⁷, ROBERT KOLLAR⁸

1 Faculty of Civil Engineering in Zagreb, Croatia, dvouk@grad.hr

2 Faculty of Civil Engineering in Zagreb, Croatia, gloncar@grad.hr

3 Faculty of Civil Engineering in Zagreb, Croatia, antonela.musa33@gmail.com

4 Faculty of Civil Engineering in Zagreb, Croatia, pandzicmateo94@gmail.com

5 Faculty of Civil Engineering in Zagreb, Croatia, avekic92@gmail.com

6 Dok-Ing Energo d.o.o, Zagreb, Croatia, morana.druskovic@gmail.com

7 Dok-Ing Energo d.o.o, Zagreb, Croatia, andjelina.bubalo@gmail.com

8 Robert Kollar, Zagreb, Croatia, robert.kollar@zg.t-com.hr

1. Summary

Electrochemical wastewater treatment technologies have been more often applied in practice, and it has been shown that the combination of electrocoagulation with advanced oxidation processes enhance the treatment efficiency. Apart from being economically viable, it must also be ecologically acceptable in order that treated water could be disposed of into the environment or reused.

This research examined the efficiency of advanced electrochemical process with combination of advanced oxidation process and electrocoagulation in urine wastewater treatment, primarily considering ammonia removal. Three electrodes of different materials were used in this research: stainless steel, aluminium and iron. The power and voltage of the electricity were regulated by a laboratory power supply unit. The results confirmed the high ammonia removal efficiency and thus possibility and justification of applying electrochemical processes for yellow (urine) wastewater treatment.

Keywords: wastewater, treatment, electrochemical processes, advanced oxidation processes, electrocoagulation, ammonia, urine.

2. Introduction

Electrochemical wastewater treatment technologies have been more often applied in practice. It has been shown that the combination of electrocoagulation with electrochemical advanced oxidation processes enhance the treatment efficiency, with relatively low investment costs as well as operation and maintenance costs.

Electrochemical wastewater treatment technologies are: electrocoagulation, electroflotation, electrochemical oxidation, electrochemical reduction, etc.

The aim of this research is to determine the efficiency of advanced electrochemical wastewater treatment processes (HEP), respectively a combination of advanced oxidation processes and electrocoagulation in urine wastewater treatment, primarily considering ammonia removal. Results of the conducted research have shown the potential of creating an innovative, modular, portable electrocoagulation (EC)

wastewater treatment. Furthermore, research have also shown the possibility of making separators/sedimentation units which ensure efficient sludge removal, which is generated as a by-product of treatment, all adapted to the treatment of yellow wastewater. In that case, the results of the research will be the guidelines for designing future EC wastewater treatment plants (WWTP), that are not limited to individual and internal sewage systems. In addition to this, by successful treatment, beside reusing treated water for different purposes (such as flushing the toilets, green watering, irrigation, washing streets, etc.), the primary aim is to protect natural water systems and all water-dependent systems, as well as protect groundwater and surface water bodies. The aim is to achieve a satisfactory treatment efficiency, up to the maximum allowed concentration of ammonia in the treated water prior to reusing or disposing it into the environment. Based on the state of the art in the field of wastewater treatment, EC and advanced oxidation processes (AOPs) have shown high efficiency for the treatment of different types of wastewater [1,2,3,5,10]. EC implies the creation of a coagulant by using an electric field and sacrificial electrodes in order to extract, aggregate and deposit pollutants of suspended particles and dissolved substances from wastewater. In addition to this, the method has been known since the end of the 19th century, however, application in municipal wastewater treatment has been explored just for the last 30 years, where researches on pilot plants and case studies with process optimization are lacking in relation to the specific composition of sanitary wastewater. Compared to conventional treatment processes, electrochemical processes generate 50% to 90% less sludge and results in high quality of treated wastewater [8,11]. In order to obtain more credible results that would contribute to the possible commercialization of the method, it is necessary to perform a significantly larger number of tests on pilot plants with raw wastewater, particularly with the actual characteristics of wastewater. Additionally, as larger hydraulic loadings require adequate space capacity at the WWTP, there is a need to shorten the sedimentation process of coagulated and flocculated sludge particles after the end of the EC operation. Therefore, this research also investigated different types of sedimentation processes for efficient removal of generated sludge, within the analyzed HEP.

3. Methods

Laboratory testing and water conditioning were done at the hydrotechnical laboratory of the Faculty of Civil Engineering, University of Zagreb. The HEP pilot treatment plant consists of several parts: 3 electrodes and 900 W laboratory power supply unit (MC Power LBN 1990) with a current range of 0-60A. Each part represents one of three electrodes made of different materials: stainless steel (inox), aluminium and iron (Figure 1.), and are attached to a laboratory power supply unit.

Moreover, a 5-liter sample is injected into plastic containers of a certain volume in which the electrodes are placed (Figure 2.). Tests were performed on pure urine (collected at the student toilet at the Faculty of Civil Engineering, University of Zagreb), synthetic urine (the sample contains a certain amount of NH_4^+ initial concentration of 100 mg/l) and dilute urine (water mixed with a small amount of pure urine). Since testing was carried out in plastic containers, it was not possible to achieve a constant flowrate, however, because of the small number of samples at each experiment, the flow was simulated by constant mixing.

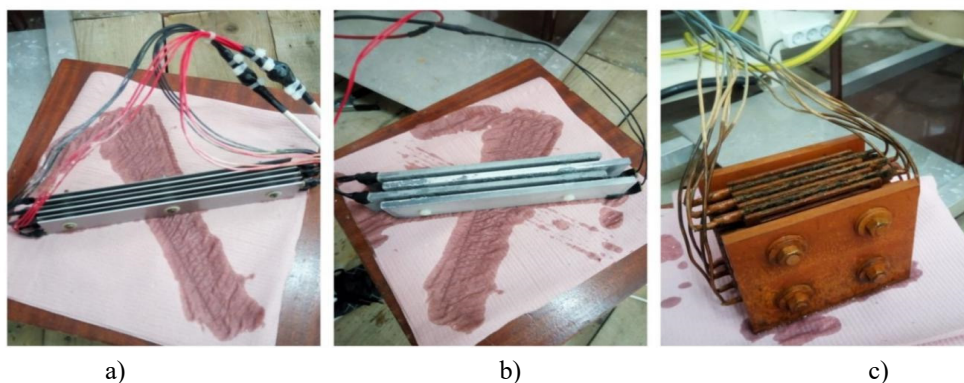


Figure 1. Electrode design: a) stainless steel/inox, b) aluminium, c) iron electrodes

Each of the procedures started with the reaction of stainless steel electrode, which actually presents a part of the research related to advanced oxidation processes. The stainless steel electrode promotes oxidation and allows the removal of ammonia to the maximum, while Al and Fe electrodes allow the formation of flocculants, as a part of the electrocoagulation process. Therefore, the process generated certain amount of sludge. After finished cycle on the stainless steel electrode in duration of 5, 10, 15, 20 or 60 minutes respectively, depending on the experiment, in the same sample, a Fe or Al electrode was set in duration of 2, 5, 7.5 or 30 minutes, where the first phase is conducted with Fe electrode and afterwards Al electrode (in the cases with serial testing). The first sample was taken at the beginning of the experiment on raw wastewater. Furthermore, NH_4^+ , PO_4^{3-} , pH, electrical conductivity, dissolved oxygen, temperature and COD were determined.



Figure 2. Electrodes in operation in 5-liter volumes in plastic containers

Subsequently, the stainless steel electrode was put into operation and at the end of that phase, a new sample was taken. In the case of a 60-minute test on a stainless steel electrode, the samples were taken every 10 minutes and the same parameters were examined except the COD which is re-measured upon completion of the whole experiment. In the second phase, the process took place on the Al or Fe electrode and at the end of that phase the sample was taken again. If the retention time of these electrodes was 30 minutes, then sampling was performed every 10 minutes. For the determination of concentrations: NH_4^+ (mg/l), PO_4^{3-} (mg/l), H_2O_2 (mg/l), CrO_4^{2-} (mg/l), $\text{Fe}^{2+/3+}$ (mg/l), Al^{3+}) the tracer indicators were used (Figure 3).

The NANOCOLOR 500D (Eutech manufacturer) (Figure 4.) photometric accuracy \pm

1%, was used to measure the concentration of NH_4^+ , COD and total dissolved nitrogen.

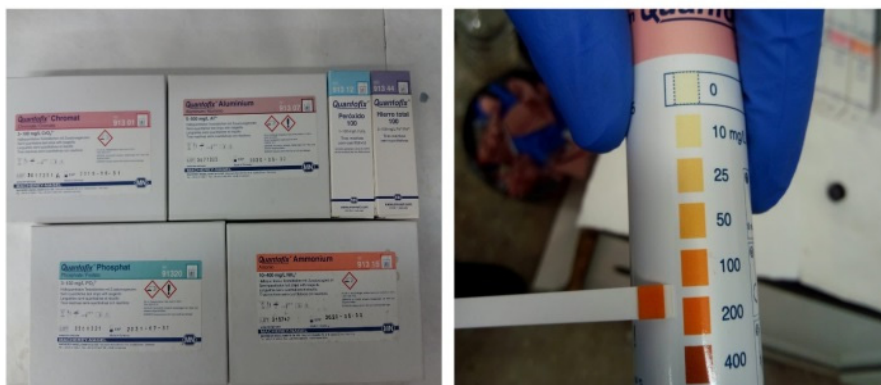


Figure 3. Tracer indicator for concentration measurement: NH_4^+ , PO_4^{3-} , H_2O_2 , CrO_4^{2-} , $\text{Fe}^{2+}/3^+$ Al^{3+} .

At the end of each experiment, generated sludge was observed. Sludge was observed in cylindrical pots with volumes of 1 liter. Two methods of sludge sedimentation were analysed: vertical sedimentation as in regular sedimentation units and sedimentation in lamella separators with lamella positioned at an angle of 45° . Sedimentation with lamella separators positioned at different angle allows the sludge flocs to touch the wall of the lamellas in a much shorter time and then sludge flocs easily slide to the bottom of the cylinder (separator), thereby proving that the sedimentation time is shortened. The sedimentation time is an important element in the dimensioning of sedimentation unit. Shorter sedimentation time results in a reduction of sedimentation unit volume and in the end reduce investment costs. However, in some tests, certain amounts of sludge flocs tend to separate at the water surface, but after some time breaks down to the bottom of sedimentation unit. Levels of separated sludge at the bottom of the sedimentation unit were recorded after 5, 10, 20 and 30 minutes of sedimentation process.



Figure 4. Photometric device NANOCOLOR 500D with samples after measurement

4. Results and discussion

4.1 Experiments made with single and in serial connected electrodes

In this research, the experiments were made with single and in serial connected reactions of electrodes, with the purpose of finding the most efficient combination in maximum ammonium removal from urine wastewater. Wastewater treatment begins with stainless steel electrode, which represents advanced oxidation process, and then is being subjected to the treatment with Fe and Al electrodes, which represents electrocoagulation processes. The purpose of using stainless steel electrode through this advanced electrochemical process is wastewater enrichment with oxygen that causes lowering in COD. Unlike advanced oxidation processes, electrocoagulation in wastewater treatment improves sedimentation. The main difference between experiments made with single electrodes and those connected in series is in fact that serial connected electrodes result in lower volume of generated sludge. Single electrodes have been divided by current intensity ($I=5, 10, 20$ A), and by the reaction time ($t=15, 22.5, 27.5$ minutes). Inlet concentration of ammonium in experiments with single electrodes was 50 mg/l. In serial connected electrodes, measurements were divided by reaction time with stainless steel electrode ($t<20$ minutes and $t=60$ minutes). Current intensity was $I=5-20$ A, and inlet concentrations of ammonium were 50-100 mg/l. Measurements have shown that maximum ammonium removal was achieved by using stainless steel electrode. One of the reasons is advanced oxidation process. Particulate matter of nitrogen is bound to oxygen and evaporate into the atmosphere. The tables below show the highest efficiency in ammonium removal in single electrode experiment number 5, with overall reaction time of 22.5 minutes and current intensity of 10 A. Stainless steel (inox) and iron electrodes have been used throughout that experiment and the efficiency of ammonium removal has been 80% of initial concentration of 50 mg/l. 40% of ammonium has been removed using stainless steel electrode, and the same amount has been removed using iron electrode afterwards.

	Retention time [min]				Electricity [A]		Retention time t [min]			Electricity[A]	Inlet concentration NH_4^+ [mg/L]
	Inox + Fe	Inox+Al						INOX	Fe		
						Experiment 10	10	5	5	10	100
						Experiment 11	15	5	5	10	100
Experiment 1	10	5	10	5	5	Experiment 12	5	5	5	10	100
Experiment 2	15	7.5	15	7.5	5	Experiment 13	5	5	5	15	100
Experiment 3	20	7.5	20	7.5	5	Experiment 14	10	10	10	10	100
Experiment 4	10	5	10	5	10	Experiment 15	10	10	10	10	100
Experiment 5	15	7.5	15	7.5	10	Experiment 16	20	10	10	10	50
Experiment 6	20	7.5	20	7.5	10	Experiment 17	20	10	10	10	50
Experiment 7	10	5	10	5	20	Experiment 18	60	5	5	10	50
Experiment 8	15	7.5	15	7.5	20	Experiment 19	60	5	5	20	50
Experiment 9	20	7.5	20	7.5	20	Experiment 20	60	20	5	20	100

Figure 5. Components of experiment

In experiments with reaction of different electrodes in serial connection, experiment number 20 has shown the highest efficiency in ammonium removal with retention time of 70 minutes, current intensity of 10 A and initial concentration of 100 mg/l of ammonium.

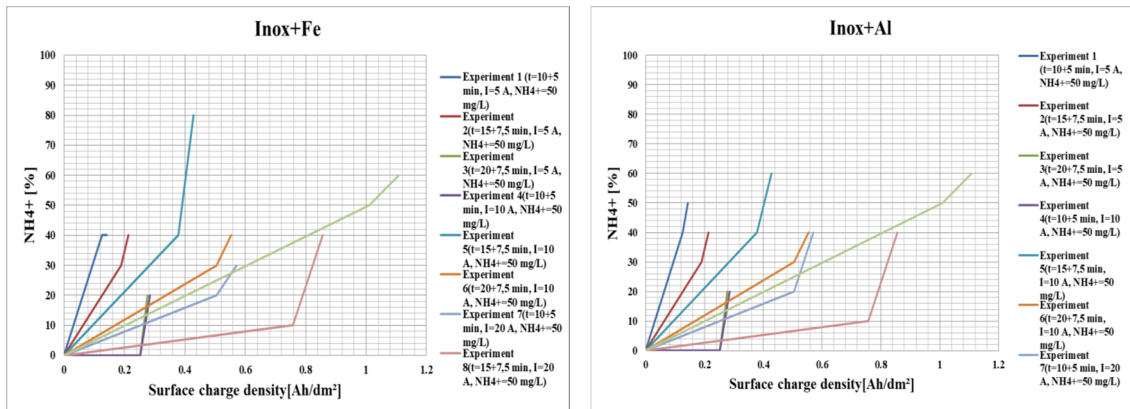


Figure 6. Efficiency of ammonium removal for reaction of single Fe or Al electrodes, connected in serial with previous reaction with stainless steel electrode

After this process, treated wastewater had good sedimentation characteristics and the turbidity of treated water was quite low. Efficiency of ammonium removal, after using stainless steel electrode, had been 50% of initial concentration. Formed sludge flocs were big in size and visible, and because of their weight they separate easily at the bottom of cylindrical pots and formed thickened sludge.

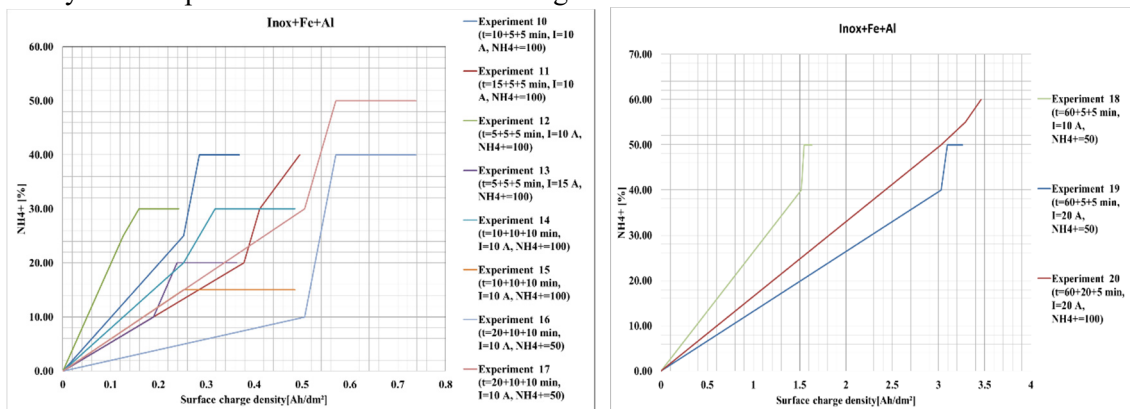


Figure 7. Efficiency of ammonium removal for serial connected electrode

4.2 Parameters influencing removal of ammonium

4.2.1 Effect of current intensity

Optimal current intensity is between 10-25 A because higher intensities can generate higher temperatures of wastewater as a result of transformation of electrical energy into thermal energy. Relation between current intensity and the size of the reactor is inversely proportional. Other than the size of the reactor, selection of current density depends on pH value as well as on temperature and flow velocity of water through reactor.

4.2.2 Effect of water pH

The effect of wastewater pH is reflected through current utilization and through effect of dissolving metal hydroxides. pH value in urine wastewater is between 7 and 8.2, while in pure urine it goes up to value of 9. This leads to conclusion that wastewater pH

primarily depends on concentration of urine, and actually on concentration of ammonium in urine. Since urine pH is usually below 9, it has higher content of ammonium rather than ammonia. Higher removal of ammonium is related with the increase in pH value. Most of ammonium in the HEP treatment plants transforms into nitrogen (gas), and it evaporates in the atmosphere.

Before discharging the treated wastewater into the environment, pH of treated water should be decreased in case of alkaline wastewater or increased in case of acid wastewater. By dissolving oxygen during cathodic reduction, pH value increases in acid media. Other than hydrogen evolution, H^+ ions are being dissolved as $Al(OH)_3$ is being formed in anode vicinity which causes decrease of pH value.



Figure 8. Sedimentation during the experiment

4.2.3 Effect of electrical conductivity

Electrical conductivity decreases with time during the HEP treatment. Electrical conductivity of pure urine was 15.8 mS/cm^3 and in diluted urine it was 1.5 mS/cm^3 . Higher water conductivity enables higher efficiency in ammonium removal. The experiments had shown the decrease of electrical conductivity in time and when it goes under 70% of initial value, ammonium removal efficiency stagnates. This leads to conclusion that value of electrical conductivity should be held at the level of inlet wastewater, if not even higher. That can be provided by adding additives, e.g. salt (NaCl). Higher electrical conductivity results with the possibility of using lower intensity currents, which makes operation costs lower.

4.2.4 Effect of reactor geometry and electrodes design

Electrocoagulation process can be affected by electrode system through electrodes design (shape and area) and inter-electrode distance. Electrodes design can either be simply composed of an anode and a cathode or be composed of many anodes and cathodes complexly settled in EC cell. The complex electrodes arrangement can be classified in monopolar (Figure 1.a) and bipolar (Figure 1.B) electrodes. Monopolar electrodes can be connected in parallel or series while bipolar are connected only in series. Bipolar electrodes require higher voltage and lower current in their work [2,3],

while monopolar operate under lower voltage and higher current. It is hard to conclude which of these arrangements presents the best solution, however, considering ratio effectiveness-costs, it can be expected for monopolar to come as a better solution since they enable higher removal of pollutants in lower electric power mode [4,5]. Polar electrodes require a little bit higher amounts of electric energy [6,7].

Besides rectangular electrodes, other shapes can also be found such as circular or cylindrical electrodes which can be positioned either horizontal (Figure 9.a) or vertical (Figure 9.b).

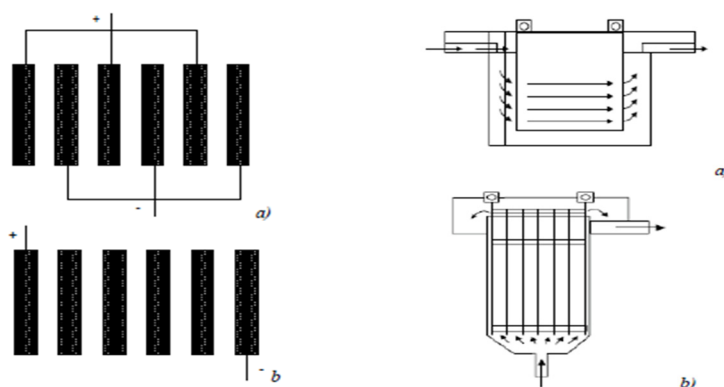


Figure 9. Monopolar and bipolar electrodes

5. Conclusion

The purpose of this research was to define optimal parameters in ammonium removal from urine wastewater using electrochemical process with combination of advanced oxidation process and electrocoagulation. In this research the main goal was to reduce concentration of ammonium from urine, using different electrodes (stainless steel, iron, aluminium) and different current intensities. Evaluating results obtained from advanced oxidation process combined with electrocoagulation, it might be concluded that this method provides removal of ammonium in value of 50% of its initial concentration in wastewater. Carrying out laboratory research in the same mentioned conditions, experiment number 5 was shown as representative experiment of the whole research. This experiment consists of two reactions using single electrodes, as a combination of stainless steel followed by reaction with iron electrode and combination of stainless steel followed by reaction with aluminium electrode. In both cases, reaction time of stainless steel electrode was 15 minutes while iron and aluminium electrodes reaction continued for another 7.5 minutes. Total time of each experiment was 22.5 minutes and was done using current intensity of 10 A. Total removal of ammonium measured at the end of the experiment was nearly 80% of its initial concentration. It is highlighted that results of this research have shown the possibility and adequacy for application of HEP treatment of urine wastewater. However, this research prove the effectiveness of used methods with usage of lower current intensity, so that these kind of systems can result in lower consumption of electric energy. As a next step in optimization of HEP wastewater treatment, it is recommended to examine the combination of HEP with different wastewater treatment technologies.

References

- [1] Ashtounkhy, S. Amina, N. and Abdelwhal, O. (2009) Treatment of paper mill effluents in a batch- stirred electrochemical tank reactor. *Chem. Eng. J.*, 146, pp 205-210.
- [2] Barrera, D. Roa, G., Avila, L. Pavan, T. and Bilyen B. (2006) Electrochemical treatment applied to food-processing industrial wastewater. *In. Eng. Chem.* 45, pp 34-38.
- [3] Borrás, C. Laredo, T. and Scharifker, B.R. (2003) Competitive electrochemical oxidation of p-chlorophenol and p-nitrophenol on bi-doped PbO₂. *Electrochimica Acta.* 48, pp 2775-2780.
- [4] Gardić, V. (2007) Primena elektrohemijskih metoda za prečišćavanje otpadnih voda: Deo 1. elektrodepozicija i elektrokoagulacija, *Zaštita materijala*, 48 (1), str. 49-58.
- [5] Gotsi, M., Kalogerakis, N., Psillakis, E., Samaras, P. and Mantzavinosa, P. (2005) Electrochemical oksidation of olive oli mill wastewaters. *Water Res.*, 39, pp 4177-4187.
- [6] Bayramoglu, M., Eyvaz, M. and Kobya, M. (2007) Treatment of the textile wastewater by electrocoagulation: economical evaluation, *Chem. Eng. J.*, 128, str. 155–161.
- [7] Golder, A.K., Samanta, A.N. and S. Ray, S. (2007) Removal of Cr³⁺ by electrocoagulation with multiple electrodes: bipolar and monopolar configurations, *J. Hazard. Mater.*, 141, str. 653–661.
- [8] Khandegar V., Saroha A.K., (2013.) Electrochemical Treatment of Distillery Spent Wash Using Aluminium and Iron Electrodes, *Chinese Journal of Chemical Engineering*, 20(3), pp 439-443
- [9] Kobya, M., Ulu, F., Gebologlu, U., Demirbas, E. and Oncel, M.S. (2011) Treatment of potable containing low concentration of arsenic with electrocoagulation: different connections mode and Fe-Al electrodes, *Sep. Purif. Technol.*, 77, str. 283–293.
- [10] Korbahati, B.K, Aktas, N. and Tanydac, A. (2007) Optimization of electrochemical treatment of industrial paint wastewater with response surface methodology, *J. Hazard Mater.*, 148. pp 83-90.
- [11] Rajkumar, K., Ganesh, K. P., Sivarasan, G., Muthukumar, M., Sivakumar, R. (2016) Studies on comparison of sludge produced from conventional treatment process and electrochemical process of soya oil refinery processing wastewater, *Jr. Of Industrial Pollution Control* 32(2), pp 562-571.
- [12] Wang C.T., Chou, W.L. and Kuo, Y.M. (2009) Removal of COD from laundry wastewater by electrocoagulation/electroflotation, *J. Hazard. Mater.*, 164, str. 81–86.
- [13] Drogui, P., Asselin, M., Brar, S.K., Benmoussa, H. and Blais, J.F. (2008) Electrochemical removal of pollutants from agro-industry wastewaters, *Sep. Purif. Technol.*, 61, str. 301–310.
- [14] Jiang, J.Q., Graham, N., André, C., Kelsall, G.H. and Nigel, B. (2002) Laboratory study of electro-coagulation- flotation for water treatment, *Water Res.*, 36, str. 4064–4078.

ELECTROCHEMICAL PROCESS FOR MUNICIPAL WASTEWATER TREATMENT – A REVIEW

HANA POSAVČIĆ¹, DRAŽEN VOUK², IVAN HALKIJEVIĆ³,

¹ Faculty of Civil Engineering, University of Zagreb, Croatia, hposavcic@grad.hr

² Faculty of Civil Engineering, University of Zagreb, Country, dvouk@grad.hr

³ Faculty of Civil Engineering, University of Zagreb, Country, halkijevic@grad.hr

1. Abstract

The choice of appropriate wastewater treatment depends on its final disposal or reuse, local environmental conditions and governmental standards. In this paper, electrochemical process as a combination of advanced oxidation and electrocoagulation is presented as an alternative to conventional wastewater treatment processes. The influence of certain operational parameters on the efficiency of reduction of COD, BOD, TSS, TN and TP has been investigated. According to previous research, electrochemical process could be a good alternative for TSS, COD and TP removal. An economic analysis is also performed.

Keywords: wastewater, treatment, electrochemical processes, advanced oxidation, electrocoagulation

2. Introduction

The protection of existing and the treatment of contaminated water bodies is essential for the development and survival of the human community. The wastewater treatment has been a necessity for decades that encourages research and development of new treatment technologies. Although the first application of electrocoagulation dates to 1889, the research related to the use of electricity in wastewater treatment, have progressed only in recent decades [1, 2].

Municipal wastewater includes sanitary and industrial wastewater, as well as rainfall runoff [3]. The choice of appropriate wastewater treatment depends on its final disposal or reuse, as well as the local environmental conditions and governmental standards. The efficiency of wastewater treatment plants depends on the degree to which the wastewater must be treated. Accordingly, conventional wastewater treatment processes are efficient but typically use several complex stages connected to a single functional unit, which are often expensive to maintain and occupy large areas [4]. Therefore, the aim of this paper is to present the electrochemical process (EC) as an alternative to conventional wastewater treatment processes.

EC process as a topic of this research is a combination of advanced oxidation, coagulation, flotation and electrochemistry in water and wastewater treatment. The EC process (Figure 1.) involves four main steps: (1) electrolytic reaction at the surface of

electrode, (2) oxidation phase, (3) formation of coagulants in the aqueous phase, (4) adsorption of soluble or colloidal particles onto coagulants and removal by sedimentation or flotation [5].

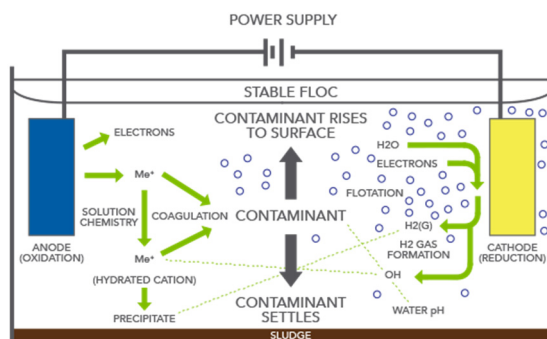


Figure 1. Electrochemical process [6]

The examples of previous studies of the EC process application is presented in this paper. The focus of the paper is to investigate the influence of the certain operational parameters such as pH, current density, electrode material, etc., on the efficiency of reduction and removal of Chemical Oxygen Demand (COD), 5-day Biochemical Oxygen Demand (BOD₅), Total Suspended Solids (TSS), Total Nitrogen (TN) and Total Phosphorus (TP) from municipal wastewater.

An economic analysis is also performed, which shows when it is feasible to use the EC process for the municipal wastewater treatment.

3. Application of electrochemical process for municipal wastewater treatment

The municipal wastewater consists of floating materials, settable solids, organic and inorganic solids, oil, dissolved gases, and microorganisms as well as COD [7]. In Croatia, the limit values of municipal wastewater emissions, before they are discharged into underground or surface waters, are prescribed by the *Ordinance on limit values of wastewater emission (Official Gazette 80/13, 43/14, 27/15 and 3/16)* [8], which is harmonized with EU Directives. The aim of this *Ordinance (80/13)* is to protect the environment from the adverse impact of wastewater discharge. The limit values of TSS, BOD₅, COD, TP and TN are shown in Table 1.

Table 1. Limit values of emissions in municipal wastewaters

PARAMETER	UNIT	LIMIT VALUE
TSS	mg/l	35
BOD ₅	mg O ₂ /l	25
COD	mg O ₂ /l	125
TP	mg/l	2,0 (for agglomerations below 100.000 PE) 1,0 (for agglomerations above 100.000 PE)
TN	mg/l	15 (for agglomerations below 100.000 PE) for agglomerations above 100.000 PE)

3.1 Removal of TSS

TSS are solid materials, organic and inorganic, that are suspended in the water. Suspended solids can result from erosion from urban runoff and agricultural land, industrial wastes, bank erosion, bottom feeders, algae growth or wastewater discharges. Common methods for TSS removal from wastewater are sedimentation, chemical treatment, biological treatment and membrane filtration [9].

According to the previous results, Table 2., EC process is highly effective in TSS removal. More than 95 % of TSS removal has been achieved in several previous research. Thus, EC process can be used as an alternative to other treatment processes. Suggested optimal operative parameters are: Al electrodes, electrode distance 3 cm, 30 min of treatment time and pH 7.

Table 2. Recent applications of EC for TSS removal

VOLUME TREATED [l]	OPTIMAL OPERATIVE PARAMETERS	% REMOVAL	REFERENCE
3	6 Al electrodes; Electrode distance: 6 mm; 30 mA/cm ² ; treatment time: 5 min; pH 8.2	98.8	[10]
1.2	2 SS electrodes; Electrode distance: 3 cm; 0.8 A; treatment time: 5 min; pH 7	95.4	[11]
1	2 SS electrodes; Electrode distance: 10 mm; 1816 A/m; treatment time: 30 min; pH 7	97.6	[12]
0.6	Al-Fe-Fe-Al electrodes; Electrode distance: 3 cm; 1 mA/cm ² ; treatment time: 30 min; pH 7.6	99.8	[13]

3.2 Removal of BOD₅

BOD₅ is the amount of dissolved oxygen consumed by aerobic bacteria in the first 5 days at 20 °C. Some of the sources of BOD₅ in wastewater are human and food waste as well as other organics that are disposed of in the sewers. It is normal for water to have some organic, but the concentration in wastewater might disturb natural biological balance in the receiving water bodies if discharged untreated. Wastewater treatment facilities have BOD₅ discharge limits which vary by each state environmental regulation, and in the EU the limit values of BOD₅ in discharge is 25 mg O₂/l. Most common method of BOD₅ removal is in conventional wastewater treatment facilities using a variety of methods in primary and secondary treatment processes [14]. Since these kind of facilities consist of several devices and occupy very large area, EC process which consists of advanced oxidation processes and electrocoagulation, is presented as an alternative (Table 3.).

In considered EC processes, SS electrodes have a crucial role for the removal of organic matter, creating an advanced oxidation process. The electrodes, whose role is the electrocoagulation (such as Fe and Al), are significantly less involved in the removal of organic matter, that is only separated by the sedimentation enhanced by electrocoagulation. Oxidation, which is possible by reacting with SS electrodes, is important for the removal of organic matter. SS electrode predominantly releases Fe²⁺

ions (Eq. (1) and (2)). The metal ions generation takes place at the anode, while hydrogen gas is released from the cathode (Eq. (3) and (4)). Freshly formed $Fe(OH)_2$ has large surface area that is beneficial for rapid adsorption of soluble organic compounds and trapping colloidal particles [15].

For SS anode:



In addition of oxygen evaluation:



For SS cathode:



Table 3. Recent applications of EC for BOD₅ removal

VOLUME TREATED [l]	OPTIMAL OPERATIVE PARAMETERS	% REMOVAL	REFERENCE
3	6 Al electrodes; Electrode distance: 6 mm; 30 mA/cm ² ; treatment time: 5 min; pH 8.2	61.5	[10]
1.2	2 SS electrodes; Electrode distance: 3 cm; 0.8 A; treatment time: 5 min; pH 7	99	[11]
1	2 SS electrodes; Electrode distance: 10 mm; 1816 A/m ² ; treatment time: 30 min; pH 7	98.1	[12]

BOD₅ removal efficiency varies from 60 % to 99 %, and since the selection of the optimal operative parameters varies significantly, it is suggested that more research needs to be done.

3.3 Removal of COD

Chemical Oxygen Demand (COD) is the amount of oxygen required to oxidize all soluble and insoluble organic compounds present in a volume of water. High COD in water indicates greater levels of oxidizable organic matter and consequently, a lower amount of Dissolved Oxygen (DO) which can decrease the amount of aquatic life forms. Reasons why it is important to determine the COD in water are to determine the concentration of oxidizable pollutants present in wastewater, to determine the overall water quality, to ascertain the effectiveness of wastewater treatment solutions and to determine the effect of wastewater disposal on the receiving environment. Two of the most common techniques for COD wastewater removal are: wastewater separation (coagulation and flocculation) and COD removal by microbial action (aerobic or anaerobic) [16]. As an alternative, electrochemical processes based on advanced oxidation are becoming more and more popular and some results of COD removal by

EC processes from the previous research are shown in Table 4. It can be noticed that the EC is highly effective for COD removal since removal efficiencies vary from 67 % to 98 %, but it is suggested that more research needs to be done. Also, removal mechanism is the same as for BOD₅ (Eq. (1) – (4)).

Table 4. Recent applications of EC for COD removal

VOLUME TREATED [l]	OPTIMAL OPERATIVE PARAMETERS	% REMOVAL	OPERATING COST [€/m ³]	REFERENCE
1.66	6 Al electrodes; Electrode distance: 1 cm; 40 A/m ² ; treatment time: 20 min; pH 7	92.0	-	[7]
3	6 Al electrodes; Electrode distance: 6 mm; 30 mA/cm ² ; treatment time: 5 min; pH 8.2	67.5	-	[10]
1	2 SS electrodes; Electrode distance: 10 mm; 1816 A/m ² ; treatment time: 30 min; pH 7	98.1	-	[12]
0.6	2 SS electrodes; Electrode distance: 3 cm; 400 mA; treatment time: 40 min; pH 7	87.0	-	[17]
0.6	Al-Fe-Fe-Al electrodes; Electrode distance: 3 cm; 1 mA/cm ² ; treatment time: 30 min; pH 7.6	98.1	-	[13]
3	6 Fe electrodes; Electrode distance: 2 cm; 30 V; treatment time: 15 min; pH 7	93.9	0,04	[18]
1.5	4 Al electrodes; Electrode distance: 15 mm; 20 A/cm ² ; treatment time: 60 min	67.2	0.06	[19]
2	2 Al electrodes; Electrode distance: 1 cm; 100 A/m ² ; treatment time: 60 min; pH 7.4; NaCl 0.5 g/L	93.8	0.25	[20]
1	4 Al electrodes; Electrode distance: 20 mm; 100 A/m ² ; treatment time: 10 min; pH 7.8	72	0.76	[21]

Further, the efficiency of EC process has been compared with other wastewater treatment processes. Figure 2. shows that EC has a similar removal efficiency as chemical coagulation and 40 % to 70 % higher removal efficiency than lime precipitation.

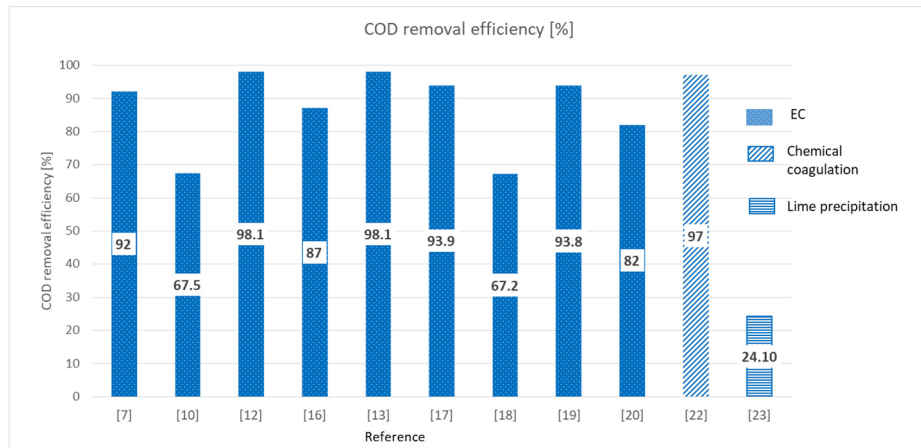


Figure 2. Comparison of COD removal efficiency

3.4 Removal of Total Phosphorus

Phosphorous is one of the major nutrients contributing to the increased eutrophication of lakes and natural waters and its controlling discharge from municipal and industrial wastewater treatment plants is a key factor in preventing eutrophication of surface waters. In addition, its presence causes many water quality problems including increased purification costs, loss of livestock and the possible fatal effect of algal toxins in drinking water. Most commonly, TP removal includes chemical precipitation, which is expensive and causes an increase of sludge volume [24]. Therefore, EC process seems as an interesting solution for TP removal, and some results are shown in Table 5. More than 86 % of TP has been removed under these conditions: Al electrodes, electrode distance 2 cm and treatment time 60 min. Further, several economy analyses has been made for TP removal by EC. Operating costs are less than 1.0 €/m³.

Table 5. Recent applications of EC for TP removal

VOLUME TREATED [l]	OPTIMAL OPERATIVE PARAMETERS	% REMOVAL	OPERATING COST [€/m ³]	REFERENCE
0.6	Al-Fe-Fe-Al electrodes; Electrode distance: 3 cm; 1 mA/cm ² ; treatment time: 30 min; pH 7.6	91.8	-	[13]
0.4	2 Al and 2 Ti electrodes; Electrode distance: 11 mm; 20 A/cm ² ; treatment time: 50 min; pH 4	99.9	0.91	[25]
1.5	4 Al electrodes; Electrode	91.1	0.06	[19]

	distance: 15 mm; 20 A/cm ² ; treatment time: 60 min			
90	Al electrodes; 75 A/m ² ; treatment time: 90 min; NaCl 2g/l	86	0.34	[26]
1	4 Al electrodes; Electrode distance: 20 mm; 100 A/m ² ; treatment time: 10 min; pH 7.8	98	0.76	[21]
5	Fe and Al electrodes; 10 A; treatment time: 2.5 min; 20°C; pH 7	100	-	[27]

3.5 Removal of Total Nitrogen

In environment, nitrogen exists in several forms, and one of them is Total Nitrogen (TN) which consists of TKN (Total Kjeldahl Nitrogen), Nitrite and Nitrate. Even though TN is an essential nutrient for many living organisms, an excess amount of TN in water may lead to low levels of dissolved oxygen and, therefore, have a negative impact on plants and animals, and some forms like ammonia are toxic for certain animal species. The main sources of TN include: municipal wastewater, fertilizer manufacturing, failing septic systems, runoff from animal manure and storage areas, and industrial discharges that contain corrosion inhibitors [28].

The main TN removal processes are biological nitrification and denitrification, and, usually, these methods require pretreatment and are sensitive to oxygen and low growth rate of microorganisms [29]. Thus, EC seems as an interesting solution for TN removal, and some results are shown in Table 6. According to the previous research, it has been shown that EC is not effective enough to meet the standards determined by the *Ordinance (80/13)* [8], and it is suggested that EC needs to be combined with other water treatment processes.

Table 6. Recent applications of EC for TN removal

VOLUME TREATED [l]	OPTIMAL OPERATIVE PARAMETERS	% REMOVAL	OPERATING COST [€/m ³]	REFERENCE
3	6 Al electrodes; Electrode distance: 6 mm; 30 mA/cm ² ; treatment time: 5 min; pH 8.2	32.4	-	[10]

0.6	Al-Fe-Fe-Al electrodes; Electrode distance: 3 cm; 1 mA/cm ² ; treatment time: 30 min; pH 7.6	82.7	-	[13]
90	Al electrodes; 150 A/m ² ; treatment time: 120 min; pH 7	36	1.95	[30]
5	SS, Fe, Al electrodes; 10 A; treatment time: 22.5 min; 20°C; pH 7.1	80	14.37	[31]

4. Economy analyses

Economy analyses, together with the removal efficiency analyses, play an important role in the selection of appropriate wastewater treatment. The economic factors, such as chemicals, membranes, electricity, men power, maintenance, etc., can affect the choice of an optimal method. Due to inconsistency of conducted economy analyses, only a rough estimation and approximate cost comparison of EC process and similar wastewater treatments can be given. Operating costs of some previous EC research are shown in Tables 4. to 6. Efficiency and cost comparisons of EC process with chemical coagulation and lime precipitation for COD removal are given in Figures 2. and 3.

According to Figure 2., EC process has a similar removal efficiency as chemical coagulation and 40 % to 70 % higher removal efficiency than lime precipitation. Operative costs of EC process vary significantly but are in range with similar treatments (Figure 3.). Therefore, it is justified to use EC process for removal of COD instead of lime precipitation or chemical coagulation.

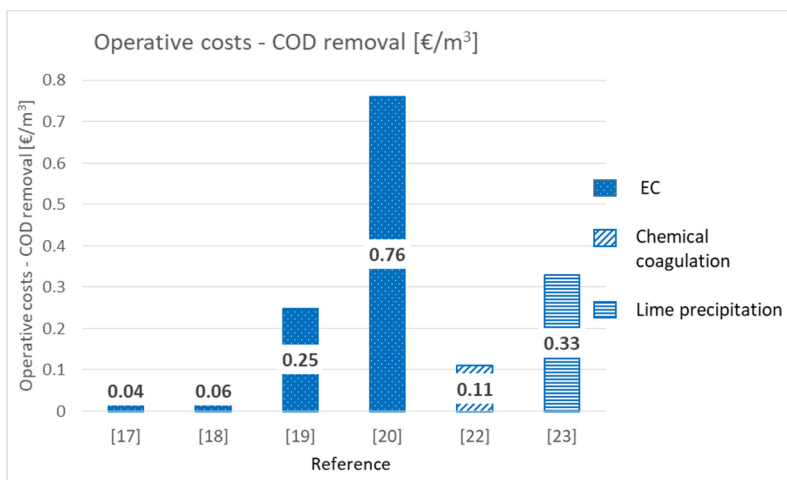


Figure 3. Comparison of operative costs for COD removal

6. Conclusion

According to previous research, EC process is suitable for removal of COD, TSS and TP. However, in cases with BOD₅ and TN, it has been shown that EC process is not effective enough to meet the limit values determined by the *Ordinance on limit values of wastewater emission* [8] and needs to be combined with other wastewater treatment processes, and it is suggested that more research on EC process needs to be done.

Even though operative costs from different EC research vary significantly, economy analyses have shown that it is feasible to use EC process for COD removal instead of chemical coagulation and lime precipitation.

Overall, most of the previous research were conducted on the small capacity units (up to 10 l), where received results (operative costs and operative parameters) significantly differ and are not applicable in real conditions. In order to obtain more credible results, more research on pilot devices need to be done.

References:

- [1] Vik, E., Carlson, D., Eikun, A., Gjessing, E.: Electrocoagulation of potable water, *Water Res*, 18, pp. 1355-1360, 1984.
- [2] Mollah, M.Y.A., Schennach, R., Parga, J.R., Cocke, D.L.: Electrocoagulation (EC) -science and application, *J. Hazard. Mater. B*, 84, pp. 29-41, 2001.
- [3] Vuković, Ž.: Vodoopskrba vodom i odvodnja I – web script, Faculty of Civil Engineering, University of Zagreb, Zagreb, http://www.grad.unizg.hr/predmet/ovio1_b, 15.02.2019.
- [4] Posavčić, H., Halkijević, I., Vuković, Ž.: Application of electrocoagulation for water conditioning, 8th International Conference WATER FOR ALL, Osijek, Croatia, 21-22 March 2019
- [5] Ozyonar, F., Karagozoglu, B.: Operating Cost Analysis and Treatment of Domestic Wastewater by Electrocoagulation Using Aluminum Electrodes, *Polish J. of Environ. Stud.*, 20, pp. 173-179, 2011.
- [6] CRS Electrocoagulation Technology, <https://www.crs-reprocessing.com/en/crs-solutions/electrocoagulation/>, 20.03.2019.
- [7] Nawarkar, C.J, Salkar, V.D.: Solar powered Electrocoagulation system for municipal wastewater treatment, *Fuel*, 237, pp. 222-226, 2019.
- [8] Official Gazette (80/13): Ordinance on limit values of wastewater emission https://narodne-novine.nn.hr/clanci/sluzbeni/2013_06_80_1681.html, 10.04.2019.
- [9] ALAR Engineering Corporation, <https://www.alarcorp.com/latest-news/2016/08/02/tss-wastewater/>, 13.06.2019.
- [10] Bhaskar Raju, G., Thalamadai Karuppiiah, M., Latha, S.S., Parvathy, S., Prabhakar, S.: Treatment of wastewater from synthetic textile industry by electrocoagulation–electrooxidation, *Chemical Engineering Journal*, 144, pp. 51-58, 2008.
- [11] Bukhari, A.: Investigation of the electro-coagulation treatment process for the removal of total suspended solids and turbidity from municipal wastewater, *Bioresource Technology*, 99, pp. 914-921, 2008.
- [12] Nasrullah, M., Singh, L., Wahid, Z.A.: Electrocoagulation/Flotation of Textile Wastewater with Simultaneous Application of Aluminum and Iron as Anode, *Environ. Process.*, 1, pp. 447-457, 2014.
- [13] Barisci, S., Turkay, O.: Domestic greywater treatment by electrocoagulation using hybridelectrode combinations, *Journal of Water Process Engineering*, 10, pp. 56-66, 2016.
- [14] ClearCove, <http://www.clearcoveystems.com/what-is-bod/>, 13.06.2019.

- [15] Santosh, P., Revathi, D., Saravanan, K.: Treatment of sludge wastewater by electrocoagulation using stainless steel electrodes, *Int. J. Chem. Sci.*, 13, pp. 1173-1186, 2015.
- [16] AOS, <https://aosts.com/how-to-reduce-chemical-oxygen-demand-cod-in-wastewater/>, 13.06.2019.
- [17] Ghanbari, F., Moradi, M., Eslami, A., Emamjomeh, M.M.: Treatment of Sewage by Electrocoagulation and the Effect of High Current Density, *Energy and Environmental Engineering Journal*, 1, pp. 27-31, 2012.
- [18] Moosavirad, S.M.: Treatment and operation cost analysis of greywater by electrocoagulation and comparison with coagulation process in mining areas, *Separation Science and Technology*, 52, pp. 1742-1750, 2017.
- [19] Makwana, A.R., Mansoor Ahammed, M.: Continuous electrocoagulation process for the post-treatment of anaerobically-treated municipal wastewater, *Process Safety and Environment Protection*, 102, pp. 724-733, 2016.
- [20] Ighilahriz, K., Ahmed, M.T., Djelal, H., Maachi, R.: Efficiency of an electrocoagulation treatment of water contaminated by hydrocarbons in a continuous mode powered by photovoltaic solar modules, *Environmental Engineering and Management Journal*, 17, pp. 1521-1529, 2018.
- [21] Ozyonar, F.: Treatment of train industry oily wastewater by electrocoagulation with hybrid electrode pairs and different electrode connection modes, *International Journal of Electrochemical Science*, 11, pp. 1456-1471, 2016.
- [22] Demirbas, E., Kobyas, M.: Operating cost and treatment of metalworking fluid wastewater by chemical coagulation and electrocoagulation processes, *Process Safety and Environment Protection*, 105, pp. 79-90, 2017.
- [23] Coskun, T., Debik, E., Manav Demir, N.: Operational Cost Comparison of Several Pre-Treatment Techniques for OMW Treatment, *Clean – Soil, Air, Water*, 40, pp. 95-99, 2012.
- [24] Lenntech, <https://www.lenntech.com/phosphorous-removal.htm>, 13.06.2019.
- [25] Omwene, P.I., Kobyas, M.: Treatment of domestic wastewater phosphate by electrocoagulation using Fe and Al electrodes: A comparative study, *Process Safety and Environment Protection*, 116, pp. 34-51, 2018.
- [26] Lončar, G., Halkijević I., Posavčić, H., Vouk, D.: Dinamički model smanjenja fosfata u vodi uporabom elektrokoagulacijskog uređaja, *Hrvatske vode*, 2018. "in press"
- [27] Petković, I.: Primjena elektrokemijskih procesa u pročišćavanju vode od pranja ruku, *University of Zagreb, Faculty of Civil Engineering*, pp. 55, 2017.
- [28] EPA, <https://www.epa.gov/sites/production/files/2015-09/documents/totalnitrogen.pdf%20>], 13.06.2019.
- [29] Khanitchaidecha, W., Nakaruk, A., Koshy, P., Futaba, K.: Comparison of Simultaneous Nitrification and Denitrification for Three Different Reactors, *BioMed Research International*, 2015, pp. 7, 2015.
- [30] Lončar, G., Halkijević I., Posavčić, H., Ban, I.: Primjena elektrokoagulacijskog uređaja s ciljem smanjenja koncentracije amonijaka, *Hrvatske vode*, 2018. "in press"
- [31] Musa, A., Pandžić, M., Vekić, A.: Pročišćavanje žutih otpadnih voda (urina) naprednim elektrokemijskim procesima, *University of Zagreb, Faculty of Civil Engineering*, pp. 71, 2019.

HYDRODYNAMIC DISPERSION IN SEWER: DETERMINATION OF DEAD ZONES PARAMETERS

YVETTA VELÍSKOVÁ¹, MAREK SOKÁČ²

¹ *Institute of Hydrology, Slovak Academy of Sciences, Slovakia*

² *Slovak University of Technology in Bratislava, Slovakia*

1 Abstract

Hydrodynamic dispersion is an important pollution transport phenomenon. Dispersion, from hydrodynamic point of view, is the spreading of mass from highly concentrated areas to less concentrated areas in flowing fluid. Mass dispersion with advection is basic motion mechanics of particles, transported in water. The main characteristics of dispersion are dispersion coefficients in relevant directions. The dispersion rate is described by the value of the dispersion coefficient in the advection – dispersion equation.

Morphological irregularities, such as small cavities existing in sand or gravel beds, side arms and embayments, bigger obstacles, bank vegetation and uprooted trees, can produce recirculating flows which occur on different scales on both the riverbanks and the riverbed. These irregularities act as dead zones for the current flowing in the main stream direction. Dead zones significantly modify velocity profiles in the main channel and affect dispersive mass transport within the river by collecting and separating part of the solute from the main current. Subsequently, the solute is slowly released and incorporated back to the main current in the stream, creating a significant distortion of the tracer concentration time course.

Strong influence of these impacts raises the question of the adequacy using standard solutions, for modelling the dispersion of pollution or other substances carried by the stream.

Paper describe the observed effect of "dead zones", which theoretically should not occur in conditions of sewer system (prismatic channel) and discuss its cause. The dead zones effect becomes evident especially in case of low discharges (dry weather flows). The reasons can be lower sewer construction quality (irregular slopes, sewer settlement due to the ground consolidation), but also obstacles, sediments and deposits in sewer pipes. The effect of dead zones was observed during field experiments, performed in a straight sewer sections under dry weather flow conditions, i.e. with relatively low pipe filling, discharges and velocities.

Paper describes also approaches how to consider the dead zones phenomenon in numerical models, simulating waste water quality in sewer networks and shows results of the dead zones parameter estimation.

Keywords: hydrodynamic dispersion, dispersion parameters, dead zones, sewer system, environmental hydraulics, pollution

2 Introduction

Dispersion, from hydrodynamic point of view, is the spreading of mass from highly concentrated areas to less concentrated areas in flowing fluid. Mass dispersion with advection is basic motion mechanics of particles, transported in water. Reductions of maximum concentrations are results of their effects. The main characteristics of dispersion are dispersion coefficients in relevant directions. Determination of these dispersion characteristics is the key task for solving problem of pollutant transport in flowing water and for modelling of that phenomenon [5, 7, 14]. Spreading and mixing processes in flowing water can be influenced with occurrence of so-called “dead zones” or “transient storage zones” in a stream [1, 13, 16]. There are zones that deform the concentration distribution of the transported substance or particles because they have been accumulated in these zones and released gradually later. That distorts the concentration time course curve, which becomes asymmetrical.

Sewer pipes are from hydraulic point of view a prismatic stream channel with relatively constant roughness of streambed. But in such hydraulic conditions the effect of “dead zones” could occur because of sediments and deposits along the pipes or because of other irregularity appearance.

It could be seen that dispersion process is not so important for the transport of substances or particles in sewer pipes, but this knowledge could be very useful in case of outlet of dangerous illegal substances and the necessity to identify the source [2, 3, 18].

3 Theoretical basis

The simplest description of the mass spreading in flowing water, especially in sewer pipes, is one-dimensional advection-dispersion equation, which describes the phenomenon in longitudinal direction x (uniform distribution of a mass concentration is required along a depth and a width of a stream). The form of this equation is:

$$\frac{\partial AC}{\partial t} + \frac{\partial QC}{\partial x} - \frac{\partial}{\partial x} \left(AD_L \frac{\partial C}{\partial x} \right) = -AKC + C_s \cdot q_s \quad (1)$$

where: C is a mass concentration ($\text{kg} \cdot \text{m}^{-3}$); D_L is the longitudinal dispersion coefficient ($\text{m}^2 \cdot \text{s}^{-1}$) - $D = df + \varepsilon$, where df is the coefficient of turbulent diffusion, ε is the coefficient of molecular dispersion, ε is often neglected, because $df \gg \varepsilon$ in flowing water streams; A is a discharge area in a stream cross-section (m^2), Q is a discharge in a stream ($\text{m}^3 \cdot \text{s}^{-1}$), K represents a rate of growth or decay of contaminant (s^{-1}), C_s is the concentration of a source, q_s is a discharge of a source, x is a distance (m), t is time (s).

Such one-dimensional approach is applicable for rivers or streams with comparatively non-wide channel or, as it was mentioned, for sewers. In this case, the pollutant spreading has markedly one-dimensional character.

As it follows from references [1, 6, 7, 8, 9, 10, 11, 12, 13, 14, 15, 19], the longitudinal dispersion coefficient DL determination is achieved by several ways: from the own experience or that from the references, over the qualified estimates, up the special calculations application.

Most of the published relations for the D_L determination are based on experimental results from laboratory physical models or directly from the field measurements at the rivers, rarely in sewers (see Table 1). Such relationships are often in the following form [7]:

$$D_L = p \cdot h \cdot u_* \quad (2)$$

where p is the empirical dimensionless coefficient, h is the mean river section depth (m), u_* is the friction velocity ($\text{m}\cdot\text{s}^{-1}$).

Other form of the equation for D_L prediction, which is based on hydraulic parameters, is expressed in the form [5]:

$$D_L = q \frac{u^2 B^2}{u_* h} \quad (3)$$

where q is the empirical dimensionless coefficient (according Fischer $q=0,011$), u is the mean velocity ($\text{m}\cdot\text{s}^{-1}$), B is the water surface width (m).

Table 1. Values of longitudinal dispersion coefficients D_L and dimensionless dispersion coefficient p from experiments.

AUTHOR	CONDITIONS	D_L [$\text{m}^2\cdot\text{s}^{-1}$]	p
ŘÍHA ET AL.	Svitava River $B=11.5\text{m}$; $h=0.9\text{m}$; $Q=(2-3)\text{m}^3\text{s}^{-1}$; $u=0.5\text{ms}^{-1}$	5.2-8.1	100-250
BRADY, JOHNSON	Wear River $B=(20-27.6)\text{m}$; $h=(0.45-1.85)\text{m}$; $Q=(1.62-3.93)\text{m}^3\text{s}^{-1}$; $u=(0.07-0.15)\text{ms}^{-1}$; $i=(0.004-0.17)\%$	4.4-87.22	94.9-2 200
VELÍSKOVÁ, PEKÁROVÁ	Ondava River (upper part) $B=12\text{m}$; $h=0.28\text{m}$; $Q=0.9 \text{ m}^3\text{s}^{-1}$; $u=0.35 \text{ ms}^{-1}$; $i=0.0033$	0.84-1.36	49.3-80
GLOVER	South Plate River meandering stream $R=0.46\text{m}$; $Q=15 \text{ m}^3\text{s}^{-1}$; $u=1.33 \text{ ms}^{-1}$; $n=0.028$	15.7	500
GLOVER	Mohawk River complicated flow conditions (power station, reservoir, tributaries, inflows...) $h=6\text{m}$; $Q=30 \text{ m}^3\text{s}^{-1}$	6.0	800
DUARTE, BOAVENTURA	Mondego River $Q=40 \text{ m}^3\text{s}^{-1}$; $u=(0.47-0.53) \text{ ms}^{-1}$	14-51	-
	$Q=(100-140) \text{ m}^3\text{s}^{-1}$; $u=(0.95-1.1) \text{ ms}^{-1}$	52-61	
	Tagus River $Q=23 \text{ m}^3\text{s}^{-1}$; $u=(1.11-1.16) \text{ ms}^{-1}$	7.3-14.8	
FISCHER	Laboratory rectangular flume	0.0072-0.063	8.7-30
FISCHER	Laboratory rectangular flume	0.123-0.415	190-640

B – width, h – depth, Q – discharge, u – flow velocity, i – longitudinal bed slope, R – hydraulic radius, n – roughness

4 Field measurements

The field measurements were performed near to the experimental hydrological base of Institute of Hydrology in Liptovský Mikuláš (Slovakia). The part of sewer network, which was built in 2004-2005 under EU Cohesion Fund project, was selected for field measurements.

The collector has profile DN 500 mm with slopes in range from 2‰ to 9,5 ‰. After more detailed reconnaissance there were selected a straight section of sewer collector for field experiments situated above Podtureň village (see figure 1).

Sewer sub-sections with various length were selected in the measured sewer part, with various tracer inlets and measuring stations (manholes). The experiment was repeated at least three times for each type of experiment to obtain valid tracer concentration time courses.

The common (kitchen) salt (NaCl) was used as a tracer. Various tracer concentrations influenced the variation of wastewater conductivity. The colouring agent (fluorescein) was added to the tracer to monitor the passage of tracer substance in manhole of measurements. The dosage of tracer was 5 l and it was discharged to sewer instantaneously.

The measurement of conductivity was performed with electric conductivity meter device in the selected manholes. The conductivity meter probe was situated in the centre of wastewater stream.

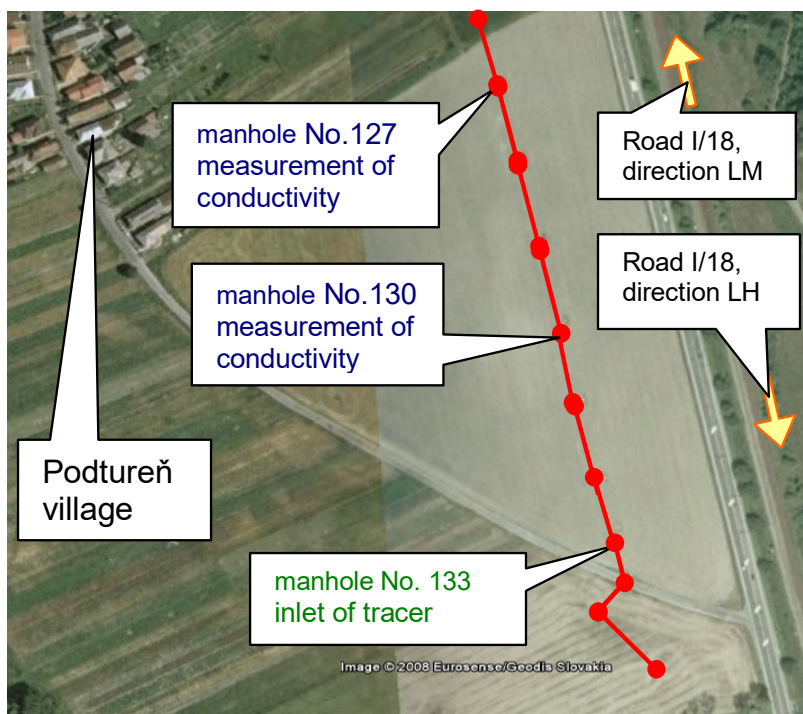


Figure 1. Scheme of the straight sewer section above Podtureň village.

All measurements were performed in dry weather conditions, so the pipe filling ranges from 10 up to 25% of the pipe diameter. Velocity in the pipe was in range from 0.25 up to 1.2 m.s⁻¹. A total of 61 tracer experiments were performed, but only about 54 datasets are identified as reliable for further data processing. The most common cause for dataset excluding was a missing part or irregular shape of the conductivity distribution in time due to measurement devices failures, etc.

5 Material and methods

The determination of longitudinal dispersion coefficient from experiment results was performed in two ways: the first one consists in simulation of tracer experiment (concentration distribution) for various values of longitudinal dispersion coefficient.

The base for this numerical simulation is the analytical solution of Eq. (1) for instantaneous injection of tracer [4]:

$$C(x,t) = \frac{G}{2A\sqrt{\pi D_L t}} \cdot \exp\left[-\frac{(x - \bar{u}t)^2}{4D_L t}\right] \quad (4)$$

where $C(x,t)$ is a mass concentration (kg.m⁻³) in a place and time; D_L is the longitudinal dispersion coefficient (m².s⁻¹); A is a discharge area in a stream cross-section (m²), G is the mass of a tracer (kg), u is a mean velocity (m.s⁻¹), x is a distance (m), t is time (s).

The difference between the measured and simulated values was evaluated. The minimum of difference squares determines the value of the longitudinal dispersion coefficient for each one of experiments.

The second way for evaluation of the longitudinal dispersion coefficient is based on direct determination of the statistical parameters (σ , standard deviation) of the acquired conductivity time courses. Principle of this method is to find the time, corresponding to the 15.87 and 84.13 percentile of the cumulative concentration curve [16]. Distance of these two points is equal to 2σ and dispersion coefficient can be determined as:

$$D_L = \frac{u^2 \sigma^2}{2t} \quad (5)$$

6 Results

Output of field measurements is the record of tracer concentration time courses, deducted from the wastewater conductivity time courses in the sewer. All results of field measurements in dimensionless form of time courses are shown on figure 2. The examples of graphic expression of a single tracer time courses records (in real units) are shown in figure 3 and 4.

The principle of experiment results evaluation was described in previous part. For experiment series at lower discharge (and thus also lower water level), the measurement processing revealed that some pipe irregularities could exist in some measurement section which influence the flow conditions and create so-called „dead zone“ in pipe flow.

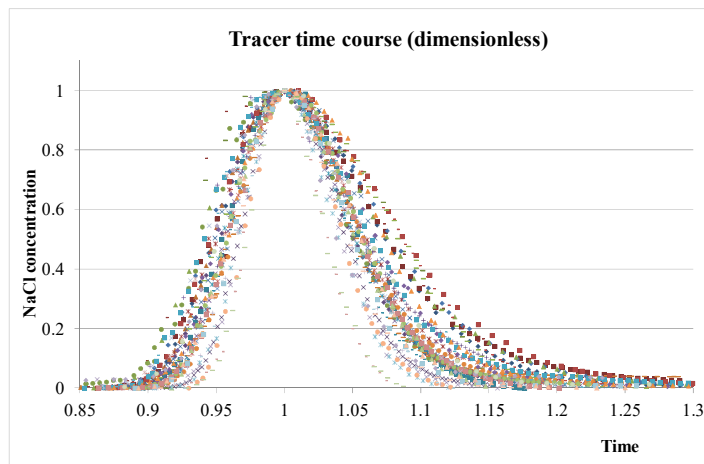


Figure 2. Dimensionless graph of all tracer experiments (max. concentration is equal to 1 in time equal to 1, background concentration is equal to zero)

In this dead zone the tracer has been accumulated and released gradually later. That skews the conductivity time course curve, it becomes asymmetrical and a „tail“ was formed because of the later tracer release. This can be seen especially on figure 4.

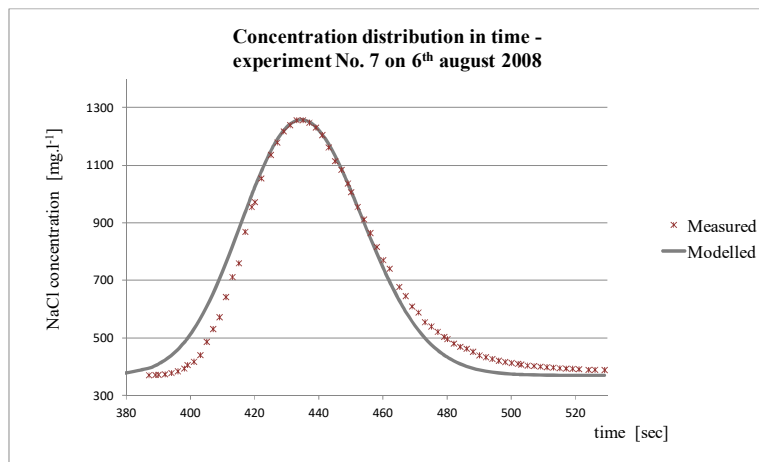


Figure 3. Behaviour of concentration distribution in manhole of measurement record (manhole Nr. 130), (inlet of tracer – manhole Nr. 133) - experiment Nr. 7

7 Discussion

It is necessary to mention a fact which occurred during the practical implementation: during evaluating the results of the measurements - it was found that the conductivity and the measured concentration of the tracer have no linear dependency in the full extent. This was verified and confirmed by conductivity meter calibration. Calibration curve was then applied for the measurement evaluation.

The result longitudinal dispersion coefficient values from the both determination ways of tracer experiments are summarized in Table 2.

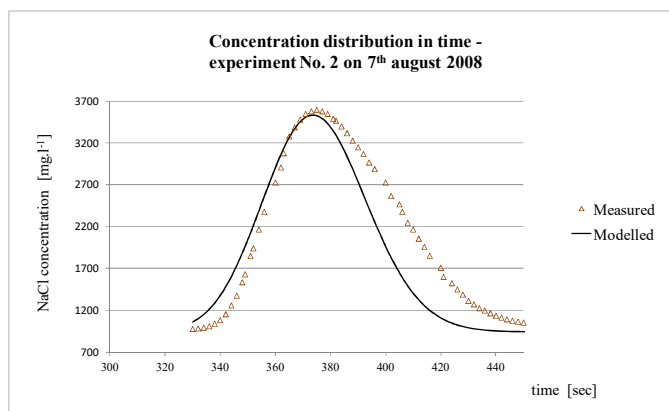


Figure 4. Behaviour of concentration distribution in manhole of measurement record (manhole Nr. 127), (inlet of tracer – manhole Nr. 133) - experiment Nr. 2

Values of longitudinal dispersion coefficients from both ways of determination were compared. It could be established that the first approach (based on numerical simulations by Eq. 4) generally gives lower values of D_L approximately by 10% (the range is from 50 to 110 %, average 89.2%), relating to the direct statistical parameter determination. Especially problematic were experiments with bigger irregularities (asymmetry) in shape of conductivity time courses.

Table 2. Statistical results of field experiments.

Evaluation method		Model approach	Statistical approach
Nr. of experiments	-	24	24
Average	$\text{m}^2.\text{s}^{-1}$	0,14	0,19
Max.	$\text{m}^2.\text{s}^{-1}$	0,20	0,65
Min.	$\text{m}^2.\text{s}^{-1}$	0,09	0,12
Std. deviation σ	$\text{m}^2.\text{s}^{-1}$	0,025	0,102

For comparison we also found empirical relationships for determination of the longitudinal dispersion coefficient value for comparable conditions in the literature.

Taylor (by [17]) derived the relationship for D_L in circular pipeline and turbulent flow condition:

$$D_L = 10.1 r u_* \quad (6)$$

where r is a radius of pipeline [m]. Using this relationship for our flow conditions, we received D_L values in the range from 0.14 to 0.23 m^2s^{-1} . It can be stated that this relatively simple relationship is applicable to the determination of longitudinal dispersion coefficient in a straight part of flows. But in case of natural streams using of this relationship has to be carefully considered.

Noticeable differences of values came from a comparison of the measured values and

the values obtained from application of relationship that was derived by Parker [12], who modified Eq. (6) to form valid for open channel:

$$D_L = 14.28 R^{2/3} \sqrt{2g i} \quad (7)$$

where R is a hydraulic radius [m], g is the gravity acceleration [$\text{m}\cdot\text{s}^{-2}$] and i is a longitudinal bed slope.

Using this relationship, the D_L values were in the range 0.69 to 0.92 $\text{m}^2 \text{s}^{-1}$. We can conclude that the use of this relationship for our conditions is limited (also considering that this relationship was derived for open channels with different cross section shape and roughness of the bed). This example also points out the importance of taking into account conditions under which and for which applied empirical relations are derived.

As it was mentioned earlier, during evaluating the results of the measurements it was found that in a series of experiments with lower discharge the measurement results showed presence of "dead zones" in the measuring section. Therefore, it was appropriate to use following relationship for D_L derived by Krenkel [10] for open channels with the appearance of "dead zones":

$$D_L = 9.1 u_* h \quad (8)$$

Using this relationship for the conditions in the sewer collector, we received D_L values in the range from 0.02 to 0.053 $\text{m}^2\cdot\text{s}^{-1}$. We can say that the range of D_L values corresponds with the range of measured values.

All mentioned examples show importance of condition evaluation for which the empirical relationships are derived and valid.

Finally, we would like to go back and discuss the "dead zones" occurrence problem and asymmetry of tracer concentration time courses. Explanation of the time course asymmetry, mentioned and described in previous part, can be as following: time course of the tracer is principle always asymmetric, because of the advection and dispersion in flowing water related to the stationary placed measurement device; it results inter alia from the form of analytical solution (4). Further asymmetry related to the analytical solution is probably caused by local backwater effects, caused by sediments or deposits in the bed of pipe or by irregular sewer pipes slope caused by damage or breakdown of pipe bed.

Such backwater acts in dry weather condition as tracer (pollutant) storage, it accumulates the tracer and slowly releases the tracer into the main stream. We assume that this phenomenon becomes evident especially in conditions of low discharges (dry weather flows) and of course in case of lower sewer construction quality (irregular slopes, sewer settlement due to the ground consolidation). These conclusions are confirmed also by fact, that in the section with lowest water depths was the time course asymmetry most evident.

8 Conclusions

This paper presents the results of longitudinal dispersion coefficients estimations from

field tracer experiments under the flow conditions in sewer pipes as in a prismatic channel with relatively constant roughness of streambed. The measurement results showed that in a given measuring section was a backwater accumulation located downstream, which resulted in the creation of "dead zones" in the examined section. Consequently, to the tracer retention and its gradual release the conductivity distribution curve was deformed, creating a tracer concentration "tail".

Comparison of D_L values obtained from experiments in sewer pipes with those one obtained in natural streams or channels shows significant differences. D_L values obtained in the sewer pipe were rather closer to the values obtained in laboratory conditions.

Acknowledgment(s)

This paper was prepared with the support of the project No. VEGA 1/0805/16 and APVV – 18 – 0205. This publication is also the result of the project H2020 “SYnergy of integrated Sensors and Technologies for urban sEcured environMents”, Acronym: SYSTEM, no: 787128.

References:

- [1] M. K. Bansal, “Dispersion in natural streams”, J. Hyd. Division, ASCE, 97(HY11), pp. 1867-1886, 1971.
- [2] C. Cassardo and J. Jones, “Managing Water in a Changing World”, Water, 3(2), pp. 618-628; 2011 (doi:10.3390/w3020618. <http://www.mdpi.com/2073-4441/3/2/618>)
- [3] D. Cuff and A.S. Goudie, “Encyclopedia of Global Change”, Oxford University Press, 2005.
- [4] J.A. Cunge, F.M. Holly and A. Verwey, “Practical aspects of computational river hydraulics”. Energoatomizdat, Moskva, 1985 (in Russian).
- [5] A. A. L. S. Duarte and R. A. R. Boaventura, “Pollutant dispersion modelling for Portuguese river water uses protection linked to tracer dye experimental data”. WSEAS Transactions on Environment and Development, 12, pp. 1047- 1056, 2008.
- [6] J. W. Elder, “Dispersion of marked fluid in turbulent shear flow”, J. Fluid Mech., 5, Part 4, pp. 544-560, 1959.
- [7] H.B. Fischer, E.J. List, R.C.Y. Koh, J. Imberger and N.H. Brooks, “Mixing in inland and coastal waters”, Academic press, New York, 1979.
- [8] G. Jolánkai, “Hydrological, chemical and biological processes of contaminant transformation and transport in river and lake systems”, A state of the art report, UNESCO, Paris, 1992.
- [9] M.J. Karcher, S. Gerland, I.H. Harms, M. Iosjpe, H.E. Heldal, P.J. Kershaw and M. Sickel, “The dispersion of 99Tc in the Nordic Seas and the Arctic Ocean: A comparison of model results and observations”, Journal of Environmental Radioactivity, 74 (1-3), pp.185-198, 2004.
- [10] P.A. Krenkel, G. Orlob, “Turbulent diffusion and reaeration coefficient”. J. Sanitary Engineering Div., ASCE, 88, SA2 - March, pp. 53-83, 1962.
- [11] K. Kosorin, “Dispersion Coefficient for Open Channels Profiles of Natural Shape”, J. Hydrol. Hydromech., 43, 1-2, pp. 93-101, 1995 (in Slovak).
- [12] F.L. Parker, “Eddy diffusion in reservoirs and pipelines”, J. Hyd. Div., 87, HY3, pp. 151-171, 1961.
- [13] P. Pekárová and Y. Velísková, “Water quality modelling in Ondava catchment, VEDA, Bratislava, 1998 (in Slovak).
- [14] J. Říha, P. Doležal, J. Jandora, J. Ošlejšková and T. Ryl, “Water quality in surface streams and its mathematical modelling”, NOEL 2000, Brno, 2002 (in Czech).

- [15] P.K. Swamee, S.K. Pathak and M. Sohrab, "Empirical relations for longitudinal dispersion in streams", *Journal of Environmental Engineering*, 126 (11), pp. 1056-1062, 2000.
- [16] S. A. Socolofsky and G. H. Jirka, "CVEN 489-501(2005) Special Topics in Mixing and Transport Processes in the Environment. Engineering Lectures", 5th Edition, Coastal and Ocean Engineering Division, Texas A&M University, M.S. 3136, College Station, TX 77843-3136.
- [17] A. Sooky, "Longitudinal dispersion in open channels", *J. Hydraulic Division, ASCE*, vol. 95, No. HY4, pp. 1327-1346. 1969.
- [18] B. Spänhoff, R. Dimmer, H. Friese, S. Harnapp, F. Herbst, K. Jenemann, A. Mickel, S. Rohde, M. Schönherr, K. Ziegler, K. Kuhn and U. Müller, "Ecological Status of Rivers and Streams in Saxony (Germany) According to the Water Framework Directive and Prospects of Improvement. *Water*, 4(4), pp. 887-904, 2012 (doi:10.3390/w4040887. <http://www.mdpi.com/2073-4441/4/4/887>).
- [19] D. Zhang, H. Lou, G. Li, X. Jia and H. Li, "Simultaneous Inversion for Dispersion Coefficients and Space-Dependent Source Magnitude in 2D Solute Transportation", *WSEAS Transactions on Fluid Mechanics*, 1, Vol. 8, pp. 31-42, 2013.

Topic no. 4 – Hydraulic structures

RESEARCH ON THE OUTLET CAPACITY OF THE LAKE MONDSEE TO IMPROVE FLOODRISK MANAGEMENT

PETR LICHTNEGER¹, HUBERT HOLZMANN², CHRISTINE SINDELAR³, JOHANNES SCHOBESBERGER⁴, HELMUT HABERSACK⁵

¹ University of Natural Resources and Life Sciences, Institute of Hydraulic Engineering and River Research, Christian Doppler Laboratory for Sediment Research and Management, Austria, Petr.Lichtneger@boku.ac.at

² University of Natural Resources and Life Sciences, Institute of Hydrology and Water Management, Austria, Hubert.Holzmann@boku.ac.at

³ University of Natural Resources and Life Sciences, Institute of Hydraulic Engineering and River Research, Christian Doppler Laboratory for Sediment Research and Management, Austria, Johannes.Schobesberger@boku.ac.at

⁴ University of Natural Resources and Life Sciences, Institute of Hydraulic Engineering and River Research, Christian Doppler Laboratory for Sediment Research and Management, Austria, Christine.Sindelar@boku.ac.at

⁵ University of Natural Resources and Life Sciences, Institute of Hydraulic Engineering and River Research, Christian Doppler Laboratory for Sediment Research and Management, Austria, Helmut.Habersack@boku.ac.at

1. Abstract

Lake Mondsee with its surface area of 13.5 km² forms a considerable reservoir for water storage and runoff retention. There is potential for downstream flood mitigation, using the flood retention capacity by pre-release strategies. The runoff release of the weir structure at the Lake Mondsee, Upper Austria, is strictly constrained by a committed release rule, according to the pre-defined hydraulic capacity of the weir structure and furthermore the weir opening is determined by the actual water level in the lake. The range of runoff control, however, is rather limited and during flood events, it is not possible to release sufficient volume of water in time, thus the retention may lead to high and fast increase of the lake water level. The extreme flood event in 2013 escalated and triggered the present investigation: What exactly is the real weir discharge capacity? Can the operation rules be improved to mitigate such extreme flooding? Which further integral aspects have to be considered? Can a drawdown of the lake water level based on rainfall-runoff forecasts improve the flood situation?

The present work focuses on technical aspects of the outlet system capacity. An interactive approach involving a hybrid modelling method (combining numerical and physical modelling) was implemented for investigating the lake stage to discharge relationship in dependence on the weir opening. The investigations revealed that the weir capacity matched the expected capacity quite well; however, the hydraulic losses between the lake and the weir structure were decisive. A rapid pre-release (drawdown) of the lake at normal water table condition is so far very limited or even impossible due to capacity constraints. An increase of the outlet reach capacity was thus identified to be the most crucial measure for any improvement of the outlet system. Moreover, tests on sediment incipient motion were carried out on the physical model to assess the bed stability and sediment transport in case of a pre-release (weir head water flushing) prior next flood events. Hence, new points were determined and placed in the Shields diagram respecting specific conditions at the outlet of the Lake Mondsee.

Keywords: Lake Mondsee, weir capacity, physical modelling, numerical modelling, sediment transport

2. Introduction

The Lake Mondsee is located in the Northern Alpine range at the border between Federal Provinces of Upper Austria and Salzburg. It was formed by glaciers in the Riss ice-age period and is part of the Salzkammergut district, which is one of the most attractive landscapes in Austria (see Figure 1). Lake Mondsee has a surface area of 13.5 km², the outlet of the lake drains an area of approx. 247 km² and releases water to the downstream lake Attersee, which is the largest lake in the region. A weir structure is situated about 225 m downstream the lake on the stream Seeache connecting the lakes Mondsee and Attersee; see Fig. 1.

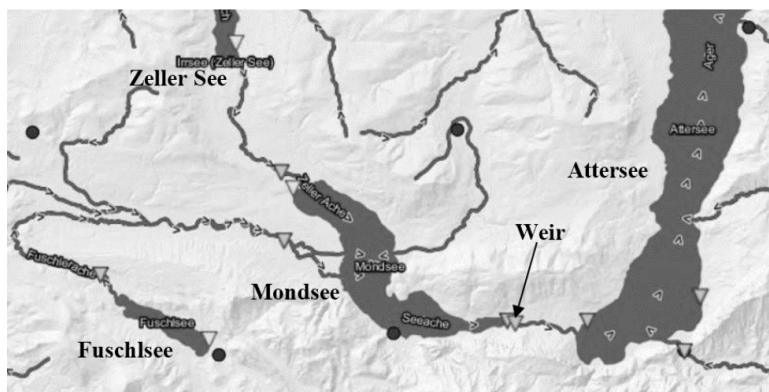


Figure 1. The hydrological system of the Lake Mondsee with Fuschlsee and Zeller See Lakes upstream and Attersee Lake downstream. The weir structure is situated on the release reach called Seeache (connection between Mondsee and Attersee) and is marked with an arrow in the image.

Current Weir Operating Regulations (WOR) of the Weir Mondsee are effective since 1982 and have been checked by Weinberger in 1994 [1] the last time. He found that there is a shortage of the outlet capacity of the weir in a flood case and proposed faster opening of two existing weir flap gates and implementing of a new remote control at tributaries from lakes Fuschlsee and Zeller See (Figure 1), as well as a creation of an additional bypass capacity at the weir structure.

A flood passed the Lake Mondsee in June 2013. Lake neighbours (ports, pensions, water sport schools, camping places, etc.) were flooded with the water table rising up to extreme 1.42 m above the normal level, whereas the maximum outlet discharge was 91 m³/s, or 104 m³/s according to the gauge station at the Seeache, or to the WOR, respectively. This approximately corresponds to a 30-years flood return period. Thus, an increase of the retention capacity, i.e. lowering of the lake water level prior to flood events (lake pre-release) is aimed by the abutting communities. In this study, the main goals were determined as follows:

1. Revision of WOR from the hydraulic point of view and with respect to the water level in the lake and downstream the weir, and options to optimise weir functions.
2. Feasibility of the WOR optimisation with respect to risk-benefit balance and hydrological tests on pre-release scenarios.

3. Applied methods

The outlet system of the Lake Mondsee can be considered to consist of three functional parts:

1. Runoff capacity of the weir itself (weir coefficient);
2. Hydraulic loss between the lake and the weir structure;
3. Runoff capacity of the reach downstream the weir (weir tail water rating curve).

Because of flow continuum, all three parts are integral and not separable with bidirectional influence. Thus, an interactive approach involving a hybrid modelling method (combining numerical and physical modelling) was implemented for investigating the lake stage to discharge relationship in dependence on the weir opening. The reach from the lake to the weir was modelled numerically with a 1D approach (HEC-RAS), the weir structure was modelled physically at a length scale of 1:17.5. The head water upstream of the weir was the interface between the numerical and physical models which were both calibrated using data from field measurements. The situation is given in Figure 2 where the main variables are defined: discharge (Q), lake water level (h_0), weir head water (h_1), weir tail water (h_2), weir head (H), and hydraulic loss of the approaching reach (Δh_1).

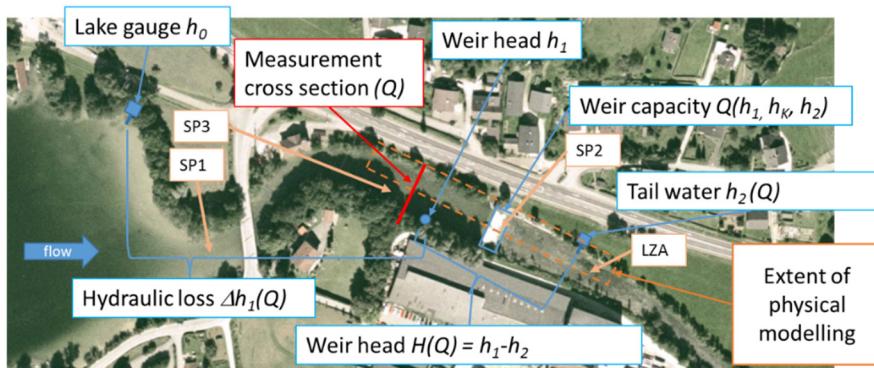


Figure 2. Outlet system of The Mondsee; Schematic presentation of variables and their relations. Discharge measuring cross-section (red), region of physical modelling containing the weir structure (orange), new head water gauge (blue circle). Further, sites where sediment probes (SP) were taken are highlighted.

3.1 Field measurements

Several measurements were done in situ: levelling of gauges, discharge measurements using acoustic methods and bed sediment samples were taken from the lake outlet part, weir approaching reach and tail water as well the weir stilling basin. Since the main weir control variable is the lake water level, there is no gauge in the head of the weir. Thus, a temporal gauge was built upstream the weir and equipped with a pressure probe. The measurement signal was adjusted and taken to the weir house and logged on a data storage. The study was conducted during 2017-2018 where a long dry period occurred. Nevertheless, few small flood events (up 1-year flood return period) occurred. Hence, the functionality between the head loss from the lake to the weir head and the flow rate could

be determined from the gauge measurements. The measured head loss was then taken for calibrating the 1D numerical model.

Flow measurements were done in the cross section upstream the weir using Acoustic Doppler Velocimeter (ADV; *FlowTracker* from SonTek) and Acoustic Doppler Current Profiler (ADCP; *StreamPro* from RD Instruments). First, ADV measurements involving the velocity-area method [2] were done to get a detailed velocity field distribution for calibration purposes of ADCP which was used for the repeated measurements. Since the ADCP leaves out regions of the flow area near the bottom and the free water surface, a slight adjustment (of about 4 %) was necessary to reflect the influence of secondary currents and respective flow field redistribution near the water surface because of the measuring section position downstream of a river bend (Figure 3; left). This was, however, practically the only site where sufficient depths and stable calm water levels were available for implementing ADCP [3]. The right bank of the measuring section suffers from sedimentation arising obviously from the flow curvature (see Figure 3) which probably negatively influences the approaching flow to the weir. Analysing historical data, a tendency in the sediment accumulation can be observed as shown in Figure 3; right.

A sieve analysis was done with sediment probes (SP) which were taken on selected places as shown in Figure 2. Big stones and rock were neglected because they were of no relevance for the sediment motion assessment. In the downstream reach there were very few small size sediments, therefore a so-called “Linienzahlanalyse” (LZA; [4]) was implemented for which a withdrawal of the stones is not necessarily required. From LZA stones up to 50 cm were registered whereas stones having a maximum size of about 10 cm could be withdrawn for sieve analyses. Fine material (sand and fine gravel) were found in the weir stilling basin (PS2) and at the flat outlet section of the lake (PS1), in the release reach stones smaller than 3 cm were rather rare (PS3, LZA). Thus, grains of at least this size should not be mobilized to preserve existing morphology in case of a future pre-release scenario. The result of sieve and LZA analyses are given in Figure 4.

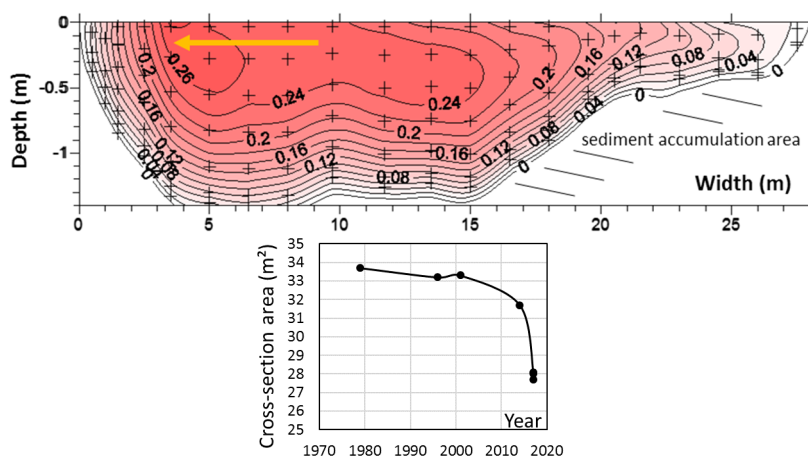


Figure 3. Left: Velocity field measured at the outlet reach of Mondsee with a FlowTracker. The arrow to the left illustrates the region with high spanwise velocity component (about 30% of the streamwise velocity). The field values are in m/s, $Q = 4.5 \text{ m}^3/\text{s}$. Right: Historical data on the cross-section area in the reach km 2.762 related to the mean water level.

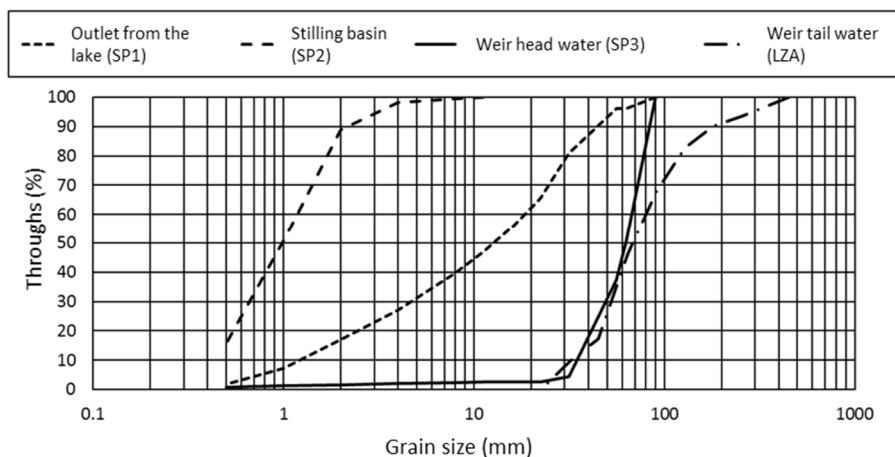


Figure 4. Grain size distribution of sieved bed probes (SP1-3) and from LZA; for probe locations see Figure 2.

3.2 Physical modelling

The physical model was built in a 1 m wide hydraulic flume. To prevent excessive size reduction and negative scaling effects a symmetry model was implemented. Hence, the left embankment, one flap gate and a half of the mid pier with the flume glass wall as a symmetry were constructed satisfying following functions: controlled opening of the flap gate, flap with spill beam baffles, aeration of the space under the flap, bypass discharge for the fish-pass, stilling basin, upper and down reach with the appropriate slope and model roughness. Total discharge, fish-pass discharge, flap gate opening and the tail water level could be controlled independently, whereas head water levels and weir wall pressures could then be measured using the water surface gauge moved on a carriage along the flume and using piezometric taps aligned with the bed in the longitudinal model axis. There is the longitudinal profile of the model with piezometric tap locations and water surface and pressure lines shown at Figure 5. The similarity of hydraulic losses and thus also of the velocity field of the approaching flow to the weir had to be achieved by applying the similarity criterion for model flow velocities v_M (according to e.g. [5]):

$$v_M \geq \frac{1908 \cdot \nu}{R^{1/6} \cdot d_s^{5/6}} \text{ for } 5 < R/d_s < 500 \quad (1)$$

In Eq. (1), there is R the hydraulic radius, ν the kinematic viscosity of water and d_s the characteristic diameter of sediment particles (values are to be used in model scale). That is why 2-3 times bigger sediment had to be used at the model to satisfy given condition for modelled characteristic velocities of about 10 – 13 cm/s, i.e. 10 – 15 mm diameter instead of 4.8 mm (all in model scale), see Figure 6, right.

In addition, investigation on incipient sediment motion was carried out for the case of pre-release conditions, i.e. flap gate is down and the head water is relatively low. Particle size mixtures of 1-2; 2-4; and 4-8 mm were used (18 – 140 mm in nature). To eliminate the effect of the oversized bed roughness (which was explained above), a flat smooth plate was placed in front of the weir sill on which the sediment probes were put, see

Figure 7, left. In this way, the hiding of particles in the sublayer was avoided and the shear stress locally increased to get higher sediment Reynolds numbers. Thus, the results depend on the weir hydrodynamics only and may be extrapolated to nature in the given length scale. The Laser Doppler Anemometry (LDA), a non-intrusive method (see e.g. [6]), was used in a 2D coincident configuration for flow velocity measurements in front of the weir (Figure 7, right).

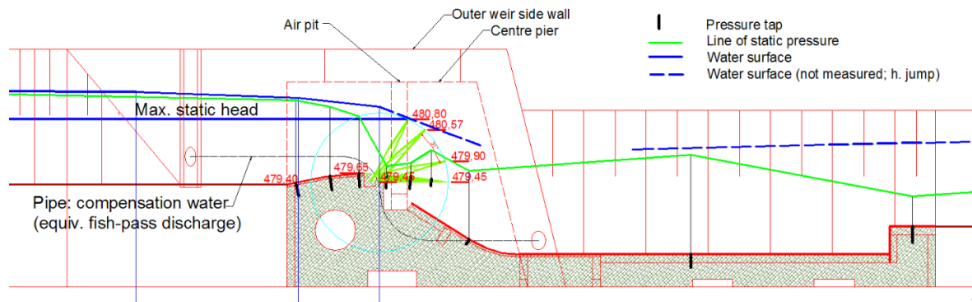


Figure 5. Longitudinal profile of the weir model. Water surface line corresponds to the flow rate of $100 \text{ m}^3/\text{s}$, the flap is down on 479.45 m ASL.

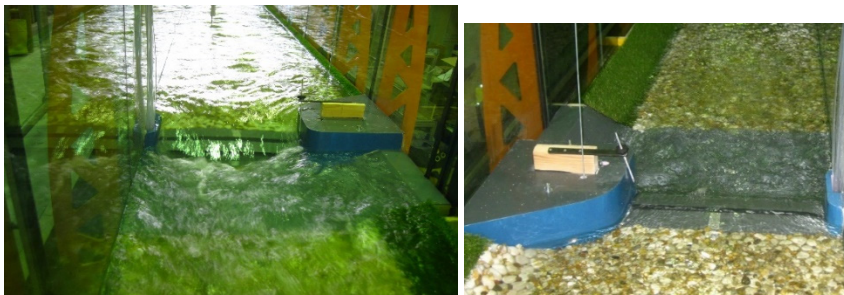


Figure 6. Example photos of the $\frac{1}{2}$ -symmetry model weir as placed in the flume and being under operation. Left: View upstream. Right: View downstream; increased roughness d_s is visible.

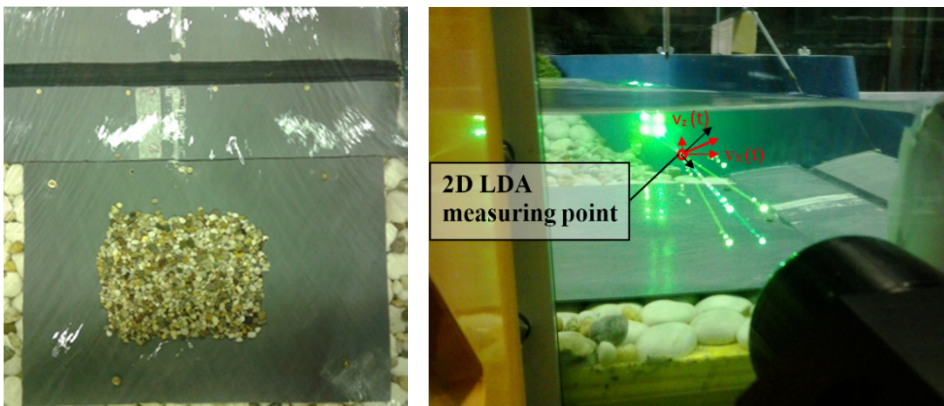


Figure 7. Left: Tests on incipient sediment motion, mixture 4-8 mm. Right: View at the hydraulic flume sidelong of the LDA probe, the measuring point and measured vectors are labelled.

3.3 Numerical modelling

A 3D numerical simulation was done to assess the influence of the glass wall symmetry. The weir flow was calculated using RANS solver and alternating the symmetry plane boundary as a symmetry (free-slip) condition and a no-slip wall condition. For the extreme flow rate of $140 \text{ m}^3/\text{s}$ and the flap laid down completely (479.45 m ASL; see Figure 5), the difference in the runoff capacity (glass wall vs. symmetry) was merely 0.13 %. The influence of the glass wall could thus be neglected. Figure 8 apparently shows a good agreement between the numerical simulation and the nature, however, there is a difference in the particular flow rate and the flap gate opening as described in the figure capture below.

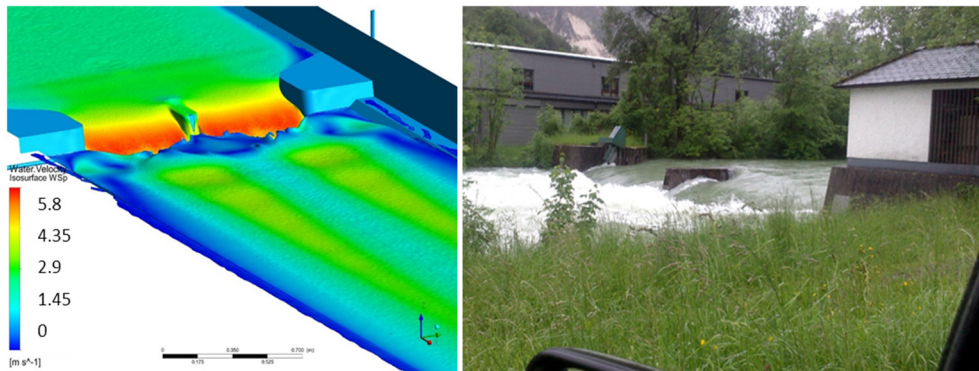


Figure 8. Left: A full width representation of numerical weir flow simulation ($Q = 140 \text{ m}^3/\text{s}$; Flap at 479.45 m ASL). Right: Onsite photograph (© Hammerl) during the flood 2013 ($Q \cong 95 \text{ m}^3/\text{s}$; Flap at 479.90 m ASL).

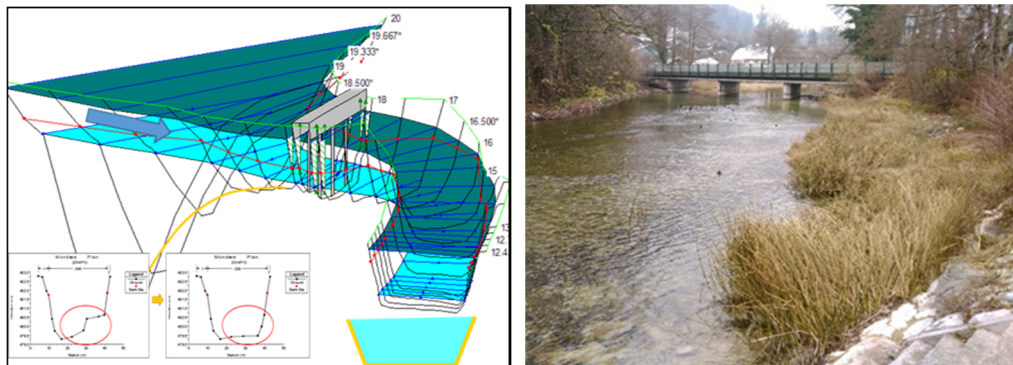


Figure 9. Left: View upstream the lake release reach where left bank side deposits are visible (photographed during extremely low water table, the grassed bank is normally flooded). Right: 3D presentation of 1D model, the restoration of cross section is highlighted, two plots with the measuring cross section show the change of the current vs. “restored” geometry.

The hydraulic loss of the approaching reach, i.e. between the lake and the weir, was simulated using the 1D model tool HEC-RAS [7]. Records of the continuously measured

water levels in the lake in the head water of the weir were taken to adjust the Manning coefficient (n). In particular, the flap gates reach their position 479.90 m ASL when the lake water level achieves 481.00 m ASL according to the weir regulations. At that moment the hydraulic energy loss is about 50 cm, which yields an overall value $n = 0.055 \text{ s/m}^{1/3}$. This represents a rather high roughness and points out that there are several sediment deposits in the lake release reach as also observed in situ (see also Figure 3, right; and Figure 9, left). These deposits, however, were not considered in the geodetic survey data, which were available. Therefore, numerical simulations with geometries introducing deposits based on observations and additional surveying were done to improve the adjustment (calibration) of the model, which yielded to a more realistic Manning's coefficient of $n = 0.035 \text{ s/m}^{1/3}$. In the next step, the improved calibration was used for further computations excavating the deposits and restoring the cross section (based on plans from 1969) to assess the potential of the release capacity improvement (Figure 9; right).

4. Results and discussion

Because of the dry period in 2018, few small floods occurred and only small absolute discharges could be measured. Nevertheless, a systematic deviation to lower values comparing with the last flow-rating curve was determined. The hybrid modelling approach was utilized for higher discharges, where the relation between both, the lake water table and the Seeache downstream the weir (at the gauge station Seeache), was known from the past (e.g. record of the flood 2013). Due to this, the tendency to lower real (measured) discharges was approved for higher discharge values; see Figure 10. It was found that the real discharge culminated with $86 \text{ m}^3/\text{s}$ (lake water table = 481.5 m ASL) instead of $91 \text{ m}^3/\text{s}$, which was stated according to the rating curve at the gauge station Seeache.

Analysing several scenarios numerically as mentioned above (sediment material deposits, dredging, complete cross-section restoration of the release reach between the lake and the weir) the potential runoff capacities and suggestions to adapting the WOR are summarized in the diagram below (see Figure 11). Both flap gates operate at higher discharges simultaneously, and if considering the current WOR, they reach their position of 479.90 m ASL if the lake water table reaches 481.00 m ASL. The discharge according to WOR should be about $25 \text{ m}^3/\text{s}$, but, unfortunately, it would be only about $21 \text{ m}^3/\text{s}$. If the present situation with gravel depositions etc. is respected, a pre-release effect may be enhanced tilting the flaps down to 479.90 m ASL earlier, i.e. when the lake water level gets at 480.80 m ASL. Thus, approximately $16 \text{ m}^3/\text{s}$ would be achieved, more than about $9 \text{ m}^3/\text{s}$ which would be released according to current WOR in the same lake water level case. Whereas the current regulation needs 27 cm of water level rising above RNW (maximum weir regulated/retained water level at low discharges), the adaption would reduce to only 7 cm; see Figure 11. Furthermore, there is practically not much difference between laying flaps on 479.90 or 479.45 m ASL, which is the constructive lowest flap gate position. On the other hand, implementing complete riverbed restoration, the absolute discharge would enhance from 16 to about $24 \text{ m}^3/\text{s}$, or $27 \text{ m}^3/\text{s}$, if the flap gates position gets at 479.90 m ASL, or 479.45 m ASL, respectively, at the same lake water level (480.80 m ASL). In case of the lake water level at 481.00 m ASL, the discharges

would rise up to about 33 or 36 m³/s, respecting the flap opening. Nevertheless, a residual hydraulic loss is remaining due to the release reach; see the patch in Figure 11. Just hypothetically, if the loss could somehow be eliminated (e.g. due to enlargement of the release reach or replacing the weir directly onto the lake reservoir) the runoff capacity would theoretically rise up to 53 or 65 m³/s, depending on the flap gate opening, if the lake water level is 481.00 m ASL.

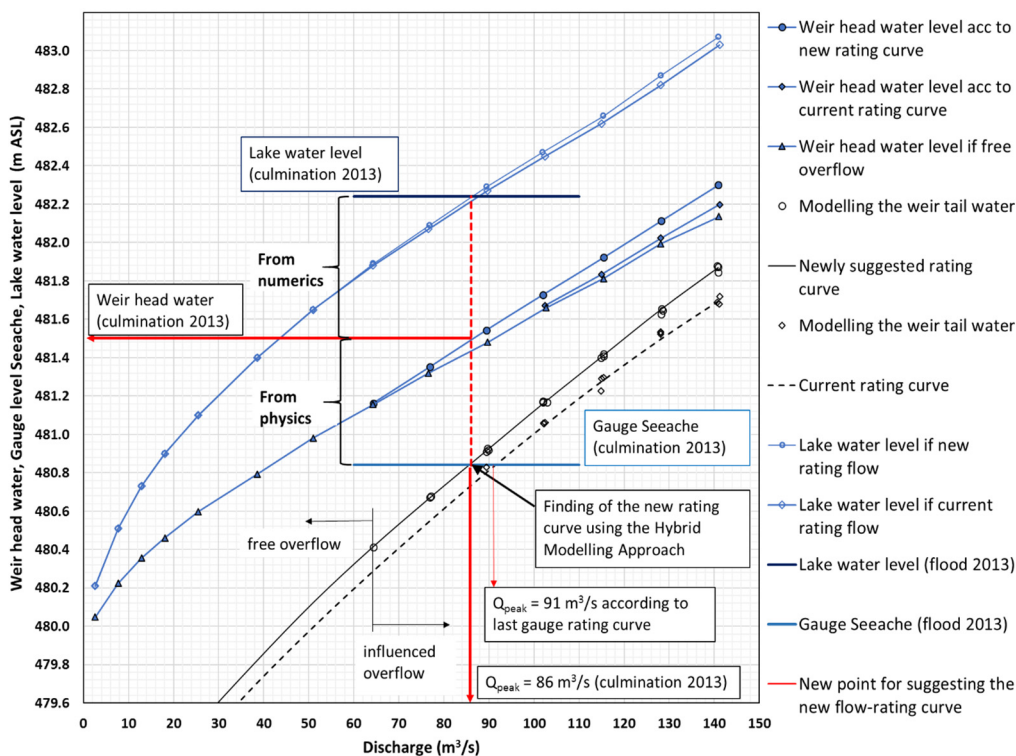


Figure 10. Water level to discharge rating curves showing the relations between the lake water, weir head and tail water levels. Using iterative approximation and hybrid modelling approach a new rating curve for the downstream gauging station was suggested. In diagram, the calibrating point showing water level culmination from the flood 2013 is depicted. In this way, a new rating curve could be suggested.

The gain of the lower flap gate opening (we consider the difference between 479.90 and 479.45 m ASL) is relatively low because of the mitigation effect of the release reach. The maximum capacity gain is available if the weir would be directly connected to the lake. The difference from the hydraulic point of view is schematically illustrated and explained in Figure 12.

Results of the investigation of the flow 1.75 m upstream the weir implementing LDA show the flow velocities and respecting Reynolds shear stresses for 9 combinations of weir openings (Y) and discharges (Q), see Figure 13. Extrapolating linear distribution of the turbulent shear stress profiles down to bed has allowed determining the bed shear stress values, and further, determining sediment Froude (Fr^*) and Reynolds (Re^*) numbers where the bed shear stress values or friction velocities (u^*) are applied.

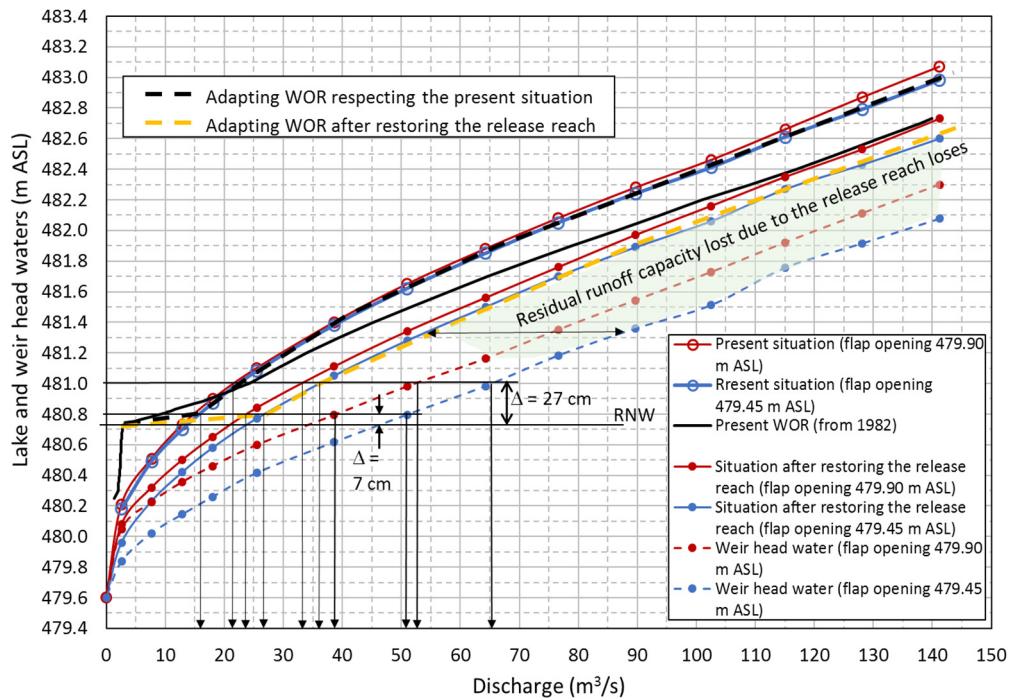


Figure 11. Resulting rating curves, present WOR and two new suggestions, first, respecting current outlet situation, second, considering the riverbed restoration. Curves of weir head water levels are plotted too for both flap gates openings, 479.90 and 479.45 m ASL. These curves represent the hypothetical maxima of the runoff capacity of the Weir Mondsee.

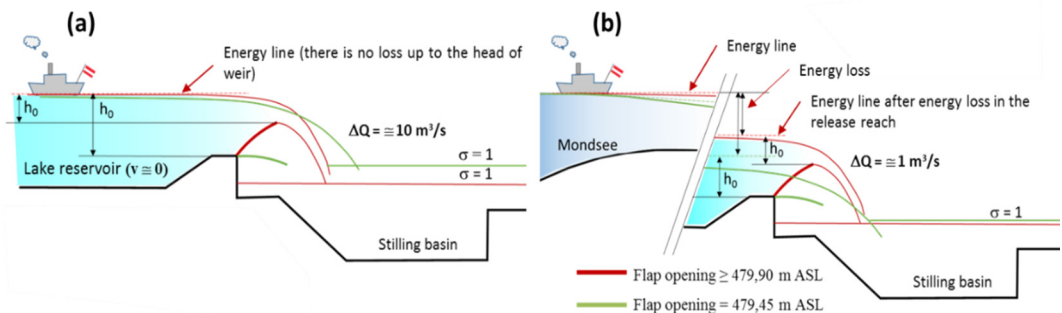


Figure 12. Principal schemes of the runoff capacity comparing a weir in direct connection to the reservoir (a) and in release reach (headrace channel) connection (b). Whereas in case (a) the lowering of the flaps effects into appropriate increase in discharge, lowering flaps in case (b) involves the increase of the flow velocity and hydraulic losses, respectively, as well as decrease of the head water level. Thus, finally, the increase of h_0 and additional runoff capacity ΔQ in case (b) is much lower than in case (a).

After collecting the knowledge of the flow and bed shear stresses in the $Y-Q$ space experiments with three sediment mixtures, $d_m = 26.5, 50,$ and 105 mm (in Nature), were done for 4 flap gate openings, i.e. 12 combinations were examined in total. The discharge was successively increased for every experiment and the incipient motion of single sediment particle up to mass sediment transport were evaluated. Results with the

determined transport thresholds are shown on the Shields diagram in relation of absolute values (diameter and discharge) depending on the flap gate opening – see Figure 14. The threshold data to sediment motion deviate from the constant line in the Shields diagram, which can be explained with the specific flow and experiment conditions. Therefore, any generalised conclusions in respect of the Shields Diagram cannot be drawn.

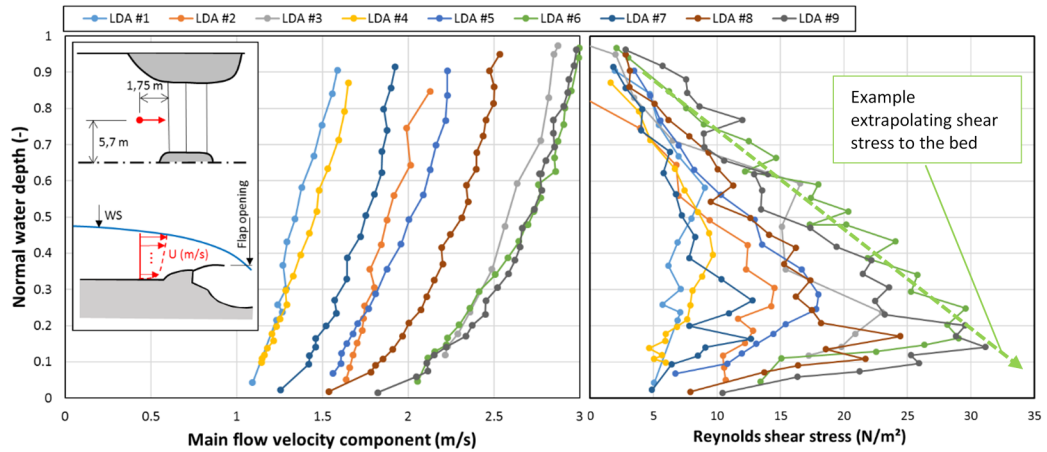


Figure 13. Results of flow measurements at the physical model using LDA.

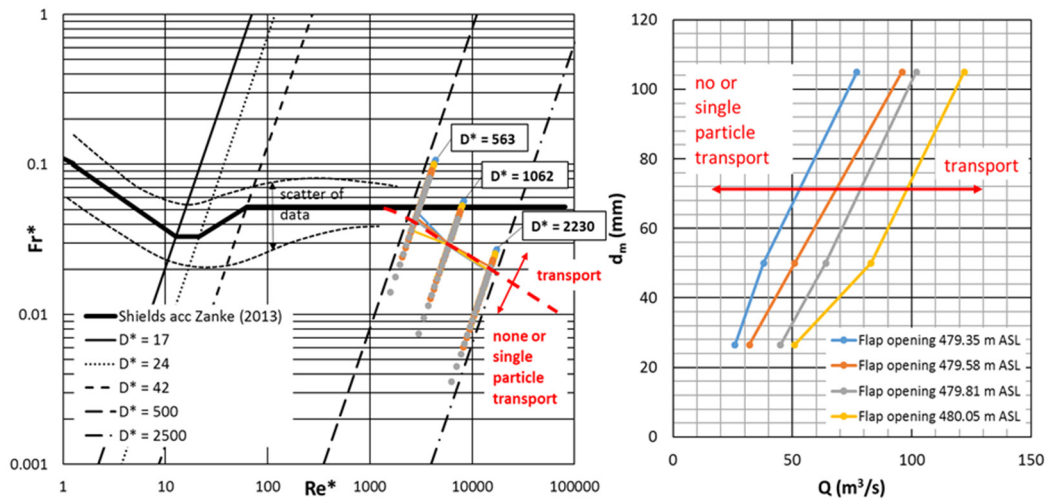


Figure 14. Results of model investigation on sediment transport at the Weir Mondsee.

5. Conclusions

It could be revealed that the weir capacity matched the expected capacity quite well; however, the hydraulic losses between the lake and the weir structure were decisive. The pre-release (drawdown) of the lake at normal water table condition is so far very limited or even impossible due to capacity constraints. An increase of the release reach capacity (connection channel between the lake and the weir) was thus identified to be the most effective measure for any improvement of the outlet system. Moreover, tests on sediment

incipient motion were carried out on the physical model to assess the bed stability and sediment transport in case of a pre-release (weir flushing). Hence, few points were determined and placed in the Shields diagram respecting specific conditions at the outlet of the Lake Mondsee. For instance, if grain size of 30 mm and flap opening 479.90 m ASL were considered, sediment transport through the weir starts at about 50 m³/s. Stones 90-100 mm big get over the weir at flood discharge 100 m³/s and the same weir opening. In case of lower flap opening (479.45 m ASL) the threshold shifts down by about 30 m³/s for the same particle size. More details including also results from hydrologic modelling can be found in [8].

Acknowledgements

The authors thank to the municipality of Mondsee for the research project award. The financial support by the Austrian Federal Ministry for Digital and Economic Affairs and the National Foundation of Research, Technology and Development of Austria is gratefully acknowledged. The authors also thank the Equipment BOKU Vienna Institute of BioTechnology-GMBH and the City of Vienna for the equipment support.

References:

- [1] Weinberger, P. (1994): Prüfbericht über die Untersuchung zur Einhaltung der Wehrbetriebsordnung des Mondseeklauswehrs (im Auftrag von Wasserverband Mondseeklaus). (Engl.: Inspection Report on Compliance with The Mondsee Weir Regulations.)
- [2] ISO 748 (2007): International Organization for Standardization. Measurement of liquid flow in open channels—Velocity-area methods.
- [3] ISO/TR 24578 (2018). International Organization for Standardization, Technical Report. Hydrometry - Acoustic Doppler profiler - Method and application for measurement of flow in open channels.
- [4] Fehr, R. (1987): Einfache Bestimmung der Korngrößenverteilung von Geschiebematerial mit Hilfe der Linienzahlanalyse. Schweizer Ingenieur und Architekt, 105. Heft 38. (Engl.: A simple determination of the sediment grain size distribution using the line count analysis.)
- [5] Novak, P., Guinot, V., Jeffrey, A. & Reeve, D. (2010): Hydraulic Modelling: An Introduction. London: CRC Press.
- [6] Ruck, B. (1987): Laser-Doppler-Anemometrie. AT Fachverlag Stuttgart. ISBN: 3-921-681-00-6
- [7] <http://www.hec.usace.army.mil/>; Hec-Ras Manuals, 2018
- [8] Habersack, H., Sindelar, C., Holzmann, H. & Lichtneger, P. (2018). Machbarkeitsstudie Wehrordnung Mondseeklaus; Phase I; Endbericht. Customer Report. Institute of Hydraulic Engineering and River Research, University of Natural Resources and Life Sciences.

POLYMERIC GEOMEMBRANES IN NEW ROCKFILL DAMS: 2 CASE HISTORIES

GABRIELLA VASCHETTI¹, VANJA VERDEL², ALBERTO SCUERO³

¹ *Carpi Tech, Switzerland, gabriella.vaschetti@carpitech.com*

² *Verdel Consulting, Slovenia, vanja.verdel@gmail.com*

³ *Carpi Group, Switzerland, alberto.scuero@carpitech.com*

1. Abstract

Polymeric geomembrane systems are since 1959 a safe, cost-effective, long-term waterproofing solution for new and existing dams. The paper discusses design, technical benefits and installation through two projects: Runcu 91 m high rockfill dam in Romania, with exposed geomembrane system substituting the concrete facing originally planned, and Zarema May Day 152 m high rockfill dam in Ethiopia, with covered geomembrane for the 15 meters of dam raise, in lieu of the bituminous core waterproofing the lower part of the dam. In both cases, the geomembrane system allowed reducing construction times and costs.

Keywords: waterproofing, dams, polymeric, geomembrane, geocomposite, sustainability.

2. Introduction

In a world with increasing needs for water and power, where climate changes may cause dramatic scarcity of water or dangerous extreme floods, dams are precious and crucial infrastructures to retain water for times of scarcity, to control water when it is in excess, and to produce power. Dams and appurtenant structures must be adequately designed and constructed, and then maintained over time to ensure their safe operation.

This paper focuses on rockfill dams that, being pervious, need a water barrier to prevent water filtration in the dam body. The barrier can be internal or upstream. Upstream water barriers have several advantages related to static and dynamic stability of the dam, to the possibility of staged construction, to maximised construction rate, and to easy accessibility for maintenance and repair of the water barrier. Traditional upstream water barriers are reinforced concrete slabs to construct what is known as a CFRD (Concrete Face Rockfill Dam), or asphalt concrete facings, to construct an ACFRD (Asphalt Concrete Facing Rockfill Dam), and, to a lesser extent, steel and wood.

In CFRDs leakage can occur through the joints or through defects in the concrete slabs. The perimeter joint is very critical and has received a great deal of attention by designers [1]. Current design foresees multiple layers of waterstops and, in some projects, a pocket of cohesionless silt or fly-ash placed over the top of the perimeter joint, which in case of

failure of the waterstop will migrate into the joint. Besides the failure of the perimeter joint, potential sources of leakage are excessive openings of the tension vertical joints or spalling at the compression vertical and horizontal joints, and cracking in the concrete slabs due to shrinkage, excessive deformations in the embankment, differential movements, problematic foundations, seismic events. Also in ACFDs major failures are related to the connection between the embankment and the concrete plinth, and to deformations of the embankment. Structural defects during service include blisters, cracking, slump and bulges related to construction, when the impervious layer is placed in more than one course. Problems associated with bitumen are stripping and instability on the slope, which can result from creep due to a too high bitumen content. In a bituminous mix, the strain at failure increases with temperature and decreases with an increase in the rate of deformation. Important temperature changes can reverse the strains and result in fatigue cracking. Bituminous concrete is subject to ageing, which can be driven by temperature and UV radiation.

The performance of these traditional water barriers may therefore in the long term not be as good as planned. Large deformations, joints ruptures, cracking of the concrete slabs in CFRDs, and the increasing rates of water losses in ACFRDs, have driven the development of flexible and deformable facings: the deformability of geomembranes and composite geomembranes, and the possibility of creating a continuous facing by watertight welding, appeared promising to survive the deformations of the embankments. Geomembranes, factory-produced with pre-established constant characteristics engineered to resist service loads and environmental aggression, and with permeability a couple of orders of magnitude lower than traditional water barriers, became in the middle of the last century a technically effective alternative to overcome the drawbacks of CFRDs and ACFRDs. Additional assets are permanent availability in the needed quality and quantity, possibility of designing systems that can be installed in stages, providing flood protection and allowing early impoundment, ease of transport, and low environmental impact of site organisation and construction, which make them a highly sustainable system.

Geomembranes have been used in rockfill dams since 1959, when a geomembrane was adopted at Contrada Sabetta rockfill dam in Italy. The geomembrane was part of the dam design and was covered, as in pioneer projects of the following decade. When manufacturing processes became more sophisticated and high-performance products became available, geomembranes were applied also in exposed position. In more than half a century, the design of geomembrane systems and their properties and performance have evolved, and they are now widely used in new construction of embankment and RCC dams, and in rehabilitation of all types of dams [2].

3. Methods

Adopting an exposed or a covered geomembrane system is a design choice. An exposed geomembrane has several advantages when compared to a covered geomembrane: the potential damages deriving from installation of any cover are avoided, the construction time and costs are minimised, and during operation it can be fully and directly inspected and if needed easily repaired, even underwater. The choice of covering the

geomembrane, partially or totally, is generally dictated by site-specific constraints, such as the possibility of large rocks falling from steep abutments, or realistic concern for wilful damage, or large fires, or for aesthetical reasons. It is to be noted that the trend is towards exposed geomembranes.

Exposed geomembrane systems require the geomembrane to be anchored to the dam face against uplift by wind and waves. Early attempts of anchorage at points were made using strips of a polymeric geomembrane embedded in the embankment and left hanging on the upstream face of the dam. The waterproofing geomembrane, unrolled over the dam face, was then heat-seamed over the protruding anchorage strips. Anchorage at points can also be done with deep earth anchors. In presence of high uplift loads, close spacing between the anchor points is needed to have the geomembrane laid flat over the subgrade and optimise its performance. A geomembrane system taut to the dam face can be more effectively obtained with continuous anchorage lines embedded in the embankment. The waterproofing geomembrane is tensioned between adjacent anchorage lines and heat-seamed to them. The anchorage lines, made of the same geomembrane material as the facing, can be embedded in trenches or in extruded curbs of low cement content concrete. The latter gathers the concept of the Itá method. The case history of Runcu rockfill dam that follows describes both methods.

In covered systems, the upstream geomembrane is anchored against uplift by the ballasting action of the cover layer. The cover layer can consist of unreinforced and cast-in-situ 0.2-0.3 m thick concrete slabs (Bovilla rockfill dam, Albania 1996), or light concrete slabs as successfully adopted at Zarema May Day dam described in the second case history, or a shotcrete layer (abutments of Bulga earthfill dam, Australia 2016). Where “natural” appearance was required, cover layers with large stones (Aubert rockfill dam, France 2010), or geocells filled with compacted soil and vegetated (Romentino reservoir, Italy 1992) have been adopted.

Regardless of the anchorage system, the waterproofing polymer liner is a composite membrane (geocomposite) formed by a geomembrane formulated with a special compound of polyvinylchloride plasticised with high molecular weight branched plasticisers. The geomembrane is laminated during fabrication to a backing geotextile that enhances tensile characteristics and provides anti-puncture protection, increased stability on inclined slopes, and some drainage capability.

3.1 Exposed geomembrane system: Runcu, Romania

Runcu is a 91m high rockfill dam in Romania, owned by Cris Water Administration, which will be used for water supply and irrigation. After construction had already started, the original CFRD design was modified to incorporate an exposed geomembrane, instead of the concrete facing, to construct a GFRD. The reasons for changing the design were related to particularly long construction times required for the support layer of the slabs and for the slabs themselves, and because of the high costs involved with the CFRD design. The solution with concrete slabs would have cost about 130% more than the solution with the geomembrane facing, because it involved constructing three different zones of granular material, made on site, as support for the slabs. The final design of the waterproofing system was developed by SC Sembenelli Consulting of Italy in association with Carpi.

The dam is a homogeneous rockfill placed in 1.5 m high compacted lifts, with quite a steep (1.4H / 1V) upstream face. The original design foresaw an about 5 m thick Zone 2 (5 to 250 mm) layer placed on the fill, followed by an about 5 m thick Zone 1 (5 to 90 mm) layer, and by a porous concrete layer acting as support for the concrete slabs. The dam was to be constructed in phases, a first phase up to elevation +681 m, a second phase up to +710 m which would allow partial operation of the dam to a water level of +700 m, and then the third phase up to crest, at elevation 736 m. When the design was modified to a GFRD, the embankment had already been constructed up to elevation +681 m, with a 0.2 m thick layer of sand and gravel placed on top of Zone 1. The design of the new waterproofing system had to adapt to the existing situation. It was decided that up to elevation +686.50 m the dam would be constructed according to the original design, while from elevation +686.50 m up to crest the Zone 1 and Zone 2 layers would be eliminated. The face would be formed by porous concrete curbs extruded by a curb extruder, placed on the fill.

The design concept for the face anchorage system of the GSS is the same for the whole dam, i.e. it is made by heat-seaming the waterproofing geocomposite liner to geocomposite anchor strips embedded in the dam. The configuration of how the geocomposite anchor strips are secured to the dam is different in the bottom section already constructed (from the plinth to elevation +686.50 m) and having a sand and gravel finishing, and in the section above it, where the face is formed by porous concrete curbs. In the bottom section the anchor strips of SIBELON® geocomposite are placed in vertical trenches excavated in the granular surface at about 12 m spacing and secured to the dam by the ballasting action of a lean concrete backfill, as outlined in Figure 1 at left. The waterproofing SIBELON® geocomposite is then seamed upon the securely fastened strips, as outlined in Figure 1 at right. From elevation +686.50 m up to crest, the Zone 1 and Zone 2 layers have been eliminated, and the face is formed by porous concrete curbs extruded by a curb extruder; SIBELON® geocomposite anchor strips are placed on each curb at about 6 m spacing, each strip overlapping the one installed on the curb underneath, as outlined in Figure 2 at left. Overlapping anchor strips are heat-seamed together to form a continuous vertical anchorage line, secured to the dam by the ballasting action of the fill placed against the curbs. The waterproofing SIBELON® geocomposite is then seamed upon the vertical anchorage line formed by the securely fastened strips, as outlined in Figure 2 at right.

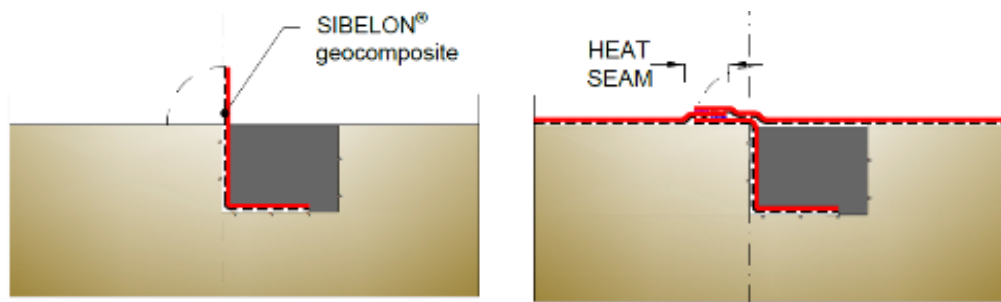


Figure 1. The geocomposite anchor strip is placed and ballasted in the anchorage trench, the SIBELON® geocomposite is then seamed upon the strip

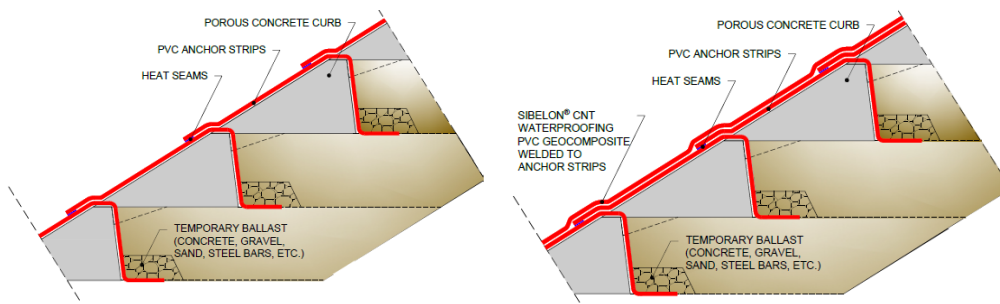


Figure 2. A geocomposite anchor strip is placed on each curb and ballasted by the fill, overlapping strips are heat-seamed horizontally, the SIBELON® geocomposite is deployed and seamed upon the strip

Figure 3 shows in the bottom part of Runcu dam a trench being formed (at right) and the white anchor strip being ballasted with lean concrete in the adjacent trench (at left). In the top section, the facing formed by curbs and the anchor strips secured to the curbs are shown.



Figure 3. Runcu dam: Anchorage lines in the bottom section are by PVC anchor strips embedded in excavated trenches, in the top section by PVC anchor strips secured to extruded curbs forming the face of the embankment

After the anchor strips are securely fastened to the dam body, the waterproofing liner is installed. The liner is the geocomposite SIBELON® CNT 3750, formed by a 2.5 mm thick extruded thermoplastic geomembrane, heat-bonded during fabrication to a 500 g/m² nonwoven, needle punched, polypropylene geotextile. The geocomposite sheets are deployed over the face and permanently anchored to the dam by heat-seaming them to the anchor strips, as shown in Figure 4. Adjacent geocomposite sheets are joined by watertight heat-seaming. All seams are checked for continuity and watertightness with appropriate standards.



Figure 4. Runcu dam: Heat seaming of overlapping anchor strips and of waterproofing liner to anchor strips

At the bottom boundary, the waterproofing system is sealed on the concrete plinth, with a mechanical watertight seal consisting of an 80x8 mm stainless-steel batten strip compressing the geocomposite onto the concrete by anchor bolts secured with chemical phials. A rubber gasket between the geocomposite and the profiles, an epoxy resin layer regularising the concrete, and splice plates at abutting profiles, complete the seal. Watertightness is obtained by the torque exerted at the anchor bolts, which squeezes all components of the seal eliminating even minimal voids that could allow water infiltration (Figure 5).

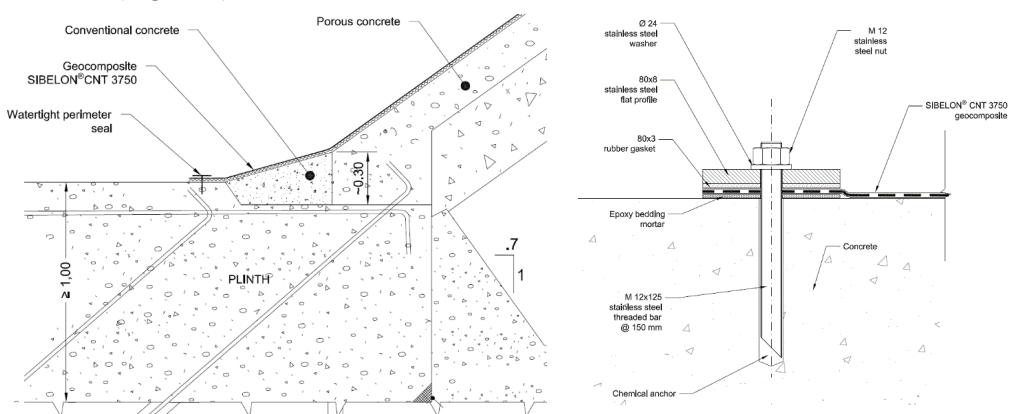


Figure 5. Runcu dam: Bottom seal at plinth

At elevation 681 m, a conventional concrete anchor beam was constructed, where an intermediate horizontal anchorage connecting the geocomposites sheets lining the top and bottom sections was placed. The anchorage consists of a 50x3 mm stainless-steel batten strip compressing the lower geocomposite onto the concrete with mechanical anchors. The top geocomposite overlaps and is heat-seamed horizontally to the lower geocomposite. The seam is covered by a strip of SIBELON® C 3250 geomembrane, identical to the one forming the waterproofing liner, but without backing geotextile, watertight seamed unto the underlying geocomposite.

In 2016 the waterproofing works were completed up elevation 711 m, where a top mechanical seal, similar to the intermediate anchorage but without cover strip, was placed. In 2017, because of economic reasons, the idea of limiting the height of the dam

immediately above elevation 711 m was advanced. Following the technical and economic studies carried out in 2017 and 2018, the idea of limiting the dam's height proved ineffective. Consequently, in 2019, the idea was dismissed, and the embankment works were resumed, including the construction of the porous concrete curbs forming the surface of the upstream face on which the waterproofing geocomposite will be applied. It is estimated that the dam will reach the projected elevation - 736 m - in autumn 2020, which will make it possible to resume the waterproofing works in the spring - summer of 2021.

3.1.1 Covered geomembrane system: Zarema May Day, Ethiopia

Zarema May Day dam is part of a large irrigation project in Ethiopia, aiming to support future export of sugar that will help the country earn hard currency and expedite the industrial revolution it is engaged in. Zarema May Day, which will irrigate a 50 thousand hectares sugar plantation, harnesses the water potential of the Zarima River, in the northern Tigray region of Ethiopia. The designers were ELC-Electroconsult of Italy, the consultants WWSDE-Water Works Design and Supervision Enterprise of Addis Ababa, and the main contractor Sur Construction P.L.C. of Addis Ababa.

The dam is a nearly 152 m high, 900 m long, rockfill embankment with a bituminous core of decreasing thickness, from 1.2 m at the foundation plinth to 0.8 m at top. The dam body is a zoned embankment with volume of around 14 million cubic meters, including a 2 million cubic meters cofferdam forming the upstream toe. The top of the grouting platform is at elevation 802 m, the crest, at elevation 954 m, is 10 m wide.

With the increasing height of the dam, the length of the crest became considerable, and forming the bituminous core in the upper part of the dam entailed long construction times: forming the bituminous core is in itself time consuming, and furthermore during its placement the core must be continuously confined and supported by the filter/transition zone on its sides, which affects the schedule and relevant cost of placement of the fill materials. Additionally, as the construction of the bituminous core must proceed at the same speed of placement of the dam body, a bituminous concrete plant must be available and continuously operational. Any disruption, due to breaking of the bitumen plant or of the finisher, or due to not constant supply of filter material, affects the whole rate of construction of the entire dam body. The main contractor and SC Sembenelli Consulting, who were performing the final design, sought a solution to reduce construction time and to reduce the project cost. Based on their wide experience in the use of synthetic geomembranes, and on the good performance of > 100 large dams where geomembranes had been adopted either as repair measure or for new construction, SC Sembenelli Consulting modified the original design to include a polymeric geomembrane as water barrier. Two different waterproofing systems were adopted: in the bottom 137 meters below elevation 939 m the original design with a bituminous core was retained, while in the 15 meters above elevation 939 m, where a longer crest would have a higher impact on construction time, the waterproofing barrier was moved at the upstream face, so to not interfere with construction of the embankment.

The top 15 meters of the dam are raised starting at the axis of the bituminous core, with a 1V:2H slope, (Figure 6). This position allowed the main contractor constructing the embankment in a quicker and simpler way since there were no constraints caused by an

impervious core placement; the waterproofing contractor could construct the water barrier independently, when the embankment had been completed. The waterproofing liner is the geocomposite SIBELON® CNT 3950, formed by a 2.5 mm thick extruded thermoplastic geomembrane, heat-bonded during fabrication to a 700 g/m² nonwoven, needle punched, polypropylene geotextile. The geocomposite extends from the crest at elevation 954 m down to elevation 939 m. The base layers on which the liner is placed are a 3 m thick layer of sedimentary rocks scalped from a quarry at 0.2 m and compacted in 0.4 m layers, and a finishing layer consisting a 1 m thick bedding made of 0-60 mm alluvial gravel properly compacted in 0.2 m layers and stabilised with cement mortar.

A special watertight connection is designed between the bituminous core and the upstream liner: a small trench excavated at the top of the bituminous core to a depth of minimum 0.5 m embeds a strip of geomembrane, of the same polymer used for the waterproofing liner but modified for contact with bitumen, and the trench is then filled with bituminous mastic. The waterproofing geocomposite is watertight heat-welded to the strip embedded in the bituminous core. At crest, the geocomposite is anchored by embedment into a 0.65 m wide and 0.3 m deep trench excavated in the rockfill embankment and backfilled with compacted red soil.

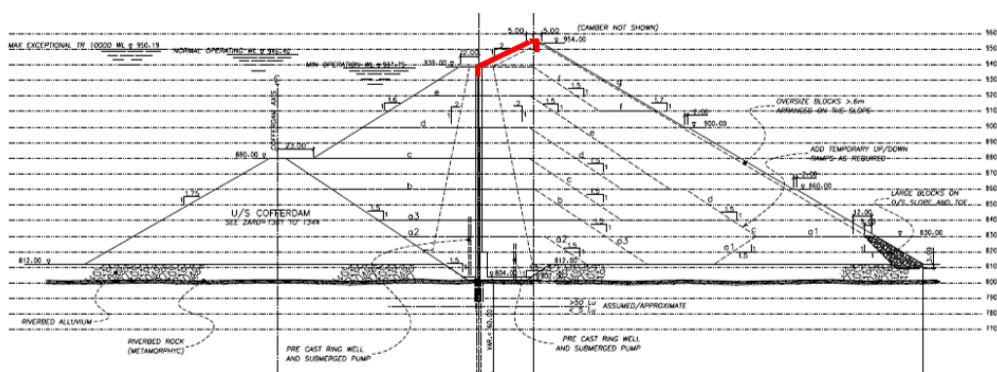


Figure 6. Cross section of Zarema May Day dam: In red, the position of the polymer liner (not to scale)

Due to the absence of the core, the main contractor could complete raising of the top 15 meters of embankment in a much shorter time. Figure 7 at left allows appreciating the fastness at which raising of an embankment without a core can proceed. Installation of the waterproofing polymer liner started on January 25, 2018, with placement of the decoupling film at the abutments, followed by deployment of the waterproofing geocomposite, as shown in Figure 7 at right.



Figure 7. Zarema May Day dam: At left, the sections under (bituminous core) and above (no core) elevation 939. At right, placement and seaming of SIBELON® CNT 3950 geocomposite sheets

The face anchorage system for the waterproofing liner consists of 4 m high x 2 m wide and 0.08 m thick unreinforced concrete slabs, cast-in-place with a staggered pattern. The slabs present alternate joints with the inclusion of three plies of 500 g/m² geotextile nailed in place, to avoid water pressure build-up under the slabs. A 1000 g/m² nonwoven, needle punched, polypropylene decoupling geotextile is placed in between the polymer lining and the concrete slabs. The protective slabs are supported on the horizontal platform at elevation 939 m by means of a 4.5 m wide and 0.25 m thick reinforced concrete toe slab. The slab presents open joints at 10 m spacing and extends 1 m up along the slope.

Installation of the geocomposite was followed by placement of the decoupling geotextile before placement of the unreinforced concrete slabs (Figure 8). The watertight seal at the concrete end-walls at the abutments was mechanical, of the type already described, while anchorage at crest was made in a trench where the waterproofing geocomposite and decoupling geotextile were placed and ballasted with backfill.



Figure 8. Zarema May Day dam: At left, placement of the decoupling geotextile on the waterproofing geocomposite, at right casting of the unreinforced ballast slabs

Installation of about 30,000 m² of watertight facing was completed in seven weeks, in March 2018. Casting of the slabs was completed about two months later, under full responsibility and control of trained and qualified local manpower. The cover slabs, besides providing permanent anchorage, will protect the liner from environmental

aggression and from vandalism.



Figure 9. Works under completion at Zarema May Day dam

4. Results and discussion

Installation of the waterproofing system in both projects proceeded at fast pace, allowing completion according to the established schedule. As planned, there was no interference between the embankment and civil works and the waterproofing works, which proceeded independently. The dams have not yet been impounded, but the successful precedents of both systems adopted allow predicting long safe future performance both for Runcu and for Zarema May Day.

5. Conclusion

Geomembrane sealing systems allow constructing safer and more economic rockfill dams. They are more durable, do not require routine maintenance, and do not interfere with construction of the embankment. Installation of an upstream geomembrane system reduces construction times and avoids possible problems and delays caused by traditional methods such as concrete facings of bituminous cores. Training of local crews can reduce construction costs.

References:

- [1] ICOLD: Concrete Face Rockfill Dams, Bulletin 141, Paris, 2010.
- [2] ICOLD: Geomembrane Sealing Systems for Dams – Design principles and review off experience, Bulletin 135, Paris, 2010.

WAVE TRANSMISSION BELOW BREAKWATERS WITH SEMI-IMMERSED CURTAIN

DALIBOR CAREVIC ¹, DAMJAN BUJAK ², KRISTINA POTOČKI ³, JURAJ DRAŠKOVIĆ⁴

¹University of Zagreb Faculty of Civil Engineering , Croatia, dalibor.carevic@grad.hr

² University of Zagreb Faculty of Civil Engineering , Croatia, damjan.bujak@grad.hr

³ University of Zagreb Faculty of Civil Engineering , Croatia, kristina.potocki@grad.hr

⁴ University of Zagreb Faculty of Civil Engineering , Croatia, juraj.draskovic@student.grad.hr

1. Abstract

Breakwaters with semi-immersed curtains are suitable for locations with low to moderate wave conditions ($H_s \leq 1,2-1,4\text{m}$, $\text{fetch} \leq 5-10\text{km}$). Such structures enable water circulations through the body of breakwater and this way better water quality in closed port basin. The wave transmission through the body of breakwater depends on the curtain immersion, water depth and wave length. Investigations on wave transmission for regular waves have already been conducted and used in engineering practice for years. The lack of the knowledge is about wave transmission for irregular waves which are in their hydrodynamics much closer to the real wind surface waves. This paper gives results of laboratory investigations in wave flume for irregular waves and their comparison to the models developed for regular waves. The paper gives relations between transmission and reflection coefficients, energy losses and transmission of wave periods.

Keywords: permeable breakwater, transmission coefficients, reflection coefficients, semi-immersed curtain, wave period transmission

2. Introduction

City ports and marinas have interest to maintain high seawater quality to attract tourists and give pleasant environment. It can be made a distinction between passive and active measures for the improvement of water quality. The active measures cover forced water circulation by pumps or water aeration where certain amount of energy should be invested. The passive measures cover several types of permeable breakwater structures such as rubble mound breakwater with flushing culverts, breakwaters with semi-immersed curtain and pontoon breakwaters. The wave transmission below breakwaters with semi-immersed curtain will be described hereafter.

To enable better circulation between outer sea and closed water basin of the port engineers used to design openings in the breakwaters' body or even applied the openings along the total breakwater length if wave climate permits such measure. One of the special structural measures is application of the semi-immersed curtain at the whole breakwater length or as just one restricted section. The most important functional parameter of such

structure is transmission of wave energy at the port side of immersed structure.

The transmission coefficient is a function of the following parameters:

$$C_T = f(T_p, L_p, H_s, d, t, H_s/L_p, t/d, t/L_p, d/L_p) \quad \text{eq. 1}$$

T_p – peak wave period [s]

L_p – peak wave length [m]

H_s – significant wave height [m]

d – water depth [m]

t – wall submergence [m]

H_s/L_p – wave steepness [-]

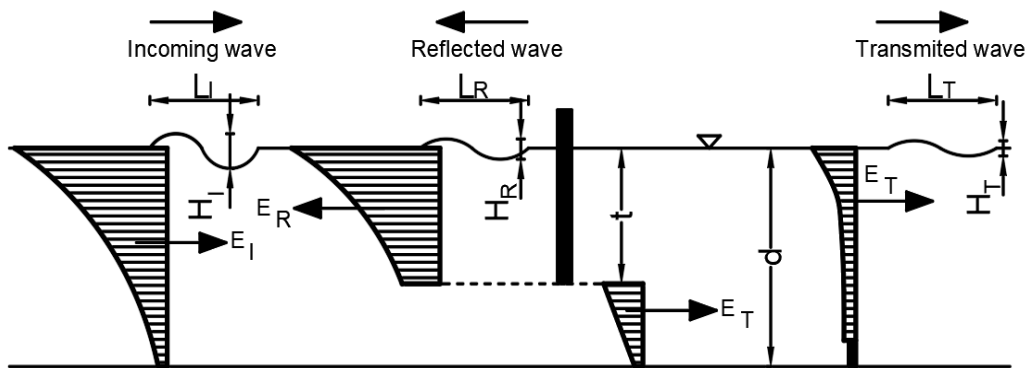


Figure 42 Definition sketch

The energy of the incoming wave (E_I) can be divided into three parts: transmitted energy (E_T), reflected energy (E_R) and the lost energy (E_V). The loss of energy on the immersed wall includes the dissipation of wave energy through internal friction and friction at the boundary between the media (e.g. on the surface of the wall), wave energy dissipation in the process of the wave breaking and energy losses due to the creation of vortex at the bottom edge of the wall.

Direct measurement of energy losses cannot be carried out. Energy losses can only be indirectly determined from the energy balance. Energetic equilibrium for the two-dimensional case of the structure takes the general form:

$$E_I = E_T + E_R + E_V \quad \text{eq. 2}$$

For the energy fraction of the individual parts of the total incoming energy, reformulating the eq. 2. gives:

$$1 = \frac{E_T}{E_I} + \frac{E_R}{E_I} + \frac{E_V}{E_I} \quad \text{eq. 3}$$

By using the first order wave theory, according to eq. 3., proportion of the individual parts of the total incoming energy can be expressed as:

$$C_T^2 = \frac{E_T}{E_I} = \left(\frac{H_T}{H_I}\right)^2 \quad \text{eq. 4}$$

$$C_R^2 = \frac{E_R}{E_I} = \left(\frac{H_R}{H_I}\right)^2 \quad \text{eq. 5}$$

$$C_V^2 = \frac{E_V}{E_I} = \left(\frac{H_V}{H_I}\right)^2 \quad \text{eq. 6}$$

Fictive loss of wave height H_V which is given in eq. 6 combines impacts of previously mentioned energy dissipation processes. Considering these relationships, the balance on the immersed wall reads:

$$1 = C_T^2 + C_R^2 + C_V^2 \quad \text{eq. 7}$$

This follows the term for energy loss E_V/E_I on the immersed wall:

$$E_V/E_I = (1 - C_T^2 - C_R^2) \quad \text{eq. 8}$$

Hoffmann (1967) promoted the Macagano expression for cuboid, which was analyzed as a semi-permeable breakwater. Introduction of an effective length l_e in this equation enabled its use for the immersed wall [1,2]. Therefore, the transmission coefficient takes form of:

$$C_T = \frac{1}{\sqrt{1 + \left(\frac{l_e \cdot \frac{2\pi d}{L} \cdot \sinh \frac{2\pi d}{L}}{2 \cdot \sinh \frac{2\pi d(d-t)}{L}}\right)^2}} \quad \text{eq. 9}$$

As previously explained, the effective length l_e does not apply only to the geometric dimensions of the semi-permeable breakwater, but also to the total energy losses. The parameter l_e/d for the transmission coefficient calculation according to eq. 9 can be found by using graph at Figure 43 [3]. The eq. 9 is valid for the relative water depth $0.10 < d/L < 0.8$, and the immersion ratio of the plate and the water depth $t/d > 0.1$.

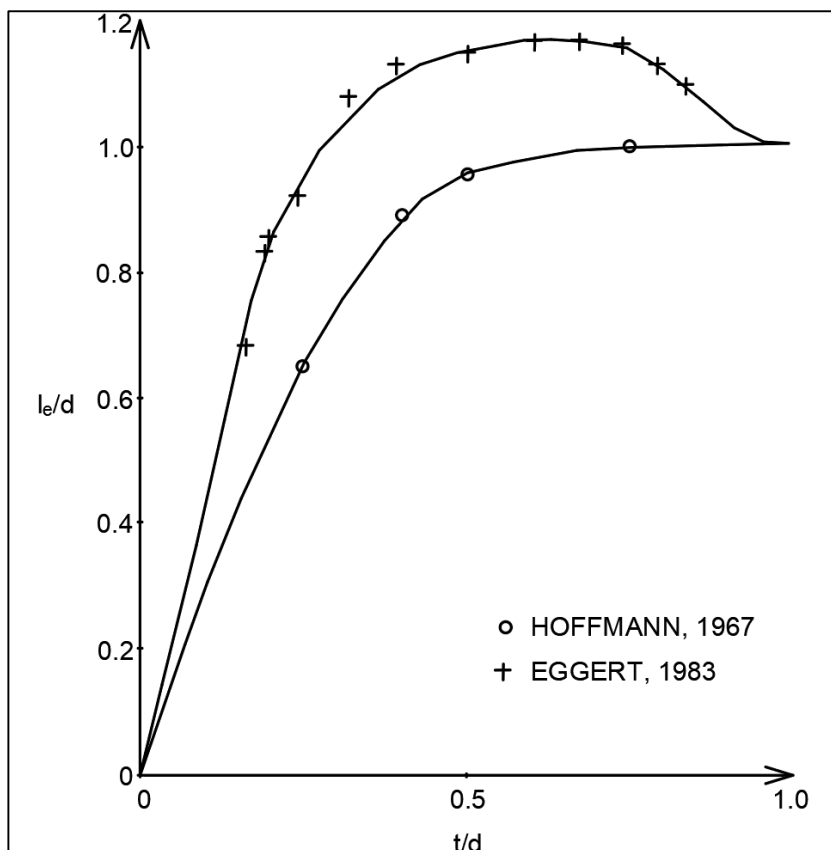


Figure 43. Comparison of the empirical functions for parameter l_e/d according to Eggert 1983 and Hoffman 1967 [1,3]

In Wiegel (1960) a simple analytic expression for the transmission coefficient was defined [4]. The term was given for monochromatic waves, without overtopping, together with the assumption that there is no energy loss (due to friction, the creation of the vortex, etc.) and has the form of:

$$K_{transm} = \sqrt{\frac{\frac{2k(d-t)}{\sinh 2kd} + \frac{\sinh 2k(d-t)}{\sinh 2kd}}{1 + \frac{2kd}{\sinh 2kd}}} \quad \text{eq. 10}$$

where k is a wave number.

The other equations similar to those presented above are developed in the past but are developed only for the monochromatic waves. Equations from Glazik (1969), Schmidt (1980), Pezzoli (1962), Lappo (1962) should be highlighted here [5–8]. The main aim of this paper is to compare measurements conducted for spectral waves and equations originally developed for monochromatic waves by Hoffman (1967) and Wiegel (1960) [1,4].

3. Methods

The wave channel model is located in the Hydraulic Laboratory of the Faculty of Civil Engineering University of Zagreb. The length of the wave channel is 18.64 [m], the width is 1 [m] and the height is 1.1 [m]. The flume has a constant column of water of 0.6 [m]. At 12.51 [m] from the beginning of the wave channel there was the semi-immersed barrier (plate) that can be vertically moved. Tests were carried out for plate immersion of $t = 0.0$ [m]; 0.05 [m]; 0.1 [m]; 0.15 [m]; 0.2 [m]; 0.25 [m]; 0.3 [m]; 0.35 [m]; 0.4 [m].

The waves were produced using a piston type wave generator with the built-in AWACS (ActiveWaveAbsorptionControl System). The electro-hydraulic servo drives the generator plate and generates waves up to $H_s=0.8$ m. The AWACS system can disable unwanted reflection effects from the rear part of the flume. A total of 8 measuring gauges were set up for measurements of water surface movement. The distances of wave gauges from the wave paddle were: G1-5.666_m, G2-6.366_m, G3-6.516_m, G4-6.626, G5-14.946_m, G6-15.646_m, G7-15.796_m, G8-15.906_m.

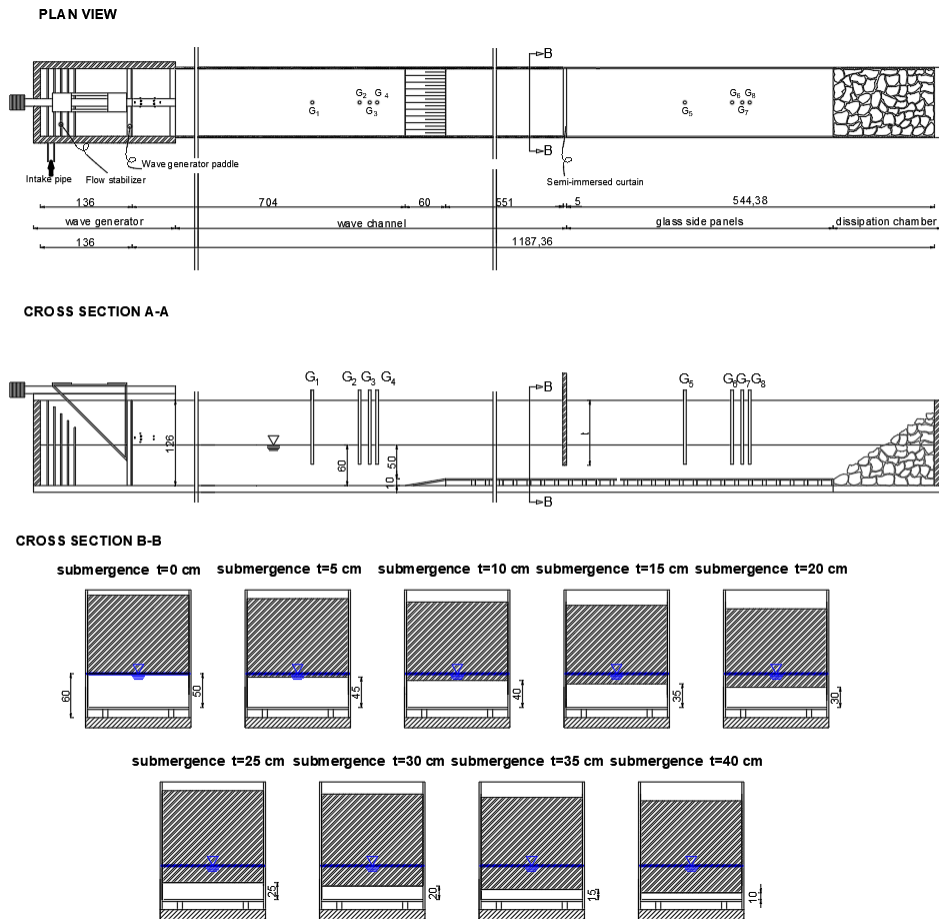


Figure 44. Sketch of the laboratory model

For the spectral (irregular) waves a total of 108 measurements were performed, i.e. 12 for each individual level of wall immersion “t”. Wave parameters of each of the tests are presented in Table 9.

Table 9 List of wave tests conducted in wave flume; H_s -significant wave height T_p -peak period for different submergences $t=0.0$ [m]; 0.05 [m]; 0.1 [m]; 0.15 [m]; 0.2 [m]; 0.25 [m]; 0.3 [m]; 0.35 [m]; 0.4 [m]

	target	
TEST	H_s [m]	T_p [s]
1	0.024	0.73
2	0.024	0.76
3	0.027	0.8
4	0.032	0.83
5	0.042	0.98
6	0.050	1.07
7	0.061	1.21
8	0.074	1.3
9	0.074	1.33
10	0.077	1.36
11	0.095	1.5
12	0.120	1.59

4. Results and discussion

The main question which arises is whether is possible to use empirical equations by Hoffman (eq. 9) and Wiegel (eq. 10), originally developed for monochromatic waves, for estimation of transmission coefficients for spectral waves (real waves in the nature) [1,4]. The comparisons are shown in Figure 45 and Figure 46. In the case of the Wiegel equation the measured values are lower than those calculated, especially in the range of smaller coefficients ($C_{T_theor} < 0.6$) [4]. So it seems that Wiegel equation does overestimates transmission coefficients for spectral waves [4].

In the case of the Hoffman equation, the measured values are lower than those calculated, especially considering the range of the coefficients ($C_{T_theor} > 0.6$) [1]. The similar conclusion should be brought that Hoffman's equation overestimates transmission coefficients for spectral waves [1]. Due to these irregularities of application of these two equations, further in this paper, the new simple approach will be proposed especially developed for spectral waves.

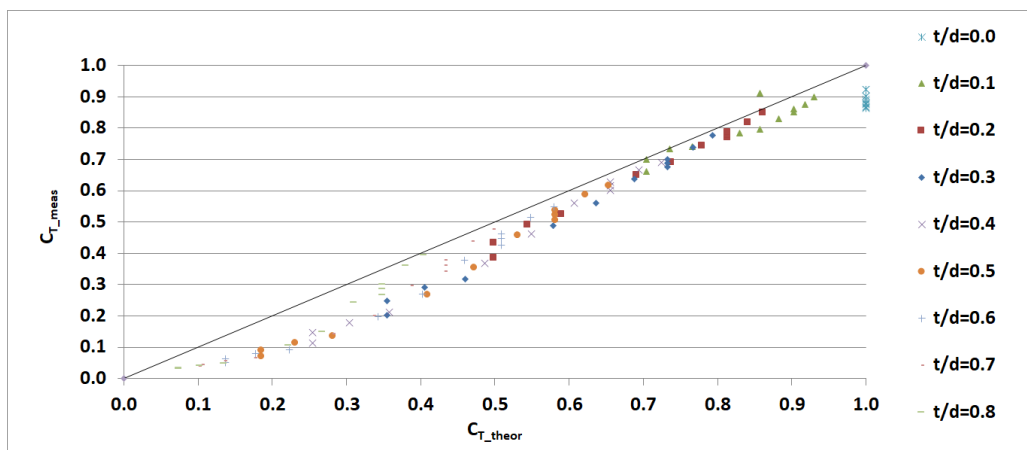


Figure 45. Comparison of the transmission coefficients $C_{T,theor}$ calculated theoretically (by Wiegel equation [4]) and measured transmission coefficients $C_{T,meas}$ in laboratory experiments for spectral waves

It should be noted also that in the case when the plate immersion is $t/d=0$, measured transmission coefficients are $C_{T,meas}=0.9$ what is different than theoretical value calculated by both theoretical equations $C_{T,theor}=1.0$. This difference is caused due to the energy losses produced in interaction between wall and wave crest. Thus, in real conditions, even for ratio $t/d=0$, there is a small amount of energy losses what is neglected by the theoretical equations.

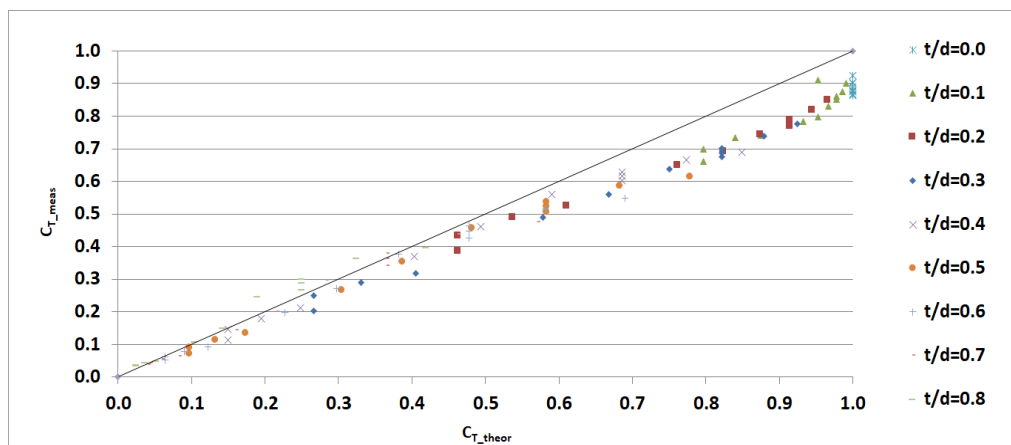


Figure 46. Comparison of the transmission coefficients $C_{T,theor}$ calculated theoretically (by Hoffman equation) and measured transmission coefficients $C_{T,meas}$ in laboratory experiments for spectral waves

According to eq. 2 there should be energy balance achieved when waves pass below the immersed plate. The comparison presented on Figure 47 show relation between measured values of transmission and reflection coefficients. The trend of data reflects clear relationship which is supported by energy balance equation (eq. 2). For the comparison, the theoretical curve of relation between C_R and C_T calculated according to eq. 7 is also presented on the graph. The theoretical curve is given taking an assumption

that energy losses are zero ($E_V/E_I = 0$).

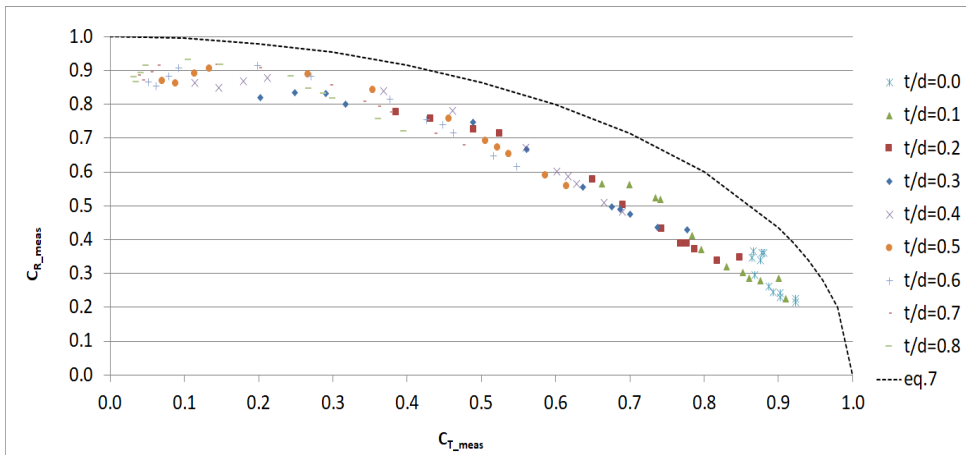


Figure 47. Comparison of the measured reflection coefficients C_{R_meas} and measured transmission coefficients C_{T_meas}

The magnitude of energy losses E_V/E_I on the immersed plate can be calculated by eq. 8 using measured data of reflected and transmitted coefficients. Values of energy losses are presented at Figure 48. In the range of small parameters $t/L_p < 0.1$ the energy losses E_V/E_I monotonically increase up to the value of 0.3 and after that each curve (for different t/d parameter) have different variation in relation to parameter t/L_p . Average value of energy losses is $(E_V/E_I)_{average} = 0.22$.

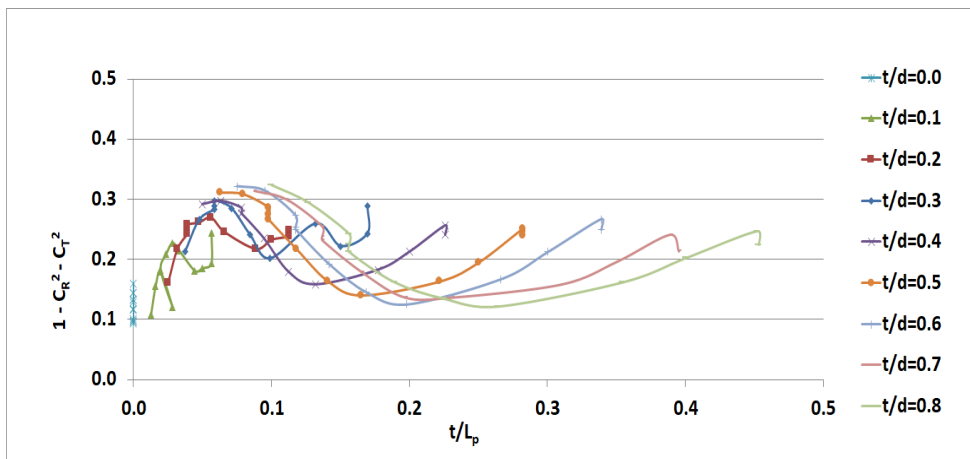


Figure 48. Energy losses values E_V/E_I calculated from measured values of reflected C_{T_meas} and transmitted C_{R_meas} coefficients

In the next section the new empirical approach will be presented for calculation of the transmission coefficient C_T in the case of spectral waves. Hoffman's (eq. 9) and Wiegel's (eq. 10) equations have been developed based on theoretical approach and validated through the experimental measurements presented in Eggert et al 1983 [1,3,4]. In the same work the relation between measured transmission coefficients C_{T_meas} and parameter t/L was investigated for monochromatic waves (from different authors

Hoffman, Glazik and Eggert) [1,3,5]. Generally, conclusion was that dispersion of data is large and that parameter t/L , singly, could not be used for description of the C_T . Eggert (1983) also concluded that C_T should be described exclusively with parameters d/L and d/t [3]. Comparison of C_{T_meas} and t/L_p is once again compared but for spectral waves measured in the scope of this research. The results are shown in Figure 49. Together with measured data the exponential empirical function fitted to the measured data is presented at the same graph. The dispersion of the data relative to the fitted curve is relatively small what is proved by high parameter $R^2=0.9826$ what means that curve describes measured data well. It should be noted that curve is valid up to the value of $C_T=0.9$ as this is a maximal (in average) recorded transmission coefficient for $t/L_p=0$. For comparison the curves which describes mean C_T for channel measurements with monochromatic waves, published by Hoffman, Glazik and Eggert are presented in Figure 49 [1,3,5].

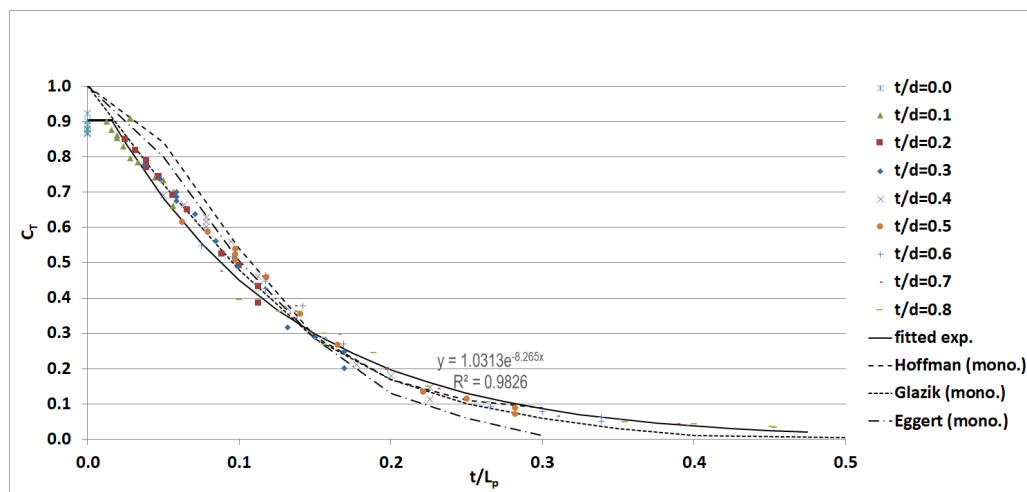


Figure 49. Dependence of the measured transmission coefficients C_{T_meas} to the ratio of the wall submergence t and peak wave length L_p

It can be concluded that wave transmission below immersed plate, for irregular (spectral) waves can be estimated using empirical equation:

$$C_T = 1.03 \cdot e^{-8.27(t/L_p)} \quad \text{eq. 11}$$

The range of the equation validity is: $0 \leq C_T \leq 0.9$; $0 \leq t/d \leq 0.8$; $0.016 \leq t/L_p \leq 0.45$; $0.13 \leq t/L_p \leq 0.57$;

Once the empirical equation for transmission coefficient is defined it is possible to define empirical equation for reflection coefficient C_R by using eq. 7 and mean value of energy loss coefficient $C_V^2=0.22$. The resulted curve is presented in Figure 50 together with the results of C_R measured in the scope of this research. It should be noted that the lowest value of reflection coefficient given by this empirical approach is $C_R=0.30$.

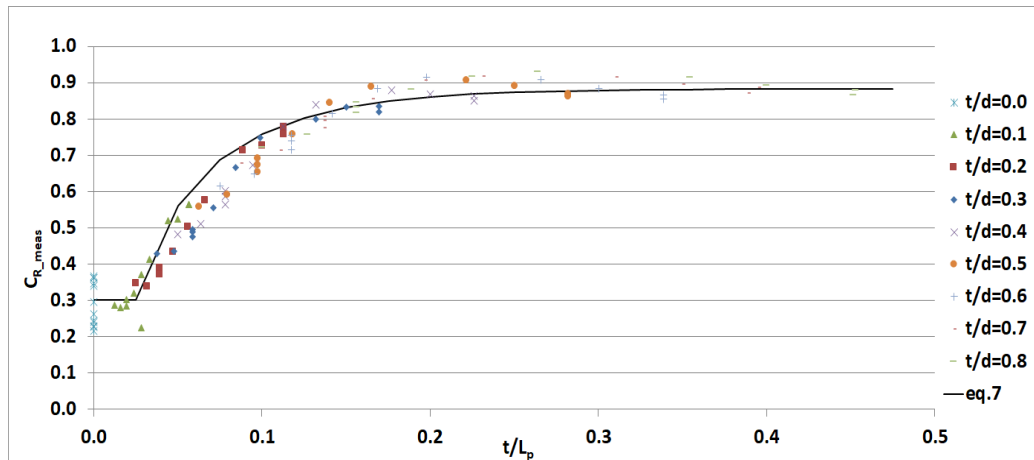


Figure 50. Dependence of the measured reflection coefficients $C_{R,meas}$ to the ratio of the plate submergence t and peak wave length L_p

In some engineering situations it is practical to have available information about transmitted wave periods. For this purpose, the measured ratio of transmitted and incident peak wave periods ($T_{p,T}/T_{p,I}$) is presented in Figure 51. From measured data it is obvious that increase of the transmitted wave periods occur in comparison to the incident one for larger ratios of t/L_p and equals in maximum 1.41. This shift of transmitted peak wave periods likely occurs due to resistances to the water flow below immersed plate and are manifested as a separation of the water vortexes.

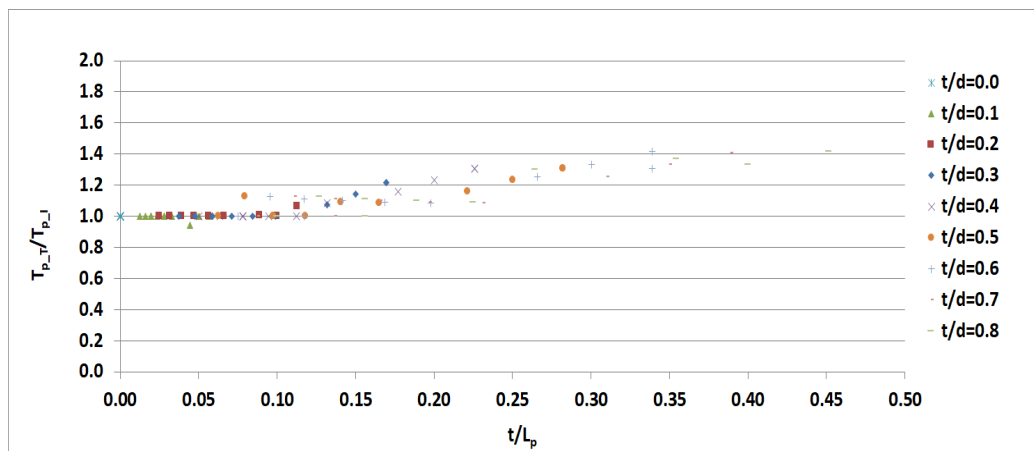


Figure 51. Change of the peak wave period ratio $T_{p,T}/T_{p,I}$ in comparison to the ratio t/L_p

The second important parameter related to wave periods is the ratio of mean transmitted period $T_{0,2,T}$ and mean incident wave period $T_{0,2,I}$. From the results presented at Figure 52, the change of parameter $T_{0,2,T}/T_{0,2,I}$ in relation to parameter t/L_p is visible. It seems that transmitted mean wave periods are larger than incident, when $t/L_p < 0.3$. This phenomenon likely occurs because, for some submergence of the plate t , shorter waves from the wave train (with smaller value of wavelength L) reflect from the plate what means that only longer waves pass below the plate and cause generally longer wave field (with greater $T_{0,2,T}$). For the ratios $t/L_p > 0.3$ this effect diminishes, and only occur

transmission of waves with smaller $T_{0,2,T}$ than incident $T_{0,2,I}$ as a result of vortexes separation from the end of the plate.

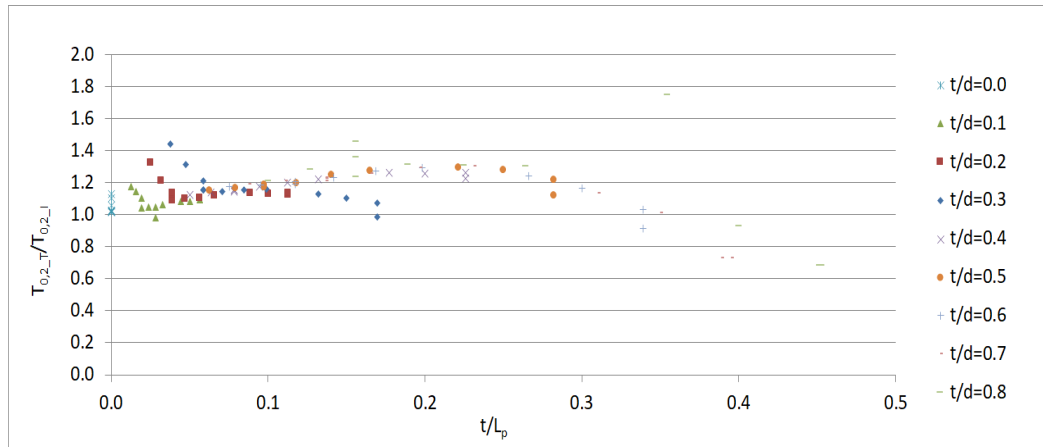


Figure 52. Change of the mean wave period ratio $T_{0,2,T}/T_{0,2,I}$ in comparison to the ratio t/L_p

5. Conclusion

Structures of permeable breakwaters are traditionally used in the seas with poor water circulation and low tidal oscillations range. One of commonly used structures is permeable breakwater with semi-immersed concrete curtain. Until now, the transmission of wave energy below the immersed plate has been investigated but only for monochromatic waves. In this paper, the wave transmission below immersed plate was investigated for spectral waves. Based on the measurements in wave channel results of wave transmission, reflection and energy losses are shown. The comparison of previously developed equations for monochromatic waves and measured waves is provided. The general conclusion is that the existing equations developed for monochromatic waves overestimate transmission coefficients for spectral waves. The new empirical equation was developed, based on measurements in wave channel, for the estimation of transmission coefficients C_T in the case of spectral waves. Also, model for estimation of reflection coefficient is developed and recommendations for transmitted wave periods estimation are given.

References:

- [3] Hoffmann H.J.: Ein Beitrag zur Ermittlung des Wellendruckgangs unter einer Tauchwand und der Wellenkraft auf dieselbe. Mitteilungen Des Instituts Fur Wasserbau Und Wasserwirtschaft Der Tech. Univ. Berlin. 64. 1967.
- [4] Macagno O.E.: Houle dans un canal present un passage au charge. Rev. e'ingenieur Hydraul. 1 1954.
- [5] Eggert W., Daemrich K.F., Grabe W., Partenscky H.W., Passlack G., Grabe W.: Diffraction and wave transfer through submersible structures. Published in the self-publishing of the Franzius Institute for Water Construction and Coastal Engineers University of Hanover. Hanover. 1983.
- [6] Wiegel R.L.: Transmission of Waves Past a Rigid Vertical Thin Barrier. J. Waterw. Hourbours Div. 86. 1960.

- [7] Glazik G.: Wirkung und Anwendung durchbrochene Molen und Wellenbrecher. Mitteilungen Der Forschungsanstalt Fur Schiffahrt. Wasser- Und Grundbau. 1969.
- [8] Schmidt R.: Modellversuche fur eine doppelwandige Tauchwandkonstruktion. Diplomarbeit am Lehrstuhl fur Verkehrswasserbau der Univesitat Hannover. 1980.
- [9] Pezzoli G.: Moti ondosi in profondita variable. L'Energia Ellettrica. 7. 1962.
- [10] Lappo D.D., Kraftwirkung von Schwerewellen auf hydrotechnische Anlagen. Moscow. 1962.

THE WATERWAY DANUBE – MORAVA – VARDAR – AEGEAN SEA, UP TO NOW REMARKS OF THE TECHNICAL DOCUMENTATION

ALEKSANDAR RADEVSKI ¹

¹ BSc Civil Engineer, North Macedonia, aradevski@mt.net.mk

1. Abstract

The idea for construction of the water way (channel) from Danube to Morava and Vardar all to the Aegean Sea is present for almost two centuries. Written records for such water way dates from 1841 from which some only for part of Morava from Danube to Kjuprija. In that period for sailing in Morava and later also in Vardar France shows interest. Such interest is intensified in the future period where as Russia also shows interest with initiative to induce interest for funding in France, as well and England and Germany. Also, there is idea in the funding America to be included. Several studies and designs are prepared in which the technical parameters of the channel are specified: route, hydrological and geological conditions, longitudinal and cross section profiles, structures of the water way and wider, that can contribute for successful operation of the water way and also the technical construction and economic feasibility was proved.

It is especially important that by such water way the distance from Danube to Aegean Sea is reduced for 1.200 km, and also the bottleneck Bosphorus is avoided.

The reactivation and realization of such project for Macedonia will mean and more rapid realization of number of structures – especially dams with reservoirs as part of the Study for integral development of the Vardar/Axios watershed, thus contributing to the successful operation of the water way.

Connected with the European grid of channels and magisterial Rhine - Main - Danube, the water way Danube-Morava-Aegean Sea will have great positive effects not only for the countries it passes through but also for great number of countries in Europe.

Keywords: Vardar, water way, Aegean Sea, economic growth

2. Introduction

Water traffic along river networks and channel constructions, with their convenient economic parameters for transport, especially transport of goods, is imposed as a problem dating from long time ago. As an example, all major rivers on the European continent have been used for sailing and transport of goods in means of their characteristics and the valleys they run through: stable water level and stable water flow, topographical elements etc. In order to increase the advantages and benefits of riverine transport, often artificial channels are built in order to bring closer production centres and interested users to this kind of transport.

In our surrounding, mainly on the Balkan Peninsula, hydrographic, hydrologic,

topographic and other conditions are different than the ones on European land. The only rivers that have the potential of being used for transport of goods are Danube, which is a borderline river on the peninsula, Sava and Drava Rivers. In the second half of the XX century, the Voivodina water system Danube – Tisa - Danube was built and sailing is part of this system's functions.

For a long time now there have been studies related on connecting Danube and Adriatic Sea by water in the north part of Balkan Peninsula. Also, for almost two centuries now there have been present thoughts and studies on connecting Danube with Aegean Sea in order to shorten the water way and reduce pressure on Bosphorus strait. Studies in this area include Danube River, Morava River and Vardar all the way to Aegean Sea. In the past almost two centuries, for this water way lot of technical documentation have been prepared, on different scale, out of which feasibility of this project – water way Danube – Morava – Vardar/Axios – Aegean Sea is elaborated and will be numbered here forward.

3. Water way Danube – Morava – Vardar/Axios – Aegean Sea at Thessaloniki

The idea of connecting Danube with Aegean Sea with one water way that would flow down the valleys of Morava River and Vardar by connecting them through the passage Preshevo and the river valley of Pcinja River dates back from the beginning of 19th century, and is based on geographic and topographic characteristics of the terrain down the valley of Morava River and Vardar. Of course, the starting idea was relying on other segments that are fundamental in water way planning such as hydrology, geology, the possibility of river restoration in function, and others. Also, economy takes great part in the previous mentioned segments. The possibility of connecting Morava River and Vardar through a relatively close passage between South Morava River and Pcinja River through Preshevo passage legitimates this water way of Danube to Thessaloniki and Aegean Sea as technically feasible. Technical documentation dating from the past is quite numbered, had been worked in different periods back in time, nevertheless, it comprises of quite serious elaboration on the topic. Most recently dated is the Study of integral development of the basin of Vardar River/Axios dating from 1978, financed and worked by UNDP program for development at United Nations. In this study, the question of finding enough water for sailing on the Macedonian side is answered and this is also in favour of the feasibility of the water way down the rivers Vardar and Pcinja. In the Study of integral development of the basin of river Vardar/Axios from 1978, technical solutions are given on most dams with reservoirs mainly considering them as multipurpose systems which of course will influence the amount of water flowing in the Vardar River, such as reservoirs on rivers Treska and Crna Reka, however, some reservoirs are directly on the water way or are located nearby in case of possible intervention. In addition, reservoirs Gradec and Veles (Bashino Selo) as well as 12 other smaller ones are directly located in the riverbed of Vardar River. Closely located to the riverbed of Vardar River, i.e. the water way, are reservoirs Vakuf on Kriva Reka just before the confluence with Pcinja River, reservoir Babuna on Babuna River before the confluence with Vardar downstream from Veles and accumulation Jarmularg on Bregalnica River, downstream from Stip. These reservoirs and other on the riverine network in Vardar basin are guaranty of delivering water for sailing in the water day

Danube – Morava – Vardar/Axios in the part through Macedonia and downstream the border with Greece to Aegean Sea. Based on existing documentation I will try to present a real picture of this vast and very significant project for the region and further, especially for Macedonia and Serbia, of course, Greece as well. If we go back in the historic idea to search for more realistic findings on this project to reduce speculation that from time to time appear in different cases, some of which are with negative opinions. Written documents on this, for our region, mega project date back from 1841 and the first documentation in this period is all about Morava River and the confluence of Morava and Danube to Kjuprija where possibilities of sailing on Morava river are suggested to be investigated and this is published in the newspaper ‘Srpske Novine’. Sailing in Morava River in this period attracts attention from French capital, so during the ruling of lord Milosh Obrenovikj a French – Serbian parasailing association on Danube – Sava and Morava. In 1844 a French – Serbian was established and it was connected to the Principal Association for sailing in France that was formed in 1850 with law by the Napoleon III. The question of restoring Morava riverbed for sailing is intensified among engineering circles and the public, in 1856. Some years later, in 1860, the Russian consulate in Belgrade shows interest in sailing on Morava. They manage to impose a wider interest of Russia for natural resources of Serbia including sailing on Morava, for which they succeed to sign a contract the same year. Russian interest is significantly larger for sailing on Morava mainly because of mineral resources in Morava basin. Serbia explores more seriously the possibilities of sailing on Morava back in 1879, but now thoughts and exploration go further towards Vardar and Aegean Sea, so the range of interest is the whole water way from Danube to Aegean Sea nearby Thessaloniki. Some 25 years later, while some activities must have had been done, in 1904 the initiative of water way Danube – Morava – Vardar – Aegean Sea is active again but this time, aside technical documentation, there are more activities into financing this project. Attempts have been made to attract interest in financing this project from England and Germany. Also, there is idea to attract interest in financing this project from America. In New Jersey (USA) in 1907 an American engineering company is established that contracts the Technical Faculty from Belgrade, i.e. professor Nikola Stamenkovic – an established expert in hydraulic structures, to conduct previous and preparation work plans and general plan for the water way Danube – Morava – Vardar – Aegean Sea, named as The Line of European Economy Gravity towards Suez Canal. The reports and the general project for the water way are given to the Serbian and Turkish governments in 1909, but also a request is delivered for concession in constructing the water way. Shortly after these activities in Europe and especially on the Balkan, political insecurities influence the project unfavourably and soon after, Balkan wars start and World War I as well with the largest battle front occurring in Macedonia area right in the river valley of Vardar, so all activities concerning the water way are stopped, an update and continuation followed in 1961.

From all studies and projects for water way Danube – Morava – Vardar/Axios – Aegean Sea, on different technical scale, some are with focus only on Morava River, but are also worth mentioning. In order to have a clear picture, names and time of preparation of the documentation is numbered as follows:

- In 1879 ‘Glasnik srpskog uchenog drushtva’ (eng. ‘Newspaper of Serbian educated society’) published the book ‘Morava – njeno sadashno stanje I

- mogukjnost ploidbeg' (eng. 'Morava – its current state and the sailing possibilities') by author Ante Aleksic – engineering officer, where technical possibilities and economic feasibility of Morava sailing project are introduced.
- In 1909, the professor Nikola Stamenkovic from the Technical Faculty in Belgrade authored a project for water way Danube – Thessaloniki. This is the project that was submitted with concession request from Serbian and Turkish governments.
 - In 1961, a 'Preliminary Design for Water Way Danube – Thessaloniki' was made by 'Proektantski zavod za rechen soobrakaj' (eng. 'Design bureau for river engineering') in Belgrade.
 - Back in that time, a 'Master plan for water resources management for Vardar River basin' is elaborated by the Water resources bureau of SR Macedonia.
 - In 1964, a 'Study on sailing possibilities on Velika, Juzhna and Zapadna Morava Rivers' is done by design bureau 'Ivan Milutinovic' in Belgrade.
 - In the same year, 1964, the 'Institute Jaroslav Cherni' and 'Directive on Morava River basin management' in Belgrade worked on the 'Study of the single water resources system in the basin of River Morava – technical and economy accounts'.
 - In 1971, a 'Water resources master plan for Morava basin' is done by the 'Opshto vodostopansko pretprijatie Morava' and the 'Vodostopanska inzenering organizacija' from Belgrade.
 - In 1973, the 'Design of Water Way Morava – Vardar/Axios – annex to the 1961 design' was made by design bureau 'Ivan Milutinovic' in Belgrade.
 - In the same year 1973 in Belgrade, a report is obtained by the UN named as 'Report on the water way Morava – Vardar/Axios'.
 - For the water way Danube – Aegean sea, the Program for countries in development from the UN, submits a report of the UN mission for the Study of integral development of Vardar/Axios river basin in Skopje, prepared in 1976 by engineers from the National company 'Roang' from France.
 - A Study for integral development of Vardar/Axios river basin is made in 1978 in Sopiye, where only the part of solving water supply for the water way on Macedonian territory is elaborated.
 - A Study for elaboration of master plan for integral development and management of water resources in Republic of Macedonia is made by an expert team of the Japanese agency for international cooperation and this study treats the water way only as a civil structure that needs water.
 - In all these studies and projects a technical feasibility is proven as well as economy feasibility of the realization of this water way. Mainly all technical parameters of the canal are defined: alignment, hydrologic and geologic specifications, longitudinal and cross section profiles, structures on the water way and auxiliary structures of a wider area of the basins of Morava and Vardar/Axios rivers that should complement the restoration and usage of water in both basins. In the end are given basic economic parameters that confirm the feasibility of constructing this water way.

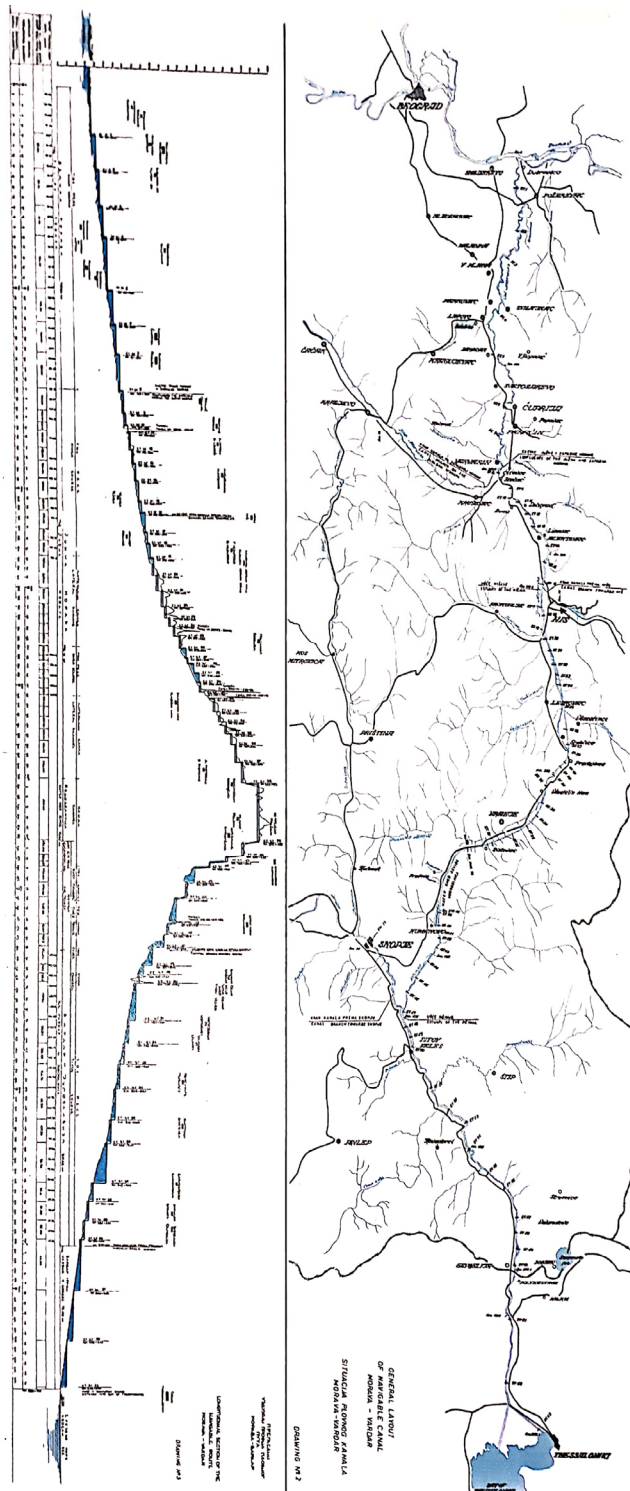


Figure 1. Display of the water way Danube- Morava – Vardar – Aegean Sea.

All these projects, although not completely sufficient of giving a final estimate on the technical solution and economy feasibility of constructing this water way mainly because of the time frame of the date of their making and today, they will serve as solid foundation for further making of more detailed studies and projects that should define the solution in details according to all technical, economy, financial, institutional and law parameters related to constructing this water way. If both Macedonia and Serbia are soon accepted as member countries in the EU, this part might simplify.

Today one can see and feel a certain distance between Danube and Aegean Sea taking under consideration its connection with European river network and its geographic proximity to Aegean Sea. Constructing the water way Morava – Vardar/Axios and its connection to the river network of European magisterial canals through the canal Rhine – Maine – Danube it will serve of great importance for the countries it goes through but also for the countries of west, middle and east Europe. From a geographic aspect and possible sailing route in today's conditions Danube is quite far away from the Mediterranean considering the distance from north to south. From Belgrade, as one of the important segments of sailing on Danube, the length of sailing route on Danube through the Black Sea and Bosphorus to Aegean Sea is 1880 km, while the length of water way from Belgrade to Aegean Sea down the valleys of Morava and Vardar rivers is a little less than 700 km. This data of shortening the water way of 1200 km compared to current route through the Black Sea significantly defines the economic effect of water way Danube – Morava – Vardar/Axios – Aegean Sea and its economy feasibility.

3.1 Hydrologic data of flows in Morava and Vardar basins

In today's conditions with natural flows in both basins, sailing is possible only on a short length on Morava River, just before the confluence with Danube, yet still with limited conditions. On the other part of the water way Morava – Vardar/Axios sailing is not possible in current conditions and aside the unfavourable topographic conditions, main disadvantage is the inconsistent hydrologic regime during the year and drought periods. Based on master plans for both basins and projects for civil structures on both rivers, Morava and Vardar/Axios will significantly change their current natural flow conditions. All these works that are to be constructed will influence in regulation the flow down future water way Morava – Vardar/Axios. Key structures for regulation and improvement of water regime will be reservoirs. With reservoirs a transformation of timely schedule of flow regime and better use of available water in quantity and time will be obtained, and by that – maintaining of sailing water levels. By constructing both reservoirs 'Konchuljg' on Binachka Morava and 'Prohor Pcinski' on Pcinja River, water will be provided for sailing on the route nearby Preshevo.

Basins of Morava and Vardar/Axios take central and south part of Balkan Peninsula. The Morava basin is under the influence of moderate continental and continental climate, whereas major part of Vardar/Axios basin is under the influence of Mediterranean climate.

Total annual precipitation in the basins of Morava and Vardar/Axios are approximately 550 – 1300 mm, or, average annual precipitation can be accounted for 600 – 800 mm (this data is from the period when projects and studies were worked on).

Characteristic flow data for Morava and Vardar/Axios rivers, as prospective routes for

the future water way, adopted back in the time, are as follows:

- Velika Morava river, at Ljubichevski bridge:
 - o 1/100 year water 3420 m³/c
 - o 1/1 year water 22.9 m³/s
- South Morava river, at Mojsinje:
 - o 1/100 year water 1694 m³/s
 - o 1/1 year water 7.6 m³/s
- Vardar river, at Veles:
 - o 1/100 year water 1600 m³/s
 - o Lowest registered flow 12 m³/s
 - o Average flow, at Gevgelija 154 m³/s

Water needs for sailing in the river channels or in lateral canals are defined in the technical documentation for the water way.

3.2 Technical solution for the water way

The idea of elaborating projects for the water way Danube – Morava – Vardar/Axios – Aegean Sea, then constructing it through Danube and connecting it with channel Rhine – Maine – Danube is to connect and fit in the European network of magisterial sailing channels. The idea is to connect the European network of sailing channels to the Mediterranean under the shortest route by constructing the Morava – Vardar/Axios channel with a canal through Preshevo and Pcija valleys. Considering these conditions and looking at all perspectives of this sailing civil structure, authors of prepared documentation so far have categorized this channel as channel of 4th category that matches the specifications that the channel Rhine – Maine – Danube has, i.e. the classification of sailing routes of international significance in the countries of the European economy chamber.

Main dimensions of the channel are:

- Width of channel at water level 43 m
- Minimal width at bottom level 28 m
- Minimal radius of curves 800 m

These dimensions are given as minimal values for sections of the canal that are solved as lateral canals. At sections of the route where the water way passes through the natural and regulated river bed of Morava and Vardar/Axios rivers, the width and depth of the water way are significantly larger. While defining the alignment of the route, it is better to maximally use the natural river beds of both rivers with some technical moderations for sailing, and where it is not possible or for other reasons it is better to predict and plan lateral canals that are diverted from the river. At sections where lateral canals serve for sailing, natural river bed serves as a recipient of large and flood water, waste water and water for irrigation needs.

Total length of the route of water way Morava – Vardar/Axios (according to the technical solution) is 650.1 km. The beginning is the confluence of Velika Morava to Danube River close to Smederevo (approximately 50 km downstream from Belgrade). From here, the canal goes down the river valley of Velika Morava to Stalakj, and then continues down the river valley of Juzhna Morava. Preshevo is the water divide. Between Morava and Vardar, where a special solution is predicted, the water continues south

down the valleys of Pcinja and Vardar/Axios.

Short summary on the route of water way Morava – Vardar/Axios – Aegean sea is given as follows:

- Total length of the route	650.1 km
- Length of the section in Morava valley	345.74 km
- Length of the section in Vardar valley	274.68 km
- Length of the water divide	29.68 km
- Total length of regulated river bed of Morava, Pcinja and Vardar/Axios	483.60 km
- Total length of lateral canals	166.50 km
- Total numbers of dams	63
o Dams with sluice canals	58
o Dams with ship lifts	5

On the route, 5 tunnels are also predicted.

Other specific civil structures on the water way Danube – Morava – Vardar/Axios – Aegean sea that need to provide continuing and secure sailing, are defined in the technical solution.

Canals for connecting three centres to the corridor of the route, are:

- Zapadna Morava to Kraljevo canal	73 km
- Nishava to Nish canal	15 km
- Pcinja – Vardar – Skopje canal	35 km

According to the calculations made in the technical solution, the mean annual transport capacity of this water way is about 20 million tons/year.

In large number of elaborated studies and projects, the cost of construction of this water way Danube – Morava – Vardar/Axios – Aegean Sea has been calculated and it is about 15 – 16.8 billion dollars. Although the numbers are quite high, compared to the total benefit of this water way, costs are not too high especially if Serbia and Macedonia become member countries of the EU soon and the canal is built as a canal of the European community.

4. Conclusion

1. From all elaborated studies and projects so far, one main and important conclusion results as construction of the water way Morava – Vardar/Axios is technically feasible and economically feasible.
2. Connected to the European network of sailing channels and magisterial route Rhine – Maine – Danube, water way Danube – Morava – Vardar/Axios – Aegean Sea will have positive effects not only for the country it passes through but also for large number of countries in Europe.
3. Shortening the route from Danube to the Aegean sea for 1200 km, i.e. shortening the time of transport, as well as:
 - a. Stimulation, promotion and acceleration of total economic development

- of the region and wider, as well as savings on transport compared to other transportation on land.
- b. Construction, exploitation and maintenance in the water way and ports will influence activities in production of raw materials, means and equipment.
 - c. Increase and improvement of water supply in areas where the water way passes through and benefit that comes from water supply to the residents in neighborhoods and industries, electricity production, water quality improvement with requirements of building waste water treatment stations, as well as retaining flood.
 - d. Significant enlargement of possibilities of employment of people from different professions and raising people's knowledge through contacts and in general by major continuum movement.
 - e. Enlargement of selling extra products from the countries that the canal passes through/
 - f. Enlargement of price and value of land down the route of the water way and larger.

From all above mentioned and many other segments that are contained in the technical documentation, as well as other segments such as economy of countries that the water way passes through, the water way Danube – Morava – Vardar/Axios – Aegean is a civil structure with high benefit and priority in constructing.

CONSTRUCTION OF DAMS AND HYDROPOWERS, AS A MEASURE FOR THE LEVEL OF DEVELOPMENT OF THE STATE

SLAVKO MILEVSKI ¹,

¹ AD ESM, HPP “Crn Drim”, Struga, Employment for dam monitoring at dams and other civil structure in AD ESM, Republic of North Macedonia, slavko.milevski@elem.com.mk

1. Abstract

The role of dams and reservoirs for sustainable development has been widely emphasized and accepted by the international public. Based on comparative studies on aquatic resources per capita, the generation of energy per capita is closely related to a country's HDI (Human Development Index), proposed by the United Nations. Hydropower as the main profit from dams and reservoirs is the best choice for recovering the invested assets compared to other types of energy production. However, dams and reservoirs are also a way to better manage and address the consequences of global climate change.

In the abstract, what is the current situation with the recently built reservoirs and hydropower plants in the Republic of North Macedonia and the impact of the construction of new reservoirs and hydropower plants on the human development index which is an indicator of the development of the country.

Keywords: dam, reservoir, hydropower, sustainable development, socioeconomic development, the Human Development Index (HDI)

2. Introduction

We are witnesses that the world's population is rapidly rising. (Figure 1) shows a population increase in the world.

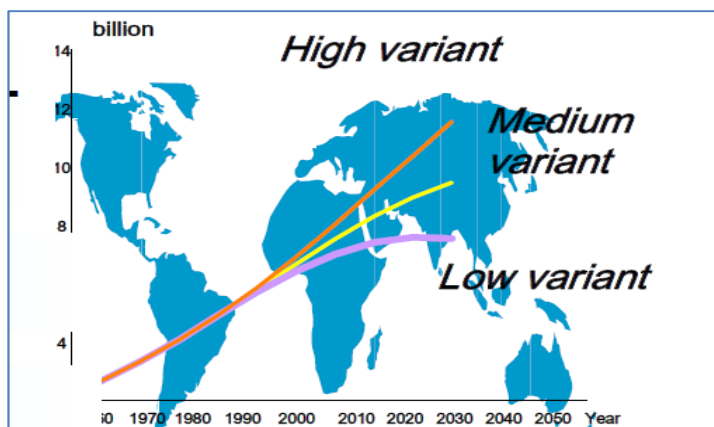


Figure 1: Population growth in the world

The increase in the population of the country also entails an increase in socioeconomic security, provision of safe water and food, increased energy production as well as increased protection and care for the environment, as with the population growth the available quantity of drinking water is also reduced. In Figure 2, the available water per capita in the past and projections for the future.

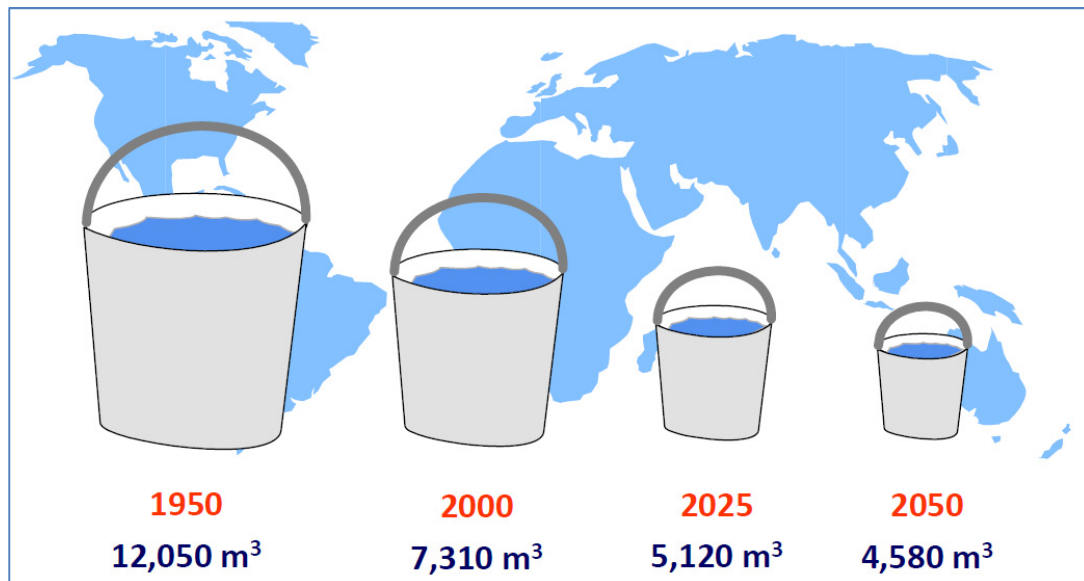


Figure 2: Population growth in the world

From this it is noted that the rational use of water in all aspects will be very important in the future.

3. The role of Hydropowers

Hydropower plants are the best choice for returning the invested funds compared to other power plants.

Multipurpose dams and reservoirs provide protection from drought, flood water supply in rural and urban settlements, sailing, recreation as well as energy supply.

Water reserves are also energy reserves. They play an important role in modern energy systems. Currently, at the global level, hydropower participates with 20% of the total energy production, which is the second generation after the production of energy from fossil fuels (Figure 3).

In Macedonia, hydropower plants give up about 20%, and thermal power plants account for 80% of the domestic electricity.

Compared to various types of energy, hydropower has a high return on money and low ozone-harmful gas emissions that are responsible for global climate change.

Given that in many countries around the world energy is generated from fossil fuel and oil power plants, many countries are looking for ways to replace these capacities with

other energy sources to meet energy needs and reduce greenhouse gas emissions.

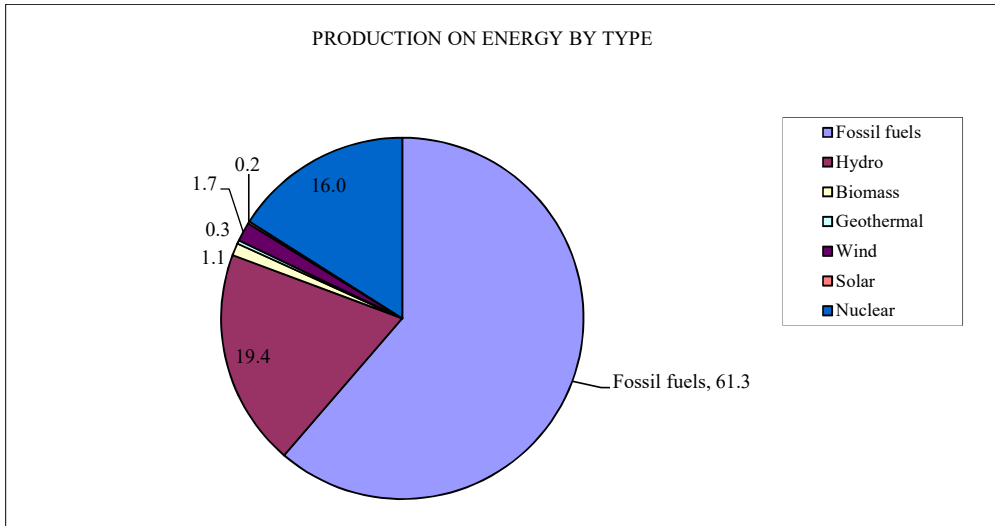


Figure 3: Production of energy by type

One way to compare the various energy options is the use and the re-calculation of the so-called Energy Payback Ratio (Energy Payback Ratio). This coefficient is the ratio of the total energy produced during the whole working life with the money for construction, maintenance and energy needed for energy converted into energy. Higher values of this coefficient indicate good performance.

The percentage of energy returns for different modes of energy development is around: 208-280% for hydropower plants with reservoirs, 170-267% for power plants, 18-34% for wind power plants, 3-5% for biological fuel, 3-6% for solar energy, 14-16% for nuclear energy, 2.5-5.1% for classical thermal power plants and only 1.6-3.3% for thermal power plants (Figure 4).

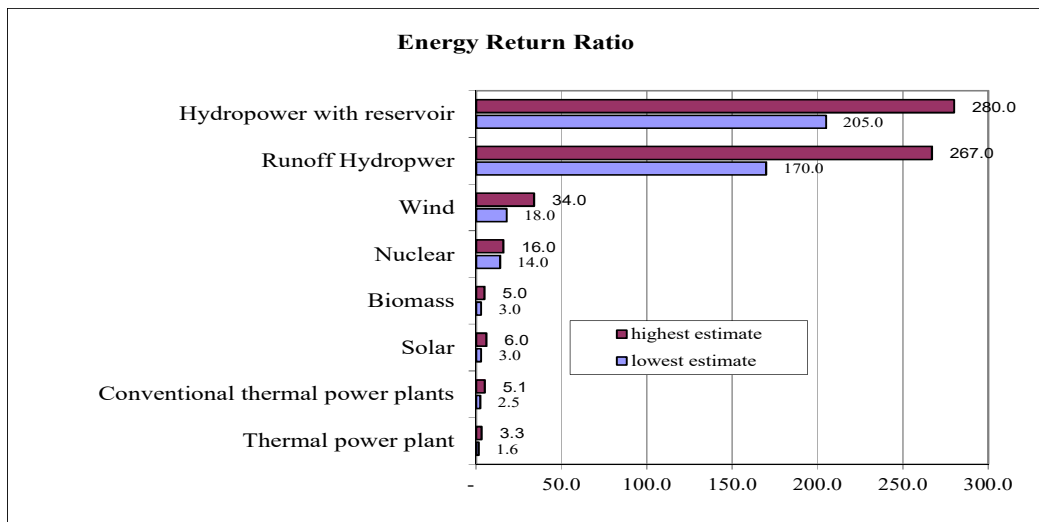


Figure 4: Energy return on investment by type of power plant

Hydropower as a source of energy also has the lowest emissions of ozone-harmful gas (Figure 5).

According to the calculations, the emission of CO₂ per GWh is about 941-1022 tons for classical thermal power plants, 649-787 tons for diesel, 220-300 tons for thermal power plants, 38-121 tons for solar energy, 51-90 tons for energy from biological fuels, 10-33 tons for hydropower, 9-20 tons for wind power plants, 6-16 tons for nuclear power and 3-4 tons for power plants that have the lowest CO₂ emission in terms of GWh.

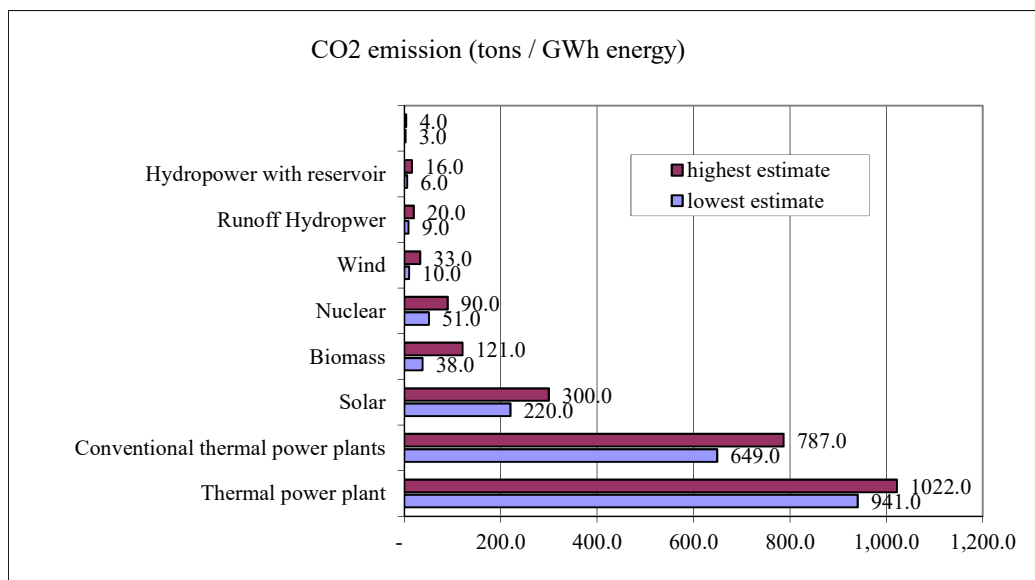


Figure 5. Ozone-harmful emissions by type of power plant

4. Relation between development and hydroelectricity HDI (Human development index)

Dams and hydropower plants are closely related to the socio-economic development of the countries. The International Committee for Large Dams (ICOLD) made a comparison of the volume of reservoirs and the production of hydro energy for the country's inhabitant with the Human Development Index (HDI) in more than 100 countries around the world. The analysis shows that it has a close connection with the socioeconomic development of the country. The results clearly indicate how the development of dams / reservoirs and hydropower is related to socioeconomic development.

HDI is a weighted average of gross national income, health and education in relation to a resident and reflects the quality of human development as a comprehensive index used to measure the level of socioeconomic divergence of member states of the United Nations. The index avoids differences in gross income per inhabitant, and is merely a measure of human development. The following figure 6 is the components that make up the Human Development Index.

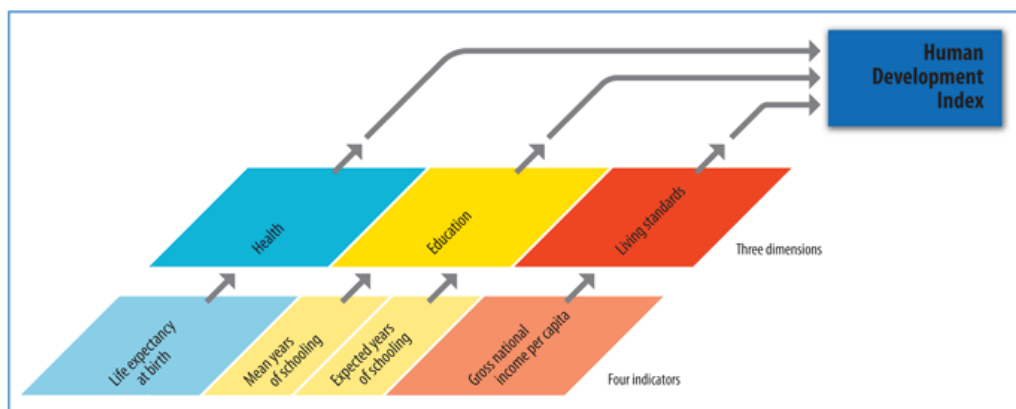


Figure 6: Components of the Human Development Index (HDI)

The HDI index ranges from 0 to 1. The closer to 1 there is a higher level of human development. Countries with high levels of HDI, greater than 0.9 are the most developed countries Australia (0.970), United States (0.956), Great Britain (0.947) Those with HDI between 0.8 and 0.9 are relatively developed. Argentina (0.866), Russia (0.817), Brazil (0.813), while those with HDI less than 0.5 are the least developed Asian and African countries. For example, Rwanda (0.46), Burkina Faso (0.389) and Afghanistan (0.352). Macedonia in 2014 has an index of HDI of 0.747 (<http://hdr.undp.org/en/data#>).

Table 1: HDI index, the volume of the accumulation and the production of energy from hydropower plants per capita

HDI	Volume per accumulation per inhabitant (m ³)	Energy per capita from hydropower plants (kWh)
>0.9	2924	1461
0.8-0.9	2476	982
0.7-0.8	571	350
0.6-0.7	212	106
0.5-0.6	173	86

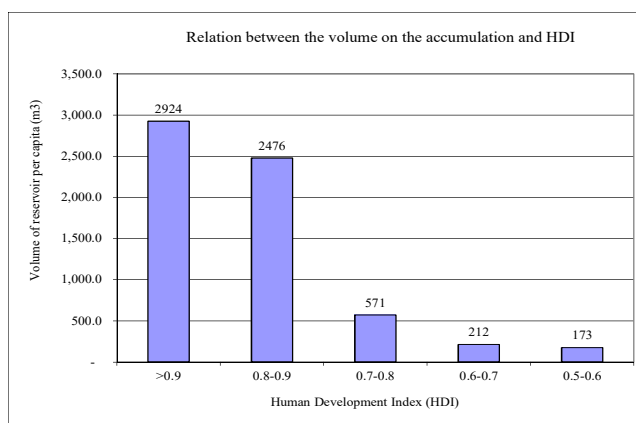


Figure 7: Connection between volume of reservoir per inhabitant and HDI

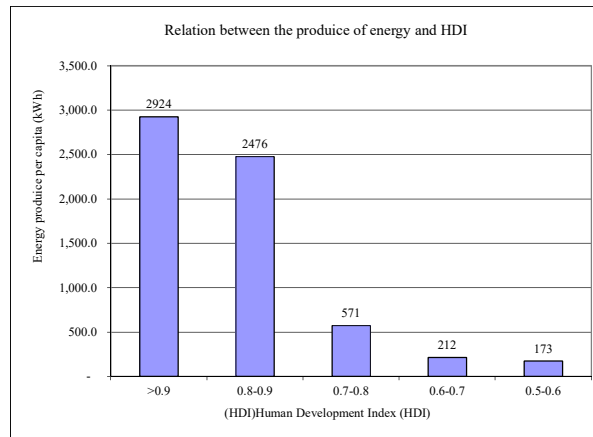


Figure 8: Connection between power generation from hydropower plants per inhabitant and HDI

As can be seen from the previous tables and graphic representations, developed countries have a reliable basis for water supply and energy production by shifting and modifying water resources, while developing countries still have a long way to reach developed and are limited by financial, technical and human resources. With some exceptions, such as Israel with a high HDI of 0.935 per capita, there is a volume of reservoir of 27 m³ per inhabitant, while Zimbabwe with 0.481 HDI has an reservoir volume of 1072 m³ per inhabitant, the level of dam development in the country or region is directly proportional to the Human Development Index HDI. It coincides with the results of the United Nations that the global distribution of water infrastructure is inversely proportional to the global distribution of the risk of water insecurity.

In Macedonia, the total volume of the existing reservoirs is 2447.63 (106 m³) or 244763 million m³, which comes to 1223.82 m³ of water from reservoirs per capita in the Republic of Macedonia, while the average annual production of electricity from hydropower plants in Macedonia is 1200 GWh or 600 kWh per capita electricity from hydroelectrics.

According to this data, it turns Macedonia into the HDI index of approximately 0.750, which responds to the official index of the Republic of Macedonia from 0.747 for 2011.

Table 2: Dams and reservoirs in Macedonia in use (given are those dams that are in the registry of the International Committee for Large Dams ICOLD).

Id.	Name	River	Year of constr.	Type	H	Hs	L	VD	VR	Purpose
					[m]	[m]	[m]	[m ³ ×103]	[m ³ ×106]	
1.	Matka	Treska	1938	AR	29.5	38	64	3	3.55	HEP
2.	Mavrovo	Mavrovska	1952	EAR	54	62	210	777	357	HEP,IR
3.	Lipkovo	Lipkovska	1958	AR	29.5	40	203	13	2.25	IR,WS
4.	Gratce	Kocanska	1959	AR	29	43	150	12	2.4	WS,IR
5.	Mladost	Otovica	1962	AR	27	34	73	2.56	8	IR
6.	Globocica	Crn Drim	1965	E-R	82.5	90	196	998	58	HEP
7.	Vodoca	Vodoca	1965	E-R	4	48.7	185	316.8	26.7	IR,WS

8.	Prilep	Oreovacka	1966	MA	35	38.5	408.5	25.5	6	IR
9.	Tikves	Crna Reka	1968	E-R	104	113.5	338	2722	475	IR,HEP
10.	Kalimanci	Bregalnica	1969	E-R	85	92	240	1389	127	IR,HEP
11.	Spilje	Crn Drim	1969	E-R	101	112	330	2699	520	HEP
12.	Ratevska	Ratevska	1972	AR	49	53	194	21.7	10.5	WS,IR
13.	Turija	Turija	1972	E-R	77.5	93	417.3	1978	48	IR,WS,HP
14.	Glaznja	Lipkovska	1972	AR	71.5	80	344	168	22	IR,HEP
15.	Mantovo	Lakavica	1975	E-R	37.5	49	138	261	47.5	IR,WS
16.	Strezevo	Semnica	1982	E-R	76	84.6	632	4300	112	IR,WS,HEP
17.	Paljurci	Luda Mara	1982	EAR	21.1	21.5	310	185	2.9	IR
18.	Suvodol	Suvodolska	1982	EAR	33.9	38.3	941	1740	7.88	R,WS
19.	Podles	Vodnik	1985	AR	18	22.5	92	6.7	0.31	IR
20.	Mavrovica	Mavrovica	1999	EAR	24	29	360	400	2.8	WS,IR
21.	Ilovica	Ilovicka	2004	E-R	27.8	29.8	274	131	0.5	WS,IR
22.	Kozjak	Treska	2005	E-R	114	126	300	3340	550	R,HEP,WS
23.	Losana	Losana	2006	R-F	41	45.2	165	260	1.08	WS
24.	Markova R.	Markova R.	2006	E-R	26	30	72.5	64.6	0.66	WS
25.	Lisice	Topolka	2008	ERT	66	76.9	579.6	3295	23	WS,IR
26.	Knezevo	Zletovska	2011	E-R	75	83	290	1550	23.5	WS,IR,HEP
27.	Sveta Petka	Treska	2012	AR	41	66	115	32.5	9.1	HEP

H – height above ground; Hs – structural height; L – length of dam crest; VD – dam volume; VR – maximum reservoir capacity; EAR – earthfill dam; E-R – earth-rock dam; R-F – rock-fill dam; AR – arch dam; MA – multiarch; WS – water supply; IR – irrigation; HEP – hydroelectric power; R – retention

In Macedonia, construction of dams and reservoirs "Lukov Pole" and "Boskov Most" is planned, and dams and reservoirs "Cebren" and "Galiste" are planned to be built. The total volume of reservoirs to be formed with these reservoirs is 1309.4 (106 m³) or 1309400000 m³ or 654.7 m³ per inhabitant. Thus, the total volume of reservoirs will be 3724.3 (106 m³) or 3724300000 m³, which is 1862.15 m³ per capita.

Table 3: Dams and reservoirs in Macedonia that are being built or need to be built (they are big in accordance with the criteria of the International Committee for Large Dams ICOLD).

Id.	Name	River	Year of construction	Type	H [m]	Hs [m]	L [m]	VD [m ³ ×103]	VR [m ³ ×106]	Purpose
1	Lukovo Pole	Radika	2025	E-R	71.0	84.9	321.0	1641.8	39.0	HEP
2	Boskov Most	Radika	2025	E-R	33.0	33.8	129.5	158.4	2.3	HEP
3	Cebren	Crna Reka	2027	AP	180.0	192.5	500,0	1214.7	915.0	HEP
4	Galiste	Crna Reka	2027	E-R	138.5	141.5	477.0	7380,0	344.0	HEP

H – height above ground; H_s – structural height; L – length of dam crest; VD – dam volume; VR – maximum reservoir capacity; EAR – earthfill dam; E-R – earth-rock dam; R-F – rock-fill dam; AR – arch dam; MA – multiarch; WS – water supply; IR – irrigation; HEP – hydroelectric power; R – retention

The average annual production of electricity from the new hydropower plants in Macedonia would be 659.9 GWh or 330.1 kWh per capita electricity from hydroelectric power plants, which together with the production from the existing hydro power plants would be 1860.2 GWh or 930.1 kWh per capita.

The total energy increase would be around 32% of the current one.

This would significantly affect the increase in the Human Development Index HDI, which would reach 0.8. That would bring Macedonia closer to the developed countries.

5. Impact of dam reservoir in the reduction of the consequences of climate change

In the last period, we witness the impact of climate change on people's lives.

Because of the varying degree of effect, climate change has different impacts and consequences on countries at different stages of development. The most vulnerable to the impact of climate change are those who live the poorest parts of the world. Also poor or underdeveloped countries were not a cause, no reason, nor could they significantly influence the increase in ozone-harmful gases blamed for global climate change. Climate change of the poor countries has the greatest impact, and their adaptability is the worst. Countries of varying degrees of development have different goals and priorities with the possibilities of water reservoirs and also different concerns. For least developed countries, climate change impacts are often catastrophic due to the inadequate capacity of reservoirs to respond to extreme weather events that are occurring more often and with worse consequences.

The construction of reservoirs is an essential part of their survival and reliability, and even more in these countries, both the energy needs and the needs of water are very important, and therefore the construction of hydro systems is of multiple benefit. The effects of climate change mitigate the needs of drinking water and energy. Water used for irrigation increases food production and thus reduces food shortages. Therefore, the construction of hydropower systems is of great importance.

In Macedonia, we are also witnessing altered climate change, with warm summers occurring with little rain, and on the other side we are witnessing heavy torrential rains with a lot of precipitation in a short time. In such conditions for reducing these consequences, the reservoirs have great influence when serving as retention areas during torrential rains and discharge of water during dry periods.

6. New period in the building of dams and reservoirs

In conditions of rapid growth of the world's population and economic development it is necessary primarily to provide drinking water and energy to meet the constant demand for raw materials and energy. Water is an essential natural resource, but it also has an

important impact on the environment. With growing population, drinking water needs increase. There will also be an increase in the effects of climate change including floods and droughts.

It should be noted that there is a change in the structure of energy sources for energy production. In the future, the leading role of fossil fuels in the structure will be reduced due to the reduction of emissions of harmful gases. According to some predicting the capacities for the production of electric energy from fossil fuels, they will completely stop production in 2050, Figure 9)

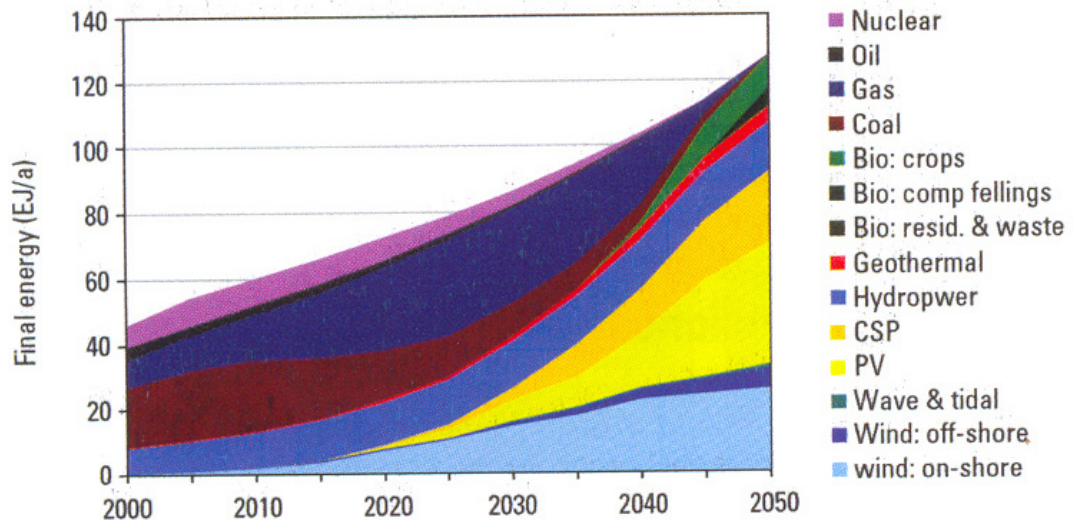


Figure 9. Percentage distribution of energy production by type by 2050 (Hidropower & Dams 3-2011)

In such conditions, it is required to increase the capacity and the possibility of regulating with engineering measures. Adopting a consensus on the role of dams and reservoirs in preventing the consequences of climate change should be done with international cooperation. More and more people recognize water infrastructure as crucial to achieving sustainable development. Insufficient aquatic facilities will slow our ability to respond to climate change and meet the Millennium Development Goals.

Supporters and opponents for building large water reservoirs must return to the negotiating table and discuss global development projects in a friendly manner in order to find a consensus on development requirements. From that point of view, it is emphasized that the side of the World Bank has formed a Defense Committee that advocates the termination of the dam construction and removal of the built. In 2014, at the meeting between the ICOLD World Bank in Marseille during the World Water Conference, it was realized that the construction of the dams should continue, and the World Bank continues to finance this construction, as the big dams are the basis for ecological development. The Dam Committee has issued a Manual for the Sustainable Development of Dams and Hydro Power Plants and it is used in practice (guidelines for sustainable development of dams and hydropower)

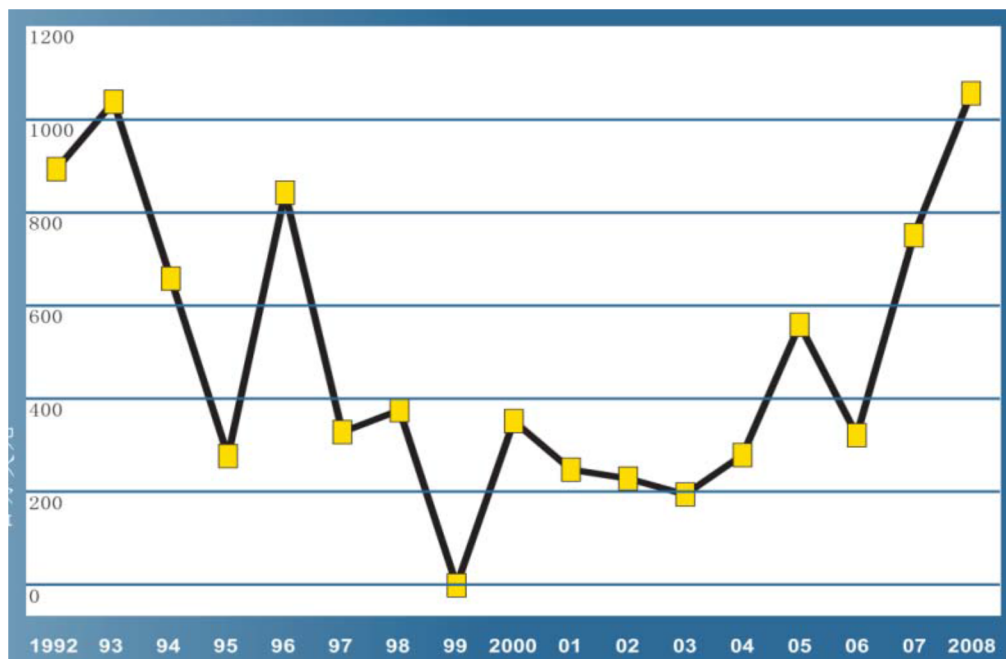


Figure 10. Investing in World Bank hydrology (WBG, 2009)

Country development plans are a new era in the development of dams and reservoirs and the development of hydropower. Many infrastructure investments and other measures taken as a result of dams will help each country individually deal with climate change and economic crises. But nevertheless, these countries face many difficulties or obstacles in the process of developing hydropower and the construction of dams and accumulators

In Macedonia, the dam s "Lukovo Pole" and "Boskov Most" is planned to be built. In the near future, the construction of the dams "Cebren" and "Galiste" should start, and it is planned to start with the Vardar Valley project and several projects for water supply and irrigation.

This will certainly contribute to the development of Macedonia and to more easily deal with climate change through a more even distribution of the excess and lack of water at different times of the year through the planned construction of dams and reservoirs.

However, it is of great importance to meet the criterion of safety through quality long-term monitoring.

7. Long-term security of dams, basis for development of dams and reservoir

Today, the sustainable development and sustainability of life in many parts of the world is affected by the lack of drinking water, food and energy. Aquatic reservoirs are practically involved in the safety of drinking water and energy security. It is therefore necessary to build even more dams and reservoirs. But even by taking all the things that are available, the effects of global climate change are still felt. On the other hand, it is necessary for those already built to function normally and securely.

Experiences from developed countries where regular monitoring of dams is carried out and where there is good safety of the dams indicate that the long-term security of the dams is the basis for the development of hydropower and dams, and with the monitoring it can be prevented and prevented by the worst problems and incidents on the dams and the reservoir.

The planning of dam monitoring should be done during design, construction and exploitation in order to obtain long-term safety of the dams and in doing so, the following things should be considered:

- the safety of the dams should not be understood only from a technical point of view, but should also be the concern of society. In addition to the responsibility for the security of the dam from the technical expertise, the security of the dams should be a very big responsibility for the state;

- The ageing of the dam and the possible problems of the dam, the remediation measures should be provided during the design, the expropriation and the exploitation. The designer, contractor and owner should not say that the dam will probably be in place for hundreds of years in the future. Consequently, the construction and the materials must be durable or anticipate the rehabilitation of a certain time during the lifetime of the dam;

- Evaluation (review of the results) of long-term monitoring by taking into account all the factors affecting the dam, can be used to plan when to repair the dam;

- The lifespan of the dam and its constituents may be different. The life span of well-designed, well-constructed and well-monitored dam can reach 100 years. But hydromechanical elements such as clips and their engines should be replaced every 30-50 years. The lifespan of the turbines is 40 to 60 years. Automatic monitoring equipment 5-7 years. The normal renewal and replacement of the old complements is very important for the reliability of the entire dam project;

- Watershed management plans are important for avoiding environmental problems in the normal use of water from reservoirs;

- For risk management, an emergency plan should be drawn up containing all the factors that may affect the safety of the dam. The demolition of a dam associated with the hydro power plant can also be considered as a risk. Many hydroelectric damages cause an interruption in the supply of electricity, which is very important for the operation of the safety devices such as the stoppers not overflowing behind the turbine valves at the dams. Thinking should take into account political and economic crises and natural disasters such as earthquakes and which will guarantee the safety of the dam and people downstream if this happens.

In the new century, the construction and use of dams and hydroelectric plants can not be considered for a long time only purely from a scientific and technical point of view. In order to minimize disputes over dams and to ensure support for global development globally, long-term security of major dams is fundamental.

In Macedonia, treating the dam safety is through the Law on Waters. The performance of the dam monitoring is compulsory for all major dams that are in accordance with the criteria of the International Committee for Large Dams (ICOLD). The user of the dam

must also prepare an annual monitoring report on the dam and send one copy to the competent Ministry.

In Electro Power Company there is an introductory ISO 9001 standard for monitoring of dams. The quality of the monitoring of the dams in Electro Power Company has been confirmed by numerous foreign experts.

8. Conclusion

From the previous it is seen that dams and hydroelectric power plants largely influence the development of one country. The ratio of the total volume of reservoirs to the country's inhabitants is an indicator of the development of that country and is very close to the development index HDI which officially indicates the degree of development of a country.

Likewise, dams and reservoirs affect the consequences of global climate change.

Therefore, in Macedonia, new dams are being built and hydroelectric plants are necessary, and the problems between the opposing sides should be resolved on the table in a common acceptable way in the interest of the entire population. But it is of great importance to meet the criterion for safety of dams and reservoirs through quality long-term monitoring.

SOLUTIONS FOR THE REHABILITATION IN THE HYDROTECHNICAL TUNNEL

ZLATKO ZAFIROVSKI ¹, VASKO GACEVSKI ², IGOR PESHEVSKI ³, MILORAD
JOVAONVSKI ⁴,

¹ University „Ss. Cyril and Methodius“, Faculty of Civil Engineering – Skopje, Macedonia,
zafirovski@gf.ukim.edu.mk

² University „Ss. Cyril and Methodius“, Faculty of Civil Engineering – Skopje, Macedonia,
vaskogacevski@yahoo.com

³ University „Ss. Cyril and Methodius“, Faculty of Civil Engineering – Skopje, Macedonia,
pesevski@gf.ukim.edu.mk

⁴ University „Ss. Cyril and Methodius“, Faculty of Civil Engineering – Skopje, Macedonia,
jovanovski@gf.ukim.edu.mk

1. Abstract

Tunnel engineering is a special area i.e. science discipline of the underground structures where the experience and knowledge from other areas are applied, such as: geology, rock mechanics, soil mechanics, fluid mechanics, theory of structures, reinforced concrete, geodesy, etc. Hydrotechnical tunnels are widespread throughout the world. They are used for different purposes, such as water supply, sewage, diversion (outlet) and melioration. Long existing tunnels require proper maintenance and rehabilitation so they may keep their stability and functionality. Hydrotechnical tunnels can be especially challenging from several aspects. Most often they are under constant effect of the water, which can be very destructive. Therefore depending on the structure and the conditions, adequate solutions for different problems are conducted during the service period of the tunnel. Any intervention in a hydrotechnical tunnel requires significant financial investments and proper team of experts from different scientific areas. In nowadays tunnels are placed under densely populated cities, under rivers, lakes, seas and tall mountains on large depths below the surface. In addition, the tunnel dimensions in the world are increasing. This makes the construction, maintenance and rehabilitation of tunnels more complex. A part of the solutions for the rehabilitation of the hydrotechnical tunnel on Saska River are shown in this paper. They include technical measures for the existing support and also construction of a new support. The proposed solutions are based on the current state of the tunnel, made with investigations and on-site inspection in the tunnel and the information about previous problems, interventions and rehabilitations. The analyses of the variant solutions are conducted through a numerical model simulated in multiple phases using the software PLAXIS 3D.

Keywords: tunnel engineering, hydrotechnical tunnel, rehabilitation, numerical analysis, PLAXIS 3D

2. Introduction

The hydrotechnical tunnel on Saska River represent a diversion tunnel which is part of

the mine for lead and zinc Sasa. The mine is located in the eastern part of the country, near the town Makedonska Kamenica at altitude of 1000 m.

The tunnel is in service since 1971. With length of 1925 m and longitudinal slope of 5-7 %, part of the tunnel is based under the tailing and the other part under the surrounding mountain. The cross section dimensions vary (≈ 3 m) depending on the tunnel support and the geological conditions.

Because of the long tunnel existence and usage, throughout the years several interventions i.e. rehabilitations have been done. This includes: rehabilitation of the primary and secondary support, injection of cracks and holes, rehabilitation of the invert arch etc.

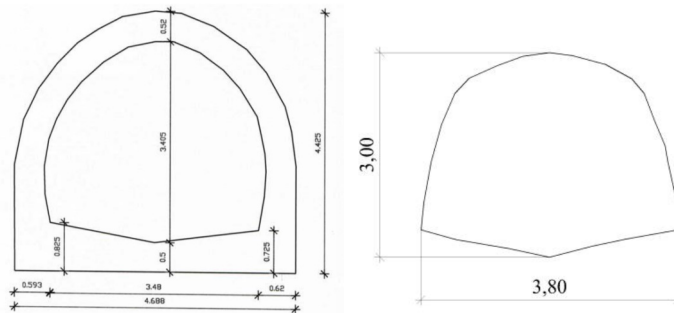


Figure 1. Characteristic cross sections

The information and data about the geological and geotechnical conditions of the terrain in the zone of the tunnel are gained throughout several phases of investigations.

In the zone of the tunnel there are two lithological compositions present, natural materials such as gneiss rock and sandy gravel and artificial materials which include the tailings sand (floatation pulp).

The represented rock masses according to their hydrogeological function in the terrain assembly behave as collectors and isolators. The group of hydrogeological collectors includes the alluvium sediments and the floatation pulp. In the group of hydrogeological isolators may be considered the strongly tied rock masses (gneisses). The inflow of ground water is present only at a few sections, but the largest part of the tunnel is dry.



Figure 2. Sattelite picture of the terrain in the zone of the tunnel

3. Methods

3.1 Current state of the tunnel

Based on the investigations and on-site inspection in the tunnel, it was determined that the hydrotechnical tunnel on Saska River can continuously perform its function. But because of the observed irregularities along the tunnel in terms of identified defects, it was recommended to apply measures which will increase the tunnel construction functionality, and thus improving the overall state of the tunnel and increasing its exploitation period. Some of the defects registered along the tunnel are: deficit of primary and secondary support, deformation of the invert arch i.e. eroding and destruction of the reinforced concrete, appearance of water along the walls of the support lining, appearance of cracks and holes in the concrete.

3.2 Solutions for the rehabilitation of the tunnel

There are several characteristic sections in the tunnel, which can be divided into three major groups:

- Sections with no support (only rock mass);
- Sections with only primary support (shotcrete and rock bolts);
- Sections with primary and secondary support (shotcrete, rock bolts and reinforced concrete lining).

3.2.1 Analysis of the tunnel sections with primary support

Some sections of the tunnel have only primary support with no secondary lining i.e. reinforced shotcrete $d=20$ cm, rock bolts $L_a=2,5$ m at distance of 1,25 m and invert arch from reinforced concrete. The following solutions were considered for these sections:

- Variant 1: partial secondary lining from reinforced concrete – pillars ($d = 30$ cm);
- Variant 2: complete secondary lining above the invert ($d = 30$ cm);
- Variant 3: rehabilitation of the invert with anchors, new reinforcement and new layer of concrete ($d= 20$ cm).

The mentioned variant solutions could be implemented individually or combined with other solutions which is usually the case with tunnel rehabilitations.

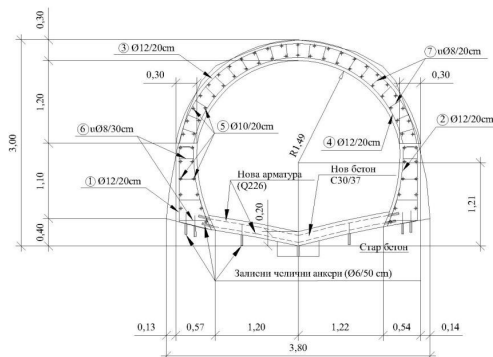


Figure 3. Tunnel cross section with combined solution of complete secondary lining and rehabilitated invert

The analysis for the proposed variant solutions was simulated in a numerical model in multiple phases:

- Phase 1: Initial stress condition in the massif before construction;
- Phase 2: Excavation of the tunnel and construction of the invert with pillars;
- Phase 3: Pseudo-static analysis.

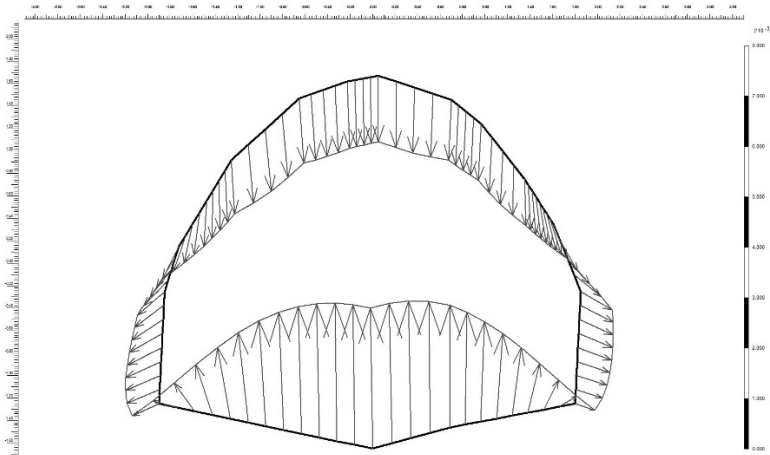


Figure 4. Deformations of the construction with complete secondary lining (2,78 mm)

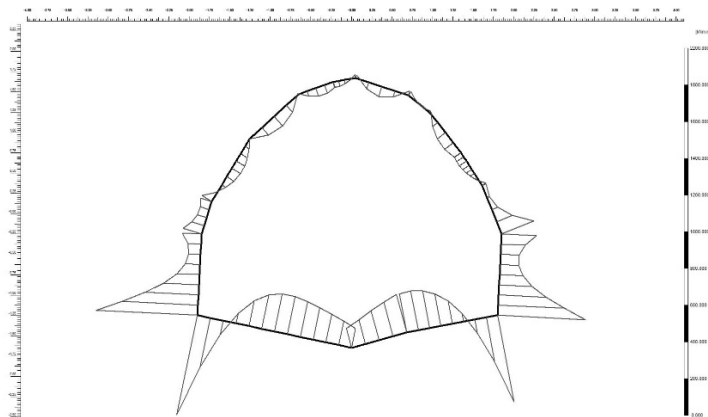


Figure 5. Diagram of bending moments ($M_{max} = -552,73 \text{ kNm/m}$)

4. Results and discussion

From conducted analysis the stability of the tunnel has been confirmed in the current state and with the proposed rehabilitation solutions. More precisely the results i.e. stresses and deformations do not threaten the stability and functionality of the tunnel.

Among the works for the rehabilitation of the tunnel it is also predicted to have a certain volume of injection works. The purpose the injections in this tunnel is to improve the characteristics of the rock mass, to establish a connection between the concrete structure and the surrounding rock mass and to disable the concentrated ground water infiltration.

On the existing concrete lining few solutions are proposed depending on the damages. These solutions include application of mortar or shotcrete. The rehabilitation of the concrete structure also includes the rehabilitation of the dilatation and work joints. After the rehabilitation, the complete concrete lining should be protected from mechanical and chemical impacts with application of appropriate materials, such as anticorrosive coatings.

5. Conclusion

Hydrotechnical tunnels are challenging structures which should be precisely and carefully designed, constructed and maintained. For long lasting exploitation the proper maintenance and rehabilitation are the key for accomplishing the adequate stability and functionality. The rehabilitation process is a complex procedure that enables the improvement of the tunnel construction and the extended service period. The solutions and analysis for the rehabilitation of the hydrotechnical tunnel on Saska River show a part from the complexed procedure.

References:

- [1] Construction design of the “Saska” river diversion tunnel, stage II, Faculty of Civil Engineering, Skopje, 2006.
- [2] Design of rehabilitation of the lining of the “Saska” river diversion tunnel from survey mark 1+200 to survey mark 1+717 and rehabilitation of the invert, Faculty of Civil Engineering, Skopje, 2003.
- [3] As built design of the “Saska” river diversion tunnel (stage II), Faculty of Civil Engineering, Skopje, 2008.
- [4] As built design of the injection works at the “Saska” river diversion tunnel, stage II, Geofluid, Skopje, 2007.
- [5] Geodetic report on the surveys conducted for special purposes, Geomer, Delcevo, 2009.
- [6] Technical solution for rehabilitation of the “Saska” river diversion tunnel at survey mark 1+150 – 1+200 km./beneath the new tsf of Sasa mine – M. Kamenica – stage I, Mining institute – Department for mineral processing – Skopje (2002)
- [7] Partial – technical solution for the accompanying facility of the diversion collector “Velkovski stream” /shaft – diversion tunnel/ after raising the “New TSF” of Sasa mine – M. Kamenica – stage I, above elevation 990.0 m, Mine institute “Zavod PMS”, Skopje, 2000.

SEDIMENTATION VELOCITY OF SAUALM CRYSTALLINE USING IMAGE PROCESSING METHODS

DOMINIK WORF¹, JOHANNES SCHOBESBERGER², PETR LICHTNEGER³, HELMUT HABERSACK⁴, CHRISTINE SINDELAR⁵

¹ *University of Natural Resources and Life Sciences, Institute of Hydraulic Engineering and River Research, Austria, dominik.worf@boku.ac.at*

² *University of Natural Resources and Life Sciences, Institute of Hydraulic Engineering and River Research, Austria, johannes.schobesberger@boku.ac.at*

³ *University of Natural Resources and Life Sciences, Institute of Hydraulic Engineering and River Research, Austria, petr.lichtneger@boku.ac.at*

⁴ *University of Natural Resources and Life Sciences, Institute of Hydraulic Engineering and River Research, Austria, helmut.habersack@boku.ac.at*

⁵ *University of Natural Resources and Life Sciences, Institute of Hydraulic Engineering and River Research, Austria, christine.sindelar@boku.ac.at*

1. Abstract

This study concerns experimental investigations of the sedimentation velocity of Saualm crystalline which is found in Carinthia/Austria. This sediment is typically flat-shaped and therefore the settling velocities were expected to differ from that of spherical particles. Due to the reflective properties of this sediment an optical measurement, using image processing, was used. After sieving a sediment sample into six grain size classes and measuring the shape factor, the sedimentation velocity was measured in standing and flowing water at five different flow velocities. The measurement method proved to be cheap, easy and accurate enough to be in good agreement with theoretical results according to the measured shape factors.

Keywords: sand trap, optical measurements, physical modeling, mica, flat shaped sediment

2. Introduction

A sand trap of a hydropower plant in the Saualm crystalline region in Austria wasn't working properly. Saualm crystalline contains mica, which has a negative impact on wear due to its hardness and a very slow sedimentation velocity due to its flat shape. This led to increased wear at turbines and other equipment. The main hypothesis was that the flat shape of Saualm crystalline slowed the sedimentation velocity and maybe showed a different behaviour to the literature [1, 2].

To test this hypothesis experiments with a sample of the Saualm crystalline were done in the hydraulic lab of the University of Natural Resources and Life Sciences, Vienna.

An important factor for sedimentation processes is the sedimentation velocity in standing water w_0 , which can be calculated by using an empirical equation [1] using a shape factor FF

$$w_0 = \frac{12\nu}{d(2.7 - 2.3FF)} \left(\sqrt{1 + (0.21D^*)^3(2.7 - 2.3FF)} - 1 \right), \quad (1)$$

$$D^* = \left(\frac{\left(\frac{\rho_s}{\rho} - 1 \right) g}{\nu^2} \right)^{\frac{1}{3}} d, \quad (2)$$

where d is the diameter of the particle, ρ_s is the density of the sediment, ρ is the density of the fluid, ν is the kinematic viscosity of the fluid and g is the gravitational acceleration. The shape factor is calculated, using the longest a , middle b and shortest axis c of the particle, with $FF = c/\sqrt{ab}$. A shape factor of 0.7 is used as a default value for fluvial sediments. Due to the flat shape of Saualm crystalline this assumption is not valid. After measurements were done a mean shape factor of 0.46 was found, with an extra cluster corresponding to the flattest parts. This cluster showed a mean shape factor of 0.2 (Figure 1, right).

For processes in sand traps the sedimentation velocity is typically reduced linearly using the flow velocity u and the height of the effective space H , according to Giesecke and Mosonyi [2],

$$w = w_0 - \alpha u \quad \text{with } \alpha = \frac{0.132}{\sqrt{H}}. \quad (3)$$

A more recent approach from Ortmanns [3] identifies the turbulent velocity in vertical direction w'_{rms} as a key factor of reducing the sedimentation velocity. Moreover this approach is considering the geometry at the inflow of the sand trap.

3. Methods

To investigate the settling behaviour/velocity of the Saualm crystalline experiments were done in three parts: (i) sieving in six different fractions of the Saualm crystalline sample, (ii) measurements in standing water and (iii) measurements in flowing water. Due to the reflective property of the sediment the experiments used an optical measurement method.

3.1 Sieve analysis

After the sample (about 10.5kg dry mass) had been dried, different sievings were done. Using smaller samples of about 100g mass each, two dry and two wet sievings were done. These led to a partitioning into six different classes of diameters,

- < 0.2mm,
- 0.2 – 0.63mm,
- 0.63 – 1mm,
- 1 – 2mm,
- 2 – 4mm ,

- > 4mm.

The relevant range of grain sizes for the planning/dimensioning of sand traps typically lies between 0.2 and 1mm. This range was represented by two classes only. The theoretical sedimentation velocities in this area vary between 2 and 12cm/s [1]. Therefore the remaining material was sieved dry in finer graded classes. Due to the available sieves the classification was

- 0.18 – 0.25mm,
- 0.25 – 0.355mm,
- 0.355 – 0.56mm,
- 0.5 – 0.71mm,
- 0.71 – 1mm,
- 1 – 2mm.

The resulting distribution can be seen in Figure 1. The finer grading showed an appropriate agreement with the results from both wet sievings. The wet sieving led to about 40% residual material under 0.2mm by mass, while the finer grading showed about 35% residual material below 0.2mm. The difference is due to the dry sieving but it was small enough as the exact results were not that relevant for the rest of the project.

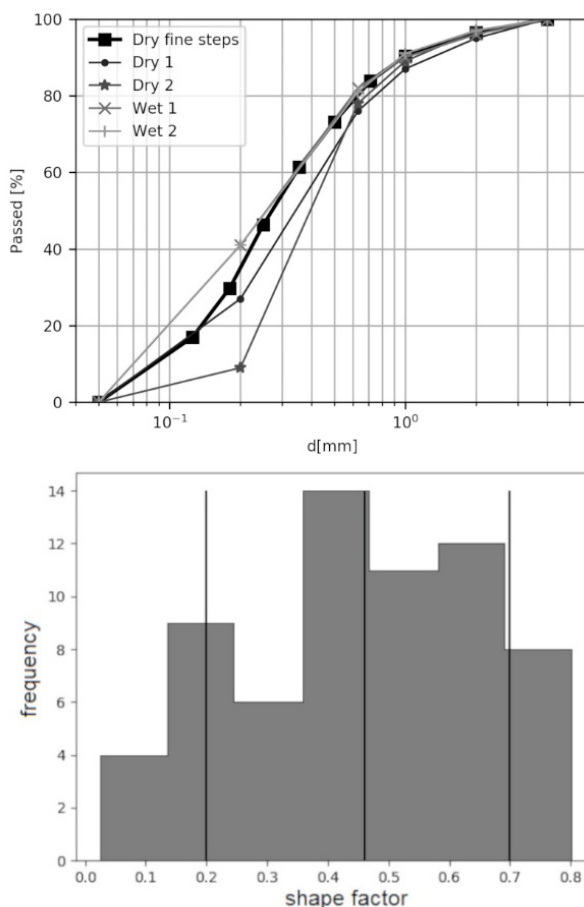


Figure 1. Upper figure: Distribution of the classes for the five different sievings. Lower figure: Histogram of the shape factors. The vertical lines describe the three considered factors $FF = 0.2$, $FF = 0.46$ and $FF = 0.7$.

Using a sample of the fraction $>1\text{mm}$ the mean shape factor was determined by measuring the three relevant axes. This led to a mean shape factor $FF = 0.46$. For the flattest particles a mean shape factor $FF = 0.2$ was measured. In Figure 1 (right), a histogram of the measured shape factors can be seen. The three vertical lines correspond to the three considered shape factors (0.2, 0.46, 0.7). An important observation is that about 30% of the sample have a shape factor below 0.36 leading to the mean shape factor of 0.2.

3.2 Standing water experiments

3.2.1 Setup

The setup for the sedimentation experiments in standing water can be seen in Figure 2. Each sediment class was put into a tank ($L \times B \times H = 60\text{cm} \times 30\text{cm} \times 30\text{cm}$) filled with water. The sediment was added wetly using a tube, to reduce the chance of floating sediment due to the surface tension. The tube was curved to a horizontal line, such that no added vertical velocity component would create a too fast velocity. The trigger for the adding of the sediment was the opening of a clamp. The fraction $>1\text{mm}$ was added dry because the large diameter clogged the tube. This did not pose a problem as this fraction didn't have the issue of floating on the water surface. The volume of the added sediment was controlled using a measuring spoon with a volume of 0.24ml. Due to the size of the particles for the largest fraction a cap with 2.4ml volume was used. The added volume was either two spoons or one cap. The particles were filmed while settling. To be able to evaluate the recordings (conversion pixel to mm) only a flat area (1.5cm wide) across the camera angle was illuminated. The rest of the water was kept without light. For the recordings a GoPro Hero 5, with 2.7k resolution and 30 frames per second was used. Per class of sediment three recordings were done.

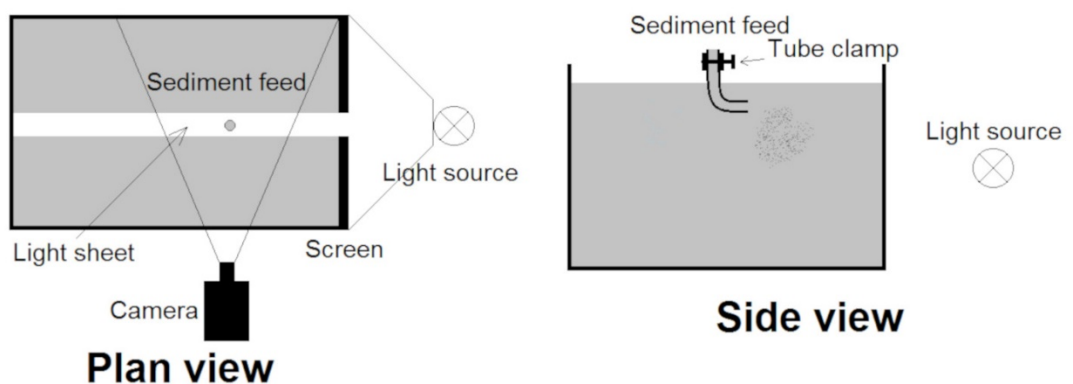


Figure 2. Setup for standing water experiments, only an about 1.5cm wide vertical area is illuminated in a water tank ($L \times B \times H = 60\text{cm} \times 30\text{cm} \times 30\text{cm}$).

3.2.2 Evaluation for standing water experiments

The evaluation was done by extracting all frames of the videos that were relevant to the

analysis. These were all frames where most particles were visible and none had left the image at the lower boundary. For all evaluation steps the programming language “Python” [4] was used. The first step for each recording was to subtract the median picture from each picture to reduce noise from sources like reflections, scratches or residual light. Afterwards the images were sharpened using the filter UnsharpMask of the Python-package “pillow”. For the evaluation the red channel was used because it showed the highest contrast between the particles and the background.

In each picture all pixels with a brightness value above a certain threshold were used to create a regression line and compute the centroid, in these experiments a threshold value of 30 was used. Using the difference of the coordinates of the centroid between two pictures the sedimentation velocity could be evaluated in pixel/frame. The different positions of the centroids and the middles of the regression line were compared for verification. Furthermore the so calculated velocities were also manually compared to the differences for a few randomly selected particles.

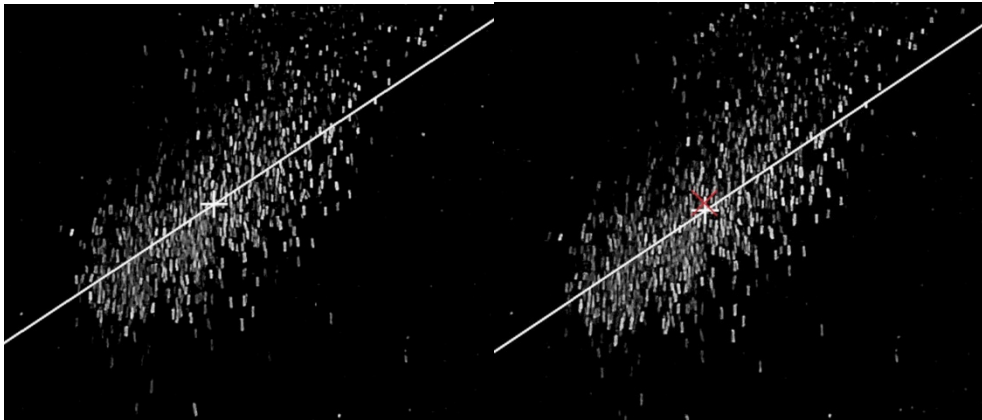


Figure 3. Two frames of video 1 of the class 0.5 to 0.71 mm, the difference between the vertical positions of the centroids (crosses) gives the velocity in pixel/frame. In the second frame the red angled cross shows the position of the centroid in the first frame.

In Figure 3 two such pictures can be seen. All pixels that are not completely black have been used for the calculation. Also the centroid and the regression line are drawn.

Using a recording with a calibration plate with a millimeter scale the length conversion was determined as $4.2\text{pixel}=1\text{mm}$. Together with the 30 frames per second this led to the velocity conversion of $4.2\text{pixel/frame}=30\text{mm/s}$.

For the final evaluation the velocities between different pairs of pictures have been averaged. Figure 4 shows results for the class 0.5 to 0.71 mm. The dots show the differences from one image to the next and the lines show the corresponding mean values. The dots labeled “middle” represent the differences in vertical position of the point on the regression line in the horizontal middle of the image. Since the midpoint of the regression line is a rather arbitrary choice, the centroid was used in the end. One can see that not all particles are in the chosen field of view yet. This leads to a certain loss in accuracy of the measurement. This effect was neglected for the evaluation as the amount of particles outside the frame was not too high. Also there are two counteracting effects due to this.

The first one is that information about slower particles is lost which increases the measured velocity. The second is due to the presence of particles in the second frame at the upper border which were not visible in the first frame. This artificially draws the centroid upwards, which lowers the velocity. Ideally the field of view should have been chosen in a way that all particles are in the frame and also have accelerated to their full velocity. This was not fully possible in the chosen setup due to the limited size of the tank.

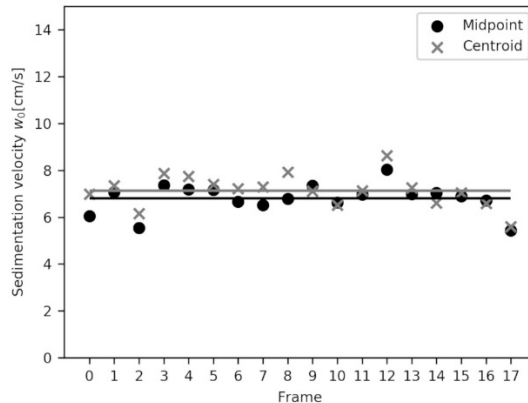


Figure 4. Comparison of the difference between frames for the fraction from 0.5 to 0.71mm. The difference is shown for the centroid and the midpoint of the regression line. The horizontal lines represent the mean values.

3.3 Flowing water experiments

3.3.1 Setup

The flowing water experiments were done in a 30cm wide, 12m long laboratory flume. The flow rate was controlled by a frequency-controlled pump and a magnetic flow meter (“Proline Promag 10D”, Endress+Hauser) with an accuracy of 0.5%. The water depth was set by a flap gate at the lower end of the flume at constant 21cm for all experiments. The setup is similar to the setup of the standing water experiments and can be seen in Figure 5. For the flowing water experiments not only videos but also long exposure photos (“Nikon D7100”, 20mm lens) were done, which could be used to track trajectories of single particles.

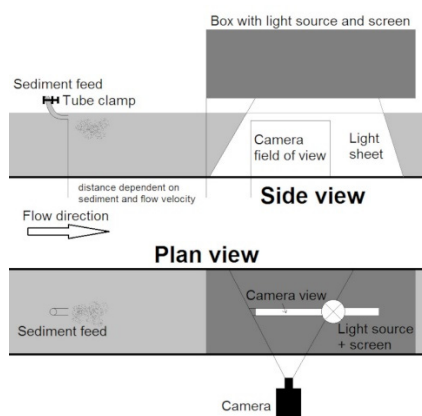


Figure 5. The setup for the flowing water experiments in a 30cm wide hydraulic flume.

The light source was placed above the flume. The sediment was added upstream of the illuminated area using a curved tube. The curvature was such that the sediment was added parallel to the flow direction. The distance between the illuminated area and the tube was adapted according to the sediment class and flow velocity, to reduce the influence of the sediment input on the sedimentation velocity. The distances are shown in Table 1. The flow velocity was varied in five equidistant steps in the area from 0.1 to 0.5m/s.

Table 1. Distances between the screen and the sediment introduction dependent on the class and flow velocity. Between the screen and the field of view of the camera is a distance of 8cm.

	> 0.18MM	> 0.25MM	> 0.355MM	> 0.5MM	> 0.71MM	> 1MM
0.1M/S	5cm	0cm	0cm	0cm	0cm	0cm
0.2M/S	15cm	10cm	5cm	0cm	0cm	0cm
0.3M/S	25cm	20cm	15cm	10cm	5cm	0cm
0.4M/S	30cm	25cm	20cm	15cm	10cm	5cm
0.5M/S	35cm	30cm	25cm	20cm	15cm	10cm

Per velocity and class different long exposure photos were taken. At first a zero-photo was taken without any sediment under the same conditions as the other photos. Afterwards 3-4 photos with sediment and 1 photo with half the amount of sediment were taken. The amount of added sediment was controlled in the same way as in the standing water experiments using a measuring spoon with 0.24ml volume and a cap with 2.4ml volume. The amount added was determined such that an optimum of photo quality was gained while keeping the added amount minimal. This was done to reduce the influence of concentration. The different amounts can be seen in Table 2. The exposure time was chosen such that the full trajectory through the camera angle was captured in the image. Also for each class a video was taken for verification of the results of the photos.

Table 2. The added amount dependent on the sediment class and the flow velocity. MS stands for measuring spoon (0.24ml) and C for cap (2.4ml).

	> 0.18mm	> 0.25mm	> 0.355mm	> 0.5mm	> 0.71mm	> 1mm
0.1m/s, 0.2m/s	2 MS	2 MS	3 MS	3 MS	3 MS	1 C
0.3m/s	2 MS	3 MS	3 MS	3 MS	3 MS	1 C

0.4m/s, 0.5m/s	3 MS	3 MS	3 MS	3 MS	3 MS	1 C
-------------------	------	------	------	------	------	-----

Furthermore for each velocity three velocity profiles in longitudinal direction in the illuminated area were measured using a current meter (“Höntzsch Mikroflügel MC20-75”).

An overview of the procedure can be found in Table 3.

Table 3. Overview of the procedure

Flow velocity target	Water depth (target = 21 cm)	Flow velocity actual	Procedure
0.1m/s	21.03cm	0.103m/s	Per class and velocity:
0.2m/s	20.94cm	0.202m/s	1 zero-photo, 3-4 photos
0.3m/s	20.92cm	0.306m/s	1 photo with half amount, 1 video
0.4m/s	21.07cm	0.406m/s	Per velocity:
0.5m/s	20.93cm	0.507m/s	3 velocity profiles measured

3.3.2 Evaluation flowing water experiments

The evaluation started by subtracting the corresponding zero-photo of each photo to reduce disturbances, e.g. scratches in the glass, or different light intensities due to standing waves on the water surface. Again the red channel was used for evaluation because it showed the highest contrast. All pixels with a value over a certain threshold were used for a linear regression line. The used threshold value had to be determined manually, such that noise was minimized without falsifying the results. Furthermore the photos were cropped to areas with the least amount of disturbances and obvious disturbances were removed manually. The inclination k of the resulting regression line together with the flow velocity u could be used for calculating the sedimentation velocity $w = -k * u$.

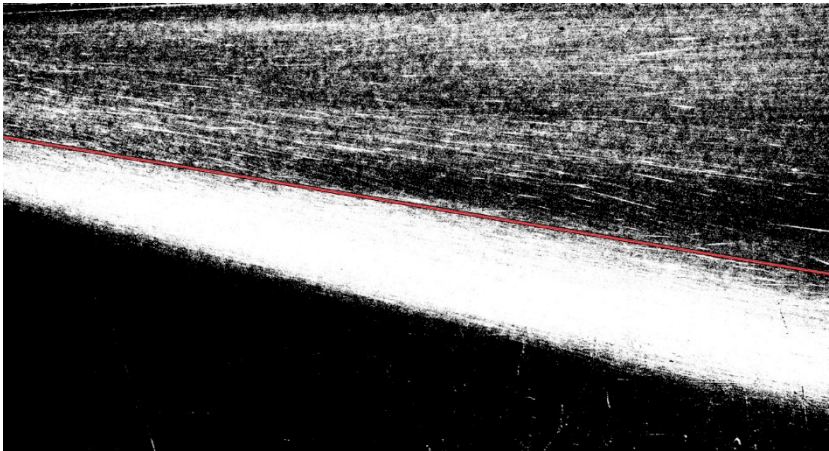


Figure 6. Exemplary evaluation for the class between 0.25 and 0.355mm with a mean flow velocity of 0.2m/s. The straight red line with black borders shows the regression line.

In Figure 6 one such evaluation can be seen. The image shows the experiment for the class 0.25 to 0.355mm at a mean velocity of $u = 0.2\text{m/s}$. Every pixel with a red value above 30 is shown. The other pixels have been set black. In this case the regression line gives an inclination of $k = -0.166$. This gives a sedimentation velocity of $w = -k * u = 0.0332\text{m/s}$.

One can also see that a considerable part of the material doesn't follow the main particle current. The trajectories are a lot flatter and sometimes even travel upwards. This behaviour can even be observed for the biggest particles at the lowest flow velocity. In the videos it can be recognized that these are very flat particles that reflect very well. During some preliminary experiments this could be observed for all classes at a mean flow velocity as low as 0.06m/s. Another way was to use the brightness values of the pixels as weighting parameters for the computation of the regression line. This didn't impact the results in any significant way.

4. Results and discussion

In Table 4 the results of the standing water experiments can be seen. They show a good agreement with each other which shows a certain robustness of the chosen method. The videos showed that some of the particles sank far slower than the rest of the sediment cloud. These were the particles with the flattest shapes, which apparently reacted to even the smallest upwards directed turbulences.

Table 4. Measured velocities in standing water showing good agreement for each sediment fraction between repeated experiments, i.e. between video 1-video3.

	> 0.18MM	> 0.25MM	> 0.355MM	> 0.5MM	> 0.71MM	> 1MM
VIDEO 1	3.18 cm/s	4.27 cm/s	5.43 cm/s	7.13 cm/s	10.12 cm/s	15.55 cm/s
VIDEO 2	3.34 cm/s	4.78 cm/s	5.21 cm/s	7.35 cm/s	10.55 cm/s	15.25 cm/s
VIDEO 3	3.48 cm/s	4.78 cm/s	5.51 cm/s	7.54 cm/s	10.20 cm/s	14.03 cm/s

The results also showed good agreement with known theoretical velocities, which can

be seen in Figure 7 left. The points are drawn in the middle of the corresponding diameter class. For the theoretical lines a temperature of 20°C is chosen because it corresponds to the water temperature during the experiments. The extrapolated points of the flowing experiments are done by evaluating regression lines of the flowing water results, which can be seen in Figure 7 right, at zero.

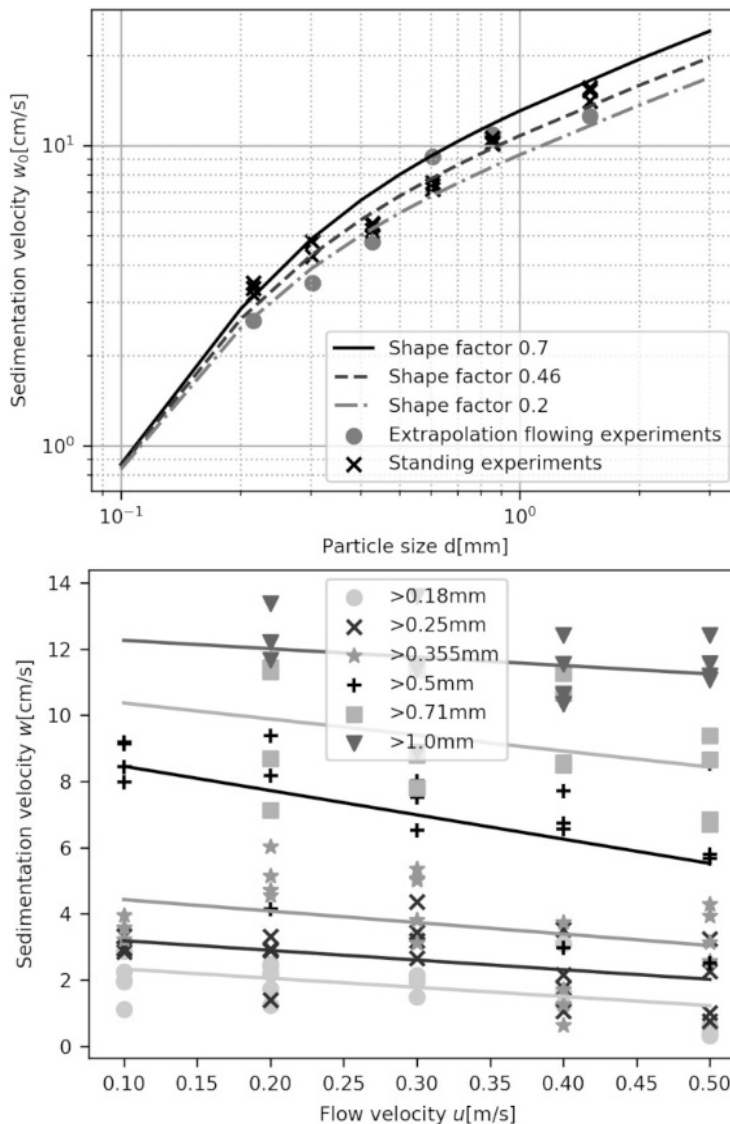


Figure 7. Upper figure: Comparison of the theoretical sedimentation velocity in standing water with the results of the experiments in standing water and extrapolated values of the flowing water experiments. Lower figure: Results of the flowing water experiments dependent on the different flow velocities with corresponding trend lines.

Results for the flowing water experiments can be seen in Figure 7 right. Trend lines are also drawn, which show the reduction in sedimentation velocity for growing flow velocities. At 0.1m/s flow velocity the sedimentation velocity of the biggest two classes

were too high to gain reliable results because their trajectories were so steep that only very small parts of the images were usable and the evaluation got very sensible to the threshold parameter and small disturbances. Thus those are not shown in this plot. This dependence on the threshold value is less for smaller sediment and higher flow velocities.

5. Conclusions

This paper deals with the measurement of the mean sedimentation velocity of Saualm crystalline. The objective was to use an inexpensive and easy method with acceptable accuracy.

A cheap and easy method, consisting of a camera (GoPro Hero 5 / Nikon D7100) and open software (Python) for measuring mean sedimentation velocities in standing and flowing water for sediment with suitable optical properties was used. In the case of Saualm crystalline, with its flat and reflective property, it was a perfect fit for this type of optical measurement. Although it seems that this property isn't necessarily needed, since non-reflective particles could be seen equally well.

Considering the shape factor the results of the measurement showed good agreement with the theoretical values. As it was expected, the sedimentation velocity of the sample was slower than for general sediment due to the flat shape. The difference between the theoretical and the measured sedimentation velocity was at most 0.015m/s for the largest diameter particles and 0.005m/s for the smallest diameter. In the standing water experiments larger particles show better agreement with the theory than smaller particles in relation to the sedimentation velocity. In the flowing water experiments the measured velocities were extrapolated to zero flow velocity. These extrapolated values also show good agreement with the theoretical values. The largest part of the sediment sinks to the floor but single particles even rise due to their flat shape.

Although the experiments have a very good agreement with the theory and also the experiments in flowing water provide plausible values, the following improvements in the experimental setup can be considered:

- The standing water experiments could use a larger tank and field of view, especially for sediment with highly varying shape factors where very different velocities are possible to occur within one sample.
- For the flowing water measurements the dependence on the threshold value should be reduced.

Due to the observed separation of particle currents (Figure 6) the adopted method has the potential to be further optimized by separately analyzing the two distinguished sediment trajectories.

Acknowledgements

The authors want to thank Lisa Schmalfuß, Julia Sandberger and Josef Pölzl for their support while carrying out the experiments.

References:

- [1] Zanke, U.: Grundlagen der Sedimentbewegung. Springer Berlin Heidelberg, 1982
- [2] Giesecke, J., Mosonyi, E.: Wasserkraftanlagen: Planung, Bau und Betrieb. Springer Berlin Heidelberg, 1998
- [3] Ortmanns, C: Entsander von Wasserkraftanlagen. PhD thesis, ETH Zürich, Zürich 2006
- [4] van Rossum, G: Python tutorial. Technical Report CS-R9526, Centrum voor Wiskunde en Informatica (CWI), Amsterdam, 1982

Topic no. 5 - Ecohydrology and Water Body Protections

NUMERICAL ANALYSIS OF ESCHERICHIA COLI TRANSPORT THROUGH THE KARST ENVIRONMENT (EXAMPLE OF BOKANJAC-POLIČNIK AQUIFER, REPUBLIC OF CROATIA)

GORAN LONČAR¹, ŽELJKO ŠRENG², HANNA MILIČEVIĆ³, SANJA OSTOJIĆ⁴,

^{1, 3, 4} *Faculty of Civil Engineering University of Zagreb, Republic of Croatia, gloncar@grad.hr*

² *Faculty of Civil Engineering and Architecture Osijek, J.J.Strossmayer University of Osijek, Republic of Croatia, zsreng@gfos.hr*

1. Abstract

This paper analyzes a pollutant transport (the principal component is E. coli) through the karst aquifer Bokanjac-Poličnik, located in pumping site of the Zadar water supply system. The main pollution sources are dysfunctional septic tanks (no public sewerage system is available) in the immediate vicinity of the pumping site. E. coli concentrations in water were monitored in the B5 well.

Numerical model Hydrus-1D was used in the analysis of the pollution transport through the vadose zone („dual-permeability“ module for flow and „physical nonequilibrium“ module for transport). The model was forced by daily precipitation data from two ombrographic stations. The model assumes flow and transport through two mutually interactive pore zones - matrix and fracture zones. The formulation is based on the Richards-Richardson equation. Transfer of dissolved or colloidal substances comprises convection processes (through water flow) and diffusion (through concentration gradient). The spatial domain of the transport model through the vadose zone was 8 m long and was discretized in vertical direction by 800 elements, each 1 cm in length. Effect of plant uptake and evaporation process was not taken into consideration. The transport through the horizontal (saturated) section was analyzed assuming that the uniform and stationary flow velocity was 1 cm/s, which corresponded to the results of an in-situ measurement of apparent horizontal flow velocity from the rural settlements to the B5 well. In the horizontal section, sorption was not taken into account due to the relatively large diameter of the fractures in the approximately horizontally fractured channels.

The results confirm that the surrounding settlements with no public drainage system and dysfunctional septic tanks are the main source of fecal contamination, which is transported to the water supply wells. The analysis shows that the increased E. coli concentrations in the well occurs after 7 days of intensive precipitation.

Keywords: karst aquifer, Escherichia coli transport, numerical model

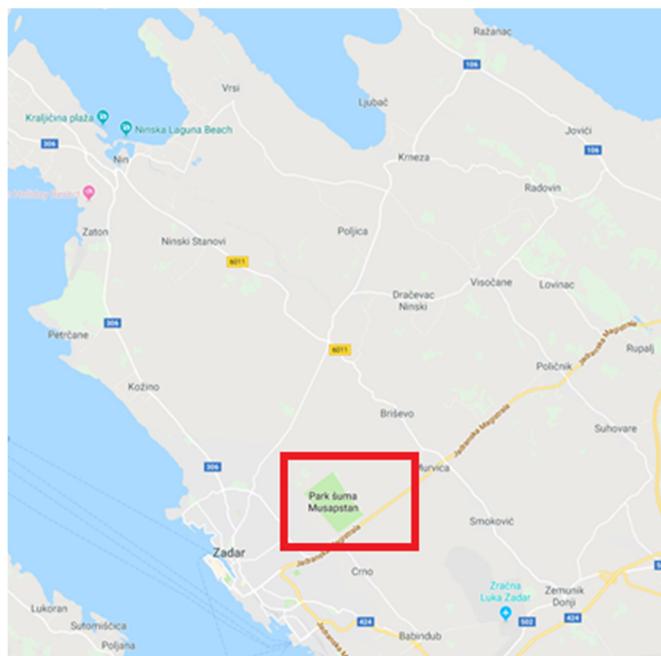
2. Introduction

Karst aquifers are very sensitive to point and nonpoint source pollution because of the existence of a preferential flows. Occasional appearance of the higher concentration of *Escherichie Coli* (*E.colli*) at the pumping sites in the Bokanjac-Poličnik karst aquifer (Zadar County, Croatia) is the indicator of fecal pollution. It is assumed that pollution infiltrate into the aquifer with the emergence of precipitation in surrounding settlements with inadequate sewage system (dysfunctional septic tanks). Determination of the pollution source is the problem which can be dealt with some of the model techniques.

The pollution from the surroundings of dysfunctional septic tanks is transported by precipitation from unsaturated (vadose) zone towards saturated zone. Unsaturated zone represents suitable surrounding for the removal of bacteria due to small percolation velocities and larger sorption potential in relation to the possibility of their removal during the transport through saturated zone.

Preferential flows in a saturated environment (macroporous soil and fractured rock) can be described by the model of dual-permeability [1,2]. The model of dual permeability includes two interactive zones, one of which is related to inter-aggregate pores (fractures), and the other one to intra-aggregate pores (matrix). The model enables the monitoring of the flow in both above-mentioned zones.

The paper shows results of the numerical simulations of *E.colli* transport from the rural settlements in the surroundings of pumping site of the city of Zadar to the B5 well (Figure 1) after intensive precipitation events (period 19/11/2018 – 1/1/2019). The transport model is divided into unsaturated (vertical) zone and saturated (approximately horizontal) section. The model of dual permeability is used for the analysis of transport in the unsaturated zone.



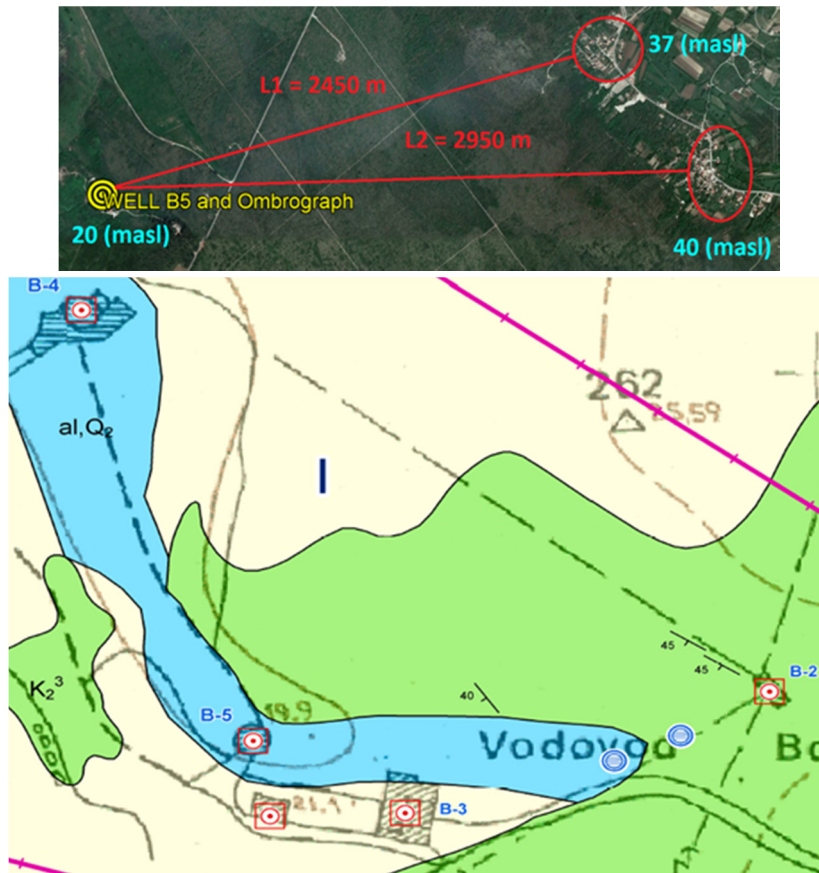


Figure 1. Positions of pumping wells (B2, B3, B4 – inactive; B5 – active), ombrograph station and surrounding settlements with the unresolved sewage system

3. Materials and methods

3.1 Implementation conditions of the in-situ experiment

During the first part of the analyzed period (19/11/2018 – 9/12/2018) from the B5 well there was no pumping. Concentration of the E.colli in raw well water was measured on 28/11/2018 and 31/12/2018. Stationary pumping of $0.105 \text{ m}^3/\text{s}$ on the B5 well were performed from 9/12/2018 until 1/1/2019. Meanwhile, the pumping was aborted in the surrounding B4 well in that period. The dates of sampling and the measured values of E.colli concentration on B5, together with the measured values of daily precipitation on the ombrograph (Lambrecht Ombrograph) and the measured water levels in the wells B2 and B5 are illustrated in Figure 2.

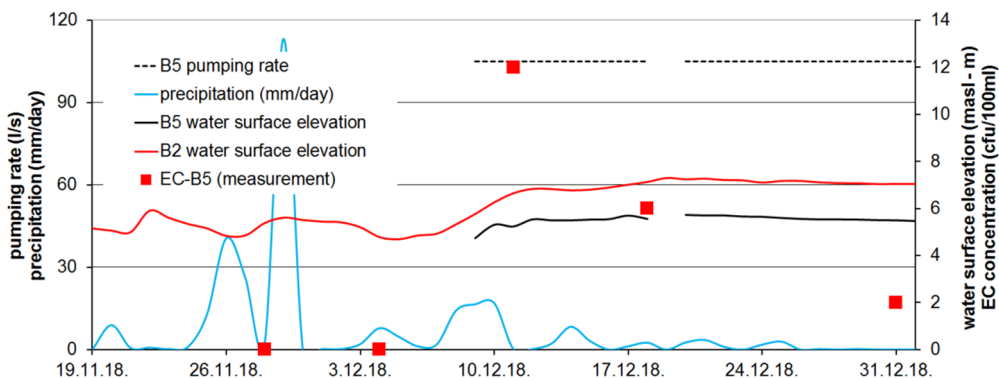


Figure 2. Measured concentration of E.colli at the pumping well B5, daily precipitation from the ombrograph and water levels in B2 and B5 wells

3.2 Groundwater levels surrounding the pumping wells

In order to determine transport through the vertical (vadose) part of the flow it is necessary to determine its length. Given the fact that there is no data on levels of the groundwater in the surrounding rural settlements (Figure 1) during analyzed period, the seepage model through the karst channel was used here [3]. The results of the implemented model indicate that the level of the groundwater in the analyzed period (19/11/2018 – 1/1/2019) was 5 – 8.2 m below the surface. It is important to emphasize that the measuring of the groundwater levels was conducted in 1996 in analyzed rural settlements [4]. The results of measuring were indicative of the fact that the level of the groundwater during November – December of 1996 was 6 to 10 m below surface.

3.3 Numerical transport model

The model Hydrus – 1D was used for vertical (vadose) part of the transport [2]. The model assumes flow and transport through two mutually interactive zones of pores – the matrix zone and the fracture zone. The founding is counted on the Richards equation [1,5]. Transfer of water between the matrix and the fractures is conducted by pressure gradient, and transfer of dissolved or colloidal matter encompasses processes of convection (conducted by water transfer) and diffusion (conducted by concentration gradient). Resolving the systems of the governing process equations is dealt with the implementation of the standard method of linear finite elements of Galerkin type.

The flow equation for fractures (subscript f) and the matrix (subscript m) in Hydrus model are:

$$\frac{\partial \theta_f(h_f)}{\partial t} = \frac{\partial}{\partial x} \left[K_f(h_f) \left(\frac{\partial h_f}{\partial x} + \cos \alpha \right) \right] - S_f(h_f) - \frac{\Gamma_w}{w}$$

$$\frac{\partial \theta_m(h_m)}{\partial t} = \frac{\partial}{\partial x} \left[K_m(h_m) \left(\frac{\partial h_m}{\partial x} + \cos \alpha \right) \right] - S_m(h_m) - \frac{\Gamma_w}{1-w} \quad (1)$$

$$K(h, x) = K_s(x) K_r(h, x)$$

where (subscript f and m refer to fractures and the matrix): w ratio of the volumes of the macropore or fracture domain and the total soil system (adopted value 0.01, Klimchouk, 2004), θ volumetric water content, h pressure head, S sink term, t time, Γ_w transfer rate

for water from fractures to matrix, K unsaturated hydraulic conductivity function, K_r relative hydraulic conductivity, K_s saturated hydraulic conductivity.

The ratio w of a fissured limestone aquifer generally ranges from 0.005% to 0.5%. However, the porosity of the epikarst can be significantly higher and estimates range from 1% to 10% [6]. The bulk hydraulic conductivity of fissured limestone volumes is about 10^{-6} m/s to 10^{-7} m/s [7].

The solution of the Richards equation (1) requires knowledge of unsaturated soil hydraulic functions and soil water retention curve $\theta(h)$ which describes relationship of the saturation level θ (ratio of the pore volume and the volume of porous environment) and pressure h and unsaturated hydraulic conductivity function $K(h)$. Unsaturated hydraulic conductivity function $K(h)$ defines hydraulic conductivity K as function h or θ . The concept of the dual permeability according to Gerke and Van Genuchten [5] is relatively complex because of the necessary characterization of retention curve and hydraulic permeability for the matrix and the fracture or channel, and also for the function of the hydraulic permeability at the fracture-matrix interface. Partial levels of saturation for the fracture θ_f and the matrix θ_m make the total saturation defined by the expression:

$$\theta = w\theta_f + (1 - w)\theta_m \quad (2)$$

Intensity of the water exchange between the fracture and the matrix Γ_w is assumed to be proportional to the pressure difference between the fracture and the matrix [5]:

$$\Gamma_w = \alpha_w(h_f - h_m) \quad ; \quad \alpha_w = \frac{\beta}{d^2} K_a \gamma_w \quad (3)$$

where: α_w first-order mass transfer coefficient, d half the fracture spacing (adopted value 0.1 cm), β shape factor that depends on the geometry (adopted value 3), γ_w scaling factor (adopted value 0.4) and K_a saturated hydraulic conductivity of the fracture-matrix interface (adopted value 10^{-5} cm/day).

DualPerm module in Hydrus-1D model relies on the retention curve of the soil according to [8] and [9]:

$$\theta(h) = \begin{cases} \theta_r + \frac{\theta_s - \theta_r}{[1 + |\alpha h|^n]^m} & h < 0 \\ \theta_s & h \geq 0 \end{cases} \quad (4)$$

$$K(h) = K_s S_e^l \left[1 - \left(1 - S_e^{\frac{1}{m}} \right)^{m-2} \right]$$

$$m = 1 - 1/n$$

Adopted values in numerical simulations are as follows: $\theta_{rm} = 0.1$ (cm³/cm³), $\theta_{sm} = 0.4$ (cm³/cm³), $\alpha_m = 0.005$ (cm⁻¹), $n_m = 1.5$ (-), $K_{sm} = 4.32$ (cm/day), $\theta_{rf} = 0$ (cm³/cm³), $\theta_{sf} = 1$ (cm³/cm³), $\alpha_f = 0.005$ (cm⁻¹), $n_f = 1.5$ (-), $K_{sf} = 8640$ (cm/day).

Formulation of the particle transport in module DualPerm of the Hydrus-1D model is based on convective-dispersive equation for the fractures and the matrix [5]:

$$\frac{\partial \theta_f c_f}{\partial t} + \rho \frac{\partial s_f}{\partial t} = \frac{\partial}{\partial z} \left[\theta_f D_f \frac{\partial c_f}{\partial z} \right] - \frac{\partial q_f c_f}{\partial z} - \phi_f \frac{\Gamma_s}{w}$$

$$\frac{\partial \theta_m c_m}{\partial t} + \rho \frac{\partial s_m}{\partial t} = \frac{\partial}{\partial z} \left[\theta_m D_m \frac{\partial c_m}{\partial z} \right] - \frac{\partial q_m c_m}{\partial z} - \phi_f \frac{\Gamma_s}{1-w} \quad (5)$$

$$\phi_f = \mu_w \theta_f c_f + \mu_s \rho s_f$$

$$\phi_m = \mu_w \theta_m c_m + \mu_s \rho s_m$$

where: (subscript f and m refer to fractures and the matrix): c and s solute concentrations in the liquid and solid phases, respectively, q volumetric flux density, ρ soil bulk density (adopted value 1.5 g/cm^3), D dispersion coefficient for the liquid phase, Γ_s mass transfer term for solute exchange between the fracture and matrix domains, ϕ sink term accounting for first-order degradation processes, μ_w first-order degradation rate constant for dissolved phase in matrix and fracture domains (adopted value 0.3 day^{-1} , [10]), μ_s is first-order degradation rate constant for solid phase in matrix and fracture domains (adopted value 0.3 day^{-1} , [10]).

Furthermore, the Hydrus model assumes disbalanced interaction between particle concentration in water (c) and the adsorbed matter on solid particles of porous media (s). Adsorption isotherm that connects s and c is described by the general nonlinear theory as follows:

$$s = \frac{K_d c^\beta}{1 + \eta c^\beta} \quad (6)$$

where: K_d , β and η are empirical coefficients.

Special cases of the above-mentioned equation are Freundlich's, Langmuir's and linear adsorption. If the values $\beta = 1$ and $\eta = 0$ are adopted, the equation represents the isotherm of the linear adsorption which is the case used when implementing numerical simulations (adopted values of coefficient for the matrix and fracture: $K_{dm} = K_{df} = 3 \text{ cm}^3/\text{g}$, [11]).

Convective- dispersive transport of the particles between the fracture and the matrix is described by the equation:

$$\Gamma_s = \alpha_s (1 - w) \theta_m (c_f - c_m) + \Gamma_w^* \quad (7)$$

where: α_s first-order solute mass transfer coefficient (adopted value 0 day^{-1}), c^* is equal to c_f for $\Gamma_w > 0$ and c_m for $\Gamma_w < 0$.

Transport through the horizontal (saturated) part is analyzed with the assumption of the uniform and stationary flow velocity with the adopted value of 1 cm/s which is correspondent to the results of the in-situ measurements of the apparent velocity of the horizontal groundwater flow from the rural settlements from Figure 1 to the B5 wells [12]. Pollution degradation in the saturated zone takes place only through the process of natural die-off, so linear theory of degradation $dC/dt = -k_w C$ is used in the model procedure. The same adopted value is used for the k_w as in the vertical part of the flow (0.3 day^{-1}). The sorption was not taken into account in the horizontal part of flow due to relatively big fracture diameters in approximately horizontal karst channels.

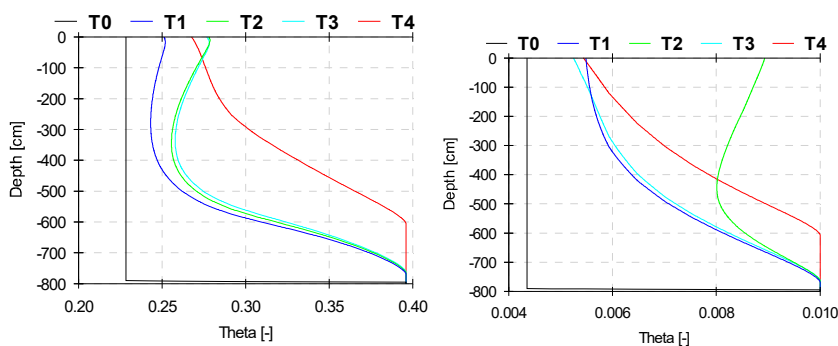
E.colli concentration dynamics entering the horizontal part of the flow is directly taken

from the results of the previously conducted numerical simulations (concentration at the end of the vadose zone transport model). The length of 2700 m was adopted for the distance between the rural settlements and B5 wells (Figure 1).

4. Results

Spatial domain of the transport model through vertical (vadose) part is adopted with 8 m which is vertically discretized with the 800 elements of 1 cm length. Non-stationary infiltration velocity with the daily intensity correspondent to the daily precipitation intensity showed in Figure 2 is used as „upper“ boundary condition. Dynamics of the water table beneath the rural settlements calculated according to methodology presented in chapter 2.2 is adopted as „lower“ boundary condition. The stationary value $c = 4E+6$ cfu/cm³ of the E.colli concentration is adopted ($4E+8$ cfu/100 ml, [12]) for the „upper“ boundary condition (at the surface level), while zero concentration gradient is used for the “lower” boundary condition. Initial conditions are expressed with the homogenous pressure value $h = -1000$ cm and E.colli concentration $c = 0$ cfu/100 ml. The impact of the vegetation roots and evaporation in all conducted simulations were not taken into account.

Figure 3 shows the vertical distribution of θ , c and the intensity of water exchange between the matrix and the fractures for the 28th, 29th and 30th of November 2018. Figure 4 shows the comparison of the measured and modelled E.colli concentration in the B5 well for the period of numerical simulation (19/11/2018 – 1/1/2019) and the calculated E.colli concentration at the end of modelled vertical part of the flow (vadose zone) with the assumption of mixing water from the matrix and the fractures in proportion defined by the parameter $w = 0.01$.



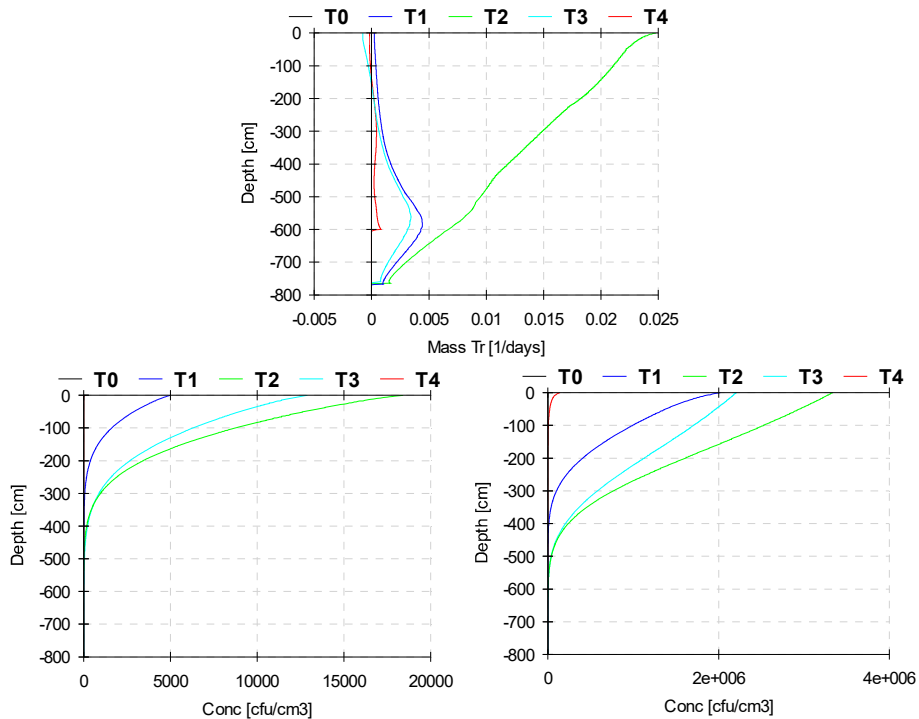


Figure 3. Vertical distribution of θ (up left – matrix, up right - fracture), c (down left – matrix, down right - fracture) and the intensity of water exchange between the matrix and the fractures (middle) for the 28th, 29th and 30th of November 2018 (T1, T2, T3) and January 1st 2019 (T4)

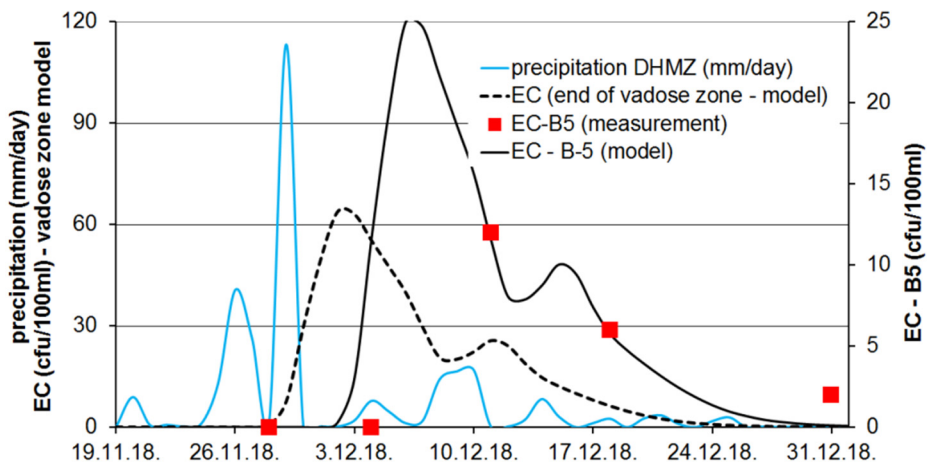


Figure 4. The comparison of measured and modelled concentration of E.colli in B5 well for the period of numerical simulation (19/11/2018 – 1/1/2019) and E.colli concentration at the bottom of modelled vertical part of the flow (vadose zone)

5. Discussion and Conclusion

Results from Figure 3 show how the saturation degree in the unsaturated zone increases

with the precipitation event. That increase is particularly pronounced in the fracture zone that is quickly filled with precipitation and generate rapid pressure increase. The green curve (T2) refers to the date 29/11/2018, the day when 113.2 mm of precipitation fell, the most in the analyzed period. The modeled increase of saturation in fractures is consistent with this data, and after that day the saturation degree drops relatively fast so that T1 and T3 have identical trend of saturation curve. This is the result of a relatively rapid percolation through the fracture zone. On the other hand, in the matrix, the increase of saturation is uniform after the first and second day (T1 and T2), and it is apparent that the more invasive precipitation from the second day does not have the same effect as in the case of fractures. On the third day (T3) recorded a slight increase in saturation due to bogging and slow drainage of water from the cracks, which continued all the way to the end of the analyzed period (T4). The water transport intensity from fractures into matrix ("+" sign) is most pronounced in the second day (T2). After the precipitation (T3) change in direction of water transport has occurred and the transport takes place from the matrix towards the fractures. This process is expressed in the first 1.5 meters from the surface of the terrain. The transport of pollution is more pronounced with the increase of the precipitation intensity, but according to the results from Figure 3 no concentration has reached the saturated zone, and the pollution has been removed to a depth of 5 m from the surface of the terrain. In the matrix zone at the end of the analyzed period (T4), no concentration has been registered, which is also a result of water transport from the matrix to the fractures.

The results in Figure 4 confirm suspicion that the surrounding settlements with unbuilt public sewage system and dysfunctional septic tanks represent the main source of fecal pollution which is then transported to the wells used for the public water supply.

References:

- [1] Šimůnek, J., N. J. Jarvis, M. Th. van Genuchten, and A. Gärdenäs, Review and comparison of models for describing non-equilibrium and preferential flow and transport in the vadose zone, *Journal of Hydrology*, 272, 14-35, 2003.
- [2] Šimůnek, J., and M. Th. van Genuchten, Modeling nonequilibrium flow and transport with HYDRUS, *Vadose Zone Journal*, doi:10.2136/VZJ2007.0074, Special Issue "Vadose Zone Modeling", 7(2), 782-797, 2008.
- [3] Lončar, G., Željko, Š., Ivezić, V.: Hydraulic-hydrology synthesis of Golubinka karst spring discharge hydrograph, *Građevinar*, 70 (2018) 4, pp. 297-303.
- [4] Geotehnika, *Vodoistražni radovi Zadar, Knjiga III – Vodostaji*, 1968.
- [5] Gerke, H. H., and M. Th. van Genuchten, A dual-porosity model for simulating the preferential movement of water and solutes in structured porous media, *Water Resour. Res.*, 29, 305-319, 1993.
- [6] Kiraly L.: Rapport sur l'état actuel des connaissances dans le domaines des caractères physiques des roches karstiques, In: Burger A. and Dubertret L. (Eds), *Hydrogeology of karstic terrains*, Int. Union of Geol. Sciences, B, 3, pp.53-67, 1975.
- [7] Milanovic, P.: *Hidrogeologija karsta i metode istraživanja*, (in Serbo-Croatian; Karst hydrogeology and methods of investigations), HE Trebišnjica, Institut za korištenje i zaštitu voda na kršu, Trebinje, 302 p, 1979.
- [8] van Genuchten, M. Th., A closed-form equation for predicting the hydraulic

- conductivity of unsaturated soils, *Soil Sci. Soc. Am. J.*, 44, 892-898, 1980.
- [9] Mualem, Y., A new model for predicting the hydraulic conductivity of unsaturated porous media, *Water Resour. Res.*, 12, 513-522, 1976.
- [10] Foppen, J.W., Herwerden, M.V., Schijven, J.: *Measuring and modelling straining of Escherichia coli in saturated porous media*, J.Contam. Hydrol., 93, 1-4, 236-254., 2007.
- [11] Bandy, A. M.: Mobility of Escherichia Coli within Karst Terrains, Kentucky, USA. 2016.
- [12] Pavičić, A., Terzić, J., 2006: *Hidrogeološki i geofizički istraživački radovi za mikrozoniranje Poslovne zone "Bokanjac" kod Zadra*. (Hydrogeological and geophysical research for the micro zoning of the Bokanjac business district near Zadar). Fond HGI 14/2006. (Technical report, in Croatian), 2006.
- [13] Paluszak, Z., Ligocka, A., Breza-Boruta, B.: *Effectiveness of Sewage Treatment Based on Selected Bacteria Elimination in Municipal Wastewater Treatment Plant in Toruń*, Pol. J. Environ. Stud. 12(3): 345-349. 2003.

Topic no. 6 - River Basin Restoration Strategies and Experiences

MULTICRITERIAL EVALUATION OF THE BÍLINA RIVER REVITALIZATION

TOMÁŠ JULÍNEK¹, JAROMÍR ŘÍHA¹

¹ Faculty of Civil Engineering, Brno University of Technology, Veveří 95, 602 00 Brno, Czech Republic,
E-mail: julinek.t@fce.vutbr.cz, riha.j@fce.vutbr.cz

1. Abstract

The Ervenice Corridor (EC) is a massive embankment of a height up to 170 m and a length of about 11 km in the area of the surface coal mine. One of the arrangements during the mining was a relocation of 3 km long river reach of the Bílina River into four steel pipelines located on the crest of the Corridor. As the mining is gradually attenuating and principal settlements have gone, the river basin authority is looking for more environmental solutions including revitalization of the Bílina River along the EC. The paper describes a formalized multi-criteria evaluation of selected variants of the revitalization of the EC.

Keywords: river revitalisation, multi-criteria analysis, surface coal mine

2. Introduction

The Ervenice Corridor (EC) is a massive embankment with a height of up to 170 m, the corridor length is approximately 11 km. Between 1964 and 1985, approximately 520 million m³ of overburden was deposited in the embankment of the corridor. Through the dump, the Bílina River is transferred through four steel pipes of 1200 mm in diameter and an emergency channel. The related waterworks (inlet, outlet, SWPP) are located on the plain of the Ervenice Corridor.

The current pipeline of the Bílina River at km 61,119 to 64,373 no longer fulfils its function for which it was built [2]. The latest complete technical safety surveillance inspection stated that the pipeline is at the end of its service life due to the annual material losses.

The river basin authority is looking for possible solutions for the revitalization of the Bílina River along the EC [1]. It is expected that the Czech Government will be presented with a regional project proposing the concept of management and use of reclaimed areas. This project will include the Bílina River revitalization along the EC as one functional unit.

The EC is a territory that has been created by human activity. The extensive earthen body was created by the depositing of secondary material produced during the mining of brown coal. The embankment body consists mainly of clay loam [5]. Since the material was deposited in the excavated area, it is referred to as the inner dump. There were relocations of road, railway and the Bílina River on this dump. The research shows the

fact that even the wider territory is formed by dumps from anthropogenic sediments of the character of clays with high to very high plasticity with fragments of claystone. These are anthropogenic sediments of the surface quarry [6].

Water management in the area of interest is addressed within the so called Water Management System of Alternative Measures for the Drinov Reservoir [4]. The Drinov reservoir was located at the site of actual quarry. The system serves to transfer water from the Ohře natural river basin to the deficit-catchment area of the Bílina River. The main purposes of the system are [4]:

- Solution of drainage conditions after disposal of the Drinov reservoir at the location of quarry.
- Protection of surface quarries from the flooding.
- Surface water supply for industry, energy, heating, drinking water, agriculture and irrigation, surface quarrying and other customers.
- Providing ecological discharge in selected profiles.



Figure 1. The Ervenice Corridor (the Bílina river)

The Water Management System consists of numerous rivers, streams and structures allowing for drainage and distribution of water within the system [4]. Table 1 provides list of main monitoring profiles on streams within the system.

Table 1. List of streams characteristics within the system

Stream	Profile	km	F	H	Q_a	q	Q_{355}	Q_{100}
			[km ²]	[mm]	[l/s]	[l/s.km ²]	[l/s]	[m ³ /s]
Podmílešský b.	downstream the confluence with Hradistsky brook	3,19	16,9	765	144	9,0	18,7	20,3
Hradistsky b.	upstream the transfer to supply system	2,20	7,94	750	67,5	8,5	8,8	10,7
Trnity b.	confluence with supply system	3,30	3,90	600	17,6	4,51	2,3	9,0
Prunerovsky b.	upstream the partitioning object	7,41	39,5	760	383	9,7	50,2	35,6
Luznicka	upstream junction to	2,55	5,54	750	41,6	7,51	4,4	11,6
Lidensky b.	confluence with supply system	0,10	2,80	730	20,5	7,32	2,2	7,8
Hutna II	confluence with supply system	5,20	10,9	750	85,7	7,90	8,4	14,1
Hacka	crossing with supply system	10,40	19,1	650	124	6,49	12,2	22,7
Brezenecy b.	confluence with supply system	0,10	7,80	680	35,0	4,49	3,7	25,0
Bílina	upstream supply sytem	66,5	106,8	663	865	8,10	90	85,4
Bílina	upstream the Jirkov dam	69,60	27,6	805	287	10,40	30	33,1
Bílina	LG Jiretin	56,31	181,5	690	1700	9,37	170	62
Luzec	confluence with supply system	1,69	16,7	750	145	8,68	15,3	30
Kundraticky b.	confluence with supply system	0,00	8,50	750	74,0	8,71	7,8	26
Vesnický b.	confluence with relocated reach	1,96	3,80	850	47,5	12,50	5	16

The water management system consists of a series of water management structures such as:

- five major reservoirs,
- pump station,
- industrial water supply network,
- emergency supply of industry,
- weirs,
- small water power plant on supply channel,
- links to other water management systems (river catchments) and connections with single reservoirs,
- a network of natural and modified watercourses, the streams are partly relocated due to mining.

This paper contains a formalized multi-criteria evaluation of selected variants of the revitalization of the Ervenice Corridor. The aim of the evaluation is to determine the most suitable variant of the arrangement and solution of revitalisation of the Bílina River on the EC in terms of seven selected and agreed criteria. The subject of the evaluation is the proposed 6 variants of the future arrangement of the EC [5]:

- VARIANT 1 (V1) - Current status.
- VARIANT 2 (V2) - Revitalization according to [1].
- VARIANT 3 (V3) - Revitalization according to [1] with modifications required by Agency of Nature and Lanscape Protection. These are mainly changes in single objects like SWPP a proposal of bolder chutes.
- VARIANT 4 (V4) - Only revitalization without energy utilization.
- VARIANT 5 (V5) - Only revitalization without energy utilization with relief of flood discharges into the abandoned quarry (newly formed lake).
- VARIANT 6 (V6) - The complete connection of the Bílina River to the quarry (newly formed lake).

3. Methods

The objective of the work is an assessment of the proposed variants using the multi-criteria analysis. The procedure consists of the following steps:

1. design and description of evaluation criteria,
2. derivation of weights for individual criteria using the pairwise comparison method and method based on respondents' preferences,
3. the description of the variants in relation to the individual evaluation criteria,
4. evaluation of individual variants (verbal and formalized),
5. comprehensive formalized assessment.

3.1 Definition and description of evaluation criteria

The determination of the individual evaluation criteria was based on the requirements of the river basin authority [7] and was refined on the basis of individual aspects characterizing the specific technical solution of each variant. The evaluation of the proposed variants takes into account the criteria described below. The importance of each criteria is emphasized by the assigned weight (Chapter 3.2.). The accepted criteria were as follows:

- C1 - Environmental impact
- C2 - Water management aspects
- C3 - Economy
- C4 - Impact on land use
- C5 - Realization aspects
- C6 - Operational aspects
- C7 - Uncertainty in a given variant

3.2 Derivation of weights for individual criteria

Firstly, weighing was done using the pairwise comparison method. The pairwise comparison of the criteria was performed by a procedure expressing preferential relations in a binary way (0, 1), when the rating "1" corresponds to the preferred criterion according to Chapter 3.1. The preferences were derived using the results of discussions with the contracting authority and professionals.

The pairwise comparison method is based on the determination of preferential relationships of the pairs of criteria (i, j). The score $d_{p,j}$ expressing the number of preferences r_{ij} belonging to the criterion j is expressed by the relation:

$$d_{p,j} = \sum_{i=1}^n r_{ij} + 1 \quad (1)$$

where r_{ij} is criterion preference j relative to i , n is number of criterions (in our case $n = 7$).

The result of the evaluation is the ranking of the criteria according to their influence on the suitability of individual variants (Table 2). The weight of the j -th criterion is determined from:

$$w_j = \frac{d_{p,j}}{d_p} \quad (2)$$

where

$$d_p = \sum_{j=1}^n d_{p,j} \quad (3)$$

The basis and description of the individual scales did not allow their "finer" differentiation, for example, by the Saaty method [3]. In order to find a better balance of the weights, the preferences resulting from the questionnaire were used for preferential method. The weight of the j -th criterion is determined from the relation (2) and (3) when:

$$d_{p,j} = \sum_{i=1}^m r_{ij}, \quad (4)$$

where

$$r_{ij} = n - h_{ij} \quad (5)$$

where h_{ij} is the rating of criterion j according to its rank (may not be a natural number) proposed by the assessor i , n is number of criterions, m is the number of responding specialists.

3.3 Evaluation of individual variants

Based on comprehensive description of each variant with respect to defined criterions, the variants were evaluated. Within the comparative analysis, the advantages and disadvantages of the individual variants were assessed in a formalized manner with respect to the individual evaluation criteria. The evaluation was performed using a scale from 1 to 5, where a higher value is assigned to a better value according to the verbal regulation:

- 1 - completely negative evaluation, completely disadvantageous variant
- 2 - negative rating, disadvantageous option
- 3 - neutral rating, neutral option
- 4 - positive reviews, preferred option
- 5 - very positive reviews, very convenient option

In assessing the variants, the difficulties arising from a certain heterogeneity of the input data as well as the different detail of the variants design (documentation), should be taken into account. The advantage is the fulfilment of the assumption that for each criterion the variants are mutually comparable, their content clearly specified, realizable and that they respect the technical possibilities and legislative limits.

3.4 Overall evaluation

The evaluation is performed by multi-criteria optimization, weighting and scoring. The significance of each criterion was quantified by expressing the weight, the size of which was derived by a pairwise comparison method and a method based on respondent preferences (Table 2).

The summary evaluation was carried out in a tabular way, whereby the $B_{i,k}$ score was assigned to individual variants according to the relevant criteria based on the evaluation of individual aspects. The final score H_i , obtained as the sum of the results of multiplying the weights w_k and the score $B_{i,k}$ for the individual criteria j in the respective variant i , expresses which variant provides the most favourable solution. Mathematically, the procedure can be expressed as follows:

$$H_i = \sum_{k=1}^7 B_{i,k} \cdot w_k \tag{6}$$

4. Results and discussion

The first step of the multi-criteria analysis was the determination of weights according chapter 3.2. Example of resulting values for preferential method is shown in Table 2. The comparison of the weights determined by both methods is shown in Figure 2. The weights are fairly similar, differences can be seen just for criterion 2 and 7.

Table 2. Weights - a method based on respondent preferences

Criterion j	Number of responding specialist										dpj	Criterion weight wj
	1	2	3	4	5	6	7	8	9	10		
C1	6	6	5	4	5,5	5,5	5	6	6	5,5	54,5	0,260
C2	5	5	6	5	5,5	5,5	6	5	5	5,5	53,5	0,255
C3	4	4	3	3	4	4	4	4	4	4	38	0,181
C4	3	3	4	2	3	2	2	2	2	0	23	0,110
C5	0	0	0	1	2	0	1	1	0	1	6	0,029
C6	2	2	2	6	1	3	3	3	3	3	28	0,133
C7	1	1	1	0	0	1	0	0	1	2	7	0,033

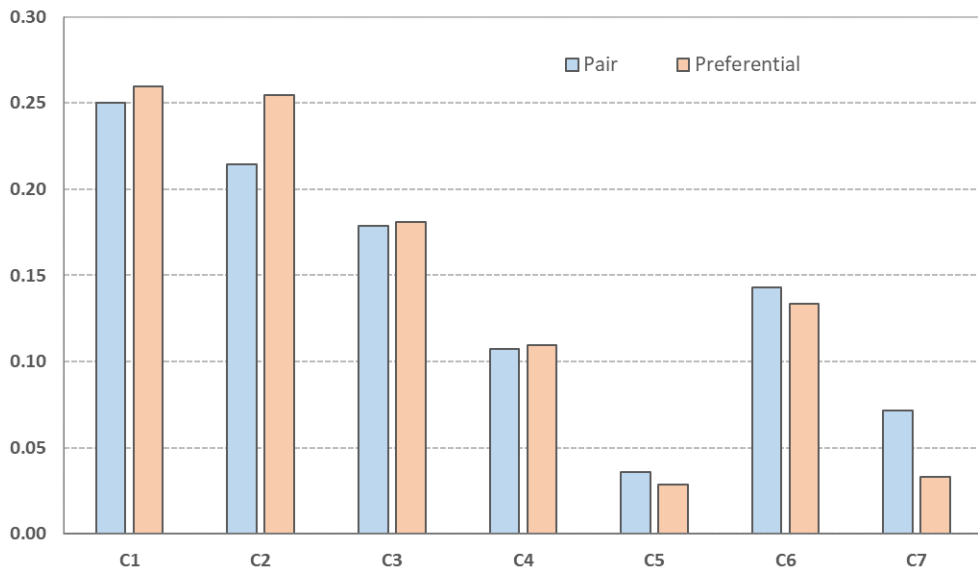


Figure 2. Comparison of resulting weights for different methods

After application of expression (6) the following resulting order of variants was reached (Tables 3 and 4):

Resulting evaluation using weights determined by pairwise comparison (Table 3)

1. V4 - Only revitalization according to requirements of Agency of Environment and Landscape Protection.
2. V5 - Only revitalization according to environmental agency requirements with overflow of flood discharges to the former mine.
3. V6 - Ccomplete connection of the Bílina river to the former mine.

Resulting evaluation using the weights determined on the basis of respondent preferences (Table 4)

1. V5 - Only revitalization according to environmental agency requirements with overflow of flood discharges to the former mine.
2. V4 - simple revitalization according to requirements of environmental agency.
3. V6 - complete connection of the Bílina river to the former mine.

The results of the multicriterial evaluation show that the most advantageous variants are V4 (simple revitalization) and V5 (simple revitalization with flood discharges overflow to the quarry).

Resulting order of the variants is summarized in Table 3. and 4. in the column "Rank". In terms of the proposed criteria, their weights and the point quantification, the most advantageous option is the highest score. The first three most preferred variants are highlighted in Tables 3. and 4. The evaluation was carried out for two variants of the criteria weights and the resulting score differs slightly as well as the resulting ranking of the judged variants. Comparison of both methods results is schematized in Figure 3.

Table 3. Formalized evaluation of the proposed variants, weights based on pair comparison

		Variant evaluation							Total	Rank
		C1	C2	C3	C4	C5	C6	C7		
Weight	w	0,250	0,214	0,179	0,107	0,036	0,143	0,071	Score	
V a r i a n t	V1	1	4	4	1	5	2	4		
	V2	2	3	3	3	4	3	5	2,929	5
	V3	3	3	3	3	4	3	4	3,107	4
	V4	5	2	4	4	3	4	3	3,714	1
	V5	5	3	3	4	3	4	2	3,679	2
	V6	4	5	1	5	2	2	1	3,214	3

Table 4. Formalized evaluation of the proposed variants, weights based on preferences

		Variant evaluation							Total	Rank
		C1	C2	C3	C4	C5	C6	C7		
Weight	w	0,260	0,255	0,181	0,110	0,029	0,133	0,033	Score	
V a	V1	1	4	4	1	5	2	4		
	V2	2	3	3	3	4	3	5	2,836	5

r i a n t	V3	3	3	3	3	4	3	4	3,062	4
	V4	5	2	4	4	3	4	3	3,688	2
	V5	5	3	3	4	3	4	2	3,729	1
	V6	4	5	1	5	2	2	1	3,398	3

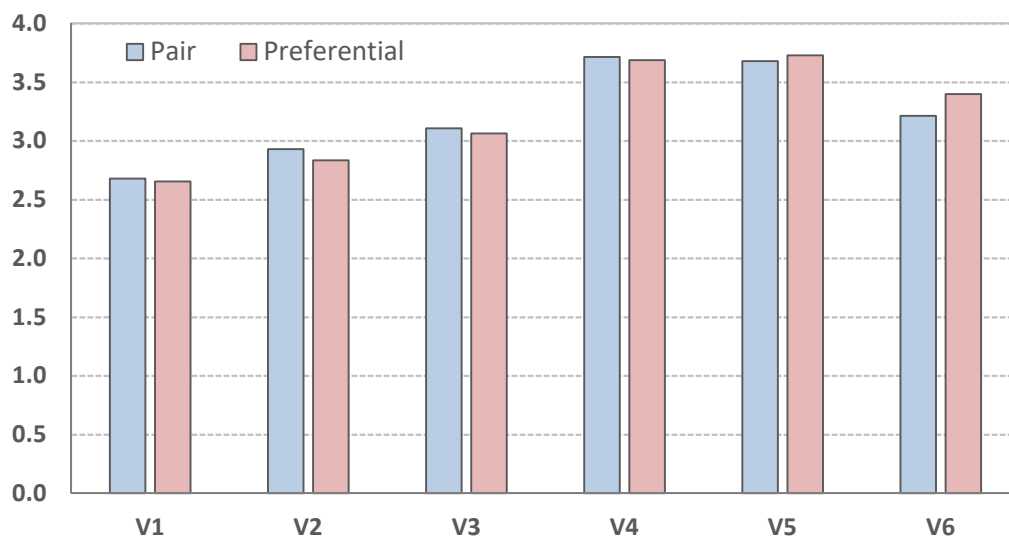


Figure 3. Comparison of final score for two variants of applied weights

5. Conclusions and recommendations

The results of the multicriterial evaluation show that the best scores were obtained for variants V4 and V5. Yet the V5 variant is based on the “more sensitive” weighting of the method using the preferences of respondents evaluating the weights of individual criteria (Table 4). The third suitable option is V6, which represents the complete redirection of the Bilina river through the former mine. Its implementation, however, suffers from a number of significant uncertainties consisting in political decisions about the fate of the mine, in the hydrological situation in the following decades and especially in the chosen method of filling the residual pit of the quarry in relation to the quantity and quality of the water source and the balance of the future lake.

During the elaboration of this work, there was a need to supplement some of the data and, in particular, the study work. The activities which would reduce uncertainties in the further procedure of revitalization on the Ervenice Corridor are:

- In advance, it will be useful to develop a variant and optimized water management solution of the actual system with the inclusion of a residual mining pit containing:
 - summary passport and summary data on the status and capacity of individual elements of the system (channels, feeders, tanks, etc.),
 - variant hydrological forecasts and assumptions,

- hydraulic calculations,
 - suggestions for modification of existing system elements,
 - derivation of a realistic filling period for former mine in individual stages.
- The water balance must include evaporative water losses, infiltration, etc.
- Exploration work is recommended for qualified estimates of evaporative water losses and infiltration. We recommend to investigate the size of the infiltration not only on the EC plan, but also on the residual pit area (some steps have already been taken).
 - Ensure long-term monitoring of water quality in all potential sources of water that could be used to fill the residual pit of the mine.
 - Elaboration of individual objects in more detail related to the variants (SWPP, inlet, outlet, spillway, etc.).

The final recommendation is to design a V4 variant with a possible extension to V5. We assume that the overflow object can be designed and built separately in the second stage of revitalization. We recommend to start the construction work for revitalization of the Bílina river until about 2022, when the end of life of pipes can be justifiably expected.

References:

- [1] VH TRES.: Bílina po Ervěnickém koridoru – revitalizace (technical documentation). DPS. České Budějovice. 04/2014.
- [2] The River Basin Ohře Authority: Bílina po Ervěnickém koridoru - revitalizace. 2017. Zpráva pro vedení Povodí Ohře, s.p. TPŘ PO. (Technical report). 02/2017.
- [3] Saaty, T. L.: Relative Measurement and Its Generalization in Decision Making Why Pairwise Comparisons are Central in Mathematics for the Measurement of Intangible Factors The Analytic Hierarchy/Network Process. RACSAM. Rev. R. Acad. Scien. Serie A. Mat. VOL. 102 (2). p. 251–318. 2008.
- [4] Manipulační řád vodohospodářské soustavy náhradních opatření za Dřínov. II.1. Manipulační řád VH soustavy NOD. (Operating regulations). Povodí Ohře, s. p., 9/2007. (aktualizace 2017).
- [5] Pichler, E., Fultner, J., Valvoda, P.: Ervěnický koridor – zakládání a konsolidace zemního tělesa za proměnlivých podmínek v dobývacích prostorech lomů Jan Šverma a velkolomu Čs. Armády – I. část., Zpravodaj Hnědé uhlí, str. 3-19, 2/2014.
- [6] Geoindustria: Geologický průzkum. Ervěnický koridor. 1982.
- [7] The River Basin Ohře Authority: Podklady pro zadání multikriteriálního hodnocení variant řešení revitalizace EK. 2018. (Digital input data).

Topic no. 7 - Climate Change and Flood Risk Management

FLOOD RISK MANAGEMENT: AN INSTITUTIONAL DEVELOPMENT PERSPECTIVE

CVETANKA POPOVSKA¹, DIMITRIJA SEKOVSKI², DARKO BARBALIĆ³,

¹ Faculty of Civil Engineering, Ss. Cyril and Methodius University, Skopje, Macedonia,
popovska@gmail.com

² Energy, Environment and Disaster Risk Management Unit, UNDP, Skopje, Macedonia,
dimitrija.sekovski@gmail.com

³ River Basin Characterization and Flood Risk Assessment, Water Management Institute "Hrvatske vode", Zagreb, Croatia: darko.barbalic@gmail.com

1. Abstract

Republic of Macedonia is highly exposed to flooding, droughts, extreme temperatures, forest fires and earthquakes, and floods are the chief hydro-meteorological hazard. Damages and losses associated with floods are on the rise in the last decades. Flood Risk Management (FRM) aims to reduce the human and socio-economic losses caused by flooding. Important part of FRM is to analyze the relationships between physical system, institutional framework and socio-economic environment. This covers a wide range of topics from drivers and natural processes to models, decisions and socio-economic consequences and institutional environment.

This paper presents the findings of an interdisciplinary review of possible country-level institutional model alternatives for adopting flood risk management in the Republic of Macedonia by harmonizing the national water management, and other related systems with the requirements of the EU Floods Directive. Based on the application of Analytic Hierarchy Process (AHP) theory, a tailor-made institutional model for integrated risk-based flood management is proposed as a substitute of the current ineffective flood management approaches that are based on purely engineering design-based standards and ad-hoc interventions to flood events. It discusses the benefits of introducing the model and outlines the key preconditions to its operationalization. Given the similarity of existing flood management systems in the countries of the wider region, these findings can be used for initiating similar improvements in line with the contemporary flood risk management principles.

Keywords: Flood Risk Management, EU Floods Directive, Analytic Hierarchy Process

2. Introduction

Republic of Macedonia is highly exposed to flooding, droughts, extreme temperatures, forest fires and earthquakes, and floods are the chief hydro-meteorological hazard, Figure 1. Damages and losses associated with floods are on the rise in the last few years. River floods in the major river basins are caused by long periods of rainfall and the intensive snow melting. River floods occur in the basins of the Vardar, Crna Reka, Treska, Strumica, Pčinja, Lepenec and Bregalnica rivers. Intensive rainfall and increase of groundwater levels in combination with poorly maintained flood control infrastructure resulted in frequent flooding of flat, mainly former wetland areas, such as Polog,

Pelagonija, Skopsko Pole and Strumičko Pole. Flash floods caused by short intensive rainfall occur in smaller river basins.

Traditionally, the main flood control activities in urban rivers comprised conventional regulations. In the majority of cities, rivers have been regulated mainly by considering hydrological and hydraulic aspects, with very little or no attention to ecological functions and aesthetic aspects.

A typical example of such ‘functional’ regulation, often referred to as a good practice from the past, has been the regulation of the Vardar River in the country’s capital Skopje. However, the flood control functionality of the regulated riverbed has been seriously diminished with the implementation of the controversial ‘Skopje 2014’ project. This massive urban infrastructure development project in the centre of Skopje comprised various new structures in the major riverbed, construction of new low placed footbridges with insufficient discharge capacity, construction of fountains and plant boxes in the basic riverbed, construction of fixed concrete/steel boats, also in the basic riverbed, as well as additional structures in the river’s floodplain.

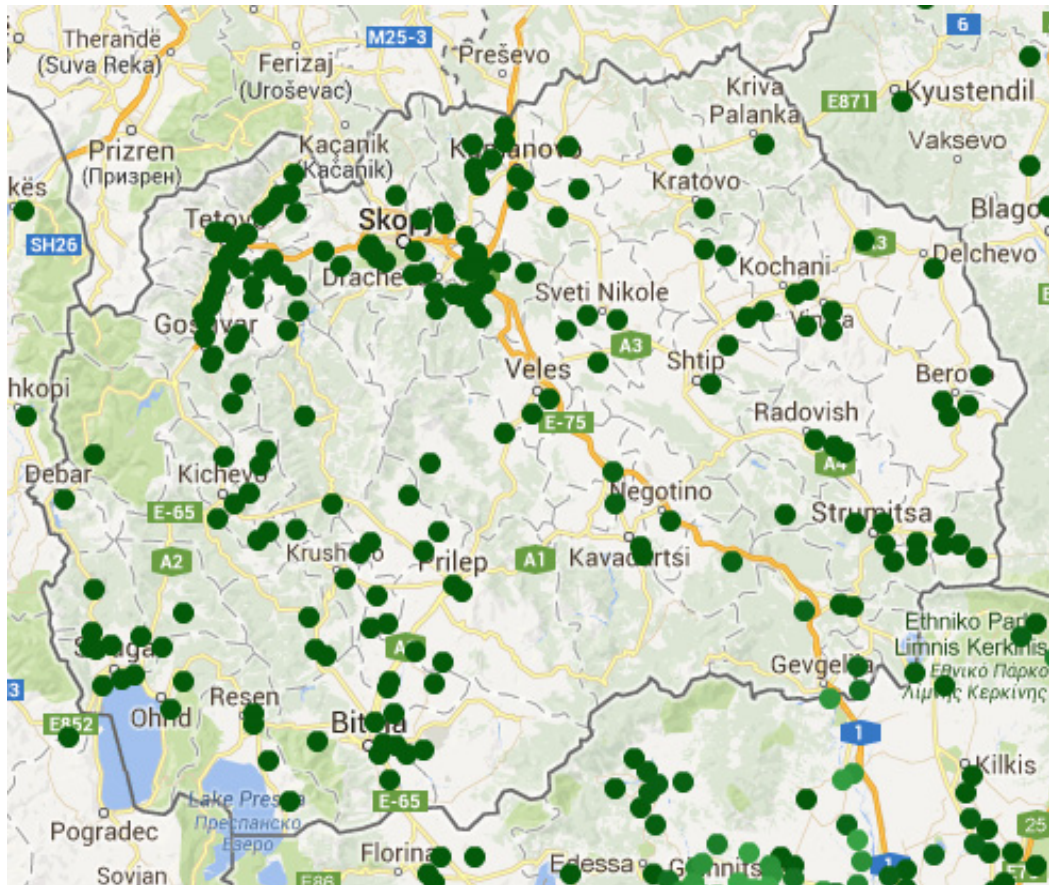


Figure 1. Registered flood events in the last 60 years (Source: <http://globalfloodmap.org/>)

Such development happened in time when the majority of EU water-related legislation has already been formally adopted – although its practical implementation is challenged

by multiple barriers – institutional, financial and human capacities. Therefore, the adoption and operationalization of the EU Floods Directive – the only piece of EU water-related legislation that hasn't been incorporated in the national systems yet – is considered particularly instrumental in preventing future similar developments that increase flood risks. The harmonization of the existing water management and other related systems in the country with the requirements of the EU Floods Directive provides the opportunity for replacing the commonly applied ad-hoc responses to flood events and the traditional approaches based on purely engineering/design-based standards with an integrated risk-based flood management.

This paper presents the findings and recommendations of the UNDP-backed interdisciplinary review of possible country-level flood risk management models aligned with the objectives of the EU Floods Directive. It proposes a tailored approach and outlines the key preconditions for its institutionalization.

2.1 Effects of and responses to significant recent flash floods

Floods participate with 44% of all disaster events in the Republic of Macedonia [1]. The Vardar river basin, which is the largest in the country, accommodates about 80% of all water resources and experiences the highest levels of exposure to flooding. The genesis of floods occurring in Skopje, for example, is specific mainly due to coincidence of flood wave peaks in Upper Vardar, Treska and Lepenec rivers. Because of this the city of Skopje was very often flooded and the most catastrophic appeared in 1778, 1858, 1876, 1895, 1903, 1916, 1935, 1937, 1962 and 1979. The floods of 1962 and 1979 resulted in economic losses of approximately 7.4% of GDP (for each year), while the floods in 1994 caused losses of 3.4% of GDP.

The occurrences of extreme hydrological events (floods and droughts) have increased in frequency and intensity over the past decades as a response to changing climate conditions. During the last three decades, flood events were caused by the largest rivers in Macedonia – Vardar, Crna Reka, Strumica, Treska, Pčinja, Lepenec, and Bregalnica. The estimated total damage worth US\$ 193.8 million.

In June 2004 alone, intensive rainfall, caused floods and activated torrential streams that affected 26 municipalities (mainly in the area of upper Vardar, but also in the central, southern and south-eastern part of the country), causing an estimated damage of EUR 15 million. The damages caused by floods directly affect the already fragile agriculture and local rural economies. 91.3 percent of the total damage caused by the flash floods in 2004 was in the agricultural production mainly in the south-east part of the country. The most severely affected were the rural communities where households and cultivated areas were flooded [1].

Severe flooding also hit much of the country in January and February 2015, causing widespread damages and economic losses. Heavy rainfall caused rivers to overflow in many locations, and 44 out of 80 municipalities experienced floods. The most affected regions were the basins of the Crna Reka, Bregalnica and Strumica rivers, which cover about 45% of the territory of the country. Roughly 170,000 people were affected in all. The floods caused major damages to roads and bridges, interrupting transport. Much agricultural land was also flooded, causing extensive losses to farming families. Drainage and irrigation systems were damaged, and private houses, industrial facilities,

schools and public facilities in some villages were flooded.

The initial impact assessment estimated the total cost of the spring 2015 floods at 35,691,672 EUR. Of this total, 62% were classified as damages and 38 percent as losses [2].

A subsequent flood-related disaster hit the country on 3 August 2015, when flash floods and mudslides struck the northwest Polog Region, killing six people and causing damage to municipal infrastructure and houses in the city of Tetovo and villages in the surrounding mountainous areas. The total damages from these floods are estimated at 21.5 million EUR [3].

Most recently, the night between 6 and 7 August 2016 heavy torrential rain affected Capital's suburbs, causing tragic loss of 23 lives and an estimated cost of over 30 million EUR, Figure 2, resulting from the severely damaged infrastructure and affected agricultural land. The Hydrometeorological Service measured 92.9 mm of rain that fell in just a few hours, which is considered an event with a return period of 1,000 years [4].

The apparent increase in the frequency and intensity of flood events indicate that the overall flood risk in the country is also increasing. The tragic consequences of the most recent extreme flood events, and the magnitude of the associated damages and losses, revealed major deficiencies in all the key components of the overall flood management system (e.g., monitoring, planning, response, and recovery). This emphasizes the need of urgent reforms in the flood management system in line with the contemporary risk-based management approaches, as elaborated in this paper at conceptual level.

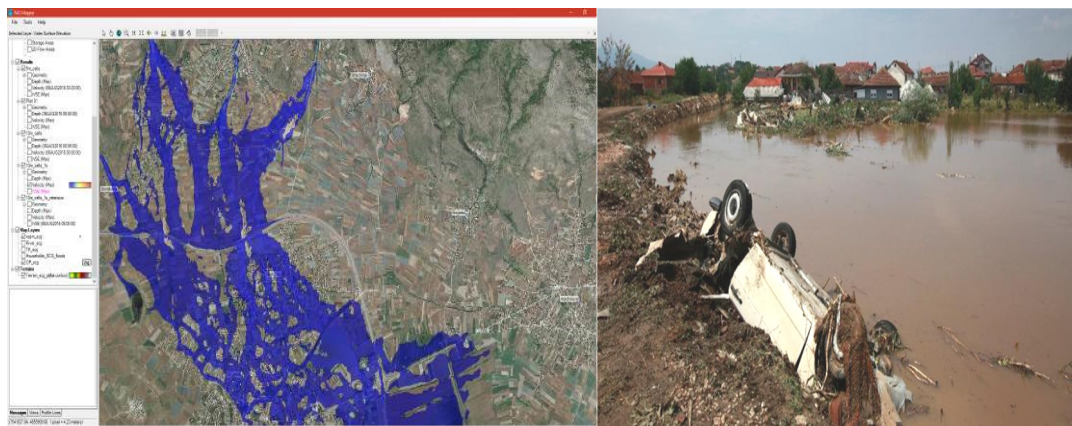


Figure 2. Skopje flood on 6 August 2016: 2D hydraulic simulation of the flooded area (left) and effects of the flood in the affected areas

3. Methodology and approach

The methodology applied is based upon an interdisciplinary assessment of possible country-level institutional model alternatives for adopting flood risk management in line with the objectives of the EU Floods Directive. The aim of the exercise was to identify the most feasible approach to incorporating additional functionality to an existing

institutional setup. For this purpose, four alternatives were formulated to consider existing administrative environment, practice and tradition, as well as interrelation with compatible, overlapping and conflicting services. The flexibility of the EU Floods Directive in terms of selection of institutional models that are adjusted to local circumstances and needs was one of the guiding principles when generating alternatives.

The limited prior work on the topic in the country, data availability constraints, and the limited possibility of formulating closed and absolutely objective assessment criteria, suggested the application of a robust and simple form of informed assessment rather than developing sophisticated models for setup assessment.

The assessment was carried out in three interlinked stages. In the first stage an interdisciplinary team of experts, practitioners and decision-makers in water and flood management, disaster risk reduction, legal and economic aspects, contributed to the gap assessment and formulated four conceptual institutional models.

In the second stage, based on the analysis of existing administrative arrangements, as well as EU-based experiences on flood risk management, the institutional setup models were subject to a SWOT analysis, and a simplified numerical assessment of the proposed alternatives. The numerical assessment provided a comparison basis, based on the most important aspects (15 criteria), as shown in Table 2 below. It consists of initial grading on how well each alternative score on each criterion (from 1 – poor to 5 – excellent), calculating the average grade for each alternative, and then applying specific weights to each criterion based on their relevance to get a weighted grade.

To provide more reasonable basis for decision-making among the proposed alternatives, the project team employed the Analytic Hierarchy Process (AHP) theory or relative ranking of alternatives based on pair-wise comparisons [5], [6].

For the needs of the AHP, the most important criteria for the numerical assessment were grouped in three major categories based on their relatedness, as follows: *Group 1 – Floods Directive (FD) Related*, consisting of: river basin approach, integrated water management, integration of FRM in River Basin Management Plans, international cooperation, and competent authority; *Group 2 – Flood Risk Management (FRM) Related*, consisting of: unified approach to risk management, conflicts of FD and operative flood defense, solidarity principle, efficiency of financing, and non-structural measures planning; and *Group 3 – Organizational*, comprising: clear responsibilities and relationships, number of additional personnel, concentration of expertise and knowledge, institutional rearrangement, and logistics benefits.

In the final stage, the outcomes of these assessment stages were presented to and discussed with key stakeholders to fine-tune the proposed optimal management arrangement and agree on the process for its institutionalization.

The functional analysis of the proposed institutional models was carried out vis-à-vis the key objectives of the Flood Risk Management (FRM) concept that has evolved from the outdated concept of Flood Protection (FP) that aims primarily to ensure flood prevention by providing a defined protection (or safety) standard, which still is the dominant way of dealing with floods in the country. The adoption of the concept in the national context is thought to be of critical importance as it will help to concentrate future flood control

efforts to high risk areas, allowing for using public funds in an economically efficient way [7]. Embedding this risk-based approach would enable the achievement of best management outcomes within available budgetary and other resources.

For the needs of this analysis the definition of flood risk as a product of the likelihood of flooding, and the associated adverse consequences (e.g., social, economic, environmental, and other impacts) is used, and as an inter-relation of hazard and vulnerability, Figure 3. Examples of corresponding flood management strategies to be applied by the newly proposed structures are provided in Table 1.

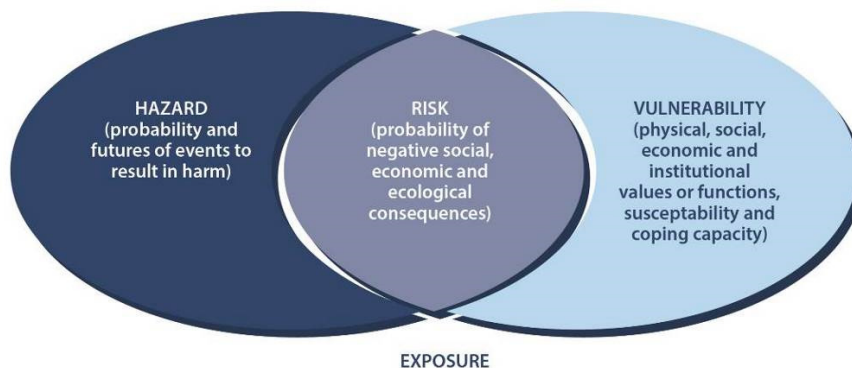


Figure 3. Risk as inter-relation of hazard and vulnerability, [8]

Table 1. Flood management strategies

STRATEGY	OPTIONS
Reducing Flooding	dams and reservoirs
	dikes, levees and flood embankments
	high flow diversions
	catchment management
	channel improvements
Reducing Susceptibility to Damage	floodplain regulation
	development and redevelopment policies
	design and location of facilities
	housing and building codes
	flood proofing
Mitigating the Impacts of Flooding	flood forecasting and warning
	information and education
	disaster preparedness
	post-flood recovery
Preserving the Natural Resources of Floodplains	flood insurance
	floodplain zoning and regulation

More specifically, flood risk management practiced by the new institutional structure will rely on the so-called “Cascade of Measures”, Figure 4, as an elementary guidance for planning of flood risk management measures based on the source-pathway-receptor principle. These include: (i) reduction of the flood source (reducing of runoff) to prevent high discharges and high flood risks downstream as the most favourable measure, (ii) reduction of the hydraulic load on flood control structures by reducing and transforming

flood wave discharges and water elevations, (iii) conventional flood control measures, (iv) zoning measures to help reducing the potential impact, (v) impact reduction measures, such as flood proofing of houses, early warning and evacuation, and (vi) residual risk reduction measures, where other measures are not sufficient.

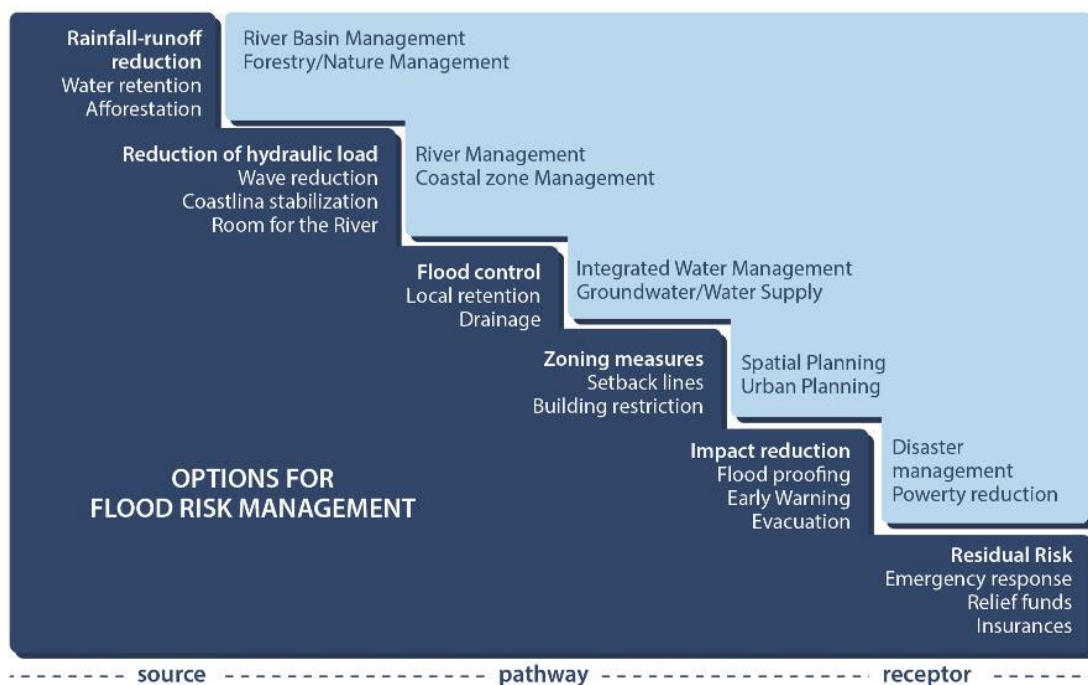


Figure 4. Cascade of measures, [9]

4. Results and discussion

Flood risk management comprises significant number of different activities interacting with numerous policies and activities. For the purpose of these analyses, the flood risk management has been approached to as a public service with significant application of the solidarity principle.

The EU Floods Directive introduces systematic approach primarily to flood risk management planning aspects and integrated water management/governance, while operative flood defence is not placed in focus. By this it provides significant freedom for shaping flood risk management to suite national needs and thus, in a broader sense, it does take into account operative flood protection in flood risk management.

The institutional arrangements are not unified and differ significantly among EU member states. Having in mind that the current institutional setting in the Republic of Macedonia is not completely defined and the responsibilities are distributed across different bodies, there is an opportunity to develop a tailor-made flood risk management system. The proposals take into consideration the existing country systems with certain competences over the management of floods (e.g., Ministry of Environment and Physical Planning which is also the EU Water Framework Directive (WF) body,

Hydrometeorological Services – HMS, Crisis Management Center – CMC and Protection and Rescue Directorate – PRD, both of them with responsibilities over the operative flood defence and multi-hazard planning).

Considering country's limited resources, area and population (area of 26,000 km², population of app. 2,100,000) the approach to institutional improvement of flood risk management is suggested to follow one of the following possible directions: (i) introduction of strong coordination mechanisms or (ii) centralisation of (at least some) management functions. Although possible approaches, with sub-options are numerous, four basic alternatives are proposed and analysed:

Alternative 1: Body dedicated to flood risk management (FRM)

This body consists of 6 units, corresponding to the six key functions of flood risk management (planning, development and implementation, operative flood defence, public and stakeholder relations, information support), as well as management and logistics. It entails all main functions of flood risk management, but integrated water management is not achieved by the introduction of such a structure.

Alternative 2: Flood risk management (FRM) integrated with WFD

In this option, in comparison to first one, major step is made towards integration of flood risk management in river basin management according to WFD. Considering the fact that certain activities of flood risk management and river basin management overlap (marked with darker blue colour in the graph), they can be aggregated and combined to achieve mutual benefits.

Alternative 3: Flood Directive (FD) integrated with WFD

This option is same as option two, except that the operative flood defence is placed outside this body. In such case development of operative flood defence and supporting activities would be entrusted to the Hydrometeorological Service (HMS), the Crisis Management Centre and the Protection and Rescue Directorate (CMC/PRD). Main benefit for FD/WFD body would be simpler organisation, and narrower scope of work (e.g., no need for operative flood forecasting activities, and other activities supporting operative flood defence, such as maintaining of equipment, ensuring additional workforce). Certain functions such as monitoring of structures and watercourses should still be preserved for maintenance purposes.

Alternative 4: Flood Directive (FD) implanted in existing institutions

This option relies on preserving existing legal and regulatory environment, as well as institutional arrangements and enhancing greatly inter-institutional cooperation. The overlapping competencies among significant number of institutions at different levels would require clear definition of extensive cooperation and coordination mechanisms. At the same time certain functions, such as planning in line with EU Floods Directive are missing and still need to be implemented. As a main disadvantage of this option, in order to achieve functional flood risk management, significant institutional rearrangements should be done, and some kind of inter-institutional body for collaboration, international cooperation, public participation, reporting and setting joint standards needs to be introduced. Based on the revealed deficiencies in the system from the most recent flood events, it is very likely that the main goal of this option (non-disturbance of existing institutional arrangements) cannot be fully achieved if an

effective flood risk management is to be introduced.

As the overall assessment was based mostly on subjective judgement of experts, decision-makers and practitioners, there was a concern on how much the selection of optimal administrative setup is sensitive to errors by subjectively defined weights and criteria assessment.

To address this, around 1,000 modified assessment tables were generated in which grades set by individuals in the original table were randomly altered in the range of ± 2 , and the weights were changed in the range of $\pm 50\%$ of the original values. The results showed that in 990 out of 1,000 (99%) generated cases, alternative 2 (Flood risk management integrated with WFD body) was superior to other options and in other 10 (1%) cases it was ranked as second best. Alternative 1 (Body dedicated to flood risk management) was superior in 8 (<1%) cases and ranked as second best in 659 (66%) cases. Alternative 3 (Flood Directive activities integrated with WFD body) was ranked as the best in 2 (<1%) cases and ranked as the second best in 331 (33%) cases. The fourth alternative (Flood Directive activities implanted in existing institutions) was the lowest ranked in all 1,000 (100%) cases.

For the application of AHP, the groups of criteria were ranked based on the same weights used to rank the individual criteria, resulting in the following matrix that illustrates the relative importance of each group of criteria in relation to each other.

Table 3. Pair-wise comparison of the main criteria

	FD RELATED	FRM RELATED	ORGANIZATIONAL
FD RELATED	1.00	1.33	2.00
FRM RELATED	0.75	1.00	1.50
ORGANIZATIONAL	0.50	0.67	1.00

Based on the comparison matrix each alternative was analyzed in view of each group of criteria; the scores for each alternative were obtained resulting in the final decision-making basis, indicating the most favourable alternative. Table 4 summarizes the results of the AHP.

Table 4. Results from the Analytic Hierarchy Process (AHP)

AHP	ALTERNATIVE 1	ALTERNATIVE 2	ALTERNATIVE 3	ALTERNATIVE 4
Group 1 Criteria	0.10940	0.17094	0.12991	0.03419
Group 2 Criteria	0.10448	0.12438	0.06965	0.03483
Group 3 Criteria	0.06093	0.06810	0.05376	0.03943
Total score	0.27481	0.36342	0.25333	0.10844
RESULTS	27%	36%	25%	11%

With an overall score of 36% the Analytic Hierarchy Process also pointed out the second alternative as the superior one compared to the other three.

5. Conclusion

The paper proposes an EU-based institutional setup model for the Republic of Macedonia that would respond to the requirements of the contemporary flood risk management approaches and as such address some of the key deficiencies in the existing flood management system.

From the flood risk management point of view, the proposed Alternative 2: FRM integrated with WFD is suggested as the optimal against the key objectives of the exercise. The participatory expert-based Analytic Hierarchy Process suggested this option as the one with the greatest potential to respond to all major requirements of the EU water-related management policies. By building upon these findings, the institutional model can be further adjusted in light of institutional development priorities, capacity strengthening needs and opportunities, as well as financial instruments in place.

As a recommendation, in any institutional development scenario, given the urgency of the issue of providing better management of floods, there are a number of preliminary activities whose implementation would be beneficial regardless on the selected option. These include, for example, development of a GIS-based spatial database on floods and flood management practices, development of flood hazard and flood risk maps, as well as flood risk management plans for the main river basins and priority areas in the country, and their use in spatial and urban planning. The introduction and development of such flood management approach is a continuous process which requires specific interdisciplinary expertise, coordination and communication instruments and major awareness rising. Therefore, priority needs to be placed on education, raising awareness at all levels in society and developing of efficient coordination mechanisms among institutions and communication with the population, especially in the areas at the highest risk of flooding.

Although complex and potentially costly, such an institutional reform can be easily justified as an absolute necessity if optimal flood risk mitigation and prevention of significant future losses is to be achieved, especially in light of the most recent catastrophic consequences of flooding in the country.

Acknowledgements

The analyses presented in this paper have been carried out by a team led by the Faculty of Civil Engineering, Skopje under the UNDP Restoration of the Strumica River Basin project, funded by the Swiss Agency for Development and Cooperation.

References:

- [1] SEE Disaster Risk Mitigation and Adaptation Initiative (2008), ISDR & World Bank, Desk Review Study
- [2] Rapid Damage and Needs Assessment (2015), Ministry of Agriculture, Forestry and Water Economy, World Bank and EU
- [3] Feasibility Study on Flood Protection in the Polog Region (2015), United Nations Development Programme (UNDP).
- [4] Flood Risk Modelling Study for the City of Skopje (2016), United Nations Development Programme (UNDP).
- [5] Saaty, T.L. (2008), Relative Measurement and its Generalization in Decision Making: Why

- Pairwise Comparisons are Central in Mathematics for the Measurement of Intangible Factors – The Analytic Hierarchy/Network Process. Review of the Royal Academy of Exact, Physical and Natural Sciences.
- [6] Saaty, T.L.; Peniwati, K. (2008), Group Decision Making: Drawing out and Reconciling Differences. Pittsburgh, Pennsylvania: RWS Publications. ISBN 978-1-888603-08-8.
 - [7] Messner, F. and Meyer, V. (2006), Flood Damage, Vulnerability and Risk Perception – Challenges for Flood Damage Research. Flood Risk Management: Hazards, Vulnerability and Mitigation Measures, Volume 67 of the NATO Science Series pp 149-167, Springer.
 - [8] Schanze, J. (2006), Flood Risk Management - A Basic Framework: Chapter 1 of Flood Risk Management – hazards, vulnerability and mitigation measures, Ed. Schanze, Zeman and Marsalek, NATO Science Series, IV Earth and Environmental Sciences – Vol. 67, Springer, Dordrecht, The Netherlands, ISBN 1-4020-4597-2.
 - [9] Guidance Document on the Integrated Assessment of Existing and Planned Civil Engineering Measures for Flood Protection (2014), EU IPA Twinning Project: Development of Flood Hazard Maps and Flood Risk Maps.
 - [10] Directive 2000/60/EC of the European Parliament and of the Council establishing a framework for Community action in the field of water policy.
 - [11] Directive 2007/60/EC of the European Parliament and of the Council on the Assessment and Management of Flood Risks, October 2007.
 - [12] Flood Management Tools Series (2008), World Meteorological Organization, http://www.apfm.info/ifm_tools.htm.
 - [13] Integrated Flood Management. Concept Paper (2009), Associated Program on Flood Management (APFM), World Meteorological Organization (WMO), Global Water Partnership (GWP).

BUILD BACK BETTER APPROACH TO RECOVERY OF FLOOD-DAMAGED TRANSPORT AND WATER INFRASTRUCTURE

CVETANKA POPOVSKA¹, MILORAD JOVANOVSKI², DIMITRIJA SEKOVSKI³

¹Faculty of Civil Engineering, Macedonia, popovska@gf.ukim.edu.mk

²Faculty of Civil Engineering, Macedonia, jovanovski@gf.ukim.edu.mk

³Energy, Environment and Disaster Risk Management Unit, UNDP, Macedonia, dimitrija.sekovski@gmail.com

1. Abstract

The frequency of disaster events, especially floods, has been on the rise globally in the past decades. This has led to a demand for improved post-disaster recovery strategies. The Build Back Better (BBB) approach involves improving the physical, social and economic aspects of affected communities to induce greater resilience.

Macedonia is also facing various types of natural hazards, and floods continue to have a growing share in the overall damages and losses. The intensity and severity of floods increases damages on infrastructure, property and economy. The country was ranked high among Eastern and Central Europe countries in terms of the overall vulnerability to climate change using an index that takes into account exposure, sensitivity, and adaptive capacity.

This paper presents some of the outcomes of the UNDP-implemented EU Recovery Programme whose main objective was to support country's recovery efforts after 2015-floods. Special emphasis is placed on the general design guidance for recovery of the most common types of flood-damaged transport and water infrastructure contained in the country's first-ever BBB manual. The manual outlines and contextualizes the BBB approach, providing an overview of its basic principles, and recovery design guidelines, aiming to enhance resilience levels and overall preparedness to future disaster events.

Keywords: Build Back Better, Post-Disaster Recovery, Transport and Water Infrastructure

2. Introduction

Most of the river basins in Macedonia are facing increased spatial and temporal variability of water resources which is among the key natural factors increasing the flooding risk, besides topographic and land characteristics. In addition, the changes in land use and land cover structure are further modifying hydrological regimes, increasing the risk of extreme flood events. Additional causes of the growing flooding risk include:

- Reduced conveyance capacity of existing regulated river sections due to poor maintenance, construction and conversion of river corridors;

- Poorly maintained hydraulic/flood control infrastructure such as drainage systems, embankments, levees;
- Operating regimes of existing multi-purpose dams and reservoirs not optimized to enable improved flood mitigation.

Common period of flood appearance in the country is November-January caused by overflow of the major rivers Vardar, CrnaReka, Treska, Strumica, and Bregalnica. Besides this kind of flooding caused by long rainy periods and intensive snowmelt (or combination of both), there are flash floods caused by short and intensive rains, most frequently in summer periods, in smaller river basins. The floods in 2004 affected 26 municipalities with an estimated damage of approximately EUR 15 million. Floods from January and February 2015 affected 43 out of 80 municipalities in the country, causing a damage of over EUR 35 million, [1]. Floods caused major damages on roads, bridges, culverts, drainage and irrigation systems, industry facilities, schools, and private houses.

A subsequent disaster occurred on 3 August 2015, when flash floods and mudslides struck the northwest Polog Region, killing six people and causing damage to municipal infrastructure and houses in the city of Tetovo and villages in the surrounding mountainous areas. The total damages from these floods are estimated at 21.5 million EUR, [2].

Moreover, the night between 6 and 7 August 2016 heavy torrential rain affected country's capital suburbs, causing tragic loss of 23 lives and an estimated cost of over 30 million EUR, resulting from the severely damaged infrastructure and affected agricultural land, Figure 1. The Hydrometeorological Service measured 92.9 mm of rain that fell in just a few hours, which is considered an event with a return period of 1,000 years, [3].



Figure 1. Effects of 2016-floods near Skopje

3. Causes for Damages to Transport and Water Infrastructure

The recent floods in the country caused major damages to transport infrastructure (roads, bridges, culverts) and water infrastructure (drainage and irrigation systems, riverbed regulation, dams). This resulted with a negative impact on many productive activities,

and access to social services in the affected areas.

Damages to transport and water management infrastructure sites can be categorized generally in two groups: natural and man-made, Figure 1. Natural damages to infrastructure are mainly caused by regional climatic and geological conditions, while man-made can be caused by technical, accidental and incidental activities. Technical damages are caused in different stages during the project development process – starting from project planning until its realization and exploitation.

3.1 Natural damages

Natural causes are often related to geological and meteorological hazards such as earthquakes, landslides, floods, droughts, etc. One of the most prominent causes of natural damages in Macedonia are floods. They make up around 44% of the natural damages, creating the biggest concern for civil engineers in the country in the last decade due to their massive increase in their frequency and intensity, [4].

3.2 Technical damages

Technical causes are far more complex than the natural ones and can be a result of deficiencies in the project development/designing or the operation and maintenance of infrastructures. Normally, it is hard to detect this type of causes considering the difficulties in tracking down cause-effect relationships. The possible causes of such technical damages that can lead to an unsuccessful project or an insufficiently resilient infrastructure to the harmful effects of the waters are: regulatory or institutional, engineering or designing.

3.3.1. Engineering causes

Engineering or design causes are related to design documentation, design reviews and quality of performance of the construction works. Some of the key engineering causes include:

- Inadequately prepared project design offers, i.e. offers without a clear methodology, without specification of necessary support and unrealistic estimated timeframe;
- Inadequate and/or insufficient background research on the necessary base data - existing and new. Namely, the necessary site investigations such as geodetic, geological, geotechnical, morphological, hydrological, ecological and water management data are without analytical scope;
- Inadequate methodological approach and/or insufficiently implemented design analyses, especially regarding throughput capability and resilience of the structures from the impact of the water;
- Inadequate technical solutions and/or design of facilities with obsolete methods and obsolete performance technologies;
- Lack of internal project monitoring;
- Inappropriate or inaccurate review of the technical designs;
- Inadequate supervision and control of construction performance and quality of materials used;

- Illegal construction of facilities, most often without valid project documentation. This especially refers to the construction of structures in the floodplains, and riverbeds themselves. It often happens that even small dams are built as illegal structures.

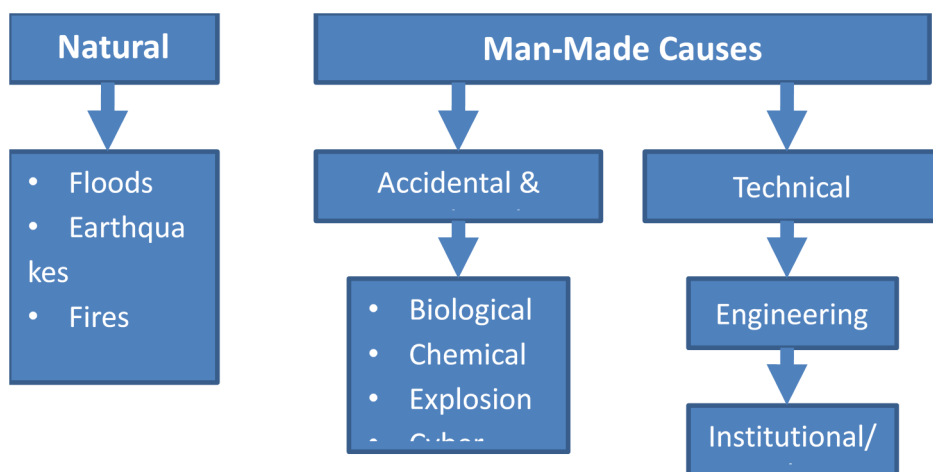


Figure 2. Causes of damages to infrastructure

3.3.2 Institutional causes

Institutional or regulatory causes are often related to institutional or specific procedural steps, for example:

- Inapplicable or insufficiently precise design requirements from the responsible institutions;
- Shortcomings in the selection of contractors. In this context, the "lowest price" practice is often accepted as the "most favorable bid", while some of the higher financial offers are a better fit in terms of the methodology, the scope of the required analyzes and the timeframe;
- Gaps in making decisions regarding changing duration of construction implementation set in the design;
- Inadequate selection of supervising engineers;
- Exclusion of the "design supervision" position in public procurement procedures, which is essential for large-scale complex infrastructure projects;
- Omissions during technical inspection and commissioning;
- Irregularities in issuing building permits;
- Inappropriate and/or no maintenance of the structures;
- Lack of operational plans and techniques for managing facilities, including with respect to the risk of flooding;
- Insufficient monitoring of structures and preventive flood protection activities. Monitoring is extremely important not only for the purpose of efficient and preventive action in protection, but also for the purpose of establishing a historical database for further analysis of the causes and damages as building blocks for developing recovery projects;

- Insufficient cooperation and coordination between institutions and overlapping of competences. For example, the water management, environmental, forestry management, energy economy ministries often lack cooperation and common interests in solving problems.

4. Key Concepts of Building Resilient Infrastructure

Infrastructure must be planned to respond to the ‘new normal’ of increasingly frequent and more intense disaster events due to climate change – building back the same is simply not enough. In order to achieve resilient infrastructure guiding principles have to be followed, [5]:

- A. Site analysis: An understanding of the site risks ensuring infrastructure elements and structures are located in the optimum building borders on the subject site (e.g. avoiding areas likely to be subject to overland floods or landslides);
- B. Risk and site assessments: Plan ahead to understand and mitigate for possible risks and hazards before a disaster to make the response more efficient;
- C. Scoping and planning of projects: Allowing enough time and resources to discuss, analyze information and consult. Utilize existing transport and water management network and land use plans to assist decision making, ensuring Disaster Risk Reduction (DRR) and Building Back Better (BBB) principles are taken into account.
- D. Engineering and spatial planning: Utilize engineering and urban/spatial planning design options to improve both the infrastructure structure’s resilience, ensuring the infrastructure structures provide equitable access and use.
- E. Materials and construction quality: Construction including inspection and testing of materials and workmanship is essential to ensure safe, functional and durable transport infrastructure. External monitoring of these quality checks by an impartial party strengthens these checks.

4.1 “Build Back Better” Principles

The frequency of disaster events worldwide, especially floods, has been increased in recent times. This led to a demand for improved post-disaster reconstruction and recovery efforts. The slogan “Build Back Better” (BBB) denotes improving the physical, social and economic aspects of communities during reconstruction and recovery to induce greater resilience. Another definition is that the “Build Back Better” signifies an ideal reconstruction and recovery process that delivers resilient, sustainable and efficient recovery solutions to disaster-affected areas, [6]. The use of the recovery, rehabilitation and reconstruction phases after a disaster to increase the resilience of nations and communities through integrating disaster risk reduction measures into the restoration of physical infrastructure and societal systems, and into the revitalization of livelihoods, economies and the environment is also one more definition of “Build Back Better” terminology.

Statistics from United Nations Environment Programme (2008) show an increase number of natural disasters over time attributing to growing populations, urban growth in risk-prone areas due to scarcity of land, global warming and other impacts. Both

natural and man-made disasters have seen nearly exponential rises in the number of disasters over time. Despite the increasing number of disaster experiences, post-disaster activities remain inefficient and poorly managed [7].

Traditionally, post-disaster reconstruction consisted of simply repairing the physical damage induced by a disaster. However, rebuilding the built environment and infrastructure exactly as they were prior to a disaster often re-creates the same vulnerabilities that existed earlier, [8]. If restored to pre-disaster standards, disaster-affected infrastructure and communities would face the same difficulties if exposed to another disaster event in the future. The reconstruction and recovery period following a disaster poses an opportunity to address and rectify vulnerability issues found in communities. As a result of witnessing the ongoing impacts of disasters on communities, a concept started to emerge where post-disaster reconstruction was to be taken as an opportunity to not only reconstruct what was damaged and return the community to its pre-disaster state but to also seize the opportunity to improve its physical, social, environmental and economic conditions.

Lessons learnt from many disaster events worldwide led to establish key considerations in post-disaster reconstruction and rebuilding for a more sustainable future [9]. Reviewing the existing guidelines and international research, the following three key concepts represent BBB approach: (i) Risk Reduction, (ii) Community Recovery, and (iii) Implementation.

4.2 International recommendations and practices

The concept of BBB proposes is a broad holistic approach to post-disaster reconstruction in order to address the wide range of prevalent issues and ensure that affected areas/communities are regenerated in a resilient manner for the future. Several guidelines directly or indirectly proposing BBB based recovery and reconstruction activities can be found, such as:

- Key Propositions for Building Back Better, (Clinton, 2006).
- Build Back Better Guiding Principles, (GoSL, 2005).
- Rebuilding for a more Sustainable Future: An Operational Framework, (FEMA, 2000).
- Recovery and Reconstruction Framework, (VBBRA, 2011).
- Build Back Better Operations Manual: A manual for the DILG and LGUs on how to design, manage and implement Build Back Better Infrastructure Projects, (AVID & DILG, 2015).

The above listed guide documents are based on experience of disaster recovery and reconstruction interventions that have been very complex/mixed including and proposing more administrative measures (regulation, capacity building, risk management, multilateral cooperation, NGOs participation) and less pure engineering approach (design, construction and monitoring the recovery and restoration projects).

4.1.1 The Sendai Framework

The “Sendai Framework for Disaster Risk Reduction 2015-2030” was prepared by United Nation International Strategy for Disaster Reduction (UNISDR) and adopted at

the Third UN World Conference in Sendai, Japan. It is the outcome of stakeholders' consultations and inter-governmental negotiations, supported by the United Nations Office for Disaster Risk Reduction. This document is the successor instrument to the Hyogo Framework for Action (HFA) 2005-2015: Building the Resilience of Nations and Communities to Disasters.

The Sendai Framework is built on elements which ensure continuity with the work done by States and other stakeholders under HFA and introduces a number of innovations. A strong emphasis on disaster risk management as opposed to disaster management is an outcome. The scope of disaster risk reduction has been broadened significantly to focus on both natural and man-made hazards and related environmental, technological and biological hazards and risks.

The Sendai Framework also articulates the following: (i) need for improved understanding of disaster risk in all dimensions of exposure, vulnerability and hazards characteristics, (ii) strengthening of disaster risk governance including national platforms, (iii) accountability for disaster risk management, (iv) preparedness to "Build Back Better", (v) recognition of stakeholders and their roles, (vi) mobilization of risk-sensitive investment to avoid the creation of new risk, (vii) resilience of infrastructure, cultural heritage and work-places, (viii) strengthening of international cooperation and global partnership, and risk-informed donor policies and programs, including financial support and loans from international financial institutions. There is also clear recognition of the Global Platform for Disaster Risk Reduction and the regional platforms as mechanisms for coherence across agendas, monitoring and periodic reviews in support of UN Governance bodies.

- A. *Scope and purpose*: The framework will apply to the risk of small-scale and large-scale, frequent and infrequent, sudden and slow-onset disasters, caused by natural or man-made hazards as well as related environmental, technological and biological hazards and risks. It aims to guide the multi-hazard management of disaster risk in development at all levels as well as within and across all sectors.
- B. *Expected outcome*: Substantial reduction of disaster risks, losses of lives and the economic, physical, social, cultural and environmental assets of persons, businesses, communities and countries.
- C. *Goals*: Prevent new and reduce existing disaster risk through the implementation of integrated and inclusive economic, structural, legal, social, health, cultural, educational, environmental, technological, political and institutional measures that prevent and reduce hazard exposure and vulnerability to disaster, increase preparedness for response and recovery, and thus strengthen the resilience.
- D. *Targets*: Substantially reduce global disaster mortality by 2030; substantially reduce the number of affected people globally by 2030; reduce direct disaster economic loss in relation to global gross domestic product (GDP) by 2030; substantially reduce disaster damage to critical infrastructure and disruption of basic services, among them health and educational facilities, including through developing their resilience by 2030; substantially increase the number of countries with national and local disaster risk reduction strategies by 2020; substantially enhance international cooperation to developing countries through adequate and sustainable support to complement their national actions for

implementation of this framework by 2013; substantially increase the availability of and access to multi hazard early warning systems and disaster risk information and assessments to people by 2030.

5. Post-flood recovery infrastructure examples

The EU Recovery Programme implemented in the country incorporated the following key goals: (i) to assist the country's recovery efforts in the aftermath of the floods that occurred in early 2015 by reconstructing damaged water infrastructure; (ii) to apply the "building back better" approach to maximize resilience to future floods and mitigate the risk of floods in the most sensitive regions. Examples of before and after recovery and reconstruction of transport and water management infrastructure systems are shown in figures below.



Figure 3. Reconstruction of spillway and stilling pool of Mavrovica Dam

Mavrovica Dam. The dam is earthfill dam constructed in 1984 near Sveti Nikole Municipality. The height of the dam is 24 m that enable volume of 2.5 million m³. Side spillway with chute canal and dissipater at the outlet were completely destroyed due to floods and lack of maintainance. The dam crest was lined with concrete plates that were also destroyed due to wave impact. Reconstruction of dam crest and spillway structures was going in phases: field investigations, design preparation, review, construction, and supervision.



Figure 4. Reconstruction of Lipa Dam

Lipa Dam. This is an earthfill dam with clay core constructed in 1988 near Negotino. The dam height is 18 m and the volume of the eservoir is 70.000 m³. The body of the dam and associate structures was damaged after couple of floods in the last decade. Reconstruction of dam, spillway and bottom outlet was going in phases: field investigations, design preparation, review, construction, and supervision



Figure 5. Reconstruction of Trabotivishte Bridge on Bregalnica River

Trabotivishte Bridge. This was a damaged bridge on the river Bregalnica in Delchevo municipality near village Trabotivishte and Razlovci. The bridge was 62 m long and with notable deformations on the lower bearing construction and the upper road structure. Due to the erosion that has severely damaged concrete piles of the bridge its reconstruction is considered an urgent matter. In the process of reconstruction in 2015 a project was developed in which besides structural solutions for strengthening of the bridge, designed measures are incorporated for mitigating the erosion and increasing the river flow capacity of the bridge openings.



Figure 6. Reconstruction of Drenska Dam.

Drenska Dam. Several floods in the last decade, especially the ones in January and February 2015, severe damaged Drenska Dam in Demir Kapija Municipality. A part of the dam was completely destroyed the accumulation is almost discharged and the facility can not be used for the basic purpose - irrigation of downstream agricultural land. The volume of the accumulation according to the 2009 project was 100,000 m³, and according to the latest geodetic surveys, for the needs of the rehabilitation project, only 20,000 m³ is the result of intensive sedimentation. The dam with a height of 12.5 m and a crown length of 45 m was built without a structure for control and evacuation of high

waters. The resulting damage is a result of infiltration through the body of the dam. The recovery project dam contained: geodetic surveys, geotechnical investigation and laboratory analyzes, hydrological analyzes, alternative solutions for consolidation of the body of the dam, an abandoned land for evacuation and control of high waters, hydraulic analysis of structures, monitoring of dam structures and body, technical conditions for performance and quality of materials.

6. Conclusion

The paper presents parts of the outcomes included in the manual that aims to outline and contextualize the “Build Back Better” concept on country level and provides an overview of its basic principles and how to ensure a greater level of resilience and preparedness to future disaster events. The main goal is to ensure effective implementation of pre and post-disaster infrastructure and aims to empower engineers, local authorities and communities to incorporate better planning measures in post-disaster recovery. The manual provides guidance to assessing the magnitude of damages on infrastructure, decision-making about recovery needs and possibilities, and recovery approaches that will ensure greater resilience of the infrastructure to future floods, also taking into consideration possible climate changes and the need to minimize environmental effects.

Country-level knowledge on “Build Back Better” principles is limited including: (i) higher investment of the long-term economic losses as a result of building inappropriate infrastructure; (ii) procedural complications and likely delays in case of significant changes in the design documentation; (iii) overall inertia of design engineers to apply new approaches and tendency to stick to the routine design practices; and (iv) no formal legal requirements.

Permitting procedures for recovery of infrastructure damaged by natural disasters are shorter and more efficient as no classical construction permit is required. However, these shortened procedures generally limit the possibility of applying substantive changes in the recovery design (e.g., by applying the “Build Back Better” approach).

References

- [1] Rapid Damage and Needs Assessment (2015), Ministry of Agriculture, Forestry and Water Economy, World Bank and EU
- [2] Feasibility Study on Flood Protection in the Polog Region (2015), United Nations Development Programme (UNDP)
- [3] Flood Risk Modelling Study for the City of Skopje (2016), United Nations Development Programme (UNDP)
- [4] South Eastern Europe Disaster Risk Mitigation and Adaptation Initiative (2008), ISDR & World Bank Desk Study Review
- [5] Build Back Better Manual: Roadmap towards resilient transport and water infrastructure (2018) EU Flood Recovery Programme, UNDP
- [6] Sendai Framework for Disaster Risk Reduction (2015-2030), UN Office for Disaster Risk Reduction
- [7] Halverson SJ, Hamilton JP. (2010), In the Aftermath of the Qa'yamat: The Kashmir Earthquake Disaster in Northern Pakistan. Department of Geography, University of Montana

- [8] Kennedy J, Morice C, Parker D.: Global and regional climate in 2010. Met Office, Exeter. 2008.
- [9] Da Silva J., (2010) Lessons from Aceh. Key Considerations in Post-Disaster Reconstruction
- [10] Mannakkara S, Wilkinson S. (2014), Re-conceptualising “Building Back Better” to improve post-disaster recovery. International Journal of Managing Projects in Business
- [11] Bridge Structure – Maintenance and Rehabilitation Repair Manual (2012), Georgia Department of Transportation
- [12] Design Guidelines for Bridge and Culvert (2004), Alberta Transportation, Technical Standards Branch

ENHANCING RESILIENCE THROUGH RECOVERY OF FLOOD-DAMAGED INFRASTRUCTURE IN MACEDONIA: AN OVERVIEW OF LESSONS AND CHALLENGES

DIMITRIJA SEKOVSKI¹, CVETANKA POPOVSKA²,

¹*Energy, Environment and Disaster Risk Management Unit, UNDP, Macedonia,*
dimitrija.sekovski@gmail.com

²*Faculty of Civil Engineering, Macedonia, popovska@gf.ukim.edu.mk*

1. Abstract

The goal of the UNDP-implemented EU Floods Recovery Programme was to assist the country's recovery efforts in the aftermath of the floods that occurred in early 2015 by reconstructing damaged transport and water infrastructure. The "building back better" approach was applied, to the extent possible, to maximize resilience to future floods and mitigate the risk of floods in the most sensitive regions throughout the country.

The Programme targeted priority damaged infrastructure in multiple locations in the country's East, West, Southeast and Pelagonija regions, with an emphasis on: a) rehabilitation of existing regulated riverbeds and drainage systems in the Crna Reka and Strumica River Basins; b) the reconstruction and better management of five priority small dams; and c) reconstruction of several priority bridges and roads, as well as the stabilization of slopes and landslides affecting roads.

Overcoming the multiple and multilayer complex challenges affecting programme implementation (e.g., legal and institutional, quality of designs, contractors' performance) has generated valuable experiences to be used in future. Besides the experience-based purely technical (engineering) recommendations, the Programme has provided multiple lessons from an overall project management perspective.

This paper summarizes the key challenges and lessons generated throughout the implementation of the EU Floods Recovery Programme, especially from attempting to apply the "building back better" approach and enhanced resilience objectives in line with the contemporary conceptual frameworks, such as the Sendai Framework for Disaster Risk Reduction.

It elaborates on such aspects as stakeholder involvement, quality assurance mechanisms, availability of expertise, requirements and constraints imposed by permitting procedures, as well as the overall challenges to applying the "building back better" requirements in the context of Macedonia. Structured in such fashion, the paper intends to contribute to overcoming challenges and helping achieve higher future implementation efficiency of such post-disaster resilience building recovery interventions.

Keywords: Post-disaster recovery, Build Back Better approach, Enhancing resilience

2. Introduction

Severe flooding hit much of the country in January and February 2015, causing widespread damage and economic losses. Heavy rainfall caused rivers to overflow in many locations, and 44 out of 80 municipalities experienced floods. The most affected regions were the basins of the Crna Reka, Bregalnica and Strumica rivers, which cover 45% of the territory of the country, Figure 1. Roughly 170,000 people were affected in all. The floods caused major damages to roads and bridges, interrupting transport. Much agricultural land was also flooded, causing extensive losses to farming families. Drainage and irrigation systems were also damaged, and private houses, private-sector industrial facilities, schools and public facilities in some villages were also flooded.



Figure 1. The country's river basins – numbers 4, 5 & 6 were most affected by the floods in spring 2015

Besides this, the country was hit by a rapid sequence of additional floods, revealing its high vulnerability to these extreme weather situations. Some of this vulnerability stems from natural causes. Most river basins experience dramatic variations in water flows over time, and the risk of floods is also exacerbated by the country's specific topography and land structure. However, human factors are also at work. Changing use of land and land cover – for example, cultivation or construction in wetland areas, and heightened erosion from logging in forests – are altering hydrological regimes, increasing the risk of floods. Other causes include neglected maintenance of regulated river segments, for example through the conversion of flood plains and river corridors for agricultural or commercial use; decaying or poorly maintained flood control infrastructure, for example by failing to clear drainage channels regularly; and insufficient use of existing dams and reservoirs to mitigate the risk of floods, [1], [2].

Vulnerability to floods contributes to a profile of the country as particularly disaster-prone. The country also faces a high risk of earthquakes, wild fires, droughts, extreme temperatures and landslides. But although earthquakes pose the largest risk in terms of the potential costs in human lives and material damages, and wildfires are the disaster that occurs most frequently, floods deserve particular attention because they are on the rise in terms of frequency and intensity.

Flooding is of particular concern owing to the impact of climate change. Of the 28

countries in Europe and Central Asia, the country comes fourth in the occurrence of climate-related natural disasters in the 1990-2008 period, [3]. And although climate-change research forecasts a rise in temperatures and 4 percent decrease in precipitation over the coming decade, the number of extreme weather events is expected to surge, bringing with them a heightened risk of flooding.

In the flood aftermath, the Government commissioned a Rapid Damage and Needs Assessment (RDNA), with the aim to assess the full impact of the disaster on the country and, on the basis of the findings, to produce a feasible and sustainable Recovery Strategy for mobilizing financial and technical resources. The RDNA was coordinated by the Ministry of Agriculture, Forestry and Water Economy, in cooperation with experts from the World Bank and the European Union (EU).

The initial impact assessment estimated the total cost of the spring 2015 floods at EUR 35.691,672 million. Of this total, 62 percent were classified as damages and 38 percent as losses, [4].

The floods caused heavy damage to the country's transport infrastructure, including roads and bridges at national, regional and local level. According to the impact assessment, total costs in the transport sector were EUR 15.276 million, or 42.8 percent of all flood damages and losses, Table 1 Damage to roads was assessed at EUR 2.27 million overall, and damage to bridges, at EUR 2.117 million. In all, 197 roads with a total length of 124 kilometers were damaged, including 7 national roads, 21 regional roads and 169 local roads. The floods also completely destroyed 11 bridges (3 regional and 8 local) and damaged 42 bridges (2 national, 6 regional and 34 local).

Damages to roads and bridges interrupted transport for short periods in many cases, and in some cases totally cut off transport. This had a negative impact on productive activities and travel between cities and villages in the affected areas.

Table 1 Summary of damages and losses by sectors

Sector	Total (EUR)	Share (%)
Agriculture	13,671,655	38.3
Industry	536,459	1.5
Transport	15,276,736	42.8
Electricity	976	--
Water and sanitation	235,439	0.7
Irrigation and drainage	4,900,680	13.7
Housing	975,504	2.7
Education	94,224	0.3
Total	35,691,673	100.0

The floods also caused heavy damage to water infrastructure including irrigation and drainage systems, dams as well as river regulations. According to the impact assessment, total costs to the water sector were almost EUR 5 million, or 14 percent of total damages and losses, Table 1.

Table 2 Estimated damages and losses to water infrastructure

Sector	Total (EUR)
Irrigation systems	855,945
Drainage systems	1,294,759
Dams	161,724
River regulation	2,588,252
Total	4,900,680

Damage affected 32 municipalities, and overall 26 percent of the country's drainage systems, 17 percent of irrigation systems and 3 percent of dams were damaged. The damaged water infrastructure plays crucial role in overall flood mitigation, making its repair and reconstruction a high priority for preventing future damages.

The RDNA identifies a wide range of immediate and short-, medium- and long-term investments in the water sector to repair the existing infrastructure and improve the prevention of and response to future extreme weather events. The short-term needs include cleaning of irrigation/drainage networks and riverbeds, preparation of technical documentation for future flood mitigation projects, capacity development assistance for Water Management Organization, as well as planning for improved emergency response in the event of floods. The total cost of the short-term needs is estimated at EUR 27,614,505, [3].

On the basis of the RDNA, the European Commission provided financial assistance through UNDP to support the recovery of priority transport (roads, bridges and culvers) and water infrastructure (dams, riverbeds and drainage systems), as part of a broader strategy to improve capacities for flood protection and mitigation in the most affected areas.

3. Methodology and approach

The EU Flood Recovery Programme (hereinafter the Programme) targeted priority damaged transport infrastructure in multiple locations in the country's East, Southeast and Pelagonija regions, Figure 2, with an emphasis on the reconstruction and rehabilitation of priority bridges and roads, as well as the stabilization of slopes and landslides affecting roads. The programme also supported the implementation of priority flood risk mitigation measures in some of the country's most affected areas/river basins. The measures were combined to optimize benefits for the population and the environment. Specific measures will include but not be limited to: a) enhancing discharge capacities of river channels at critical sections; c) improving the status of existing drainage canals; and c) reconstruction and better management of dams/reservoirs.

The relevance of the proposed specific rehabilitation projects based on RDNA has been validated by applying multiple criteria, including: a) the size of the affected population; b) access to other funding sources (all rehabilitation projects that are funded or likely to be funded from other sources, such as national and local government budgets, were not selected for funding under the EU recovery programme); c) alternative transport routes (transport infrastructure where there are no suitable alternative routes were given higher

priority for EU funding); d) the complexity of rehabilitation projects (the projects that are considered more complex were prioritized for EU financial and technical assistance); and e) the urgency of reconstruction needs (the most urgent rehabilitation projects were already started with government funding in order not to wait for approval of the EU recovery programme); f) and availability of EU funding for transport infrastructure projects.

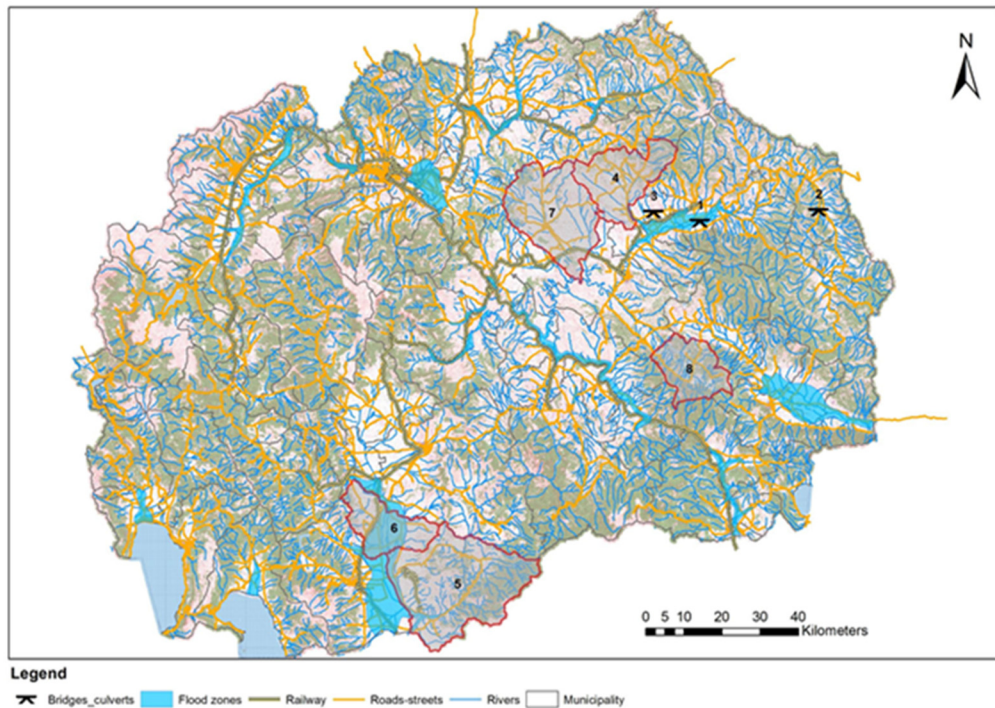


Figure 2. Geographic location of the implemented recovery projects

Great part of the necessary technical documentation (reviewed basic designs) was provided by the responsible institutions, and the remaining part was developed as part of the Programme. The Programme attempted to incorporate the ‘building back better’ concept both in the existing and newly developed technical documentation for all selected priority structures for recovery, [5].

To do so, the engineering designs have been evaluated against a number of critical parameters:

- a) Are the causes of the damages adequately studied and included in the recovery projects?
- b) Will the recovered infrastructure have any influence on future flood occurrence?
- c) Are the main design/construction standards adequately applied?
- d) Do the design process and documents adhere to national regulations for construction projects?

As a result of this comprehensive review process, wherever applicable, the technical documentation was modified in a way to take into account causes for the damages. Based on hydrological and hydraulic analyses, recovery designs were adjusted to improve

discharge capacity (e.g., of bridges and culvers), and to incorporate additional interventions such as off-site measures on nearby sources of sediment affecting the infrastructure (e.g., erosion prone areas, smaller torrents), stabilization of slopes and additional water control structures.

Considering the fact that this was country's first-ever such programme aligned with the 'build back better' principles, its implementation helped generate numerous lessons that are summarized later in this paper.

4. Results and discussion

The EU Floods Recovery Programme was successfully completed, generating multiple benefits for communities and economic activity adversely affected by the 2015 floods. In spite of the challenges of different nature and varying degree of complexity (e.g., difficult site conditions, complicated permitting procedures, capacities of contractors, financial losses due to exchange rate variations, and differences between original cost estimates of individual recovery projects and the actual cost of construction), all anticipated results were delivered in line with original objectives.

Almost 80,000 people from the eight selected flood-sensitive municipalities in the affected regions benefitted from **transport infrastructure** recovered in line with the 'build back better' principle (through restored connectivity, reduced travel time and improved discharge capacity of bridges). In addition, reconstructed infrastructure restores/improves access to social services (schools, medical care) and enables local businesses to continue to grow.

Typical interventions in line with the 'build back better' approach incorporated in the recovery designs included: a) improved conceptual designs for structures; b) reinforcement of bridges to improve structural stability in conjunction with riverbed regulations (to improve discharge capacity and reduce erosion); c) recovery of roads in combination with drainage canals that would minimize future flooding; and d) stabilization of slopes affecting recovered infrastructure.

The following figures show examples of the recovered transport infrastructure from before the start of the works and after completion of works.



Figure 3. Recovery of culvert in the municipality of Cesinovo-Oblesevo (before and after)



Figure 3. Recovery of bridge in the municipality of Delcevo



Figure 4. Recovery of bridge in the municipality of Zrnovci



Figure 5. Bridge in the municipality of Sv. Nikole and new river regulation to enhance discharge capacity

The majority of **water infrastructure recovery** interventions focused on rehabilitation of drainage systems and riverbed regulations, Table 1. The remaining interventions focused on reconstruction of five existing priority dams (Mavrovica, Drenska Reka, Lipa, Slatino and Prilep). The inclusion of rehabilitation projects for dams, despite their limited contribution in the overall estimated damages from the 2015 floods, stems from the following factors: a) dam rehabilitation projects are usually more complex and therefore are considered more suitable for external financial and technical assistance; b) they have a primary flood control role in comparison with other mechanisms; c) improvement of dam operations provides an excellent opportunity to enhance their flood mitigation potential; and d) EU/UNDP-backed rehabilitation of dams based on the “build back better” approach would provide an opportunity to create models with replication potential at national level.

A few earlier UNDP-backed flood risk assessments based on modeling work (space-oriented economic damage simulations) helped carry out a risk-based prioritization of riverbed/canal sections with most urgent recovery needs in the Crna Reka and Strumica River Basins.

The overall effects of the project recovery efforts are further complemented/upgraded by integrating early warning systems (currently under implementation as part of separate UNDP projects in the Crna Reka and Strumica River Basins). Ongoing work involves linking the dam/reservoir operation with meteorological/hydrological forecast data provided by the Hydro-meteorological Service. In practice this would mean increasing discharges from reservoirs when anticipating heavier rainfall and/or snowmelt so as to increase their capacity to absorb more water and help better protect downstream communities and assets.

Recovery/clean-up works in Crna Reka River Basin (or Pelagonija) – a flood-sensitive region with the highest investment needs – have focused on removal of vegetation from 43.4 km of flood control canals, followed by clean-up of sediment deposits on a priority canal network in total length of 23 km, Figure 6. Works also included reconstruction of damaged earth embankments on priority sections, prioritized by applying a risk-based approach. Over 230,000 people are direct beneficiaries of the improved flood control system, and the avoided average annual damage from likely floods is estimated at approximately USD 2 million, [6].



Figure 6. Canal recovery activities in the Crna Reka River Basin

The recovery/clean-up of the flood control canal network in the Strumica River Basin encompasses enhancement of the discharge capacity of over 27 km of canals by almost 50%, securing prevention of average annual economic loss of 50,000-100,000 USD from future flood events with high probability of occurrence, [7].

The Programme completed the recovery works on all five dams – Mavrovica, Lipa, Drenska Reka, Slatino, and Prilep. The dam recovery projects were confronted with major challenges throughout all stages of implementation, stemming mostly from: a) difficult conditions and access to sites; b) poor standards applied at the time of construction of the dams which had to be addressed in the recovery designs; c) severe damages on dams caused by floods and poor maintenance in the past; and d) lack of and/or poor quality technical/design documentation. All these factors increased the need of field investigations, and adjustment of technical solutions which in turn prolonged the design stages and required temporary ceases of construction activities to overcome emerging issues.

Typical interventions on the selected dams, in line with the ‘build back better’ principles involved: a) reconstruction and strengthening of dam bodies; b) (re)construction of spillways and bottom outlet structures; c) grouting techniques, use of geomembranes and clay carpets to improve geological conditions and reduce permeability.

Some examples of recovered dams under the programme are presented in the following few figures:



Figure 7. Recovery of Lipa Dam



Figure 8. New dam body and a spillway structure on Drenska Reka Dam

5. Conclusion and lessons learnt

Overcoming multiple and multilayer complex challenges affecting the implementation of the EU Floods Recovery Programme (e.g., legal and institutional, quality of designs, contractor performance) has generated valuable experiences and lessons that are now valuable countrywide. In line with the scope of this paper, the following paragraphs summarize the key findings and lessons learnt from a project management point of view. Part of the experiences stem from the attempt to apply for the first time in the country the ‘build back better’ principles in the recovery designs, as well as the need to implement multiple parallel projects considering the time limitations in funding availability:

1. There is a need of early involvement of all stakeholders (including potentially affected local communities) from the planning stages of the recovery projects to prevent possible opposition due to disruption of living routines during construction;
2. The minimum legal quality assurance mechanisms in the country (e.g., review of design and supervision of works) often turn out to be insufficient (e.g., considering low performance of contractors and need for adjustment of design during construction). High level consulting engineering support is recommended for complex projects with a high degree of uncertainty;
3. Permitting procedures for recovery of infrastructure damaged by natural disasters are shorter and more efficient as no classical construction permit is required. However, these shortened procedures generally limit the possibility of applying substantive changes in the recovery design (e.g., by applying the “build back better” approach). Another risk arises from skipping the formal consultation processes with entities in charge of adjacent infrastructure (e.g., power lines, telecommunication infrastructure, and irrigation canals) which may cause delays in the later stages of the project. As a recommendation, even when no formal permitting procedure needs to be conducted, the responsible authority needs to conduct early consultations to ensure timely planning of measures to prevent potential disruption.
4. Country-level knowledge on “build back better” principles is limited, or even when existing is not applied for a number of reasons, including: a) higher investment costs and lack of understanding of the long-term economic losses as

a result of building inappropriate infrastructure; b) procedural/permitting complications and likely delays in case of significant changes in the design documentation; c) overall inertia of design engineers to apply new approaches and tendency to stick to the routine design practices; and d) no formal legal requirements.

In conclusion, in spite of all challenges the majority of programme targets have been met by the recovery of significant transport and water infrastructure. Very importantly, the Programme has also contributed to learning processes on ‘build back better’ principles, and risk-based planning and design, in line with enhanced resilience objectives. As a result, future similar initiatives can be implemented with even higher efficiency rate.

References:

- [1] EU Floods Recovery Programme – Reconstruction and rehabilitation of transport infrastructure (2015), UNDP
- [2] EU Recovery Programme for Floods – Improvement of Flood Prevention and Mitigation Response in Affected Areas (2016), UNDP
- [3] Adapting to Climate Change in Eastern and Central Europe (2009), World Bank
- [4] Rapid Damage and Needs Assessment (2015), Ministry of Agriculture, Forestry and Water Economy, World Bank and EU
- [5] Sendai Framework for Disaster Risk Reduction (2015-2030), UN Office for Disaster Risk Reduction
- [6] Preliminary Flood Risk Assessment for the Crna Reka River Basin (2016), UNDP
- [7] Flood Risk Management Plan for the Strumica River Basin (2017), UNDP
- [8] Directive 2007/60/EC of the European Parliament and of the Council on the Assessment and Management of Flood Risks, October 2007.

DROUGHT AND PRECIPITATION CONCENTRATION INDEX (PCI) ANALYSIS IN CONTINENTAL CROATIA

LIDIJA TADIĆ¹, TAMARA BRLEKOVIĆ¹

Faculty of Civil Engineering and Architecture Osijek, Croatia. ltadic@gfos.hr, tamaradadic@gfos.hr

1. Abstract

Drought is an extreme hydrological event that causes great economic and environmental damages. There are various methods used for the identification and quantification of drought. Here will be presented Standardised Precipitation Index (SPI) which is the most common one for drought identification related to Precipitation Concentration Index (PCI). Precipitation Concentration Index is statistical parameter which can be very useful in identification of precipitation distribution. It can be applied on precipitation obtained on daily, monthly, seasonal or annual basis. It characterizes the monthly concentration of precipitation on a scale that ranges from less than 10 for evenly distributed rainfall to much higher values for extreme monthly rainfall distribution. Mapped values of the PCI provide a good visualization of relative precipitation distribution of a certain period. An unbalanced precipitation distribution indicates periods of drought or extensive rainfall. Study area of comparison Standardized Precipitation Index (SPI) and precipitation concentration index analysis is continental part of Croatia. Climate of this region is typical continental but in recent time, since middle eighties many researches confirmed changes in air temperature and precipitation regime, probably caused by climate change. The both indices are calculated for 14 meteorological stations, situated in 15 cities in continental part of Croatia in the period from 1981 to 2018. Analysis has been done on annual and seasonal basis in order to define variability in precipitation regime and its impact on drought episodes.

Key words: standardised precipitation index, precipitation concentration index

2. Introduction

Climate change due to a global warming is one of the most pronounced topics in the past few decades. There are many paper published on analysis of change in hydrological cycle and predictions of its future impacts on ecological, geomorphological and economic processes. Changes in precipitation have significant consequences on hydrological circle and availability of water resources. Changes in precipitation leads to changes in ground water recharge, water availability, modification of fluvial regimes and increased flood risk [1].

On of the climate change main characteristic is higher frequency of extreme hydrological events, such as floods and droughts. Comparing to the floods, droughts have more global character effecting whole regions, even continents [2].

According to Report of IPCC-2007, it is important to stress very frequent regional and sub-regional variabilities that need further investigations [3].

Republic of Croatia belongs to transitional area between northern Europe characterized by weak trend of precipitation increment in continental part of the country and Mediterranean characterized by more pronounced drying [4,5].

Besides, research on air temperatures of more than 50 years long period observed on 26 meteorological stations all over the country proved average increasing of air temperature of 0.84°C and the most severe drought events occurred in 2000, 2003 and 2011 in the continental part of Croatia [6,7].

Also, results of water balance analysis of previous investigations shows significant increasing of evapotranspiration in the period 1900-1995 and diminishing of run off and soil water content [8].

There are many methods to quantify precipitation variations on various time scales and evaluate the precipitation concentration.. These indices include Precipitation Concentration Index (PCI), Simple Daily Intensity Index, Precipitation Concentration Degree (PCD) and Precipitation Concentration Period (PCP), modified Fourier Index, Seasonality Index etc. [1,9]. In this paper, PCI is used to evaluate precipitation concentration.

The Precipitation Concentration Index (PCI) is indicator the temporal distribution of precipitation, which can be applied at annual, seasonal and supra-seasonal scales. The higher PCI values, the more concentrated the precipitation. Precipitation Concentration Index is descriptor of rainfall variability. Furthermore, PCI is a part of the well-known Fournier index [9,10].

Also, there will be used, well known method for drought evaluation is Standardised Precipitation Index (SPI) used all over the world regardless of climatic or topographical features. It is recommended by the World Meteorological Organisation as a method with no limitations as to its use, because the method is independent of drainage basin characteristics.

This paper analyses precipitation concentration and the occurrence of drought in the continental part of Croatia for 14 stations in period 1981-2018. Table 1 presents their geographical position (coordinates) and absolute altitude. They are situated between 15° and 19° The altitude decline from west (167 m a.s.l) to east (88 m a.s.l.). It reflects the distribution of annual precipitation which is significantly related to geographical position, what is presented on Figure 1.

Table 1. Geographical position of meteorological stations involved in the research

Town/meteorological station	Northern longitude	Northern latitude	Altitude (m a.s.l.)
Karlovac (KA)	15°34'	45°30'	110
Zagreb-Maksimir (ZG)	16°02'	45°49'	123
Varaždin (VŽ)	16°20'	46°18'	167

Sisak (SI)	16°22'	45°30'	98
Križevci (KR)	16°33'	46°02'	155
Čazma (ČA)	16°38'	45°45'	144
Bjelovar (BJ)	16°51'	45°55'	141
Đurđevac (ĐU)	17°04'	46°03'	121
Daruvar (DA)	17°14'	45°36'	161
Slavonski Brod (SB)	17°23'	45°10'	88
Našice (NA)	18°06'	45°29'	144
Donji Miholjac (DM)	18°10'	45°46'	97
Osijek (OS)	18°34'	45°30'	89
Gradište (GR)	18°42'	45°09'	97

Spatial distribution of mean annual precipitations which are the basis for PCI and SPI calculations, together with the position of observed stations, is shown in Figure 1. There is evident decreasing in annual precipitation from west to east. The highest values are around Karlovac station (>1024 mm), and the lowest for the most eastern stations Osijek and Gradište (<700 mm).

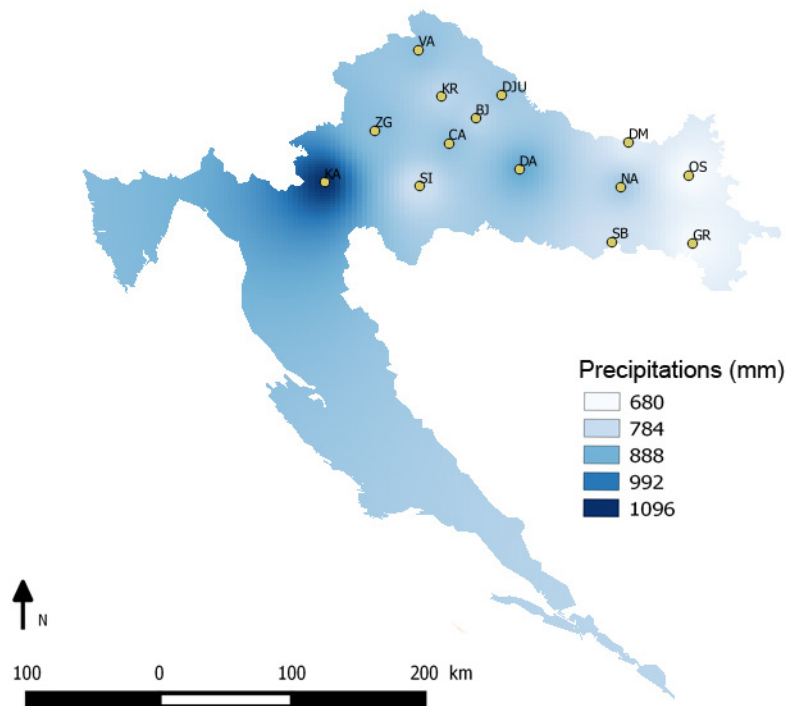


Figure 1. Location of stations and distribution of mean annual precipitations for period 1981-2018

3. Methods

3.1. Precipitation Concentration Index

Monthly precipitation data for 14 stations situated in continental part of Croatia presented in Figure 1 were used for PCI and SPI calculations. The data on monthly precipitation and air temperatures that were not available in war years on some stations (Sisak, Osijek, Našice, Čazma) were interpolated using the IDW method (Inverse Distance Weighting) by QGIS computer program. In each of these 4 incomplete series of the precipitation and air temperature data, the number of interpolated data was less than 6 (less than 2%).

The Precipitation Concentration Index (PCI), as indicator of rainfall concentration and rainfall erosivity, was calculated on an annual scale according to Eq.(1):

$$PCI_{annual} = \frac{\sum_{i=1}^{12} p_i^2}{(\sum_{i=1}^{12} p_i)^2} \cdot 100 \quad (1)$$

where p_i is monthly precipitation data [1,9,10].

PCI was also calculated on a seasonal scale for winter (December, January, February), spring (March, April, May), summer (June, July, August) and autumn (September, October, November) according to Eq.(2):

$$PCI_{seasonal} = \frac{\sum_{i=1}^3 p_i^2}{(\sum_{i=1}^3 p_i)^2} \cdot 25 \quad (2)$$

The lower values of PCI indicate uniform precipitation distribution, while higher values mean that precipitations occurred in shorter time then observed period (year or season). The higher the PCI, the precipitation distribution is more irregular. PCI range and classification are listed in Table 2.

Table 2. PCI range and classification [9]

PCI value	PCI classification
$PCI \leq 10$	Uniform Precipitation Distribution (low precipitation concentration)
$10 < PCI \leq 15$	Moderate Precipitation Distribution
$16 < PCI \leq 20$	Irregular Precipitation Distribution
$PCI > 20$	Strong Irregularity of Precipitation Distribution

The Standardised Precipitation Concentration Index (SPCI) was also calculated to analyze precipitation concentration variations [11] according to Eq.(3):

$$SPCI_{zi} = \frac{PCI_{zi} - \overline{PCI}_z}{\overline{PCI}_z} \quad (3)$$

where PCI_{zi} is PCI of i-th year at station Z; and \overline{PCI}_z is the average PCI at station Z.

3.2 Standardised Precipitation Index

The SPI is based on normalised gamma distribution of precipitation and presents a number of standard deviations with regard to an average value. The basic advantage of this method lies in the fact that it necessitates only a set of precipitation for a longer period of time (30 or more years), and that it can be used for various time scales, the most frequent ones being 1, 3, 6, 12, and 24 months. Thus the same index can be used for the evaluation of precipitation deficit in various water resources (ground water, open watercourses, soil moisture) depending on the purpose for which the drought analysis is made. One to six months time scales are appropriate for the analysis of drought in agriculture, one to two months are needed for meteorological drought, and 6 to 24 months are needed for hydrological drought (a positive SPI points to a greater quantity of precipitation with respect to the mean multiyear value, while a negative SPI is an indication of lower precipitation compared to mean value).

The standardised precipitation index has the defined limit values dependent on the relative frequency of drought, which enables comparison of values for various locations or regions, as shown in Table 3 [12].

Table 3. Limit values for standardised precipitation index (SPI) [12]

SPI value	SPI classification
≥ 2.00	Extremely wet
1.50 - 1.99	Very wet
1.00 - 1.49	Moderately wet
0.99 – (-0.99)	Normal
(-1.0) – (-1.49)	Moderately dry
(-1.5) – (-1.99)	Very dry
$\leq (-2.00)$	Extremely dry

The computer program “spi_si_6” (National Drought Mitigation Centre, USA) [13] was used for calculating monthly indices of standardised precipitation.

4. Results and discussion

PCI values on annual scale obtained according to Eq.(1) for all stations are shown in Figure 2. Calculated annual PCI values varies for analyzed stations from value 8.8 (station Našice for year 2017) to 50 (Sisak station for year 1985). For all stations, the most PCI values are between 10 and 15 which means that precipitation distributions are moderate. The percentage of PCI values between 10 and 15 (moderate precipitation distribution) varies from 71% for stations Gradište, Karlovac and Sisak to 89% for station Đurđevac. Station Našice showed the most irregular precipitation distribution with 10.5% annual PCI values higher than 16 which is the lower limit for irregular precipitation distribution (also marked on Figure 2).

PCI was also calculated on a seasonal scale. According to obtained results, on seasonal scale, for all stations the highest percentage of PCI (52-65%) is in the first category (PCI<10) which indicates uniform precipitation distribution (low precipitation

concentration).

Spatial distribution of mean values of PCI for every season, along with the mean values of PCI on an annual scale is shown in Figure 3. Distributions are obtained with IDW interpolation method in QGIS software.

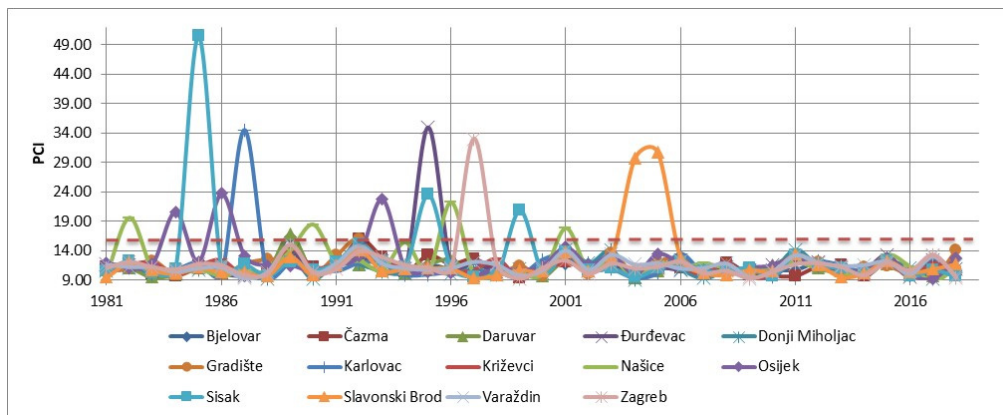


Figure 2. Annual PCI values for all stations with indicated value for irregular precipitation distribution

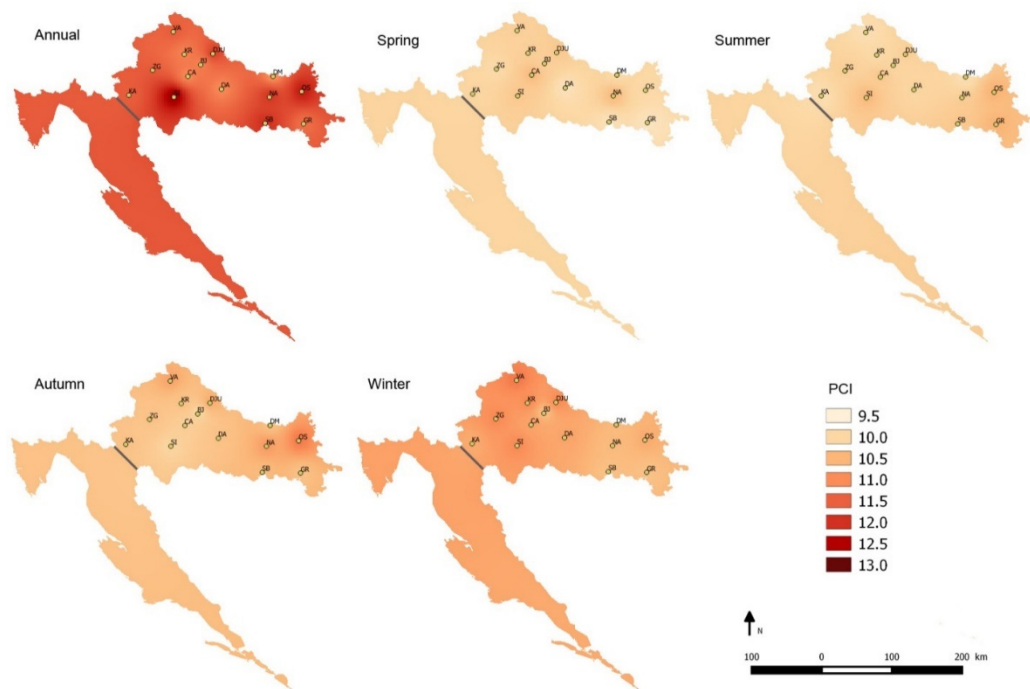


Figure 3. Mean values of PCI for annual and seasonal scale for period 1981-2018

According to Figure 3, mean PCI values indicate uniform to moderate precipitation distribution in continental part of Croatia for observed period. The highest mean PCI are obtained on annual scale, especially for Osijek and Sisak stations, while the lowest are

for spring period. There is some increasing in PCI values during winter period from east to west.

Besides PCI, SPCI is calculated for all stations to understand the variances of PCI value during observed period. Calculated annual SPCI values varies for analyzed stations from value 2.96 (Sisak station) to -0.26 (Našice station). Našice station has the biggest change in SPCI values and Đurđevac the smallest, except for the year 1995. Temporal fluctuations of SPCI for these two stations are shown in Figure 4.

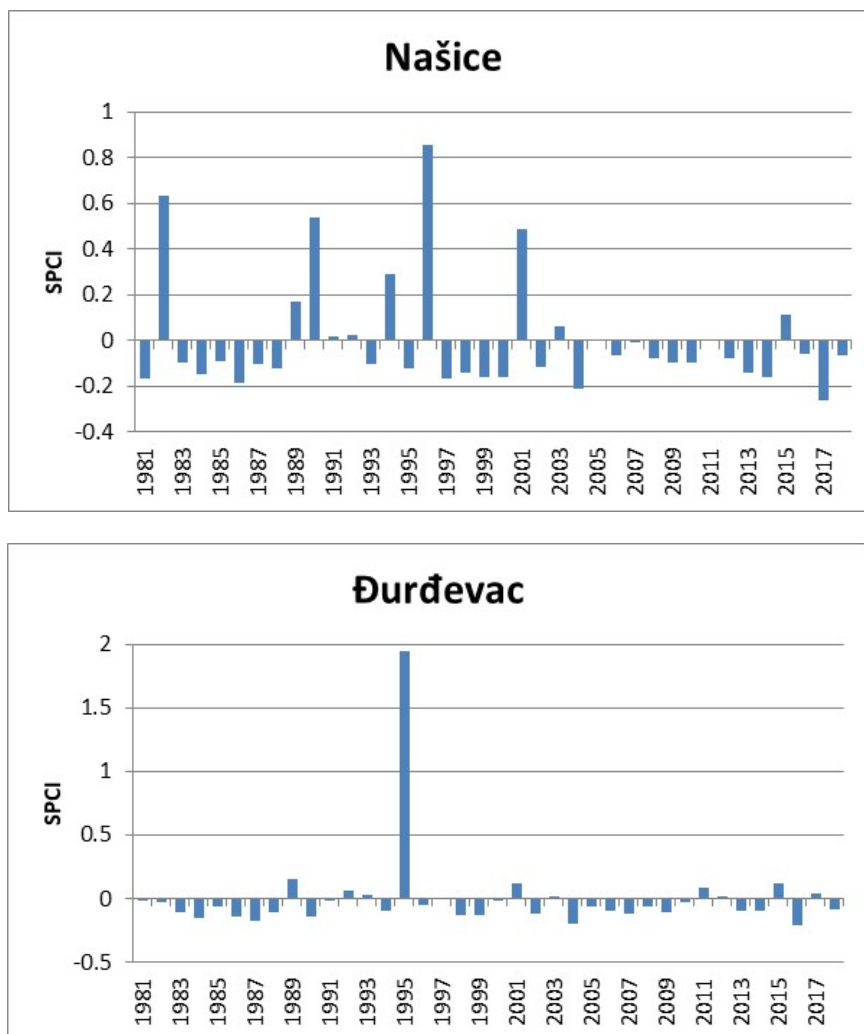


Figure 4. The variations of SPCI for stations Našice and Đurđevac

Calculation of SPI was done on monthly, seasonal and annual basis. As it was expected the greatest extremes appeared on monthly basis, in both direction - positive and negative (Figure 5).

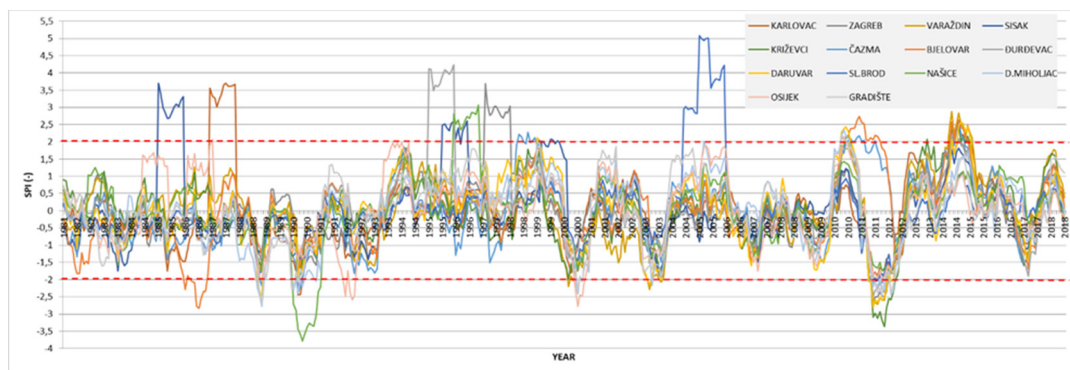


Figure 5 Monthly values of SPI in continental part of Croatia (1981-2018)

Long, extremely dry periods ($SPI \leq -2.00$) in 1987, 1989, 1990, 1992, 2000, 2002 and 2012 effected the whole continental part of Croatia especially in the 21st century. On contrary, extremely wet periods, with $SPI \geq 2.00$, appear more locally.

As it was expected, distribution of seasonal and annual SPI values is more uniform (Figure 6).

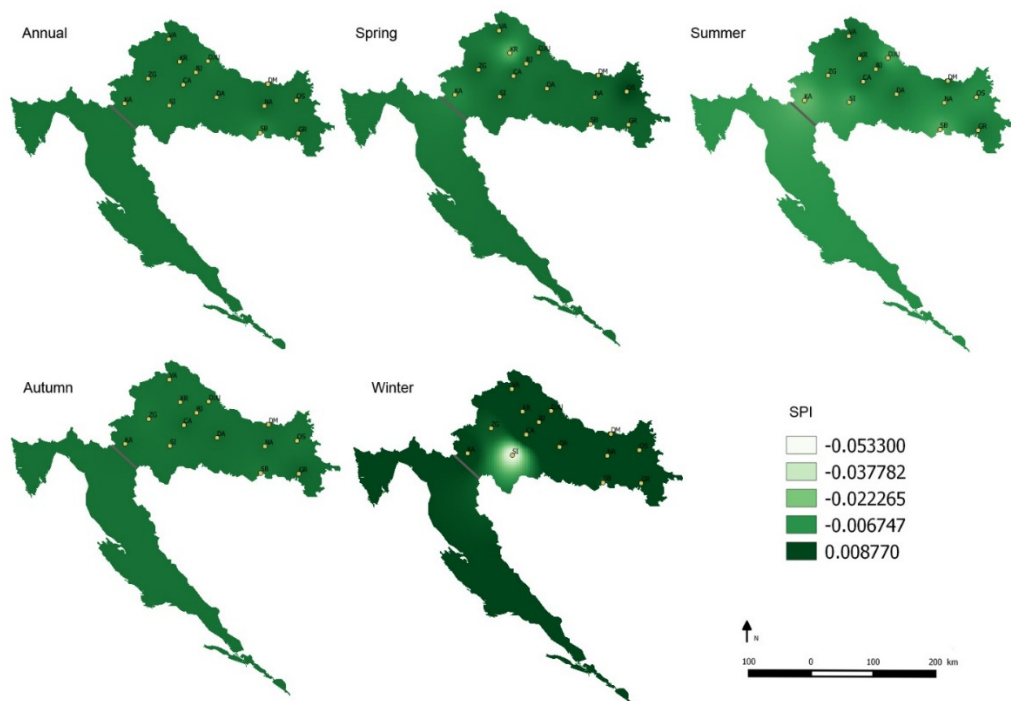


Figure 6 Mean values of SPI for annual and seasonal scale for period 1981-2018

Winters are wet all over study area and summer periods have more negative values of SPI, but both according to classification (Table 3) belong to normal wetness/dryness. On annual basis it can be concluded that there is no evidence of any irregularity on the whole observed area.

In order to compare PCI and SPI values and the possibilities of their relationship, further statistical analysis was done. Calculation of RV coefficient depicts the similarity between two matrices of quantitative variables or two configurations resulting from multivariate analysis [14]. The RV coefficient is a generalization of the squared Pearson correlation coefficient and it lies between 0 and 1. The closer to 1 the RV is, the more similar the two matrices are. Figure 7 presents results of this statistical procedure.

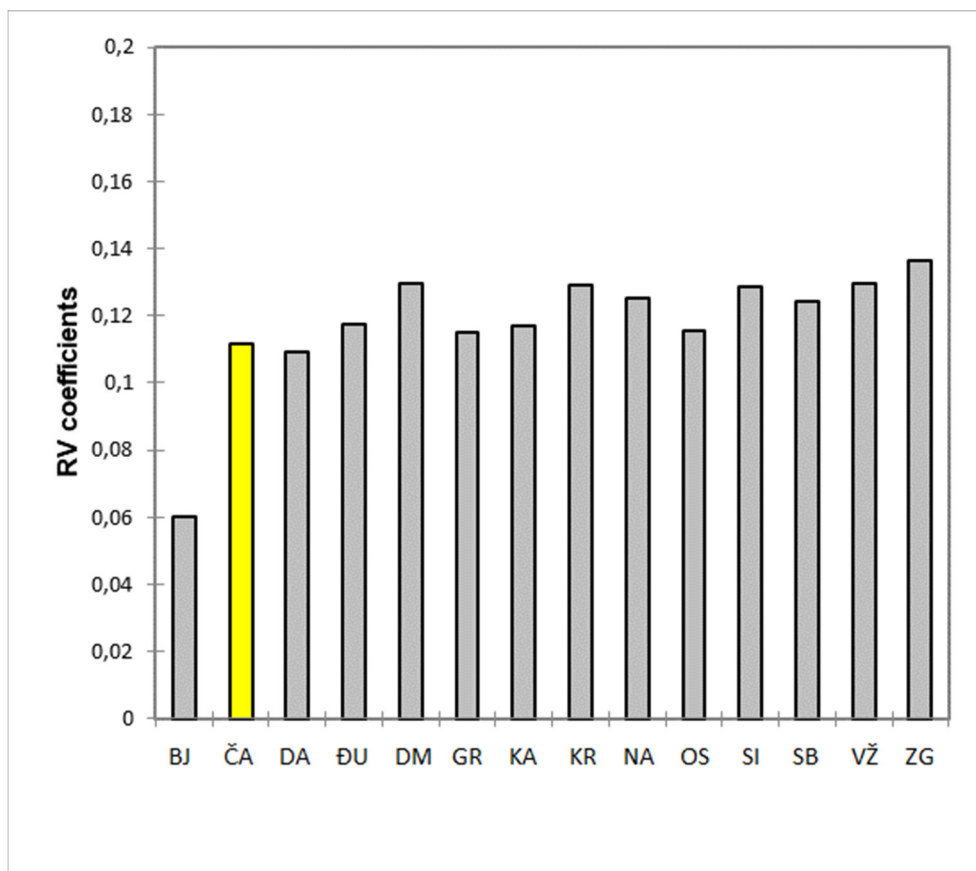


Figure 7. RV coefficients between PCI and SPI matrices for summer values

In this case RV coefficients between two matrices including all variables from both matrices were calculated for annual and seasonal values of entire period (1981-2018). Figure 7 presents RV coefficients for summer periods which are the highest but still results did not show any significant relationship. The most values are less than 0.14 with significance $p > 0.05$. Only Čazma station has slightly higher significance, designated in yellow ($0.01 < p < 0.05$).

5 Conclusion

Obtained PCI of study area in period 1981-2018 varies between 8.8 and 50. But, for all stations, precipitation distribution on an annual scale is moderate with values between 10 and 15. The highest percentage (10.5%) of $PCI > 16$ was obtained for Našice station. Even

though, this percentage is small which means that for continental part of Croatia, precipitation distribution is moderate. Obtained PCI on seasonal scale was even smaller, about 60% of obtained PCI is less than 10 for all stations which means that precipitations on seasonal scale is uniform. The smallest PCI values were obtained for spring and the highest for winter period. Even though mean annual precipitation showed decrease from west to east, mean PCI values on annual and seasonal basis did not show any spatial pattern. Also, annual and seasonal SPI values have no significant variabilities along the studied area. And there is no the similarity between PCI and SPI matrix what implies that Precipitation Concentration Index (PCI) as an indicator of temporal distribution of precipitation have no correlation with Standardised Precipitation Index (SPI) on any temporal scale.

References:

- [1] Ezenwaji E.E., Nzoiwu, C.P., Chima G.N.: Analysis of Precipitation Concentration Index (PCI) for Awka Urban Area, Nigeria, *Hydrol Current Res* ,pp. 2017. 8:4 DOI: 10.4172/2157-7587.1000287.
- [2] Lloyd-Hughes,B., Shaffrey,L.C., Vidale,P.L., Arnell, N.W.: An evaluation of the spatiotemporal structure of large-scale European drought within the HiGEM climate model, *International Journal of Climatology*,vol .33,no.8, pp.2024–2035, 2012.
- [3] Solomon,S.D., Qin,D., Manning,M., Chen, Z., Marquis,M., Averyt,K.B., Tignor M., Miller, H.L. (eds): *Climate Change 2007: The Physical Science Basis*, Cambridge University Press, New York, 2007.
- [4] Gajić-Čapka,M., Cindrić, K., Pasarić,Z.: Trends in precipitation indices in Croatia 1961-2010, *Theoretical and Applied Climatology* , vol.121, no.1-2, pp.167-177, 2015.
- [5] Perčec Tadić,M., Gajić-Čapka,M., Zaninović K., Cindrić,K.: Drought vulnerability in Croatia, *Agriculturae Conspectus Scientificus*, vol.79, no.1, pp.31-38, 2014.
- [6] Bonacci,O.: Analiza nizova srednjih godišnjih temperatura zraka u Hrvatskoj, *Građevinar*, vol. 62, no.9, pp.781-791, 2010.
- [7] Tadić,L., T. Dadić T., Bosak,M.: Comparison of different drought assessment methods in continental Croatia, *Građevinar* , vol.67, no.1, pp. 11-22, 2015.
- [8] Zaninović K., Gajić-Čapka,M.: Changes in components of the water balance in the Croatian Lowlands, *Theoretical and Applied Climatology* ,vol.65, no.1-2, pp.111-117, 2000.
- [9] de Luis, M., Gonzalez-Hidalgo, J.C., Brunetti, M., Longares, L.A.: Precipitation concentration changes in Spain 1946–2005, *Nat. Hazards Earth Syst. Sci.*, 11, pp. 1259–1265, 2011. doi:10.5194/nhess-11-1259-2011.
- [10] Rasel, A.H., Islam, Md. M., Keramat, M.: Analysis of Annual and Seasonal Precipitation Concentration Index of North-Western Region of Bangladesh, *International Conference on Computer, Communication, Chemical, Materials and Electronic Engineering IC4ME2-2016*, 2016.
- [11] AL-Shamarti, Hasanain K.A.: The Variation of Annual Precipitation and Precipitation Concentration Index of Iraq, *Journal of Applied Physics*, 8, 4, pp. 36-44, 2016. DOI: 10.9790/4861-0804033644.
- [12] McKee, T.B., Doeskin, N.J., Kleist J.: Drought Monitoring with Multiple Time Scales, *Conference of Applied Climatology*, American Meteorological Society, Boston, pp. 179-184, 1995.
- [13] <http://drought.unl.edu/MonitoringTools/DownloadableSPIProgram.aspx>
- [14] Robert P. and Escoufier Y.: A unifying tool for linear multivariate statistical methods: the RV-coefficient. *Applied Statistics*, 25, pp 257–265, 1976.

POSSIBILITIES OF DESIGN OF FLOOD PROTECTION MEASURES ON THE ONDAVA RIVER

JAKUB MYDLA ¹, ANDREJ ŠOLTÉSZ ¹ MARTIN ORFÁNUS ¹

¹ *Slovak University of Technology in Bratislava, Faculty of Civil Engineering, Department of Hydraulic Engineering, Radlinského 11, 810 05 Bratislava, Slovakia, jakub.mydla@stuba.sk, andrej.soltesz@stuba.sk, martin.orfanus@stuba.sk*

1. Abstract

Contribution is dealing with run-off conditions on lower part of one of rivers – the Ondava River – flowing through East Slovak Lowland. Although the Ondava River has its protection dykes (coming from 1848), the capacity of the river bed is – especially - at high flow rates insufficient. The reason for the proposed research were flood situations from 2004 and 2010 when flood protection dykes collapsed and the flowing water endangered municipalities close to the river. To improve the flood protection a 250 m long lateral spillway was constructed on the left-hand protection dyke close to pumping station (PS) Ladislav. It should serve for controlled water release into adjacent agricultural land in period of flood progress.

For modelling purposes a digital terrain model has been utilized together with numerical tools of HEC-RAS modelling software package combining 1-D with 2-D modelling procedure. The necessary hydrological data have been obtained from the Slovak Hydrometeorological Institute as well as morphological and technical data have been obtained from Slovak Water Authority in the East Slovak Region. Other morphological data have been gathered by geodetic survey in situ. Results of the mathematical modelling of surface water level regime in the Ondava River were compared with measured values and afterwards used for design of further flood protection measures utilized existing drainage channel system and pumping station, as well.

Keywords: flood wave, numerical modelling, lateral spillway, river bed capacity, protection dyke

2. Introduction

Motivation for starting to investigate the run-off conditions on the lower part of the Ondava River were floods which occurred in year 2004 and 2010 in East Slovak Lowland [1], [2] and the non-traditional release of flood flow rates utilizing the solid lateral spillway which was constructed on left-side flood protection dyke [3]. The research consisted of two separate parts, the first was the 1-D mathematical modelling of surface water flow on the Ondava River in the adjacent reach and the second was the 2-D modelling of the extent of the released water through lateral spillway into agricultural utilized territory determined for the elimination of the flood wave [4], [6].

Protection dykes of the Ondava River were built in the past to protect the adjacent territory against the 20-year flood discharge. The history of them is going back to 1848.

The first larger flood in 1888 has damaged the dykes on several reaches and therefore a concrete wall was built into the dyke as a core. It is shown clearly in Figure 1 when the left-side protection dyke was damaged in 2004 [4], [7].

From hydrologic point of view can this region be defined as a region with very complicated run-off conditions due to confluence of more rivers. Especially, the Topla River which is the most important tributary stream of the Ondava River has a larger basin area than the Ondava River. The run-off process is significantly affected by snowmelt of solid precipitation in upper parts of the watershed connected by rainfall process. That is the reason for maximum water levels in the spring time and the minimum in the autumn. This status is valid for both of mentioned rivers – Ondava River as well as Topla River. Positive impact on reduction of flood waves on the Ondava River was achieved by building-up of Domaša Water Structure (1962 – 1967) with its retention volume of 21,0 mil. m³.

There are several pumping stations (PS) on both sides of the Ondava River which were constructed in the second half of the 20th century. They enable the pumping of internal water in flood periods into the Ondava and Latorica rivers [4], [5].



Figure 1. Damaged left side protection dyke on the Ondava River in 2004

In July 2004 after heavy rainfalls came to a significant increase of water levels on all rivers in east Slovak Lowland. Almost in all reaches of the Ondava and Topla rivers the surface water overflow the river bed and after permanently unceasing rainfall the protection dyke on the left side was broken approximately 600 m over the PS Ladislav. The width of the dyke breakage was at the beginning 90 m and finally more than 130 m. The water flooded gradually 3.920 hectares of agricultural land. The aerial photo of the dyke breakage is shown in Figure 2 [1].



Figure 2. Protection dyke breakage on the Ondava River (July, 2004)

At the reconstruction of the protection dyke a solid lateral spillway (Figure 3) with the crest approx. 1 m below the dyke crest was constructed which should serve for releasing flood discharges coming in the future, i. e. for controlled release of flood waves into agriculturally utilized territory [4], [6].



Figure 3. Illustration of the constructed 250 m long solid lateral spillway in the left-side protection dyke

The same situation (even worse) happened in May and June 2010 when the flood wave exceeded the maximum flood from 2004. In this case the right-side protection dyke was overflowed and afterwards broken very close to dyke breakage profile on the other side from 2004.

3. Methods

For 1-D mathematical simulation of the run-off process morphological and geodetic data about the river bed and floodplain of the Ondava River was obtained from water board operator – Slovak Water Management Enterprise (SWME). The necessary hydrological data about the flood wave propagation was achieved by Slovak Hydro-meteorological Institute (SHMI). Next data which was necessary for the hydraulic analysis was about parameters of the realized lateral spillway.

Cross-section profiles of the lower reach of the Ondava River are available from different periods – some of them were from the year 1968, next from the year 1983 and the last which have been used for the simulation are coming from the year 2004 (Figure 4).

For 2-D modelling of the flow through the solid lateral spillway (Figure 3) into the flooded agricultural land data about the overall morphology was necessary. It was given by digital terrain model (DTM) with measured network 20 x 20 m supplemented by break lines. Detail of the DTM is illustrated in Figure 5. Red dots are representing measured points, green outlines are break lines and blue coloured lines is the water level in the river and channels in the period of survey. To check the accuracy and reliability of the DTM own survey was realized in the area of interest with special attention to realized lateral spillway (shadows in Figure 3).

Hydrologic data were obtained from two gauging stations – Horovce (SHMI, above the lateral spillway) and at PS Hraň (SWME, below the lateral spillway). The record of both floods (2004, 2010) was available and one of this is presented in Figure 6. In this figure can be noticed a rapid increase of the flood on both gauging stations and consequently a rapid decrease on Horovce gauging station and gradual decrease of water level on Hraň gauging station, as well. The difference is caused by the dyke breakage (31.7.2004).

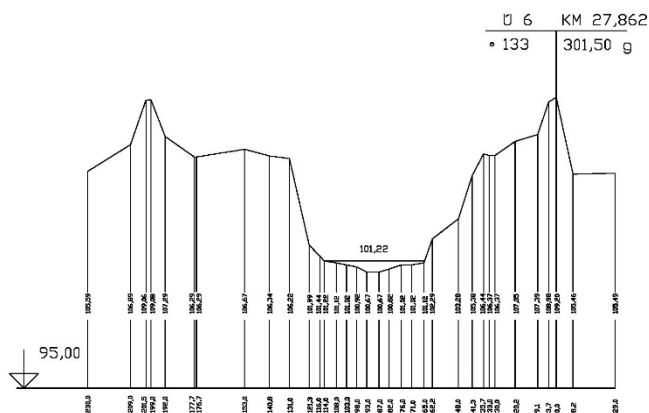


Figure 4. Cross-section profile of the lower Ondava River from 2004

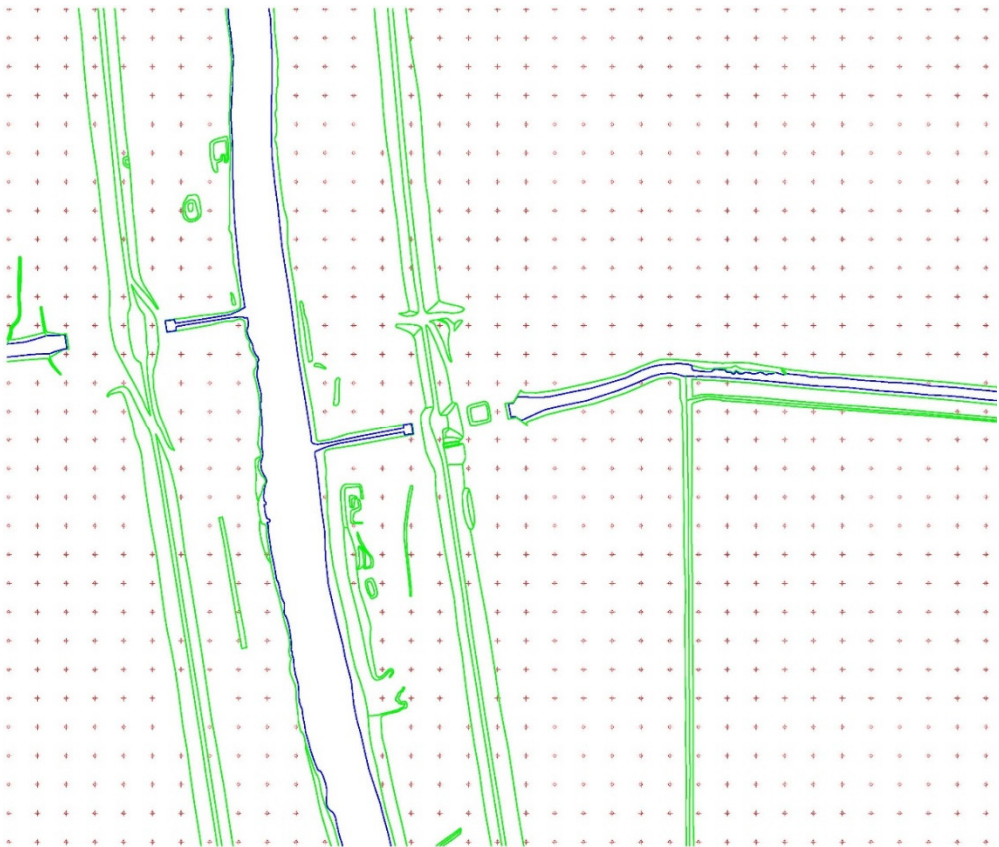


Figure 5. DTM detail of the area of interest close to lateral spillway.

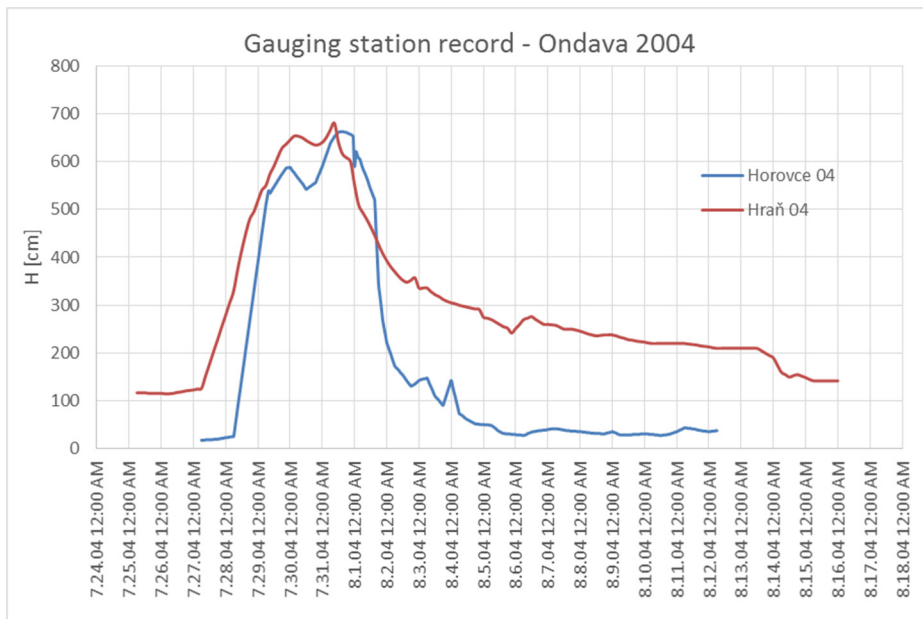


Figure 6. Records on gauging stations Horovce and Hraň during the flood in year 2004

For investigation of the water level regime in the Ondava River the HEC-RAS (Hydrologic Engineering Center – River Analysis System) program, version 5.0.6 has been used [8]. It makes available to investigate 1-D as well as 2-D model and to interconnect them when necessary. 1-D model was used for the progress of water level regime in the Ondava River and 2-D was used for flooded territory outside of the river bed.

1-D simulation model was established, imported into geometry of the HEC-RAS program and afterwards calibrated for both flood situations. Illustration of the calibration is presented in Figure 7.

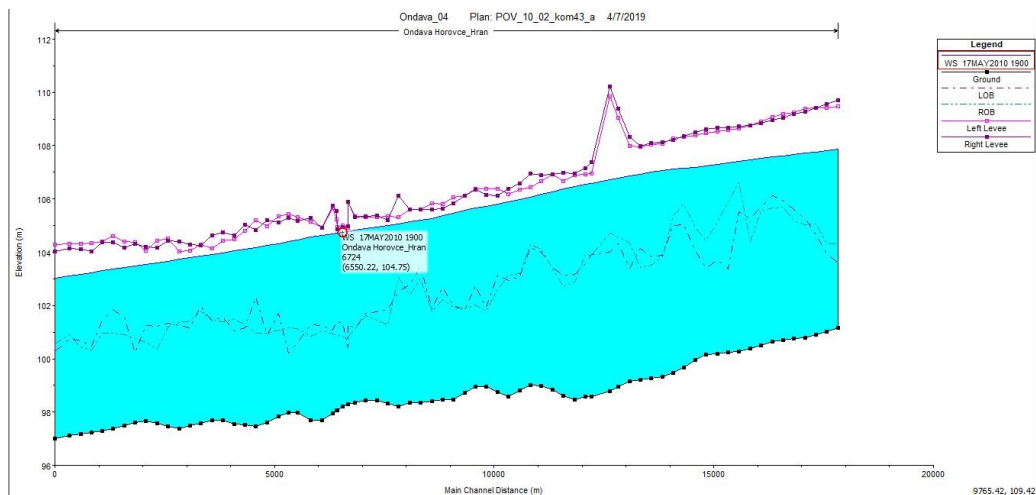


Figure 7. Longitudinal profile of the Ondava River reach Horovce – Hraň, calibration for 2010

2-D model was assembled according to the given DTM generated in ArcGIS program with allocated uniform value of roughness after Manning $n = 0,045$. The model was not calibrated due to lack of data [4], [9].

4. Results and discussion

The simulation calculations itself were realized for several scenarios of the capacity of the lateral spillway. According to them different flooded areas have been obtained in adjacent area, one of them is illustrated in Figure 8a. The territory is mostly limited by existing drainage channels. Lateral spillway is marked by red ellipse.

After preparing calculation scenarios some flood protection measures could be designed in the flooded region for faster run-off of the flooded water in drainage channels towards the PS Kamenná Moľva situated in the south of the flooded area (blue coloured circle). One of them was to built up a rectifying low earth dyke along the Molviansky channel (Figure 8b) or to surround a larger territory to create a detention reservoir for surface water storage and subsequent release of it using existing drainage system. The flooded area would be significantly smaller with no danger for inhabitants in the surrounding [4], [9].

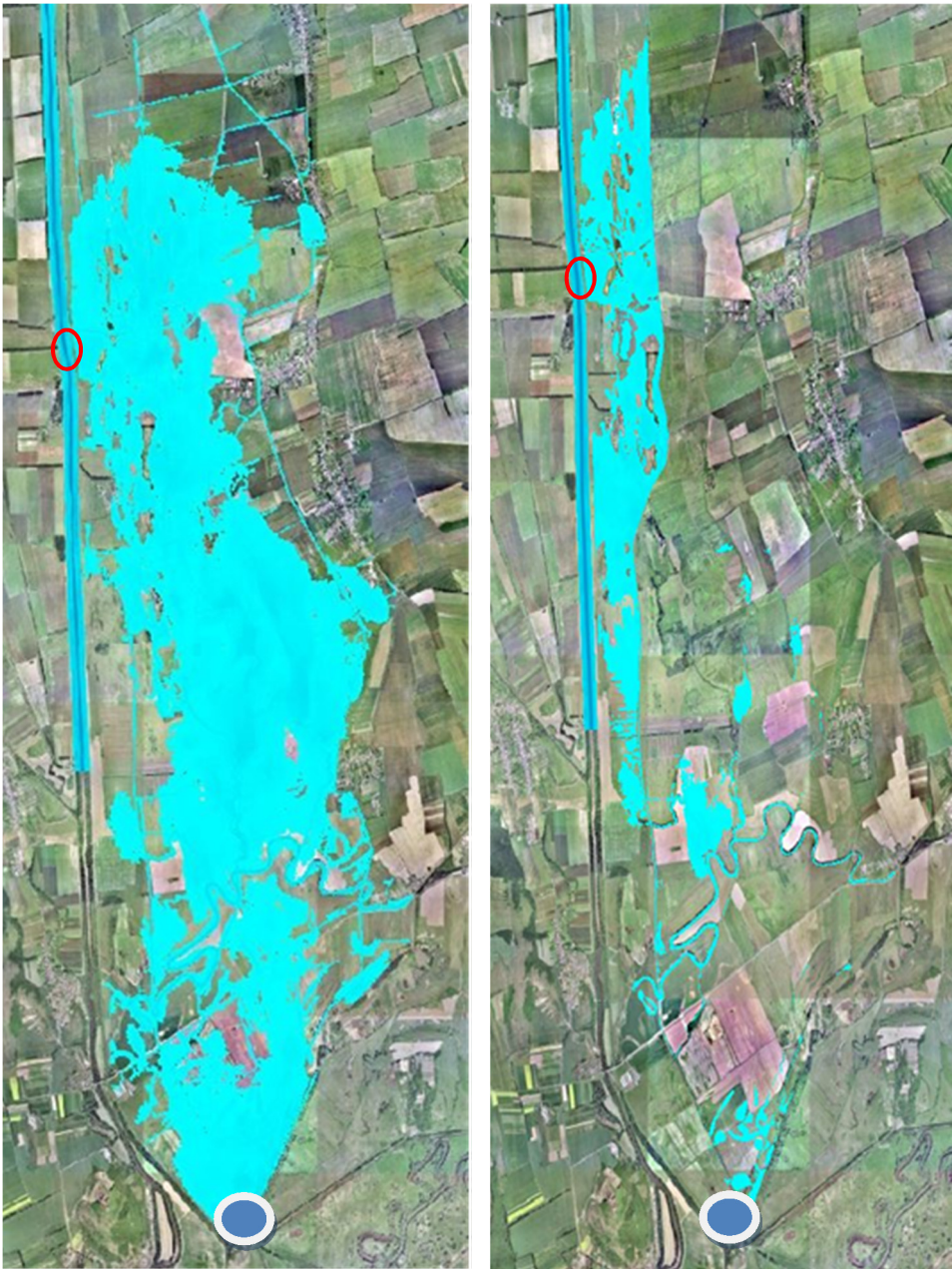


Figure 8a. Presentation of the flooded area during the flood in 2010

Figure 8b. The same area during the flood in 2010 after introducing a rectifying dyke along the channel

5. Conclusion

The flood protection on the lower Ondava River in East Slovak Lowland is despite of enormous human activities insufficient. Mainly, it is due to high accumulation of

sediments in the river bed as well in the flood plain of the river. The consequence is the decreased capacity of the Ondava River during flood situations. Secondly, it is caused by material (mostly sand) which was used during the history for building up earth fill protection dykes along the Ondava River.

Therefore, it is quite appropriate to try to find another possibilities for release and storage of the surface water during flood periods and to divert them afterwards to pumping station using existing system of drainage channels. The goal of research activities of the Department of Hydraulic Engineering in this region is to analyze the water level regime during floods, release the water through hydraulic structures (lateral spillway) and consequently divert it to recipients using pumping or due to gravity.

Acknowledgements

The paper was developed within the frame of and based on the financial support of the VEGA 1/0800/17 project “Optimization of the flood protection of municipalities in river basin of mountain streams” and of the Slovak Research and Development Agency under Contract No. APVV-16-0278 project „Use of hydromelioration structures for mitigation of the negative extreme hydrological phenomena effects and their impacts on the quality of water bodies in agricultural landscapes”.

References:

- [1] Tkáč, J.: General report on flood protection activities on streams in the period 2004 – 2005, SWME Trebišov, 2005.
- [2] Kolesárová, E.: General report on flood behavior, its consequences and realized measures on water streams in the period 2010 – 2011, SWME Trebišov, 2011.
- [3] Květon, R., Šoltész, A., Baroková, D.: Mathematical modelling of flood protection on the Ondava River, *Acta Hydrologica Slovaca*, vol. 12, No. 2, pp. 304- 311, 2011.
- [4] Mydla, J.: Possibilities of mitigation of flood discharges on the lower Ondava River (Diploma thesis). STU Bratislava, 56 p., 2019.
- [5] Šoltész, A., Květon, R., Baroková, D.: Dewatering system in East Slovakian lowland and its hydrologic-hydraulic assessment. In *Colloquium on Landscape Management Mendel University Brno*, pp. 151 – 158, 2016.
- [6] Orfánus, M., Šoltész, A.: The CFD analyses of the lateral spillway using different turbulence models. In: *Proc. of 14th International Symposium on Water Management and Hydraulic Engineering*, Brno, pp. 121 – 130, 2015.
- [7] Kunderát, V., Prosba, J. et al.: *Water management association on the Ondava River in Trebišov, Košice*, ISBN 80-7132-012-9, 1998.
- [8] Brunner, G. W. *HEC-RAS River Analysis System, Hydraulic Reference Manual*, 2016.
- [9] Šoltész, A., Orfánus, M.: Hybrid modelling in flood risk management. In *SGEM2014, GeoConference on water Resources, Forest, Marine and Ocean ecosystem*, Sofia, STEF 92, pp. 345 – 352, 2014.

CLIMATE CHANGE IMPACT ON IRRIGATION WATER REQUIREMENTS: CASE STUDY OF IRRIGATION SYSTEM IN SKOPJE VALLEY

KATERINA DONEVSKA¹, ANGELCO PANOV², ...

1 Professor, University Ss Cyril and Methodius, Faculty of Civil Engineering, Republic of North Macedonia, email: donevska@gf.ukim.edu.mk

2 Project Manager, Pointpro Consulting, Republic of North Macedonia, email: angel.panov@pointpro.com.mk

1. Abstract

The aim of the paper is to present the impact of eventual climate changes on irrigation water requirements by analyses of historical data and generated synthetic unsteady sequences of climate-meteorological data that include forecasted climate variability. Climate change impact on irrigation water requirements is assessed for irrigation system located in Skopje Valley for time period until 2050. Historical data for climate and meteorological elements from the Meteorological Station (MS) Skopje for the period 1961- 2005 are used in the assessment. The study area, mostly in the valley is under an influence of the Continental and Mediterranean type of climate, experiencing very hot and dry summer periods and average cold and wet winters.

Series of monthly and temperature data are generated to 2050 in compliance with the official climate change scenarios for Macedonia using data from Third National Communication on Climate Change to UNFCCC (2014). Official climate change scenarios for the country suggest that there will be continuous increase in temperature in the period 2025- 2100. The predicted changes of the temperature will be most intense in the warmest part of the year. A decrease of precipitation is predicted in all seasons and at annual level, with the maximal decrease in the summer season.

Irrigation water requirements for the actual cropping pattern are calculated on a monthly basis for a period of 45 years (1961 to 2005) using FAO's CROPWAT computer program and climate and meteorological data for the MS Skopje (baseline condition). Adopted regression model (based on statistical tests) is applied to forecast irrigation water requirements for the period from 2016 to 2050 for the same cropping pattern using generated synthetic climate data series like precipitation, temperature data and solar radiation and wind speed as well. The results indicate that climate change being expected in the future may cause increase of irrigation water requirements for 8% for the particular irrigation system in the Skopje Valley.

Keywords: climate change, irrigation water requirements, water management

2. Introduction

In recent decades more intense rainfall events have occurred in parts of Europe as well

as extreme weather events like severe droughts, floods and heat waves. Climate change scenarios forecast more intense changes in temperature and precipitation and therefore increase of the possibility of occurrence of extreme weather events. Decrease of precipitation combined with increase of temperatures will impact both the quantity and quality of the water resources. However, uncertainties persist regarding the magnitude of the climate change impacts to water resources, the timeframe of occurrence, as well as their interactions with human activities.

Climate change scenarios for the country (Climate Change Scenarios, 2012) suggest that there will be continuous increase in temperature in the period 2025- 2100. The predicted changes of the temperature will be most intense in the warmest part of the year. A decrease of precipitation is predicted in the period 2025- 2100, in all seasons and at annual level, with the maximal decrease in the summer season, expecting in July and August there may be no precipitation at all. In winter season, decreases of precipitation of up to 40% of the average monthly quantities are foreseen (Third National Communication on Climate Change, 2014).

Regarding surface water resources, analyses of the variations and trend lines of the minimal, average and maximal annual discharges for all river basins in the country are showing that there is a general trend of reduction of all discharges, most expressed in the central and south-eastern part of the country (Donevska and Gorsevski, 2011). Water resources in the country are highly vulnerable to climate change with regard to both their quantity and quality. The annual water resources per capita are about 3,150 m³/year, classifying the country in the middle category of the European countries upon the available water resources per capita (Second National Communication on Climate Change, 2008). However, this data is close to the limit threshold of water resources needed for sustainable development.

The aim of the paper is to present the impact of climate changes on irrigation water requirements for an irrigation system located in Skopje Valley until 2050. Analyses include generation of series of monthly and annual temperature and precipitation data in compliance with the official climate change scenarios prepared for the Third National Communication on Climate Change (2014) and analysis of the irrigation water requirements taking into consideration climate characteristics in climate change conditions, the cropping pattern (current and foreseen), characteristics of the crops (period of planting, development period, crop coefficients), etc. The research presents a part of the project Climate Change Strategy for the City of Skopje (Resilient Skopje, Climate Change Strategy, 2017).

3. Materials and methods

3.1 Background and study area

The City of Skopje is situated in the central part of the Skopje Valley (Figure 1), covering an area of 571 km². The region relief is complex, comprised of a valley and surrounding mountains on the north-west and on the south and east, forming a border between them and the flat zone of the valley. The main direction of the valley is from the north west to the south east, being shaped by the action of the River Vardar. The River Vardar is the largest river in the country with catchment area of 22,290 km², which covers nearly 80

% of total land area (25,713 km²) of the country. The River Vardar within the Skopje valley is one tenth of total length and located in the upper and middle stretch. The ground elevation of the valley ranges from 340 masl to 220 masl (Spatial Plan of Skopje Region 2005-2020 (draft), 2009).

The valley geology is represented with Neogene and Quaternary sediments, while the surrounding mountains and hills are built of rocks formations of different age. There are two main groundwater aquifers: the first one is high yield semi-confined aquifer of superficial sand and gravel with clay horizons and the second one low yield aquifer in underlying marls. The superficial aquifer is in direct continuity with the River Vardar, while the depths of groundwater level vary depending on the local conditions. In the lower part of Skopje Valley the same aquifer – compacted alluvial sand and gravel – continues with reduced thickness and similar conductivity.

Pedological composition of Skopje Valley is heterogeneous. Different soil types are represented such as: regosols, coluvial, deluvial soils, vertisols, chromium cambosols (cinamonic forest soils), cambosols (brown forest soils), fluvisols (alluvion soils), fluvial-meadow soils (humus flovsoils) etc. Generally, the major part of the soil in the valley is mixed clay and alluvial with high organic contents. The soils in the lower parts of the valley are fertile having a high agricultural value.

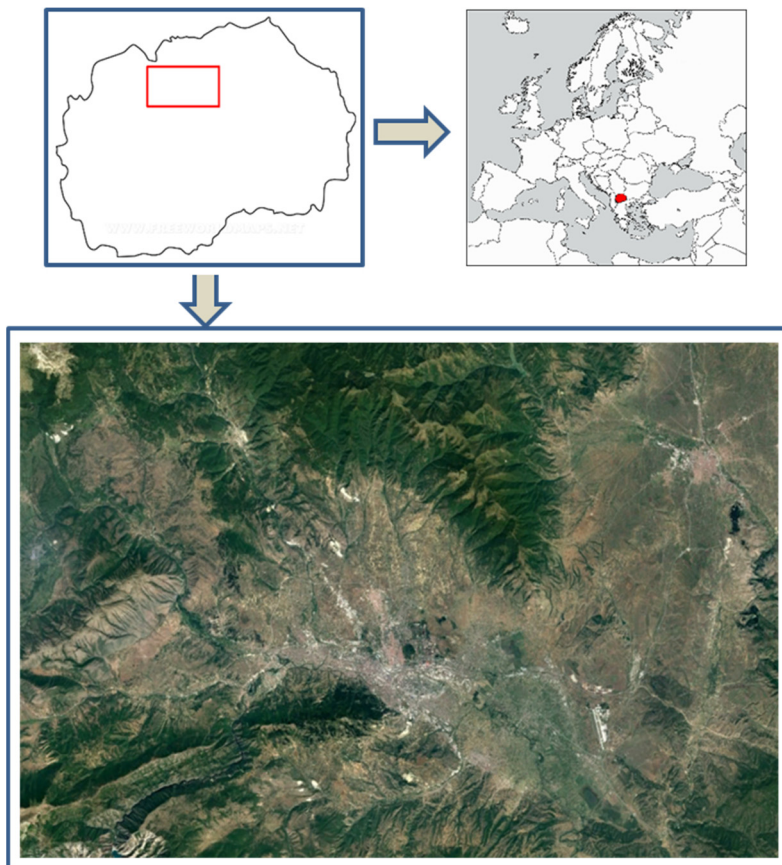


Figure 1. Location of the study area

The study area, mostly in the valley is under an influence of the Continental and Mediterranean type of climate, as well as under an influence of the mountain climate on higher elevations. Lower parts of the valley are experiencing very hot and dry summer periods and average cold and wet winters. The average annual air temperature for the valley is 12.9 °C, the highest monthly temperatures are recorded in July and August, while the lowest in January. Average annual temperatures for the period from 1978 to 2015 show an increasing trend. In Skopje there are usually short heat waves that last for up to six days. Heat waves have been most frequent in the last ten years.

Average annual sum of precipitations is 484.8 mm. The uneven spatial and temporal distribution of precipitation results in long dry periods, from July to September, lasting often continuously more than 60 days. On the other hand, there are abundant precipitations between October and December and limited precipitation between March and May.

According to the De Martonne index of drought, greater percentage of the years can be classified to have characteristics of dry and semi arid climate. Of great importance is the declining trend line of the annual values of De Martonne index till 2008, presenting the trend of increasing the aridity of the region (Figure 2). However, the humid 2009, 2010 and 2014 result in increase of the trend line of the annual values of De Martonne index after 2008.

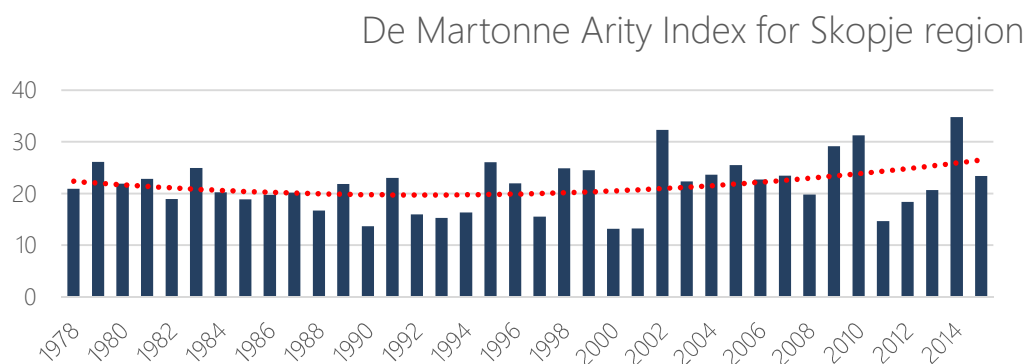


Figure 2. Temporal distribution of De Martonne index of drought for period 1978 - 2015

3.2 Methodology and Data

The research is based on the data series for: average monthly and average annual temperatures for period 1978 – 2015; monthly and annual sum of precipitation for period 1978 – 2015; data for predicted changes of air temperature and precipitation according to climate change scenarios (Climate Change Scenarios, 2012). Analysis of the climate elements of main meteorological station (MS) Skopje are performed, as a representative of the climate condition in the project area.

Table 1 presents a summary of meteorological data for MS Skopje used for calculation of irrigation water requirements. Due to the large amount of data, presentation of the results is performed with three characteristic empirical probabilities (25%, 50% и 75%), with minimal, maximal and average values.

Table 1. Average monthly meteorological data (MS Skopje for the period of 1978-2015 for temperature and precipitation and for the period 1961-2005 for RH, WS, SR)

	Jan	Feb	Mar	Apr	May	Jun	Jul	Aug	Sep	Oct	Nov	Dec
P (%)	31,9	30,1	31,2	42,8	51,8	42,9	34,0	31,9	42,1	49,9	49,9	46,3
Tav(°)	0,9	3,4	8,2	12,7	17,6	21,9	24,4	24,1	19,2	13,3	6,9	2,2
RH (%)	82.2	75.9	68.7	65.3	65.3	60.6	56.4	57.0	63.2	72.2	80.3	84.0
WS(m/s)	1.0	1.2	1.0	1.1	0.8	0.8	0.7	0.7	0.7	0.8	0.9	1.0
SR (h)	74	113	137	175	213	226	307	286	212	181	92	61

P – Precipitation; Tav – Average air temperature;

RH – Relative humidity; WS – Wind speed; SR – Solar radiation

In order to evaluate the impact of possible climate changes for the forthcoming period on the water crop and irrigation water requirements, data analyses are made for climate elements and their changes according to the study “Climate Change Scenarios for Macedonia” (Third National Communication on Climate Change, 2012). The prognosis of possible climate changes is performed by the method of proportional reduction (downscaling) of Global models at regional level.

3.2.1 Generating Synthetic Sequences of Climate Series

The values of the average scenario are entered in the historical climate data series, new sequences are generated, and consequently calculation of irrigation water requirements is carried out.

Time allocation during one year of the projected seasonal climate values of the characteristic elements is performed by means of fourth degree polynomial equations. In fact, polynomials have been developed for transferring the seasonal into monthly values for all climate elements, for the two time section 2025 and 2050. Adaptability of the anticipated dependence is significant, with extremely high values of correlation coefficients.

The second step is to complete series filling them with monthly values of climate elements between the two characteristic time sections. Filling is performed with direct interpolation between the reference values from 2025 and 2050, setting zero value to be 2000.

These distributed time series of climate elements define only differences in terms of change of the characteristic temperatures expressed in °C or decrease of precipitation expressed in %. Finally, time distributed changes of climate elements are added to the historical climate data; thus calculation of future irrigation water requirements with the influence of climate change is performed.

Assessment of other climate elements, such as solar radiation and wind speed, is generally performed at national level. For both elements the relative expected changes are small and do not exceed 5%. Minor increase in solar radiation is expected throughout the year, with extreme incidence during summer months. There is practically no change in speed of the dominant winds.

All analyses are conducted on a monthly basis for a period of 45 years. To represent the large amount of data more visibly, the presentation of the characteristic values is through appropriate assistance of empirical probability of average monthly values for the feature. The presentation of the results is performed with three characteristic empirical

probabilities (25%, 50% and 75%), with minimum and maximum value and in some cases by average value of the feature. Table 2 shows the average values of projected monthly precipitation, average air temperature, wind speed and solar radiation for MS Skopje for the period from 2006 to 2050.

Table 2. Average projected monthly climate data (MS Skopje, 2016 - 2050)

	Jan	Feb	Mar	Apr	May	Jun	Jul	Aug	Sep	Oct	Nov	Dec
P(%)	35.0	33.1	37.5	41.6	52.1	40.1	31.3	25.6	34.3	42.5	52.4	51.1
Tav(oC)	0.9	3.2	7.9	13.1	18.4	22.6	25.0	24.6	19.9	13.7	7.0	2.0
RH	82.2	75.9	68.6	65.2	65.2	60.5	56.2	56.9	63.1	72.1	80.3	84.0
WS(m/s)	1.0	1.2	1.0	1.1	0.8	0.8	0.7	0.7	0.7	0.8	0.9	1.0
SR (h)	74	114	139	178	218	232	314	291	215	183	93	61

P – Precipitation; Tav – Average air temperature;

RH – Relative humidity; WS – Wind speed; SR – Solar radiation

3.2.2. Cropping Pattern -Current Practice

Agriculture production in the project area is very restricted, which is conditioned by the dry conditions. Although some parts of the cultivated areas are covered by well-fed irrigation, they are planted with crops that require less quantities of water. Presentation of different crops for the Skopje region according to the agriculture census 2007 and Statistical bulletin for Agriculture, Orchards and Viniculture (2014), is given below:

Table 3. Crop representation in Skopje Region by Statistical Bulletin for Agriculture, Orchards and Viniculture (2014)

	Skopje	Ilinden	Petrovec	Arachinovo	Zelenikovo	Sopishte	Studenichani	Chucher Sandevo	Total (ha)
Cereals	6860	2112	1432	681	634	1084	576	832	14.211
Industrial crops	104	50	39	52	31	0	313	2	591
Vegetables	4346	715	272	213	117	451	636	648	7.398
Fodder crops	1664	265	243	123	96	401	226	118	3.136
Meadows	516	346	88	128	195	132	428	1941	3.774
Pastures	37151	148	625	161	215	515	395	1898	41.108
Orchards	393	61	96	21	35	34	113	35	788
Vineyards	1200	85	160	5	38	68	62	425	2.043
Area	52.234	3.782	2.955	1.384	1.361	2.685	2.749	5.899	73.049
Net Area	14.567	3.288	2.242	1.095	951	2.038	1.926	2.060	28.167

According to statistics, in the project area, agricultural activity currently is spread approximately on 28,000 hectares.

Irrigation water requirements for the system are calculated for a period of 45 years and presented as discrete values for one day. Water requirements are determined by reference evaporation, calculated by the Penman – Monteith method.

Besides the historical data used to determine irrigation water requirements synthetic data series are also applied, which include possible climate changes until 2050 according the average scenario. Crop water requirements are determined based on the FAO Irrigation and Drainage paper 24, No 25 and No 56. The FAO software CROPWAT 8.0 is used for the analysis. Initially, the reference evaporation is determined in accordance with the modified Penman - Monteith method. Consequently, the reference evaporation method is used for determination of irrigation water requirements with application of crops coefficients given in the FAO reference adapted for the local conditions.

4. Results

Irrigation water requirements for the historical period 1961 to 2005 are presented on Figure 3.

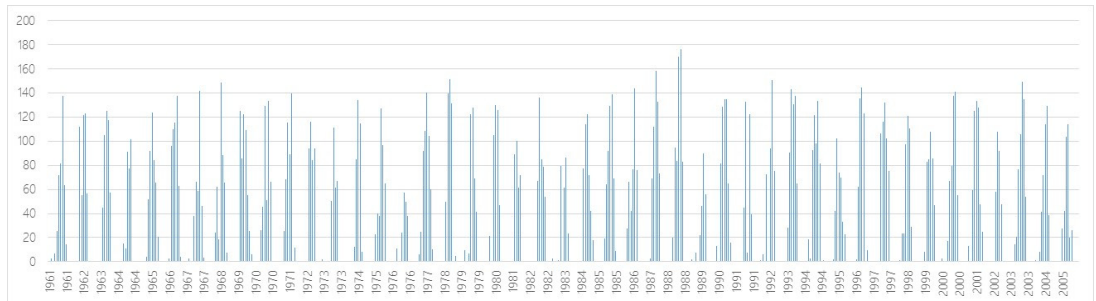


Figure 3. Historical irrigation water requirements for the period 1961 to 2005

The total annual and monthly irrigation water requirements with various empirical probabilities are represented in the Table 4.

Table 4. Irrigation water requirements for Skopje for the period of 1961 – 2005 (in mm)

IWR	Jan	Feb	Mar	Apr	May	Jun	Jul	Aug	Sep	Oct	Nov	Dec	Sum
min	0.0	0.0	0.0	0.0	0.0	0.0	7.5	19.7	0.0	0.0	0.0	0.0	180
25%	0.0	0.0	0.0	0.0	41.8	79.8	81.9	86.5	28.8	0.0	0.0	0.0	358
50%	0.0	0.0	0.0	2.4	62.5	103.9	121.0	117.8	53.8	0.0	0.0	0.0	430
75%	0.0	0.0	0.0	20.3	81.4	116.1	132.5	134.8	65.2	7.4	0.0	0.0	521
max	2.9	2.9	18.9	28.0	125.4	143.0	170.3	176.6	83.2	25.4	6.3	1.7	629

Reference evaporation (E_{To}) depends on the average maximum and minimum air temperature, relative humidity, solar radiation and wind speed. Main goal in this section is calculation of E_{To} , however as a function of climate elements that contain the potential changes. The average annual value of potential evaporation for the analyzed period is 886 mm.

More significant air temperature increase during the summer months with special emphasis of the temperature difference between summer and winter periods and the obvious extreme temperatures change, where the maximum is greater than the minimum gradient, directly reflects the potential evaporation.

Comparing the entire sequences, predicted water requirements for crops according to climate changes are extremely high in the summer months. In general, the increase of potential evaporation almost linearly reflects on irrigation water requirements to the crops.

Table 5. Irrigation water requirements for Skopje for the period of 2016 – 2050 (in mm)

IWR	Jan	Feb	Mar	Apr	May	Jun	Jul	Aug	Sep	Oct	Nov	Dec	Sum
min	0.0	0.0	0.0	0.0	0.0	0.0	35.9	46.8	0.0	0.0	0.0	0.0	217
25%	0.0	0.0	0.0	0.0	53.9	99.0	92.5	93.6	31.9	0.0	0.0	0.0	406
50%	0.0	0.0	0.0	4.5	74.4	115.6	132.6	124.8	51.7	0.0	0.0	0.0	477
75%	0.0	0.0	0.9	23.1	90.8	127.2	143.1	141.6	68.0	4.0	0.0	0.0	578
max	3.7	1.7	18.0	30.7	116.0	151.1	181.7	185.1	88.7	26.2	0.9	2.1	679

Estimated irrigation water requirements for the forthcoming period 2016- 2050 including climate change scenarios are presented on Figure 4.

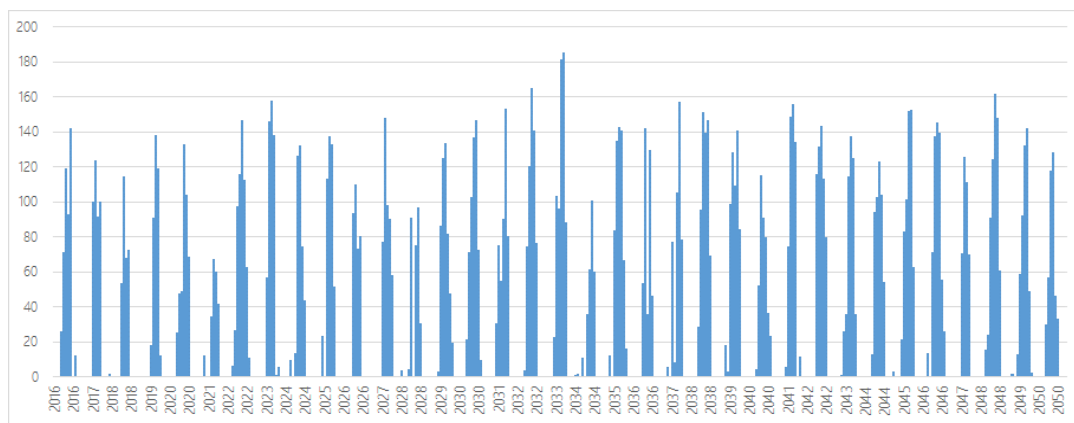


Figure 4. Predicted irrigation water requirements for period 2016- 2050

The average annual value of required water for irrigation over the analyzed period is 467 mm and is 8% greater than the reference historical period.

5. Conclusions

The research presents the impact of predicted climate change on the irrigation water requirements up to 2050 for an irrigation system located in the Skopje Valley. It is based on historical data and generated synthetic unsteady sequences of climate-meteorological data that include forecasted climate variability. All data used for climate and meteorological elements are obtained from MS Skopje for the period of 1961- 2005. Incomplete climatic historical and meteorological data series are correlative with one or more independent variable values. Correlation coefficients that define model adaptiveness are very high.

Irrigation water requirements are calculated based on: the FAO methodology (Irrigation and Drainage Paper 24, No 25 and No 56), using the programming package CROPWAT 8.0, and based on previously defined input file with climate elements and assumed cropping pattern. Calculated results are presented for specific probability of appearance in terms of considered series. Daily values of the crops irrigation water requirements are obtained by linear discretization of subsequent additional decade values. Assuming that according to the cropping pattern presented in Statistical bulletin for Agriculture, Orchards and Viniculture (2014), all areas except those planted with cereal crops are irrigated, agriculture consumes approximately 77 million m³ of water.

Possible climate changes that are expected in the future resulting in decrease of precipitation and increasing of air temperature, may cause increasing of irrigation water requirements for 8%.

References:

- [1] Climate Change Scenarios, 2012 Ministry of Agriculture, Forestry and Water Economy,

- Administration for Hydro-Meteorological Services, Skopje, Republic of Macedonia.
- [2] Donevska K., Gorsevski P., 2011, Climatic Influence on Surface Water Resources in the Republic of Macedonia, 12th International Symposium on Water Management and Hydraulic Engineering, Proceedings Ecohydrological Methods in Water Management pp. 5-14, Gdansk, Poland, ISBN 978-83-7348-376-7.
 - [3] Resilient Skopje, Climate Change Strategy, 2017 City of Skopje, Republic of Macedonia (UNDP funded project).
 - [4] Second National Communication on Climate Change, 2008 Ministry of Environment and Physical Planning, ISBN 978-9989-110-69-6
 - [5] Spatial Plan of Skopje Region 2005-2020 (draft), 2009 Ministry of Environment and Physical Planning of the Republic of Macedonia, Agency of Spatial Planning, Skopje, Republic of Macedonia.
 - [6] Third National Communication on Climate Change, 2014 Ministry of Environment and Physical Planning of the Republic of Macedonia, Skopje, Republic of Macedonia, ISBN 978-9989-110-89-4.

PROTECTION FROM EROSION AND RIVER SEDIMENTS BY TORRENTIAL RIVERS AND GULLIES NEAR LOCAL ROADS IN THE MUNICIPALITY OF KONCHE

DRAGAN DIMITRIEVSKI¹, SANJA STOSHEVSKA², DARKO ILIEVSKI³, LJUBENKA
S. TRENDAFILOVA⁴, KATERINA VELESKA⁵

¹ GEING, Skopje, North Macedonia, dragan@geing.com.mk

² GEING, Skopje, North Macedonia, sanja@geing.com.mk

³ GEING, Skopje, North Macedonia, darko@geing.com.mk

⁴ GEING, Skopje, North Macedonia, stojanova.lj@geing.com.mk

⁵ GEING, Skopje, North Macedonia, veleska.k@geing.com.mk

1. Abstract

The section from the regional road Konce to Strumica which was built in 1980, in the winter of 2015, was hit by flood, and the road was interrupted due to heavy damages from sediments from the flowing rivers and the traffic was stopped.

After detailed site prospection was performed, a concept of anti-erosion regulation was prepared which is based on the analysis of the current situation in the catchment areas, primarily the factors affecting the regime of flow, the potential of erosion and the regime of transport of the erosive sediments and proposed measures and solutions for mitigation and remediation of damages and consequences.

Keywords: Anti-erosion, anti-torrential, barrier, afforestation, environment, riverbanks.

2. Introduction

The torrential series Volvov Dere - Gabreshka River is located in the southeastern part of the Republic of Macedonia, on the territory of the municipality of Konche. This torrential series covers 7 (seven) torrential watercourses: Volov Dere, Makreshka River, Rakitec River, Rakichka River, Dedinska River, Dukov Dol and Gabreshka River. For the first three torrential watercourses: Volov Dere, Makreshka River and Rakichka River, a technical solution on a level of conceptual, then basic design was prepared, while for the other three torrential watercourses: Dedinska River, Dujkov Dol and Gabreshka River, only a technical solution on a level of conceptual design was prepared.

The catchment area of the torrential series is approximately 5.0 km south of Radovich, i.e. 5.0 km east of the village of Konche which is also the headquarters of the municipality of the same name.

The source parts of the catchment areas are mainly flattened, slightly to moderately inclined, with a multitude of small ridges and plateaus. The middle parts of all basins of the torrential series have a strongly developed hydrographic network and almost all the

watercourses in these parts of the watersheds flow into steep and narrow, and partly rocky beds. One of the most significant features of the watercourses of this torrential series are the wide, ie, long and wide valleys.

Basically, the torrential watercourses of this series have a moderately dense to distinctively dense hydrographic network, which has a strong influence on the water flow regime. The basins of Makreshka River, Dedinska River and Gabreshka River have the form / shape of a had fan, which has a very adverse effect on the surface water flow regime. At these three watercourses there are orographic-hydrographic conditions and possibilities for rapid and simultaneous concentration of the extracted waters from the catchment areas.

The concept of anti-erosion protection of the catchment areas was based on the application and implementation of biological, biological-technical agrotechnical measures and works, primarily afforestation, grass planting, irrigation and anti-erosion agricultural technology. Anti-erosion works and measures are in accordance with the intensity of erosion, the types and forms of erosion present and the natural / environmental conditions present at the sites. Hydrotechnical structures - barriers, have the role of "sediment tank" and they are expected to achieve rapid effects. Their location is conditioned by the morphology of the torrential riverbeds, primarily the widths of the alluvial fan.

The purpose of the envisaged anti-erosion and counter-measures and works is to mitigate and repair the present erosion processes, and above all, the processes with higher intensity-potential, dominance III and much less category II erosion. By reducing the potential for erosion in the catchment areas of the torrential watercourses of the torrential series, the impacts and damages on the road infrastructure will be reduced or fully remedied and at the same time a major contribution to extending the life of the Mantovo reservoir and the hydro system will be achieved.

By investing in the anti-erosion management of catchment areas, it is also investing in the sustainable development and improvement of natural resources (water, forests, soil, wildlife pastures, etc.) and the development of the area as a whole.

Given the enormous importance of the hydro system and the necessity for its long-term use, continuous monitoring of the erosion process intensity, intensity and dynamics of filling the accumulation with erosive sedimentary material should be carried out and adequately planned and implemented appropriate anti-erosion and anti-storm works and measures to regulate watersheds and riverbeds.

The implemented measures and works with this technical solution are aimed at protecting the road infrastructure, which is the basic task, but at the same time in order to increase the life span and use of the Mantovo reservoir and hydro system as a whole.

3. Methods

In order to determine the most appropriate method of problem solving and to propose a technical solution for the erosion of torrential series, it was necessary to analyze and study the existing basin erosion and to determine flood water quantity.

3.1 Regime of erosion in the basin and regime

3.1.1 Erosion mapping and determination of erosion coefficient

In order to determine the amount of produced erosive material in the catchment area of the torrential series: Volov Dere - Gabreshka River and the amount of transported (transported) erosive sediment in the torrential series, the existing documentation was used.

From the time of preparation of the Erosion Map of R. Macedonia, to this day, has undergone some changes in the catchment area. These changes result from the realization of planning and other projects for management of natural resources (forests, pastures, agricultural land, water, etc.) in the public sector and daily activities in the private sector.

Since no opportunities and conditions were provided for permanent updating of the Erosion Map, the working team performed a new erosion mapping in the watershed. The mapping was performed in October 2016.

Looking at topographic maps made in 1970 and 2004, significant changes can be observed in the watershed. The torrent series stream: Volvov Dere - Gabreshka River is in the immediate vicinity of the Mantovo reservoir. Prior to and during the construction of the reservoir, more anti-erosion biotechnical works and measures have been carried out (building objects in the riverbed and afforestation in the basin). Nowadays the watershed is significantly covered with vegetation which plays an important role in protecting the eroding ground from erosion.

On the other hand, the pressure on nature is much lower, the population is reduced and thus there is no intensive use of natural resources (forest cutting, livestock grazing and intensive agricultural production). These are factors that influence the reduction of erosion processes in the watershed.

The erosion map of the Republic of Macedonia, which means the erosion map for the watershed area of the torrential series, was prepared according to the methodology of S. Gavrilovic, who for the conditions of this area, has been modified to some extent. The mapping of the erosion processes and the preparation of the Watershed Erosion Map is done according to the same methodology. That is, methodological and otherwise, there are no differences in the approach of mapping and map preparation. The production and transport of erosive sedimentary material for the torrential series watershed are determined by the methodology of S. Gavrilovic.

During preparation of erosion map were used data, backgrounds and knowledge of: climate and climate elements and factors, topographic maps, data and maps of surface structure by purpose and method of use, vegetation maps, (forest management plans), engineering-geological map R . Macedonia, research and findings on pedological construction of the substrate and existing project documentation (studies, conceptual and main designs, research papers and designs) etc. The Erosion Map shows the status of the present erosion processes in the watershed, classified into five categories of erosion.

Based on the Erosion Map, the structure of the surfaces affected by different types of erosion, ie categories of erosion, is determined.

According to the presence of the identified areas with the corresponding types of erosion,

the average erosion coefficient "Z" for the torrent series watershed: Volov Dere - Gabreshka River "is: $Z_{sr} = 0.46$.

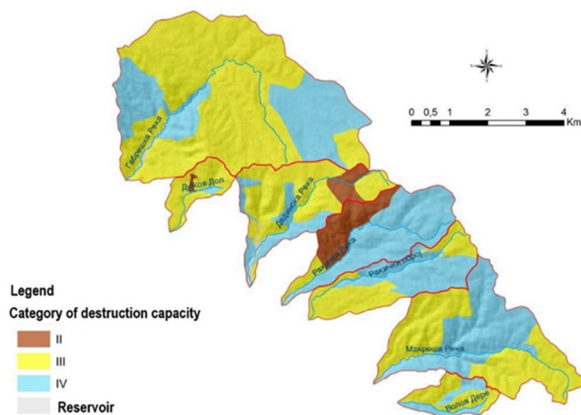


Figure 1. Categories of erosion processes in torrential series

In the catchment area of the torrential series: Volvov Dere-Gabreshka River, the most frequent are Category III processes of destruction. They cover an area of 30.08 km^2 or 56.74% of the total catchment area. Deep and mixed erosion processes of category IV, with an erosion coefficient of 0.25-0.35 are present at an area of 20.13 km^2 or 37.6%. The least represented in the watershed is the strong erosion (category II) of mixed character and is represented by 2.33 km^2 or 4.4%.

The strongest erosion of category II is mainly located in the basin of Rakichka River in the middle part of the basin on the right bank of the river and a small part of it is in the upstream of Dedinska River. Erosion of Category III and Category IV destruction is present in all basins of the torrential series. Occurrences and processes of Category III destruction are present on more than half of the surface in the catchments of the following torrents: Gabreshka River, Dujkov Dol (more than 80%), Dedinska River and Volvov Dere. In the other basins, more than half of the total area is dominated by category IV destruction.

From the foregoing it can be concluded that more intensive erosion processes take place in the lower and middle part of the basin, mainly in the vicinity of the villages.

3.2 Determination of flood water quantities

Determination of the flood waters of the torrential watercourses Gabreshka, Volov Dere Makreshka, Raklicka, Dedinska, Djukov Dol, as there are no measurement data, was carried out by parametric and empirical formulas. Flood water was calculated according to the natural conditions and characteristics of the watercourse, which gives results that are most appropriate to the watershed situation.

The quantification of water will be carried out by the following methods:

I method - Parametric method SCS (Synthetic Hydrogram). The application of synthetic hydrogram eliminates certain possible geologically undefined basins, which have a specific impact on high waters and their occurrences. This method uses the probability distribution of maximum precipitation for the most appropriate Demir Kapija

meteorological station. This method is best suited for calculating flood waters for catchments with large inclinations.

II method - Study on the flood waters in the partitions in the Vardar River Watershed, developed by the Jaroslav Cherni Institute.

III method - Gavrilovic's empirical formula

Table 1. Flood waters with probability of 1% according to all three methods for each watercourse in m³/s

	I METHOD	II METHOD	III METHOD
GABRESHKA	36.65	51.41	39.26
DJUKOV DOL	6.65	5.88	10.72
DEDINSKA	11.22	19.59	19.58
RAKICHKA	10.30	19.81	21.49
MAKRESHKA	13.30	29.41	29.01
VOLOV DERE	5.24	6.70	11.88

4. Results and discussion

As a result, to all these analyses a concept was prepared of anti-erosion protection measures.

The concept consists of the following:

- Proposal of measures and solutions for rehabilitation / reconstruction of existing performed anti-erosion and anti-torrential works and structures (biological, biological-technical and hydrotechnical);
- Proposal of measures and works for biological, biological-technical and agro-technical anti-erosive arrangement, according to the current situation and
- Proposal of hydrotechnical solutions for counter-arrangement of the riverbeds, according to the present situation (reconstruction of existing and construction of new).

Following figures best describe the anticipated measures.

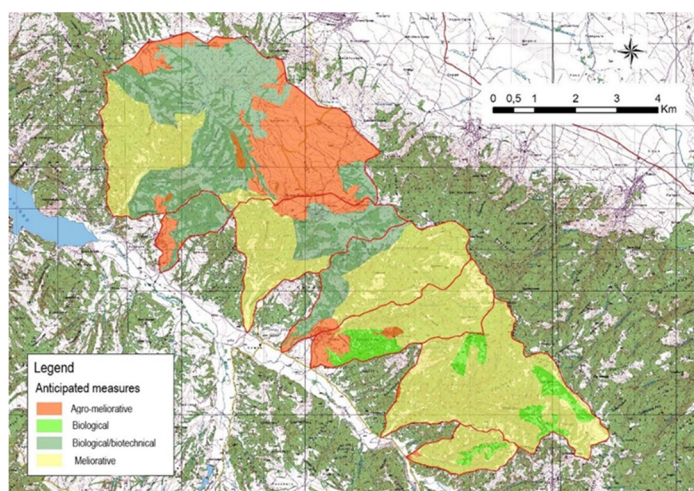


Figure 2. Anticipated measures and works for biological and biological-technical anti-erosion arrangement

4.1 Biological/technical, meliorative and agrotechnical – agro-meliorative measures and works

Biological-technical measures and works in the last decades in the Republic of Macedonia have been completely neglected. These are measures and activities that can be successfully implemented by all entities, both at the state, regional and local levels, as well as the owners of agricultural land and forests. The following types of protection can be successfully used for reinforcement of deep furrows, ravines, small landslides, shorelines, etc.: single and double wattle dams, rustic walls, small balconies, gabion walls, use of fascines (tied bundles of rods obtained during the orchard harvest, etc.). The choice of material, type and dimensions of these constructions should be determined according to the needs and purpose.

In locations where there is a greater presence of stone at the site or in the immediate vicinity, rustic objects, gabion walls and obstacles and rows of thrown stone were planned to take precedence. In locations where there is no stone and there is material for making wattle dams, "live" or dead, the advantage is given to them. Single-row wattle dams were planned on the steep and erosive slopes where the soil layer is very shallow and skeletal, and therefore there are no opportunities and conditions for direct afforestation. Double-sided wattle dams were envisaged in ravines and gullies.

Biological technical works are in the function of biological works, primarily reforestation and remediation and mitigation of ravine-fluvial erosion. These works are aimed at reducing the erosion intensity and reducing the amount of sediment transported and deposited. Typically, as in this case, they are in the function of reforestation (single plates) and combined with reforestation.

Significant agro-meliorative measures and things that have positive effects in the fight against erosion are: plowing by contour lines, crop rotation, contour furrows, plowed terraces and so on.

All proposed biological, biological-technical and agro-technical / meliorative measures and works are at recommendation level. In many countries, the application of these measures and matters is regulated by laws and bylaws and projects developed and adopted by all stakeholders at the state, regional and local level - the municipality. The application of measures and matters is the obligation of all entities, regardless of ownership.

4.2 Construction and hydro-technical structures

In this case two types of hydro-technical structures were anticipated: transverse and longitudinal.

Basically, all transverse hydrotechnical structures: barriers and threshold have a combined effect, i.e. they are intended for remediation and mitigation of fluvial erosion, stabilization of the bottom and banks of the riverbeds, improvement of the regime of torrential water flow and retention of significant amounts of sediment in the riverbeds of the watercourses.

Two types of barriers were suggested: barriers from stone in cement mortar and a concrete barrier, and according to the financial value the relevant institutions chose the second one, so a proper number of concrete barriers were planned for each watercourse.

Besides the transverse, also a longitudinal hydrotechnical structures were planned. Building regulations along the course of torrential watercourses from this torrential series is a costly, irrational, and inevitable solution. The slopes are spacious, both in length and width. When selecting "partitions" for the new facilities, we chose the narrowest transverse profiles, which are mainly concentrated in the most opposing parts of the slopes, which is logical according to the terrain and the configuration of the terrain.

In order to direct the torrential waters to the crossings through the roads, that is, the ravines (bad solution), we propose to make adjustments in the most upstream sections of the slopes, 150-200 meters upstream of the culverts "bridges", at the following torrents: Volov Dere, Makreshka River and Rakichka River. The beginning of the regulations cannot be provided with classical barriers due to the large width of the slopes. Therefore, the beginnings of the regulations will be secured by low barriers, whose shoreline walls will enter 2-3 meters in the "shores" of the riverbeds.

The "banks" of the regulated riverbed will be assured with fascines, dominated by orchards, and will be strengthened in the shores with a gabion wire. The embankments will be formed from local material, i.e. the sediment from the basin itself. After forming the embankments and the shore protection from the fascines, a shallow layer of fertile soil can be applied and sown with non-native grass and shrubby vegetation, in order to provide natural protection of the banks from the effects of fluvial erosion, especially if present given the fact that the fascines have a short shelf life (2-3 years).

5. Conclusion

The subject was anti-erosive protection of areas affected by erosion processes and anti-torrential protection of the riverbeds of the Volvov Dere - Gabreshka River flood series.

Basically, objectives can be defined through the following points:

- Protection of road infrastructure and reduction of damages and consequences from future torrential floods;
- Extension of the life cycle of the reservoir and hydro system "Mantovo";
- Definition of the erosion processes present, types and categories of erosion;
- Defining the intensity-potential of the erosive processes present in the catchment areas of the torrential series;
- Defining the regime and erosive sediments (production and transmission);
- Proposal of measures and works for anti-erosive regulation;
- Anti-torrential regulation of erosion in the riverbeds;
- Expansion and improvement of the forest fund;
- Protection of land from erosion;
- Enhancement of biodiversity;
- Nature enrichment;
- Sustainable development and improvement of the environment;
- Improvement of the surface water regime (flow);
- Improving the microclimate;
- Creation of new forests and new orchards with protective function;

- Improvement of micro natural conditions;
- Mechanical and biological stabilization of eroded soils and erosive surfaces and
- Soil revitalization and accelerating the process of pedogenesis.

References:

- [1] Erosion Map of the Republic of Macedonia, Water Management Institute of the Republic of Macedonia, 1993;
- [2] Watershed erosion map prepared by the study design team, based on direct mapping, October 2016.
- [3] Intensive Rainfall in the Republic of Macedonia, Faculty of Civil Engineering - Institute of Hydrotechnics, June 1993
- [4] Phd. Trendafilov, A.: Erosion and torrential watercourse, Faculty of Forestry – Skopje, 2003
- [5] Popovska, C., Gjeshovska, V., Donevska, K.: Hydrology, Faculty of Civil Engineering, 2004
- [6] Conceptual design for protection from erosion and river sediments from torrential rivers and gullies near regional roads in Municipality of Konche, Geing Krebs und Kiefer International and others DOO, December 2016
- [7] Main design for protection from erosion and river sediments from torrential rivers and gullies near regional roads in Municipality of Konche, Geing Krebs und Kiefer International and others DOO, June 2017

REDEFINITION OF FLOOD WATERS FOR THE KALIMANCI DAM

VIOLETA GJESOVSKA¹, IVANA LEFKOVA², GOCE TASESKI³

¹ *University Ss. Cyril and Methodius, Faculty of Civil Engineering, Skopje, R. Macedonia
violetag@gf.ukim.edu.mk*

² *University Ss. Cyril and Methodius, Faculty of Civil Engineering, Skopje, R. Macedonia
taseski@gf.ukim.edu.mk*

³ *University Ss. Cyril and Methodius, Faculty of Civil Engineering, Skopje, R. Macedonia
ivana.lefkova@hotmail.com*

1. Abstract

Definition of flood waters, their intensity and duration is the most important factor in defining the relevant flood waters for proportioning hydro-technical structures and protection against flood waters.

Due to changes of natural factors and changed conditions under the influence of anthropogenic factors taking place at already constructed hydrotechnical structures, redefinition of flood waters is an extremely important measure in forecasting floods and timely undertaking of corresponding activities for prevention or reduction of their consequences.

Presented in this paper are the results of the hydrological analysis of the Kalimanci dam basin carried out for the purpose of redefining flood waters. The analyses of the physical-geometrical characteristics of the drainage area carried out by use of DTM (Digital Terrain Model) and application of SWAT (Soil & Water Assessment Tool), a hydrological analysis module from the Geographic Information Software (GIS), are presented further in the text. Flood waters with different return periods will be redefined by use of statistic methods based on data from measurements of "Bregalnica" river flow (1961-2005) and "Kamenichka Reka" river flow (1986-2005). Shown further in the paper will be the results of the calculation of the maximum flood waters (MPF-Maximum Probable Flood waters) in the basin. MPF will be calculated by taking into account a series of data on maximum annual daily rainfall, measured at the dam itself, in the period 2005 to 2017. The results of these analyses will be presented in a tabular and graphic form.

Keywords: hydrological analysis, watershed, flood, discharge, precipitation

2. Introduction

Water is an essential component of life on our planet. However, at the time of increased CO₂ emissions and global planetary environmental pollution, man faces the negative impacts of water. We are witnessing more frequent extreme meteorological and hydrological phenomena that result in enormous damage and loss of human lives. Under global warming effects, the conditions for the formation of natural hydrological

phenomena have changed. Noticeable is the occurrence of non-characteristic high and low temperatures, heavy precipitations and increased humidity as well as periods without precipitations. These phenomena are manifested by extremely dry and extremely wet periods at previously uncharacteristic locations.

Floods as extreme events are the reason for the increased level and flow of water in river beds, lakes and seas. The appearance of flood water in nature is a natural phenomenon. It takes place due to an increased quantity of water in a given area within a relatively short period of time. In hydrotechnics and, generally, in construction, determination of flood waters with a certain return period is one of the key elements in design of such facilities.

Due to climate changes, but also due to anthropogenic activities in the catchment areas, conditions for formation of flood waves are changing. Therefore, redefinition of flood waters at already constructed hydrotechnical objects is necessary from the aspect of timely and precise forecasting of occurrence of flood waters and taking certain activities in order to prevent unwanted consequences.

In this paper, the subject of analysis is the catchment area of the Kalimanci dam and redefinition of flood waters.

The "Kalimanci" dam was built in 1969. It is located in the eastern part of the Republic of Macedonia, on "Bregalnica" river, northeast of the city of "Kochani", at 23 km from "Makedonska Kamenica". To the North, where "Kamenicka Reka" river empties into the water mirror of the "Kalimanci" reservoir, there starts the mining town of "Makedonska Kamenica". To the south, below the reservoir body, the hydroelectric power plant "Kalimanci" and "Istibanje" settlement were built. To the East, there stretches the "Kalimanci" field. Locations of "Kalimanci" dam is shown on Figure 1.



Figure 1 Locations of "Kalimanci" dam (Source: Google Earth)

The "Kalimanci" was built as an earthfill dam of a combined type constructed of a rock-shale fill, while its middle part is composed of a thin waterproof clay core and upstream and downstream filters. The height of the dam measured from the river terrace is 85 m, while its design height is 95 m. The dam length is 232 m, while the dam width is 10 m,

Figure 2. With the construction of the dam, the artificial "Kalimanci" lake was formed to accumulate the waters of "Bregalnica" and "Kamenicka Reka" rivers. The volume of the reservoir up to the overflow (515 mNV) is 115.6 million m³, of which 113.8 million m³ represents effective space.

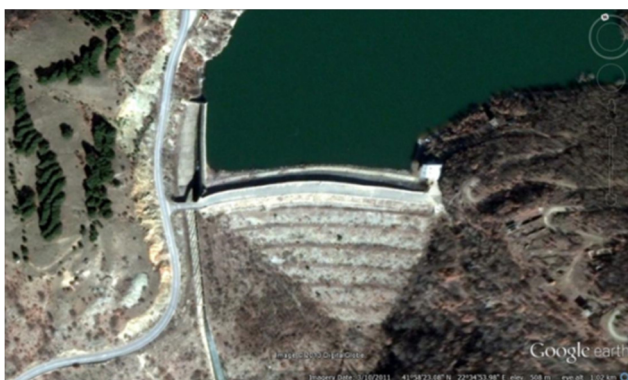


Figure2 "Kalimanci" Dam (Source: Google Earth)

The purpose of the "Kalimanci" Dam is to accumulate water for irrigation of agricultural land with total area of 28 000 ha from "Kocansko Pole", "Vinichko Pole", "Shtipsko Pole" and "Ovce Pole", to produce electricity and flood protection.

2. Physical-geographical characteristics of the watershed

The determination of the physical geometric characteristics of the watershed was done by use of DTM (Digital Terrain Model) (30x30 m) and application of SWAT (Soil & Water Assessment Tool), hydrological analysis module from GIS (Geographic Information Software). To define the geometric characteristics of the watershed from the "Bregalnica" river to the "Kalimanci" dam, using the ArcSwat program, the DEM base of the Republic of Macedonia was used. Plotting of the watershed and definition of the size of the drainage basin on the "Bregalnica" river was done for the profile of the Kalimanci dam, with coordinates xy (631 529; 4648885). Output results through graph display of the watershed from "Bregalnica" river to the dam and separately for the "Kamenichka Reka" river are given in Figure 3 and Figure 4, respectively. The geometric characteristics are shown in Table 1.

Table 1 The geometric characteristics of the watershed upstream the dam, watershed of "Bregalnica" and "Kamenicka reka" river

Watershed	A [km ²]	H _{min} [mNV]	H _{max} [mNV]	dH	L _t [m]	L _s [m]	S _t [%]	S _s [%]
upstream the dam	1123	498	860	362	85,6	61,9	4,23	5,85
"Bregalnica" river	1007,3	498	860	362	62,6	41,8	5,78	7,42
"Kamenicka reka" river	115,7	506	1200	866	23	17	3,76	4,85

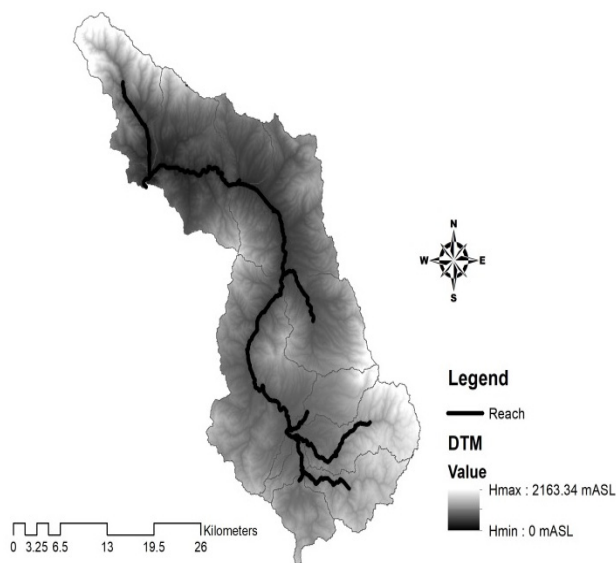


Figure 3 Watershed of the "Bregalnica" river



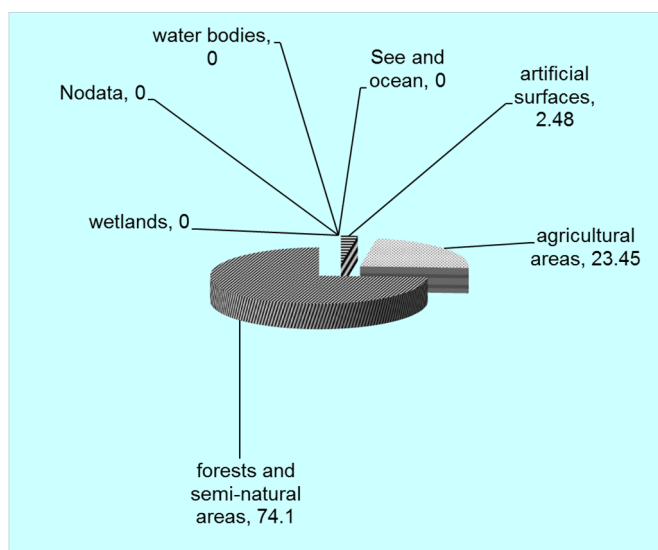
Figure 4 Watershed of the "Kamenicka reka" river

3 Use Land

Analysis of land use and representation of certain classes for the purpose of hydrological modeling of the drainage basin of the "Bregalnica" river, from its spring to the "Kalimanci" dam, was carried out by application of CORINE Layer Classification. The data were processed and interpreted using the GIS software modules, Table 2. The most common in the basin covering more than 832.18 km² (74.1%) are the so called forests and semi-natural areas. Out of these, 799.04 km² (71.2%) are under forests. The structure of the forests is dominated by coniferous, then broadleaf and small mixed forests. Grassland and grassland vegetation is present both in the transitional areas and in the higher parts of the watershed. In this group, the most present is the natural grass with approximately 33.05 km² (2.9%) of the total surface of the basin and there is a negligible presence of rare vegetation of 0.1 km² (0.01%). The agricultural areas with 263.35 km² (23.45%) are fairly present in the basin and cover pastures of 120.04 km² and dominant mixed agricultural areas, i.e., an agricultural area with natural vegetation of 143.31 km² (12.80%). Within the basin, the so-called artificial surfaces (urban areas, industrial, commercial and transport facilities, then mines, landfills and construction sites) account for 27.47 km² (2.45%) of the total surface of the basin. Urban areas are represented by 5.52 km² (0.49%), industrial and commercial buildings cover 0.84 km² and the most dominant are mines covering 21.11 km² (1.88%). The scale of the network used (250x250 m) did not allow exact determination of the individual categories of the third level, such as roads, railways and alike that exist in the basin. For these reasons, no wetlands, muddy areas and water bodies were detected. Therefore, this analysis of presence of individual categories of land use should be taken only as indicative and for the needs of the hydrological analysis of the watershed. Figure 4 shows the sectoral presentation of presence of different categories of land.

Table 2 Category of Use land

Classe 1	Classe 2	second level		first level	
		[km ²]	[%]	[km ²]	[%]
artificial surfaces	urban areas	5.52	0.49	27.47	2.48
	industrial, commercial and transport units	0.84	0.07		
	mine, dump and construction sites	21.11	1.88		
	artificial, non-agricultural vegetated areas	0.00	0.00		
agricultural areas	arable land	0.00	0.00	263.35	23.45
	permanent crops	0.00	0.00		
	pastures	120.04	10.7		
	heterogeneous agricultural areas	143.31	12.8		
forests and semi-natural areas	forests	799.04	71.2	832.18	74.10
	scrub and/or herbaceous vegetation associations	33.05	2.9		
	open spaces with little or no vegetation	0.09	0.01		
wetlands	inland wetlands	0.00	0.00	0.00	0.00
	maritime wetlands	0.00	0.00		
water bodies	inland waters	0.00	0.00	0.00	0.00
	marine waters	0.00	0.00		
Nodata	Nodata	0.00	0.00	0.00	0.00
see and ocean	see and ocean	0.00	0.00	0.00	0.00
		1123.00	100	1123.00	100

**Figure 5** Categories of use land, sectoral presentation

4. Redefining flood waters

In order to determine the flood wave from the basin upstream the dam, the flood waters from the "Bregalnica" river and particularly the flood waters from the "Kamenichka Reka" river were analyzed since these are the two main rivers that flow directly into the reservoir.

To define the flood waters from "Bregalnica" river, a series of maximum annual flows at the measuring point of the dam profile was used. This series (1961-2005) was obtained

in correlation with the series of maximum annual flows measured at the "Ochi Pale" measurement profile (source: UHMR).

A series of maximum annual flows (1986-2005) measured at the measuring profile in "Kamenica" was used to determine the flood wave from "Kamenichka Reka" river. The series of maximum annual flows of "Bregalnica" river and "Kamenichka Reka" river are shown in the form of hydrograms in Fig. 6 and 7.

All these data were statistically processed and the main statistic parameters (number of measured data (N), characteristic values of the sequence: average discharge (Q_{sr}), minimum (Q_{min}) and maximum discharge (Q_{max}), mean square deviation (σ), variation coefficient (C_v) and asymmetry coefficient (C_s)) were computed, Table 2. Statistical methods were used to determine the flood waters using three theoretical distribution functions (Gumbel, Pearson III-type and Log-Normal distribution[2], [3], [5])). To determine which distribution best adapts to the empirical probability of the array of measured data, the results obtained were tested. For this purpose, the (χ^2) test was applied. For the "Bregalnica" river, the best adapted was the Pearson III type distribution, while for the "Kamenichka Reka" river, the Gumbel distribution was best fitted. Lines of distribution of flood waters for "Bregalnica" river are shown in Figur 8 and lines of distribution of flood waters for "Kamenicka reka" river are shown in Figur 9. Hydrographs of a flood water with a different return period for "Bregalnica" river are shown in Figur 10 and hydrographs of a flood water with a different return period for "Kamenicka reka" river are shown in Figure 11.

Table 2 - - Statistic parametars for seria of data on maximum annual flows "Bregalnica" river and "Kamenicka Reka" river

discharge	N	Q_{sr}	Q_{min}	Q_{max}	σ	C_v	C_s
"Bregalnica" river	45	124,66	16,68	357,37	85,29	0,68	0,83
"Kamenicka reka" river	23	7,82	1,34	19,2	4,03	0,515	0,861

Table 3 – Flood waters calculate according to the three distribution functions for the "Bregalnica" river and "Kamenicka Reka"river

Return period T [years]	Probability p [%]	Bregalnica river			Kamenicka Reka river		
		Gumbel distribution	Log-Normal distribution	Pisrson-III-type distribution	Gumbel distribution	Log-Normal distribution	Pisrson-III-type distribution
10000	0,01	698,96	1834,87	710,58	34,96	57,64	31,84
1000	0,1	545,83	1119,63	558,77	27,72	40,32	26,08
100	1	392,29	606,23	403,55	20,47	25,87	19,99
20	5	283,85	352,65	290,12	15,34	17,48	15,40
5	20	186,06	184,96	185,21	10,72	10,96	10,88
2	50	110,69	94,71	105,90	7,16	6,75	7,17

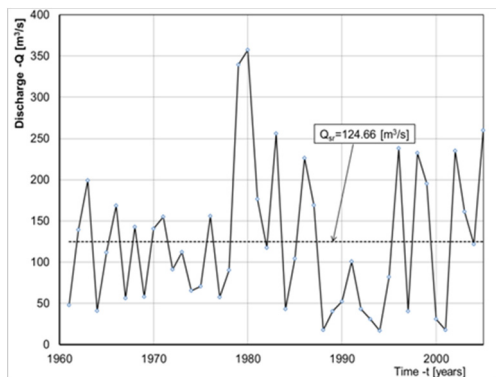


Figure 6 Hydrogram on maximum annual flows in "Bregalnica" river (1961-2005)

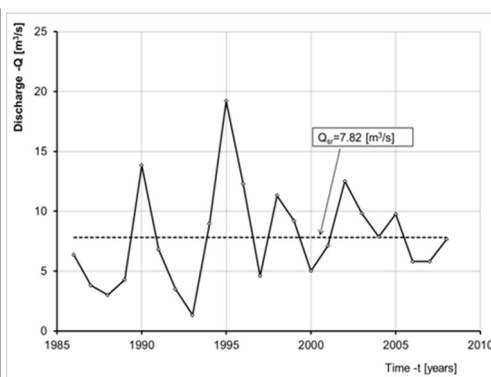


Figure 7 Hydrogram on maximum annual flows in "Kamenicka Reka" river (1986-2005)

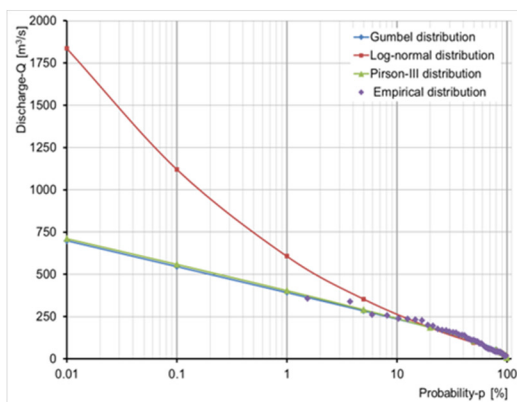


Figure 9 Lines of distribution on flood waters in the "Bregalnica" river

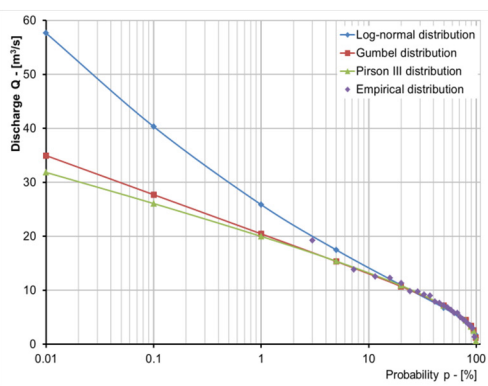


Figure 10 Lines of distribution on flood waters in the "Kamenicka reka" river

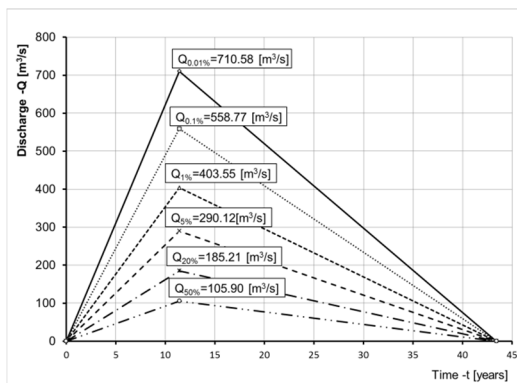


Figure 11 Hydrographs of a flood water with a different return period for "Bregalnica" river

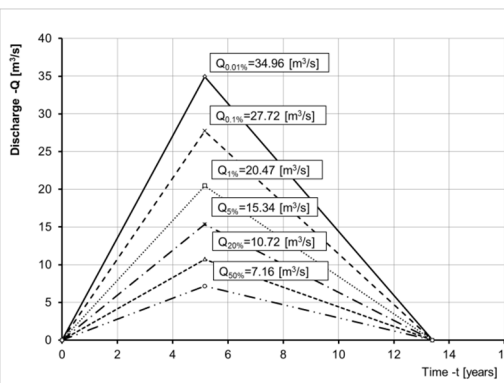


Figure 12 Hydrographs of a flood water with a different return period for "Kamenicka reka" river

5. Maximum Probable Flood (MPF)

A widely accepted practice in hydro-engineering was proportioning of spillways of large dams (dams higher than 15 m) by consideration of flood waters with a probability of occurrence of 0.01% (i.e., a return period of $T = 10000$ years) for bulk dams and 0.1 % ($T = 1000$ years) for concrete dams. More recently, this rule has been accepted and applied in our country and has been subjected to an extensive revision. Namely, from the statistics made by ICOLD (International Commission of Large Dams) regarding collapsed dams and reasons for their collapse, one can see that the most common reason for failure of large dams (even for 34% of the total registered collapsed large dams) is overflowing of the dam crown, which is mainly due to the low capacity and the insufficient throughput of the evacuation facilities (overpass). Due to this, in recent times and worldwide, an obligation has been introduced to design the spillway facilities of all major dams and dams of greater significance by consideration of the Maximum Probable Flood (MPF). This obligation is not only consistently observed in a large number of countries, but already built dams are subjected to revision, as well.

According to the U.S. Corps of Engineers, the Maximum Probable Flood (MPF) is the flood wave that can be expected as a consequence of the most unfavorable combination of critical meteorological and hydrological conditions in the analyzed basin. A dominant role in the formation of the MPF have the meteorological conditions combined with the hydrological state of the watershed (the previous humidity conditions of the soil that depend on the geological structure of the terrain). The physical geographical characteristics of the considered basin are practically unchangeable and do not have a dominant role in the formation of the MPF. Deterministic or parametric methods are used to determine the MPF. Used as an input in these methods are the probable maximum 24-hour precipitations (PMP₂₄-Maximum Probable Precipitation) at the geographical point of the basin where the measurement is carried out and at the average height of the layer of the probable maximum 24 –hour precipitations (PMP_{24, A}) in the basin.

Due to incomplete data and substrates (air humidity, wind, map of PMP), an alternative way of determining the probable maximum precipitation or a statistical empirical method prepared by the US meteorologist David Hershfield, [1], will be used to determine the maximum flood wave (MPF) for the "Kalimanci" dam basin. The procedure itself is simple, easy and fast and gives satisfactory results. This method used data in seria of maximum annual daily rainfall in the watershed for the period from 2005 to 2017 measured at the dam itself. The statistics for this seria (P_n) and the seria without the highest value (P_{n-1}) are shown in Table 4.

Table 4 - Statistical parametars for seria of data on maximum annual daily rainfall (2005-2017)

	N	P_{sr}	P_{min}	P_{max}	σ	C_v	C_s
P_n	13	40.45	25.1	55.2	8.57	0.21	0.23
P_{n-1}	12	39.22	25.1	54.0	7.54	0.19	0.13

To calculate the 24-hour maximum precipitations, the corrected values $P_{cor} = P_n \cdot f_1 \cdot f_2 = 43,33$ (mm/den) and $\sigma_{cor} = f_3 \cdot f_4 \cdot \sigma_n = 10.84$ are used, where: $f_1 = 1.04$, $f_2 = 1.03$, $f_3 = 1.1$, factors that depend on the length of the array, and $f_4 = 1.15$, the factor in function of the (σ_{n-1}/σ_n) relationship and the length of the array. $PMP = P_{cor} + k_{max} \cdot \sigma_{cor} = 203.05$ (mm/24h), where $k_{max} = 15$ is the generalized probability of

the maximization factor and depends on P_{cor} , [1]. Since precipitation values are read at fixed time intervals, every day at 7 a.m., the observed values represent 24-hour precipitation. PMP_{24} is obtained if PMP is increased by 13%, namely: $PMP_{24}=1.13PMP=237.89$ (mm/24h).

PMP_{24} represents precipitation at a point, but for a basin, it is corrected by a reduction factor that decreases with the increase of the catchment area, i.e., $f_6=f(A, t_k)$. For the basin upstream the Kalimanci dam covering an area of $A=1123$ km², with rain duration $t_k=8.22$ h [?], $f_6=0.755$, while: $PMP_{24,A}=f_6 \cdot PMP_{24}=179.6$ (mm/24h). The maximum probable flood waters (MPF) are calculated according to the empirical formula: $Q_{max}=MPF=(PMP_e \cdot A)/T_b=1458.87$ m³/s where: $P_e=(PMP_{24,A}-0.2d) / (PMP_{24,A} + 0.8d) = 101.51$ mm, d- humidity deficit, which is in function of CN, which, on the other hand, is in direct relation with the categories of land use within the basin. For the basin upstream the "Kalimanci" dam, it is $CN = 73$, [2]. $T_b = 43.41$ h.

6. Conclusions

Definition of flood waters with different return periods, early warning about their arrival, as well as undertaking activities in order to safely accept them and prevent adverse consequences, is extremely important for the security of the populated areas downstream the dams. For high quality analyses and calculations, it is necessary to have adequate hydrological data (data on measured flows at appropriate hydrological measuring stations, measured precipitation data on the entire drainage area, etc.). In order to provide these data, it is necessary to establish an effective monitoring network and to maintain, develop and improve it according to the recommendations of the World Meteorological Organization (WMO).

In this paper, using statistical and statistical-empirical methods, based on available data, the flood waters and the Maximum Probable Flood for the "Kalimanci" dam basin have been defined/redefined.

Using statistical data and based on data from measurements of flows, the flood waters with different return periods have been defined for "Bregalnica" river and "Kamenichka Reka" river up to the profile of the "Kalimanci" dam. From the conducted analyses, it can be concluded that the "Kalimanci" lake is dominantly influenced by the surface waters that come from the "Bregalnica" river basin in respect to the surface waters coming from the "Kamenichka Reka" river basin. The flood wave from the "Bregalnica" river, i.e., the maximum flood water from the "Bregalnica" river basin upstream the profile of "Kalimanci" dam arrives in the lake for 11.42 hours, while that from "Kamenichka" river arrives in the lake in 5.16 hours.

According to these analyses, the Maximum Probable Flood (MPF) is 1458,87 m³/s or almost twice the wave with a return period of 10,000 years (710,58 for the "Bregalnica" river basin and 34,96 m³/s for the "Kamenichka Reka" river basin).

For further analyses aimed at checking the capacity of the facilities within the frames of the Kalimanci dam regarding acceptance of flood waters and safety of the downstream populated places against flooding, the maximum probable flood waters are recommended to be used.

References:

- [1] Zelenhasic, E., Ruski, M.: Engineering Hydrology, Naucna knjiga, Belgrad, (1991)
- [2] Popovska, C., Gjesovska, V.: Hydrology-Theory with solved problems, Faculty of Civil Engineering, ISBN 978-608-4510-11-6, Skopje, (2012)
- [3] Prohaska, S., Hidrology - prvi deo, Faculty of Mining and Geology, Belgrad, (2003)
- [4] Climate and Hydrology of the Republic of Macedonia, Annual Reports. Hydrometeorological Service. Skopje, Macedonian, (1999)
- [5] Wilfried Brutsaert, Hydrology an Introduction, Cambrige University Press, (2005)
- [6] Energoproekt,. Main project for the dam Kalimanci, Beograd, (1962)
- [7] Hydrological-hydraulic analysis for determination of flood waters and flood wave through the reservoir, Lefkova, I., Master thesis, Faculty of Civil Engineering, Skopje, (2019)

Topic no. 8 - Geotechnical aspects of Hydraulic Engineering

EXPERIMENTAL AND NUMERICAL MODELLING OF RAINFALL-INDUCED SLOPE INSTABILITIES IN UNSATURATED SANDY SOIL

JOSIF JOSIFOVSKI ¹, BOJAN SUSINOV ², MAGDALENA TASEVSKA ³,

¹ Prof. PhD. Faculty of Civil Engineering – Skopje, “Ss Cyril and Methodius” University, Skopje, R. N. Macedonia, jjosifovski@gf.ukim.edu.mk

² Assist. MSc, Faculty of Civil Engineering – Skopje, “Ss Cyril and Methodius” University, Skopje, R. N. Macedonia, susinov@gf.ukim.edu.mk

³ BCh, Faculty of Civil Engineering – Skopje, “Ss Cyril and Methodius” University, Skopje, R. N. Macedonia, tasevska@yahoo.com

1. Abstract

The behaviour of natural or engineered slopes is controlled by the thermo-hydro-mechanical conditions and soil–atmosphere interaction. The consequences of the climate change regarding the slope stability are ever more present in different parts of the world. Therefore, most of the research on this topic nowadays is concentrated to determine the climate influence on the slope stability. They atmospheric perturbations are often manifested with short and intense rainfalls sometimes reaching even a value of monthly precipitation. The increasing rate, size and frequency of the slope instabilities in the past couple of years is becoming quite alarming, thus more decisive steps have to be made to define the risk.

Among the atmospheric perturbations beside the sharp temperature change, hence the intense rainfall is considered as a key factor which directly relates to soil sliding or erosion. The rainfall water partially infiltrates in the soil, thus changes the porewater pressure within a slope leading to an overall decrease of the available soil strength and suction with depth and, ultimately, to a progressive slope collapse.

This paper presents an analysis of ideal slope example subjected to heavy short duration rainfall. For this purpose, both physical and numerical model were employed. First, a small-scale physical model of unsaturated sandy slope was used to determine the rainfall infiltration rate into the slope and other hydraulic properties for which the slope was adequately instrumented with suction and water content sensors. The monitoring showed that the infiltrated water sharply increases the volumetric water content which generally reduces the strength and suction of the soil.

In terms of numerical modelling, a coupled hydro-mechanical analysis was performed to simulate the slope-atmospheric interaction. For the hydraulic part a van Genuchten model was assumed which requires definition the soil water retention curve and hydraulic conductivity function obtain from the laboratory and experimental testing, while for the mechanical part two different soil models were used a standard with Mohr Coulomb criteria and Basic Barcelona as advanced able to describe the unsaturated nature of the soil. The two-dimensional finite element stability has been evaluated for a slope inclination of 1:1 and 1:2. Moreover, different rainfall scenarios were examined with an objective to determine the influence of infiltration rate and duration of rainfall. It was proven that relatively short of few hours up to 12 hours rainfall with intensity of 10 to 30 mm/h have significant influence on the overall stability.

The prediction of future climate scenarios and forecasting of slope–atmosphere interaction processes are a challenging task. Nevertheless, the study results re-assure that the presented approach and models are able to re-evaluate the reliability and stability of the existing natural and engineered slopes on measured precipitations, because in future they will be more frequent and more instabilities could be expected.

Keywords: Unsaturated soil, Slope stability, Rainfall, Infiltration, Suction, Porewater pressure, Failure.

2. Introduction

The slope behaviour depends of many factors, such as: the lithological and morphological conditions, mechanical properties etc. In principle, beside the mechanical conditions the slope behaviour will be governed also by climate conditions, atmospheric perturbations. Among them the rainfall is seen as key factor which directly relates to soil sliding or erosion. Therefore, in the recent period the research is concentrated on definition of climate change influence. The climatic perturbations or so-called soil-atmospheric interaction is seen as deterministic factors in the slope stability in many regions around the world (Zhang et al. 2011). Montoya-Dominguez et al. (2016) studied the effect of rainfall infiltration on the hydraulic response and failure mechanisms of four sandy slope models with changing the initial water content, rainfall intensity and duration of rainfall. They found out how the change of water content or level of saturation reduces the soil strength. Moreover, the rainfall intensity and the filtration coefficient significantly influence the deformation processes. The rainfall-induced slope failure in unsaturated soil is mainly due to rainfall infiltration and loss in shear strength when soil suction decreases (Fourie et al. 1999, Fredlund & Rahardjo, 1993). Eckersley (1990), Shimoma et al. (2002) and Chaminda (2006) presented results of slope model tests, subjected to prescribed rainfall, and instrumented with pore pressure and moisture content sensors. They found that failure was initiated when the soil at the toe of the slope becomes fully saturated, and excess positive pore water pressure developed. Another influencing factor is surely the soil suction. Orense (2003) explained how soil suction is reduced when rainwater infiltrates through the soil profile.

In general, the slopes are controlled by soil–vegetation–atmosphere interaction, hence, porewater pressure changes within a slope related to variable meteorological settings which can lead to an overall decrease of the available soil strength with depth and, ultimately, to a slope collapse. Thus, soil degradation and deformation processes such as soil erosion, shrinkage–swelling, cracking and sliding can be induced (Figure 1).

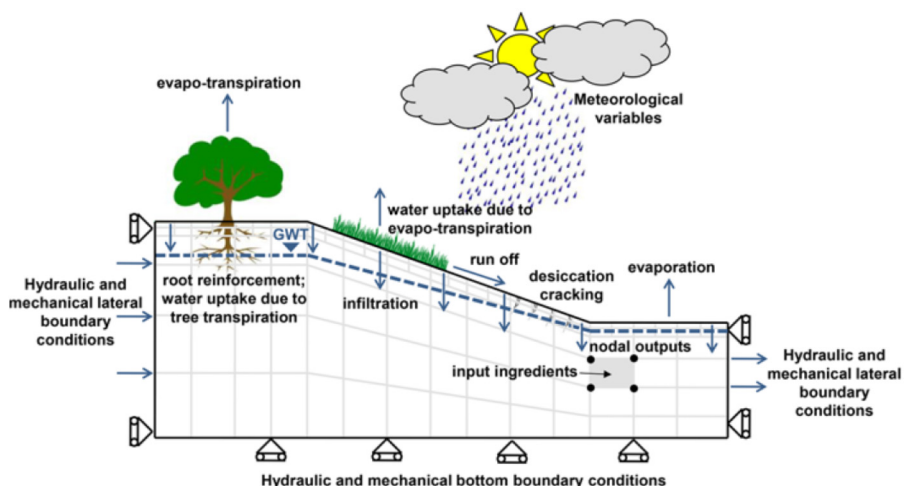


Figure 1. Schematic slope model and potential slope–vegetation–atmosphere interaction phenomena (Elia et al, 2017)

The modelling has shown that suction responses to rainfall vary on a number of different timescales (Casini et al, 2013). On shorter timescales (ranging from minutes to hours and days) heavy rainfall which was of primary interest in this study produced very interesting results. The rainfall infiltration effects in the literature (Cotecchia et al, 2013) are usually critical for shallow landslides, especially when real short durations triggering fast sliding shallow mechanisms.

Hence, the rainfall water infiltrates fast in the soil slope thus influences the ground water table and distribution of pore water pressure. In the areas where the upward flux (i.e. evaporation and evapotranspiration) exists, suction above phreatic level increases (and degree of saturation decreases) and the water level is lowered with time while in the case of downward flux (i.e. precipitation) suction decreases (and degree of saturation increases) and the water level rises with time.

In the case of zero net surface flux, the pore water pressure profile become in equilibrium at a hydrostatic condition (Figure 2).

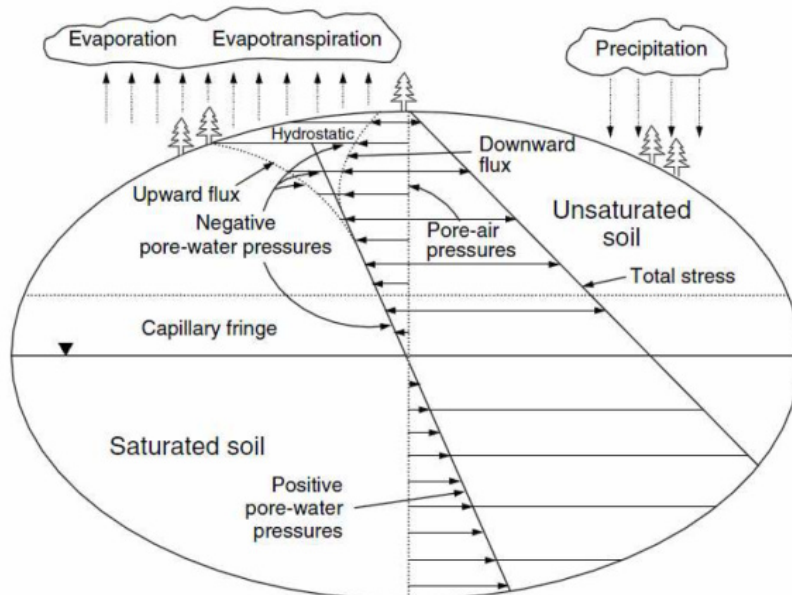


Figure 2. A visualization of soil mechanics showing the role of the surface flux boundary conditions (Fredlund, 1996)

3. Physical model

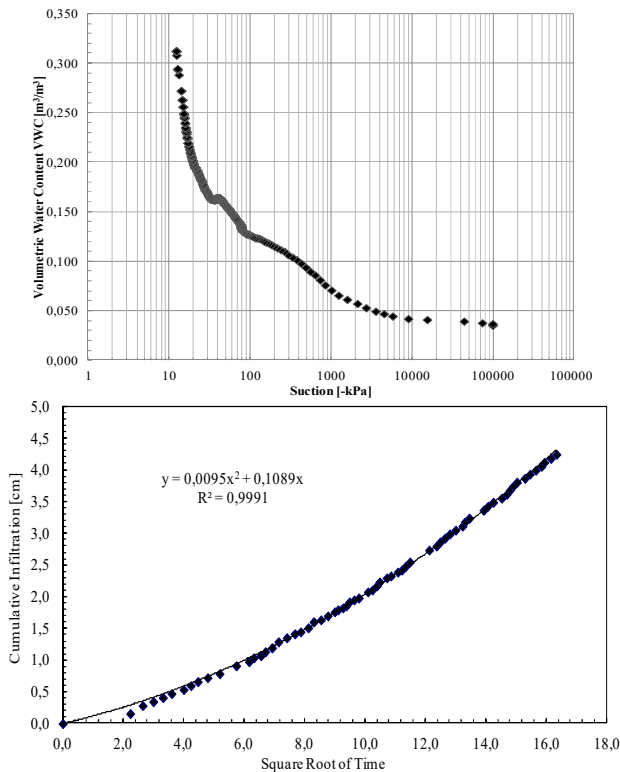
A small-scale physical model of 45 degrees slope was constructed from uniform fine sand material a by-product of the copper and flotation of a mine near Radovis, Macedonia. Originally the material was used for construction of the Topolnica tailing dam. A series of appropriate laboratory tests were carried out to define the mechanical as well as the hydraulic properties of the material. According them the following values were assumed for further analysis.

Table 1. Soil properties

Property	Value
Specific gravity G_s	2.72
Dry bulk density γ_d	15.5 kN / m ²
Optimum humidity ω	22.5%
Internal friction angle ϕ	33 °
Cohesion c	0 kPa
Compressibility modulus Mv 25-800 kPa	1459.3-16814.7 kPa
Hydraulic conductivity $k=$	0.0207 cm/s

The sieve analysis has produced a granulometric curve (Figure 2) with grain size distribution of the investigated soil. The material contains 82.5% sand and 17.5% silt which classify this soil as silty sand. The coefficient of uniformity $C_u=4.29$ and the coefficient of curvature $C_c=1.51$.

To define the hydraulic behaviour of the silty sand, the unsaturated hydraulic conductivity measured with Mini Disk Infiltrometer (Susinov & Josifovski, 2018). The obtained results are plotted as a function of volumetric water content and suction, see Figure 3a.



a)

b)

Figure. 3 Measured curves of (a) VWC versus Suction and (b) Cumulative infiltration versus Time

The suction sensors began to respond after the volumetric water content (VWC) reaches $0.038 \text{ m}^3/\text{m}^3$ decreasing sharply with the level of saturation. For this material realistic value should be in range between 10 and 100 kPa. Figure 3b presents the relationship between the cumulative infiltrations and time later used to determine the soil hydraulic conductivity through the method for dry soils proposed by (Zhang, 1997), hence a value of $k=0.0207\text{cm/s}$ is calculated.

After the material definition an experimental test was conducted on a small-scale physical model with slope inclination of 45 degrees. The dimensions of the model box were: 92cm in length, 48cm in height and 28cm, see Figure 4a.

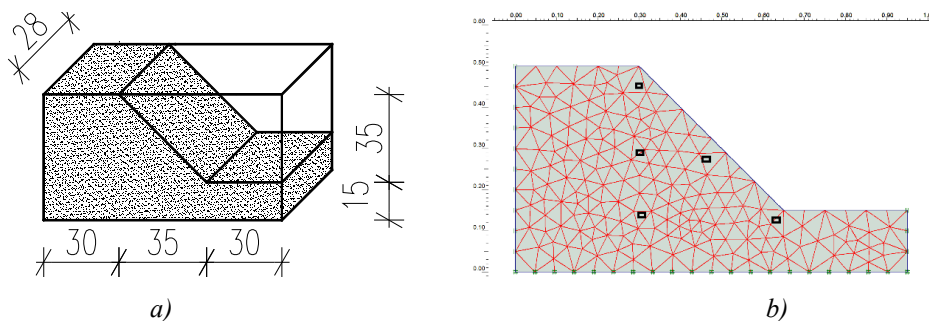


Figure. 4 Ideal slope example (a) Small-scale physical and (b) Finite element model

The material was confined in the transparent glass box where geotextile with few holes were used to drain excess water. A quadratic grid $5 \times 5 \text{ cm}$ helped to observe the water infiltration, saturation and deformation of the slope. The changes in soil moisture and suction during rainfall was monitored in real time through a system of four (I to IV) EC-5 and four (I to IV) MPS-6 sensors, respectively (Figure 4).

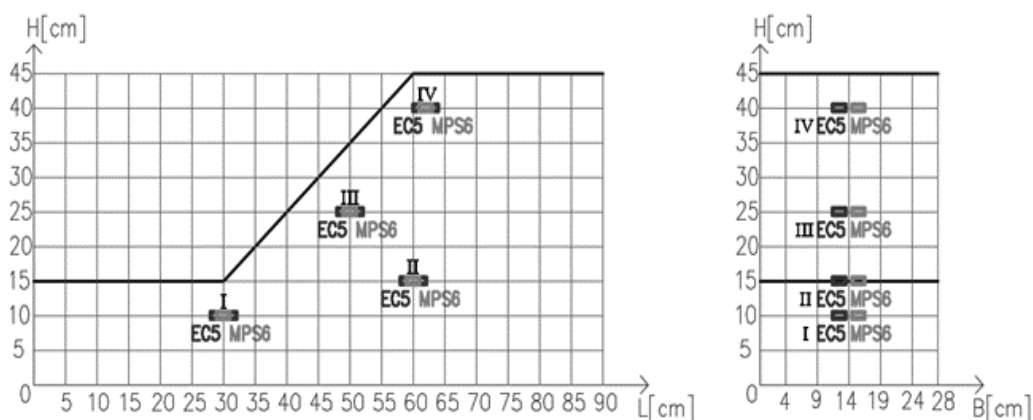


Figure. 5 Longitudinal and transverse views of the model, location of sensors

A rainfall intensity of 15 mm/h to 30 mm/h was simulated with sprinklers positioned above the model and controlled by pressure regulator. In Figure 6 the progress of the experiment is shown.

The monitored data of VWC and suction for rainfall intensity of 28mm/h with duration of 135 min. are presented in Figure 7a and b, respectively.

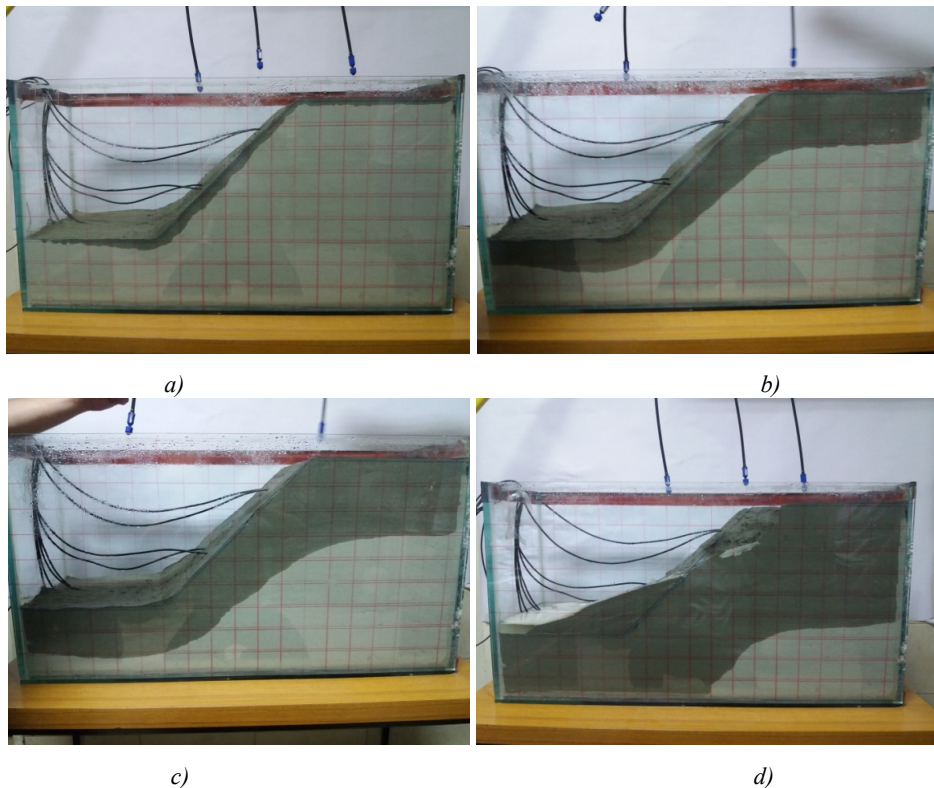


Figure. 1 Test progress: a) photo taken 5 minutes after rainfall starts, b) after 40 min., c) after 65 min. and d) after 135 min (end of rainfall)

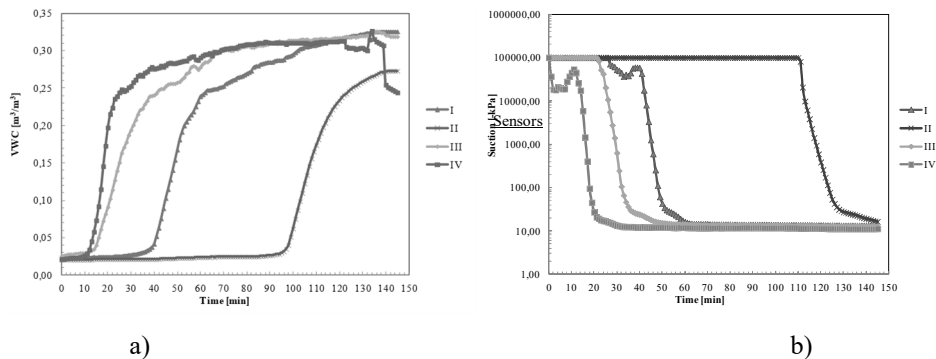


Figure. 2 a) Time dependence of volumetric water content and b) Changes in suction over time

The initial registered volumetric water content (Figure 7a) of the soil before the rain was around $0.025 \text{ m}^3/\text{m}^3$. Upon rainfall initiation, VWC sensors IV placed near the crest and III placed at the mid-height show water content indicating the rainfall infiltration and development of the wetting front. After 15 minutes in sensors III and IV the increase in VWC was sharp with up to ten times of the initial value. After approximately 60 minutes, VWC remains constant indicating saturation of the surface ground. The significant increase in VWC at sensor I begins after 40 minutes and continues until the end of the test but not with the same increment. The deepest placed sensor II begins to react after 95 minutes prolonged as a result of time necessary for saturation

In the same manner Figure 7b presents the suction changes with the time. The suction is affected when the infiltrated water reaches the sensor depth. After that point, the suction significantly decreases and reaches approximately 20 kPa after 20-30 minutes depending on sensor position. After 110 minutes as the rainfall continues, the slope surface reached nearly fully saturation and failure occurred at the slope crest i.e. the runoff water begins to down the slope surface and drains through the downstream holes. This causes concentrated surface flows which erode the slope surface, see Figure 8.

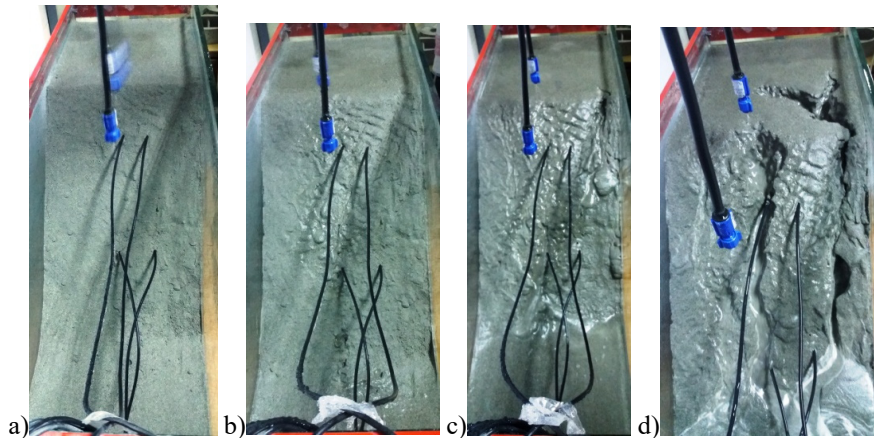


Figure. 3 Slope condition: a) after 30 min., b) after 100 min., c) after 120 min. and d) after 135 min (end of rainfall)

3. Numerical model

In terms of numerical modelling for calculation of partially saturated slope stability a wide range of approaches have been proposed in the literature (Elia et al, 2017). The more advanced approaches, although more rigorous, require input data such as the soil water retention curve and the hydraulic conductivity function, which in some cases are difficult to be determined. To analyse the mechanical behaviour of saturated or partially saturated soils by means of numerical methods in proper manner, it is necessary to take into account both deformation and groundwater flow. For time dependent behaviour, this leads to mixed equations of displacement and pore pressure, called coupled hydro-mechanical approach, which have to be solved simultaneously.

In the present study the task has been to employ a constitutive hydraulic and mechanical model which will be able properly to evaluate the effects of rainfall and water infiltration on slope stability. The shear strength of the unsaturated soil has been examined based on Bishop's effective stress concept considering suction. The Van Genuchten hydraulic model was used in the analysis. Also, the shear strength reduction technique was employed to evaluate the factor of safety (FOS). As the ultimate limit states were of primary interest, but additionally the comparison between the elastoplastic Mohr Coulomb (MC) and more advanced Basic Barcelona model (BBM) constitutive model was made. In contrast, MC model which looks for definition of only 5 parameters the BBM takes 18 usually defined by laboratory or experimental tests. Therefore, this study has been devised into two parts. The first one deals with the calibration the BBM after

the MC model parameters on relatively simple benchmark example of slope inclined by angle of 45 degrees, see experimental model (Figure 4). In the second step an ideal slope of Hamdhan & Schweiger (2011) is used as benchmark example, thus comparison of BBM with much simpler MC model was made. In particular, stability of slope 10 m and 20 m height with inclination of 1:1 and 1:2 was analysed. The two-dimensional finite element model used is presented in Figure 10.

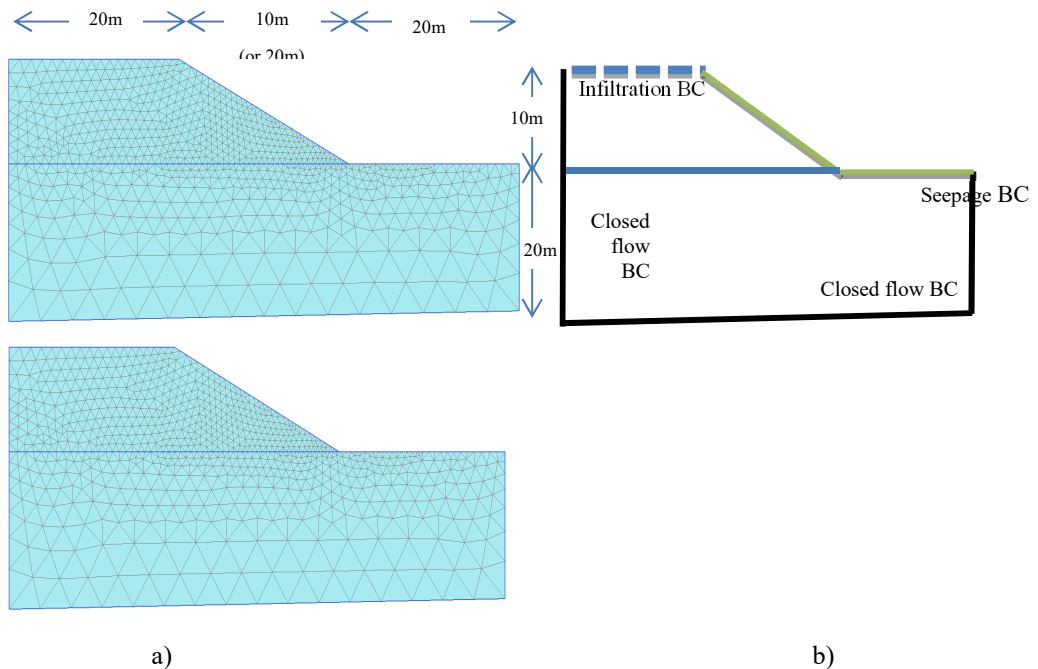


Figure. 10 (a) Geometry and finite element mesh of the slope and (b)Hydraulic boundary conditions of the model

A two-sensor system, one for suction and one for water volumetric weight (VWC) were used on a specimen of the silty sand material to directly measure the relationship between these two parameters, in order to determine the so-called Soil water retention curve (SWRC) only in continuous wetting, see Figure 11.

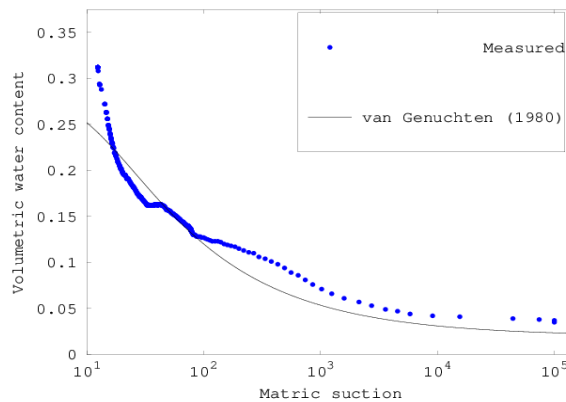


Figure. 11 Soil water retention curve for definition of the Van Genuchten model

The parameters of the Van Genuchten hydraulic Model are determined by fitting of the measured SWRC curve, see in Table 2.

Table 2. Hydraulic data of Van Genuchten model obtained from SWRC fitting

Parameter	θ_s	θ_r	α	n	R^2
Sand	0.297	0.0198	0.0806	1.480	0.854

To implement an advance material model such as BBM in Plaxis requires application of a user-defined soil model (USDMM) with six state variables: Pre-consolidation pressure of the saturated soil (P_o); Actual suction value (S), Actual degree of saturation (S_r), Pre-consolidation pressure of Unsaturated soil (P_c); Tensile strength due to suction (p_t) and Value of yield function (F_{result}). Those 6 state parameters will be determined in different time dependent steps following on the 18 model parameters defined in Tab. 3.

Table 3. Soil Parameters for Barcelona Basic Model

Parameter	Description	Symbol	Unit	Value
Program name(1)	Poisson ratio	μ	-	0,3
Program name(2)	Slope of the unload/reload line of saturated soil	κ	-	7,7E-3
Program name(3)	Slope of the normal compression line of saturated soil	λ_o	-	0,075
Program name(4)	Elastic stiffness due to suction	κ_s	-	2,1
Program name(5)	Parameter to control the tensile strength due to suction	K	-	0
Program name(6)	Slope of the Critical state line	M	-	1,2
Program name(7)	Friction angle at CS	$cs\phi$	degrees	25
Program name(8)	Initial void ratio	e_o	-	1
Program name(9)	Pre-consolidation pressure of saturated soil	P_o	[kPa]	200
Program name(10)	Reference mean stress	P_r	[kPa]	100
Program name(11)	Parameter to control infinite suction	R	-	0,25
Program name(12)	Parameter to control soil stiffness with suction	β	[kPa-1]	20
Program name(13)	Van Genuchten Parameter	a	[kPa]	14,5
Program name(14)	Van Genuchten Parameter	B	-	2,68
Program name(15)	Van Genuchten Parameter	C	-	0,5
Program name(16)	Parameter of non-associated flow rule	α_g	-	0,3
Program name(17)	Coefficient of earth pressure at rest	K_o	-	0,577
Program name(18)	Overconsolidation ratio	OCR	-	1

All values were chosen accordingly to the performed laboratory tests and recommendations by Galavi (2010) and Scientific Manuel (Plaxis 2D, 2012). The initial ground water level was assumed as horizontal at level of the toe of the slope. A rainfall with different intensity ranging between 10 and 30 mm/h was applied for a period of few to 12 hours. All other, left, bottom and right boundaries were assumed as no flow or impervious boundaries, see Figure 10b.

The results of the suction, relative permeability, excess pore and total displacement after the 12h of rainfall event presented in Figure 11, respectively.

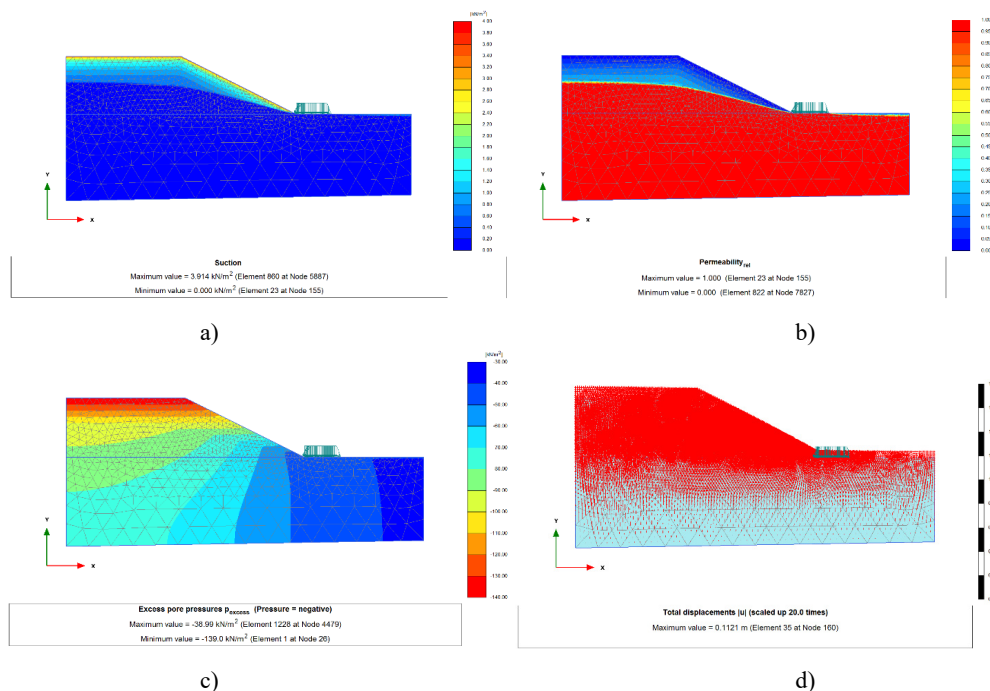


Figure. 11 BBM results: (a) Suction, (b) Relative permeability, (c) Excess pore pressure and (d) Total displacements (arrows)

The suction profile has significantly change when compared to the initial, hence the saturation level and zero suction line is raised 5m to 6m above the stationary GWL. This effect is depicted in the diagram of relative permeability and degree of saturation. To the initial active pore pressure an excess pore pressure (negative) is added with highest concentration at the top of the profile (surface) from where the water infiltration the slope. Finally, the VWC increase linearly above ground water level is reducing the soil strength and suction by adding excess pore water pressure until the ground surface exhibits an upward displacement (sliding) of around 0.11m. In general, the infiltrated rainfall water in different timescales has determining effects on the slope stability. In the presented results the FOS is practically one.

4. Conclusion

The influence of climate change on natural and engineered slope stability can be significant. The rate, size and frequency of the slope instabilities although difficult can be predict. On the other hand, many of them in the past couple of years are seen as a direct consequence of climate change and extreme rainfall. This fact questions the need for re-evolution of the existing risk land sliding maps based on recent atmospheric perturbations, temperatures and precipitations.

This paper presents an analysis of unsaturated stability of ideal slope using both physical and numerical model. The intense and short duration rainfall through the infiltrated water can trigger shallow sliding mechanisms, thus the main interest of this study its effects on the stability. Among the parameters analysed are the infiltration rate, water content,

suction and strength of the slopes. In particular, the research relates to hydro-mechanical coupling processes in soils, nowadays used as approach which can precisely account of climate effects in slope stability and as serviceability analyses. However, given their mathematical complexity and the in-depth knowledge of soil constitutive behaviour they are seldom used in practice.

In the first stage, a small-scale physical model was constructed to evaluate the effects of the extreme rainfall. Through this model a hydro-mechanical soil behaviour was studied by measuring of volumetric water content and suction during water infiltration at different locations. Through the experiment the slope was subjected to 28 mm/h rainfall intensity in duration of 135 min. The results had confirmed that the water starts to infiltrate very fast increasing the volumetric water content and pore water pressure from the top to bottom of the model. This causes reduction of the shear strength and suction which after saturation of the lower zone starts to deform and slide. Moreover, at the final stages a concentrated surface flows erode the slope surface and form gullies.

In the second stage, the experimental results were used to calibrate the numerical model. In the study a coupled hydro-mechanical analysis was used to describe the influence of the rainfall intensity, duration, initial water content and slope angle on the stability. A two-dimensional finite element stability has been evaluated for a slope inclination of 1:1 and 1:2 for different rainfall intensity and duration. It was proven that even relatively short of few hours up to 12 hours rainfall with intensity of 10 to 30 mm/h can have significant influence on the overall (global) stability. They were able precisely to simulate a timeline of slope behaviour in good agreement with the results of the physical model. Other modelling aspects of -soil-vegetation-atmospheric interaction, such as: influence of cracks and fissures, root water uptake were not considered, thus there are still but a few improvements in the model.

Finally, it can be concluded that it is possible to predict the unsaturated slope behaviour during rainfall. Obviously, the even short intense rainfall through infiltration and change of pore pressure and suction can trigger shallow slope instabilities and erosion. The study results re-assure that the presented approach and models are able to re-evaluate the reliability and stability of the existing natural and engineered slopes on recently measured precipitations, because in future they will be more frequent and more instabilities could be expected.

References

- [1] Vahid Galavi, Internal report: Groundwater flow, fully coupled flow deformation and undrained analysis in Plaxis 2d and 3D, 2010.
- [2] Gaetano Elia et al. (2017) Numerical modelling of slope–vegetation–atmosphere interaction: an overview, *Quarterly Journal of Engineering Geology and Hydrogeology* (2017),50(3):249
- [3] Indra Noer Hamdhan and Helmut F. Schweiger (2011) Slope Stability Analysis of Unsaturated Soil with Fully Coupled Flow-Deformation Analysis, Peer-reviewed IAMG 2011 publication (doi:10.5242/iamg.2011.0063)
- [4] Ayman A. Abed, Pieter A. Vermeer: Numerical Simulation of Unsaturated Soil Behaviour, First Euro Mediterranean Conference on Advances in Geomaterials and Structures – Hammamet
- [5] L. Nguyen Tuan, T. Schanz, M. Datcheva: Landslide Hazard: A Coupled Hydro-Mechanical

- Analysis With Variation Of Suction And Soil Stiffness During Wetting Process - Ma River Case Study
- [6] Amin Askarinejad: Failure mechanisms in unsaturated silty sand slopes triggered by rainfall, diss. Eth no. 21423, 2013.
- [7] Cotecchia, F., Pedone, G., Bottiglieri, O., Santaloia, F. & Vitone, C. 2014. Slope-atmosphere interaction in a tectonized clayey slope: a case study. *Italian Geotechnical Journal*, 1, 34–61. [8] Francesca Casini, Victor Serri, and Sarah M. Springman: Hydromechanical behaviour of a silty sand from a steep slope triggered by artificial rainfall: from unsaturated to saturated conditions, *Can. Geotech. J.* **50**: 28–40 (2013) [dx.doi.org/10.1139/cgj-2012-0095](https://doi.org/10.1139/cgj-2012-0095)
- [8] Amin Askarinejad, Francesca Casini, Patrick Bischof, Alexander Beck, Sarah M. Springman: Rainfall induced instabilities in a silty sand slope: a case history in northern Switzerland, Institute for Geotechnical Engineering, Swiss Federal Institute of Technology, ETH Zurich
- [9] Josifovski, J. & Lenart, S. (2016) Some experience in numerical modeling of unsaturated slope instabilities
- [10] Josifovski, J., Susinov, B. & Lenart, S. (2017) Unsaturated analyzes of extreme rainfall influence on the landslide stability, WMHE 2017 15th International Symposium on Water Management and Hydraulic Engineering
- [11] Susinov, B. & Josifovski, J. (2018) Investigation of the hydro-mechanical properties of silty sand material from Topolnica tailings dam, XVI Danube - European Conference on Geotechnical Engineering, 07-09 June 2018, Skopje, R. Macedonia, Paper No. 099
- [12] Susinov, B. & Josifovski, J. (2018) Investigation of the hydro-mechanical properties of silty sand material from Topolnica tailings dam
- [13] Chaminda, G. P. K. (2006) Real time prediction of rain-induced embankment by minimum measurements with back-analysis for SWCC parameters. University of Tokyo, Japan.
- [14] Fourie, A. B., Rowe, D. & Blight, G. E. (1999) The effect of infiltration on the stability of the slopes of a dry ash dump, *Geotechnique*. Vol 49, No. 1, 1-13.
- [15] Fredlund, D. G. & Raharjo, H. (1993) *Soil Mechanics for Unsaturated Soils*. Wiley, New York, USA.
- [16] Green, W. H. & Ampt, C. A. (1911) Studies on soil physics: flow of air and water through soils, *Journal of Agricultural Science*, No. 4, 1-24.
- [17] Mein, R. G. & Larson, C. L. (1973) Modelling infiltration during a steady rain, *Water Resources Research*, Vol 9, No. 2, 384-394.
- [18] Montoya-Domínguez, J. D., García-Aristizábal, E. F., & Vega-Posada, C. A. (2016) Effect of rainfall infiltration on the hydraulic response and failure mechanisms of sandy slope models, *Facultad de Ingeniería*, Vol 25, No. 43, 97-109.
- [19] Shimoma, S., Orense, R. P., Honda, T., Maeda, K. & Towhata, I. (2002) Model tests on slope failures caused by heavy rainfall, *Proc. Interpraevent 2002 in the Pacific Rim: Protection of Habitat against Floods, Debris Flows and Avalanches*, Vol 2, 547-557.
- [20] Zhang, L. L., Zhang, J., Zhang, L. M. & Tang, W. H. (2011) Stability analysis of rainfall-induced slope failure: a review, *Proc. of the Institution of Civil Engineers, Geotechnical Engineering*. Vol. 164, Issue GE5, 299-312.

COMPARISON OF CALCULATED AND MEASURED FILTRATION RATES

JURAJ ŠKVARKA ¹, EMÍLIA BEDNÁROVÁ ²

¹ Faculty of Civil Engineering STU in Bratislava, Slovakia, juraj.skvarka@stuba.sk

² Faculty of Civil Engineering STU in Bratislava, Slovakia, emilia.bednarova@stuba.sk

1. Abstract

Quality and reliability of the data about hydraulic structures play an important role in their safety of their components. The paper focuses on the hydraulic structure located on the Hron River, which consists of a weir, a small hydropower plant and systems of dykes. Later, additional anti-seepage measures had to be built, seepage canal and cut-off wall, to reduce excessive seepage from the reservoir. Groundwater and seepage water level are regularly monitored in adjacent observation wells. In addition to regular measurements, special measurements of filtration rates were carried out during the construction and after putting the hydraulic structure into permanent operation. For the measurement of filtration rates, an indicator method was used based on principle of monitoring the vertical movement of water in a borehole. After the construction of the anti-seepage measures, higher values of filtration rates were observed in the well T-4, which reached given limit value. Therefore, a characteristic cross section, which goes through T-4, was selected for detailed FEM analysis. We used Geostudio 2018 - SEEP / W, which is a finite element software suited for modelling groundwater flow in porous media. Input material characteristics were obtained from available data - coefficients of filtration determined mainly from grain size curve analyses. For that reason, several alternatives of real input parameters have been considered in the numerical model in order to model actual conditions when filtration rate measurements were carried out as accurately as possible. The paper deals with the comparison of results of measured and calculated values of filtration rates and also, we discuss reasons of occurred deviations between measurements and calculations and their possible interpretation.

Keywords: coefficient of permeability, filtration rate, dyke, subsoil, drainage coefficient of borehole

2. Introduction

The safety of hydraulic structures and their components are mainly determined by the quality and reliability of the data of the hydraulic structure and the natural environment. It is possible to optimize their design by using numerical modeling - to predict their behavior under different conditions and under different load conditions, thus to solve their interaction with the natural environment. Also, numerical modeling should be used if the hydraulic structure is already in operation, e.g. to determine the causes of some anomalous phenomena that may occur during its operation, or to verify the assumptions

that were available during the design of the hydraulic structure. The paper deals with the influence of the hydroelectric power plant, built on the Hron River, on the groundwater regime in the affected environment. We chose this hydraulic structure due to its problems with seepage through the dyke subsoil which appeared during the verification operation. We used Geostudio 2016 [1] software to solve the problem in the form of a parametric study. The model of the subsoil was constructed on the basis of data, acquired from geological surveys and available project documentation. We analyzed the impact of the hydraulic structure on groundwater regime in the adjacent environment, provided: without anti-seepage measures (so-called original state), with drainage channel and channel along with cut-off wall of various depths. Attention is focused on comparison of measured values of filtration rates in observation well with computed filtration rates using the numerical model.

3. Methods

3.1 Geological composition of the examined area

The geological composition of the area was investigated as part of the exploratory works prior to the hydraulic structure construction and also during the verification operation [2]. The depth of the exploratory wells ranged from approximately 10 up to 22 m below ground level (b.g.l.) and from taken soil samples were examined their geotechnical parameters. Coefficients of permeability of individual layers were determined by empirical formulas. The cover layer consists of loamy-clay soil materials (F6, F8) with the thickness of approximately 20 cm. However, in the vicinity of the dyke system, this layer is not present. Respectively, it was removed during construction and thus it was not considered in the model. The dyke body is made of gravel with trace of fines (G-F) or silty gravel (GM). The subsoil of the dykes is formed by a layer of gravel with trace of fines (G-F) and poorly graded gravel (GP) with locally occurring sandy soils S3 and S5 to a depth of about 9 up to 12 m b.g.l. Results of pumping tests for this layer were also included in the survey. Recommended coefficient of permeability for gravel sediments is $2.3 \cdot 10^{-4} \text{ m}\cdot\text{s}^{-1}$. Under this layer there is cemented and very dense layer with the thickness about 2.0 m. The drill core from this layer was formed by cemented, dry cylinders in the center. The surface of the cylinders was wet, which may indicate their possible water-bearing, but the used drilling technology could not exclude groundwater inflows from higher levels. Under this layer, there is a further aquiferous layer of similar nature as the layer above the cemented layer, possibly with clay pods. Under this watered layer there is again cemented and very dense layer from the depth about 20-21 m b.g.l.

3.2 Methodology of measurement

To measure groundwater flow rates in the area of interest, we used a single-borehole indicator method on the principle of monitoring the vertical movement of water in the borehole. Permeability coefficients are calculated from Darcy's law using the hydraulic gradient values from the surrounding. For vertical water flow in boreholes an immersion probe is used with pneumatic hydraulic jetting dosage equipment and two conductivity meters fitted above and below the jetting place at a distance of 0.5 m. The immersion probe is connected to the computer transducer with a cable and then to a portable computer. Concentration curves can be seen directly on the computer screen as well as

flow direction and time for the following calculations. Scheme of the measuring device is depicted on the following figure (Fig. 1).

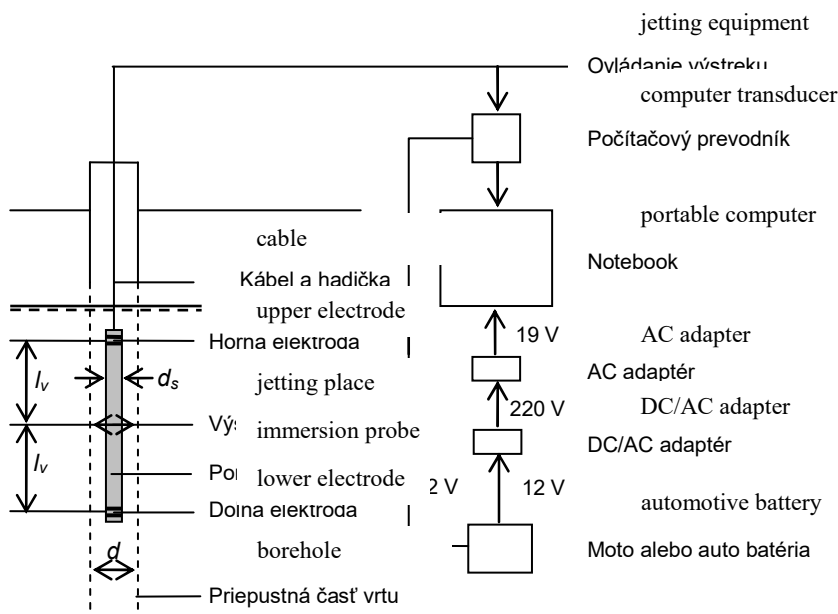


Figure 1. Scheme of the device for measuring vertical water flow in boreholes

From the vertical water flow measurement in the borehole, the value of water flow filtration velocity in the surrounding medium (approximately in the horizontal direction) is calculated by the formula:

$$v_f = \frac{\Delta q_v}{\bar{\alpha} d \Delta h} \quad (1)$$

Where Δq_v is the vertical flow increase or decrease in the part with height Δh ; $\bar{\alpha} = 20$ is the vertical flow borehole drainage influence coefficient; d is the inner diameter of the observation well.

Filtration rates calculations are performed on personal computers and results are graphically depicted as dependencies of filtration rates on depth. The approach enables the researcher to monitor "natural" water flow in boreholes due to interconnection of different pressure horizons, but they also enable the monitoring of vertical flow caused by artificial influences such as pumping or water introduction into boreholes. For illustration we present results of these measurements in Fig. 2. There are three separate measurements: the first one - 14.12.2013 during the verification operation and the others during constant operation after the remedial measures were built.

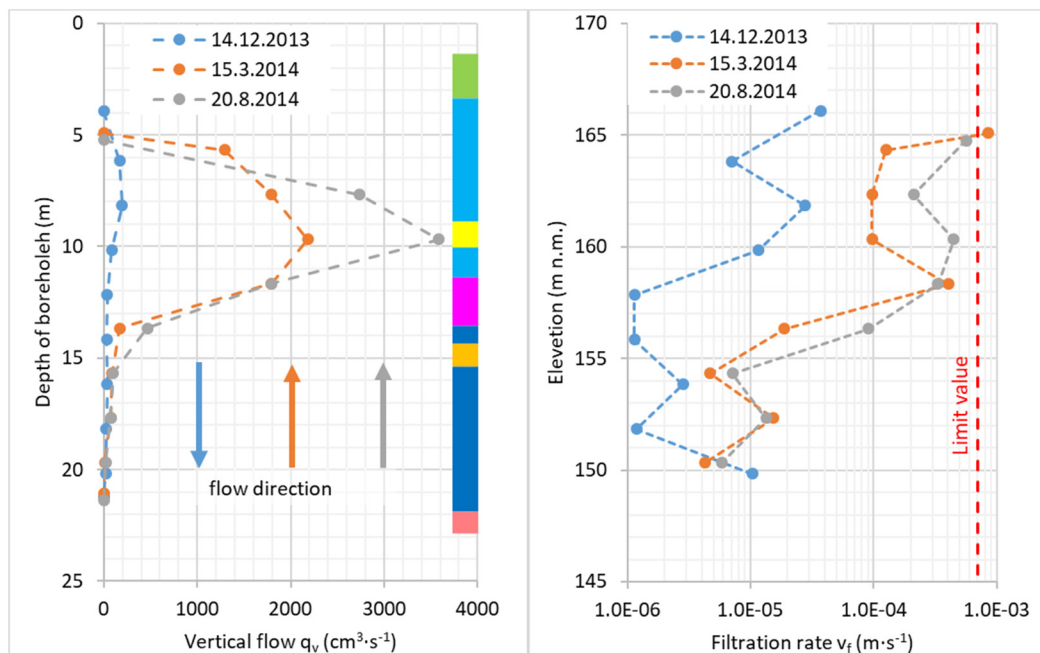










Figure 2. Vertical flow rates and filtration rates in well T-4 during measurements

3.3 Numerical model

The computational model was created on the basis of reports of geological surveys and characteristic sections taken from the project documentation of the structure. We used 2D model for the calculation because previous analyzes of the groundwater level regime showed that the dominant direction of water flow is from reservoir directly to seepage canal from where seepage water is drained away [4]. After the construction of the seepage canal, there is a steady state of the levels in the observation boreholes. All materials considered in the numerical model are shown in Tab.1.

Table 1. Materials considered in the model

Material - layer	Coefficient of permeability ($\text{m}\cdot\text{s}^{-1}$)	Color
dyke	$3\cdot 10^{-5}$	
dyke's protection	$1\cdot 10^{-4}$	
aquifer 1	$2,3\cdot 10^{-4}$	
sandy layers 1	$1\cdot 10^{-4}$	
upper cemented layer	$1\cdot 10^{-7}$	
aquifer 2	$1,1\cdot 10^{-5}$	
sandy layers 2	$1,2\cdot 10^{-6}$	
lower cemented layer	$1\cdot 10^{-7}$	

Coefficients of permeability were determined using empirical relationships and pumping test results. Seepage rates are measured in seepage canal with a length of 706 m in two sections. Based on the length and inclination of the channel, we determined the specific leakage, which approximately coincided with the calculated values from the numerical model. However, it is not possible to exclude locally more permeable positions, since the selected profile (at T-4 borehole) is located at the site of the old river bed. Since

leakage rates are measured only in two sections, it is not possible to determine the specific leakage more accurately in individual profiles. All measurements are carried out by automatic probes. In order to check the accuracy of the measurements, the operators of the hydraulic structure measure the levels in all observation wells once a week and also the levels in the reservoir and in the channel under the reservoir [5]. Also, precipitation and water levels were available in the observation wells of the Slovak Hydrometeorological Institute, located near the water structure. Several alternatives were examined, at three different water levels in the reservoir:

- original level - 164.89 m above sea level (a.s.l.),
- operating level - 166.11 m a.s.l.
- and level at Q100 - 167.26 m a.s.l.

In the parametric study, 8 alternatives were considered to investigate the effectiveness of anti-seepage measures - drainage channel and cut-off wall. The effect of the drainage channel and the efficiency of the cut-off wall with different lengths was investigated. The results from the model were then compared with in situ one-borehole tracer measurements. States at which the measurements of filtration velocities were realized: alternative 0 - original state, 1 – without anti-seepage measures, 2 - with drainage channel, 7 and 8 - with drainage channel and cut-off wall of 9 m and 10 m. Following figure depicts a part of the model of characteristic section no. 11.

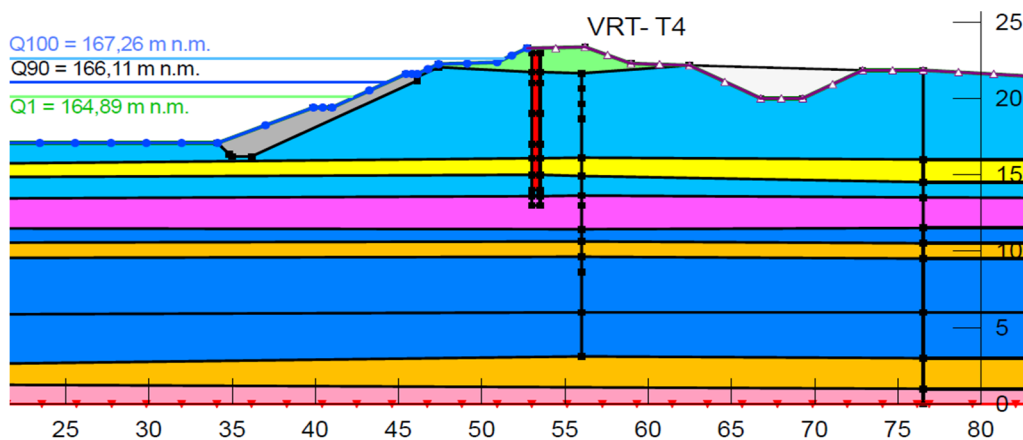


Figure 3. Detail of the reservoir dyke of characteristic profile no. 11

4. Results

The paper presents the results of the calculation for characteristic profile no. 11, where the observation well T-4 is located. This profile was chosen because there were measured the highest values of filtration rates in the well T-4, which were close to the limit values. If the filtration rate values are lower than the limit values, the filtration stability of the soils is not endangered. The limit value for gravel soils at the site was set at $7 \cdot 10^{-4} \text{ m.s}^{-1}$ [6]. After the construction of the cut-off wall, we observed change in the direction of vertical movement of water in the well from descending to ascending (Fig. 2). This phenomenon may indicate a leakage underneath of the cut-off wall, or it indicates the

occurrence of preferred leakage paths at the place of the old river bed. For the illustration purpose - in the graphical form - the values of the filtration velocities in the X and Y directions are presented in dependence on the depth (Fig. 4).

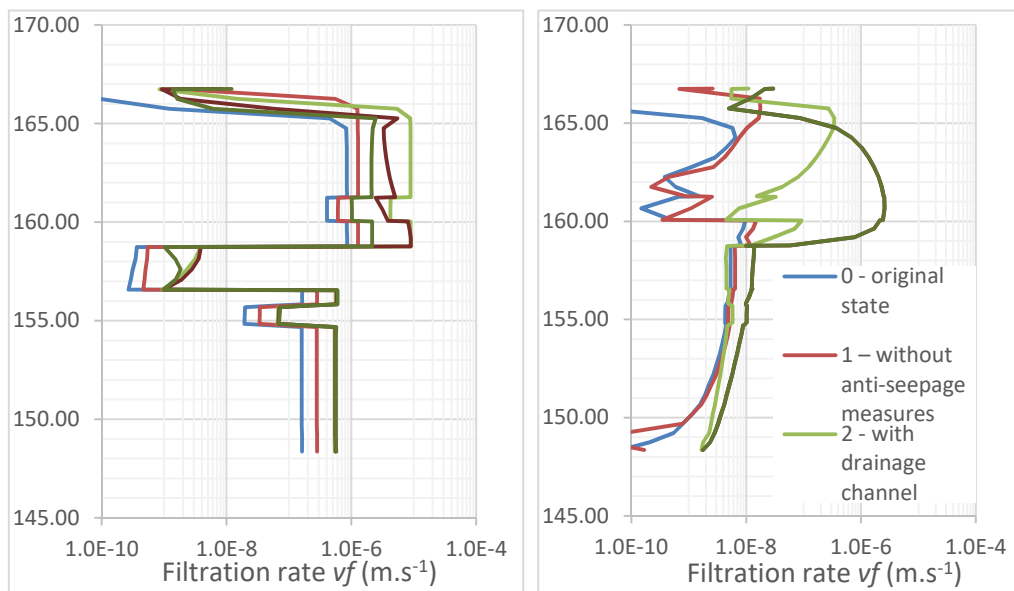


Figure 4. Detail of the reservoir dyke of characteristic profile no. 11

The calculation results show that the more dyke dominant flow direction is in the X-axis direction. The flow in the Y-axis affects the flow at the length of the cut-off wall from 6 m and the flow field begins to deform considerably. Cut-off wall is much less permeable than gravel and sandy soils in the dyke, so water flows beneath its lower edge. This phenomenon is shown in Fig. 3, which is a comparison of the filtration rates for a drainage channel and a drainage channel with 9 m deep cut-off wall.

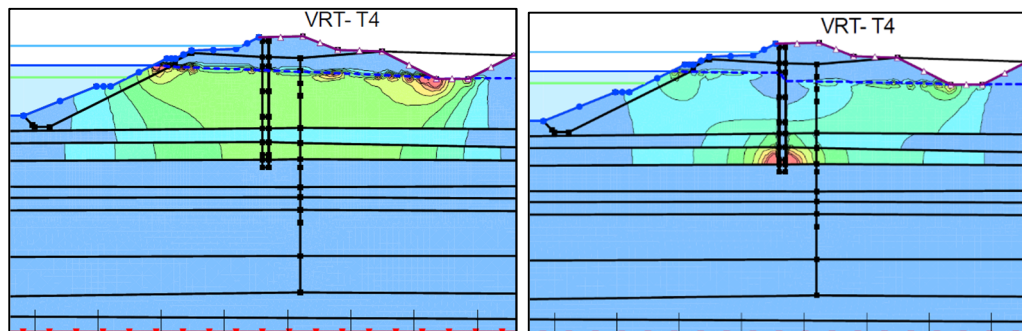


Figure 4. Detail of the reservoir dyke of characteristic profile no. 11

For more detailed analysis and comparison of the measured and calculated values of filtration rates, we chose only those alternatives that correspond to the real conditions on the hydraulic structure [7]: 14 December 2013 - without anti-seepage measures, 15 March 2014 and 20. August 2014 - with drainage channel and cut-off wall (Fig. 5). The outputs from the numerical model indicate that if the cut-off wall is embedded in the cemented layer, then the dyke subsoil is completely sealed. However, measurements

showed that there more intense flow in boreholes, as calculated for a wall depth of 10 m. Therefore, it is possible that the cut-off wall, which was built by Mixed-in-Place technology, is not embedded in the cemented layer (Fig. 4) or two separate aquifers were interconnected by the creation of observation wells. This hypothesis can also be confirmed by measurements, which show that descending flow was observed in the well prior to the cut-off wall construction and the flow has changed to ascending after its construction. Also, we observed higher values of the measured filtration rates as they were before its construction. However, it would also be beneficial to carry out further measurements to monitor the trend in the development of vertical water flow in the well - along with the trend in the development of filtration rates in terms of assessing filtration stability of soils.

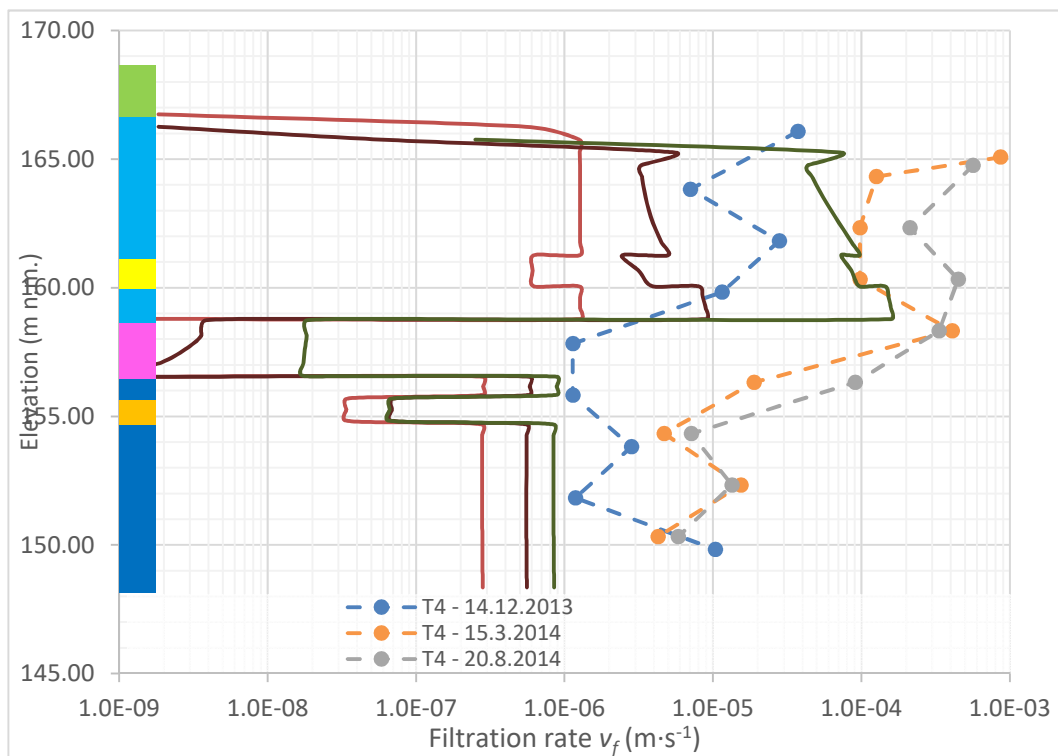


Figure 5. Measured and calculated filtration rates in well T-4

By comparing measured and calculated filtration rates (Fig. 5), the deviation is considerable between them – measured are more than ten times higher than calculated values. This difference can be allocated to several factors. One of them is the value of the drainage coefficient of borehole α . This coefficient expresses the deformation of the flow field around the borehole and its value depends on several parameters, such as: the vertical flow rate, the hydraulic gradient and the coefficient of permeability of given the environment. Since in complex, spatially changing geological and hydrogeological conditions, its exact determination is unrealistic. Therefore, its values have been determined experimentally. Usually, its values are considered from 2 to 20 in the rock environment of dams in Slovakia, but under special conditions even higher values are not excluded. At presented hydraulic structure we considered $\alpha = 20$.

5. Discussion

From the comparison of measured and calculated filtration rates, we can conclude:

- Measured and calculated filtration rate values have a similar pattern. It is clear that there is more intense flow in the upper aquifer than in the lower aquifer under the cemented layer.
- Calculated and filtration rate values are approximately ten times smaller than the measured filtration rates. This deviation may be caused by the fact that realization of the observation well deformed the flow field, which is a spatial phenomenon. This is taken into account - in determining the filtration rates from the tracer measurements - as effect of coefficient of drainage influence α . In 2D numerical models, this spatial phenomenon is not able to take into account. We can consider only the heterogeneity of the environment.
- In numerical modeling of filtration rates, the most important role is played by the quality and reliability of input data - coefficient of permeability. Coefficients of permeability of the individual layers in the model were determined from grain-size distribution curves of the soils by empirical formulas. Their variance was within several orders. Consequently, the real coefficients of permeability of a given environment may be different than our assumptions.
- The results of the measured filtration rates show more intense flow in the lower aquifer than we calculated. One option is that the construction of observation wells has connected two previously separated aquifers. This connection is not considered in the numerical model, and therefore the filtration rates are smaller. The second option is that these two aquifers are connected upstream the hydraulic structure. Then considered boundary conditions in the lower aquifer have to be changed, but hypothesis could not be confirmed from the available data. An additional geological survey would be needed to confirm it.
- It is not possible to accurately determine the heterogeneity of a given environment by measuring filtration rates. Measurements in wells were carried out every 2 m, despite that some sandy layers are only about 1 m thick according to geological survey and also cemented layer has thickness only about 2 m. Various layers have been connected after the well construction, which can partially affect the measurement results.
- Anisotropy of the environment is also very important factor. In the geological environment, permeability may be higher in the horizontal direction than in the vertical. However, anisotropy is not considered in the present model.
- Observation well T-4 is located in the place of old buried river bed where the preferred leakage paths can be found. From the available geological data, it is not possible to confirm their existence, but in the case of their existence, the measured filtration rates may be higher than calculated.

To verify mentioned causes of deviations between the measured and calculated filtration rate values, it will be necessary to model more characteristic profiles with observation wells where filtration rate measurements were carried out. By comparing several models with in situ measurements, it will be possible to better assess the deviations between the measured and calculated filtration rate values, to determine possible cause of deviations and to make necessary corrections.

6. Conclusion

During the design and operation hydraulic structure, it is necessary to have sufficient data of the natural environment of the site. The most important geotechnical parameter is the coefficient of permeability of soil when modeling the groundwater flow and seepage through the subsoil. In general, the exact determination of the coefficient of permeability is a complex task, since soil is a natural material and several factors affect its value. Therefore, the results of the numerical modeling of groundwater flow may differ from the measured values.

The paper focuses on the comparison of calculated filtration rates using a numerical model with measured in-situ filtration rates. By comparing the results, we found relatively good match of the filtration rate distribution over the borehole depth. The differences between the measured and calculated filtration rate values affect several factors which we described in the paper. In our opinion, these differences may be caused by reliability of input parameters - the coefficient of permeability of the environment and the chosen value of the borehole drainage coefficient. These hypotheses will be need further analyze.

If extreme leakage is detected or the limit values are exceeded during operation of the hydraulic structure, it is advisable to use numerical models. The causes of these anomalies can be simulated and analyzed by inverse modeling. With numerical model of the cross-section at T-4 borehole, we were able to confirm the hypothesis of the probable existence of seepage paths under the cut-off wall. From the safety and reliability point of view, these leakage rates do not pose a risk to the filtration stability of the soil because measured and calculated filtration rate values are lower than the limit values.

To verify the impact of possible cross connection of two aquifers by creation observation wells, it would be appropriate to use 3D groundwater flow modeling software. However, from a practical point of view, 3D models are demanding on the amount and quality of input data such as the spatial distribution of observation wells. For most of smaller hydraulic structures such as small hydropower plants on the rivers, we do not have conditions for such solution.

Acknowledgements

The paper is a part of the project VEGA 1/0452/17.

References:

- [1] GEO-SLOPE INTERNATIONAL Seepage Modeling with SEEP /W 2007. 2010. 307 s.
- [2] Šikula, G., Škvarka, J., Filo, J.: MVE – Tekov, pozorovacie sondy, Správa geologického dozoru za obdobie november – december 2013. Bratislava, EKOGEOS– zakladanie, s.r.o., 2013.
- [3] Hulla, J. Bednárová, E.: Zdokonalené indikátorové metódy na sledovanie rýchlostných zložiek priesakových režimov v podloží priehrad, Přehradní dny 2008. Brno, ISBN 978-80-02-02017-2
- [4] Škvarka, J.: Vplyv prevádzky MVE Tekov na hladinový režim podzemných vôd. [s.l.]: STU, 2015.
- [5] Fábik,: Hodnoty z meraní hladín v sondách a z hĺbok vody v potrubíach. MVE Tekov, 2015.

- [6] Hulla, J. Cábél, J.: Analýza kritérií pre filtračnú stabilitu. Inžinierske stavby. 1997. Vol. 45, no. 4-5s. 145-149.
- [7] Hulla, J., Takáčová, M.: Vplyv MVE Tekov na podzemné vody, Záverečná správa. Bratislava, apríl 2014.

STABILIZATION OF SURFACE EROSION ON SLOPES USING POLYMERS AND VEGETATION

ALEKSANDRA NIKOLOVSKA¹, JOSIF JOSIFOVSKI², BOJAN SUSINOV³

¹ *Ss Cyril and Methodius University, Civil Engineering Faculty - Skopje, R. N. Macedonia, alexandranikolovska@hotmail.com*

² *Prof. Dr. Ss Cyril and Methodius University, Civil Engineering Faculty - Skopje, R. N. Macedonia, jjosifovski@gf.ukim.edu.mk*

³ *Assist.MS. Ss Cyril and Methodius University, Civil Engineering Faculty - Skopje, R. N. Macedonia, susinov@gf.ukim.edu.mk*

1. Abstract

Nowadays, the use of natural micro-organisms for stabilization surface erosion are catching the attention of the researchers because of their presence in nature and their environmentally friendly structure. With the microbes renewable, biodegradable, possess high absorption sticky extracellular polymer substances (biopolymers) are produced which are able to change the hydraulic characteristics of the soil. In suspensions the biopolymers bind together soil grains, fill in the pores of the soil with viscous hydrogels to improve the mutual adhesion of the gel-coated beads resulting in the formation of a solid surface crust.

In this study we use biopolymer solutions of Xanthan gum, Cationamyl, Potassiumnitrate, Carboxy methyl cellulose, with concentration 0.5%-1.0%.

The design of the biopolymer binder of biopolymer solutions is in the direction of the selection of long nano-molecular structures that form strong bonds between individual soil grains.

There are designed 12 biopolymers binders on soil which are combination of two or more biopolymer solutions with different number of biopolymer coat, number of components, viscosity, intensity of absorption, crust thickness, elastic-plastic, rubbery and frangible crusts, retain a varying percentage of moisture, uneven growth of vegetation, etc.

The optimum choice of biopolymer binder is made by a multi-criteria analysis based on scoring criteria that are observed in the formation of the surface crusts. The two binders with the highest points of the multi-criteria analysis named Binder No. 1 and Binder No. 2, latter the strength of the crust is tested with one-axial loading and laboratory vane test.

The choice of one of the two biopolymer binders is based on the results of the laboratory tests of erosion with rain simulation, and the vegetation penetrating through the crust. The ability of the biopolymer crust to prevent wash out of the eroded material is tested by the experiment of erosion of rain and the planting of vegetation.

Finally, with the chosen binder we made an analysis on surface erosion of the influence of rain at slopes 1:2 made out of fine grained sand.

This test confirms the ability of the biopolymer binder to prevent the occurrence of surface erosion with the formed hydrophobic surface crust. We made a conclusion that hydrophobic crust allows reduced infiltration, increased capacity in retaining the water on the surface without washing the eroded material, and retaining the natural moisture of the soil by which the potential of vegetation growth is increased.

These results can be implemented in analysis of slope stability, planning of stability measurements, and protection of surface erosion.

Keywords: biopolymers, binders, surface erosion, stability, slopes, vegetation.

2. Introduction

Soil erodibility is a complex concept, it is influenced by many factors such as soil properties and human activities. Soil erosion is the process of detachment and transport of soil particles caused by water and wind [1]. Soil erosion occurs once shear stress exerted by moving fluids exceeds a critical value, referred to as the critical erosion shear stress [2]. The rainfall which is runoff from slopes is recognized as the main source for surface erosion. Some soils are more erodible than others, but climate change can bring more frequent and intense rainfall that will cause increased soil erosion regardless of soil type. Soil water is an important water source for vegetation development. Vegetation dynamics largely depend on soil water availability, which, in turn, results from a number of complex and mutually interacting hydrologic processes [3]. Different vegetation and soil types have different water infiltration capacities. The root systems make the soil more resistant to external influences. Climate change can cause severe dry periods that create difficult conditions for survival of vegetation.

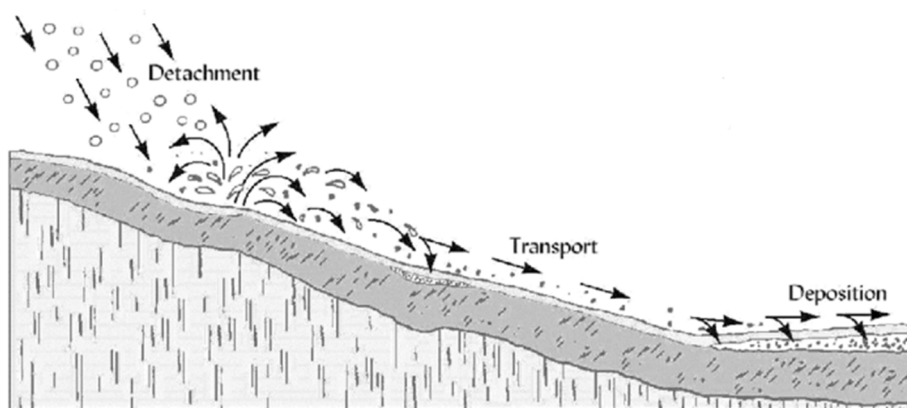


Figure 1. Process of creation soil erodibility

Ground enhancement methods have been intensively studied and developed over centuries. Application of natural soil enhancers will ensure stabilization of surface erosion and will create optimal conditions for maintaining vegetation during dry periods that are of great interest. In fact, the use of biopolymers is not entirely a new development in geotechnical engineering. Organic polymers such as natural bitumen, straw and sticky rice have been used in ancient civilizations and can also be classified as biopolymers. Polymers and biopolymers have been recognized as viable soil conditioners, because they stabilize Soil surface structure and pore continuity. In the past decade water soluble polymers were identified as high effective erosion preventing and infiltration enhancing polymers [4]. The synthetic and natural polymers when blended show possible applicability to improve properties of soils by binding particles together and retain water.

Today there is an increasing number of biopolymer applications for environment-friendly soil improvement and erosion prevention. For lower cost and human safety, biopolymers with agar, guar, xanthan, casein, gellan, and sodium alginate have been commonly studied to improve strength and to decrease the hydraulic conductivity of highly permeable soil materials. Among those, xanthan gum is known to perform better

in terms of lowering permeability [5]. Biopolymers are natural polymers produced by living organisms and are considered environmentally friendly and sustainable materials; however, the physical properties of biopolymers widely vary for different biopolymer types and compositions. They consist of monomeric units that are bonded into larger formations. Among the three types of biopolymers are: polynucleotides (for example, RNA and DNA), polypeptides (for example, amino acids) and polysaccharides, the most commonly used biopolymer in different practices are polysaccharides [6]. Polysaccharides can be found in nature, in plants, animals and microorganisms. Polysaccharides are widely used as stabilizing agents, such as thickeners for food, cosmetics, medicinal products, etc [7]. The biopolymers can easily be found in nature and they are known to be harmless and can be eaten. Biopolymers are considered to be environmentally eco- friendly products for improving the soil. When the biopolymers are mixed with the soil they can produce increased soil strength, improve cohesion, reduce permeability of water, but also retain moisture in the soil, and can produce greater resistance to erosive forces.

3. Methodology for design and optimum choice of biopolymer binder

3.1 Design of biopolymer binder

In this study, biodegradable and water-soluble polymeric materials (biopolymers) that do not have adverse effects on the environment are used for the analyzation of surface erosion. For analysis biopolymer solutions were used such as Xanthan gum, Cationamyl, Potassium Nitrate, Carboxymethyl cellulose, with concentration 0.5%-1.0%. Biopolymer solutions have binding properties of soil grains which are coated with a gel coating from the solution. Hence, using biopolymer solution and soil surface biopolymer crust can be formed. From the biopolymer solutions are designed 12 biopolymer binders of soil. Biopolymer binders of soil are a combination of two or more water-soluble biopolymers. Binders are different by number of biopolymer coat, number of components, viscosity, intensity of absorption, crust thickness, elastic-plastic, rubbery and frangible crusts, retain a varying percentage of moisture, uneven growth of vegetation, etc.

In the Petri dishes, the process of forming biopolymer crust is followed, as well as the criteria necessary for the optimal choice of biopolymer binder (Fig. 2).



Figure 2. Example by formed and frangible biopolymer crust in Petri dish

3.2 Multi-criteria analysis

For optimum choice of 1 from 12 biopolymer binders' multi-criteria analysis was used [8]. The multi-criteria analysis is based on scoring of the 9 criteria observed in the formation of biopolymer crusts (Table 1). Each criterion is reduced by a factor of importance for that criteria. The sum of points each biopolymer binder on soil classifies it into the I-X class of binder. This analysis makes an optimum choice of 2 by 12 biopolymer binders of soil. The results of this analysis showed that the binders with the most points are binder 6 and binder 11.

Table 1. Multi-criteria analysis for optimal choice of biopolymer binder

Criteria:		Importance of criteria	Number of biopolymer binders											
			1	2	3	4	5	6	7	8	9	10	11	12
1	Number of components	0.03	1		2-4			>4						
	Points		10		8			4						
2	Description of solution	0.03	no shreds, no bubbles			no shreds, with bubbles			with shreds, no bubbles		with shreds, with bubbles			
	Points		10			8			5		2			
3	Viscosity	0.06	high		viscous		middle		low					
	Points		1		3		8		10					
4	Absorption	0.06	very rapid		rapid		average		slow					
	Points		10		9		7		5					
5	Number of layers	0.15	1				2			3				
	Points		10				9			5				
6	Moisture [gr]	0.15	≥1				1-0.5			<0.5				
	Points		10				7			3				
7	Crust thickness [mm]	0.25	7-5						5-1					
	Points		10						9					
8	Cracks	0.02	surface				in depth				combination			
			shallow + long		shallow + short		deep + long		deep + short		shallow + deep + short		shallow + deep + long	
	Points		4		5		1		2		3		2	
9	Elastic-plastic crusts	0.25	very high		high		middle		short		very short		none	
	Points		10		9		5		2		1		0	

4. Effects and mechanisms of biopolymer binders for soil improvement

4.1 Strength characteristics

A small concentration of biopolymer solutions (0.5%-1.0%) can produce significant strengthening effects. In general, biopolymers have high specific surfaces with electrical chargers, which enable direct interactions between the biopolymers and fine particles of soil. The strengths characteristics of the biopolymer solutions were tested with unconfined compressive strength (UCS) and laboratory vane shear strength. For prepared UCS samples, the biopolymer solutions from binder 6 and binder 11 are mixed with dry soil and samples were compacted in accordance with standard proctor test. The prepared specimens were tested between a period of 1 and 7 days. All geometric dimensions were measured, such as specimen mass, specimen diameter and height. In order to prevent stress localization, filter paper was placed above and below the samples during testing. Samples were loaded until failure and the residual compressive strength was observed.

Table 2. Unconfined compressive strength of treated and untreated samples

	Samples with binder 6	Samples with binder 11	Untreated samples	Days
Maximal normal strength [kpa]	211.59	148.44	90.45	1
	876.56	358.35	39.47	7

Table 2 presents the results from unconfined compressive strengths testing. Untreated specimens were prepared to see the strengthened effect from UCS specimens prepared with binder. The specimens with binder showed the highest values of UCS than untreated specimens. The strength of biopolymers specimen is increased with moisture decrease, whereas the strength at the untreated specimens is decreased. The treated samples with binder 6 showed a higher compressive strength (876.56 kPa) than the binder 11 (358.35 kPa). All treated samples show higher UCS value than untreated samples tested at same curing time. The effect of curing time is evident when we compare the results for 1 and 7 days. The specimens tested on 7 day show higher UCS than the specimens tested on 1 day. We can also conclude that UCS samples tested on day 7 contain moisture inside the biopolymer solution (Fig. 2).

Laboratory vane shear tests are used to determine soil surface shear strength. For this testing, vane with dimension 12.70 mm of height, 12.70 mm of width, 0.5 mm vane thickness was used. The vane was pushed 30.0 mm into the soil from the top surface to place the blade directly in the middle of the specimens and then rotated constantly with a 10°/min angular velocity. Vane specimens were prepared with mixed dry soil and biopolymer solutions. Specimens with dimension 60.00 mm of diameter and 70.00 mm of height are tested on 1, 2 and 3 days. Figure 3 presents results from laboratory vane shear strengths for different days of testing. The value of shear strength is increased when moisture content of the binders is decreased.

Results from unconfined compressive strength and laboratory vane share test show that samples strength is increased when moisture from biopolymer solutions is decreased. Also, it shows that the biopolymer crust can be strong in dry periods and can keep a

long-time content of water in the soil.



Figure 2. Example from UCS sample with moisture (7 day)

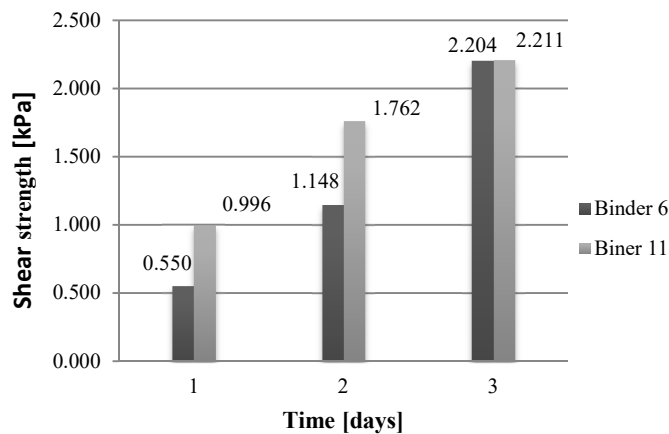


Figure 3. Vane shear strengths of biopolymer binders

4.2 Erosion resistance

Biopolymer binders of soil fill pores into the soil do not allow infiltration, but allow the leak of water on the formed surface crust without the occurrence of surface erosion.

The resistance of rain erosion is checked on the 2 binders from multi-criteria analysis. Erosion of rain was tested 20 minutes with rainfall simulation through sprinkler system with intensity of 12 l/h.

In contact with water, biopolymer crust can have different characteristics. Specimens were prepared from binder 6 and binder 11 which were tested for erosion from rain. Also, the crusts formed by these binders were analysis on rainfall. The effects of the

biopolymer crust to prevent soil washing and the appearance of surface erosion is proven with erosion of rain on untreated soil (Figure 4).

This analysis of the crust show that the crust of binder 6 has a weaker strength from the crust of binder 11. This crust is more elastic, the interior is elastoplastic and the crust is connected with interior. The binder 11 created strong crust which is connected with interior and is elastoplastic.

Finally, these crusts do not allow wash on materials because water slides on the surface.

With this test, effects from the biopolymer binders were shown which do not allow soil wash of soil such as example with untreated soil.

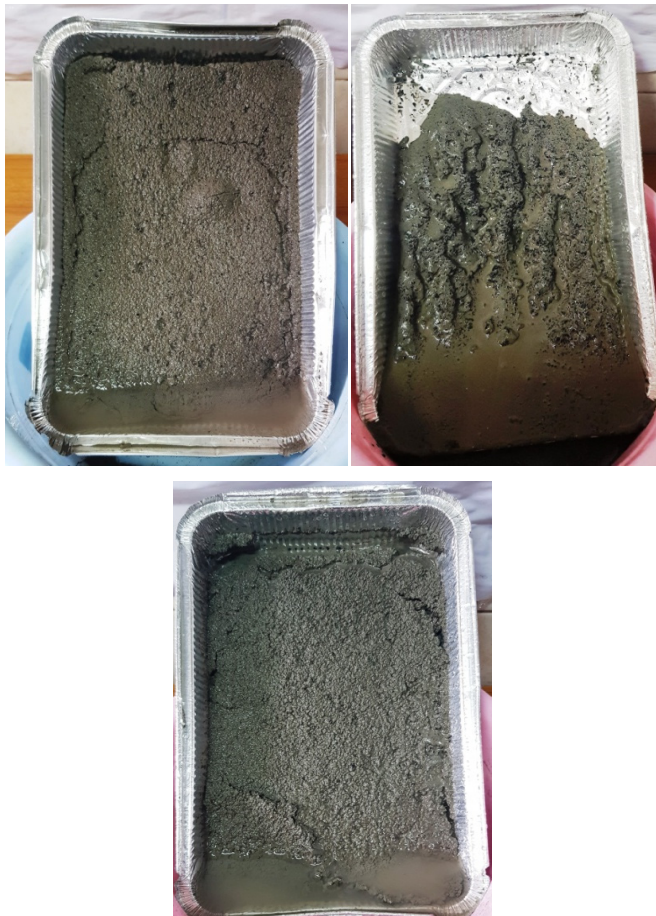


Figure 4. Crust from binder 6, binder 11 and untreated soil tested of erosion of rain (from left to right)

The strength of biopolymer-treated soils significantly degrades in the presence of water. Biopolymers tend to increase the viscosity of pore fluids due to hydraulic absorption. With biopolymer hydrogels the pore spaces within the soil are filled with highly viscous hydrogels enhances the inter-particle adhesion [9]. This hydrogel induced inter-particle bonding characteristic increases the erosion resistance of soils even in the presence of severe fluid (i.e., water or air) flow conditions.

4.3 Vegetation growth

Soil moisture has a direct influence on vegetation growth. Vegetation can play an important role in preventing shallow instability in slopes such as for surface erosion. Vegetation can provide tensile reinforcement through the roots. However, on the steepened slopes the lack of available moisture is a major problem in successfully maintaining the required vegetation for stability on surface layer. The biopolymers which are a produce of natural polymers are primarily composed of glucose, which provides nutrition to the vegetation. In addition, biopolymers are highly hydrophilic hydrogels which can hold water for extended periods of time compared to the soils [9]. Soils treated with biopolymers contain more water and with this are provides the vegetation with plenty of water and nutrition and that promotes growth. On the two models with dimension 29.00 cm of length, 8.00 cm of width and 5.00 cm of height seed of vegetation was planted. The specimen prepared with binder 11, vegetation growth is observed after 5 days of planting. The crust of binder 6 is very firm because the growth of vegetation through the crust is very slow and vegetation is observed after 10 days of planting.

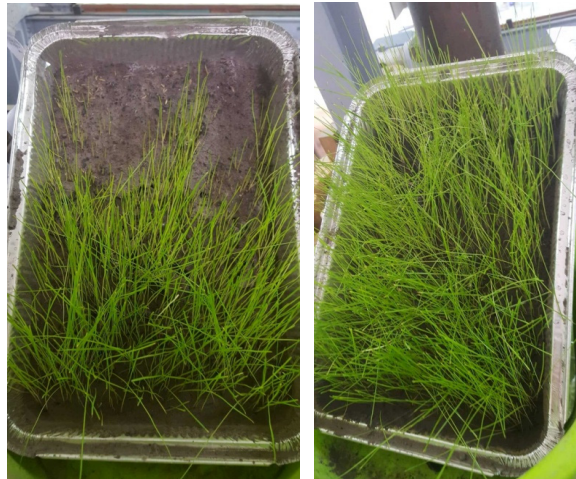


Figure 5. Vegetation 20 days after planting – models with binder 6 and binder 11 (from left to right)

The primary objective of this analysis was to design the biopolymer binder which can form crust with grains of soil. Also, will prevent the occurrence of surface erosion and will stimulate the growth of vegetation through the biopolymer crust. With the study results, erosion of rain and vegetation it can be decided which biopolymer binder of soil is better. The biopolymer binder 11 showed better resistance of the rainfall and provide rapid vegetation growth.

5. Slopes treated with biopolymer solution

From different binders are applied on surface at slope 1:2. In this experiment, three models with dimension 50.00 cm of length, 50.00 cm of width and 10 cm of height were tested. The models represent slopes with slope 1:2, namely: 1st model - soil, 2nd model

- soil and binder and 3rd model - soil, binder and vegetation. The 1st and 2nd models were prepared out of fine grained sand defined with granulometric analysis. In the 3rd model measurement systems were used for measuring suction and moisture in the soil. On the bottom they have holes through which water will flow out when the material is saturated. Also, on the bottom an adhesive mesh is positioned for better contact between the soil and the model.

The 1st and 2nd slope were tested for 120 minutes (12 phases) with simulation of rain (Fig. 6). In the initial phase, visual difference cannot be seen, but only if formed crust from binder is touched. Rain drops that are remained on the surface are not absorbed in the crust because the hydrophobic crust allows the accumulated water to leak along the slope without washing the material. In the 4th phase, 40 minutes after the rainfall starts, it can be seen that the material is saturated. From this phase the water starts to flow out of the holes in the bottom of the model. After this slope, from 5th to 12th phase another change cannot be seen.

The other model, slope only with soil, when the rainfall started small knots with material are saturated and washed. Also, on the surface larger sandy grains can be seen which are washed, and smaller grains change their location. From the 8 phase, pats of movement of eroded material are known. In the penultimate stage, all material is saturated because water flow out of from holes in bottom.

When the testing was finished it was made cross section on two models. The soil in the 1st model, was completely saturated and eroded material was seen only on the surface. The section in the 2nd model indicates that the water which flows through the holes is the water slipping down the stairs of the model. Soil in the bottom and crust is saturated. Under the crust and in the middle the soil was partly dry.

The viscosity properties of biopolymer hydrogels and their ability to entangle soil particles have been shown to have a positive effect on the hydraulic conductivity reduction of soils [10]. When biopolymers come into contact with water, this results in the formation of a highly viscous hydrogel in the pore spaces in the soil. These hydrogels tend to have strong water holding capabilities and slow the transport of water through the pores in the soil. When biopolymers are mixed into soil, the hydraulic conductivity of the soil is significantly reduced.

In the 3rd model, system of water content and suction sensor was used to monitor the changes in soil moisture and suction during the rainfall infiltration and the growth of vegetation. These types of mixture seed of vegetation were planted: *Festuca rubra*, *Poa pratensis*, *Lolium perene* and *Trifolium repens*. The model, 27 days after planting the seeds of vegetation were tested 60 minutes with simulation rainfall. The measuring systems were taken out from model 4 days after the test. Figure 7 presents the response of the volumetric water content (VWC) sensor during the watering for vegetation and rainfall event. Significant changes for VWC can be seen when sensor is covered with soil (6/7/19), application of binder (6/10/19) and all changes of the VWC from (6/12/19) to (7/4/19) are observed during watering of the vegetation. Upon rainfall initiation VWC sensor showed increase in water content in soil. The maximal registered volumetric water content of the soil is $0.218 \text{ m}^3/\text{m}^3$. The sensor were taken out from model 4 days after the test and then volumetric water content of the soil is $0.151 \text{ m}^3/\text{m}^3$.



Figure 6. Slopes untreated and treated 120 minutes after rainfall (from left to right)

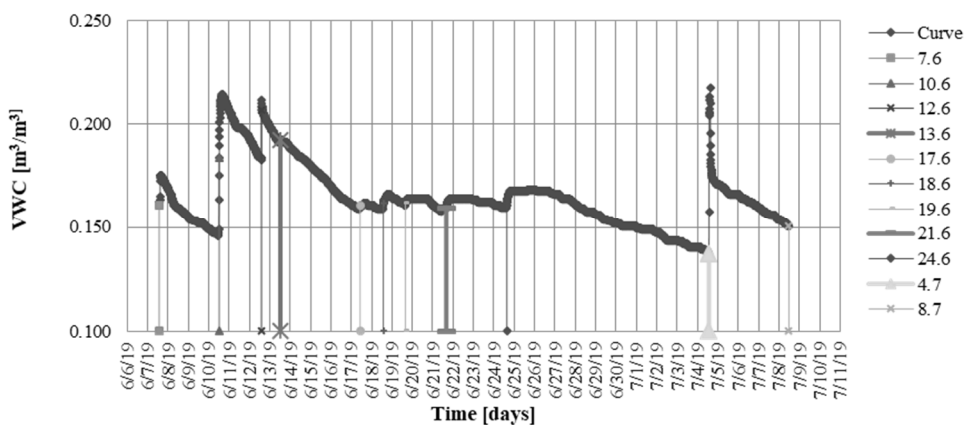


Figure 7. Time dependence of volumetric water content

The maximum value of the soil suction or negative pore water pressure which this sensor can measure is 100000 kPa. The suction is effected when the infiltrated water reaches the sensor depth. The value of suction significantly decreased when water content of the soil increased. The initial suction value of the sensor when is covered with soil is 46876.9 kPa (6/7/19). After 1 day the value of suction significantly decreased to 15.9 kPa (6/8/19) due to natural soil water content. The cycles of watering does not affect the suction significantly. Before the rainfall event the samples were not watered for 7 days. During this period the suction increases from 10.70 kPa (6/28/19) to 21.00 kPa (7/4/19) due to loss of moisture content. When the rainfall starts the suction immediately decreased to final value of 11.5 kPa (7/5/19) which is sensor minimum value (Fig. 8).

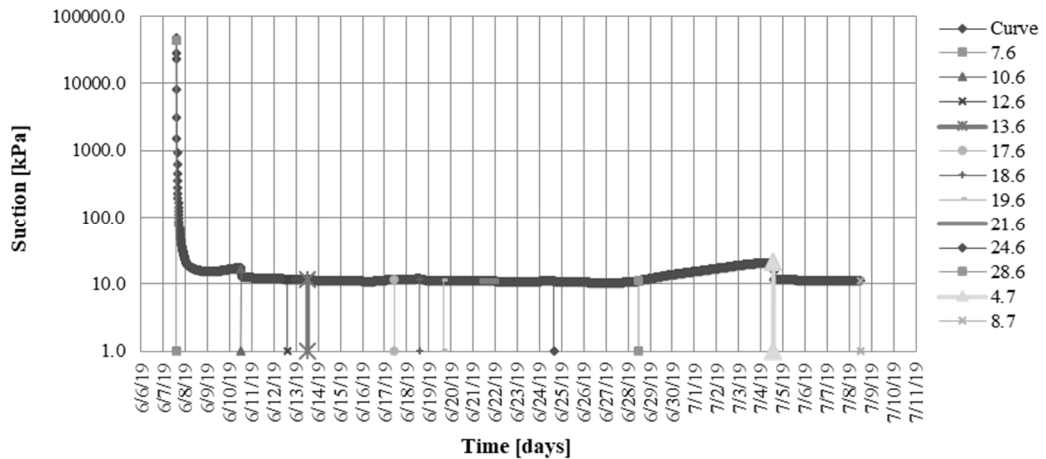


Figure 8. Changes in suction over time

6. Conclusion

The use of biopolymers has shown an increase in the erosion resistance of soils in the presence of fluid flow conditions. Moreover, biopolymer hydrogels restrict the rapid infiltration of water into the soil. Although the strength of biopolymer-treated soils significantly degrades in the presence of water, biopolymers generally tend to increase the viscosity of pore fluids due to hydraulic absorption. And thus, accompanying biopolymer hydrogel formation in which the pore spaces within the soil are filled with highly viscous hydrogels enhances the inter-particle adhesion.

Combined with their water retaining properties in soil, biopolymers are thought to be capable of promoting vegetation growth overall, a wide variety of methods can be applied to improve the mechanical properties of biopolymer treated soils, and as such, the use of biopolymers is emerging as a possible eco-friendly, sustainable method for soil improvement and stabilization.

Although their benefits are numerous, several challenges related to the use of biopolymers remain to be addressed, including sensitivity to water and market costs. Overall, given the wide variety of available biopolymers, the flexibility of their modification, and the numerous advantageous properties that they possess, the use of biopolymers in geotechnical engineering appears to have a promising future.

References:

- [1] Song, Y., Liu, L., Yan, P., Cao, T.,: A review of soil erodibility in water and wind erosion research, *Journal of Geographical Science*, 15 (2), 2005.
- [2] Soo-Min, H., Chang, I., Dong-Hwa, H., Tae-Hyuk, K., Balasingam, M.,: Improvement of surface erosion resistance of sand by microbial biopolymer formation, *Journal of Geotechnical and Geoinverimental Engineering*, pp. 144 (7), 2018.
- [3] Chen, L., Huang, Z., Gong, J., Fu, B., Huang, Y.: The effect of land cover/vegetation on soil water dynamic in the hilly area of the loess plateau, China, www.elsevier.com/locate/catena, pp. 200-208, 2007.

- [4] Lentz, R. D., Sojka, R. E.,: Field results using polyacrylamide to manage furrow erosion and infiltration, *Soil science*, Vol, 150, No. 4, 1994.
- [5] Tran, T, P, A., Im, J., Chom G-C., Chang, I.,: Soil-water characteristics of xanthan gum biopolymer containing soils, *Proceedings of the 19th International Conference on Soil Mechanics and geotechnical Engineering*, Seoul 2017.
- [6] Kalia, S., Averous, L.,: *Biopolymers: Biomedical and Environmental Applications*, pp. 3-34.
- [7] Saha, S., Bhattachatya, S.,: Hydrocolloids as thickening and gelling agents in food: a critical review, *Journal of Food Science Technological*, 47 (6), pp. 587-597, 2010.
- [8] Susinov, B., Zileska, P, Z.,: Multi-criteria analysis for selecting the most favourable method of ground improvement for local road construction in Veles industrial zone, *Annual conference at the school of doctoral studies at UKIM*, 2016.
- [9] Bouazza, A., Gates, W, P., Ranjih, P, G.,: Hydraulic conductivity of biopolymer-treated silty sand, *Geotechnique* 59 (1), pp. 71-72, 2009.
- [10] Chang, I., Im, J., Prasadhi, A, K., Cho, G-C.,: Effects of Xantan gum biopolymer on soil strengthening, www.elsevier.com/locate/conbuildmat, 74, pp. 65-75, 2015.

HYDROGEOLOGICAL ASPECT IN DETERMINING THE PROTECTION ZONES OF THE “NEREZI – LEPENEC” WELL SYSTEM

ZLATKO ILIJOVSKI¹, STOJAN MIHAILOVSKI², MARIJA MAKESHOSKA³,

¹*Civil Engineering Institute MACEDONIA, Republic of North Macedonia, geozlatko@gim.mk*

²*Civil Engineering Institute MACEDONIA, Republic of North Macedonia, stojan.mihailovski@gim.com.mk*

³*Civil Engineering Institute MACEDONIA, Republic of North Macedonia, marija.makeshoska@gim.com.mk*

1. Abstract

The “Nerezi-Lepenec” well system consists of seven wells that range in depth from 27 m to 70 m, with capacity between 150 l/s and 230 l/s. The total well system capacity is 1200 l/s.

This well system provides additional amounts of water for water supply of the city of Skopje, and it is used when the capacity of Rasche spring does not meet the city's requirements.

It is located near the mouth of the river Lepenec where it flows into the river Vardar. The aquifer, tapped with these seven wells, is an alluvial deposit at the rivers Vardar and Lepenec that fills in the 3 km long, 1.2 km wide and 130 m deep neotectonic depression. This depression accumulates $72 \times 10^6 \text{ m}^3$ of water.

Three protection zones were formed in order to protect the groundwater in this well system by having zone borders and prohibitions and restrictions for different activities which may have negative impact on the water quality.

The well system is located in an urban area. The high level of vulnerability, the high population density, the industry, the cultivation of agricultural land, the number of liquid and solid industrial and communal waste, put serious pressure and present high-risk factor for the groundwater contamination.

The hydro geological aspect is a very important factor in establishing the protection zones borders of this spring.

Keywords: protective, zones, sediments, vulnerability, pollution, water, river

2. Introduction

The renovation of the protection zones at the springs, which serve for public water supply, is inevitable and needs to be done every 20-25 years. The “Nerezi – Lepenec” well area with its 1200 l/s capacity used as additional water supply for the city of Skopje, set up protection zones in 1992. The intensive economic development, population

growth, urbanization and utilization of the agricultural land, have greatly increased the pressure to maintain the groundwater quantitative and qualitative status. Taking this into consideration, and the fact that 25 years have passed since the establishment of the protection zones, urgent action is required for the renovation of the spring protection zones, since this spring is extremely important for the city of Skopje.

The hydrogeological properties of the terrain are extremely important for the protection zones, because they have a huge impact on defining the protection zones borders, as well as the planned measures, prohibitions and restrictions.

3. Methods

3.1 Geological and Tectonic Features

The wider area of the location in question, the “Nerezi-Lepenec” well system with its 7 (seven) wells in total, is located in Skopje Valley. Regarding the tectonics, Skopje Valley is a neotectonic depression which appeared and was formed due to the lowering of the area during the Neogene – Quaternary period, and, simultaneously, the raising of the surrounding terrain (Vodno and Skopska Crna Gora). The peripheral parts and the Paleosurface of the depression are made of rock masses of different ages and different geological formation. The central part of Skopje Valley i.e. the Paleosurface, is covered with Neogene and alluvial Quaternary sediments.

The Neogene sediments are mainly presented by siltstone marl facies, and the Quaternary sediments are presented by alluvial deposits mainly made of variously granulated sands and gravels.

The microsite itself is about 3 km long, 1.2 km wide and 130 m deep Quaternary elliptical depression, which appeared as a result of an intense young tectonics. The depression is entirely filled with alluvial sediments.

The alluvial sediments at the location in question are mainly made of variously granulated sands and gravels with dominant presence of gravel fraction, where cobbles and boulders are detected in large quantity. The cobbles and boulders are well processed and can reach up to 100 – 200 mm. Based on the hydrogeological function, the alluvial and terrace sediments are groundwater collectors where unconfined type of aquifer is formed, with good filtration properties, water-bearing and yield of the wells.

3.2. Hydrogeological Properties

An extensive hydrogeological exploration was conducted in the past, especially after the 1963 Skopje earthquake, which included drilling of a number of exploratory boreholes and quite detailed geophysical research. However, in the past 30 years, the exploration was not as extensive as before.

Based on the analysis of the hydrogeological documentation from the investigated terrain and the wider area in Skopje Valley, it was stated that in terms of the groundwater reserves, the aquifers formed in the alluvial and terrace sediments in river Vardar are the most important ones. They are unconfined type of aquifers with intergranular porosity. The alluvial sediments in Skopje valley have fairly uniformed lithological composition, made up of variously granulated fairly pure fractions of sands and gravels. This results

in fairly equal values for filtration coefficient.

The yield of the wells depends on the thickness of the alluvial sediments, or the thickness of the aquifer zone, so the highest level of yield is at the "Nerezi - Lepenec" well area, where the thickness of the alluvial and terrace sediments is more than 100 m and sometimes up to 130 m. Depending on the thickness of the alluvial sediments and the analysis of the parameters of the wells (yield, GWL, depth, diameter), a hydrogeological regionalization was carried out on the territory of the city of Skopje, as presented in Figure 1.

During the regionalization, the main emphasis is placed on the division of alluvial sediments regarding their thickness and the yields of the wells. Based on this regionalization, the city of Skopje is divided into 6 regions, where the alluvial sediments have suitable hydrogeological properties.

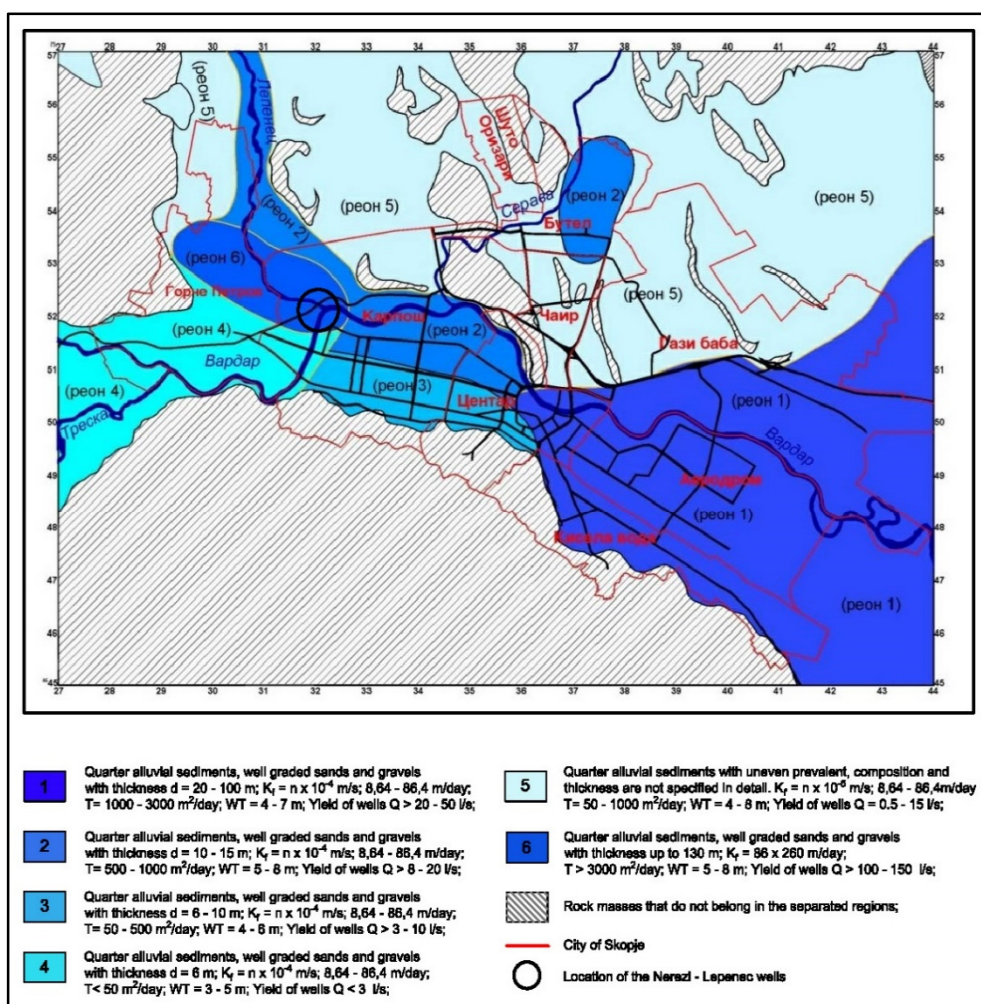


Figure 1. Hydrogeological model of Skopje region (Methodology for investigating groundwater vulnerability, Z.Ilijovski, 2013).

The lithological units shown on the hydrogeological map and the hydrogeological profiles (A-A', B-B') have intergranular porosity: pre-Quaternary Miocene and Pliocene sediments and Quaternary mainly alluvial, and diluvial and proluvial sediments along the rims. The pre-Quaternary Miocene and Pliocene sediments are mainly impervious, and based on the hydrogeological function they are hydrogeological isolators which contour the underground reservoir and create semi-closed hydrogeological system. On the other hand, the Quaternary sediments, especially the alluvial ones, have intergranular porosity where unconfined type of aquifer is formed.

In this area, the aquifer is continuous with continuous hydraulic connection. The previous investigations and the drilling of the wells in “Nerezi – Lepenec”, have not shown continuous layers or interbeds of clay and clayey materials that could horizontally and vertically interrupt the connections, except rare and low-power clayey layers which are not in continuity i.e. they wedge out in certain places.

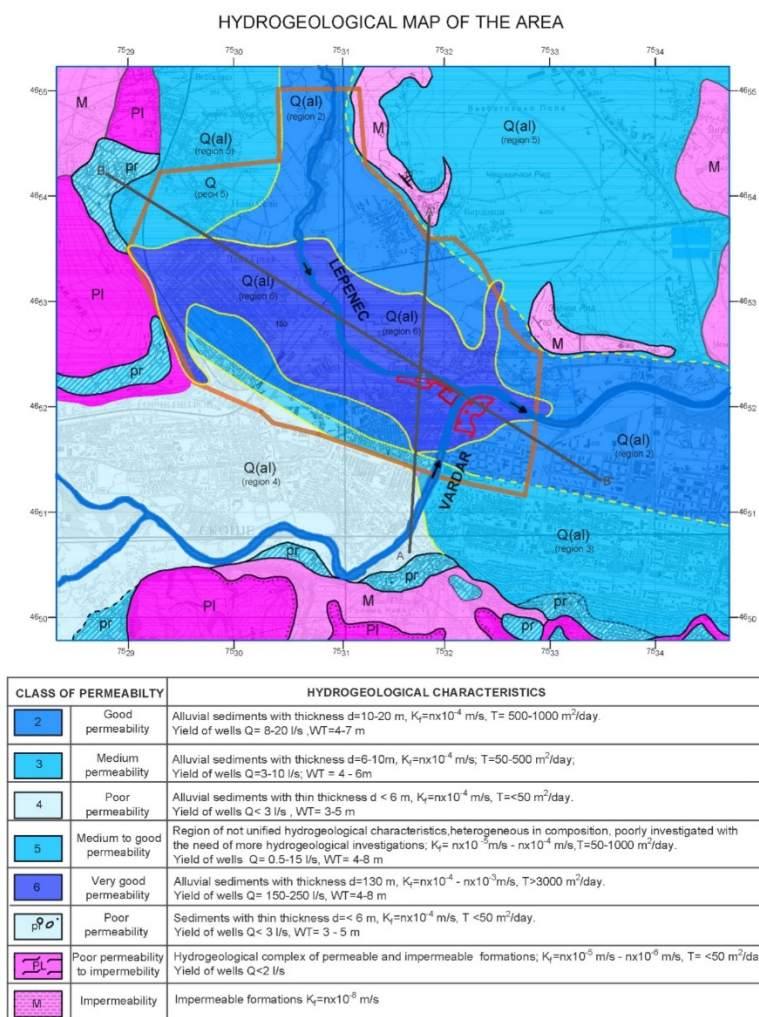


Figure 2. Hydrogeological map of Skopje region M 1:50 000

The sixth region is the so called neotectonic depression Lepenec, where the river Lepenec flows into the river Vardar. It covers the area of the villages Zlokukjani, Novo Selo and Bardovci in northwest – southeast direction, in length of about 3 km and width from 750 to 1 200 m. The maximum depth of this depression is 130 m. The thickness of the Quaternary alluvial sediments in this region is up to 130 m, the groundwater level is within the limits 3-6 m, the filtration coefficient $K_f = nx10^{-4} - nx10^{-3}$ m/s (86-260 m/day), the water-permeability coefficient $T > 3000$ m²/day, and the yield of the wells $Q = 150 - 250$ l/s. The specific yield is q_{sp} 14-47 l/s/m'. Due to the coarse granulation, the sediment at the river Lepenec has increased collector properties. Boulders greater than 300 mm were detected during the drilling of the wells. The general groundwater flow directions follow the river flows with different partial gradients, depending on the local morphology and the filtration properties.

The Vardar and Lepenec rivers recharge the aquifer along their courses, and in that way, they help a great deal with the renewal of groundwater reserves in the Nerezi-Lepenec well system and beyond, but at the same time they increase the groundwater contamination risk.

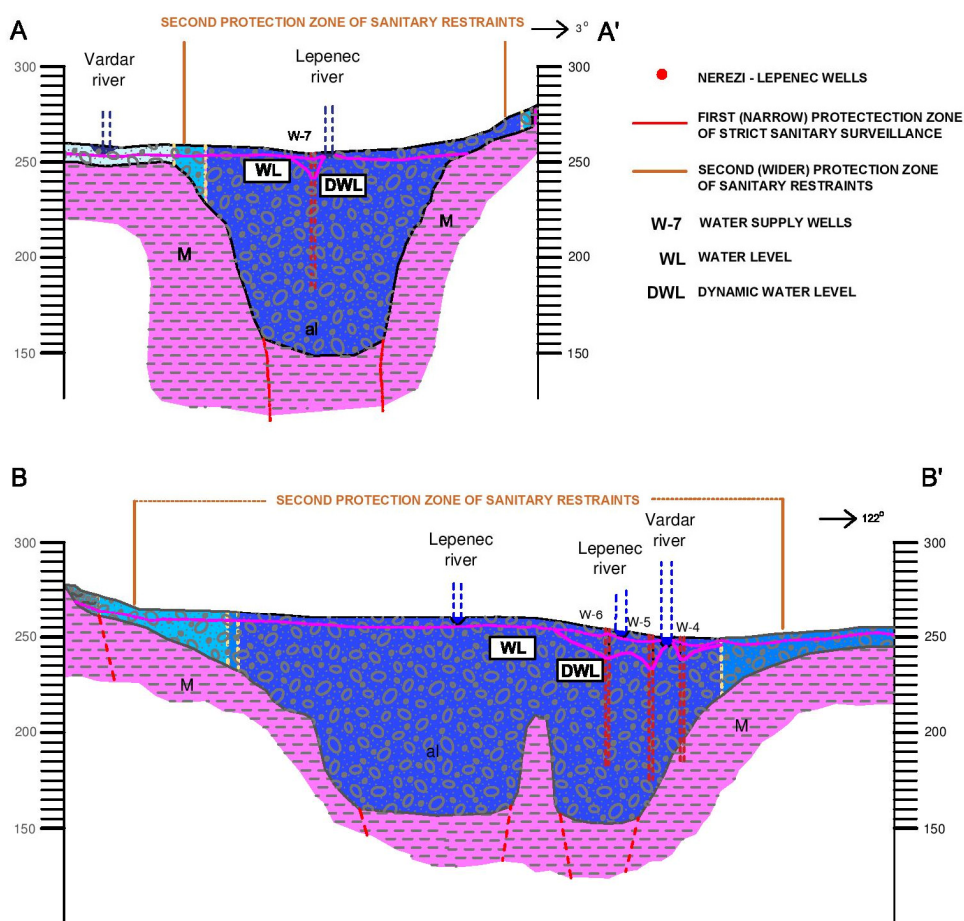


Figure 3. Hydrogeological profiles M 1:50 000/4000

3.3 Type, Location and Hydraulotechnical Properties of the Wells

“Nerezi – Lepenec” well system is located in an area near the mouth of the river Lepenec where it flows into the river Vardar i.e. the western part of the city of Skopje.

These wells are managed by PE "Water supply and sewage" - Skopje and are particularly important for the following reasons: high groundwater availability, water quality, consumer proximity, possibility to replace Rasche spring in case of natural, technical or intentional disaster at the intake and the pipeline (length 17 km).

The “Nerezi – Lepenec” well system includes 7 (seven) wells used for groundwater exploitation.

On the right side, downstream of river Vardar, i.e. on the opposite side of the mouth of the river Lepenec where it flows into the river Vardar, 4 (four) wells (W-1, W-2, W-3 and W-4) were drilled. In addition, three wells were drilled (W-5, W-6 and W-7) starting from the mouth of the river Lepenec, on the right side, upstream along the river Lepenec, in length of about 500 m.

The wells at the site “Nerezi” were drilled in 1964. The drilling of the wells was conducted with a diameter of \varnothing 1000 mm, and a steel well structure in diameter of \varnothing 600 mm was placed into the wells, Table no. 1.

The wells at the site “Lepenec” were drilled in 1991 with identical structure. The structure of the wells was made so that the filter was placed at a greater depth of 40 m in order to extract good-quality groundwater. This was detected in all wells except for the well W-1.



Figure 4. Google Earth location map of the well system

Table 1. Basic technical data for the “Nerezi - Lepenec” well system

Wells	Depth [m]	Drilling diameter (mm)	Well structure diameter (mm)	Filter pipes diameter (m)	Exploitation capacity Q (l/s)	Lowering (m)	Specific yield q (l/s/m)
W-1	27	1000	600	17-25	150	4,50	33.3
W-2	64.2	1000	600	50-62	230	5,40	42.59
W-3	67	1000	600	47-67	230	4,90	46.93
W-4	64	1000	600	43,6-59,7	150	10,60	14.15
W-5	74.5	1000	600	45,5-71,5	122	1.6	76.25
W-6	70	1000	600	40,5-66,5	130	1.64	79.26
W-7	69.5	1000	600	40,5-66,5	131	1.58	82.91

The total exploitation capacity for all of the 7 (seven) wells at the site “Nerezi – Lepenec” is $Q = 1210$ l/s.

3.4. Groundwater Reserves Analysis in the Well Area “Nerezi-Lepenec”

Based on the available data and the usual hydrogeological procedures, the following is estimated:

Q_{st} – static reserves

Q_{dyn} – dynamic reserves

Q_{exp} – exploitable reserves

Static reserves: are estimated for the narrow drainage basin of the wells i.e. the Neogene depression area is covered, which is the main groundwater reservoir used for groundwater exploitation from the wells "Nerezi - Lepenec" for the needs of the City of Skopje. The water reservoirs are estimated based on the vertical parallel profiles method which gives the total aquifer volume. The water reservoirs are calculated based on the following formula:

$$Q_{st} = \mu \times V \quad (1)$$

where:

μ – specific yield coefficient (effective porosity),

V – aquifer volume (aquifer layer);

From the extracted parallel profiles made on the basis of previous hydrogeological and geophysical investigations in this area, the input parameters are:

$$\mu = 0.25$$

$$V = 289.0 \times 106 \text{ m}^3$$

$$Q_{st} = 72.25 \times 106 \text{ m}^3$$

Dynamic reserves: are estimated as underground flow size of the representative profile through the reservoir which goes through the well area. The following formula is used

for the calculation:

$$Q_{\text{dyn}} = Kf_{\text{av}} \times H_{\text{av}} \times B \times I \quad (2)$$

where:

Kf_{av} – average filtration coefficient (280m/day)

H_{av} – average thickness of the aquifer zone (40m)

B – width of aquifer flow (2.000m)

I - average value of the hydraulic gradient (0,0032)

$$Q_{\text{dyn}} = 7.2 \times 104 \text{m}^3/\text{day} = 0,833 \text{m}^3/\text{s}$$

Exploitable reserves: based on the present knowledge about the characteristics of the aquifer and the practically achieved yield of the wells, at this moment only one strict orientational calculation for the available exploitation possibilities of the wells can be given, using the formula:

$$Q_{\text{exp}} = (Q_{\text{dyn}} + Q_{\text{st}}/T) \times \alpha \quad (3)$$

where:

Q_{dyn} – dynamic reserves of the groundwater

Q_{st} – static reserves of the groundwater

T - time of the exploitation period

α – coefficient of utilization of reserves(30%)

$$Q_{\text{exp}} = 1,35 \times 105 \text{m}^3/\text{day} = 1.56 \text{m}^3/\text{s}$$

These exploitable reserves are of an orientational nature so they are not completely reliable. For more accurate calculation of the exploitable reserves, it is necessary to carry out detailed monitoring, additional control extraction and afterwards to make additional calculations and analyses. The determination of the hydraulic connection between the surface watercourse (a river) and the groundwater is exceptionally important for the quantity and quality of groundwater at this site.

The exploitable reserves of groundwater must be aligned with the study of hydrogeological issues of the aquifer, additional urban and economic conditions, optimal yield of the wells, results of the proposed monitoring, as well as set goals and limitations of quality protection.

4. Results and Discussion

4.1. Determining Protection Zones Borders

In accordance with the legislation and the rulebook for determining the protection zones borders, there are three protection zones: first, second and third protection zone.

The first protection zone is the immediate location of the wells. It is surrounded with a wire fence, under constant security by the guard service and under permanent video

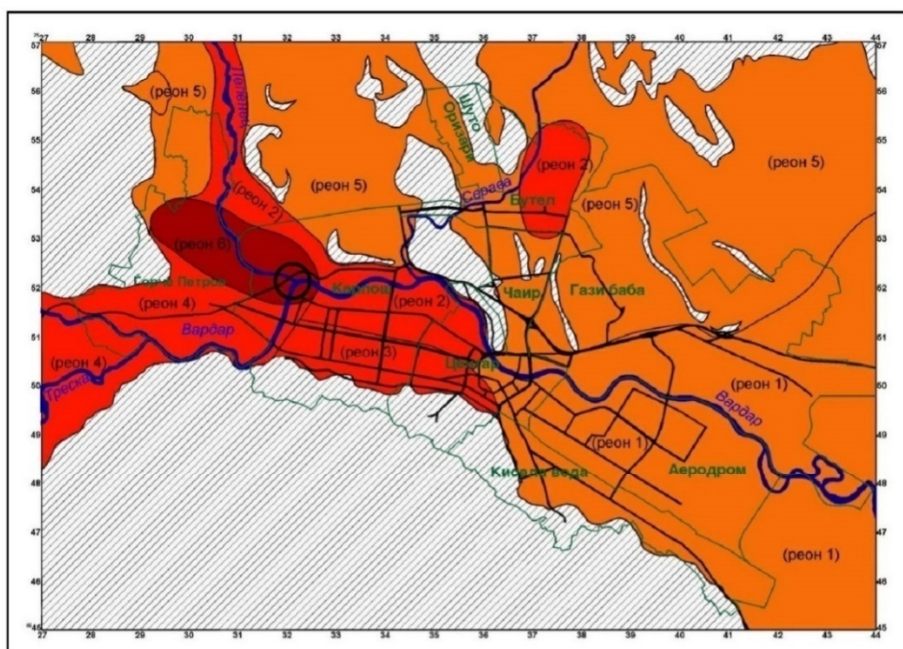
surveillance. The second protection zone for groundwater intake in intergranular porosity is determined by a period of 50 days of underground flow of the water from the site of possible microbiological, biological, physical, chemical, radiological and other contamination, to the site of the intake in conditions of exploitation of the spring.

Table 2. Significance and rating of the DRASTIC and MVCRS methodology

DRASTIC	Symbol	Meaning	Max. Rating	MVCRS	Symbol	Meaning	Max. Rating
	D	Depth to water	125		D	Depth to water	25
	R	Recharge to the aquifer	60		R	Recharge to the aquifer	15
	A	Aquifer media	60		A	Aquifer media	20
	S	Soil media	30		T	Topography (slope)	10
	T	Topography (slope)	10		SI	Lithology of the vadose (unsaturated) zone	15
	I	Impact of vadose (unsaturated) zone	75		C	Conductivity of the aquifer	15
	C	Conductivity of the aquifer	45		Total maximum rating:		100
	Total maximum rating:				405		




Table 3. Analysed parameters and points for determining the vulnerability (region 6 - Neotectonic depression Lepenec, Nerezi) according to MVCRS and DRASTIC methodology

Aquifer type	Water-permeability class	HG region	Ranking according to the MVCRS- methodology and definition of total rating and vulnerability class						Total rating	Vulnerability class	
			D	R	A	T	SI	C			
Quaternary alluvial sediments – unconfined type of aquifer	14	Neotectonic depression Lepenec, Nerezi	20	14	20	10	12	51	91	<u>Very high</u>	
			Ranking according to the DRASTIC - methodology and definition of the DRASTICindex and vulnerability class								
			D	R	A	S	T	I	C	Total rating	Vulnerability class
			100	56	60	24	10	60	45	355	<u>Very high</u>



LEGEND

Category of vulnerability

	Moderate 55 - 70
	High 70 - 85
	Very high 85 - 100




	Rock masses that do not belong in the separated regions
	City of Skopje
	Location of the Nerezi - Lepenec wells

Figure 5. Vulnerability map of groundwater according to MVCRS

In addition to this criterion that was defined by the development of the hydro-geological mathematical model, the hydrogeological limits of the represented aquifers, the vulnerability class and the contamination risk class, were taken into account. The hydrogeological criterion in this case is crucial for the vulnerability of the aquifer, which according to the MVCRS methodology is classified in a very high vulnerability class, while the presence of pollutants, densely populated areas, usage of agricultural land and other pressures define the groundwater contamination risk under which this area is in a category of a very high risk.

Having this in mind, the second protection zone boundary follows the hydrogeological boundary of the hydrogeological region 6 and part of the hydrogeological region 2 on the upstream side along the flow of the river Lepenec where alluvial sediments are formed.

5. Conclusion

The Nerezi – Lepenec well system is essential as a source for additional water supply

for the city of Skopje. The neotectonic activity towards the end of the Neogene created excellent conditions for positioning a large aquifer with very favourable hydrogeological characteristics regarding the groundwater exploitation.

The hydrogeological structure of the terrain and the hydrogeological characteristics of the represented lithological formations are essential for the formation of the protection zones boundaries at the water supply springs, especially in this case. The hydrogeological structure on the terrain is an important factor in determining the aquifer vulnerability, and also together with the pressures on the groundwater quality, they are an important factor for defining the risk level of groundwater contamination.

According to detailed analysis of the hydrogeological characteristics of the terrain, vulnerability, quantity and quality pressures and possible contamination risks, three protection zones were established. The protection zones have borders, prohibitions and restrictions. All of this, should help the long-term protection of groundwater quality of this important water supply spring for the City of Skopje.

References:

- [1] Civil Engineering InstituteMacedonia: Expertise on updating the boundaries of the protection zones in the well area “Nerezi – Lepenec” and the determination of protection measures,Skopje, 2017.
- [2] Ilijovski Z. : Methodology for investigating groundwater vulnerability, Skopje, 2015

HAZARD AND RISK ASSESSMENT OF EARTHQUAKE GEOTECHNICAL INSTABILITIES

JULIJANA BOJADJIEVA¹, VLATKO SHESHOV², KEMAL EDIP³ TONI KITANOVSKI⁴,
JORDANKA CHANEVA⁵, DEJAN IVANOVSKI⁶

¹ *Institute of earthquake engineering and engineering seismology (IZIIS), Macedonia, jule@iziis.ukim.edu.mk*

² *Institute of earthquake engineering and engineering seismology (IZIIS), Macedonia, vlatko@iziis.ukim.edu.mk*

³ *Institute of earthquake engineering and engineering seismology (IZIIS), Macedonia, kemal@iziis.ukim.edu.mk*

⁴ *Institute of earthquake engineering and engineering seismology (IZIIS), Macedonia, tonik@iziis.ukim.edu.mk*

⁵ *Institute of earthquake engineering and engineering seismology (IZIIS), Macedonia, dance@iziis.ukim.edu.mk*

⁶ *Institute of earthquake engineering and engineering seismology (IZIIS), Macedonia, ivanovski@iziis.ukim.edu.mk*

Abstract

Landslides and liquefaction as secondary earthquake hazards are causing some patterns of soil failure that are often considered among the most destructive ones. In fact, the impact from triggered landslides and liquefaction has sometimes exceeded damage directly related to strong shaking and fault rupture.

The objective of this research study is to present applicable methodology for hazard and risk assessment of landslides and liquefaction through two case studies in Macedonia. This approach, through the GIS database can be easily upgraded by adding different hazard for ex. floods, erosion and analyze the area of concern by multi hazard assessment under different scenarios of interest. The first case study is landslide hazard and risk assessment considering different water saturation and earthquake scenarios, for a selected area in a suburban hilly part of Skopje—the capital of Macedonia. The final product is represented by digital maps of expected permanent displacements for a defined earthquake scenario, in different water saturation conditions of the instable soil layer. Qualitative landslide risk assessment is performed taking into consideration the exposure map of the habitants and local road of the area. As to the target area, it can be concluded that it has the potential for instability that, under certain scenarios, could result in economic and social damage (vulnerability of individual houses, vulnerability of infrastructure and alike). The results from this study referring to potentially affected population and infrastructure present solid base for preventive mitigation activities for reducing the consequences of geotechnical hazards in Skopje City associated with earthquakes.

The second case study is focused on hazard assessment of liquefaction potential using in-situ methods, particularly SPT investigations for a characteristic location - Ohrid city, Republic of Macedonia. Being on the Coast of Ohrid Lake, the soils of this location are with near surface water tables, and are also characterized by layers of relatively loose saturated sand, with low to high content of fines. A liquefaction potential assessment by means of an F_s (factor of safety) and PL (probability of liquefaction), was carried out for a number of locations with available results from geotechnical investigations, using the deterministic and probabilistic relations proposed by Boulanger & Idriss. The dynamic inputs for deriving the CSR (cyclic stress ratio) were parameters of PGA and M_w for two selected seismic scenarios, in accordance with the seismic hazard for the selected location. The results served as a basis for deriving a methodology for local zoning of this type of hazard, using the GIS methodology. The final product are 4 maps of factor of safety against liquefaction and probability map of liquefaction for the two analyzed scenario, which refer to the critical layer with potential of liquefaction. The results led to several conclusions related to the soil conditions and characteristics, the advantages of the in-situ methods, the need for additional terrain investigations as well as comparison between deterministic and probabilistic approaches. Also, they highlight the necessity for this type of investigations as a prevention measure for urban planning.

Keywords: landslides, liquefaction, earthquake, GIS, hazard, risk.

2. Hazard and risk management methodology

For many natural landslides the risk posed by the landslide is managed by zoning to avoid the hazard, or installing early warning systems so the population at risk can be evacuated from the hazard. For small natural landslides and resulting debris flows, etc, this is the only practical management system, because it is impractical to calculate the factors of safety of each slope (and in any case, they will often be approaching 1.0 under certain circumstances eg. heavy rain, or snow melt), or to monitor the deformations of each slope. The risk management process formally requires considerations of the likelihood of sliding, the consequences, and hence the risk; and comparison of these calculated risks to risk acceptance criteria, accounting for financial and loss of life issues.

In many situations it will be sufficient to simply assess the likelihood of sliding in very approximate terms, and assess the travel distance, elements at risk, potential damage and loss of life using simple and empirical methods. The advantage of the risk management approach is that the process requires the formal consideration of the question “if the landslide did happen to occur, how far could it travel, how fast, and could it kill people” [1]. Figure 1 presents the difference in the risk management approach and the deterministic approach. Often, if the answer is yes, it may be that there are too great uncertainties in the understanding of the slope, or too great a reliance on observational approaches, so more detailed investigations, or defensive measures to reduce the hazard, on the consequences, are needed.

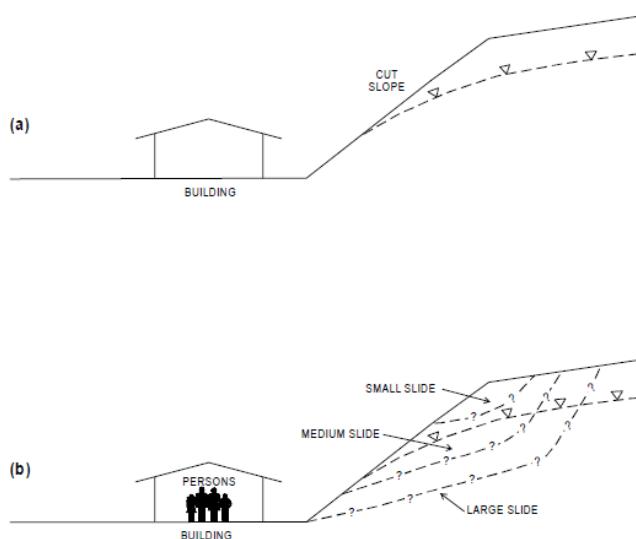


Figure 1. Deterministic (a) and risk management (b) approach [1]

For the deterministic approach the questions are:

What is Geometry, Geology, Hydrogeology? Shear Strength? Pore Pressure? What is factor of safety and sensitivity to assumptions? Is this acceptable? Taking into account the consequences?

For the risk based approach, the questions are: What is Slope Geometry, Geology,

Hydrogeology? Where? How big? And what is the probability of sliding? What will the slide mechanism be? How far will the slide travel? And how fast? Will there be warning signs? Will the slide reach the house/ How big? How fast? Will there be persons in the house? What is the vulnerability of the persons and the house? What is the risk to life and property? Is the risk acceptable?

In earthquake conditions, problems of geotechnical hazards occurrence become superior, wherefore additional attention is needed to understand the mechanism, define the critical parameters, assess, and mitigate the damage potential. Therefore, an interactive and integrated procedure—methodology for assessment of potential terrain instabilities is necessary. Practical and fast updating of different parameters of a given model, multiple mathematical tools and functions to combine data, and possibilities for data visualization by means of graphic characteristics are only part of the possibilities offered by geographic-information systems (GIS) in managing risks pertaining to geotechnical hazards. Nowadays, earth scientists mainly make use of (GIS)-based techniques and remote sensing data in order to map the geotechnical hazards and evaluate the risk within an area. In this paper GIS based approach is applied for two case studies for landslide and liquefaction potential assessment triggered by earthquake excitation.

3. Case study 1 – Hazard and risk assessment of earthquake induced landslides

3.1 Case study and methodology

Skopje - the capital of the Republic of Macedonia covers 1,854 km², has a population of 700 000 citizens (density of population of 273 citizens/km²) and represents an administrative, political and financial center of Macedonia. The intensive development of Skopje city, particularly after the 1963 earthquake [2], has been one of the main causes for the increase of the risk related to natural disasters. Namely, the built structures on steep terrains and the concentration of population and material property on potentially unstable locations considerably increase the risk pertaining to geotechnical hazards. In addition to the seismic activity of the territory of Macedonia, which can be one of the main triggering factors of loss of stability of slopes, there are also uncontrolled creation of landfills (that have lately created potentially unstable steep slopes), construction activities that do not comply with technical regulations and standards (cuttings, vertical excavation, etc.), intensive cutting and destruction of forests and vegetation in the terrain (contributing to occurrence of erosion and instability of surface soil layers), improper management of outflows, channels (increase of underground water table that causes reduction of effective strength of soil materials), etc.

The selected study area is squared proportioned 5 km x 5 km within the coordinates 7533000 meters to 7538000 meters, from west to east, and 464300 to 464800 from south to north and is located in a sub-urban area of the city of Skopje, in the southeast foothill of the Vodno mountain.

To create the necessary data base and documentation in GIS, from aspect of geotechnical parameters data in order to calculate the safety factor and critical acceleration, there have been collected and used data from a number of reports, geotechnical reports boreholes data from each geological unit, main and working designs on repair of already occurred instabilities in this area elaborated by IZIIS and other firms dealing with geotechnical

field investigations and measurements. Regional geotechnical properties such as the unit weight, cohesion, internal angle of friction and depth of soil failure were assigned to the geologic units of the 1:25,000 digital geologic map (Figure 2, a), based on the available data from boreholes and geotechnical reports. Based on these values, raster maps have been created which are involved directly into calculation of the safety factor and critical acceleration maps, (cohesion map, unit weight of soil material map, depth of slope failure map and internal angle of friction map, Figure 2, b).

The selected location is characterized by slope instabilities, poor infrastructure conditions and rapid growth [3]. Among the recent recorded landslides is the landslide in the municipality of Rakotintsi village that took place in 2005 causing serious damage to 45 family houses. The impact and the consequences of these instabilities are for now, on local scale but the possible consequences which arrive with taking into account the moderate to high seismic potential that is present at this region, than it can be concluded that this minor problems with the instabilities might cause a significantly larger destructive events in earthquake conditions such as earthquake triggered landslides. The main focus of this study is to verify that additional research is needed to evaluate the real risk that comes to the instability of the terrains in earthquake conditions especially in areas where there are already noticed instabilities in static conditions. Even though the presented slope instabilities are not associated with earthquake, this work focuses on the assessment of the landslide hazard and risk in earthquake conditions, having in mind the earthquake conditions in Republic of Macedonia which inevitably will increase the possible damages.

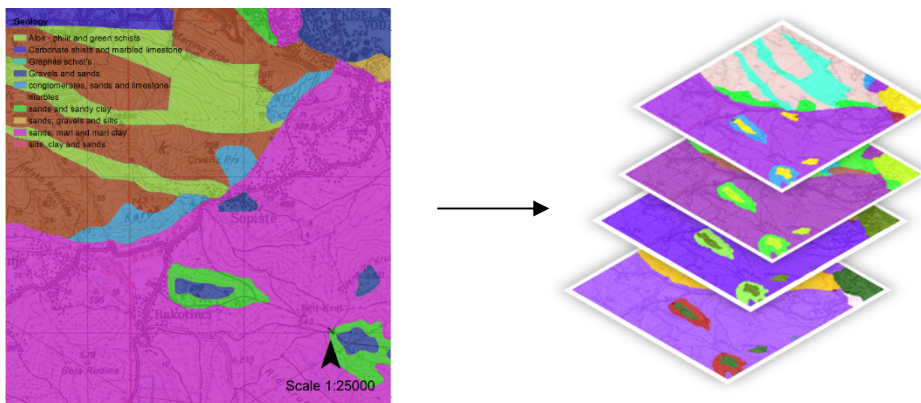


Figure 2. a) Geology map and **b)** Created raster maps of soil parameters (internal friction angle, material unit weight, cohesion and depth of instable soil layer)

From geological aspect, the study area in one part, along the Vodno slope, there is predominant presence of marbles, cypolines and shales that can be classified as stable media, whereas, in the foothill, there is presence of marlstone and marly clays that behave as stable in static and dry conditions and have a potential to be instable in water saturated and seismic conditions. Due to this reason, the following scenarios have been defined:

- Period with relatively low intensity of rains, i.e., natural dry conditions ($m = 0$). This corresponds to a height of the water level equal to zero;
- Period of moderate intensity of rains or snow melting i.e., conditions of relatively intensive precipitation ($m = 0.5$). This corresponds to a height of the water level that is equal to half of the height of the instable soil layer;
- Period of complete water saturation ($m = 1$) of the instable soil layer, which is a scenario with the greatest potential for occurrence of instabilities. This corresponds to a height of the water level that is equal to the height of the instable soil layer.

Pixel based computation of the safety factor formula (1), (Figure 3, b) for the three different scenarios of ground water saturation of the instable soil layer:

$$F = \frac{c' + (\gamma - m \gamma_w) z \cos^2 \beta \tan \phi}{\gamma z \sin \beta \cos \beta} \quad (1)$$

Where,

$m = z_w/z$ (nondimensional ratio of water height to the height of the instable soil layer)

β = slope of the terrain [$^\circ$] – (Figure 3, a).

z = the height of the instable soil layer [m]

z_w = the height of the water table above the surface failure [m]

By incorporating the module for computation of critical acceleration (eq. 2), maps have been created with the value of critical acceleration for the three scenarios of water saturation (Figure 3, c).

$$a_c = (FS - 1)g \sin \alpha \quad (2)$$

where, FS – safety factor, g = ground acceleration (m/sec²); α - slope of terrain ($^\circ$)

This parameter is explained as the value necessary for motion of the potentially instable soil mass. These maps describe, in fact, the level of susceptibility of the terrain to landslides in earthquake conditions. To obtain results as to how many of these landslides will occur under a given earthquake scenario, it is necessary to compare these maps with the expected accelerations for a certain analyzed area.

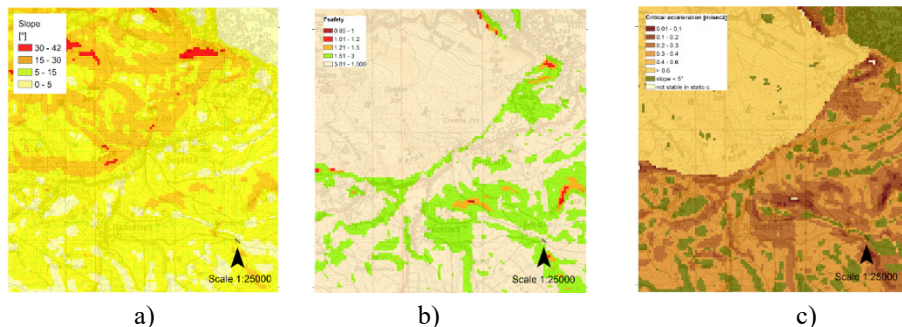


Figure 3. Slope map (a), factor of safety map (b) and critical acceleration map (c) for 50 % water saturation of the instable soil layer

3.2 Results and discussion

In this study, a simple qualitative approach was used to create an exposure map from the aspect of physical (direct) and systemic (indirect) vulnerability, Figure 4. The exposure map is of a unique value and simply represents the exposed elements at risk (houses, roads). The populated settlements of Sopsishte and KiselaVoda municipalities presented with individual houses and properties show the direct exposure of the area (the damage potential), while the only road that connects these settlements with the city center presents the indirect vulnerability of the region (social, economic vulnerability). The no exposure parts are the uninhabited parts of the city.

Based on the exposure map and the hazard maps for the three conditions of saturation, final risk maps with three levels of risk were created. Figure 5 shows the landslide risk map in earthquake conditions for 50 % water saturation ratio of the instable soil layer. The overlay method was used for creation of the risk maps as follows:

High risk = High hazard * exposure

Medium risk = Medium hazard * exposure

Low risk = Low hazard * exposure

The performed risk analysis provides a general overview of the possible affected areas in case of earthquake triggered landslides. In order to calculate the quantitative values of the risk, a detailed vulnerability analysis (extent of damage due to a certain hazard level) which should include typology of the buildings, social vulnerability in terms of exact information on population, economic analysis, etc, should be carried out. Still, the results obtained in this research provide an insight into the potential impact of the analyzed natural phenomena and the serious need for further investigations and measures to be taken toward dealing with them in future.

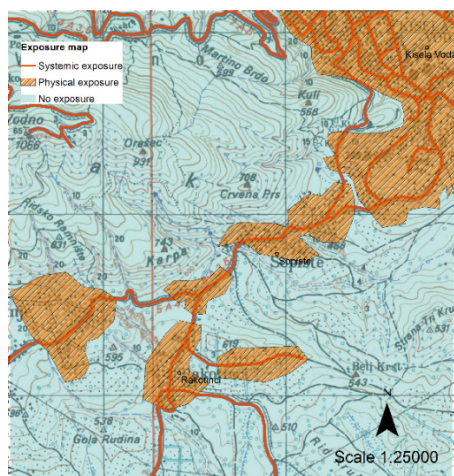


Figure 4. Exposure map of elements at risk

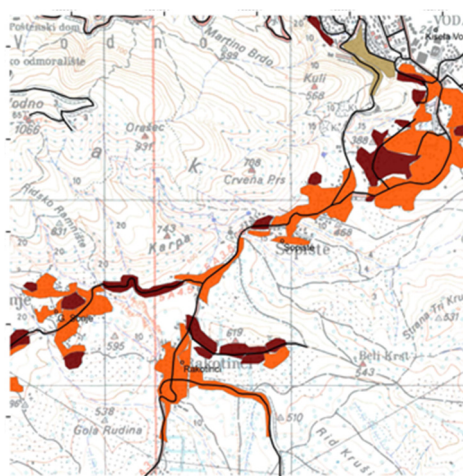


Figure 5. Landslide risk map in earthquake for 50 % saturation of unstable soil layer

The risk map can contribute to management of the development of the city by providing insight into the most critical points for the selected scenario of water saturation and

earthquake. As to the target area, it can be concluded that it has the potential for instability that, under certain scenarios, could result in economic and social damage (vulnerability of individual houses, vulnerability of infrastructure and alike). Facts that can increase the risk pertaining to the analyzed region are the following [4]:

- Uncontrolled construction of structures in potentially instable parts;
- Insufficient road infrastructure. There is only single road that connects the populated places with the main resources of Skopje city. If this road is affected by large geotechnical instabilities (landslides), it would be very difficult to provide urgent medical aid and evacuation of the injured from the isolated area;
- Individual houses that are located in the potentially instable zones are directly exposed to increased risk of destructive effects of landslides caused by earthquakes.

4. Case study 2 – Liquefaction hazard assessment

4.1 Applied methodology for zonation

In situ methods (SPT, CPT) for liquefaction assessment can be considered as most popular approach to define the liquefaction potential for several reasons. Namely is practical, it has an advantage over the difficulties and costs associated with high-quality undisturbed sampling for high-quality laboratory testing. Moreover, the same factors that affect SPT, CPT resistance also affect the liquefaction resistance (i.e., overconsolidation, non-uniformity, density, fines content etc.). As a methodology it has been analyzed by several authors [5], [6], [7], [8] and it relies and is based on selected case histories.

The liquefaction potential can be expressed by the factor of safety (F_s) or as probability for liquefaction (PL). The probabilistic liquefaction triggering models are crucial for developing the relatively new framework for evaluating liquefaction hazards - the performance-based liquefaction assessment procedure [9].

The relationships obtained by the probabilistic approach are to some extent recent, and their development is needed for the purpose of more representative evaluation of locations of moderate seismicity for which the deterministic relationships have proved to be a kind of an upper bound.

Namely, the results obtained from deterministic methods for locations of a moderate hazard considerably over predict the liquefaction hazard – the safety coefficients are around 1, which points to a liquefaction potential, but still, that value of the safety coefficient is associated with relatively small probabilities for liquefaction occurrence.

So far, in the R. Macedonia, several investigations have been carried out for definition of the liquefaction potential by application of field methods and use of the deterministic approach [10], [11], [12], [13], [14] (Cubrinovska, 2009, Sesov et al. 2012, Bojadjeva et al. 2013, Bojadjeva et al. 2016, Chaneva, 2018). Considering the fact that R. Macedonia is a country characterized by moderate to high seismicity, the extension of knowledge and investigations in the field of these methods where the probability for occurrence of liquefaction is included would be of an extraordinary importance for further application in a number of additional activities and investigations for more

detailed definition of the liquefaction hazard. Namely, recent history has seen a number of earthquakes with a magnitude greater than 5 in the territory of R Macedonia, without recorded cases of liquefaction occurrence. It is exactly at this point that a question is posed as to the probability for occurrence of such type of soil instability in the case of different magnitudes, i.e., earthquakes with different return periods.

SPT is the most frequently applied field investigation in the engineering practice in R. Macedonia. This and the fact that the methods for evaluation of the liquefaction potential based on these investigations have continuously been developed and updated in literature and the fact that they have been “favored” in EUROCODE 8 has made them the subject of the investigation presented in this paper.

The location used as a case study is in Ohrid, as a specific area with high underground water table, complex geological conditions and moderate level of seismicity. The liquefaction potential was computed for all layers of the selected soil profile. The city of Ohrid is in southwest Macedonia, in the northeastern part of the Ohrid Lake. The available results from geological investigations and maps show that the soil in and around the city generally consists of surface Quaternary and deep Pliocene sediments. For the selected area, 16 locations for which results from geotechnical investigations within SPT investigations were made available by the geotechnical company GEING Krebs und Kiefer International, Skopje, were analyzed. These are in different parts of the city of Ohrid, but most of them lie along the lake coast, i.e., in the part where the underground water table is the highest. All 16 locations were analyzed in respect to their susceptibility and the liquefaction potential was assessed.

The evaluation of liquefaction potential has three major steps:

- 1) Calculating the liquefaction resistance (CRR)
- 2) Calculation of the cyclic stress (CSR)
- 3) Calculation of safety against liquefaction (FSL)

4.2 Created GIS maps for selected seismic scenarios

In table 1 classification of zones for maps with presentation of the coefficient of safety against liquefaction occurrence (F_s) is presented. The proposed classification is done according to the recommendations given in EUROCODE 8 (EN 1998-5-2004 (E)) Article 4.1.2.: *The liquefaction potential is small and no improvement of the soil for safety coefficient $F_s > 1.25$ is necessary.* Table 2 represents the classes for zonation of the probability maps.

Table 1. Zonation of the factor of safety for liquefaction potential

$F_s \leq 1$	Locations with very high liquefaction potential	(Red zone)
$1.01 \leq F_s \leq 1.25$	Locations with moderately high liquefaction potential	(Yellow zone)
$F_s \geq 1.25$	Locations with low liquefaction potential	(Green zone)

Table 2. Zonation of the probability for liquefaction (Pl)

Probability [%]	Safety coefficient	Zoning
PL < 10	$F_s < 1,03$	
10,01 - 50	1,03 – 0,87	

$50,01 < PL < 70$	$0,87 - 0,82$	
$70,01 < PL < 95$	$0,82 - 0,70$	
$95,01 < PL < 100$	$0,70 - 0,50$	

It is necessary to comment that, due to the fact that the maps are created by interpolation among the values of the parameters (F_s и PL), their exactness for the areas for which there are no available geotechnical reports or the available ones refer to a greater distance, can be increased by updating the database of the maps, i.e., increasing the number of geotechnical investigations whose results are used as basic documentation.

Still, Ohrid is a location where, magnitudes around $M_w = 5$, are most typical, and there is no liquefaction case yet registered. This goes in favour of the results from the probabilistic triggering models.

As final product from the analysis 4 maps were created which are presented in Figure 6 and 7:

1. F_s (against liquefaction) of the critical layer for seismic scenario – $M_w = 5$, $a_0 = 0.15g$;
2. F_s (against liquefaction) of the critical layer for seismic scenario – $M_w = 6$, $a_0 = 0.25g$;
3. PL (probability of liquefaction) for seismic scenario – $M_w = 5$, $a_0 = 0.15g$;
4. PL (probability of liquefaction) for seismic scenario – $M_w = 6$, $a_0 = 0.25g$.

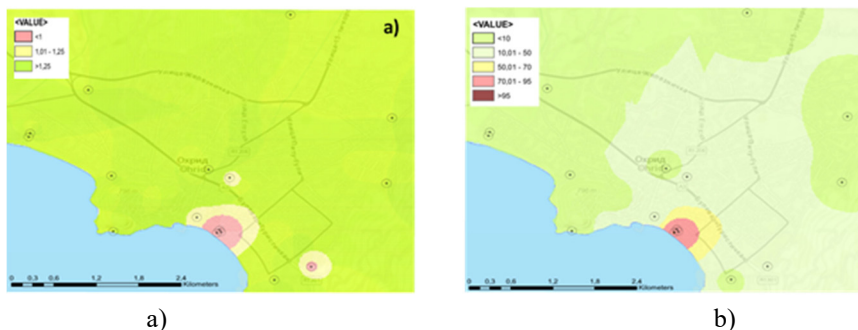


Figure 6. (a) Factor of safety against liquefaction map (b) Probability of liquefaction map for Ohrid, Macedonia for seismic scenario $M_w=5$, $a_g=0.15g$

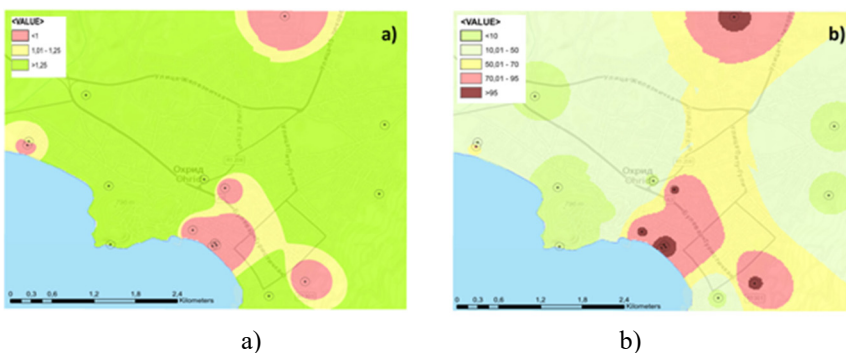


Figure 7. (a) Factor of safety against liquefaction map (b) Probability of liquefaction map for Ohrid, Macedonia for seismic scenario $M_w=6$, $a_g=0.25g$

Based on the investigations presented in this paper the following conclusions can be made:

So far, in several case studies in R. Macedonia where field methods for evaluation of liquefaction potential were used, the analyses were done by use of the deterministic approach, i.e., through coefficient of safety against liquefaction occurrence.

The probabilistic models include a probability factor in the analysis where $F_s < 1.2$. In other words, they perform a new classification of zones per percentage [%] of probability where the deterministic ones indicate a red zone. This has been the main motivation for the performance of such an evaluation of a site that has recently been affected by a series of earthquakes among which an earthquake with a magnitude of $M_w=5.2$, with no record of liquefaction occurrence.

The results show that, for some locations that are in the red zone, according to F_s map, the probability for liquefaction occurrence in compliance with the Boulanger & Idriss model is very low to moderate. Thus, the probabilistic approach give improved insight to the real associated risk of liquefaction damage to a certain site.

5. Conclusion

The results on the potential instabilities, i.e., level of hazard for a given analyzed location would have no significance if, no human or material property were at stake. The main purpose of risk assessment is to define, by connecting the information on hazard with the vulnerability level from economic, social and physical aspect, the level of risk pertaining to the natural hazard for a given location. By defining the risk for a given area, a safer urban development can be achieved by avoiding or managing the potential instable zones.

In general, local roads and transportation system are crucial parts of infrastructure in the post-earthquake relief operations. In advance planning and more resources should therefore be allocated for their seismic retrofitting. The purpose of retrofitting is to provide all the communities in the concerned area with an appropriate access to at least one transport connection after a strong earthquake.

Generally, this type of maps should serve as indicators of the red zones of geotechnical instabilities or different hazards in general. For further decision, additional laboratory and numerical analyses of the critical soil layers for greater accuracy in evaluating the potential of liquefaction and landslides and the possible consequences are recommended.

References:

- [1] Fell, R., Hungr, O., Leroueil, S., Riemer, W., (2000). Keynote lecture-Geotechnical engineering of the stability of natural slopes, cuts and fills in soil. *Geo Eng 2000*, 1. Technomic, Lancaster, pp. 21–120.
- [2] Petrovski, Jakim T. "Damaging effects of July 26, 1963 Skopje earthquake." *Middle East Seismological Forum, Cyber Journal of Geoscience Volume Two*. 2004.
- [3] Blinkov I., Mincev I. and Trendafilov B. (2008). *Erosion Risk Analyses on the Vodno Mountain and Impact to the Surrounding Areas*. BALWOIS 2008, Ohrid, Republic of Macedonia.

- [4] Bojadjieva, J., Sheshov, V., & Bonnard, C. (2018). Hazard and risk assessment of earthquake-induced landslides—case study. *Landslides*, 15(1), 161-171.
- [5] Youd et. al., April 2001 – “Liquefaction Resistance of Soils: Summary Report from 1996 NCEER/NSF Workshops on Evaluation of Liquefaction Resistance of Soils”, *Journal of Geotechnical and Geoenvironmental Engineering*.
- [6] Cetin K.O., Seed R. B., Der Kiureghian A., Tokimatsu K., Harder Jr. L. F., Kayen R. E., Moss R.E.S., “Standard Penetration Test-Based Probabilistic and Deterministic Assessment of Seismic Soil Liquefaction Potential”.
- [7] Idriss I. M., Boulanger R. W., December 2010, “SPT-BASED LIQUEFACTION TRIGGERING PROCEDURES” Report no. UCD/CGM-10/02 University of California at Davis.
- [8] Boulanger R. W., Idriss I.M. (2014), “CPT and SPT Based Liquefaction Triggering Procedures”, Report no. UCD/CGM-14/01, University of California at Davis.
- [9] Kramer, S. L., Mayfield, R. T., & Huang, Y. M. (2006). Performance-based liquefaction potential: a step toward more uniform design requirements. In *Proceedings of the US-Japan workshop on seismic design of bridges*. Bellevue, WA.
- [10] Cubrinovska, E., (2009), “Foundation of Structures in Urban Media with Liquefaction Potential”, (in Macedonian), master thesis, UKIM-IZIIS.
- [11] Bojadjieva J., Sesov V., Edip K. and Gjorgjiev I., 2013 “Evaluation of the Liquefaction Potential in Complex Geological Conditions” 15th International Symposium of Macedonian Association of Structural Engineers (MASE) 18-21, Struga, Macedonia.
- [12] Bojadjieva J., V. Sesov, K. Edip. 2016. “A Case Study of Liquefaction Assessment for Business Center in City of Skopje” ACUUS, Ss. Petersburg, Russia, 2016.
- [13] Chaneva, J., Bojadjieva, J., Sheshov, V., Edip, K. and Kitanovski, T. (2018), Application of deterministic and probabilistic - SPT based liquefaction assessment triggering models. *ce/papers*, 2: 603-608. doi:10.1002/cepa.736.
- [14] Sesov V., Edip K., Cvetanovska J., September, 2012, “Evaluation Of The Liquefaction Potential by In-Situ Tests And Laboratory Experiments in Complex Geological Conditions”, 15th World Conference on Earthquake Engineering, Lisbon, Portugal, 24 – 28.

NUMERICAL SIMULATION OF SOIL CONSOLIDATION AS A GEOTECHNICAL PHENOMENON

KEMAL EDIP¹, VLATKO SHESHOV², JULIJANA BOJADJEVA³ TONI KITANOVSKI⁴,
JORDANKA CHANEVA⁵, DEJAN IVANOVSKI⁶

¹ Institute of earthquake engineering and engineering seismology (IZIIS), Macedonia,
kemal@iziis.ukim.edu.mk

² Institute of earthquake engineering and engineering seismology (IZIIS), Macedonia,
vlatko@iziis.ukim.edu.mk

³ Institute of earthquake engineering and engineering seismology (IZIIS), Macedonia,
jule@iziis.ukim.edu.mk

⁴ Institute of earthquake engineering and engineering seismology (IZIIS), Macedonia,
tonik@iziis.ukim.edu.mk

⁵ Institute of earthquake engineering and engineering seismology (IZIIS), Macedonia,
dance@iziis.ukim.edu.mk

⁶ Institute of earthquake engineering and engineering seismology (IZIIS), Macedonia,
ivanovski@iziis.ukim.edu.mk

Abstract

In recent years many problems in geotechnical engineering remain unsolvable, in spite of the impressive progresses attained in numerical analysis, discretization techniques and computer science during the last decade, because their numerical complexity is simply incomprehensible. In simulation of water flow problems in geotechnical problems the geo-materials are considered by taking into account both the mass transport and water flow equations. This part of geomechanics considers the transport problems in aquifers, displacements due to soil consolidation, design of safe containers etc. Simulation of such problems using the finite elements concludes the full interaction of the pore pressure with the soil skeleton. It is to be stated that these models based on fully coupled formulation require the simultaneous solution of fluid flow equations and equilibrium equations in terms of displacements. Thus the degrees of freedom per node correspond to both displacement and pore pressures. The form of the stresses used in this type of simulations assumes the soil skeleton as incompressible which is a common assumption in soil mechanics. To account for compressible grains, the Biot coefficient α should appear in front of the pore pressures in order to account for the compressibility factors. The soil medium has various components such that it can be also called a multiphase body. It follows that observed at a macroscopic scale soil media can be considered as mixtures.

The objective of this study is to present the applicable numerical simulations in order to consider both soil skeleton stress development and pore pressure distribution in soil media. The model is developed as a coupled displacement-pressure formulation in which the porous medium is composed of a soil skeleton and water in the pores. The considered problem in this paper is the consolidation of a saturated soil layer subjected to uniform pressure at the top. The coupled mathematical model addressed in this work considers both drained and undrained boundary conditions in the consolidation problem. The consequent mathematical model involves equations of mass and momentum balance for the whole system. Interesting outcomes are achieved from the numerical simulation in which it is clearly seen that the water flow influences the overall consolidation results.

Keywords: soil consolidation, numerical simulation, multiphase flow.

1. Introduction

In geotechnical problems the geo-materials are considered by taking into account both the mass transport and flux equations. This part of geomechanics considers the transport problems in aquifers, displacements due to soil consolidation, design of safe containers etc. Simulation of such problems using the finite elements includes the full interaction of the pore pressure with the soil skeleton. It is to be stated that these models based on fully coupled formulation require the simultaneous solution of fluid flow equation and equilibrium equations in terms of displacements. Thus the degrees of freedom per node correspond to both displacement and pore pressures. The soil medium has various components such that it can be also called a multiphase body. It follows that observed at a macroscopic scale soil media can be considered as mixtures [1]. A detailed description of the porous media is not the scope of this paper although consolidation problem has been taken into consideration. The consolidation problem of a soil layer is known since the work of Terzaghi [2] and Biot [3]. In classical fully saturated consolidation the boundary conditions are drained during the entire calculation while the flow of water out of the region of interest is considered. In the work of Zienkiewicz [4] it is shown that any constitutive relations of the soil skeleton can be defined incrementally since it is assumed that changes in the pore pressure do not cause any strain change in the porous solid material. In the literature different versions of effective stress principles are proposed [5]. Therefore, the effective stress principle in saturated soils is considered following the work of Verruijt [6].

In the present work, the analysis of water flow through saturated soil, coupled with the mechanical behavior of the soil skeleton is considered. A mathematical framework assuming porous medium in which the voids of the medium are filled with water is considered and the solution of the partial differential equation system is solved using the finite element method. The numerical model involves both momentum and mass balance equations.

2. Governing equations

In saturated porous media the governing equations considering the dynamic problem are the mass balance and the momentum conservation equations. Following the work of Oettl [7] the momentum balance and mass conservation equations of fluid saturated medium are combined yielding the following two equations.

$$\nabla \cdot \dot{\mathbf{u}} + \left(\frac{1-n}{K_s} + \frac{n}{K_f} \right) \dot{p} + \nabla \cdot \mathbf{v} = 0 \quad 2.1$$

$$\rho \ddot{\mathbf{u}} = \nabla \cdot \boldsymbol{\sigma} + \rho \mathbf{b} \quad 2.2$$

In equation 2.1 the term $\dot{\mathbf{u}}$ stands for the solid velocity, K_s and K_f denote the bulk modulus of solid and fluid phases. In equation 2.2 the term $\ddot{\mathbf{u}}$ is the acceleration of the solid phase, \mathbf{b} is the body force and $\boldsymbol{\sigma}$ is the Cauchy stress tensor. The term ρ denotes the density of the medium and can be written as

$$\rho = (1-n)\rho_s + n\rho_f \quad 2.3$$

In equation 2.3. the terms ρ_w and ρ_s denote the densities of water and solid phases. The effective stress tensor is given as:

$$\boldsymbol{\sigma}' = \boldsymbol{\sigma} - p\mathbf{I} \quad 2.4$$

The relative fluid velocity \mathbf{v} is governed by the Darcy's law and can be written as:

$$\mathbf{v} = -\frac{\mathbf{k}}{\rho_f \mathbf{g}} \cdot (\nabla p - \rho_f \mathbf{b} + \rho_f \ddot{\mathbf{u}}) \quad 2.5$$

where \mathbf{k} is the permeability tensor, \mathbf{g} is the gravity and ∇p is the gradient of pressure.

In order to derive the finite element matrices the weighted residual ^{method} is applied to the formulas above. The displacement vector \mathbf{u} of the solid skeleton and the pore pressure \mathbf{p} are chosen as the basic variables of the problem. The finite element discretization in space is presented by the following system of equations:

$$\begin{bmatrix} 0 & 0 \\ \mathbf{C}_{sw}^T & \mathbf{P}_{ww} \end{bmatrix} \begin{bmatrix} \dot{\mathbf{u}} \\ \dot{\mathbf{p}} \end{bmatrix} + \begin{bmatrix} \mathbf{K} & -\mathbf{C}_{sw} \\ 0 & \mathbf{H}_{ww} \end{bmatrix} \begin{bmatrix} \mathbf{u} \\ \mathbf{p} \end{bmatrix} = \begin{bmatrix} \mathbf{f}_u \\ \mathbf{f}_w \end{bmatrix} \quad 2.6$$

In the equation 2.6 the matrix \mathbf{C}_{sw} stands for coupling between solid and water phases. The matrix \mathbf{P} stands for compressibility, matrix \mathbf{H} for permeability. More detailed explanation for the derivation of the constituent matrices can be found in the work of the author [8].

3. Numerical examples

The coupled finite element method has been implemented into the finite element software ANSYS [9]. As a verification example a consolidation problem for water saturated soil is simulated. Similar investigations concerning the consolidation of a saturated soil layer have been done in the works of other authors such as Hwang [10], Fredlund [11], Oettl [12] etc. The application of the proposed model is tested in a problem of elastic consolidation for which two different initial boundary conditions are defined. The model used in this example is taken from the work of Oettl [12]. In this example a consolidating soil layer with a height of 8.0m is taken into consideration. In the horizontal direction the model has a width of 40.0m. The length of the loaded area is long as the depth of the soil layer. The lower boundary is fixed while on the side boundaries the horizontal displacements are impeded. Considering the coupled analysis, the water flow is not allowed on the bottom and side boundaries. The contact of soil layer and the applied stress on the top boundary is considered as a) drained and b) undrained boundary conditions. The boundary and initial conditions are given in the figure below:

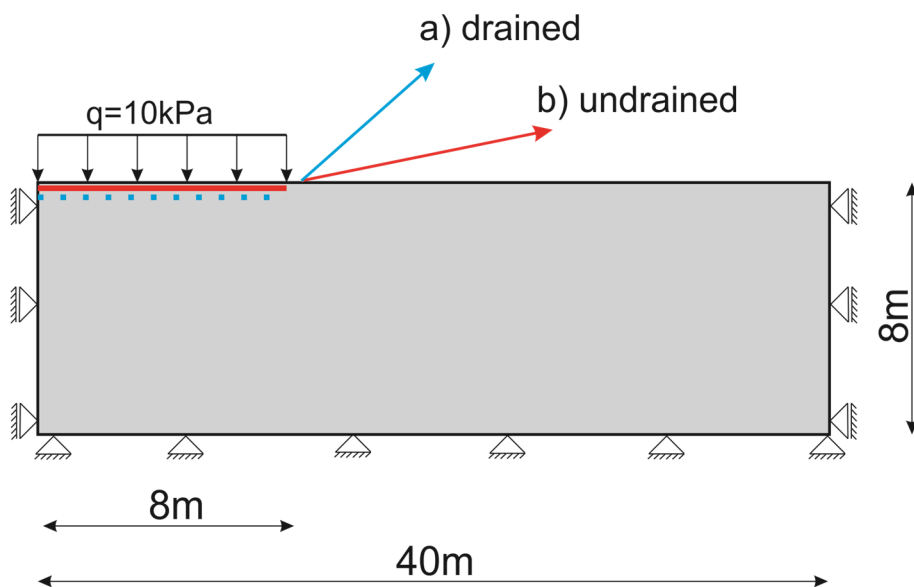


Fig. 1. Model of soil layer with boundary conditions

The initial stress that is applied on the soil layer is a uniform stress of 10kPa. The consolidation analysis of the soil layer is done until the water has flowed out totally from the soil layer. In the numerical simulation the consolidation analysis is performed for 1000 seconds. The soil layer parameters are given in the table below.

Table 1. Material properties for analysis of soil consolidation

Young's modulus of elasticity	$E = 5000 \text{ kPa}$
Poisson's ratio	$\nu = 0.1$
Density of solid phase	$\rho = 2.7 \text{ ton/m}^3$
Density of water	$\rho = 1.0 \text{ ton/m}^3$
Initial porosity	$n = 0.5$
Permeability	$k = 1.5 \times 10^{-13} \text{ m/s}$

Two cases of analysis are performed. In the first case a drained boundary is considered at the top layer.

In the second case the same domain is simulated by applying undrained boundary conditions on the region where force is applied. In both cases analysis has been performed beginning from time $t=0.001$ seconds. The results concerning the pore pressure for both cases are given in Fig. 2 below. As can be seen from the Fig.2 in the case of drained boundary there is sudden increase in the pore pressure at the mid height of the soil layer. On the other hand, in the undrained case the sudden increase in the pore pressure is hindered although there is an increase in the pore pressure. This clearly shows that in the case of drained boundaries the load is carried by the water in the pores totally. In the undrained case the load carrying is shared between the solid particles and water in the pores.

When concerning the effective stress development during the consolidation stage the effective stress development through time takes longer than in the case of drained boundary conditions.

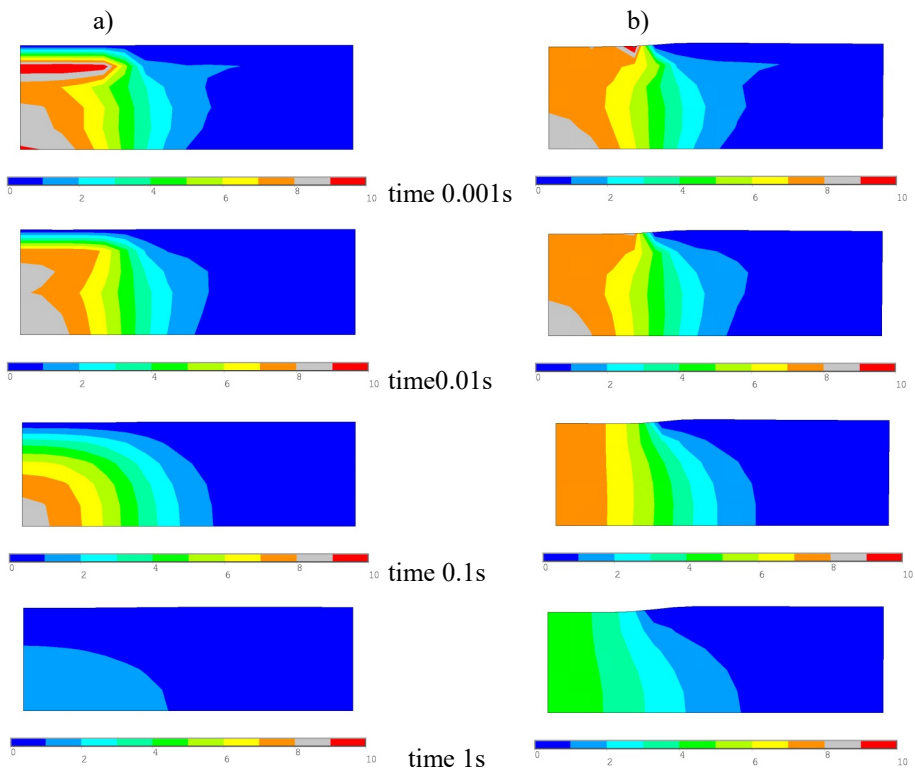
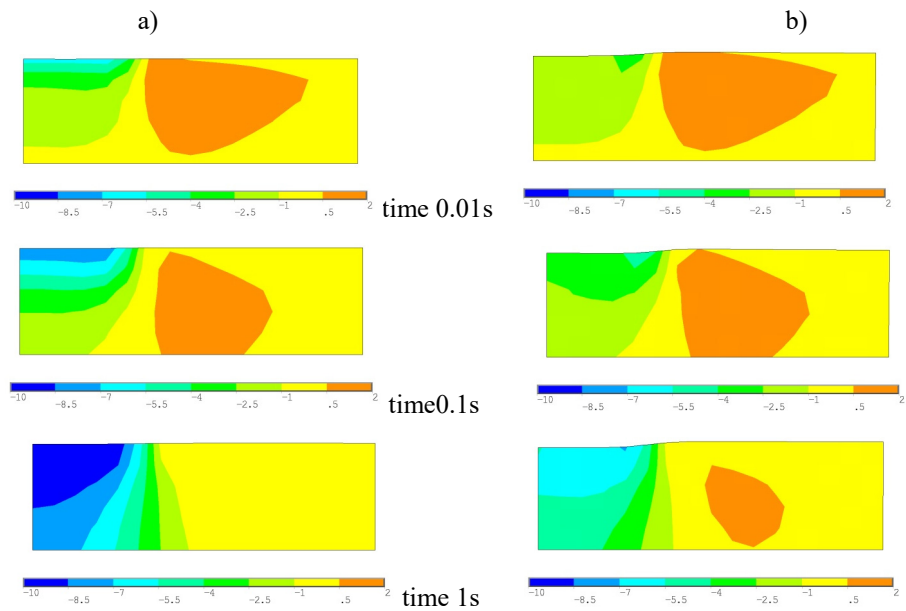


Fig. 2. Development of pore pressure in consolidation process



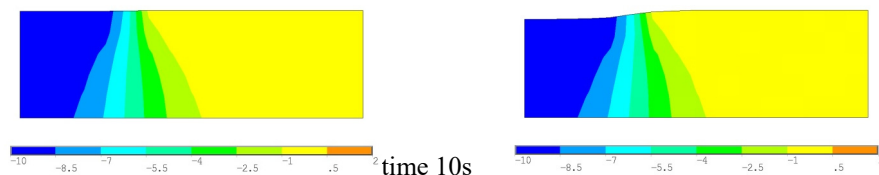


Fig. 3. Development of effective stress in consolidation process

From Fig.3 it is seen that the effective stress in consolidation stage of drained and undrained boundary conditions reveal the same end result although the time to reach the final effective stress is different. This is due to the boundary conditions of the consolidation process. In the first case of drained boundary condition the time needed for total consolidation is 2 seconds. On the other hand, in the case of undrained boundary conditions the time needed for total consolidation is 10 seconds. The stress distribution is in correlation with the deformation during the consolidation process.

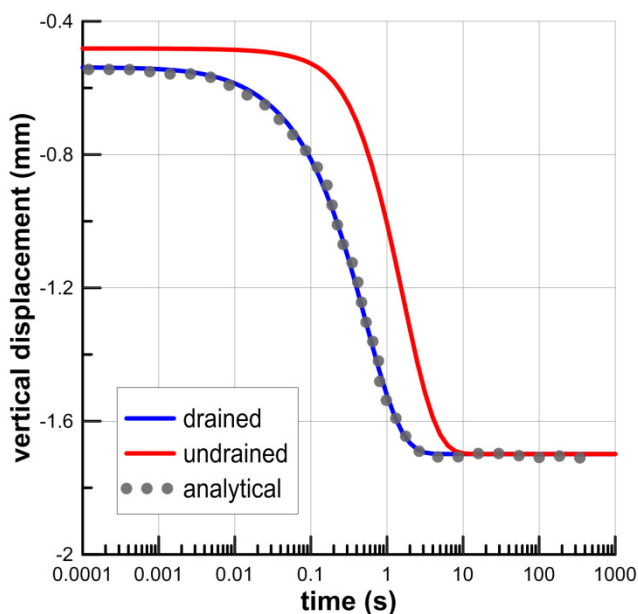


Fig. 4. Comparison of vertical displacement in drained and undrained and analytical drained results

As can be seen from Fig. 4 the consolidation at the end time has the same value in both cases of drained and undrained boundary conditions. The difference is in the time to develop the final consolidation. The obtained values correspond with the analytical results as given in the work of Lewis et. al [13]. Thus it can be stated the model predicts the analytical values in a good manner. The difference in vertical displacement development time proves the correctness of the applied numerical model.

4. Conclusion

In this paper a numerical model concerning the porous medium is presented by considering the interaction between the solid displacement and pore pressure in porous

medium. The model is applied to a plane strain consolidation of a saturated soil layer subjected to uniform loading at the top of the soil layer. The investigation in this particular paper has shown that the boundary conditions do play an important role in defining the consolidation of the soil layer. As can be seen from the results the drained boundary at the contact with the applied force consolidates faster when compared with the undrained boundary condition. Although the end results are same the development of the effective stress development at a point in a saturated medium depends on the pore pressure at that particular point.

References

- [1] Alcoverro, J., The effective stress principle. *Mathematical and Computer Modelling*, 2003. 37(5–6): p. 457-467.
- [2] Terzaghi, K., *Theoretical soil mechanics*. 1943.
- [3] M.A.Biot, Theory of elasticity and consolidation for porous anisotropic solid. *Journal of Applied Physics*, 1955. 26(2): p. 182-185.
- [4] Zienkiewicz, O.C., C. C.T., and P.Bettess, Drained, undrained, consolidating and dynamic behaviour assumptions in soils. *Geotechnique*, 1980. 30(4): p. 385-395.
- [5] Boer, R. and W. Ehlers, The development of the concept of effective stresses. *acta mechanica*, 1990. 83(1-2): p. 77-92.
- [6] Verruijt, A., *Consolidation of Soils*, in *Encyclopedia of Hydrological Sciences* 2006, John Wiley & Sons, Ltd.
- [7] Oettl, G., R. Stark, and G. Hofstetter, Numerical simulation of geotechnical problems based on a multi-phase finite element approach. *Computers and Geotechnics*, 2004. 31(8): p. 643-664.
- [8] Edip, K., *Development of three phase model with finite and infinite elements for dynamic analysis of soil media*, 2013, Ss. Cyril and Methodius: Institute of Earthquake Engineering and Engineering Seismology.
- [9] ANSYS. *Fem Software*. 2006.
- [10] Hwang, C., N. Morgenstern, and D. Murray, On solutions of plane strain consolidation problems by finite element methods. *Canadian Geotechnical Journal*, 1971. 8(1): p. 109-118.
- [11] Fredlund, D.G. and J.U. Hasan, One-dimensional consolidation theory: unsaturated soils. *Canadian Geotechnical Journal*, 1979. 16(3): p. 521-531.
- [12] Oettl, G., *A Three-Phase FE-Model for Dewatering of Soils by Means of Compressed Air*, 2003, Universitaet Innsbruck.
- [13] Lewis, R.W. and B.A. Schrefler, *The finite element method in the static and dynamic deformation and consolidation of porous media*, 1998: Second Edition, Wiley Verlag.

HYDROLOGICAL ANALYSIS OF HIGH INTENSITY RAINFALLS OVER TOPOLNICA TAILING DAM

BOJAN SUSINOV¹, MIHAIL NAUMOVSKI², JOSIF JOSIFOVSKI³,

¹ Ss Cyril and Methodius University, Faculty of Civil Engineering - Skopje, R. N. Macedonia,
susinov@gf.ukim.edu.mk

² Ss Cyril and Methodius University, Faculty of Civil Engineering - Skopje, R. N. Macedonia,
naumovskimgf@outlook.com

³ Ss Cyril and Methodius University, Faculty of Civil Engineering - Skopje, R. N. Macedonia,
jjosifovski@gf.ukim.edu.mk

1. Abstract

This paper presents the results from the hydrological analysis of the intensive rainfalls over the area of the Topolnica tailing dam. The main objective was to define extreme rainfall events and to obtain the basic parameters for analyzing the stability of the dam and the influence of the intensive rainfalls. In other words, to define the characteristic values of the intensive rainfalls of a given duration and probability of occurrence. A precipitation hydrograph in 10 minutes' intervals for a three-year period from 2016 to 2019 was created. To analyze the pluviographic measurements, a standard methodology was proposed. Thus, rainfall data series of monthly precipitation were formed. In order to determine the probability distribution function for each data series, a standard methodology based on methods of mathematical statistics and probability theory was used. A relationship between the probability of occurrence of the maximum intensive rainfall is also plotted in function of the amount of precipitation and characteristic durations. Finally, this paper provides information on the extreme rainfall events over the investigated area, which can be used not only to analyze the dam stability and slopes erosion control, but also for hydrological analysis of flood wave propagation in the catchment area necessary for the design and maintenance of the drainage and overflow systems, determining the risk level of damage by extreme events etc.

Keywords: intensive rainfalls, tailing dam, probability distribution, rainfall data series, probable maximum precipitation

2. Introduction

We still have fresh memories of the Skopje flood in August 2016 which caused great damage to human lives and properties. This hydrological extreme event was caused by short-duration rainfall of over 100 l/m² for 4 hours or 46 l/m² in just one hour. High intensity and short-duration rainfalls is one of the areas in hydrometeorology that is relatively rarely investigated in our engineering experience. Nowadays, the study of rainfall characteristics in terms of climate change has attracted everybody's attention. Rainfalls as a stochastic process are studied with statistical methods and probability

theory. The results are useful when solving various technical and scientific problems in the field of hydrology agriculture, water management, etc. [1]. Several researchers have so far investigated the intensity rainfalls as meteorological phenomena. K. Milosavljevic studied short-duration rainfalls in 1952 with a probability of occurrence from once a year to once in 5 years for Prilep weather station. A. Lazarevski in 1967, as a member Hydro Meteorological Institute, used long-term data to analyze the intensive rainfall at standard intervals of 5, 10, 15, 20, 45, 60, 80, 100 and 120 minutes, for 7 meteorological stations: Skopje, Bitola, Ohrid, Prilep, Kriva Palanka, Demir Kapija and Struga [2]. His study gives pluviographic measurements; intensive rainfall events curves as well as other comparative graphs for the mentioned stations. Z. Shkoklevski and B. Todorovski in 1993 defined the intense extreme precipitation with duration from 5 minutes to 1440 minutes (24 hours), based on measurements with pluviographs and formed database, by forming intensive rainfall ranges for meteorological stations.

The aim of this paper is to process the measurements from the meteorological station of Topolnica tailing dam and to provide a solid basis for analyzing the stability of the dam and the influence of the intensive rainfall.

3. Measurements and location

In this paper, the rainfall measurements over the Topolnica tailing dam will be processed. The data refers to relatively short period of three years from 2016 to 2019. Topolnica tailing dam is built within the copper-mine Bucim which is located between the city of Stip and Radovis, East part of N. Macedonia. With its height of 134.0 m (654.0 m a.s.l) is one of the highest tailings dam in Europe [3]. The dam is constructed by pulp hydro cycling method. Namely, a downstream dam is created from the sand and the spillway from the hydro cyclones is realized in the upstream deposit lake. Figure 1 shows a typical cross section of the tailings dam Topolnica.

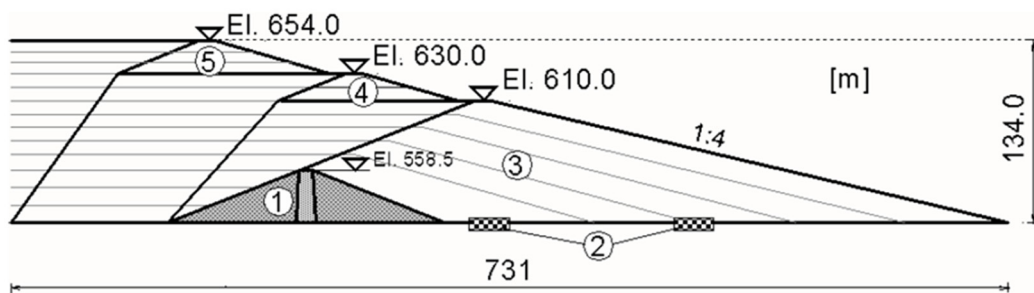


Figure 1. A cross section of Topolnica tailings dam. (1) Initial dam; (2) Longitudinal base drainages; (3) First phase sand dam constructed using downstream method; (4) Second and (5) Third phase sand dam constructed using upstream method

The meteorological station is located 654 m a.s.l. on the right side of the dam crown. The coordinates of the station are $X=41.668927^\circ$ and $Y=22.370122^\circ$.

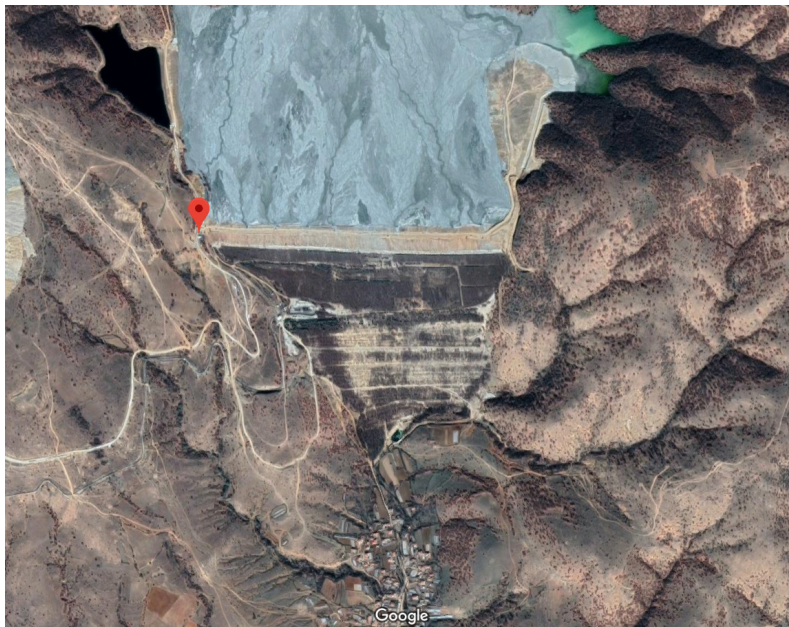


Figure 2. Ground plan of the tailing dam and meteorological station location (source: <https://www.google.com/maps>)

The analyzed rainfalls are measured by the weather station PCE-FWS 20 with the ability to measure temperature, humidity, atmospheric pressure, wind and precipitation [4]. It is also equipped with data logger for data storage and software for results analysis in real time. The shortest recording time interval is 10 minutes.



Figure 3. Weather station PCE-FWS 20 (source: <https://www.pce-instruments.com>)

4. Methodology

The pluviograms processing methodology from which the rainfall intensity can be calculated includes:

- A preliminary selection of pluviograms for a designed period, for which major rainy episodes or intensive rainfalls are recorded. From such selected pluviograms, the highest rainfall levels h_i of a given duration t_i (10, 20, 40, 60, 90, 120, 180, 300, 720 и 1440 minutes);
- Forming a table from basic processing data – pluviographs readings. Once the pluviogram for 24 hours in 10 minutes' time intervals is formed, the records of characteristic transversal points are read in 10 minutes' accuracy. The time is inserted in the first column of the Table 1. The second and third column present the time interval duration in minutes and the rainfall height recorded between two time points t_i and t_{i+1} in mm, respectively. The last column shows the calculated rainfall intensity i in the interval between t_i and t_{i+1} in mm/min;
- Forming a table (data series) of monthly (annual or daily) maximum rainfall heights. Based on the results from the preliminary selected pluviograms, a data series of monthly maximum rainfall heights h_i [mm] of a specified duration $t=10, 20, \dots, 1440$ min. Within any analyzed month or year, the maximum amount of precipitation with a specified duration must be greater than the maximum rainfall height whose designated duration is lower;
- Forming a data series of monthly precipitation empirical probability from which the statistical parameters of the data series can be calculated. The probability of occurrence of maximum intensive rainfall is calculated using probability density functions. For selecting the best-fit probability distribution, the choice of probability distribution models is crucial. The Gumbel distribution can be used when analyzing a maximum process;

5. Data processing

A precipitation hydrograph in 10 minutes' intervals for the selected three-year period was constructed.

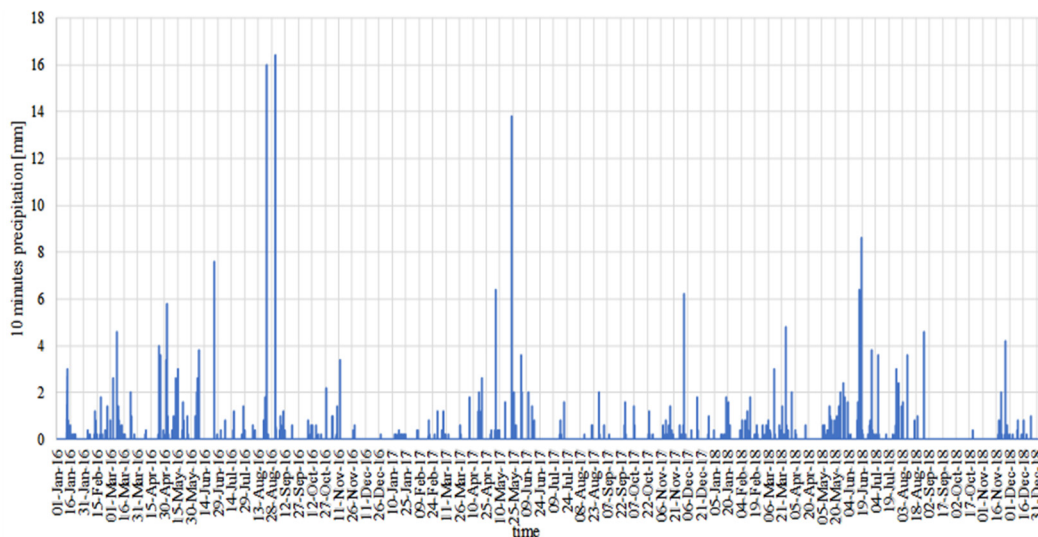


Figure 4. 10-minute rainfall hydrograph between 1 January 2016 and 31 December 2018

From the presented hydrograph, a processed pluviogram was selected for a 24-hour period for which maximum daily precipitation was observed (23.5.2017, 17:10 h - 24.5.2017, 17:10 h.). The results are shown in Table 1.

Table 1. Pluviogram processed data for 24-hour period

Time	Time interval Δt	Rainfall height h_i	Rainfall intensity i
[h:min]	[min]	[mm]	[mm/min]
1	2	3	4
19:10-19:20	10	13.8	1.38
19:10-19:30	20	15.4	0.77
17:20-18:00	40	29.6	0.74
17:20-18:20	60	32.0	0.53
17:20-18:50	90	32.0	0.36
17:20-19:20	120	46.4	0.39
17:20-20:20	180	52.4	0.29
17:20-22:20	300	57.0	0.19
17:20-06:20	720	57.6	0.08
17:10-17:10	1440	59.0	0.04

The maximum rainfall intensity for the considered pluviogram of 1.38 mm/min was observed for 10 minutes' interval. The maximum one-hour intensive rainfall of 32.0 mm was recorded in another time interval. By analyzing the pluviogram data, the maximum monthly rainfall data series are formed and presented in Table 2.

The one-hour rainfalls are the most important parameter when analyzing the dam stability as well as stabilization and erosion protection measures. From the three-years analyzed period, a maximum of 34.6 mm one-hour intensive rainfall was observed in September 2016. Similar intensive rainfall was observed in May 2017, when the one-hour precipitation was 32.0 mm, but also 46.4 mm in 2 hours. The maximum 24-hour precipitation of 59.0 mm was measured the same day. In 2018, the maximum one-hour intensive rainfall was 13.2 mm which is significantly lower. There is also a month without precipitation.

6. Statistical analysis of intensive rainfall, results and discussion

In order to define the distribution function of probability for each data series, the composed data series are analyzed by methods of mathematical statistics and probability theory. The statistical parameters of the data series are defined using the data series of monthly precipitation empirical probability presented in Table 3.

The method of moments (MOM) estimators are used for parameter estimation of the distributions. The following distributions can be used: The Gaussian or N distribution, Log-Normal, Pearson Type 3, Log-Pearson Type 3, Exponential, Gumbel, Generalized Extreme Value, Weibull, Generalized Pareto etc. The extreme value type 1 distribution, also called Gumbel distribution, is often used as the best-fit distribution to represent maximum rainfall or flood [6].

Table 2. Monthly maximum rainfall for characteristic time intervals

Year	Month	10'	20'	40'	60'	90'	120'	180'	300'	720'	1440'
2016	I	3.0	3.0	3.4	4.2	5.0	5.6	5.8	7.6	13.0	14.0
	II	1.8	2.4	3.4	3.8	4.2	4.4	5.2	5.4	5.4	7.8
	III	4.6	8.0	12.4	15.8	20.8	22.8	23.6	23.6	25.8	40.4
	IV	4.0	4.8	6.4	8.0	10.0	10.2	10.8	11.8	17.0	17.6
	V	5.8	7.0	7.8	9.2	11.2	13.6	16.4	20.8	34.2	40.2
	VI	7.6	8.4	10.4	12.4	12.6	13.8	18.2	22.8	22.8	22.8
	VII	1.4	2.6	2.8	2.8	2.8	3.0	3.0	3.0	3.0	3.0
	VIII	16.0	18.6	19.2	19.2	19.2	19.2	19.4	19.8	19.8	19.8
	IX	16.4	22.6	31.2	34.6	35.6	35.6	36.4	37.6	37.6	37.6
	X	2.2	2.6	3.2	3.6	4.2	4.6	6.6	8.6	9.4	9.8
	XI	3.4	4.8	5.4	6.0	7.0	7.8	8.0	8.2	15.4	18.0
	XII	0.2	0.2	0.2	0.2	0.2	0.2	0.2	0.2	0.2	0.2
2017	I	0.4	0.8	1.2	1.6	1.8	2.0	2.4	2.6	3.0	3.2
	II	0.8	1.2	1.6	2.2	2.4	2.4	2.4	3.0	3.6	3.6
	III	1.2	1.2	2.2	2.8	3.2	3.2	3.8	4.2	5.2	6.2
	IV	2.6	4.0	6.0	7.2	9.0	11.6	13.4	16.8	16.8	19.0
	V	13.8	15.4	29.6	32.0	32.0	46.4	52.4	57.0	57.6	59.0
	VI	3.6	4.6	4.8	6.6	8.4	8.4	10.4	10.4	10.4	20.2
	VII	1.6	1.8	1.8	2.6	3.6	4.4	5.0	5.0	6.4	7.4
	VIII	2.0	3.0	4.2	5.0	6.6	7.0	7.2	9.4	10.0	10.0
	IX	1.6	1.6	1.6	2.4	3.4	4.6	6.0	6.6	8.2	8.8
	X	1.4	2.2	4.0	4.6	5.2	6.0	6.8	8.0	10.2	10.2
	XI	1.4	2.6	4.6	6.4	8.6	9.4	9.6	10.6	17.4	25.8
	XII	6.2	6.2	7.6	9.4	11.0	12.8	14.0	17.6	22.4	37.6
2018	I	1.8	3.2	6.2	8.6	11.8	13.2	13.6	13.6	13.8	13.8
	II	1.8	2.2	2.4	3.4	4.2	5.2	6.6	8.8	11.6	16.0
	III	4.8	5.4	6.2	6.4	6.8	7.0	7.0	8.6	9.0	9.6
	IV	2.0	3.4	4.6	5.4	6.6	6.6	6.6	6.8	7.4	7.4
	V	2.4	3.8	6.2	6.6	9.4	9.8	10.0	11.4	13.0	13.0
	VI	8.6	12.8	13.2	13.2	13.4	13.6	13.8	14.2	14.2	17.4
	VII	3.6	4.4	5.0	5.0	5.0	5.0	5.0	5.0	5.0	5.0
	VIII	4.6	5.6	7.4	7.8	8.0	8.0	8.0	10.2	10.6	10.6
	IX	0.0	0.0	0.0	0.0	0.0	0.0	0.0	0.0	0.0	0.0
	X	0.4	0.6	0.6	0.6	0.6	0.6	0.6	0.6	0.6	0.6
	XI	4.2	5.0	6.4	7.0	8.6	11.0	15.6	18.6	22.4	26.4
	XII	1.0	1.8	3.0	3.6	4.4	5.4	7.8	8.6	9.4	11.0

Table 3. Data series of monthly precipitation empirical probability

No.	10'	20'	40'	60'	90'	120'	180'	300'	720'	1440'
1	16.4	22.6	31.2	34.6	35.6	46.4	52.4	57.0	57.6	59.0
2	16.0	18.6	29.6	32.0	32.0	35.6	36.4	37.6	37.6	40.4
3	13.8	15.4	19.2	19.2	20.8	22.8	23.6	23.6	34.2	40.2
4	8.6	12.8	13.2	15.8	19.2	19.2	19.4	22.8	25.8	37.6
5	7.6	8.4	12.4	13.2	13.4	13.8	18.2	20.8	22.8	37.6
6	6.2	8.0	10.4	12.4	12.6	13.6	16.4	19.8	22.4	26.4
7	5.8	7.0	7.8	9.4	11.8	13.6	15.6	18.6	22.4	25.8
8	4.8	6.2	7.6	9.2	11.2	13.2	14.0	17.6	19.8	22.8
9	4.6	5.6	7.4	8.6	11.0	12.8	13.8	16.8	17.4	20.2
10	4.6	5.4	6.4	8.0	10.0	11.6	13.6	14.2	17.0	19.8
11	4.2	5.0	6.4	7.8	9.4	11.0	13.4	13.6	16.8	19.0
12	4.0	4.8	6.2	7.2	9.0	10.2	10.8	11.8	15.4	18.0
13	3.6	4.8	6.2	7.0	8.6	9.8	10.4	11.4	14.2	17.6
14	3.6	4.6	6.2	6.6	8.6	9.4	10.0	10.6	13.8	17.4
15	3.4	4.4	6.0	6.6	8.4	8.4	9.6	10.4	13.0	16.0
16	3.0	4.0	5.4	6.4	8.0	8.0	8.0	10.2	13.0	14.0
17	2.6	3.8	5.0	6.4	7.0	7.8	8.0	9.4	11.6	13.8
18	2.4	3.4	4.8	6.0	6.8	7.0	7.8	8.8	10.6	13.0
19	2.2	3.2	4.6	5.4	6.6	7.0	7.2	8.6	10.4	11.0
20	2.0	3.0	4.6	5.0	6.6	6.6	7.0	8.6	10.2	10.6
21	2.0	3.0	4.2	5.0	5.2	6.0	6.8	8.6	10.0	10.2
22	1.8	2.6	4.0	4.6	5.0	5.6	6.6	8.2	9.4	10.0
23	1.8	2.6	3.4	4.2	5.0	5.4	6.6	8.0	9.4	9.8
24	1.8	2.6	3.4	3.8	4.4	5.2	6.6	7.6	9.0	9.6
25	1.6	2.4	3.2	3.6	4.2	5.0	6.0	6.8	8.2	8.8
26	1.6	2.2	3.0	3.6	4.2	4.6	5.8	6.6	7.4	7.8
27	1.4	2.2	2.8	3.4	4.2	4.6	5.2	5.4	6.4	7.4
28	1.4	1.8	2.4	2.8	3.6	4.4	5.0	5.0	5.4	7.4
29	1.4	1.8	2.2	2.8	3.4	4.4	5.0	5.0	5.2	6.2
30	1.2	1.6	1.8	2.6	3.2	3.2	3.8	4.2	5.0	5.0
31	1.0	1.2	1.6	2.4	2.8	3.0	3.0	3.0	3.6	3.6
32	0.8	1.2	1.6	2.2	2.4	2.4	2.4	3.0	3.0	3.2
33	0.4	0.8	1.2	1.6	1.8	2.0	2.4	2.6	3.0	3.0
34	0.4	0.6	0.6	0.6	0.6	0.6	0.6	0.6	0.6	0.6
35	0.2	0.2	0.2	0.2	0.2	0.2	0.2	0.2	0.2	0.2
36	0.0	0.0	0.0	0.0	0.0	0.0	0.0	0.0	0.0	0.0

The statistical parameters of each data series x_i with n observations in the data set are defined as follows:

- Arithmetic average

$$\bar{x} = \frac{x_1 + x_2 + x_3 + \dots + x_{n-1} + x_n}{n} = \frac{\sum_{i=1}^n x_i}{n} \quad (1)$$

- Modular coefficient

$$k_i = \frac{x_i}{\bar{x}} \quad (2)$$

- Standard deviation (for data series with $n \geq 30$)

$$\sigma = \sqrt{\frac{\sum_{i=1}^n (x_i - \bar{x})^2}{n}} \quad (3)$$

- Variation coefficient (for data series with $n < 60$)

$$c_v = \frac{\sigma}{\bar{x}} = \sqrt{\frac{\sum_{i=1}^n (k_i - 1)^2}{n - 1}} \quad (4)$$

- Asymmetry coefficient

$$c_s = \frac{\sum_{i=1}^n (k_i - 1)^3}{n \cdot c_v^3} \quad (5)$$

The calculated statistical parameters are presented in Table 4.

Table 4. Statistical parameters of monthly precipitation data series

Parameter	10'	20'	40'	60'	90'	120'	150'	300'	720'	1440'
\bar{x}	3.84	4.94	6.56	7.51	8.52	9.57	10.60	11.86	13.66	15.92
σ	4.03	4.98	6.94	7.50	7.71	9.21	10.03	10.81	11.42	13.12
C_v	1.06	1.02	1.07	1.01	0.92	0.98	0.96	0.92	0.85	0.84
C_s	1.87	1.96	2.23	2.20	1.91	2.27	2.32	2.21	1.75	1.28
α	0.32	0.26	0.18	0.17	0.17	0.14	0.13	0.12	0.11	0.10
β	3.36	4.48	6.08	7.05	8.11	9.13	10.17	11.45	13.28	15.54

In the next step, to estimate the probable maximum precipitation, the values were fitted by the Gumbel distribution suitable to analyze extreme values. The Cumulative distribution function (CDF) and Probability density function (PDF) are expressed as:

- Cumulative distribution function (CDF)

$$f(z) = e^{-e^{-z}} \quad (6)$$

- Probability density function (PDF)

$$p(z) = e^{-z - e^{-z}} \quad (7)$$

Where data series parameters from Table 4 are: normalized variable z , scale parameter α dependent on standard deviation, location parameter β dependent on standard deviation arithmetic average, and can be calculated as:

$$z = \alpha \cdot (x - \beta) \quad (8)$$

$$\alpha = \frac{1.282}{\sigma} \quad (9)$$

$$\beta = \bar{x} - 0.45 \cdot \sigma \quad (10)$$

The obtained results from this analysis which represents the probability of not exceeding the value of the rain height by that random variable [5] are presented in Table 5.

Table 5. Probability of maximum precipitation p (z) [%] of a given duration

No.	10'	20'	40'	60'	90'	120'	180'	300'	720'	1440'
1	1.56	0.94	0.96	0.90	1.03	0.56	0.45	0.45	0.69	1.42
2	1.77	2.60	1.29	1.39	1.86	2.48	3.43	4.40	6.32	8.44
3	3.54	5.83	8.48	11.77	11.40	13.85	16.43	21.07	9.11	8.59
4	17.19	11.08	23.55	20.06	14.62	21.81	26.45	22.90	21.75	10.94
5	22.84	30.54	26.74	29.48	33.95	40.65	30.10	28.09	29.07	10.94
6	33.29	33.23	36.25	33.00	37.73	41.52	36.29	31.01	30.18	29.25
7	36.86	40.70	51.70	48.78	41.79	41.52	39.31	34.82	30.18	30.72
8	46.86	47.38	53.00	49.96	45.01	43.29	45.81	38.24	38.19	38.86
9	49.03	52.73	54.32	53.56	46.11	45.10	46.66	41.13	46.73	46.97
10	49.03	54.56	61.03	57.26	51.82	50.77	47.52	51.39	48.25	48.29
11	53.48	58.29	61.03	58.50	55.37	53.72	48.39	53.91	49.01	50.99
12	55.77	60.17	62.38	62.27	57.78	57.74	60.24	61.66	54.53	54.45
13	60.41	60.17	62.38	63.52	60.21	59.77	62.12	63.41	59.42	55.86
14	60.41	62.06	62.38	66.04	60.21	61.82	64.00	66.89	61.06	56.56
15	62.75	63.96	63.74	66.04	61.44	66.93	65.88	67.76	64.37	61.56
16	67.42	67.73	67.81	67.29	63.88	68.96	73.27	68.62	64.37	68.73
17	72.02	69.61	70.49	67.29	69.96	69.97	73.27	72.04	70.10	69.44
18	74.27	73.29	71.81	69.78	71.16	73.94	74.17	74.55	74.10	72.24
19	76.47	75.09	73.12	73.45	72.35	73.94	76.81	75.37	74.88	78.95
20	78.60	76.85	73.12	75.82	72.35	75.87	77.67	75.37	75.66	80.22
21	78.60	76.85	75.70	75.82	80.26	78.68	78.53	75.37	76.42	81.46
22	80.67	80.25	76.96	78.14	81.32	80.49	79.36	76.99	78.68	82.06
23	80.67	80.25	80.60	80.37	81.32	81.37	79.36	77.79	78.68	82.66
24	80.67	80.25	80.60	82.51	84.33	82.23	79.36	79.36	80.14	83.25
25	82.65	81.87	81.76	83.53	85.29	83.08	81.80	82.36	82.94	85.52
26	82.65	83.44	82.89	83.53	85.29	84.71	82.59	83.08	85.55	88.12
27	84.53	83.44	83.99	84.54	85.29	84.71	84.85	87.10	88.52	89.09
28	84.53	86.37	86.09	87.36	87.97	85.50	85.58	88.33	91.12	89.09
29	84.53	86.37	87.08	87.36	88.80	85.50	85.58	88.33	91.59	91.72
30	86.32	87.73	88.96	88.24	89.60	89.80	89.54	90.57	92.05	93.92
31	88.00	90.23	89.83	89.08	91.10	90.43	91.80	93.43	94.84	95.97
32	89.56	90.23	89.83	89.89	92.46	92.20	93.28	93.43	95.80	96.45
33	92.32	92.41	91.47	92.11	94.26	93.26	93.28	94.24	95.80	96.68
34	92.32	93.38	93.61	95.09	96.94	96.23	96.66	97.32	98.42	98.65
35	93.51	95.07	94.82	96.03	97.60	96.87	97.20	97.75	98.70	98.86
36	94.58	95.79	95.37	96.45	97.88	97.17	97.45	97.95	98.82	98.96

The estimation of the probable maximum precipitation PMP (statistical approach) in relation with the rainfall heights for given characteristic durations is presented in Figure 5.

In case when rainfall heights differ from the ones presented are needed, it is recommended to obtain them from the above presented diagram using linear interpolation. Thus, the rainfall heights presented in Table 6 are obtained for probabilities of 50, 20, 10, 4, 2 и 1 %, which correspond to the return period T of 2, 5, 10, 25, 50 и 100 months, respectively.

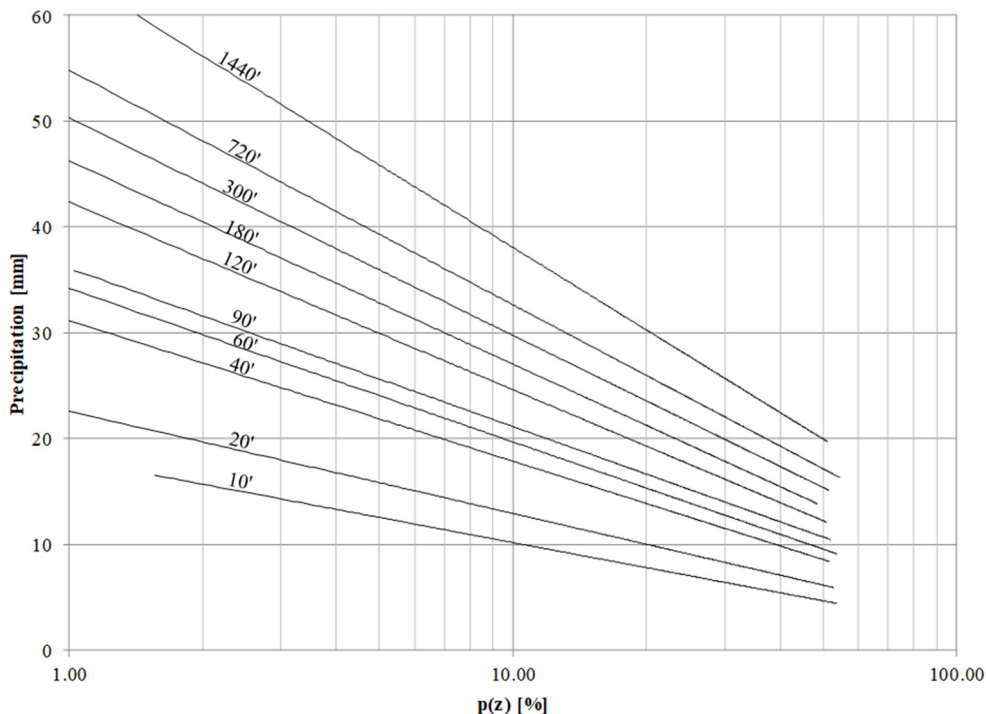


Figure 5. Probability distribution of monthly maximum rainfall data

Table 6. Monthly maximum rainfall [mm] for characteristic probabilities

$p(z)$ [%]	T [months]	10'	20'	40'	60'	90'	120'	180'	300'	720'	1440'
50	2	4.51	5.91	8.09	9.19	10.32	11.76	13.05	14.55	16.55	19.29
20	5	8.10	10.78	14.61	15.83	17.58	20.02	22.10	24.50	26.97	32.06
10	10	11.34	13.33	18.60	21.38	22.45	27.13	29.94	32.89	33.61	38.64
4	25	13.62	17.22	25.68	28.78	29.49	33.89	35.84	39.55	45.83	52.16
2	50	15.72	20.05	28.58	31.25	31.84	38.28	44.09	49.38	52.94	57.47
1	100		22.45	30.02	34.05		43.90	49.45	54.29	56.49	

7. Conclusion

This paper provides information on the short-duration intensive rainfalls over Topolnica tailing dam. The analyzed data refers to relatively short period of three years.

From the precipitation hydrograph in 10 minutes' intervals, a processed pluviogram was selected for a 24-hour period for which maximum daily precipitation was observed. The

maximum rainfall intensity is 1.38 mm/min, observed for duration of 10 minutes. The goal was to define the extreme values in a smaller time window, as the one-hour rainfalls are the most important parameter for such analysis. The results from data series show a maximum of 34.6 mm one-hour intensive rainfall observed in September 2016. Similar intensive rainfall was observed in May 2017, when the one-hour precipitation was 32.0 mm, but also 46.4 mm in 2 hours. The maximum 24-hour precipitation of 59.0 mm was measured the same day.

To represent the monthly precipitation data, the extreme value Gumbel probability distribution was used. As a result, the proposed diagram can be used for estimation of the probable maximum precipitation PMP for given durations and rainfall heights or vice versa.

The obtained results from this study can be used not only to analyze the dam stability and slopes erosion control, but also for hydrological analysis of flood wave propagation in the catchment area necessary for the design and maintenance of the drainage and overflow systems, determining the risk level of damage by extreme events etc.

Acknowledgements

The authors would like to express their thanks to management and technical staff of copper-mine Bucim who unselfishly shared the measurement data and support this work.

References:

- [1] Shkoklevski, Z., Todorovski, B.: Intensity rainfalls in Republic of Macedonia, Ss. Cyril and Methodius University, Faculty of Civil Engineering, Skopje, 1993.
- [2] Lazarevski, A.: Intensity of heavy precipitation in Macedonia, Republic Hydro Meteorological Institute, Skopje, 1967.
- [3] Susinov B., Josifovski J.: Investigation of the hydro-mechanical properties of silty sand material from Topolnica tailings dam, XVI Danube - European Conference on Geotechnical Engineering, Skopje, 2018.
- [4] PCE-FWS 20 Weather Station, www.pce-instruments.com, 05.05.2019.
- [5] De Paola F., Giugni M., Topa M.E., Bucchignani E.: Intensity-Duration-Frequency (IDF) rainfall curves, for data series and climate projection in African cities, SpringerPlus, 2014.
- [6] Alam, M., Emura, K., Farnham, C. and Yuan, J.: Best-fit probability distributions and return periods for maximum monthly rainfall in Bangladesh, *Climate*, 6(1), pp. 9, 2018.

MANAGEMENT, EXPLOITATION AND MONITORING OF THE GROUNDWATER

DRAGAN DIMITRIEVSKI ¹,

¹ *PhD, BSc.Civ.Eng., Geing Krebs und Kiefer International & others Ltd., Str. Boris Trajkovski 111, 1050 Skopje, Republic of North Macedonia; dragan@geing.com.mk*

1. Abstract

The groundwater development, management and monitoring proposes a long-term investment in the infrastructure for groundwater exploitation. In the world's developed countries, the groundwater management is maintained by implementation of advanced tools for hydrogeological modelling and quality monitoring systems. The trends in this field identify that the groundwater should be placed higher on the political agenda and that administrative units who are competent for groundwater management should be in charge for its future use. The groundwater is better protected from contamination than surface water, its quality is higher and the groundwater requires less treatment- which contributes to increased economic growth. Of course, the sustainable exploitation and controlled contamination as desired goals of the whole process are possible only by proper planning and strategic approach. The monitoring of the data for the groundwater status and their interpretation into respective technical documentation is a continuous and uninterrupted process, where the requirements of the European directives and international standards for North Macedonia as a candidate country for EU membership are not only recommended, but mandatory. The components of the Water Framework Directive that refer to the groundwater include a few different steps for reaching a good quantitative and chemical status of the groundwater. The member states of EU are supposed to encourage participation of all involved parties in the implementation of the Water Framework Directive, ensure that the price policy would stimulate efficient use of water resources and that the economic departments will contribute to the decrease of the water costs, including the ones that refer to the environment and resources.

Keywords: groundwater, management, monitoring, contamination, European directives.

2. Introduction

The groundwater is a "hidden resource" which is quantitatively bigger source than the surface water. Its prevention, monitoring and sustainability is more difficult due to their "hidden" character which makes the understanding of the pollution influences more complex. This often results with lack of awareness and/or evidence in terms of the level of risks and pressures.

In the developed countries of the world, the groundwater management is maintained by implementation of advanced tools for hydrogeological modeling and quality monitoring systems. In today's world there is a huge demand for this type of expertise as well as for

the accompanying technologies which include geodetic investigations, integrated by modeling of the water resources and the decision making systems.

Effective usage of data is essential for successful groundwater mapping, but interpretation of the data alone is not enough. The results of groundwater mapping must eventually be used for the management and protection of aquifers.

The groundwater development, management and exploitation proposes a long-term investment in the infrastructure for groundwater usage. The sustainable exploitation and the avoidance of contamination as desired goals of the whole process are possible only by proper planning and strategic approach. The implementation of the international experiences and practices of the developed countries in this field can be highly significant.

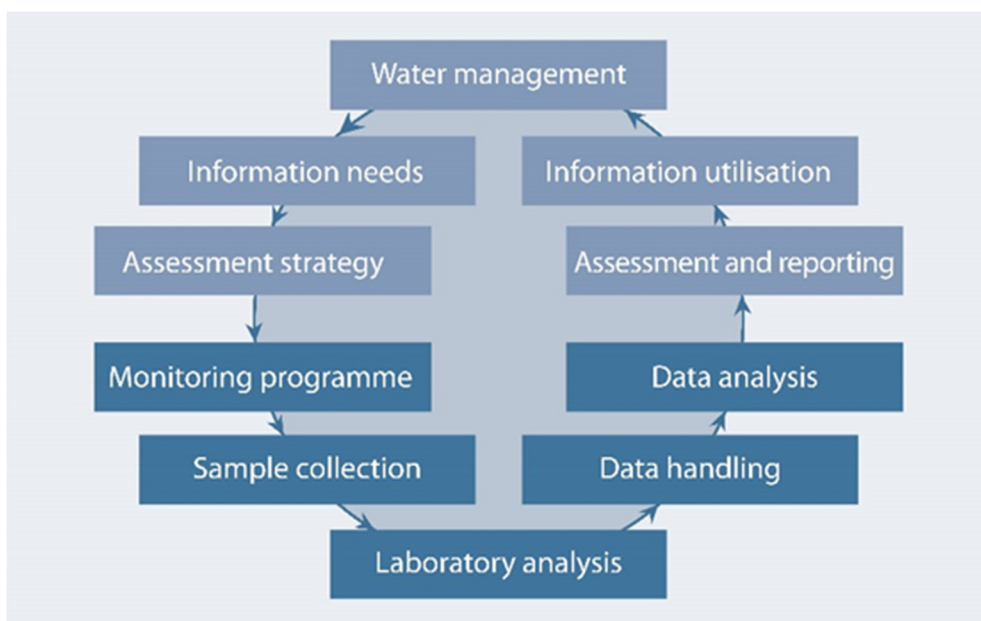


Figure 1. Water management cycle

The monitoring of the data for the groundwater status and their interpretation into respective technical documentation is a continuous and uninterrupted process, where the requirements of the European directives and international standards for North Macedonia as a candidate country for EU membership are not only recommended, but are mandatory.

The components of the Water Framework Directive that refer to the groundwater include a few different steps for reaching a good quantitative and chemical status of the groundwater.

Appendix VII from WFD formulates the Groundwater strategy which generally observes the following two subjects:

- Mapping of the locations and boundaries of groundwater bodies
- Groun/dwater status (chemical and quantitative)

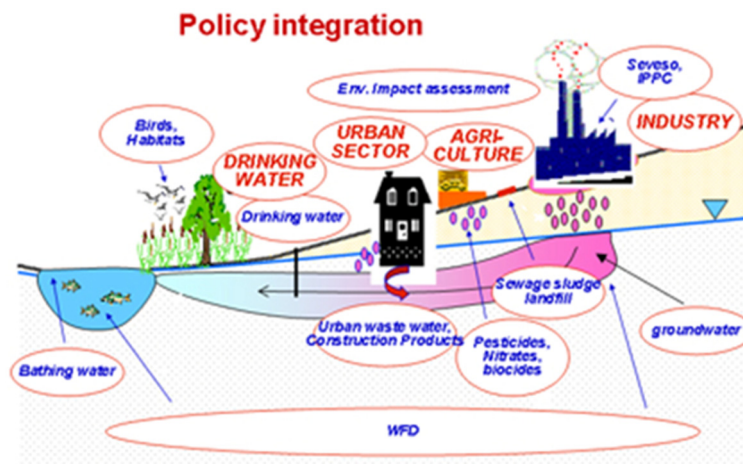
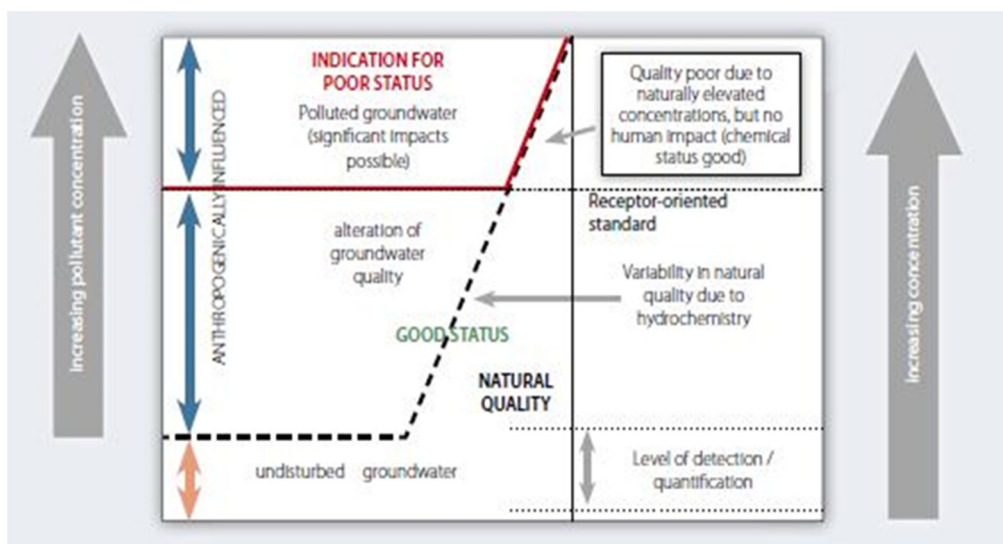


Figure 2. Policy of integration of the directives for environmental protection

Apart from the other integrated directives related to WFD in the part of the groundwater (Figure 2), the Groundwater directive (2006/118/EC) is sort of a scientific answer to the WFD requirements since it takes into account the estimations of the groundwater chemical status as well as the identification and correction of significant and constant upward trends in the concentrations of the pollutants.

The Charter established by the EU points out that the Research Framework Programmes must be developed considering two main strategic goals. First of all, it provides scientific and technological basis for the industry and encourages the international competitiveness. Secondly, it promotes research activities for support of other EU policies.



Picture 3. Elements for classification of the groundwater chemical status analyzed by the so-called project MOST (financed by the sixth Framework Programmes for Research and Technological Development)

Finally, the framework programmes (as part of the activities of the Union in this field) are created to assist during the problem solving stage and to respond to the major socio-economic challenges facing the society. Therefore, the Framework Programmes for Research (*Picture 3*) are a main instrument of the European Union for support of the research and development in the field of groundwater.

3. Methods

The establishment of a monitoring network is compulsory as per the Water Framework Directive of the European Union (WFD EU, 2000) and the Groundwater Directive (2002, 2006) for all member states and the candidates for EU membership. In ideal conditions, this network can be the basis for development of the groundwater monitoring in the countries where the groundwater resources have a significant influence.

The EU member states have an obligation to establish networks for groundwater monitoring on the basis of the results from the characterization and the estimation of the risk for providing a comprehensive review of the chemical and quantitative status of the groundwater. They had to create monitoring programmes which came into force at the end of 2006. In this context, the data from the monitoring comprise a significant element of the whole management cycle.

The monitoring programmes must contain information necessary for estimation of the achievement of objectives from the Directives which refer to the environment. This means that it is necessary to clearly understand the environmental conditions which are required for achieving the objectives and how the human activity can influence these, in order to prepare an effective monitoring programme. For that reason, the monitoring programmes should be designed on the basis of the procedure for characterization and estimation of the risks and the conceptual model (understanding of the groundwater system). The table below gives a short review of the objectives and requirements of the groundwater monitoring programmes established with Appendix 5 from WFD.

It is important to emphasize that the purpose of the monitoring as per the WFD is to focus on the phenomenon that influence the overall status of the groundwater body. The processes of local pollution levels that do not impact the overall status of the groundwater bodies should be objectives of different monitoring activities carried out by different competent institutions (local, regional), they are not relevant for the network on European level until their time and spatial development becomes dangerous for the qualitative objectives on the level of the macro system.

Data collection methods

Effective usage of the methods for data management is essential for successful groundwater mapping, but interpretation of the data alone is not enough. The results of groundwater mapping must eventually be used for the management and protection of aquifers.

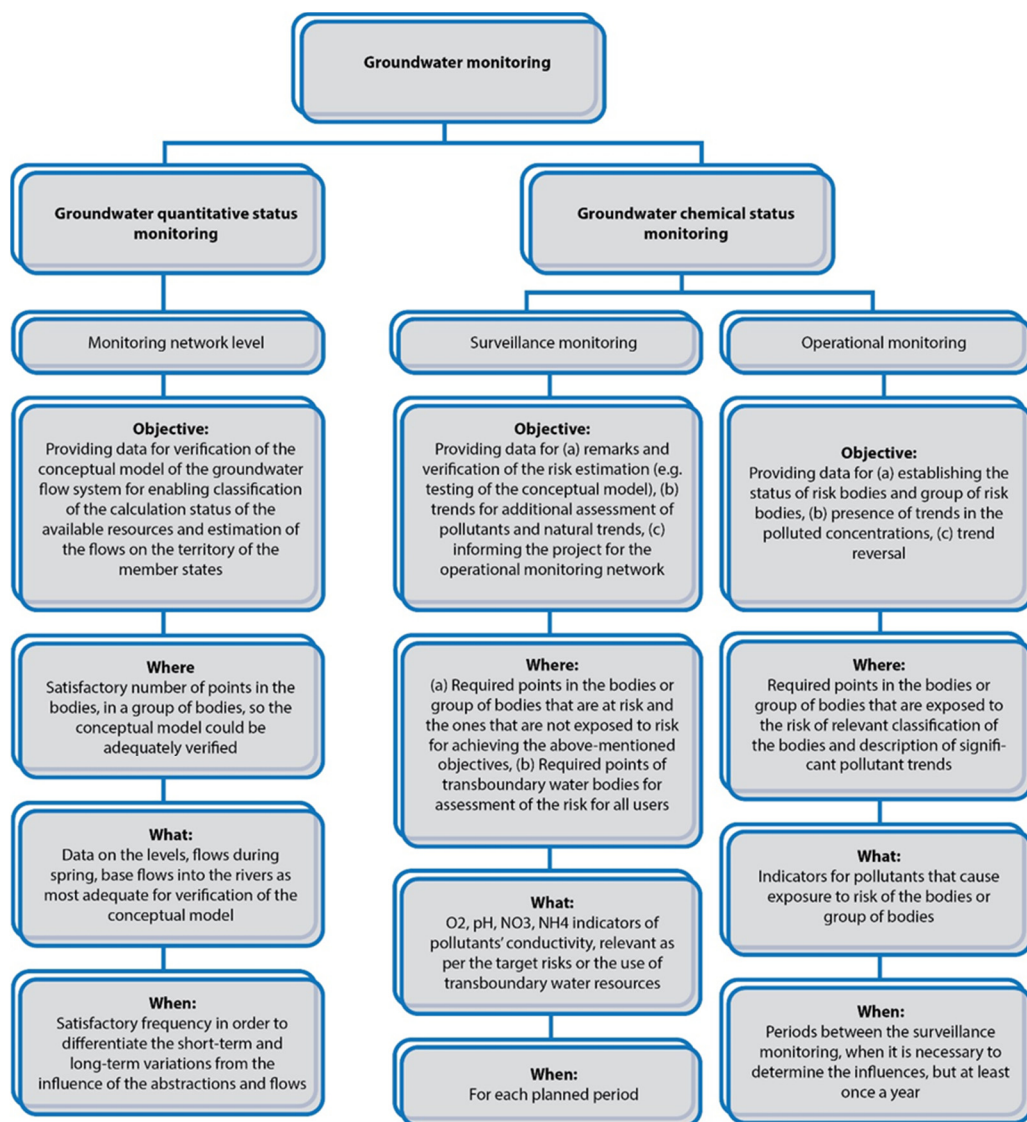


Figure 5. Objectives and requirements of the groundwater monitoring programmes

The water levels are expressed as heights above the sea level. All of the wells have a recommended point whose height is obtained with geodetic surveying or precise and sophisticated GPS equipment. The field workers determine the depth of the water from the reference height point. The water level is further calculated by subtracting the water depth from the referent height point. In many cases, the measure point of the well casings (i.e. the appropriate point of the well casing where the water depth is measured from) is not same with the referent point. When this occurs, the measured water depth is adjusted so it gives the water depth from the referent point. The data regarding the water levels are collected by monitoring the project, using manual and automatic techniques. The final product is a water level measured in meters above sea level. These heights are used for preparation of maps that show the flow direction of the groundwater, the gradients and the number of other obtained hydrogeological parameters that are known (hydraulic

conductivity, transmissivity, saturation etc.).

The monitoring programmes must contain information which is necessary in order to validate the risk estimation procedure and to estimate the achievement of the objectives set in the Groundwater Directive. It should be emphasized that it may be necessary to amend the programmes by adding additional monitoring in order to meet the requirements for the protected areas (i.e. Drinking Water Protection Areas - DWPA)

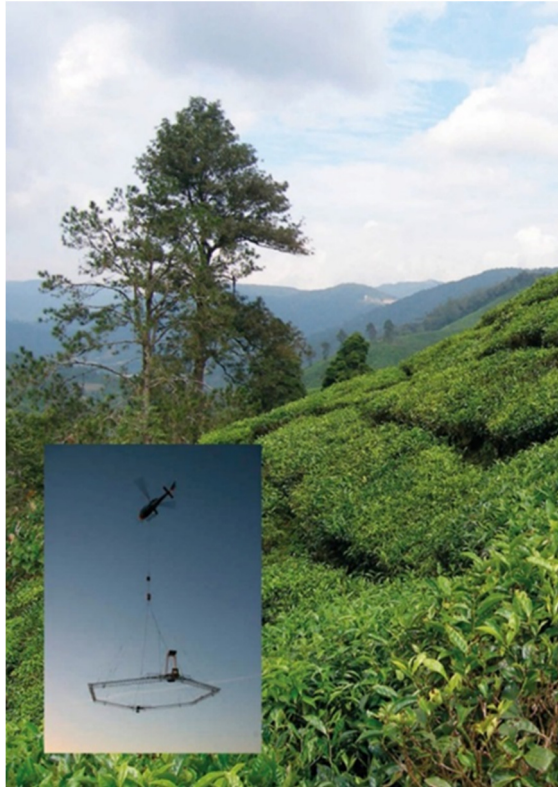


Figure 4. Regional mapping, Malaysia. New technology makes it possible to map water and minerals from the air. In Southeast Asia, in Malaysia, airborne technology has been used for very large geophysical surveys of groundwater. These involved flying over 15,000 kilometers (9,000 miles) in 30-40 kilometers (18-25 miles) long parallel tracks, covering an area of 3,000 square kilometers (1,100 square miles). Several Danish companies worked together in order to carry out drilling, down hole logging, water-quality testing, well field design, geological and hydrological modelling. The survey revealed a potential source of 500 million liters of groundwater per day (130 million US gallons). (Source: SkyTEM Surveys and EnviDan International)

Sustainable use of the groundwater

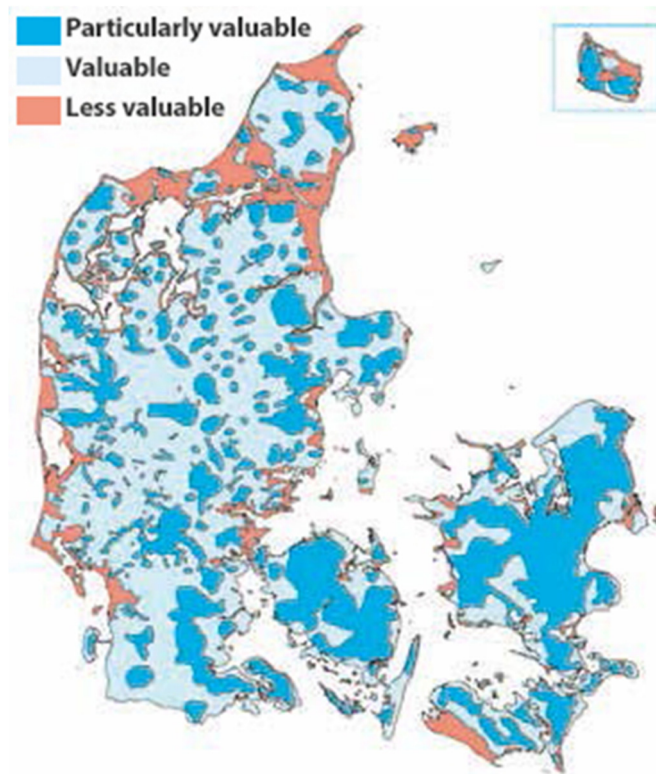


Figure 3. Classification. Groundwater classification map with subdivision of Denmark into highly valuable, valuable, and less valuable groundwater abstraction areas. (Source: GEUS).

Groundwater can be located very efficiently with advanced airborne geophysical mapping methods, and groundwater management can be achieved sustainably with groundwater modelling technologies and monitoring systems. The key is a credible groundwater model, which guards against over-extraction from the wells. Over-exploitation of the resource will come at the expense of future generations.

4. Results and discussion

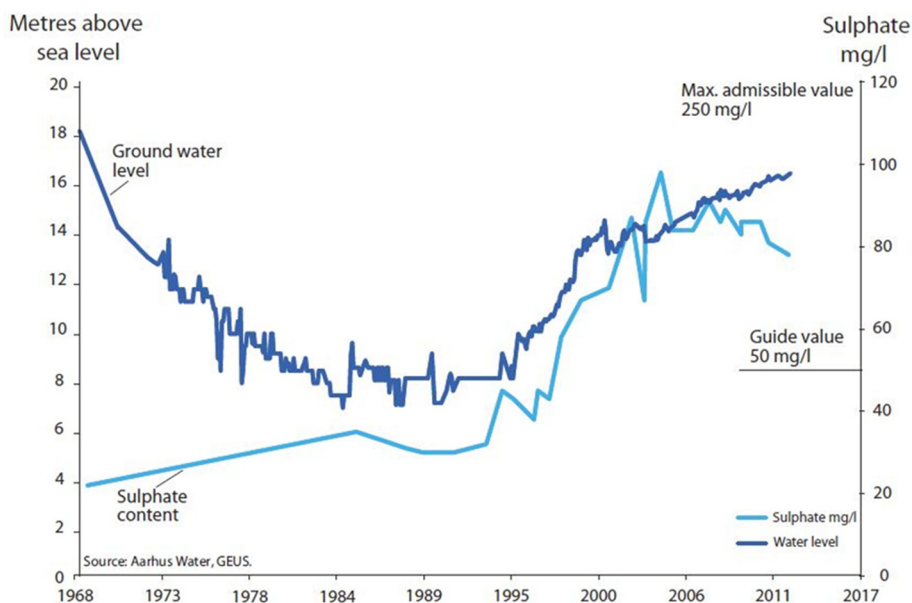
The results from the monitoring should be used for:

- Assistance during the categorization of the groundwater bodies;
- Validation of the risk estimation;
- Determining the chemical and quantitative status of groundwater bodies (including the estimation of the disposable resources of groundwater);
- Verifying the direction and the rate of flow in the groundwater bodies which cross the member states borders;
- Assistance during the designing of programme measures;
- Evaluation of the programme measures efficiency;
- Displaying the complementarity with DWPA and other objectives for the protected areas;

- Characterization of the natural quality of the groundwater including the natural trends (main line); and
- Identification of anthropogenic induced trends in the pollution concentrations and their interruption.

Some recent reports of the European Commission show that the pollution from the household, agricultural and industrial sources, despite that advancement in some areas, is still a major problem, whether directly by discharges (effluents), indirectly by extensive use of nitrogen fertilizers and pesticides or by discharge from old contaminated industrial lands or landfill sites (e.g. landfills, mines, heavy manufacturing industry, etc.). While the point sources have caused the largest part of the identified pollution until now, there is evidence that the diffuse sources have an increased impact on the groundwater. For example, the existing nitrate concentrations exceed the proposed nitrate values in almost one third of the groundwater bodies in Europe.

The groundwater mapping programme in Denmark is financed directly by those using the water. Public and private water consumers pay an additional costs per cubic meter of water. In 2015, when the programme ended, more than 25% of the total money was invested in geophysical mapping.



Picture 6. Sustainable yield, Denmark. The capacity of a water pumping station in Beder in Denmark was originally calculated using traditional hydrogeological analysis of the borehole data, combined with a short-term pumping test. These methods provided an incomplete understanding of the complexity of the aquifer dynamics, and as a result the capacity of the pumping station was overestimated. After pumping began in 1968 the water table fell by over 10 meters and the sulphate concentration increased. Based on advanced geophysical mapping and 3D hydrological modelling the sustainable yield estimate was reduced in 1990 by 35 percent. The water table has now risen to a sustainable level and the sulphate content has stabilized. (Source: GEUS)

5. Conclusion

Benefits of investing in groundwater supply

A key argument for using groundwater — besides the obvious argument of there being a shortage of surface water — is that groundwater is better protected from contamination than surface water. The quality is higher and the water requires less treatment. It is important to take care that aquifers (water-bearing formations) do not get contaminated, which can lead to high clean-up costs. Otherwise, in many places, using groundwater can be economically beneficial and secure a safe and stable water supply across both public and commercial sectors. There are also potential financial benefits for water utilities who supplement a water supply based on surface water resources with new groundwater resources. They may be better able to plan long term. They may also be able to postpone major investments in surface water infrastructure, or in assuring a higher level of water security. The treatment process for groundwater is simpler and cheaper compared with that for surface water, and increasing the volume of supply is much easier, since there is no need to build dams. . That is why groundwater should be placed higher on the political agenda and administrative units should be in charge for the future use of mapping results. Public entities should also be designated to monitor the groundwater resources that have been mapped and ensure that they are protected.

The continuous monitoring, groundwater mapping and sustainable management enable a better understanding of the available groundwater resources which is a crucial factor in terms of attracting new industrial companies and production. The companies can benefit from the improved water efficiency, the better quality and the safe water supply. The mining, food industries and the agricultural sector are often in conflict with other sectors and groups due to water. The groundwater can be a solution for this. Besides, the collection of the groundwater leaves a lesser mark on the environment if it is conducted appropriately. Also, all of the above-stated contributes to increased economic growth.

References:

- [1] <http://ec.europa.eu/environment/water/water-framework/groundwater/framework.htm>
- [2] <http://ec.europa.eu/environment/water/water-framework/groundwater/resource.htm>
- [3] <http://ec.europa.eu/environment/water/water-framework/groundwater/pdf/brochure/en.pdf>
- [4] http://ec.europa.eu/environment/water/participation/map_mc/map.htm
- [5] <http://inspire.ec.europa.eu/>
- [6] <http://inspire.ec.europa.eu/index.cfm/pageid/2/list/7>
- [7] <http://inspire.ec.europa.eu/index.cfm/pageid/48>
- [8] <http://inspire.ec.europa.eu/index.cfm/pageid/381>
- [9] <http://vandmodel.dk/vm/uk/index.html>
- [10] <https://stateofgreen.com/files/download/8291>
- [11] http://ec.europa.eu/environment/water/water-framework/facts_figures/pdf/2007_03_22_gwb_no_risk.pdf
- [12] http://ec.europa.eu/environment/water/water-framework/facts_figures/pdf/Groundwater%20monitoring%20stations-2012.pdf
- [13] <http://eur-lex.europa.eu/legal-content/EN/TXT/?uri=CELEX:32014L0080>
- [14] Common Implementation Strategy for the Water Framework Directive (2000/60/EC). Groundwater summary report. Technical report on groundwater body characterisation, monitoring and risk assessment issues as discussed at the WG C workshops in 2003–2004.

- December 2005, https://ec.europa.eu/environment/water/water-framework/pdf/groundwater_report.pdf
- [15] Convention on the protection and use of transboundary watercourses and international lakes; Helsinki, 17 March 1992
- [16] Jovanovski M., Gapkovski N., Pesevski I.: Engineering geology, Ss. Cyril and Methodius University, Faculty of Civil Engineering – Skopje, 2012
- [17] Dimitrievski D.: Enclosure to the continuous monitoring for the status of the groundwater, Ss. Cyril and Methodius University, Faculty of Civil Engineering – Skopje, 2017

Symposim Supporters



Ss. Cyril and Methodius University in Skopje

Bld. Coce Delchev no. 9, 1000 Skopje, N. Macedonia

www.ukim.edu.mk | ukim@ukim.edu.mk



**КОМОРА НА ОВЛАСТЕНИ АРХИТЕКТИ
И ОВЛАСТЕНИ ИНЖЕНЕРИ НА МАКЕДОНИЈА**

The Macedonian Chamber of certified architects and
certified engineers

Bld. Partizanski odredi no. 29, Skopje, N. Macedonia

<https://www.komoraoadi.mk> | contact@komoraoadi.mk

Become a student of the Faculty of Civil Engineering and a part of the impetus that creates and build the world! Step in the world of the successful people, because even the longest roads start with the first step. You will spend a part of your youth with us, and the youth is expensive to be misspent in vain. Your choice is an exceptional profession, for people who do believe in themselves, profession that requires prompt and courageous decisions. This profession will provide you with great privileges: your actions will remain an eternal record in the space and in the time being.

- STRUCTURAL ENGINEERING
- HYDRO-TECHNICAL ENGINEERING
- ROADS AND RAILWAYS ENGINEERING
- GEODESY
- GEOTECHNICAL ENGINEERING

SS. CYRIL AND METHODIUS UNIVERSITY
FACULTY OF CIVIL ENGINEERING
 gf.ukm.edu.mk

БЕТОН

ГРАДЕЊЕ * КОНСАЛТИНГ * ПРОЕКТИРАЊЕ * ИНЖЕНЕРИНГ

ДГ "БЕТОН" АД - Скопје, ул.Јуриј Гагарин бр.15, Скопје, тел: +389 2 55 13 700 +389 2 30 80 888.



Excellence in Engineering

Проектирање, Надзор, Ревизија и Консултанство во областите на:

ГЕОТЕХНИКА | геомеханички елаборати | потпорни ѕидови | геологија и хидрогеологија | бунари за вода | истражни дупчења | депонији, јаловишта, брани | санација на свлечишта | подобрување на почви | инјекциони работи | оскултација и мониторинг | геотехнички анализи на рудници и каменоломи | одводнување | **ХИДРОТЕХНИКА** | хидроенергетски системи | водоснабдителни и канализациски системи | хидрометеоролошки системи | регулација на речни корита | брани и акумулации | пречистителни станици | хидрологија | **ПАТИШТА И ЖЕЛЕЗНИЦИ** | инфраструктурни и основни проекти за патништа и железници | ревизија на проектна документација | оптимизација на проектни решенија | надзор под одржување на патништа | надзор под реконструкција на патништа | **ЕНЕРГЕТИКА** | хидроцентрали | надзор под реконструкција на патништа | соларни системи | фотоволтајски системи | ветерни електрани | термоелектрани | гасни дистрибутивни системи | инсталации | далсководи и електрични инсталации | **РУДАРСТВО** | главни и дополнителни рударски проекти | студии и елаборати од областа на водене и надзор над работи | проекти за заштита на косини | анализа на јаловишта | менаџмент и бонификација на јатлен | **ЖИВОТНА СРЕДИНА** | студии за оцена на влијанието врз животната средина (EIA) | профитбилитет и фазибилитет студии | елаборати за заштита на животна средина | мерни и технолошки за енергетска ефикасност и имплементација на обновливи енергетски извори | **АРХИТЕКТУРА И УРБАНИЗАМ** | инженерска архитектура | ТИРЗ | урбанистичко планирање | техничко-економска анализа | изработка на комплетна проектна документација | проект менаџмент | **ГЕОДЕЗИЈА** | геодетско снимање | дигитални геодетски подлоги | оскултација и мониторинг | дигитални планови и тематски мапи | ГИС апликации | **ЛАБОРАТОРИЈА** | геомеханички испитувања | испитувања за асфалт, агрегат и бетон | теренска лабораторија | испитувања на бучава и вибрации | **КОНСУЛТАНСТВО** | проект менаџмент | контрола менаџмент | финансиски менаџмент | физикални студии | правни консултации | контрола на квалитет |



Адреса
ул. Марко Среванец бр.1/1-1
1000 Скопје, Македонија
Тел: +389 (0)2 3109 795
Факс: +389 (0)2 3246 281

Email: info@geing.com.mk
ONLINE: www.GEING.com.mk
Контактирајте нв.
Веруваме дека ќе ги надминеме
Вашиите очекувања.



ADING
состојка на секоја градба
ingredient of each construction

Деловен систем за производство, примена и
пласман на хемиски материјали за градежништво

www.ading.com.mk

Business system for production, application and sale of
chemical materials for construction industry



ADING AD - Скопје,
1000 Скопје, R.Macedonia
ul. Novoselski Pat b.b.
tel: +389 2 2034 820;
+389 2 2034 840;
fax: +389 2 2034 821
e-mail: ading@ading.com.mk

Автомат, Западна Европа - Западна Кина*, Казахстан
Вграднување на бетонски колбови
Highway, Western Europe - Western China*, Kazakhistan
Concrete pavement installation



CIVIL ENGINEERING INSTITUTE "MACEDONIA"

CONTACT

GEOTECHNICAL DEPARTMENT
Tel: +389 02 30 63 040
gimgso@gim.com.mk

ENGINEERING DEPARTMENT
Tel: +389 02 30 66 836
gimn@gim.com.mk

CONSTRUCTION DEPARTMENT
Tel: +389 02 30 66 836
gim_operative@gim.com.mk

LABORATORY DEPARTMENT
Tel: +389 02 30 66 821
gim_laboratorija@gim.com.mk

MARKETING SECTOR
Tel: +389 (0)22091 994
priprema@gim.com.mk

FINANCE AND HR SECTOR
info@gim.com.mk
Tel: +389 (0)23091 988

CIVIL ENGINEERING INSTITUTE "MACEDONIA"
ul.Drezdenska br.52, 1000 Skopje
R. of Macedonia
Tel: +389 (0)23066 833
Fax: +389 (0)23066 828
[e-mail: info@gim.com.mk](mailto:info@gim.com.mk)
www.gim.com.mk



**УНИВЕРЗИТЕТ
"СВ. КИРИЛ И МЕТОДИЈ"
С К О П Ј Е**

**ЗАВОД ЗА
ИСПИТУВАЊЕ НА
МАТЕРИЈАЛИ И
РАЗВОЈ НА НОВИ
ТЕХНОЛОГИИ
" СКОПЈЕ "**

Тел: 02/3116 610;3213 718;
3222 308;3221 363
Телефакс: 02/3211 996
**Ул. Раде Кончар бр. 16,
1000 Скопје, Македонија**
<http://zlm.com.mk>
E-mail: zlm@f.ukim.edu.mk

- **ДИРЕКТОР**
- **ТЕХНИЧКИ
РАКОВОДИТЕЛ**
- **ЗАЕДНИЧКИ
СЛУЖБИ**
- **ИНСТИТУТИ**
- **МАТЕРИЈАЛИ
ТРАНСПОРТ И
ЕКОЛОГИЈА**
- **РАЗВОЈ НА
НОВИ
ТЕХНОЛОГИИ**
- **ЛАБОРАТОРИИ**
- **СЕКТОРИ**



Инженеринг при конструкција на прелив



Инженеринг при конструкција на ретновале и пат



Инженеринг при конструкција на автопат

